



C-H & C-O FUNCTIONALIZATION BY SILICON-HETEROATOM INTERELEMENT LINKAGES

Yiting Gu

ADVERTIMENT. L'accés als continguts d'aquesta tesi doctoral i la seva utilització ha de respectar els drets de la persona autora. Pot ser utilitzada per a consulta o estudi personal, així com en activitats o materials d'investigació i docència en els termes establerts a l'art. 32 del Text Refós de la Llei de Propietat Intel·lectual (RDL 1/1996). Per altres utilitzacions es requereix l'autorització prèvia i expressa de la persona autora. En qualsevol cas, en la utilització dels seus continguts caldrà indicar de forma clara el nom i cognoms de la persona autora i el títol de la tesi doctoral. No s'autoritza la seva reproducció o altres formes d'explotació efectuades amb finalitats de lucre ni la seva comunicació pública des d'un lloc aliè al servei TDX. Tampoc s'autoritza la presentació del seu contingut en una finestra o marc aliè a TDX (framing). Aquesta reserva de drets afecta tant als continguts de la tesi com als seus resums i índexs.

ADVERTENCIA. El acceso a los contenidos de esta tesis doctoral y su utilización debe respetar los derechos de la persona autora. Puede ser utilizada para consulta o estudio personal, así como en actividades o materiales de investigación y docencia en los términos establecidos en el art. 32 del Texto Refundido de la Ley de Propiedad Intelectual (RDL 1/1996). Para otros usos se requiere la autorización previa y expresa de la persona autora. En cualquier caso, en la utilización de sus contenidos se deberá indicar de forma clara el nombre y apellidos de la persona autora y el título de la tesis doctoral. No se autoriza su reproducción u otras formas de explotación efectuadas con fines lucrativos ni su comunicación pública desde un sitio ajeno al servicio TDR. Tampoco se autoriza la presentación de su contenido en una ventana o marco ajeno a TDR (framing). Esta reserva de derechos afecta tanto al contenido de la tesis como a sus resúmenes e índices.

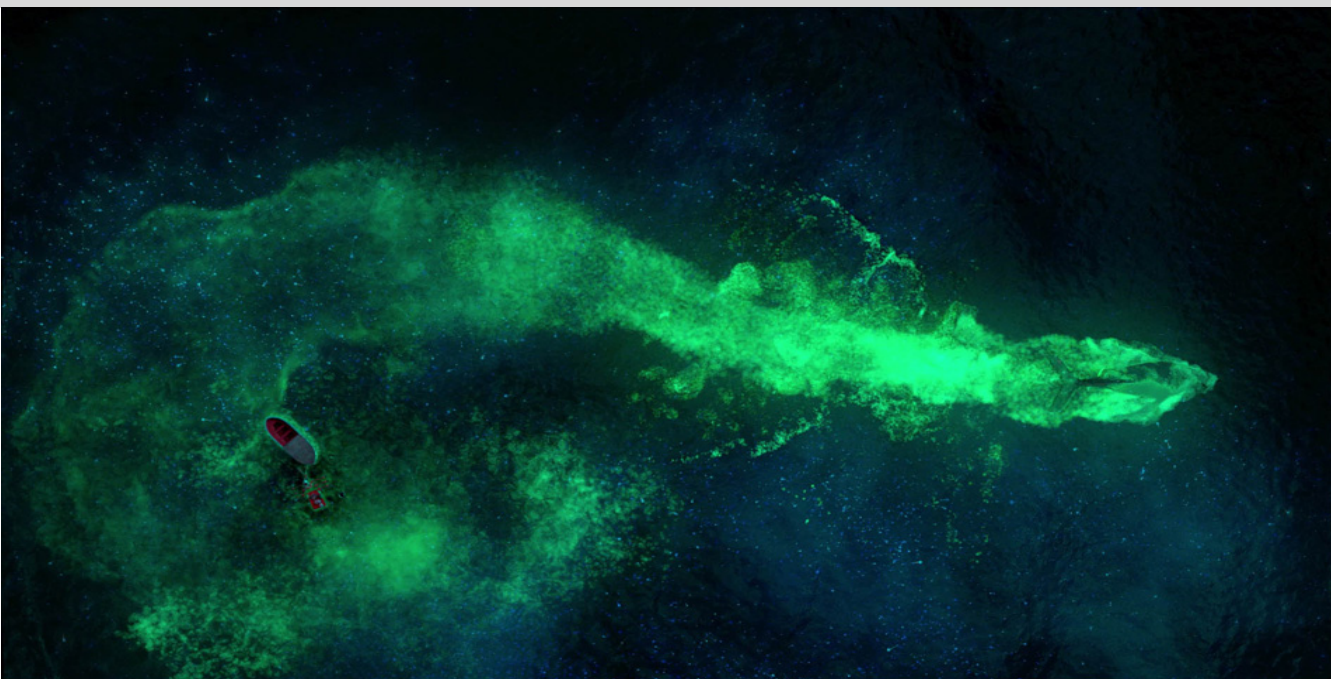
WARNING. Access to the contents of this doctoral thesis and its use must respect the rights of the author. It can be used for reference or private study, as well as research and learning activities or materials in the terms established by the 32nd article of the Spanish Consolidated Copyright Act (RDL 1/1996). Express and previous authorization of the author is required for any other uses. In any case, when using its content, full name of the author and title of the thesis must be clearly indicated. Reproduction or other forms of for profit use or public communication from outside TDX service is not allowed. Presentation of its content in a window or frame external to TDX (framing) is not authorized either. These rights affect both the content of the thesis and its abstracts and indexes.



UNIVERSITAT
ROVIRA I VIRGILI

C-H & C-O Functionalization by Silicon-Heteroatom Interelement Linkages

Yiting Gu



TESI DOCTORAL – TESIS DOCTORAL- DOCTORAL THESIS
2019

C-H & C-O Functionalization by Silicon-Heteroatom Interelement Linkages

Yiting Gu

Doctoral Thesis

Supervised by Prof. Rubén Martín

Institut Català d'Investigació Química (ICIQ)

Universitat Rovira i Virgili (URV)

Department of Analytical Chemistry & Organic Chemistry



**UNIVERSITAT
ROVIRA i VIRGILI**





Prof. Rubén Martín Romo, Group Leader at the Institute of Chemical Research of Catalonia (ICIQ) and Research Professor of the Catalan Institution for Research and Advanced Studies (ICREA),

STATES that the present study, entitled “C–H & C–O Functionalization by silicon–Heteroatom Interelement Linkages”, presented by Yiting Gu for the award of the degree of Doctor, has been carried out under my supervision at the Institute of Chemical Research of Catalonia (ICIQ).

Tarragona, October 2019

Doctoral Thesis Supervisor

Ruben Martin

Prof. Rubén Martín Romo

List of Publications

1. Yiting Gu, Yangyang Shen, Cayetana Zarate, Ruben, Martin*
“A Mild and Direct Site-Selective sp^2 C–H Silylation of (Poly)Azines”
J. Am. Chem. Soc. **2019**, *141*, 127-132.
2. Yangyang Shen, Yiting Gu, Ruben, Martin*
“ sp^3 C–H Arylation and Alkylation Enabled by the Synergy of Triplet Excited Ketones and Nickel Catalysts”
J. Am. Chem. Soc. **2018**, *140*, 12200-12209.
3. Yiting Gu, Ruben, Martin*
“Ni-Catalyzed Stannylation of Aryl Ester via C–O Cleavage”
Angew. Chem. Int. Ed. **2017**, *56*, 3187-3190.
4. Yiting Gu, Yaya Duan, Yangyang Shen, Ruben, Martin*
“Stereoselective Base-Catalyzed 1,1-Silaboration of Terminal Alkynes”
Submitted

Table of Contents

Acknowledgement	I
Preface	III
Abbreviations & Acronyms	IV
Abstract of This Doctoral Thesis	VI
Chapter 1. General Introduction	1
1.1. General Background.....	2
1.2. Synthesis of Si-B and Si-Sn Compounds	3
1.3. Activation Modes of Si-B and S-Sn Bonds.....	6
1.4. Application of Si-B and Si-Sn Reagents in Organic Synthesis.....	7
1.4.1. Monofunctionalization technologies using Si-B and Si-Sn reagents.....	7
1.4.2. Difunctionalization events using Si-B and Si-Sn reagents.....	15
1.5. General Objectives of This Doctoral Thesis.....	23
1.6. References.....	24
Chapter 2. Ni-Catalyzed Stannylation of Aryl Ester via C-O Bond Cleavage	31
2.1. C-O Electrophiles as Counterparts in Cross-Coupling Reactions.....	32
2.1.1. Challenges in using C-O electrophiles in Ni-catalyzed cross-coupling reactions.....	32
2.1.2. Ni vs Pd in cross-coupling reactions.....	33
2.2. Ni-Catalyzed Cross-Coupling of Aryl Pivalates via C-O Cleavage.....	35
2.2.1. C-C bond formation via <i>sp</i> ² C-O cleavage.....	35
2.2.2. C-heteroatom bond formation via C-O cleavage.....	39
2.3. General Aim of the Project.....	43
2.4. Ni-Catalyzed Stannylation of Aryl Pivalates.....	44
2.4.1. Optimization of the reaction conditions.....	44
2.4.2. Preparative substrate scope.....	51
2.4.2.1. Scope of naphthyl pivalates.....	51
2.4.2.2. Scope of phenyl pivalates.....	52
2.4.2.3. Scope of benzyl and allyl pivalates.....	52
2.4.2.4. Unsuccessful substrates.....	53
2.4.3. Synthetic applicability and orthogonal strategy.....	54
2.5. Mechanistic Considerations: Catalytic Cycle and Discussions	56
2.6. Conclusions.....	58
2.7. References.....	59
2.8. Experimental Section.....	63
2.8.1. General considerations.....	63
2.8.2. Synthesis of starting materials.....	63
2.8.3. General procedure for Ni-catalyzed stannylation of aryl pivalates via C-O cleavage.....	64

2.8.4. Gram scale reaction and synthetic applicability.....	75
2.8.5. Synthesis of oxidative addition complex Ni-1.....	66
2.8.6. Bibliography of known compounds.....	77
2.8.7. NMR spectra.....	78
Chapter 3. A Mild and Direct Site Selective sp^2 C-H Silylation of (Poly)Azines.....	117
3.1. General Characteristics of (Poly)Azines.....	118
3.2. C-H Functionalization of Pyridine.....	119
3.2.1. Overview on C-H Bond functionalization of pyridine	119
3.2.2. C-heteroatom bond-formation via C-H functionalization with transition metal.....	123
3.2.3. Selectivity control in C-H functionalization of pyridine	125
3.2.4. sp^2 C-H silylation of pyridine.....	127
3.3. General Aim of the Project.....	132
3.4. KHMDS Mediated Direct Site-Selective C-H Silylation of (Poly)Azines.....	133
3.4.1. Optimization of the reaction conditions.....	133
3.4.2. Substrate scope and late-stage silylation of functional azine.....	136
3.4.3. Regiodivergent C-H silylation.....	139
3.4.4. Application of silylated pyridine.....	140
3.5. Mechanistic Studies and Proposal	141
3.6. Conclusions.....	146
3.7. References.....	147
3.8. Experimental Section.....	152
3.8.1. General considerations.....	152
3.8.2. Synthesis of starting materials.....	152
3.8.3. General procedure for site-selective sp^2 C-H silylation of (poly)azines.....	153
3.8.4. Synthetic application profile.....	167
3.8.5. Orthogonal strategies and intermediacy of silyl anion species.....	168
3.8.6. ICP-OES analysis and ring opening reaction with epoxide.....	170
3.8.7. NMR experiments.....	171
3.8.8. X-ray crystallography.....	172
3.8.9. Bibliography of known compounds.....	196
3.8.10. NMR spectra	197
Chapter 4. Stereoselective Base-Catalyzed 1,1-Silaboration of Terminal Alkynes.....	255
4.1. 1,1-Difunctionalization of Terminal Alkynes.....	256
4.1.1. TM-catalyzed three-component 1,1-difunctionalization of terminal alkynes.....	257
4.1.2. Transition-metal-catalyzed 1,1-diboration of terminal alkynes.....	260
4.2. 1,2-Metallate Shift from Boron to sp Center.....	265
4.3. General Aim of the Project.....	269
4.4. Catalytic Base-Catalyzed Site-Selective 1,1-Silaboration of Terminal Alkynes.....	270
4.4.1. Optimization of the reaction conditions	270

4.4.2. Preparative substrate scope.....	273
4.4.3. Synthetic applicability of 1-boryl-1-silylalkene.....	275
4.4.4. Mechanistic considerations.....	277
4.5. Conclusions	279
4.6. References.....	280
4.7. Experimental Section.....	284
4.7.1. General considerations.....	284
4.7.2. General procedure for base-catalyzed 1,1-silaboration of terminal alkynes.....	284
4.7.3. Synthetic application profile	291
4.7.4. Mechanistic studies.....	294
4.7.5. X-ray diffraction	297
4.7.6. Bibliography of known compounds	305
4.7.7. NMR spectra.....	306
Chapter 5. General Conclusions.....	339

Acknowledgements

First and foremost, I would like to express my deepest gratitude to my supervisor **Rubén Martín**, for giving me strong supports, useful suggestions and inspiring talks during my PhD studies. I always feel lucky to have you as our supervisor. It is the day I went to Germany for the short stay, I suddenly recognize my changes after joining in MartiNis group. I'm feeling more confident and mature when dealing with new projects or moving to a new country. I still remember that day I was so excited and can't wait to email you and share my feelings. Looking back to the first year in your group, I'm surprised about all the magic you have performed on me.

Secondly, I would like to thank the members of the jury, **Prof. Elena Fernández**, **Prof. Mariola Tortosa** and **Prof. Igor Larrosa** for accepting to be part of my examination committee. **Prof. Marcos G. Suero**, **Prof. Arkaitz Correa Navarro**, **Prof. Francisco Juliá Hernández**, **Prof. Manuel Van Gemmeren**, **Prof. Xueqiang Wang** are also warmly thanked for taking time to evaluate this thesis as external reviewers.

Thanks **Ingrid** for all administrative support and ordering our solvents and chemicals. And **Miriam!** You make our group run more efficiently. It is great to have you around. Also **Sope!** Thanks for solving all the problems with GC and GC-MS and I will never forget your happy face when enjoying dumplings and spicy source. Special thanks to the ICIQ Supporting Units. Without all their kind help, I will not able to collect my data efficiently.

I would like to offer my heartfelt thanks to **Prof. Alois Fürstner**. It is a great experience to spend six months in your amazing lab. I learned a lot and truly enjoyed our chemistry discussion. During these months, I met amazing people like **Zhanchao**, **Ling**, **Pol**, **Sebastian**, **Marc**, **Lee**, **Kown**, **Lorenz**, **Chunxiang**, **John**, **Xiaobin** and **Hongming**.

I also would like to express my deep appreciations to the current and past members of the Martin group, I really enjoyed working together with all of you.

Rosie, a big thank for you for helping me correct the drafts and thesis. I will never forget the girls night until midnight in Vienna. You always think about other people's feelings and ready to be helpful. I wish the world had more people like you. **Elo**, I'm really cherish our friendship. I miss you so much! I've told many people about our crazy hiking. Thanks for always supporting me and sharing your feelings. I'm sure we will be good friends for our whole life. **Bart**, Thanks for your kindness and inviting me to the BBQ; it is amazing to overlap with you in Germany. Take care of my Elo!

Yaya! The world is so small. We met in Germany, then you became my labmate, and now you are my roommate, and project partner! Thank you so much for sharing your chemistry knowledge with me. You are a fantastic and patient guitar teacher. I will be safe when walking home very late, because you will always be on my side. **Caye**, "the queen of C-O cleavage", always with big small and endless energy. Your curiosity about chemistry really impressed me. Thanks for leaving me all the legacy from your C-O projects.

Shangzheng, crazy "column boy". You are clever and the most hardworking student I've ever seen. It has been a great pleasure to work next to you. I'm sure you will do a great job in chemistry on the years to come. **Hongfei**, thank you for taking over the project and trying to ski down the mountain with me. I had a lot of fun on the ski trip. **Basudev** and **Paco**, thanks so much for all the help, chemistry discussions and kindness to answer my stupid questions. **Reddy**, it was great to share the lab for 2 years with you; we all miss your Indian

food, palipoli ??? **Bradley**, unique “Young Macmillan” in our lab, always has sharp questions. I wish you all the best and good luck with your chemistry. **Marino, Andreu, Raul**, you are such nice guys. Thanks for helping me with the Spanish phone call, and all the helpful discussions and advice. I wish all the best for your thesis. And also I truly appreciate Andreu for sharing fume hood before I moved to the lab 2.12. Two more hardworking and smart PhD students **Fei** and **Craig**, I’m pretty sure you will do amazing job with your projects. **Laura, Carlota**, new blood in our team, it has been a pleasure meeting you. Thanks Laura for driving me home at that crazy rainy night. Good luck with your PhD studies.

Jacob, thanks for baking tasty cookies and bringing us fresh oranges. I like your Christmas gift a lot! It has been a pleasure to work with you. **Liang** (Prof. Xu), thanks for sharing interesting stories. Don’t worry! Hongfei will keep you safe in Tarragona. **Jessica**, thanks for your kind heart. I really enjoy our conversation about the plastic pollution and environment protection. Also I would like to thank all others: **Tiago, Ciro**. I wish the lab is not so far way and I could have more time to know you better.

Toni & Morgane, thank you for being very nice lab mates. **Masaki**, thanks for explaining me HTE. It was really nice to work with you. **Alicia**, it was great to have you in our lab, I hope you enjoy the new job in ICIQ. **Daniel**, a knowledgeable postdoc. I wish you all the best with your career. **Antonio**, my favorite Master so far. I really enjoy our short talks when you were waiting the glovebox. And I also want to mention some friends who did short stay in our group. **Lilly, Riccardo, Georgios, Tim, Yutaka, Philipp, Jonas, Pascal, Alberto**. I hope you enjoyed the time in our group and all the best for your respective future!

A specious mention goes to **Yangyang**, you have taught me how important it is to know what your strength and weakness are. Thank you for your unconditional love, companion, and understanding. You make these four years more enjoyable and full of happiness.

I also would like to express my deep appreciations to many friends in ICIQ for sharing their experience and giving me supports all the time. An additional gratitude to **Chang** and **Sijing** for encouragement, care, all the moments of gossips and Masaji. It was awesome sharing the weekend with you. Your friendship means a lot to me!

Last, but not at least, I am indebted to my parents and sister for supporting me and sharing my worries, frustrations, and happiness. This thesis certainly would not have been possible without the love, support and understanding of my family. 最后, 我要感谢我最亲爱的父母。是他们无条件的支持, 爱护和理解, 让我可以安心在西班牙完成学业。在过去的四年中, 他们从来都是报喜不报忧, 默默的为我们付出, 并始终关心着我是否开心, 健康和安。同时也要感谢我贴心的妹妹顾怡钰, 在我不在国内时经常陪伴着爸爸妈妈; 和我相互吐槽学习的压力, 和我分享生活和工汇中的点点滴滴。在博士期间, 最好的事情就是遇到了沈阳阳。感谢你无条件的支持和鼓励, 让我变得更加自信和快乐。一起加油吧!

It is a long journey and my PhD study enriched by all of your companions. The road to obtaining PhD could not have been possible without the kindness of the people I met during my past four years. Thank you all for appearing in my life, for all the encouragement and support through my hard times, and all the trust on every step and decision I have made.

Preface

The whole work presented in this dissertation has been carried out at the Institute of Chemical Research of Catalonia (ICIQ), during the period of December 2015 to October 2019 under the guidance of Professor Rubén Martín. The thesis contains five chapters: a general introduction, three research chapters, and a last chapter with a general conclusion of all the research work. Each of the research chapter includes an introduction and an aim of the presenting project, followed by a discussion of experimental results, mechanistic analysis, conclusions, and experimental sections.

The first chapter includes the general background of silicon-based interelement linkages. A brief overview of the preparation and activation pathways of silicon-heteroatom compounds, and their application in functionalization reactions are discussed.

The second chapter, ‘*Ni-Catalyzed Stannylation of Aryl Ester via C–O Bond Cleavage*’, describes the synthesis of arylstannanes via sp^2 C–O bond cleavage of aryl pivalates. Preliminary mechanistic studies and control experiments have indicated that a canonical catalytic cycle consisting of oxidative addition, transmetalation and reductive elimination comes into play. The results of this chapter have been published in *Angew. Chem. Int. Ed.* **2017**, *56*, 3187-3190.

The third chapter, ‘*A Mild and Direct Site Selective sp^2 C–H Silylation of (Poly)Azines*’, describes the synthesis of silylated azines through C–H functionalization of unactivated azines in the presence of stoichiometric amounts of base. This technology allows to access valuable silylated azines under mild conditions that are not easily within reach by traditional cross-coupling methodologies. Preliminary mechanistic studies and control experiments have indicated a silyl anion pathway, with site-selectivity modulated by the denticity of the solvent. The results in this chapter have been published in *J. Am. Chem. Soc.* **2019**, *141*, 127-132, with Dr. Yangyang Shen as co-author.

The last chapter, ‘*Stereoselective Base-Catalyzed 1,1-Silylation of Terminal Alkynes*’, presents our efforts toward the direct, atom-economical 1,1-difunctionalization of sp C–H bonds catalyzed by KHMDS. Our method allows to incorporate both a silyl and a boron fragment across an alkyne with an exquisite site-selectivity pattern, representing a complementary approach to traditional silylboration of π -components that require the utilization of transition metals and that operate with a different selectivity pattern. Additionally, we demonstrate the synthetic versatility of the corresponding silylborane adducts in a series of orthogonal C–C bond-forming reactions. The manuscript of this chapter is submitted, and it has been possible due to the collaboration with Dr Yaya Duan and Dr Yangyang Shen.

Abbreviations & Acronyms

acac = acetylacetonate

BDE = bond dissociation energy

Bpin = 4,4,5,5-tetramethyl-1,3,2-dioxaboronic ester

Cy = cyclohexyl

cod = 1,5-cyclooctadiene

DME = ethylene glycol dimethyl ether

DMF = N,N-dimethylformamide

DABSO = 1,4-Diazabicyclo[2.2.2]octane bis(sulfur dioxide)

equiv = equivalent

h = hour(s)

HMPA = hexamethylphosphoramide

Int = intermediate

KHMDS = potassium bis(trimethylsilyl)amide

o = ortho

m = meta

p = para

NHC = N-heterocyclic carbene

NFSI = N-Fluorobenzenesulfonimide

Piv = pivalate

rt = room temperature

SET = single electron transfer

t = tert

THF = tetrahydrofuran

Ts = tosyl

S_EAr = electrophilic aromatic substitution

S_NAr = nucleophilic aromatic substitution

TBS = tert-butyldimethylsilyl

DTBP = di-tert-butyl peroxide

Tmp = 2,2,6,6-tetramethylpiperidyl

Abstract of This Doctoral Thesis

Synthetic chemistry is almost unimaginable without three main group elements, namely, boron, silicon, and tin. When attached to a carbon atom of any hybridization, these functional groups serve as exceptionally versatile linchpins in synthesis, selectively transforming into an enormous breadth of C–C and C–X bonds. Therefore, the means to discover new methods to forge valuable C–Si, C–B and C–Sn bonds are always in high demand. In line with the research interest of Martín’s group in the activation of strong σ -bonds, this doctoral thesis will be focused on the development of novel techniques to make use of silicon-heteroatom interelement linkages to functionalize inert C–O & C–H bonds via either nickel catalysis or transition metal-free protocols. We hope that the transformations described in my PhD thesis will inspire others for the development of cross-coupling reactions and functionalization techniques that make use of interelement linkages as coupling partners.

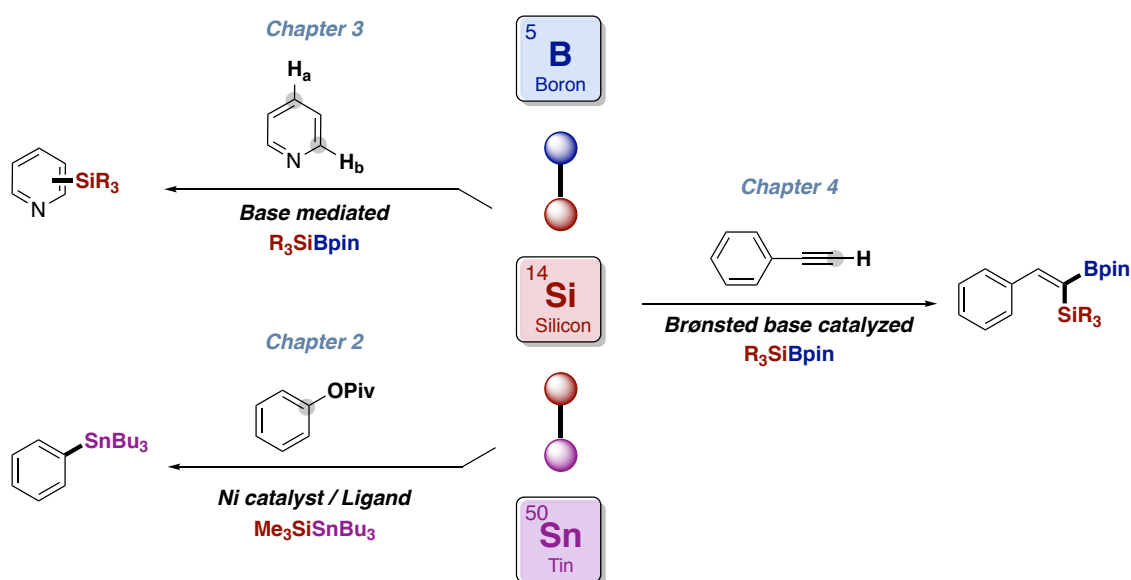


Figure 1. General abstract of this doctoral thesis

Our first effort on interelement linkages was focused on a nickel-catalyzed stannylation of aryl esters via sp^2 C–O functionalization aided by silicon-tin nucleophiles. In this project we chose sterically bulky aryl pivalates as precursors, as these are less likely to undergo hydrolysis compared with their corresponding acetate congeners. In addition, the electronegativity difference of silicon and tin allows for chemoselective activation of the Si–Sn bond, allowing to transfer selectively the tin fragment. This protocol was distinguished with its wide scope and mild conditions, thus representing a useful entry to synthetically versatile aryl stannane building blocks. Following up our interest on interelement linkages, chapter 2 will be based on the utilization of silylboranes for the development of a rather unusual site-selective sp^2 C–H silylation of (poly)azines in the absence of transition metal. Our method is characterized by its mild conditions, wide substrate scope, switchable regioselectivity by subtle modulation of the solvent denticity and its application

in late-stage functionalization in (poly)azine drugs. Mechanistic studies suggest the intermediacy of silyl anion species and the involvement of contacted or separated ion pairs depending on the solvent utilized. Our last project deals with the difunctionalization of alkynes with silylboranes in the absence of transition metals. Specifically, we have found a rather abnormal 1,1-difunctionalization event that has allowed us to unlock a new pathway for forging $C(sp^2)$ -B and $C(sp^2)$ -Si bonds in an atom-economical manner in the presence of catalytic amounts of KHMDS. This transformation is distinguished by its excellent site-selectivity, exploiting a previously unrecognized opportunity that complements existing 1,1- and 1,2-difunctionalization events of alkynes. Additionally, such a platform provides a new strategy for streamlining the synthesis of geminal dimetallic reagent with high stereoselectivity and preparative utility in organic synthesis. Mechanistic experiments suggest that a 1,2-shift on the boron center to *sp* carbon comes into play.

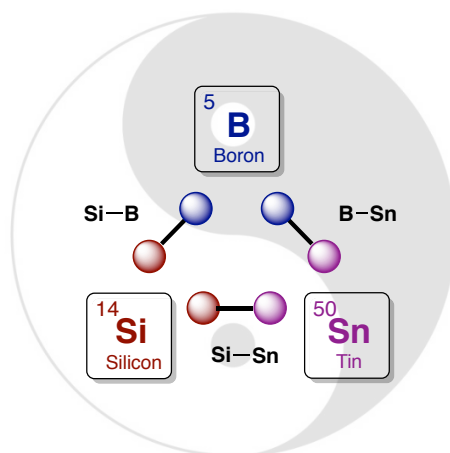
In conclusion, we have developed three new methods towards the functionalization of inert C-O & C-H bonds by using silicon-based interelement linkages. All the above transformations display excellent chemoselectivity profile under mild conditions. Preliminary mechanistic studies have been carried out, allowing to understand how these reactions operate at the molecular level. We believe these protocols will contribute to a more systematic utilization of silicon-heteroatom reagents in the arena of inert chemical bond functionalization.

Chapter 1.

General Introduction

1.1. General Background

Main group elements such as boron, silicon, and tin have revolutionized the way synthetic chemists build up C–C and C–heteroatom bonds. Apart from the inherent versatility and application profile of organoboron, organosilicon and organotin compounds, it is worth noting that these building blocks have found immediate application in material science, pharmaceuticals and agrochemical settings.¹⁻³ The term “interelement linkage” was introduced for chemical bonds constructed by these three elements, which are mutual linkages within the heavy main group elements and linkages between the main group elements and the transition metals.⁴ There are six different combinations of these three elements. Among these, silylboranes and silylstannanes rank amongst the most widely used reagents in these endeavors.

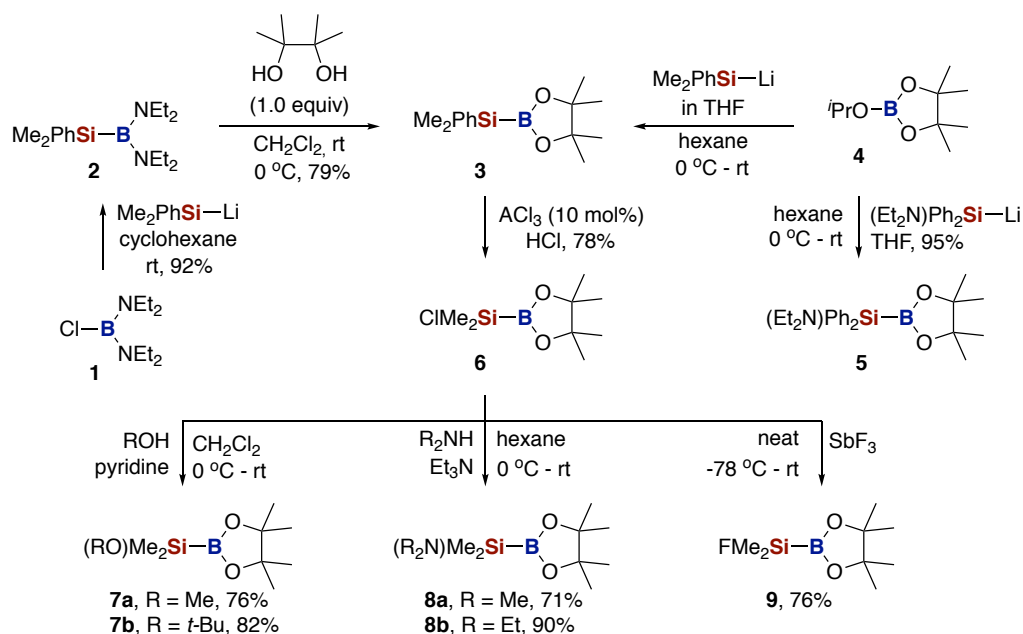


Scheme 1.1. Interelement linkages from boron, silicon and tin

Nonpolarized Si–Si bonds are thermally stable, with a bond dissociation energy (BDE) of 55 kcal/mol in average. In contrast, the electronegativity difference of the two elements in silylboranes and silylstannanes ($\chi_{\text{B}} = 2.04$, $\chi_{\text{Si}} = 1.90$, $\chi_{\text{Sn}} = 1.96$) makes the activation of the Si–B and Si–Sn viable. In addition, the inherent distinct reactivities of boryl, silyl and stannyl groups suggest that interelement linkages might be used to selectively introducing these moieties into organic molecules with high levels of regiocontrol. As Si–B and Si–Sn interelement reagents are not naturally-occurring, the next sections summarize known protocols for preparing silylboranes and silylstannanes. Although silylstannanes have comparatively been less-studied, the different pathways known to activate the Si–B bond might a priori be employed to functionalize the Si–Sn linkage as well. As it will become evident from the data compiled in the following sections, silylboranes and silylstannanes might serve as a gateway to build up molecular diversity in a rapid and reliable manner while allowing to generate useful building blocks that would a priori be difficult to reach via other synthetic routes.

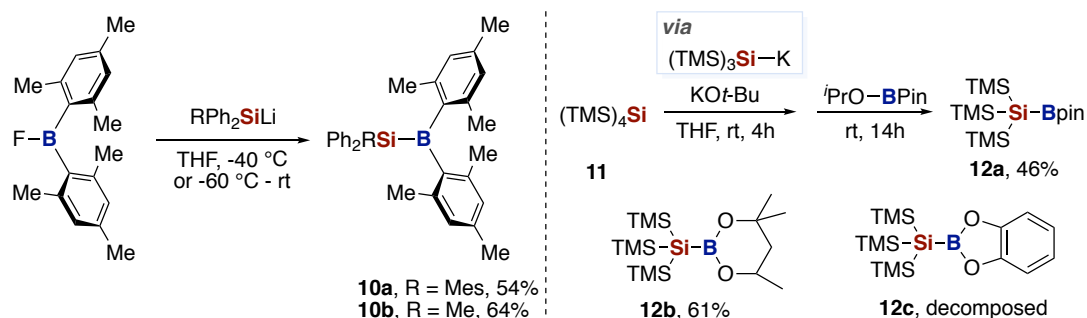
1.2. Synthesis of Si-B and Si-Sn Compounds

Pioneering studies by Nöth and co-workers allowed chemists to have a platform to prepare stable silylboranes. Specifically, the Si-B bond was formed by transmetalation of silyl lithium reagent with electrophilic boron halides (**1** to **2**).⁵ Silylboranes with amino groups directly attached to the boron atom increase the stability of the Si-B bond due to electronic shielding effect of the lone pairs of the nitrogen atoms to the adjacent boron atom, whereas the presence of alkyl groups at boron lowers down the stability of the corresponding silylborane. Nöth also disclosed that various oxygen-substituted Si-B compounds could easily be prepared by ligand exchange of the corresponding amine-containing silylboranes with an appropriate diol (**2** to **3**).^{6,7} The wide applicability and enhanced stability of **3** prompted Suginome and Ito to find a more convenient synthetic pathway for its preparation, ending up in a platform that makes use of silyl lithium reagents (**4** to **3** and **5**).⁸



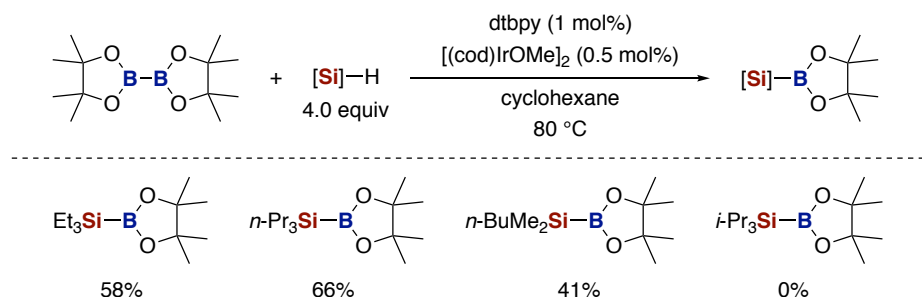
Scheme 1.2. Synthesis of functionalized silylboranes

In 1981, Suginome and co-workers elaborated the syntheses of several XR₂SiBpin compounds from PhMe₂SiBpin (**3**).⁹ The phenyl group in PhMe₂SiBpin was able to be displaced by a chlorine substituent to afford ClMe₂SiBpin (**6**) due to β-silicon effect.¹⁰ The resulting ClMe₂SiBpin served as a platform for preparing a wide variety of functionalized silicon-substituted Bpin derivatives, including the formation of Si-O bonds (**7**), Si-N (**8**) and Si-F (**9**) in reasonable yields via nucleophilic attack. Such modulation of the silicon atom is particularly relevant, setting the stage for the utilization of silylboranes in a broader spectrum of cross-coupling reactions and oxidative-type transformations.



Scheme 1.3. Synthesis of bulky silylboranes

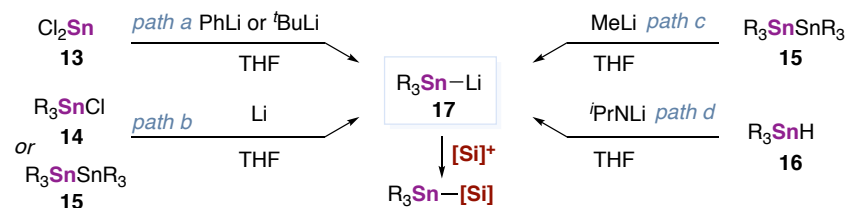
As $\text{PhMe}_2\text{Si-Bpin}$ is sensitive to air and moisture, significant decomposition of silylboronate esters is typically observed upon storage. Driven by the prevailing perception that the inclusion of steric bulk at boron or silicon atom would make the corresponding silylboronate esters much more stable and particularly resistant to air and moisture, Birot and co-workers prepared a series of sterically-encumbered silylboranes possessing mesityl groups at the boron atom by reaction with appropriately substituted silyl lithium reagents **10** (Scheme 1.3).^{11,12} Recently, a new family of bulky, air- and moisture-stable tris(trimethylsilyl)silylboranes were made by the reaction of tris(trimethylsilyl)silylpotassium with the corresponding boron electrophiles.¹³ While tris(trimethylsilyl)silylboronic acid (**12a**) hexylene glycol ester $\text{TMS}_3\text{Si-Bhg}$ (**12b**) could be prepared by this route, this protocol failed to prepare related catecholato (Bcat) and neopentylglycolato (Bnep) motifs due to the decomposition upon purification.



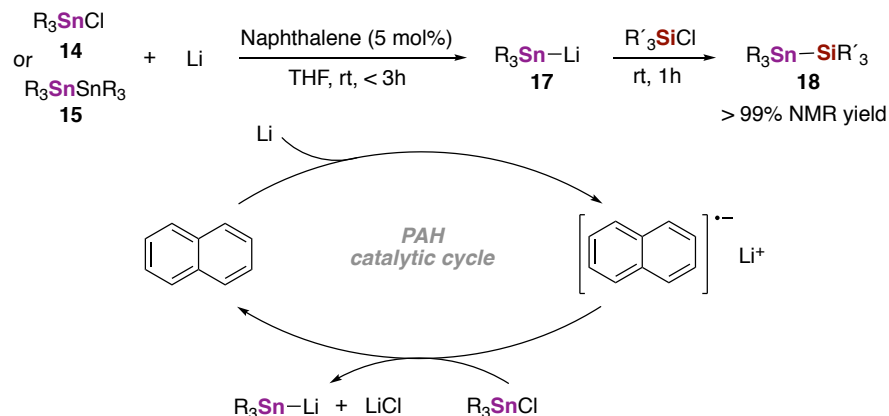
Scheme 1.4. Synthesis of trialkylsilylboronic esters

A significant limitation of Ito and Suginomé's methods is the requirement for silyl-metal reagents, which are prepared from the corresponding chlorosilanes, inevitably resulting in the formation of significant amounts of disilanes as by-products. Although trialkylsilyl lithium reagents can be prepared from disilanes, only a limited number of disilanes are commercially available. Taking this into consideration, Hartwig and co-workers reported an Ir-catalyzed Si-B bond formation by reaction of trialkylsilanes with B_2pin_2 , thus resulting in the formation of a wide variety of trialkylsilylboronate esters, including Et_3SiBpin (Scheme 1.4).¹⁴ These trialkylsilylboranes are fairly stable and could be easily purified by regular column chromatography over silica gel.

A. Classical methods to the synthesis of stannylithium



B. PAH-catalyzed synthesis of stannylithium

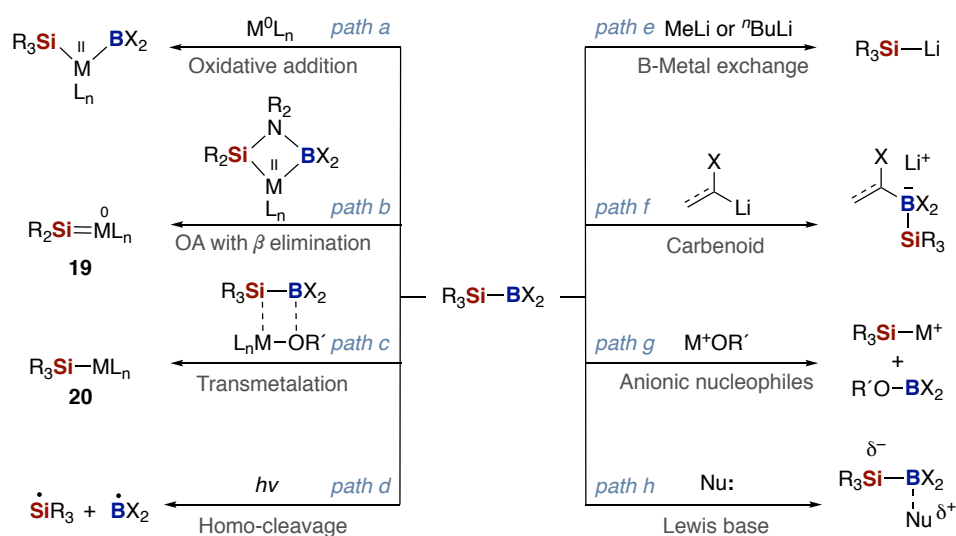


Scheme 1.5. Synthesis of silylstannanes

Since the seminal studies by Wittig, Gilman and Still, among others, stannyl lithium compounds have been utilized as heavy analogues to C–Li reagents in a myriad of functionalization reactions.¹⁵⁻¹⁸ As for silylboranes, silylstannanes can also be prepared by generating a tin anion and subsequent reaction with an appropriate silyl chloride. However, typical protocols for preparing Sn–Li reagents have several disadvantages such as large excess of Sn sources, low yields, and long reaction times (Scheme 1.5).¹⁹ In addition, the inherent toxicity of organotin compounds have prevented their full adoption in industry, where the toxicity partly comes from the undesired byproducts and remaining excess of Sn. For example, paths a and b lead to the formation of rather toxic byproducts such as R_4Sn or R_3SnCl ,^{20,21} and the corresponding Sn–Si bond is formed in low yields (33-75%). In path c, the use of distannanes inevitably result in the loss of 50% of the Sn content, and large amounts of toxic MeR_3Sn are generated as byproduct.²² In path d, an excess of highly toxic R_3SnH is needed to obtain satisfactory yields. In this manner, the utilization of paths a-c unfortunately result in a low Sn transfer, leading to the generation of a non-negligible number of toxic byproducts.²³ To such end, Uchiyama and co-workers came up with a simple and practical protocol that results in the formation of Sn–Li bonds by using polycyclic aromatic hydrocarbons (PAH) as catalysts as electron acceptors (Scheme 1.5, B).²⁴ In addition, the corresponding Sn–Li reagents prepared by this route show superior reactivity and high stability under ambient conditions, enabling the formation of the targeted silylstannanes upon reaction with chlorosilanes in quantitative yield, thus allowing to reduce the toxicity of protocols en route to the formation of Si–Sn interelement linkages.

1.3. Activation Modes of Si-B and Si-Sn Compounds

As summarized in Scheme 1.6, various scenarios are conceivable when utilizing silylboranes as coupling partners, ranging from oxidative addition pathways with transition metal catalysts to stoichiometric processes mediated by Lewis acid activation, among others. For example, Ito and co-workers discovered that Si-B bond can undergo oxidative addition to various low-valent transition metal complexes such as Pt(0), Pd(0) or Ni(0) (path a).²⁵⁻²⁷ Subsequently, migratory insertion of the oxidative addition metal species to C-C multiple bonds might occur, allowed to form both C-B and C-Si bonds while regenerating back the active metal species upon reductive elimination. Later on, Suginome and colleagues reported the generation of a Pd-stabilized silylene possessing a leaving group at the silicon center of **8**, establishing the basis for triggering a β -elimination pathway to transition metal-stabilized silylene (**19**, Path b).²⁸ Alternatively, transition metal-based silicon nucleophiles **20** could be easily formed upon transmetalation with metal alkoxides via metathesis-type transition state due to the Lewis acidity of the boron atom (path c).²⁹ An otherwise similar scenario accounts for the utilization of organolithiums via boron-metal exchange (paths e).³⁰ Furthermore, photochemical homolytic Si-B bond cleavage through UV irradiation could also be applied under specific reaction conditions (path d).³¹ Another well-investigated transformation is the activation of the Si-B reagent by in situ generated organometallic derivatives (path g).³² Indeed, Hiyama and co-workers demonstrated that 1,2-migration can take place in several alkylidene-type and allylic carbenoids,³³ setting the stage for accessing 1,1-difunctionalized compounds. Recently, it has been reported that *N*-heterocyclic carbene catalysts enable a metal-free intermolecular silyl transfer to Michael acceptors (path h).³⁴⁻³⁶ Despite the advances realized with silylboranes, the utilization of silylstannanes as coupling partners have received much less attention. However, the similarity of the Si-B bond and Si-Sn bond suggests that silylstannanes could be employed in related transformations, including oxidative addition and transmetalation (path a, c).^{37,38}

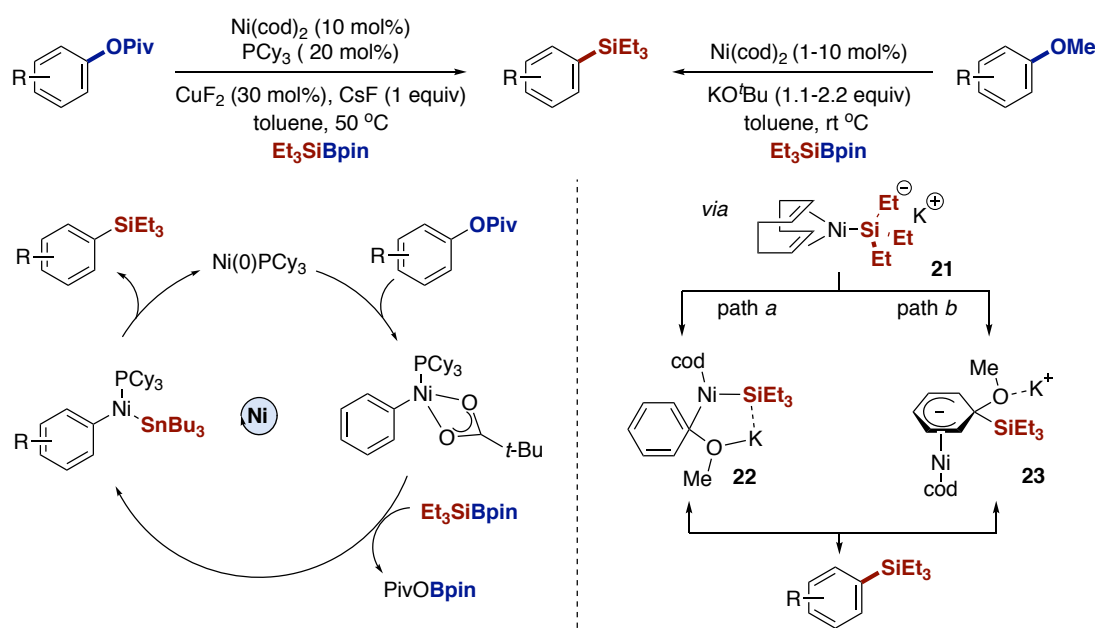


Scheme 1.6. Activation of Si-B bonds in silylboranes

1.4. Application of Si-B and Si-Sn Reagents in Organic Synthesis

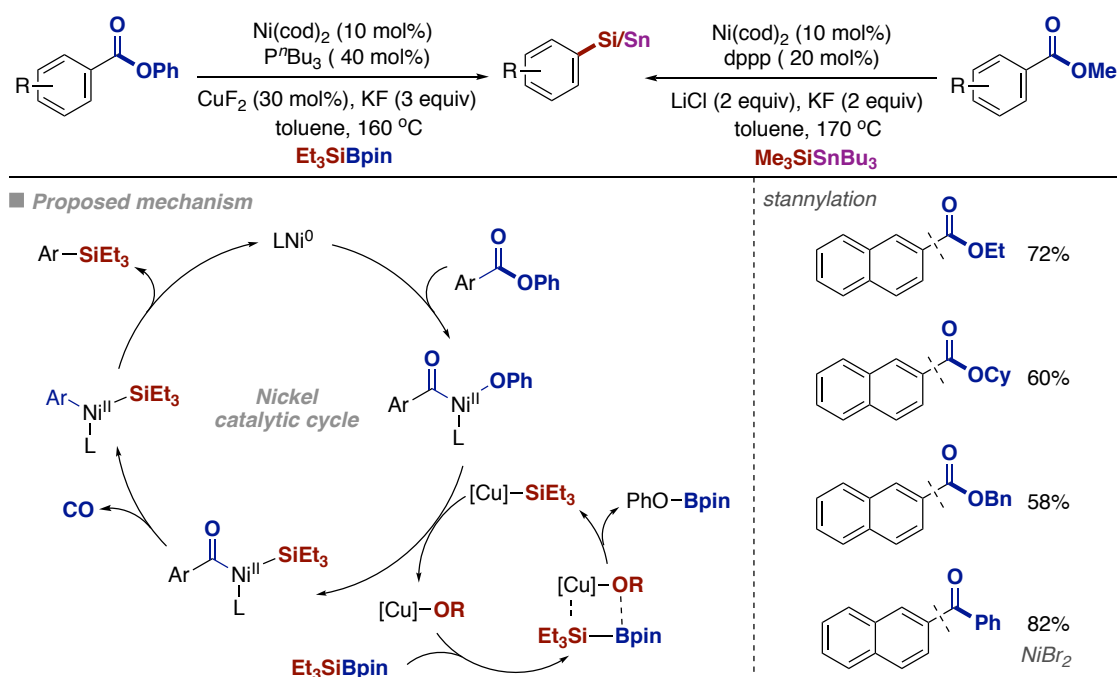
1.4.1. Monofunctionalization technologies using Si-B and Si-Sn reagents

With the increasing demand for silicon-, boron-, and tin-containing compounds in organic synthesis as well as in material sciences, a non-negligible number of methodologies have been described that make use of silylboranes and silylstannanes as counterparts.³⁹ For example, our group reported that aryl silanes can be prepared via Ni-catalyzed silylation of aryl pivalates and aryl methyl ethers via C–O bond-cleavage using Et₃SiBpin as coupling partner (Scheme 1.7).⁴⁰⁻⁴² In the former,⁴⁰ we found that a bimetallic platform based on Ni/PCy₃ and Cu catalysts allowed for the dual activation of the C–O and Si–B bond in the presence of an appropriate fluoride source. Very recently, in depth mechanistic studies conducted by our group has allowed to identify dinickel complexes bearing monodentate PCy₃ deriving from oxidative addition and comproportionation as key intermediates within the catalytic cycle.⁴¹ In the latter, a ligand-free protocol enables the targeted silylation in a more demanding C–OMe bond-cleavage.⁴² Importantly, such a transformation proceeds at room temperature, with catalyst loadings as low as 1 mol%. Gratifyingly, in contrast to other C–OMe bond scission protocols, this reaction could be applied to either π-extended or regular aromatic backbones with equal ease. Although we were unable to isolate any putative nickel intermediates within the catalytic cycle, we proposed that the reaction operates via the formation of Ni(0)-Si ate-complexes (**21**) that are reminiscent of the complexes reported by Pörschke.^{43,44} Subsequently, a K⁺ assisted C–O bond activation via either five-membered ring intermediate **22** or an internal nucleophilic aromatic substitution mechanism (I-S_NAr) would lead to the formation of the targeted aryl silane while transferring the methoxide anion to the potassium center.



Scheme 1.7. Ni-catalyzed silylation via C–O bond cleavage

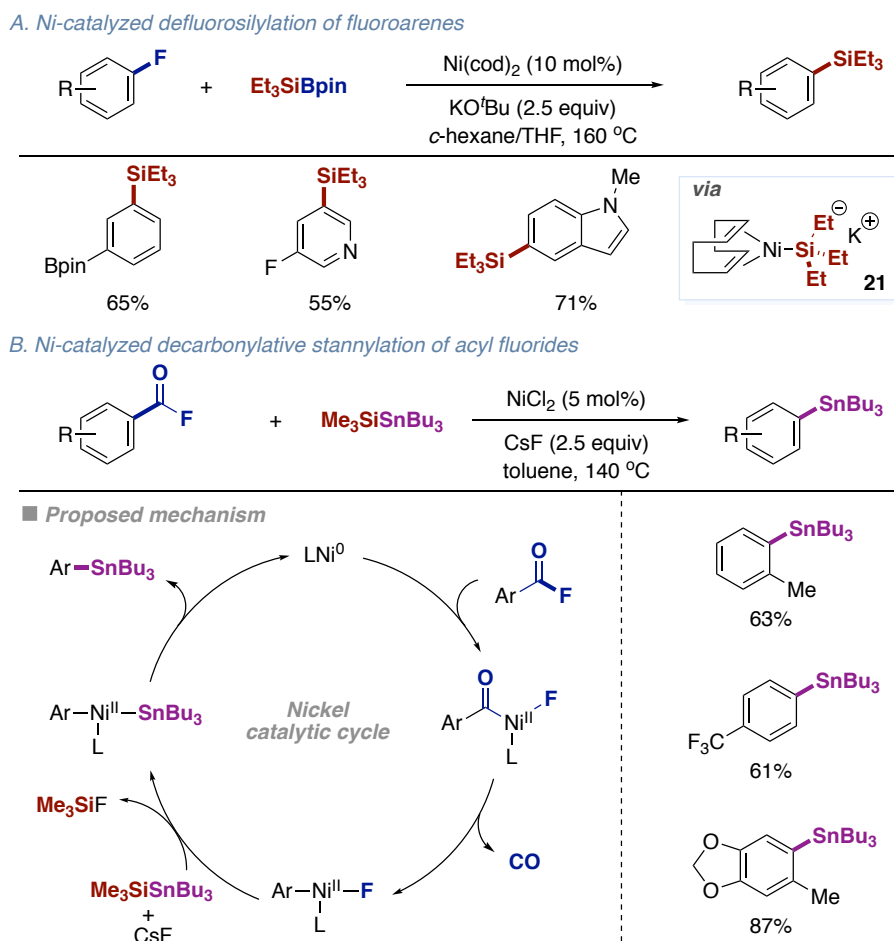
Prompted by our silylation of aryl esters,⁴⁰ chemists have focused their attention in related silylation events. Among these, particularly interesting is the ability to trigger a Ni-catalyzed decarbonylative silylation reaction upon exposure of the targeted aryl esters to a similar Ni/Cu bimetallic system (Scheme 1.8).^{45,46} In this case, the protocol utilized catalytic amounts of Ni(cod)₂ (10 mol%) and PⁿBu₃ (40 mol%) in the presence of CuF₂ and KF. The mechanism of this transformation is believed to proceed via initial oxidative addition of the C–O bond to the Ni(0) center, setting the basis for a transmetalation with an *in situ* generated copper silane complex. A subsequent CO extrusion and a reductive elimination releases the targeted aryl silane while regenerating the Ni(0) species.⁴⁷ Few months after we reported our Ni-catalyzed stannylation of aryl esters,⁴⁸ Rueping and co-workers reported the utilization of the reagent we employed in our stannylation reaction (Me₃SiSnBu₃) in a related decarbonylative stannylation of aryl methyl esters under Ni catalysis.⁴⁹



Scheme 1.8. Ni-catalyzed decarbonylative silylation and stannylation

Driven by the high bond-dissociation energy of the *sp*² C–F bond (125 Kcal/mol), chemists have been challenged to design catalytic cross-coupling technologies via C–F cleavage. For example, Ni-catalyzed defluoroborylation technologies have recently been implemented independently by our group and Hosoya, demonstrating that the cleavage of C–F bonds with subsequent C–B bond-formation can be within reach.^{50,51} Driven by the observation that the B–F bond ranks amongst the strongest bonds in organic chemistry (183 Kcal/mol), it comes as no surprise that this observation has been turned into a strategic advantage for activating C–F bonds. In 2018, Shibata and co-workers described a novel *ipso*-silylation of aryl fluorides via C–F bond cleavage in the presence of Ni catalyst and silylboranes as silylated reagents under relatively high temperatures (Scheme 1.9, A).⁵² In line with our mechanistic proposal when using aryl methyl

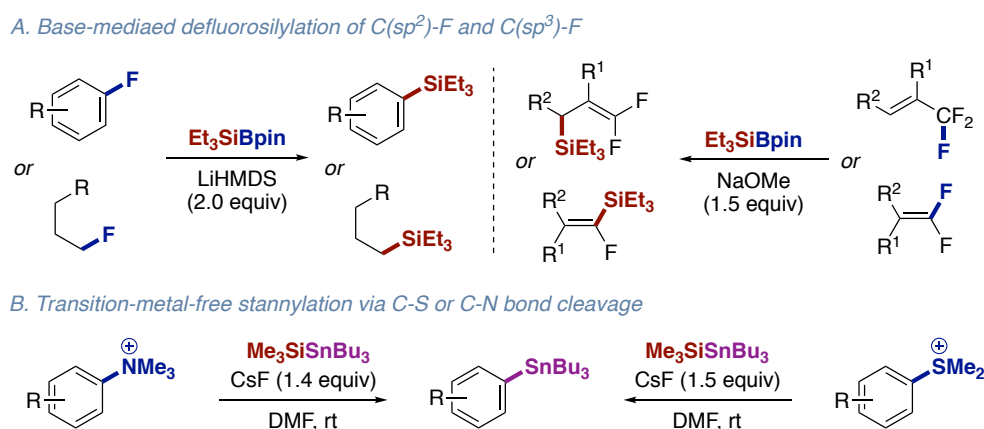
ethers,⁴² the reaction was believed to proceed via Ni(0)-silyl ate complexes (**21**). Very recently, and inspired by the development of our stannylation of aryl esters (see chapter 2), Nishihara has reported the means to effect a Ni-catalyzed decarbonylative stannylation of acyl fluorides with Bu₃SnSiMe₃ at high temperatures (Scheme 1.9, B).⁵³ In this case, the proposed mechanism proceed via oxidative addition of acyl fluoride to Ni(0) species. Then subsequent extrusion of CO to form ArNi(II)F intermediate, followed by transmetalation with silylstannane assisted by CsF. Finally, reductive elimination occurred to deliver arylstannanes and regenerate Ni(0) catalyst.



Scheme 1.9. Ni-catalyzed silylation and stannylation via C–F bond cleavage

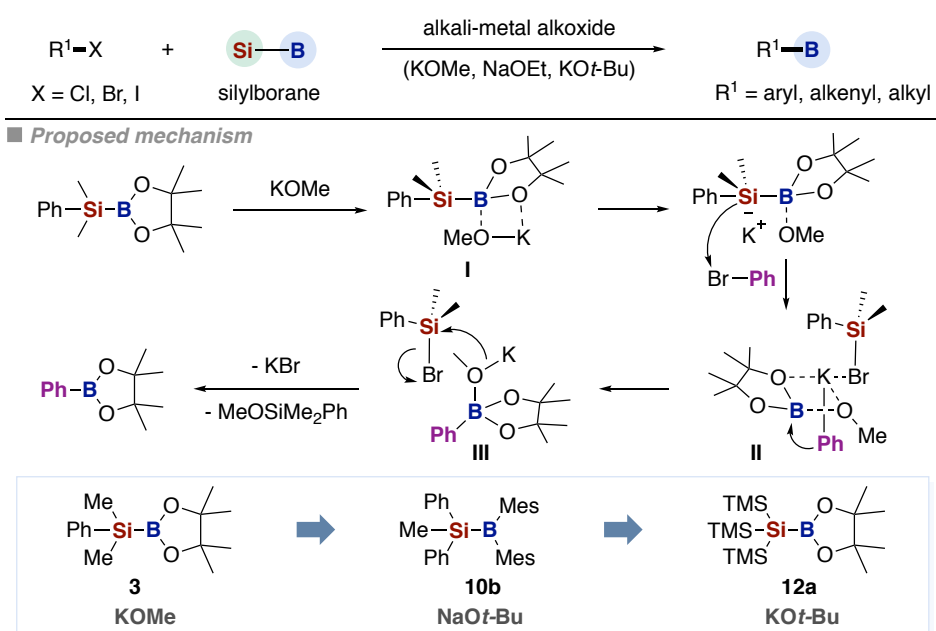
Driven by the observation that high temperatures are generally required for effecting silylation events at *sp*² C–F bonds,⁵² our group has recently described a transition-metal-free defluorosilylation of aryl fluorides promoted by LiHMDS (Scheme 1.10).⁵⁴ The reaction was proposed to proceed via a concerted nucleophilic substitution at the *ipso* C–F site by solvent coordinated silyl anion species. Importantly, this technique could be extended to the implementation of defluorosilylation techniques at much more unactivated aliphatic *sp*³ C–F bonds. Shortly afterwards, Shi and co-workers report a defluorosilylation of a variety of fluoroalkenes with silylboronates in the presence of alkoxides as bases.⁵⁵ Density functional

theory (DFT) calculations showed that transient silyl anion species undergo S_N2' or S_NV substitution, which is responsible for such base-mediated defluorosilylation event.⁵⁶



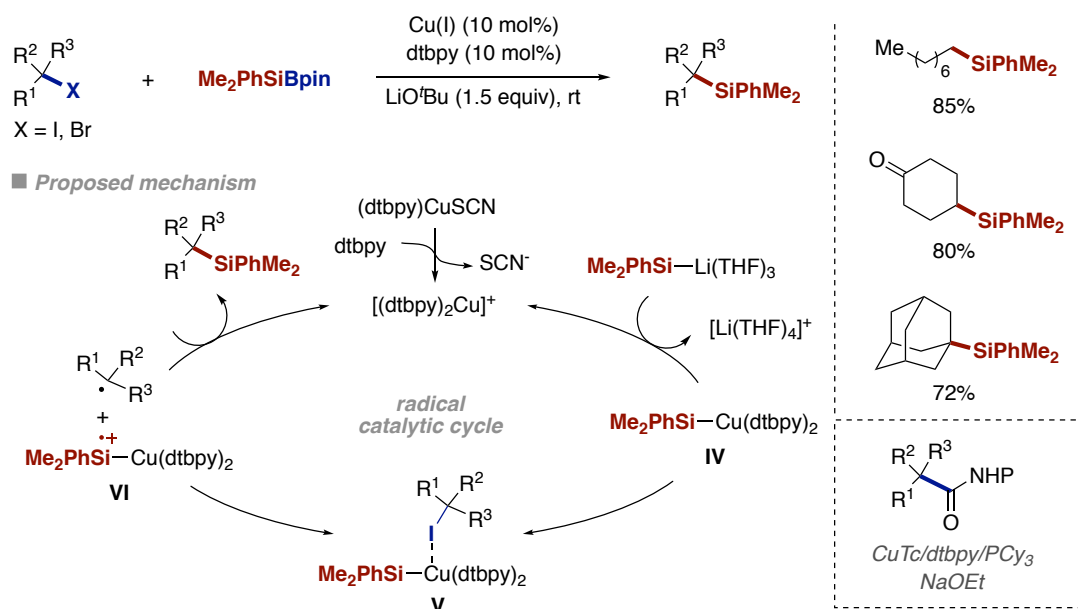
Scheme 1.10. Base-mediated defluorosilylation and stannylation

In 2019, Zhang and co-workers established a convenient and efficient approach to construct C–Sn bonds using arylammonium salts as counterparts.⁵⁷ Various C–Si, C–Ge and C–Se bonds could also be within reach with appropriately substituted nucleophilic partners. The method was successfully applied within the context of late-stage functionalization of existing antibiotic drugs, fluorescent probes and molecules for drug discovery. Transformations of arylsulfonium salts via S_NAr mechanisms was also realized, allowing to forge C–O, C–S, C–Sn, C–Si and C–Se bonds.⁵⁸ In particular, the stannylation efficiently proceeded at room temperature with $Me_3SiSnBu_3$ in the absence of transition metal catalyst, whereas the use of aryl sulfonium as substrates found application in a number of bioactive natural products and drug-like molecules.



Scheme 1.11. Boryl substitution of organic halides with silylboranes and alkoxy bases

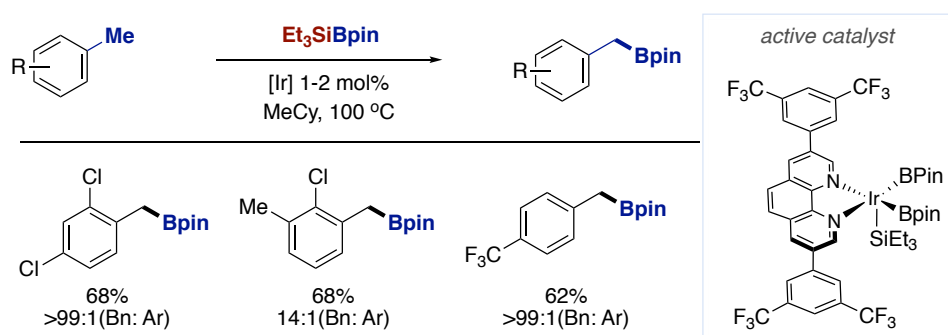
Ito and co-workers showed that silylboranes can be employed as vehicles for triggering borylation events for a variety of aryl, alkenyl, and alkyl halides, including sterically hindered substrates in the presence of alkoxy bases without transition-metal catalysts (Scheme 1.11).⁵⁹⁻⁶¹ This system offers a novel and convenient route to access aryl, heteroaryl, alkenyl and alkyl boronates from the corresponding organohalides with high borylation/silylation ratios. A representative reaction pathway of this formal nucleophilic boryl substitution was proposed based on experimental observations and DFT studies.⁶² Specifically, a silylborane/KOMe complex (I) is initially formed with PhMe₂SiBpin and KOMe. Subsequently, nucleophilic attack of the silyl moiety of complex I to PhBr leads to the formation of an anionic phenyl species (II) via metal-halogen exchange. Attack of the carbon nucleophile to the Lewis-acidic boron atom gives the corresponding organoborate salt [PhBpinOMe]⁻K⁺ (III), which finally delivers phenyl boronate ester, PhMe₂SiOMe and KBr as byproducts. This borylation event was then applied to the synthesis of aryldimesitylboranes with Ph₂MeSiBMe₂,⁶³ which have numerous potential applications in the field of material science.^{64,65} For instance, such boron-containing π -conjugated systems show intriguing optical properties due to the p - π^* conjugation between the vacant p orbital of the boron center and the π^* orbital of the attached phenyl moiety. However, the application of this strategy can be hampered by the formation of both borylation and silylation products (67:33 to 96:4 ratios). Notably, the B/Si ratio could be significantly improved if bulky tris(trimethylsilyl)silyl groups are employed.¹³ As expected, the utilization of (TMS)₃Silyl boronate esters resulted in the corresponding borylation of organic halides in high yields and B/Si ratios (up to 99/1) as well as the silaboration of styrene with catalytic KOMe.⁶⁶⁻⁶⁸



Scheme 1.12. Copper-catalyzed radical silylation of unactivated alkylhalides

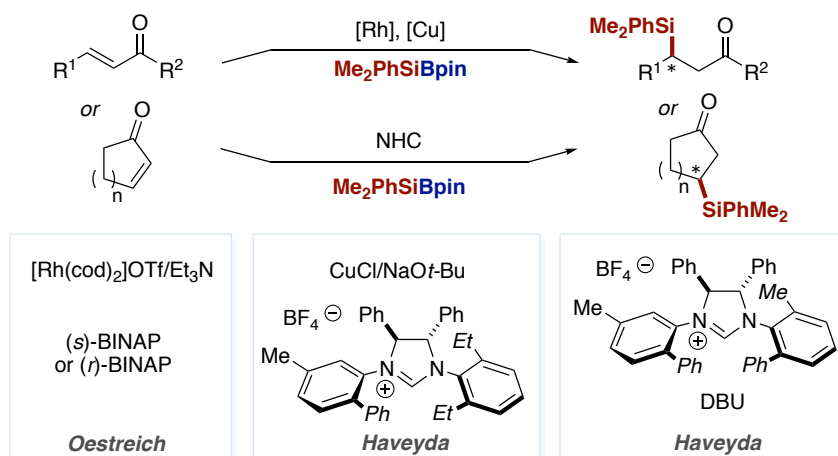
Recently, Oestreich showed that a CuSCN/dtbpy protocol that utilizes LiOt-Bu as base in THF/DMF (9:1) enables the implementation of a silylation event of tertiary alkyl halides with Si-B reagents (Scheme 1.12).⁶⁹ In this particular case, a radical pathway was proposed due to the

epimerization observed with diastereomerically pure substrates as well as the inhibition found in the presence of TEMPO. In addition, 5-*exo*-trig cyclization and DFT calculations reinforced the notion that open-shell intermediates come into play. It was additionally proposed that a highly solvated Li cation led to an elongation of the Si-B bond upon coordination of the tertbutoxy anion to the boron center, thus setting the basis for a rapid transmetalation with the Cu catalyst en route to (dtbbpy)₂Cu-Si species (IV). Subsequently, binding with the alkyl iodide to form a loose dative Cu...I bond enables a single electron transfer (SET) to form a transient alkyl radical with concomitant formation of a cationic intermediate VI. Final *sp*³ C-Si bond-formation was proposed to occur via radical recombination. A useful addition to this dehalogenative *sp*³ C-Si cross-coupling is recently reported by the same group using aliphatic N-hydroxy-phthalimide esters (NHPI) as radical precursor. The alkyl radical is generated by single-electron-transfer reduction with [Cu]-Si species followed by decarboxylation.⁷⁰



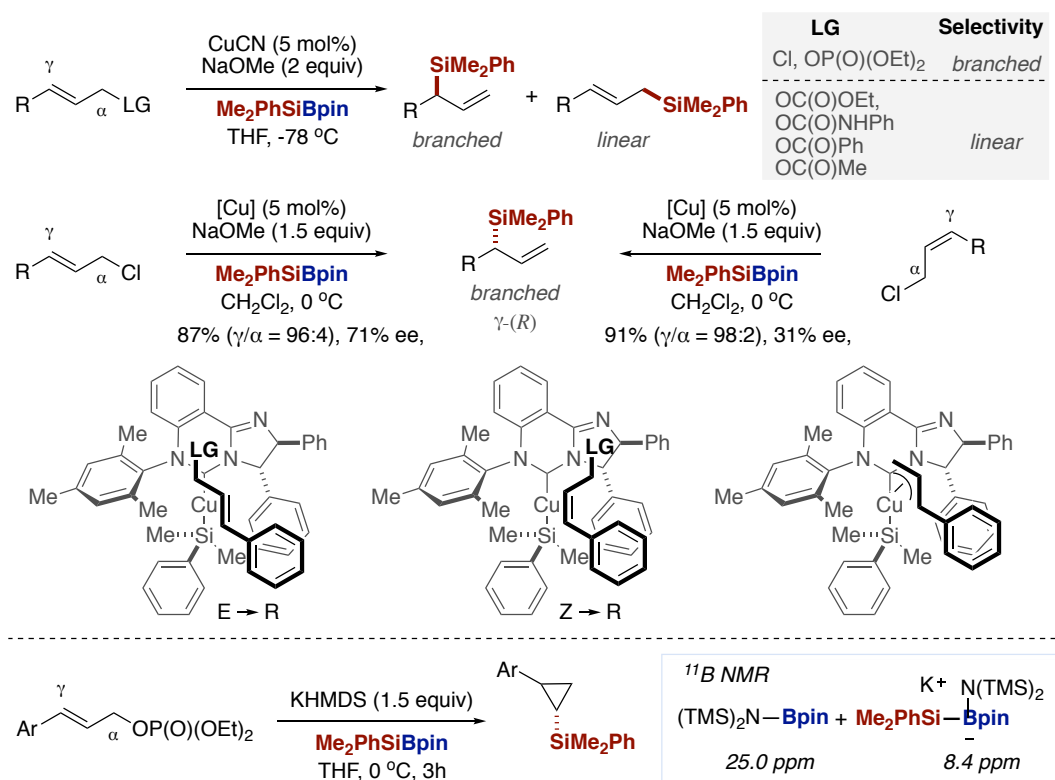
Scheme 1.13. Iridium-catalyzed C-H borylation with silylboranes

Unlike the vast majority of borylation events enabled by B₂pin₂, Hartwig developed a *sp*² C-H borylation using Et₃SiBpin under Ir/bipyridine catalyst system.¹⁴ This method could successfully be applied to trigger a borylation of primary benzylic *sp*³ C-H bonds.⁷¹ Critical for success was the discovery of an iridium diborylmonosilyl complex that is more electron-deficient than the previously reported iridium trisboryl complex employed in related C-H borylations.⁷² Mechanistic studies showed that the rate of *sp*² C-H borylation decreases upon decreasing electron density at the Ir center, whereas the rate of benzylic *sp*³ C-H borylation was less sensitive to the degree of electron density at the Ir metal center.



Scheme 1.14. Conjugate addition of silyboranes to α,β -unsaturated carbonyl compounds

Addition of diboron to α,β -unsaturated carbonyl compounds are well studied by many groups including enantioselective variants which are promoted by transition-metal species, phosphines or NHC catalysts.⁷³⁻⁷⁵ Subsequently, enantioselective conjugate silyl addition to cyclic and acyclic unsaturated carbonyls in presence of rhodium(I) catalyst and (s) -BINAP were introduced by Oestreich and co-workers.⁷⁶ Apart from rhodium(I) catalyst, Lee and Hoveyda succeeded in developing a enantioselective conjugate silyl transfer that relies on a combination of CuCl, chiral carbene precursor, and NaOt-Bu.⁷⁷ In these transition metal-involved reactions, the nucleophilic M-SiMe₂Ph species would be initially delivered followed by insertion of the α,β -unsaturated acceptor into the M-Si bond. In 2011, the same group found a complementary metal-free method for the enantioselective conjugate addition of the silyl group to α,β -unsaturated carbonyls catalyzed by a readily accessible chiral imidazolium salt (NHC) and a common organic base (DBU). The reaction could be conducted in an aqueous solution (3:1 mixture of water and THF) and was operationally simpler to perform than the NHC-Cu-catalyzed variant.⁷⁸ Despite moderate yields for some substrates, high enantiomeric purities were obtained throughout. Stoichiometric amounts of the NHC/DBU with Me₂PhSiBpin resulted in the formation of the sp^3 -hybridized borates via nucleophilic attack to the more Lewis acidic boron atom. Detailed spectroscopic evidences demonstrated that the proton source could influence the efficiency and/or enantioselectivity of NHC-catalyzed enantioselective transformations.⁷⁹

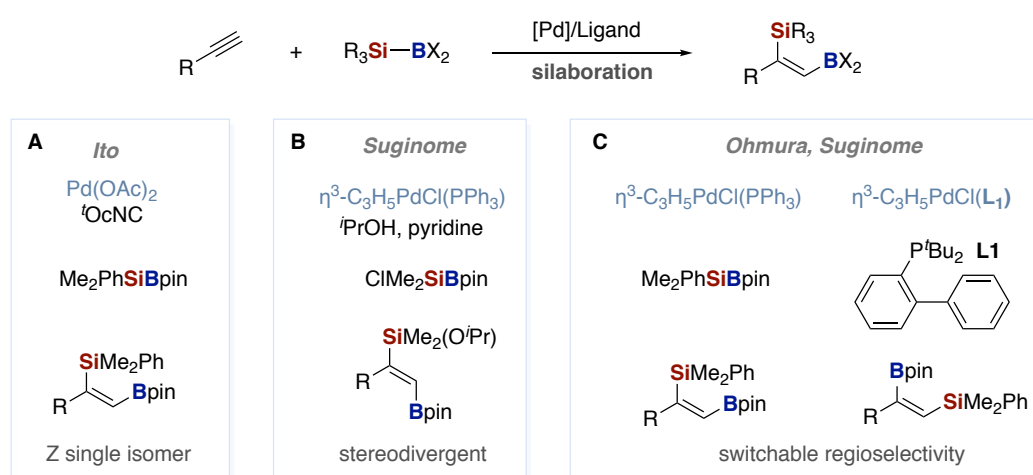


Scheme 1.15. Allylic silylation with silyl nucleophile

Oestreich and co-workers have recently elaborated a branched-selective allylic substitution of linear allylic chlorides, yielding α -chiral allylic silanes in racemic form (Scheme 1.15).⁸⁰ The reaction was realized by exploiting a Cu(I)-induced generation of silicon nucleophiles that are transferred to various acceptors via C–Si bond formation. γ -selectivity was observed for halides and phosphates, while α -selectivity was obtained for carbonates, carbamates, and carboxylates albeit with eroded α -selectivity for the latter. The Oestreich group also present an enantio- and regioselective allylic substitution of linear allylic chlorides, and phosphates catalyzed by a copper(I) complex containing a chiral N-heterocyclic carbene (NHC) ligand.⁸¹ This catalyst also exhibits a preference for the same face of both (*E*)- and (*Z*)-alkenes, providing stereoconvergent outcomes.⁸² However, enantioconvergence is also an indication of the catalysis passing through a common intermediate η^3 π -allyl copper(III) complex. Later on, Nozaki and Shintani developed a KHMDS-mediated cyclopropanation of allyl phosphates with a silylboronate. Unlike the previously reported copper-catalyzed allylic substitution reactions, the nucleophile selectively attacks at the β -position of the allylic substrates.⁸³ Investigation of the mechanism showed that a silylpotassium species could be the active nucleophilic species as tetracoordinated anionic boron species ($\delta = 8.4$ ppm) and the desilylated three-coordinate boron species ($\delta = 25.0$ ppm) were observed from ¹¹B NMR.

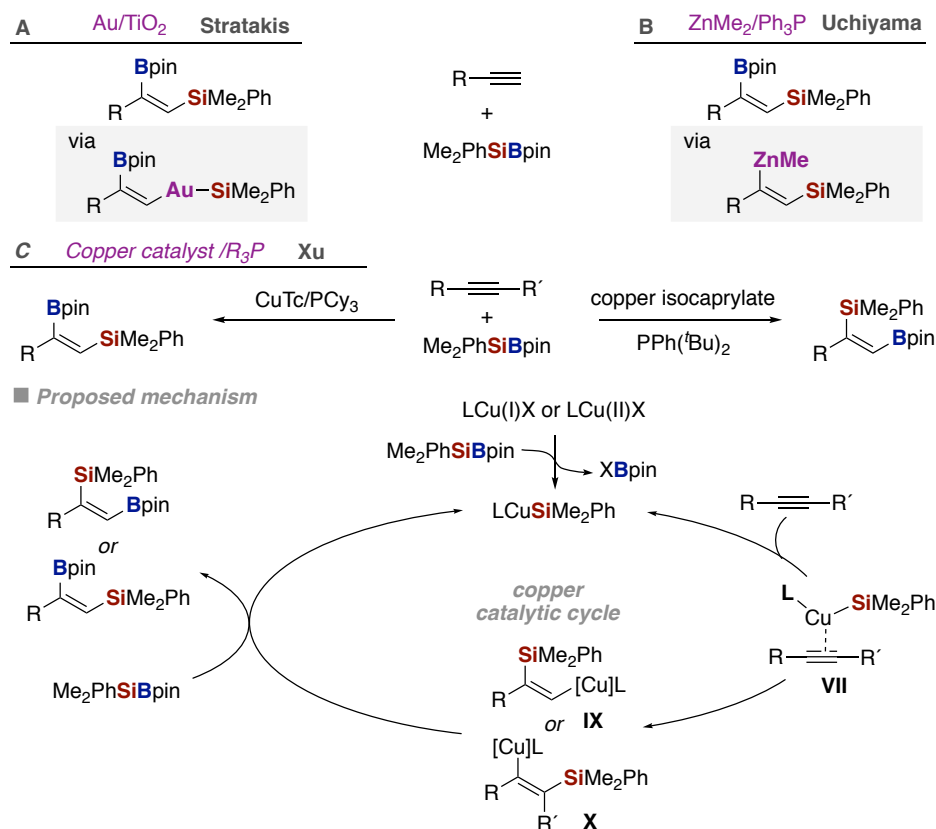
1.4.2. Difunctionalization events using Si–B and Si–Sn reagents

Despite the significant advances realized with interelement linkages, the vast majority of coupling reactions that make use of silylboranes or silylstannanes result in either a silylation, borylation or stannylation event, thus constituting a drawback from an atom-economical standpoint. To such end, chemists have been challenged to incorporate both the Si/B or Si/Sn unit into an organic molecule. Among various scenarios, the utilization of π -components as precursors is particularly attractive, as it will provide access to organic molecular possessing multiple organometallic bonds that could be used in synthetic applications while resulting in a highly atom-economical technique with great potential in synthetic chemistry.⁸⁴



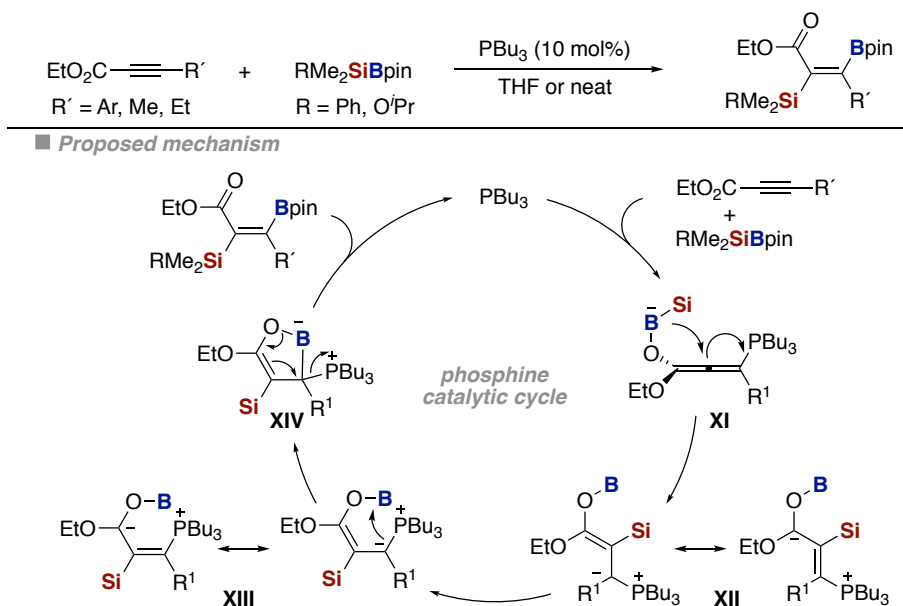
Scheme 1.16. Regioselectivity in Pd-catalyzed silaboration of terminal alkynes

The utilization of alkynes as coupling partners in combination with silylboranes could provide an useful entry point to generate valuable vinyl boranes and vinyl silanes. This approach was shown by Ito and co-workers using a palladium–isonitrile catalytic system that resulted in a highly regio- and stereoselective silaboration of terminal and internal alkynes, with the boryl group attached to the terminal carbon atom whereas the silyl group was connected to the internal position (Scheme 1.16 A).⁸⁵ Moreover, the reaction gave the *Z* isomer as major product, corresponding to a formal *syn*-addition of the Si–B bond across the triple bond. Subsequently, Suginome and co-workers found that a *Z/E* isomerization occurred in the presence of excess amounts of $\text{ClMe}_2\text{SiBpin}$ and *i*-PrOH/pyridine (Scheme 1.16, B).⁸⁶ A Pd-catalyzed regioselective silaboration of terminal alkynes was found by Ohmura and Suginome by tuning the phosphine ligand (Scheme 1.16, C).⁸⁷ Specifically, it was found that the boryl group was transferred to the alkyne terminus if Ph_3P is used, whereas bulkier (biphenyl-2-yl) $t\text{Bu}_2\text{P}$ (**L1**) resulted in a regioselectivity switch. Specifically, it was suggested that C–B bond formation occurs prior to the formation of the C–Si bond by insertion of the alkyne into the B–Pd bond.⁸⁸ The steric bulk of the phosphine accounts for the regioselectivity switch in a ligand-controlled regioselective alkyne insertion into the Pd–B bond.



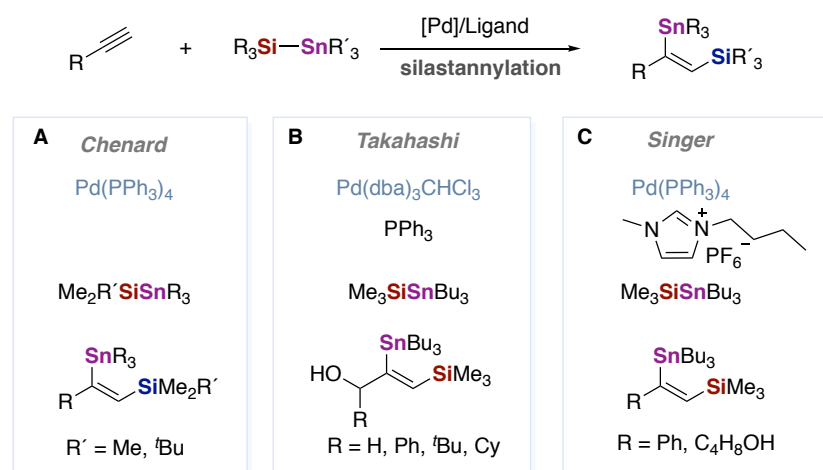
Scheme 1.17. Transition-metal-catalyzed silaboration of terminal alkynes

Regioselective silaboration of alkynes with PhMe₂SiBpin was also documented by Stratakis's group using gold nanoparticles supported on TiO₂ (Scheme 1.17, A).⁸⁹ No additional additives or ligands are required, resulting in an abnormal regioselectivity switch that could only be within reach in homogeneous conditions using bulky phosphines and Pd catalysts.⁸⁷ Such regioselectivity profile is attributed to steric factors imposed by Au nanoparticles during the 1,2-addition of silylborane to the alkyne. Subsequently, Uchiyama and co-workers developed a dimethylzinc-catalyzed regioselective silaboration of terminal alkynes (Scheme 1.17, B).⁹⁰ Silylzinc species were generated *in situ* by Si–B bond activation in the presence of dimethylzinc/phosphine catalyst system. Notably, it was found that a regioselectivity switch was observed in the absence of phosphine ligand to yield 2,1-silaborated alkenes, suggesting that different species account for such selectivity profile. A ligand -controlled Cu-catalyzed regio- and stereoselective silaboration was reported by Xu and co-workers (Scheme 1.17, C).⁹¹ The utilization of Cu(OAc)₂ and CuTc resulted in 2-boryl-1-silyl-1-alkenes as major product whereas a protocol based on copper isocaprylate and PPh(*t*-Bu)₂ in heptane led to a selectivity switch. Interestingly, protosilylation occurred smoothly when phenylacetylene was used instead of alkyl-substituted acetylene. A plausible mechanistic rationale is depicted in Scheme 1.17. It was believed that the LCuX catalyst reacts with silylborane to generate **VII** prior to coordination to the π-cloud of the acetylene moiety. Subsequently, a *cis* insertion generates vinyl cuprate intermediates **IX** or **X**, setting the stage for a transmetalation event, leading to an alkynyl boronic ester while turning over the catalytically competent LCuSiMe₂Ph species within the catalytic cycle.



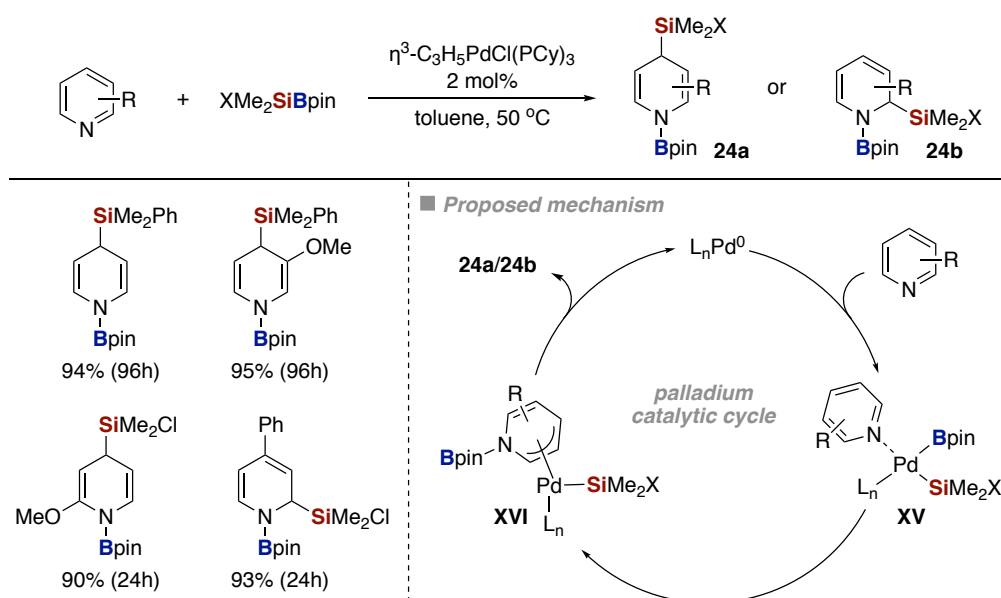
Scheme 1.18. Phosphine-catalyzed *anti*-selective vicinal silaboration

In 2015, Sawamura disclosed an *anti*-selective vicinal silaboration of alkyneates enabled by trialkylphosphine catalyst to produce β -boryl- α -silyl acrylates (Scheme 1.18).⁹² Notably, the two vicinal C-heteroatom bonds could be differentiated and converted to unsymmetrical tetrasubstituted alkenes. The reaction was believed to proceed via conjugate addition of the phosphine to the alkyne fragment assisted by Lewis acidic activation of the carbonyl group to form a zwitterionic allenolate intermediate **XI**.⁹³ Then, the terminal silyl fragment migrates to the *sp* carbon center of the allene moiety to form ylide intermediates **XII**, which will isomerize to **XIII**. The ylide carbon of **XIII** then attacks the B-atom bound to the oxygen atom to form cyclic borate **XIV**. Finally, elimination of Bu_3P with concomitant B-O cleavage affords the desired product.



Scheme 1.19. Regioselectivity in Pd-catalyzed silastannylation of terminal alkynes

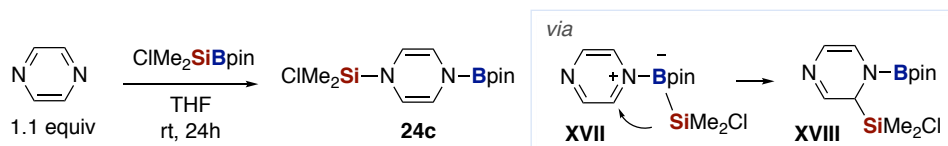
The first examples of silastannylation of terminal alkynes were reported by Chenard in presence of Pd(PPh₃)₄.⁹⁴ Under the best reaction conditions, a high regio- and stereoselectivity was observed, obtaining selectively *cis*-adducts with the silyl group attached to terminal carbon (Scheme 1.19, A). Remarkable improvement of catalytic activity was realized by using Ito's palladium-isonitrile catalyst system; unlike the utilization of Pd(PPh₃)₄ catalyst that required heating, the use of Ito's protocol allowed the silylstannylation to occur at room temperature. Unfortunately, the reaction could not be employed with internal alkynes. The presence of a propargylic ether enhanced the reactivity of the internal triple bonds, resulting in a regio- and stereoselective formation of products bearing a tin fragment at the internal vinylic position (Scheme 1.19, B).⁹⁵ Interestingly, the utilization of ionic liquids allowed to improve the recyclability up to 10 times without loss of activity (Scheme 1.19, C).⁹⁶ While the nature of the active catalyst is unknown, it was suggested that either palladium-imidazolylidene carbene complexes or palladium metal nanoclusters may be responsible for the observed reactivity.



Scheme 1.20. Pd-catalyzed dearomatization of pyridines with silylboranes

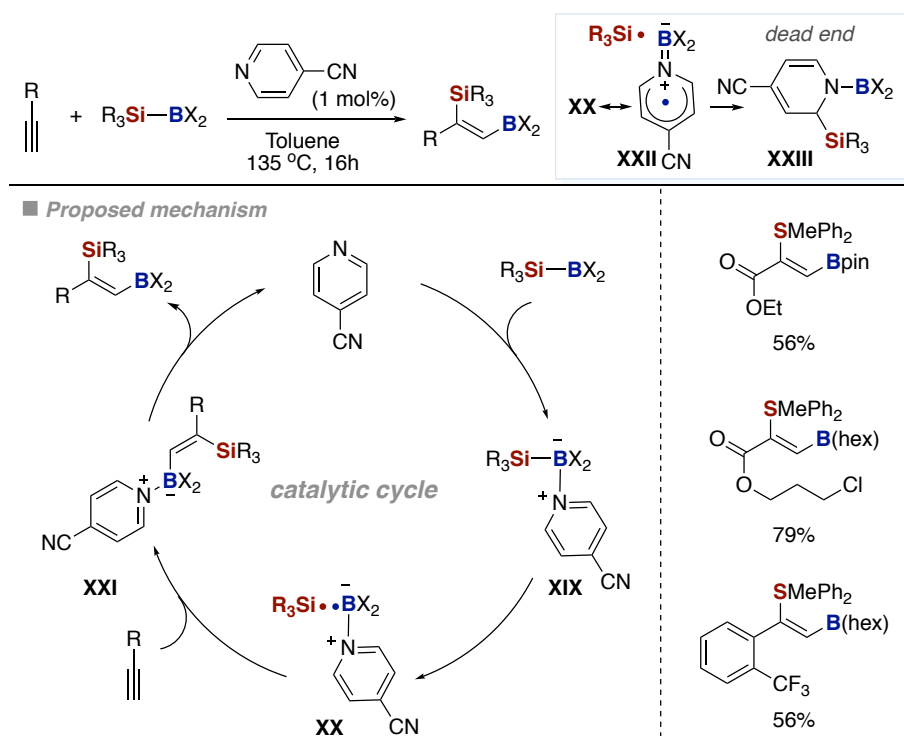
Oshima, Ohmura and Suginome described the addition of Si–B bonds across a pyridine ring by means of Pd catalysis (Scheme 1.20).⁹⁷ Specifically, it was found that the ($\eta^3\text{-C}_3\text{H}_5$)PdCl(PCy₃) complex promoted the silaboration of pyridine (10 equiv) with XMe₂SiBpin as a limiting reagent, thereby delivering a dihydropyridine derivative with a boryl group at the nitrogen atom and a silyl group at the C4-position. Pyridines bearing 3-methoxy or 3-ester substituents reacted smoothly with Me₂PhSiBpin to afford the corresponding 1,4-adducts in good to high yields. The use of ClMe₂SiBpin dramatically improved the reaction efficiency to deliver N-boryl-4-silyl-1,4-dihydropyridine. Unlike C2- or C3-substituted pyridines, 4-substituted pyridines were silaborated in a 1,2-fashion, thereby delivering 4-substituted 1,2-dihydropyridines at the C2-position. The mechanism of the transformation was believed to proceed via oxidative addition of the silylboronic ester to the Pd(0) species, followed by the coordination of pyridine to form

complex **XV**. These species presumably underwent a regioselective insertion of Pd–B bond into the to form a π -allyl-palladium complex **XVI** followed by a reductive elimination to afford dihydropyridine (**24a** or **24b**) while regenerating the $L_nPd(0)$. The regioselectivity C2/C4 pattern could be controlled by the positional selectivity of the substituents at the pyridine ring. DFT calculations were carried out by Yates and co-workers which indicated the dearomatization step to be rather facile (4.3 kcal/mol), presumably due to the formation of a strong covalent bond between the nitrogen and boron atoms in the final product, while reductive elimination was suggested to be rate-determining.⁹⁸



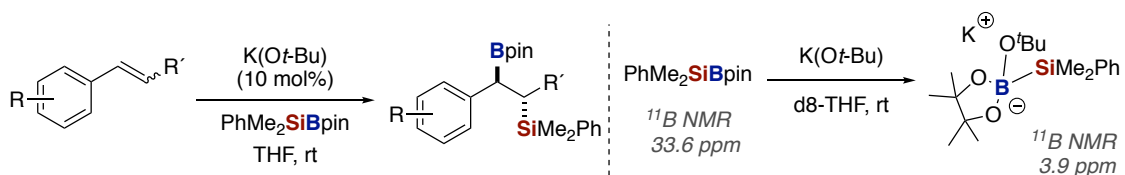
Scheme 1.21. TM free dearomatization of pyrazines

Pyrazines could undergo addition towards Si–B bond under transition-metal-free conditions, leading to N-borylated 1,4-dihydropyrazines.⁹⁹ The Si–B bond was activated by coordination of one of the nitrogen atoms of pyrazine to the boron to form a tetracoordinated boron intermediate **XVII**, and intramolecular nucleophilic attack of silyl group on the C2 carbon takes place to give 1,2-adduct **XVIII**. Rearrangement of **XVIII** resulted in the final product **24c**. High yield was observed in the dearomatizing addition reactions, which may be attributed to the formation of B–N bond, as mentioned above and also observed in the hydroboration of pyridines.^{100,101} Very recently, Suginome and Ohmura reported an organocatalytic silaboration of terminal alkynes and allenes using 4-cyanopyridine as catalyst (Scheme 1.22).¹⁰² The reaction undergoes regio- and stereoselective 1,2-addition of silaboranes in toluene. It was revealed that 4-cyanopyridine is capable to homolytically cleave the B–B bond to generate pyridine boryl radicals.¹⁰³ The authors assumed a mechanism as shown in Scheme 1.22. The Si–B bond is activated by 4-cyanopyridine coordinated onto the boron atom. The mechanism involves homolytic cleavage of the Si–B bond, which forms a stabilized boryl radical. The generated radical pair **XX** rapidly adds to the carbon–carbon triple bond in a *syn* manner. This addition may take place in an almost concerted fashion. The absence of reactive alkyne may result in the formation of **XXIII** as a dead end product. It is also suggested that the more nucleophilic pyridine-boryl radical preferentially attacks the more electron-deficient alkyne terminus, resulting in the observed regioselectivity.

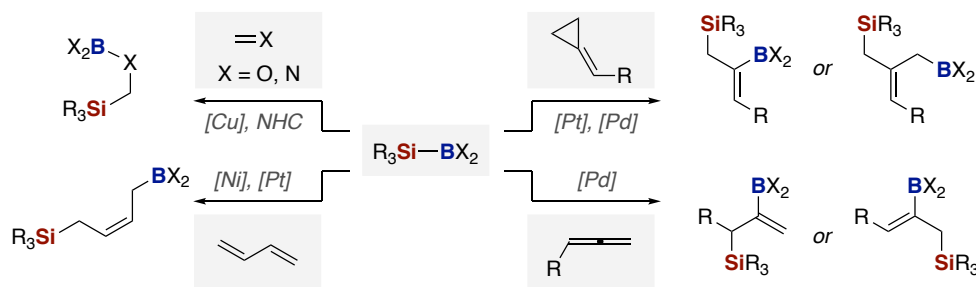


Scheme 1.22. Pyridine-based organocatalyst for *syn*-1,2-silaboration of terminal alkynes

Silaboration of aromatic alkenes was first reported by Ito and co-workers, in which a regio- and diastereoselective 1,2-silaboration proceeded in the presence of a catalytic amount of KO*t*-Bu (Scheme 1.23).¹⁰⁴ It was found that *anti*-product was the major product, which is in contrast to the results found in transition-metal-catalyzed silaboration reactions. Although the authors can't provide a clear reaction mechanism, the preliminary studies indicated an adduct of silaborane and the alkoxide rather than free silyl anion species. Further detailed studies on the reaction mechanism are required to understand the stereospecificity of the reaction.

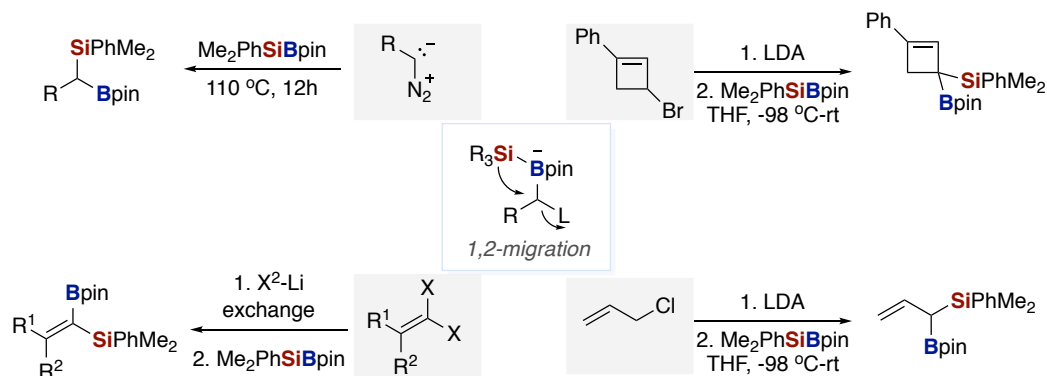


Scheme 1.23. KO*t*-Bu mediated regioselective silaboration of aromatic alkenes



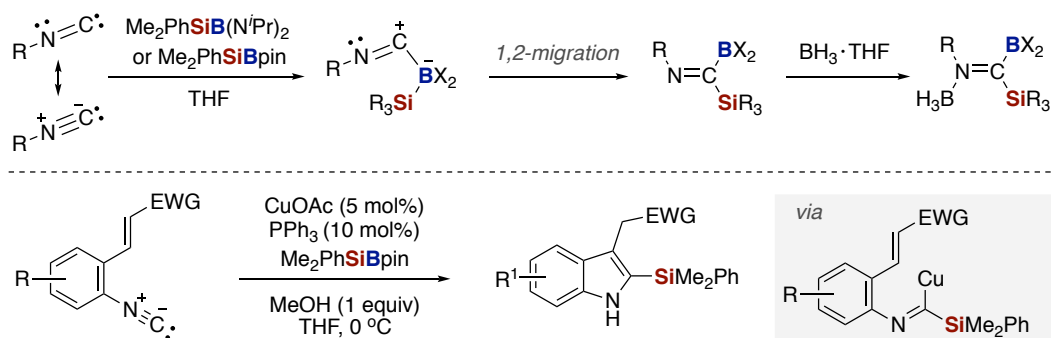
Scheme 1.24. Silaboration of other unsaturated organic compounds

Other silaboration of unsaturated compounds such as imines,¹⁰⁵ aldehydes,¹⁰⁶ dienes¹⁰⁷, allene¹⁰⁸ have also been developed with/without transition metal catalysts (Scheme 1.24).^{27,39} These transformations can also proceed in a highly regio- and stereoselective manner, leading to the formation of organic compounds bearing silyl and boryl groups that can be used for diverse synthetic applications.



Scheme 1.25. 1,1-difunctionalization of carbenoid and related compounds via 1,2-migration

In order to keep both silyl and boryl group in the molecule, another strategy could be the utilization of 1,2-migration in which the silyl group from the boron center is added at the adjacent carbon atom. If the carbon atom is substituted with an appropriate leaving group, the neat outcome will be generation of geminal functionalized compounds (Scheme 1.25). This has been applied to many transformations involving the use of as 1,1-dihalalkenes, diazo compounds, allyl chloride or 3-bromocyclobutene.^{109-112, 39}



Scheme 1.26. Insertion of isonitriles

Insertion of isonitriles into the Si-B bond of several Si-B compounds without transition metal was also reported by Ito and co-workers (Scheme 1.26). A large number of isonitriles reacted with silaboranes at elevated or even room temperature, obtaining the corresponding (boryl)(silyl)iminomethanes as their borane complexes.¹¹³ Chatani developed a copper(I)-catalyzed indole synthesis involving the utilization of isonitriles.¹¹⁴ The mechanism of this domino reaction probably began with an intermolecular silyl transfer from the catalytically generated monosilyl copper(I) species onto the isocyano group. Subsequent intramolecular 1,4-addition led to the formation of the indole ring. Hydrolysis of copper(I) enolate with MeOH generated the indol moiety and regenerates the copper(I) methoxide catalyst.

1.5. General Objectives of This Doctoral Thesis

The last decade has witnessed an impressive knowledge in the implementation of silylboranes and silylstannanes as coupling partners as vehicles to prepare densely functionalized organosilicon, organoboron and organostannane reagents in a high chemo-, regio- and stereoselective manner. Despite the significant advances realized, the ability to employ interelement linkages within the context of the functionalization of particularly strong σ sp^2 C–O or sp^2 C–H bonds still remains less explored. Driven by the inherent interest of the Martin group for designing new methods for activating strong σ -bonds, this thesis is aimed at discovering new C–heteroatom bond-forming reactions by using silicon-heteroatom interelement linkages as coupling partners. To such end, the following objectives will be pursued:

- To expand the toolbox of C–O bond functionalization techniques to trigger a stannylation event with ***Me₃SiSnBu₃***.
- To develop a direct site-selective sp^2 C–H silylation of (poly)azines using ***Et₃SiBpin*** as silyl reagent under transition-metal-free conditions, ending up in a new tool for rapid diversification via late-stage functionalization of drug-type molecules.
- To explore the viability of conducting an atom-economical 1,1-difunctionalization of terminal alkynes with ***Et₃SiBpin*** via 1,2-metallate shift from boron atom to sp carbon centers.
- To unravel the mode of action by which silicon-based interelement linkages results in the formation of C–heteroatom bonds via the functionalization of strong σ -bonds.

1.6. References

1. A. G. Davies, M. Gielen, K. H. Pannell, E. R. Tiekink, *Tin Chemistry : Fundamentals, Frontiers and Applications*, 1st ed. , Wiley, Chichester, **2008**.
2. *Synthesis and Application of Organoboron Compounds*; Fernández, E.; Whiting, A.; Eds.; Springer: Berlin, **2015**.
3. Ramesh, R.; Reddy, D. S. Organosilicon Molecules with Medicinal Applications *J. Med. Chem.* **2018**, *61*, 3779.
4. Tamao, K.; Yamaguchi, S. Introduction to The Chemistry of Interelement Linkage. *J. Organomet. Chem.* **2000**, *611*, 3.
5. Nöth, H.; Höllerer, G. *Angew. Chem. Int. Ed. Engl.* **1962**, *1*, 551.
6. Nöth, H.; Höllerer, G. Organylsilyl-borane. *Chem. Ber.* **1966**, *99*, 2197.
7. Biffar, W.; Nöth, H.; Schwerthöffer, R. *Liebigs Ann. Chem.* **1981**, 2067.
8. Suginome, M.; Matsuda, T.; Ito, Y. Convenient Preparation of Silylboranes. *Organometallics* **2000**, *19*, 4647.
9. Ohmura, T.; Masuda, K.; Furukawa, H.; Suginome, M. Synthesis of Silylboronic Esters Functionalized on Silicon. *Organometallics* **2007**, *26*, 1291.
10. The β -silicon effect or silicon hyperconjugation is the stabilizing effect of a silicon atom located at β position to carbocations.
11. Bonnefon, E.; Birot, M.; Dunogues, J.; Pillot, J.-P.; Courseille, C.; Taulelle, F. *Main Group Met. Chem.* **1996**, *19*, 761.
12. AraujoDaSilva, J. C. ; Birot, M.; Pillot, J.-P.; Pétraud, M. Regio- and Stereoselective Addition of Sterically Hindered Silylboranes to Terminal Alkynes. *J. Organomet. Chem.* **2002**, *646*, 179.
13. Yamamoto, E.; Shishido, R.; Seki, T.; Ito, H. Tris(trimethylsilyl)silylboronate Esters: Novel Bulky, Air- and Moisture-Stable Silylboronate Ester Reagents for Boryl Substitution and Silaboration Reactions. *Organometallics* **2017**, *36*, 3019.
14. Boebel, T. A.; Hartwig, J. F. Iridium-Catalyzed Preparation of Silylboranes by Silane Borylation and Their Use in the Catalytic Borylation of Arenes. *Organometallics* **2008**, *27*, 6013.
15. Wittig, G. Über metallorganische Komplexverbindungen. *Angew. Chem.* **1950**, *62*, 231.
16. Gilman, H.; Rosenberg, S. D. The Preparation of Triphenyltin-lithium and Some of Its Reactions. *J. Am. Chem. Soc.* **1952**, *74*, 531.
17. Still, W. C. Stannylation/destannylation. New syntheses of Carbonyl Compounds via Organotin Intermediates. *J. Am. Chem. Soc.* **1977**, *99*, 4836.
18. For selected reviews, see: (a) *Organotin Chemistry*, 2nd ed.; Davies, A. G., Ed.; Wiley-VCH: Weinheim. **2004**. (b) Compounds with Tin- Metal Bonds. *Organotin Chemistry*; pp 311–332, *ibid.* (c) Glockling, F. In *Chemistry of Tin*; Smith, P. J. , Ed.; Blackie: London, **1998**.
19. Sharma, S.; Oehlschlager, A. C. Scope and Mechanism of Stannylation of 1-Alkynes. *J. Org. Chem.* **1989**, *54*, 5064.
20. Gilman, H.; Rosenberg, S. D. The Preparation of Triphenyltin-lithium and Some of Its Reactions. *J. Am. Chem. Soc.* **1952**, *74*, 531.
21. Gilman, H.; Cartledge, F. K.; Sim, S.-Y. The Analysis of Organic-Substituted Group IVB Lithium Compounds. *J. Organomet. Chem.* **1963**, *1*, 8.
22. Still, W. C. Stannylation/destannylation. New Syntheses of Carbonyl Compounds via Organotin Intermediates. *J. Am. Chem. Soc.* **1977**, *99*, 4836.
23. Still, W. C. Stannylation/destannylation. Preparation of α -alkoxy Organolithium Reagents and Synthesis of Dendrolasin via a Carbinyl Carbanion Equivalent. *J. Am. Chem. Soc.* **1978**, *100*, 1481.
24. Wang, D.-Y.; Wang, C.; Uchiyama, M. Stannyll-Lithium: A Facile and Efficient Synthesis Facilitating Further Applications. *J. Am. Chem. Soc.* **2015**, *137*, 10488.
25. Suginome, M.; Ito, Y. Transition-Metal-Catalyzed Additions of Silicon-Silicon and Silicon-Heteroatom Bonds to Unsaturated Organic Molecules. *Chem. Rev.* **2000**, *100*, 3221.

26. Suginome, M.; Ito, Y. Regio- and Stereoselective Synthesis of Boryl-substituted Allylsilanes via Transition Metal-Catalyzed Silaboration. *J. Organomet. Chem.* **2003**, *680*, 43.
27. Oestreich, M.; Hartmann, E.; Mewald M. Activation of the Si-B Interelement Bond: Mechanism, Catalysis, and Synthesis. *Chem. Rev.* **2013**, *113*, 402.
28. Ohmura, T.; Masuda, K.; Suginome, M. Silylboranes Bearing Dialkylamino Groups on Silicon as Silylene Equivalents: Palladium-Catalyzed Regioselective Synthesis of 2,4-Disubstituted Siloles. *J. Am. Chem. Soc.* **2008**, *130*, 1526.
29. Hartmann, E.; Oestreich, M. Transition Metal-Catalyzed Addition of Interelement Bonds Across Unsaturated C-C Bonds Involving Transmetalation. *Chim. Oggi* **2011**, *29*, 34.
30. Kawachi, A.; Minamimoto, T.; Tamao, K. Boron-Metal Exchange Reaction of Silylboranes with Organometallic Reagents: A New Route to Arylsilyl Anions. *Chem. Lett.* **2001**, *30*, 1216.
31. Matsumoto, A.; Ito, Y. New Generation of Organosilyl Radicals by Photochemically Induced Homolytic Cleavage of Silicon-Boron Bonds. *J. Org. Chem.* **2000**, *65*, 5707.
32. Hata, T.; Kitagawa, H.; Masai, H.; Kurahashi, T.; Shimizu, M.; Hiyama, T. Geminal Difunctionalization of Alkenylidene-Type Carbenoids by Using Interelement Compounds. *Angew. Chem. Int. Ed.* **2001**, *40*, 790.
33. Shimizu, M.; Kitagawa, H.; Kurahashi, T.; Hiyama, T. 1-Silyl-1-boryl-2-alkenes: Reagents for Stereodivergent Allylation Leading to 4-Oxy-(E)-1-alkenylboronates and 4-Oxy-(Z)-1-alkenylsilanes. *Angew. Chem. Int. Ed.* **2001**, *40*, 4283.
34. O'Brien, J. M.; Hoveyda, A. H. Metal-Free Catalytic C-Si Bond Formation in an Aqueous Medium. Enantioselective NHC-Catalyzed Silyl Conjugate Additions to Cyclic and Acyclic α,β -Unsaturated Carbonyls. *J. Am. Chem. Soc.* **2011**, *133*, 7712.
35. Oshima, K.; Ohmura, T.; Suginome, M. Dearomatizing Conversion of Pyrazines to 1,4-Dihydropyrazine Derivatives via Transition-Metal-Free Diboration, Silaboration, and Hydroboration. *Chem. Commun.* **2012**, *48*, 8571.
36. Kleeberg, C.; Borner, C. On the Reactivity of Silylboranes toward Lewis Bases: Heterolytic B-Si Cleavage vs. Adduct Formation. *Eur. J. Inorg. Chem.* **2013**, 2799.
37. Suginome, M.; Ito, Y. Transition-Metal-Catalyzed Additions of Silicon-Silicon and Silicon-Heteroatom Bonds to Unsaturated Organic Molecules. *Chem. Rev.* **2000**, *100*, 3221.
38. Beletskaya, I.; Moberg, C. Element-Element Addition to Alkynes Catalyzed by the Group 10 Metals. *Chem. Rev.* **1999**, *99*, 3435.
39. Cuenca, A. B.; Shishido, R.; Ito H.; Fernández, E. Transition-Metal-Free B-B and B-interelement Reactions with Organic Molecules. *Chem. Soc. Rev.* **2017**, *46*, 415.
40. Zarate, C.; Martin, R. A Mild Ni/Cu-Catalyzed Silylation via C-O Cleavage. *J. Am. Chem. Soc.* **2014**, *136*, 2236.
41. Somerville, R.; Hale, L.; Gomez-Bengoa, E.; Bureš, J.; Martin, R. Intermediacy of Ni-Ni Species in sp^2 C-O Bond Cleavage of Aryl Esters: Relevance in Catalytic C-Si Bond Formation. *J. Am. Chem. Soc.* **2018**, *140*, 8771.
42. Zarate, C.; Nakajima, M.; Martin, R. A Mild and Ligand-Free Ni-Catalyzed Silylation via C-OMe Cleavage. *J. Am. Chem. Soc.* **2017**, *139*, 1191.
43. Jonas, K.; Pörschke, K. R.; Krüger, C.; Tsay, Y.-H. Carbanion Complexes of Nickel(0). *Angew. Chem. Int. Ed.* **1976**, *15*, 621.
44. Kaschube, W.; Pörschke, K.-R.; Angermund, K.; Krüger, C.; Wilke, G. diorganylmagnesium-komplexe von Nickel(0): (TMEDA)MgCH₃(μ -CH₃)Ni(C₂H₄)₂ *Chem. Ber.* **1988**, *121*, 1921.
45. Guo, L.; Chatupheeraphat, A.; Rueping, M. Decarbonylative Silylation of Esters by Combined Nickel and Copper Catalysis for the Synthesis of Arylsilanes and Heteroarylsilanes. *Angew. Chem. Int. Ed.* **2016**, *55*, 11810.
46. Pu, X.; Hu, J.; Zhao, Y.; Shi, Z. Nickel-Catalyzed Decarbonylative Borylation and Silylation of Esters. *ACS Catal.* **2016**, *6*, 6692.
47. Guo, L.; Rueping, M. Decarbonylative Cross-Couplings: Nickel Catalyzed Functional Group Interconversion Strategies for the Construction of Complex Organic Molecules. *Acc. Chem. Res.* **2018**, *51*, 1185.

48. See Chapter 2 of the present thesis: Gu, Y.; Martin, R. Ni-Catalyzed Stannylation of Aryl Ester via C–O Cleavage. *Angew. Chem. Int. Ed.* **2017**, *56*, 3187.
49. Yue, H.; Zhu, C.; Rueping, M. Catalytic Ester to Stannane Functional Group Interconversion via Decarbonylative Cross-Coupling of Methyl Esters. *Org. Lett.* **2018**, *20*, 385.
50. Liu, X.-W.; Echavarren, J.; Zarate, C.; Martin, R. Ni-Catalyzed Borylation of Aryl Fluorides via C–F Cleavage. *J. Am. Chem. Soc.* **2015**, *139*, 12470.
51. Sakaguchi, H.; Uetake, Y.; Ohashi, M.; Niwa, T.; Ogoshi, S.; Hosoya, T. Copper-Catalyzed Regioselective Monodefluoroborylation of Polyfluoroalkenes en Route to Diverse Fluoroalkenes. *J. Am. Chem. Soc.* **2017**, *139*, 12855.
52. Cui, B.; Jia, S.; Tokunaga, E.; Shibata, N. Defluorosilylation of Fluoroarenes and Fluoroalkanes. *Nat Commun.* **2018**, *1*, 4393.
53. Wang, X.; Wang, Z.; Liu, L.; Asanuma, Y.; Nishihara, Y. Nickel-Catalyzed Decarbonylative Stannylation of Acyl Fluorides under Ligand-Free Conditions. *Molecules.* **2019**, *24*, 1671.
54. Liu, X.-W.; Zarate, C.; Martin, R. Base-Mediated Defluorosilylation of C(sp²)–F and C(sp³)–F Bonds. *Angew. Chem. Int. Ed.* **2019**, *58*, 2064.
55. Gao, P.; Wang, G.; Xi, L.; Wang, M.; Li, S.; Shi, Z. Transition-Metal-Free Defluorosilylation of Fluoroalkenes with Silylboronates. *Chin. J. Chem.* **2019**, *37*, 1009.
56. Bernasconi, C. F.; Rappoport, Z. Recent Advances in Our Mechanistic Understanding of S_NV Reactions. *Acc. Chem. Res.* **2009**, *42*, 8993.
57. Wang, D.-Y.; Wen, X.; Xiong, C.-D.; Zhao, J.-N.; Ding, C.-Y.; Meng, Q.; Zhou, H.; Wang, C.; Uchiyama, M.; Lu, X.-J.; Zhang, A. Non-transition Metal-Mediated Diverse Aryl–Heteroatom Bond Formation of Arylammonium Salts. *iScience*, **2019**, *15*, 307.
58. Zhao, J.-N.; Kayumov, M.; Wang, D.-Y.; Zhang, A. Transition-Metal-Free Aryl–Heteroatom Bond Formation via C–S Bond Cleavage. *Org. Lett.* **2019**, *18*, 7303.
59. Yamamoto, E.; Izumi, K.; Horita, Y.; Ito, H. Anomalous Reactivity of Silylborane: Transition -Metal-Free Boryl Substitution of Aryl, Alkenyl, and Alkyl Halides with Silylborane/Alkoxy Base Systems. *J. Am. Chem. Soc.* **2012**, *134*, 19997.
60. Yamamoto, E.; Ukigai, S.; Ito, H. Boryl Substitution of Functionalized Aryl-, Heteroaryl- and Alkenyl Halides with Silylborane and an Alkoxy Base: Expanded Scope and Mechanistic Studies. *Chem. Sci.* **2015**, *6*, 2943.
61. Yamamoto, E.; Maeda, S.; Taketsugu, T.; Ito, H. Transition-Metal-Free Boryl Substitution Using Silylboranes and Alkoxy Bases. *Synlett*, **2017**, *28*, 1258.
62. Uematsu, R.; Yamamoto, E.; Maeda, S.; Ito, H.; Taketsugu, T. Reaction Mechanism of the Anomalous Formal Nucleophilic Borylation of Organic Halides with Silylborane: Combined Theoretical and Experimental Studies. *J. Am. Chem. Soc.* **2015**, *137*, 4090.
63. Yamamoto, E.; Izumi, K.; Shishido, R.; Seki, T.; Tokodai, N.; Ito, H. Direct Introduction of a Dimesitylboryl Group Using Base-Mediated Substitution of Aryl Halides with Silyldimesitylborane. *Chem. Eur. J.* **2016**, *22*, 17547.
64. Zhao, C.-H.; Wakamiya, A.; Inukai, Y.; Yamaguchi, S. Highly Emissive Organic Solids Containing 2,5-Diboryl-1,4-phenylene Unit. *J. Am. Chem. Soc.* **2006**, *128*, 15934.
65. Entwistle, C. D.; Marder, T. B. Applications of Three-Coordinate Organoboron Compounds and Polymers in Optoelectronics. *Chem. Mater.* **2004**, *16*, 4574.
66. Ito, H.; Horita, Y.; Yamamoto, E. Potassium tert-butoxide-mediated Regioselective Silaboration of Aromatic Alkenes. *Chem. Commun.* **2012**, *48*, 8006.
67. Bonet, A.; Pubill-Ulldemolins, C.; Bo, C.; Gulyás, H.; Fernández, E. Transition-Metal-Free Diboration Reaction by Activation of Diboron Compounds with Simple Lewis Bases. *Angew. Chem. Int. Ed.* **2011**, *50*, 7158.
68. Pubill-Ulldemolins, C.; Bonet, A.; Bo, C.; Gulyás, H.; Fernández, E. Activation of Diboron Reagents with Brønsted Bases and Alcohols: An Experimental and Theoretical Perspective of the Organocatalytic Boron Conjugate Addition Reaction. *Chem.–Eur. J.* **2012**, *18*, 1121.

69. Xue, W.; Qu, Z.-W.; Grimme, S.; Oestreich, M. Copper-Catalyzed Cross-Coupling of Silicon Pronucleophiles with Unactivated Alkyl Electrophiles Coupled with Radical Cyclization. *J. Am. Chem. Soc.* **2016**, *138*, 14222.
70. Xue, W.; Oestreich, M. Copper-Catalyzed Decarboxylative Radical Silylation of Redox-Active Aliphatic Carboxylic Acid Derivatives. *Angew. Chem. Int. Ed.* **2017**, *56*, 11649.
71. Larsen, M. A.; Wilson, C. V.; Hartwig, J. F. Iridium-Catalyzed Borylation of Primary Benzylic C-H Bonds without a Directing Group: Scope, Mechanism, and Origins of Selectivity. *J. Am. Chem. Soc.* **2015**, *137*, 8633.
72. Larsen, M. A.; Hartwig, J. F. Iridium-Catalyzed C-H Borylation of Heteroarenes: Scope, Regioselectivity, Application to Late-Stage Functionalization, and Mechanism. *J. Am. Chem. Soc.* **2014**, *136*, 4287.
73. Calow, A. D. J.; Batsanov, A. S.; Pujol, A.; Solé, C.; Fernández, E.; Whiting, A. A Selective Transformation of Enals into Chiral γ -Amino Alcohols. *Org. Lett.* **2013**, *15*, 4810.
74. Lillo, V.; Geier, M. J.; Westcott, S. A.; Fernández, E. Ni and Pd Mediate Asymmetric Organoboron Synthesis with Ester Functionality at the β -position. *Org. Biomol. Chem.* **2009**, *7*, 4674.
75. Bonet, A.; Gulyaś, H.; Fernández, E. Metal-Free Catalytic Borylation at the β -Position of α,β -Unsaturated Compounds: A Challenging Asymmetric Induction. *Angew. Chem. Int. Ed.* **2010**, *49*, 5130.
76. (a) Walter, C.; Auer, G.; Oestreich, M. Rhodium-catalyzed enantioselective conjugate silyl transfer: 1,4-addition of silyl boronic esters to cyclic enones and lactones. *Angew. Chem. Int. Ed.* **2006**, *45*, 5675. (b) Walter, C.; Oestreich, M. Catalytic asymmetric C-Si bond formation to acyclic α,β -unsaturated acceptors by Rh(I)-catalyzed conjugate silyl transfer using a Si-B linkage. *Angew. Chem. Int. Ed.* **2008**, *47*, 3818.
77. Lee, K.-s.; Hoveyda, A. H. Enantioselective Conjugate Silyl Additions to Cyclic and Acyclic Unsaturated Carbonyls Catalyzed by Cu Complexes of Chiral N-Heterocyclic Carbenes. *J. Am. Chem. Soc.* **2010**, *132*, 2898.
78. O'Brien, J. M.; Hoveyda, A. H. Metal-Free Catalytic C-Si Bond Formation in an Aqueous Medium. Enantioselective NHC-Catalyzed Silyl Conjugate Additions to Cyclic and Acyclic α,β -Unsaturated Carbonyls. *J. Am. Chem. Soc.* **2011**, *133*, 7712.
79. Wu, H.; Garcia, J. M.; Haefner, F.; Radomkit, S.; Zhugralin, A. R.; Hoveyda, A. H. Mechanism of NHC-Catalyzed Conjugate Additions of Diboron and Borosilane Reagents to α,β -Unsaturated Carbonyl Compounds. *J. Am. Chem. Soc.* **2015**, *137*, 10585.
80. Vyas, D. J.; Oestreich, M. Copper-Catalyzed Si-B Bond Activation in Branched-Selective Allylic Substitution of Linear Allylic Chlorides. *Angew. Chem. Int. Ed.* **2010**, *49*, 8513.
81. Delvos, L. B.; Vyas, D. J.; Oestreich, M. Asymmetric Synthesis of α -Chiral Allylic Silanes by Enantioconvergent γ -Selective Copper(I)-Catalyzed Allylic Silylation. *Angew. Chem. Int. Ed.* **2013**, *52*, 4650.
82. Park, J. K.; Lackey, H. H.; Ondrusek, B. A.; McQuade, D. T. Stereoconvergent Synthesis of Chiral Allylboronates from an E/Z Mixture of Allylic Aryl Ethers Using a 6-NHC-Cu(I) Catalyst. *J. Am. Chem. Soc.* **2011**, *133*, 2410.
83. Shintani, R.; Fujie, R.; Takeda, M.; Nozaki, K. Silylative Cyclopropanation of Allyl Phosphates with Silylboronates. *Angew. Chem. Int. Ed.* **2014**, *53*, 6546.
84. Beletskaya, I.; Moberg, C. Element-Element Additions to Unsaturated Carbon-Carbon Bonds Catalyzed by Transition Metal Complexes. *Chem. Rev.* **2006**, *106*, 2320.
85. Suginome, M.; Nakamura, H.; Ito, Y. Regio- and Stereo-Selective Silaboration of Alkynes Catalysed by Palladium and Platinum Complexes. *Chem. Commun.* **1996**, 2777.
86. Ohmura, T.; Oshima, K.; Suginome, M. Palladium-Catalysed cis- and trans-Silaboration of Terminal Alkynes: Complementary Access to Stereo-Defined Trisubstituted Alkene. *Chem. Commun.* **2008**, 1416.
87. Ohmura, T.; Oshima, K.; Taniguchi, H.; Suginome, M. Switch of Regioselectivity in Palladium-Catalyzed Silaboration of Terminal Alkynes by Ligand-Dependent Control of Reductive Elimination. *J. Am. Chem. Soc.* **2010**, *132*, 12194.

88. Abe, Y.; Kuramoto, K.; Ehara, M.; Nakatsuji, H.; Suginome, M.; Murakami, M.; Ito, Y. A Mechanism for the Palladium-Catalyzed Regioselective Silaboration of Allene: A Theoretical Study. *Organometallics* **2008**, *27*, 1736.
89. Gryparis, C.; Stratakis, M. Nanogold-Catalyzed cis-Silaboration of Alkynes with Abnormal Regioselectivity. *Org. Lett.* **2014**, *16*, 1430.
90. Nagashima, Y.; Yukimori, D.; Wang, C.; Uchiyama, M. In Situ Generation of Silylzinc by Si-B Bond Activation Enabling Silylzincation and Silaboration of Terminal Alkynes. *Angew. Chem. Int. Ed.* **2018**, *57*, 8053.
91. Zhao, M.; Shan, C.-C.; Wang, Z.-L.; Yang, C.; Fu, Y.; Xu, Y.-H.; Ligand-Dependent-Controlled Copper-Catalyzed Regio- and Stereoselective Silaboration of Alkynes. *Org. Lett.* **2019**, *21*, 6016.
92. Nagao, K.; Ohmiya, H.; Sawamura, M. Anti-Selective Vicinal Silaboration and Diboration of Alkynoates through Phosphine Organocatalysis. *Org. Lett.* **2015**, *17*, 1304.
93. Methot, J. L.; Roush, W. R. Nucleophilic Phosphine Organocatalysis. *Adv. Synth. Catal.* **2004**, *346*, 1035.
94. Chenard, B. L.; Laganis, E. D.; Davidson, F.; RajanBabu, T. V. Silyl Stannanes: Useful Reagents for bis-Functionalization of α,β -Unsaturated Ketones and Acetylenes. *J. Org. Chem.* **1985**, *50*, 3666.
95. Nielsen, T. E.; Le Quement, S.; Tanner, D. Palladium-Catalyzed Silastannylation of Secondary Propargylic Alcohols and their Derivatives. *Synthesis* **2004**, 1381.
96. Hemeon, I.; Singer, R. D. Silylstannylation of Terminal Alkynes Using a Recyclable Palladium(0) Catalyst Immobilised in an Ionic Liquid. *Chem. Commun.* **2002**, 1884.
97. Oshima, K.; Ohmura, T.; Suginome, M. Palladium-Catalyzed Regioselective Silaboration of Pyridines Leading to the Synthesis of Silylated Dihydropyridines. *J. Am. Chem. Soc.* **2011**, *133*, 7324.
98. Ariafard, A.; Tabatabaie, E. S.; Monfared, A. T.; Assar, S. H. A.; Hyland, C. J. T.; Yates, B. F. Theoretical Investigation into the Palladium-Catalyzed Silaboration of Pyridines. *Organometallics* **2012**, *31*, 1680.
99. Oshima, K.; Ohmura, T.; Suginome, M. Dearomatizing Conversion of Pyrazines to 1,4-Dihydropyrazine Derivatives via Transition-metal-free Diboration, Silaboration, and Hydroboration. *Chem. Commun.* **2012**, *48*, 8571.
100. Oshima, K.; Ohmura, T.; Suginome, M. Regioselective Synthesis of 1,2-Dihydropyridines by Rhodium-Catalyzed Hydroboration of Pyridines. *J. Am. Chem. Soc.* **2012**, *134*, 3699.
101. Cuenca, A. B.; Shishido, R.; Ito, H.; Fernández, E. Transition-metal-free B-B and B-Interelement Reactions with Organic Molecules. *Chem. Soc. Rev.* **2017**, *46*, 415.
102. Morimasa, Y.; Kabasawa, K.; Ohmura, T.; and Suginome, M. Pyridine-Based Organocatalysts for Regioselective syn-1,2-Silaboration of Terminal Alkynes and Allenes. *Asian J. Org. Chem.* **2019**, *8*, 1092.
103. Wang, G.; Zhang, H.; Zhao, J.; Li, W.; Cao, J.; Zhu, C.; Li, S. Homolytic Cleavage of a B-B Bond by the Cooperative Catalysis of Two Lewis Bases: Computational Design and Experimental Verification. *Angew. Chem. Int. Ed.* **2016**, *55*, 5985.
104. Ito, H.; Horita, Y.; Yamamoto, E. Potassium tert-butoxide-Mediated Regioselective Silaboration of Aromatic Alkenes. *Chem. Commun.* **2012**, *48*, 8006.
105. Vyas, D. J.; Fröhlich, R.; Oestreich, M. Activation of the Si-B Linkage: Copper-Catalyzed Addition of Nucleophilic Silicon to Imines. *Org. Lett.* **2011**, *13*, 2094.
106. Kleeberg, C.; Feldmann, E.; Hartmann, E.; Vyas, D. J.; Oestreich, M. Copper-Catalyzed 1,2-Addition of Nucleophilic Silicon to Aldehydes: Mechanistic Insight and Catalytic Systems. *Chem.—Eur. J.* **2011**, *17*, 13538.
107. Suginome, M.; Matsuda, T.; Yoshimoto, T.; Ito, Y. Stereoselective 1,4-Silaboration of 1,3-Dienes Catalyzed by Nickel Complexes. *Org. Lett.* **1999**, *1*, 1567.
108. Suginome, M.; Ohmori, Y.; Ito, Y. Palladium-Catalyzed Regioselective Silaboration of 1,2-dienes. *J. Organomet. Chem.* **2000**, *611*, 403.
109. Buynak, J. D.; Geng, B. Synthesis and Reactivity of Silylboranes. *Organometallics* **1995**, *14*, 3112.
110. Hata, T.; Kitagawa, H.; Masai, H.; Kurahashi, T.; Shimizu, M.; Hiyama, T. Geminal Difunctionalization of Alkenylidene-Type Carbenoids by Using Interelement Compounds. *Angew. Chem. Int. Ed.* **2001**, *40*, 790.
111. Murakami, M.; Usui, I.; Hasegawa, M.; Matsuda, T. Contrasteric Stereochemical Dictation of the Cyclobutene Ring-Opening Reaction by a Vacant Boron p Orbital. *J. Am. Chem. Soc.* **2005**, *127*, 1366.

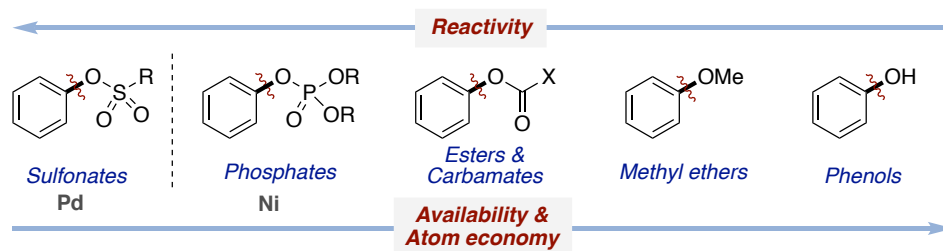
112. Shimizu, M.; Kitagawa, H.; Kurahashi, T.; Hiyama, T. 1-Silyl-1-boryl-2-alkenes: Reagents for Stereodivergent Allylation Leading to 4-Oxy-(E)-1-alkenylboronates and 4-Oxy-(Z)-1-alkenylsilanes. *Angew. Chem. Int. Ed.* **2001**, *40*, 4283.
113. Suginome, M.; Fukuda, T.; Nakamura, H.; Ito, Y. Synthesis of (Boryl)(silyl)iminomethanes by Insertion of Isonitriles into Silicon–Boron Bonds. *Organometallics* **2000**, *19*, 719.
114. Tobisu, M.; Fujihara, H.; Koh, K.; Chatani, N. Synthesis of 2-Boryl- and Silylindoles by Copper-Catalyzed Borylative and Silylative Cyclization of 2-Alkenylaryl Isocyanides. *J. Org. Chem.* **2010**, *75*, 4841.

Chapter 2.

Ni-Catalyzed Stannylation of Aryl Ester via C–O Bond Cleavage

2.1. C–O Electrophiles as Counterparts in Cross-Coupling Reactions

Transition-metal-catalyzed cross-coupling reactions have provided new dogmas for bond-construction, changing logics in retrosynthetic analysis when building up molecular complexity.¹⁻⁴ Indeed, their use is so pervasive that it is difficult to advance any advanced total synthesis or target lead in drug discovery approaches that do not take recourse to these methodologies. At present, the vast majority of transition metal-catalyzed C–C and C–heteroatom bond-forming reactions rely on the utilization of organic halides as coupling partners.⁵ Despite the advances realized in preparative terms, it is worth noting that accessing advanced aryl halides in a both chemo- and regioselective manner is not particularly facile and that the toxicity associated to the inevitable halide waste can be problematic, particularly in late-stage diversification techniques. Prompted by these observations, chemists have been challenged to look for alternative coupling partners with improved flexibility, practicality and generality. Among the different alternatives, the utilization of C–O electrophiles have gained tremendous momentum since the first seminal work by Wenkert in 1979,⁶ becoming powerful alternatives to commonly employed organic halides in transition metal-catalyzed cross-coupling reactions.⁷⁻¹¹ Their popularity arises from their bench-stability and ease of synthesis from abundant and non-toxic phenols. In addition, the utilization of C–O electrophiles as coupling partners might offer the possibility of designing orthogonal bond-forming reactions in the presence of organic halides.⁹ Scheme 2.1 summarizes the most commonly employed C–O electrophiles in cross-coupling reactions ranging from particularly activated sulfonate derivatives to rather unreactive phenols or aryl methyl ethers.

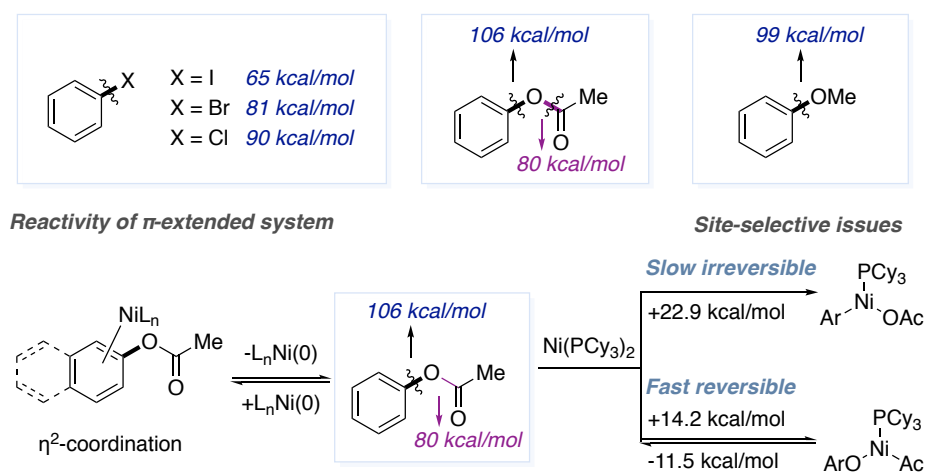


Scheme 2.1. Phenol derivatives as modern electrophiles in cross-coupling

2.1.1. Challenges in using C–O electrophiles in Ni-catalyzed cross-coupling reactions

While the utilization of aryl sulfonates have become routine in Pd-catalyzed cross-coupling reactions,¹² chemists have turned their attention to the employment of simpler, less-activated and more atom-economical aryl ester motifs as counterparts (Scheme 2.1). Although one might argue that this would be a trivial extension, a close look at the literature data indicates otherwise. First, the bond-dissociation of sp^2 C–O bonds in aryl esters is rather uphill when compared to both aryl halides or even aryl sulfonates,¹³ making these counterparts particularly reluctant to react via canonical oxidative addition events.¹⁴ Intriguingly, Pd catalysts have shown to be inert

towards C-O cleavage of aryl esters, whereas the employment of nickel catalysts have proven particularly effective for such purposes. In addition, the presence of weaker acyl sp^2 C-O bond in aryl esters raise the question on whether it would be possible to effect a site-selective functionalization of the targeted sp^2 C-O bond (Scheme 2.2). Seminal studies by Yamamoto, however, indicated that the oxidative addition of these moieties to $Ni(0)_n$ was reversible, suggesting that the design of catalytic cross-coupling reactions by means of functionalizing the sp^2 C-O bonds would not be a chimera. These studies set the basis for exploring whether steric effects might exert a role on site-selective C-O bond-functionalization. Indeed, it was shown that bulky pivaloyl groups are particularly suited for sp^2 C-O bond-functionalization by preventing the cleavage of the proximal and a priori weaker acyl sp^2 C-O bond.¹⁵ Unfortunately, a non-negligible number of cross-coupling reactions with C-O electrophiles are somewhat restricted to the utilization of π -extended arenes, suggesting that η^2 -coordination of the π -extended system to the low valent metal center might be a prerequisite for tackling C-O bond-cleavage, probably due to a partial retention of aromaticity.¹⁶



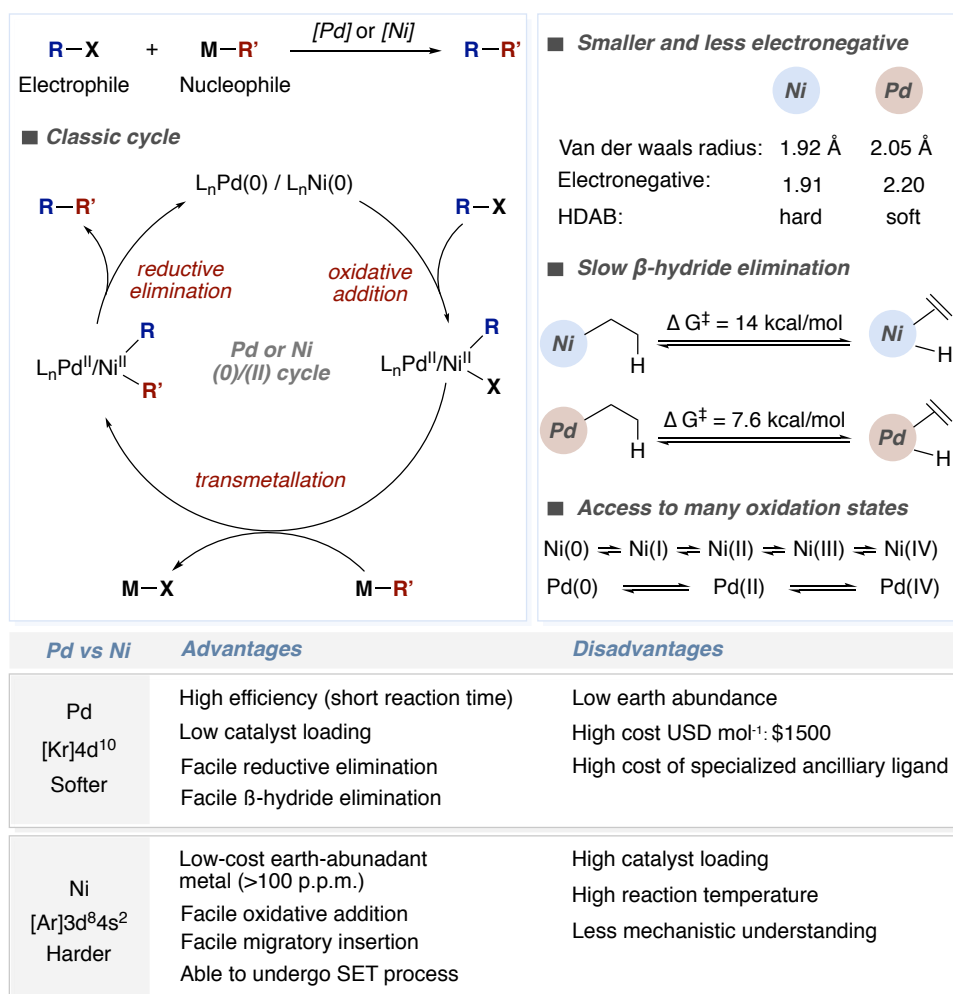
Scheme 2.2. Challenges in using C-O electrophiles in Ni-catalyzed reactions

2.1.2. Ni vs Pd in cross-coupling reactions

In line with the known literature data on C-O cleavage, one might wonder why nickel promotes effectively these transformations whereas Pd fails to provide the targeted bond-forming event. Both Pd and Ni catalysts have their advantages and disadvantages, which are highlighted in Scheme 2.3.¹⁷⁻¹⁹ Alongside these advantages, nickel has a smaller center, lower electronegativity than Pd. The propensity of the nickel center to lose electron density facilitates oxidative addition while a more facile reductive elimination is observed with palladium. As result, electron-rich Ni(0) can activate strong σ -bonds such as C-F²⁰ and C-N²¹ bonds via oxidative addition. Furthermore, π -back donation is more favorable from Ni(0) compared to Pd(0) resulting in a stronger binding to π systems ($d-\pi^*$ back donation). This also explains the

particular reactivity of Ni catalysts towards C–O bond activation, in which Ni(0)-arene η^2 -complex formation is essential to cleave the C–O bond of phenol derivatives.

Two factors contribute to slower β -H elimination of Ni-alkyl compounds. The lower electronegativity of Ni results in a weaker agostic interaction relative to Pd – the main contribution for the agostic interaction with electropositive metals is the σ -donation of the C–H bond to the metal center – and the smaller radius of Ni leads to a more strained geometry in the transition state. Due to the slow β -H elimination of Ni, cross coupling reaction with Ni could tolerate alkyl coupling partners that will undergo decomposition through β -H elimination with Pd. However, in comparison to Pd catalyzed cross-coupling reactions, those catalyzed by nickel are more likely to undergo SET processes, which is likely a result of the higher pairing energy of Ni due to a more condensed electron cloud.²² The stability of open-shell Ni(I) and Ni(III), in combination with the use of N-containing ligand gives rise to Ni-mediated radical pathways which could be merged with photoredox and electrochemical reactions. From these aspects above, Ni shows complementary reactivity to Pd, and thus could be applied in the development of alternative transformations and expand the scope of cross coupling reactions.²³

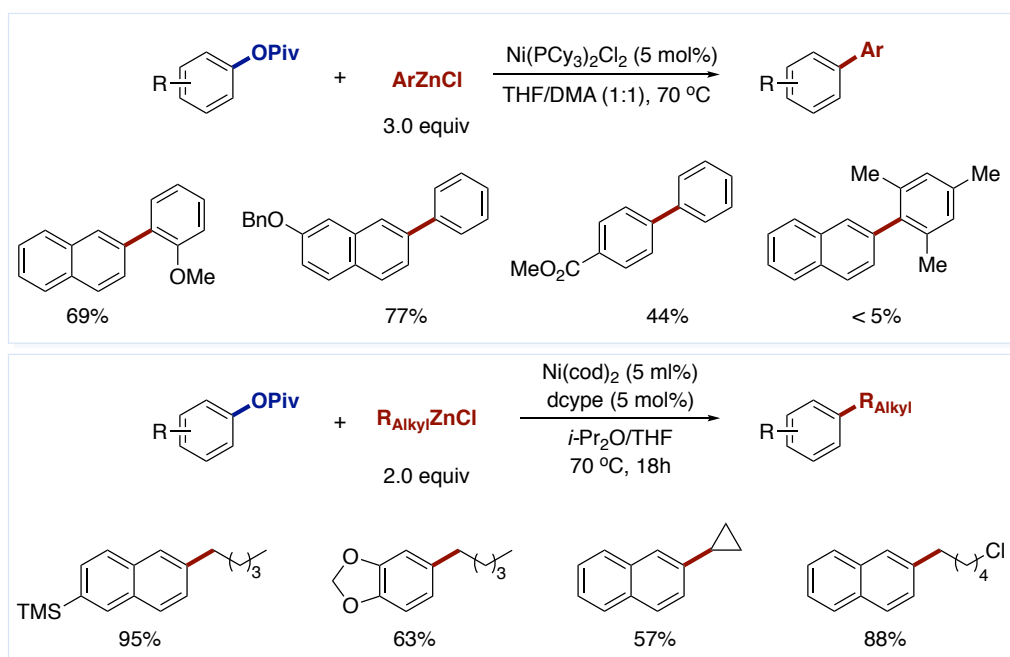


Scheme 2.3. General characteristics of Ni and Pd catalysts.

2.2. Ni-Catalyzed Cross-Coupling of Aryl Pivalates

2.2.1. C–C bond formation via sp^2 C–O cleavage

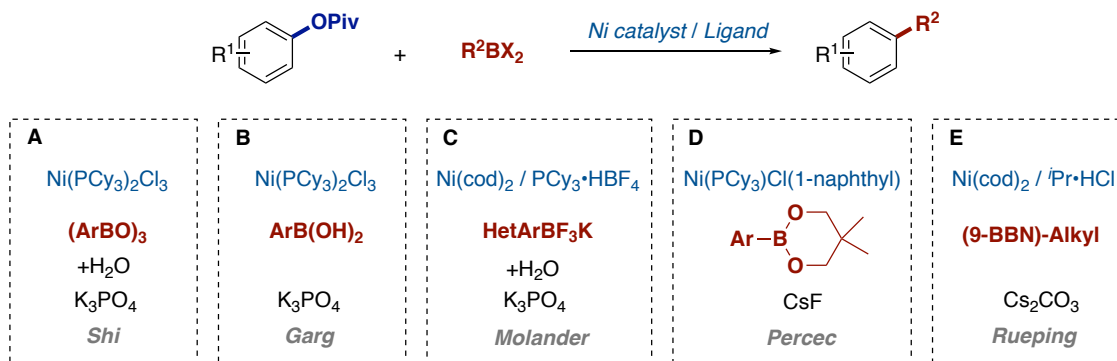
While Kumada-Corriu cross-coupling reactions of vinyl pivalates or vinyl acetates with Grignard reagents could be conducted within the context of Fe catalysis,^{24,25} extensions to aryl esters were found to be particularly problematic, probably due to competitive addition of the Grignard reagent to the acyl sp^2 C–O bond. This observation prompted the utilization of less-basic, yet less-reactive, organozinc reagents as coupling partners (Scheme 2.4). In particular, Shi described that air-stable $\text{Ni}(\text{PCy}_3)_2\text{Cl}_2$ could be used for such purposes, resulting in the targeted C–C bond-forming reaction in good yields.²⁶ In line with other C–O bond-functionalization reactions,^{26–29,61} the targeted cross-coupling only occurred efficiently when π -extended aryl pivalates were employed as substrates. In addition, steric effects played also a role on reactivity, as bulky arylzinc reagents were found to be incompetent in the targeted C–C bond-formation.



Scheme 2.4. Ni-catalyzed Negishi-type reactions of aryl pivalates

Aiming at extending the scope of these reactions, Rueping group reported a Negishi cross-coupling reaction between aryl pivalates and alkylzinc reagents catalyzed by $\text{Ni}(\text{cod})_2$ and a bisphosphine ligand (dcype).³⁰ Interestingly, various β -hydrogen-containing alkylzinc reagents could be coupled without problems. The absence of isomerization products in this endeavor is certainly intriguing, as such parasitic pathways have typically been observed in related cross-coupling techniques catalyzed by Pd catalysts. Additionally, alkylzinc reagents bearing substituents such as ester and chloride all proceeded smoothly with high efficiency. As for Shi's protocol,²⁶ however, this disclosure did not include mechanistic data, leaving a reasonable doubt

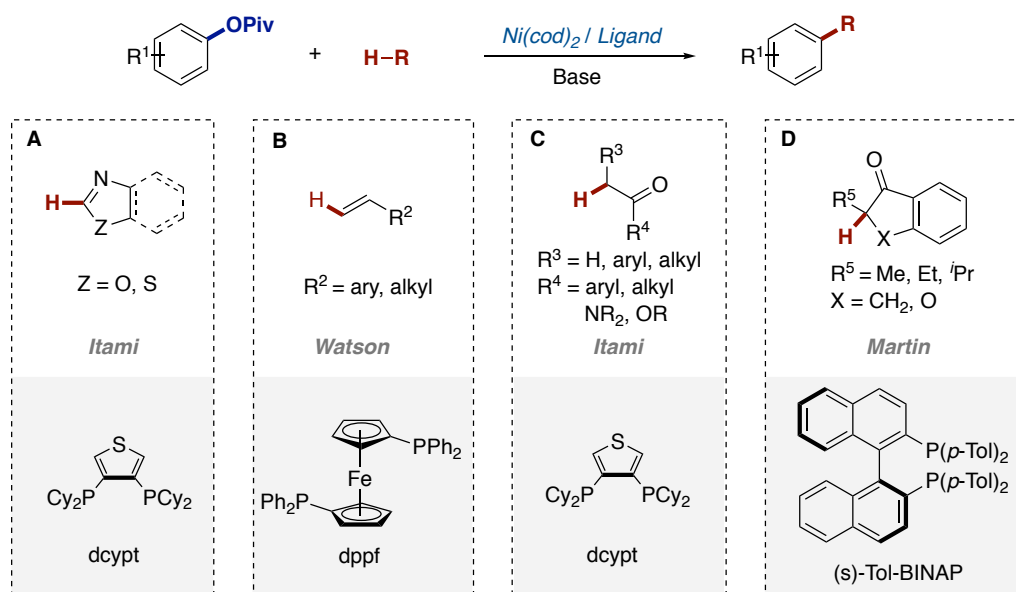
on whether the reactions follow a classical pathway consisting of oxidative addition followed by transmetalation and reductive elimination. Undoubtedly, shedding light into these mechanisms will not only clarify how the C–O bond is functionalized, but also will open up new vistas for exploring other reactivity within this field of expertise.



Scheme 2.5. Ni-catalyzed Suzuki-Miyaura reactions of aryl pivalates

Prompted by the air-sensitivity of organozinc reagents or Grignard reagents, chemists have turned their attention to the employment of organoboron reagents due to their air- and moisture stability and high functional group compatibility. To such end, Shi and Garg independently disclosed the first Suzuki-Miyaura reaction of aryl pivalates using Ni(PCy₃)₂Cl₃ as precatalyst.^{31, 32} While Shi employed arylboroxines – a cyclic trimer of arylboronic acids – in combination with water (Scheme 2.5, A), Garg used arylboronic acids without additional water (Scheme 2.5, B). The latter conditions allowed for the arylation of aryl acetates; this is particularly noteworthy if one takes into consideration that the vast majority of aryl ester cross-coupling reactions are conducted with rather bulky aryl pivalates to suppress the attack into the acyl C–O bond. In 2010, Molander expanded the range of Suzuki-Miyaura couplings of aryl esters when employing potassium heteroaryltrifluoroborates, even at particularly low catalyst loadings (Scheme 2.5, C).³³ As for other cases, however, the scope was limited to π-extended systems. Later on, a bench-stable Ni(II)PCy₃Cl(1-naphthyl) precatalyst was discovered by Percec, showing its competence in Suzuki-Miyaura cross-coupling reactions of aryl boronic esters (Scheme 2.5, D).³⁴ More recently, Rueping reported an aryl-alkyl cross-coupling of aryl esters catalyzed by a Ni(cod)₂/NHC catalyst system based on the utilization of B-Alkyl-9-borabicyclo[3.3.1]nonanes (Scheme 2.5, E).³⁵ Although a wide range of alkyl boron reagents possessing β-hydrogens could be utilized, these transformations could not be applied to either secondary or tertiary alkylboranes. Unfortunately, no mechanistic data was provided in all these cases, thus leaving a halo of mystery on the reaction mechanism.

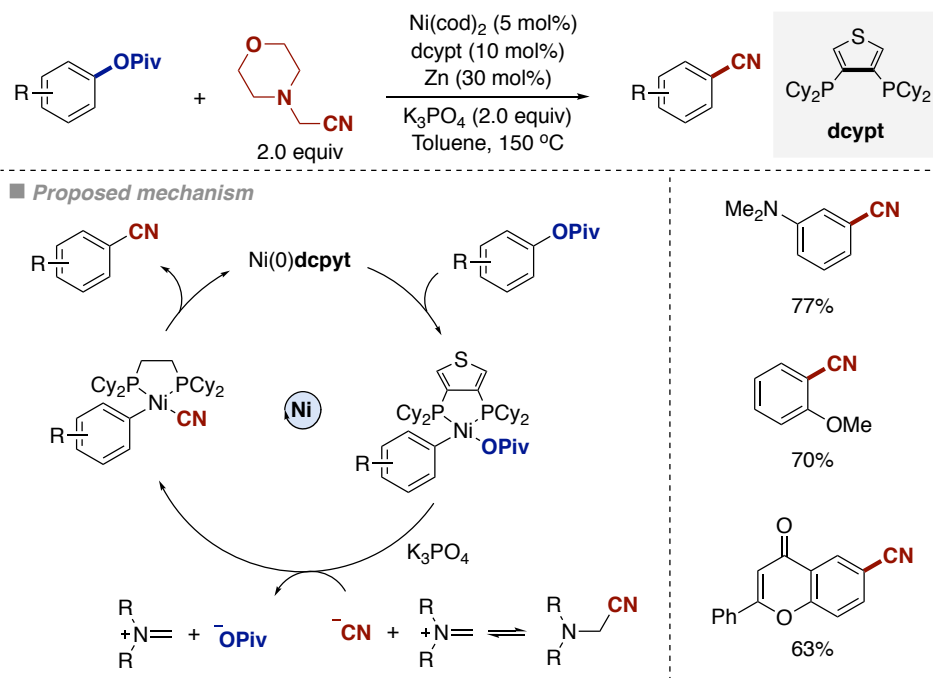
Ni-Catalyzed Stannylation of Aryl Ester via C–O Bond Cleavage



Scheme 2.6. Ni-catalyzed C–O/C–H cross-coupling reactions of aryl pivalates

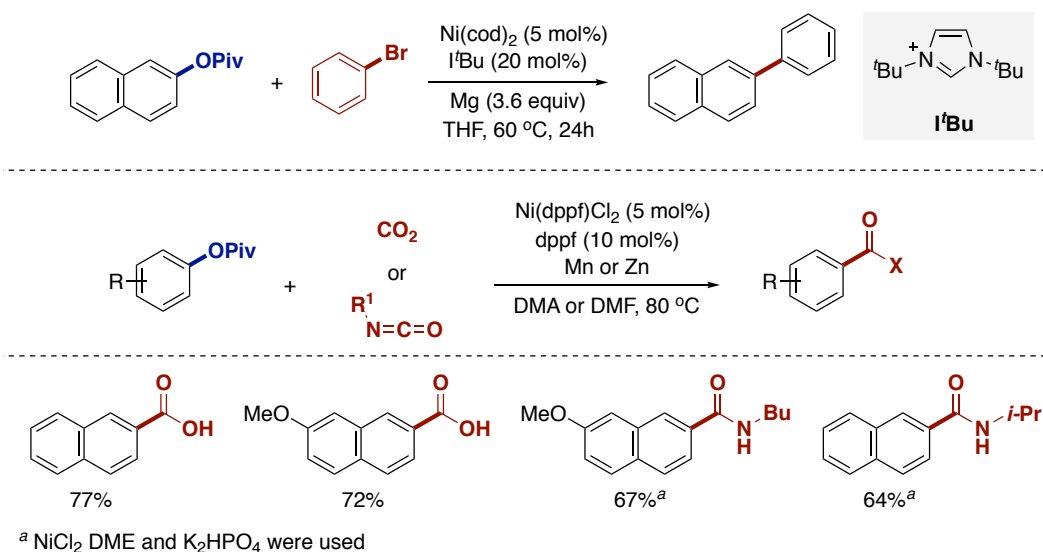
Despite the advances realized in C–O bond-cleavage, the vast majority of catalytic cross-coupling reactions of aryl esters rely on the utilization of well-defined organometallic reagents as coupling partners. From a conceptual and practical standpoint, it would be particularly attractive the development of a technique aimed at enabling C–C bond-formation of aryl esters within the context of C–H functionalization. This transformation was described by Itami, Yamaguchi and co-workers in which the utilization of $\text{Ni}(\text{cod})_2/\text{dcypt}$ was critical for success (Scheme 2.6, A).³⁶ Note, however, that the reaction could only be conducted efficiently with rather acidic sp^2 C–H bonds and with π -extended aryl pivalates at high temperatures. The mechanism of this transformation was studied by density functional theory (DFT) calculations and experimental studies.^{37, 38} While the former suggested that a Cs-cluster intervenes to assist C–H nickelation, there exists certain ambiguity on whether this rather sophisticated pathway comes into play. Indeed, no experiments were performed to determine the involvement of these species. More interestingly, it was found that the oxidative addition complex $\text{Ar-Ni}(\text{dcypt})\text{OPiv}$ could be isolated in pure form, allowing to rationalize that a canonical $\text{Ni}(0)/\text{Ni}(\text{II})$ pathway takes place under these reaction conditions. Extending this reaction to alkenes could be tackled by employing a $\text{Ni}(\text{cod})_2/\text{dppf}$ system at high temperatures (Scheme 2.6, B),^{39, 40} giving access to *E*-olefins and with an excess of alkene. Care should be taken when generalizing this, as the reaction is better visualized as a Heck-type endeavor rather than a C–H functionalization. Later on, Itami disclosed the α -arylation of carbonyl compounds and aryl pivalates by employing the Ni/dcypt couple (Scheme 2.6, C).⁴¹ Although these transformations suggested that the means to promote C–C bond-forming reactions with aryl esters should be conducted at high temperatures and/or specialized ligands, our group described that an enantioselective α -arylation was within reach by using prochiral ketones and simple (*s*)-Tol-BINAP as ligand, thus

allowing to generate enantioenriched quaternary stereocenters in high yields and selectivity (up to 99:1 e.r.) under remarkable mild conditions (Scheme 2.6, D).⁴²



Scheme 2.7. Ni-catalyzed cyanation of aryl pivalates with aminoacetonitriles

Following up their interest in C–O functionalization of aryl esters, Itami and Yamaguchi described a catalytic cyanation of aryl ester derivatives by using aminoacetonitrile as cyanide source with a Ni/dcpyt couple (Scheme 2.7).⁴³ Unlike related C–C bond-formations, this technique could be extended to non- π -extended arenes. The authors favored a pathway consisting of oxidative addition of aryl pivalate to Ni(0)_{L_n} followed by anion exchange with the nitrile and a final reductive elimination. Still, however, no mechanistic studies were performed.

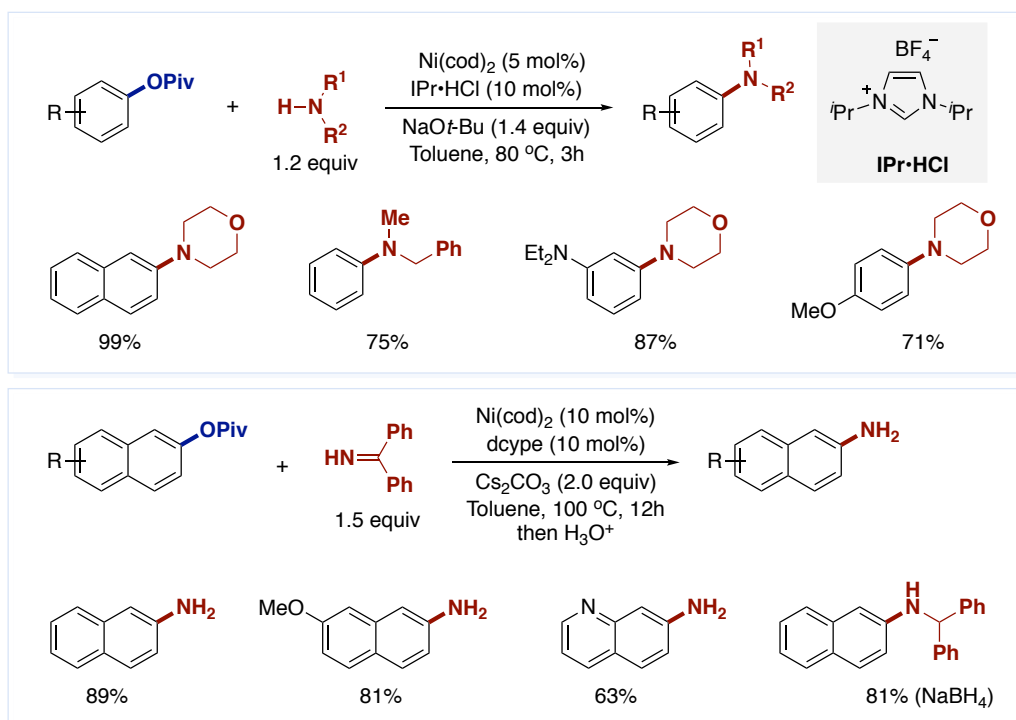


Scheme 2.8. Ni-catalyzed reductive cross-coupling with aryl bromides, CO₂ and isocyanates

Aiming at providing an alternative to the utilization of well-defined organometallic reagents in Suzuki-Miyaura, Negishi or Kumada-Corriu couplings, Shi reported a formal cross-electrophile coupling between aryl pivalates and aryl halides that is viable in the presence of Mg as stoichiometric reductant (Scheme 2.8, *top*).⁴⁴ Although preliminary experiments suggested that this reaction does not proceed through the formation of a Grignard reagent, it was not particularly clear the role of Mg in the reaction media. While a step-forward, the utilization of stoichiometric amounts of Mg does not represent a bonus from a chemoselectivity standpoint when compared to organozinc or organoboron reagents. In addition, and as for other C-O cross-couplings,²⁷⁻²⁹ this reaction turned out to be limited to π -extended aryl pivalates. As part of a program aimed at designing catalytic carboxylation reactions with abundant and inexpensive CO₂,⁴⁵ our group described a Ni-catalyzed reductive carboxylation of aryl and benzyl pivalates, representing a powerful alternative to the classical carboxylation protocols based on stoichiometric amounts of Grignard reagents or organozinc derivatives (Scheme 2.8, *middle*).⁴⁶ This protocol was based on the use of Ni/dppf as catalyst and cheap Mn as stoichiometric reductant, offering a superior chemoselectivity profile when compared with other carboxylation techniques based on well-defined aryl metal reagents. This transformation was believed to operate via initial oxidative addition followed by SET reduction mediated by Mn, generating the corresponding ArNi(I)L_n species *in situ* prior to CO₂ insertion. The targeted carboxylic acid was obtained after SET reduction, allowing to turn over the catalytically competent Ni(0)/dppf species. As expected, an otherwise related Ni-catalyzed amidation of aryl pivalates was accomplished by the use of isoelectronic isocyanates in the presence of Zn as reductant (Scheme 2.8, *bottom*).⁴⁷

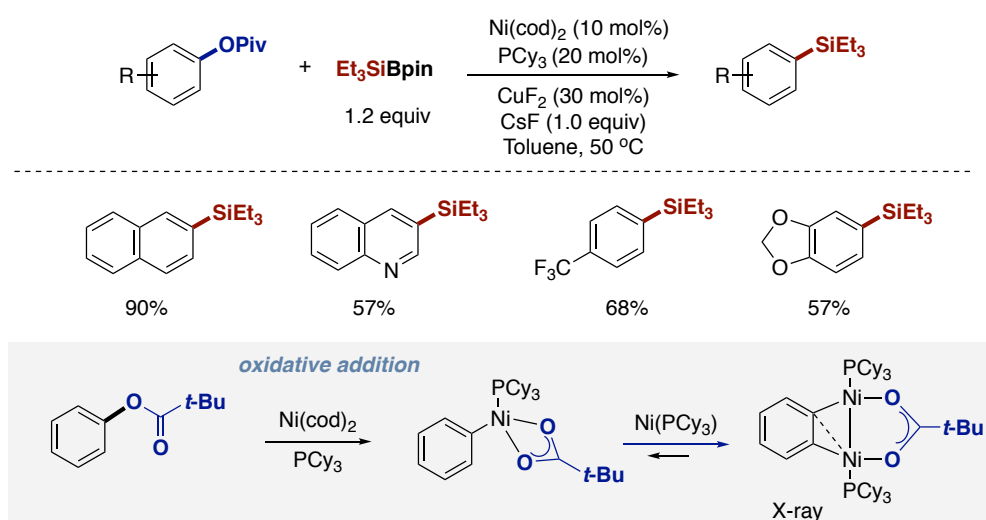
2.2.2. C-heteroatom bond formation via C-O cleavage

Unlike Pd-catalyzed cross-coupling reactions,⁴⁸ Ni-catalyzed C-heteroatom bond-forming reactions are not as commonly practiced as one might initially anticipate. This is particularly the case when employing C-O electrophiles as coupling partners. This paucity is probably associated to (a) the lower nucleophilicity of heteroatom-based nucleophiles and (b) the inherent difficulty of enabling C-heteroatom bond-reductive elimination. The first protocol that demonstrated the viability for triggering such a reaction was described by Chatani and Tobisu in the presence of Ni(0)/IPr and using secondary amines as pronucleophiles (Scheme 2.9, *top*).⁴⁹ The use of a pivalate leaving group is crucial to preventing undesired C_{acyl}-O bond cleavage, which becomes a major pathway resulting in hydrolysis when aryl acetates and benzoates are used as substrates instead. A range of secondary amines can be used to form the corresponding aminated products. In comparison to their previously described amination of aryl methyl ethers via C-OMe bond-cleavage, the new protocol has better generality as it allows the amination of unbiased regular aryl pivalates to be conducted under comparatively milder conditions.



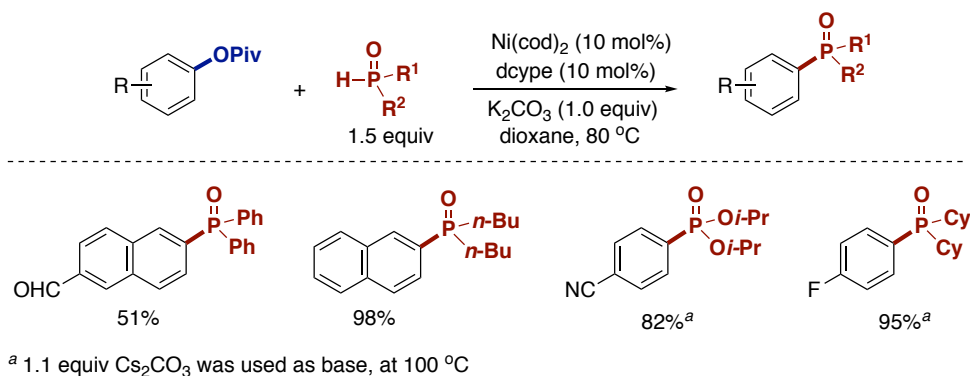
Scheme 2.9. Ni-catalyzed amination of aryl pivalates

Prompted by Chatani and Tobisu's amination,⁴⁹ Rueping developed an amination technology that resulted in the formation of anilines (Scheme 2.9, *bottom*).⁵⁰ Key for success was the utilization of benzophenone imine, a strategy already employed by Buchwald when promoting an otherwise analogous amination of organic halides by means of Pd catalysis.^{xx} In this case, the transformation was promoted by Ni(0)/dcype in combination with Cs₂CO₃ at relatively high temperatures, resulting in the corresponding imine that subsequently was reduced in the presence of sodium borohydride (NaBH₄) to the targeted aniline.



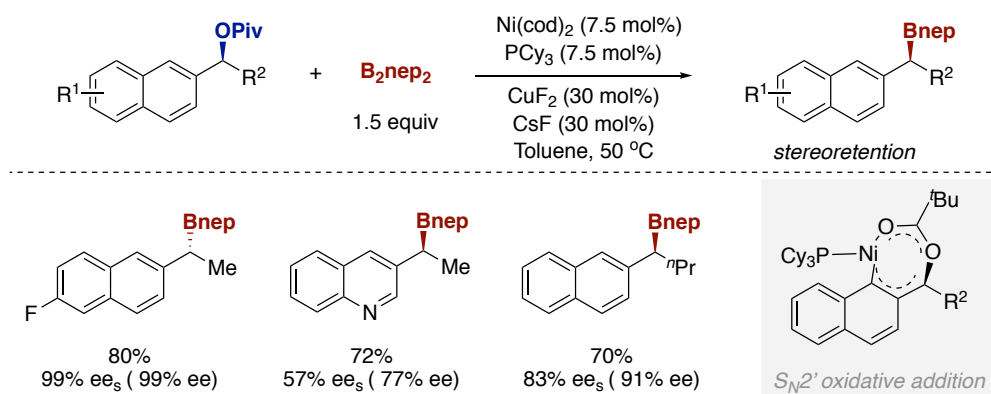
Scheme 2.10. Ni-catalyzed silylation of aryl pivalates

In 2014, our group described a catalytic silylation of aryl esters by means of C–O functionalization with silylboranes (Scheme 2.10, *top*).⁵¹ Interestingly, this transformation was promoted by both Cu and Ni catalysts with PCy₃ as supporting ligand, allowing to effect the targeted transformation at remarkable low temperatures (50 °C). This was particularly important, as it allowed the reaction to be extended to non- π -extended aryl pivalates, including those bearing sensitive functional groups. While originally the transformation was believed to proceed via the intermediacy of silylcopper species as pronucleophiles, recent mechanistic studies described by our group indicated that a different pathway came into play.⁵² Specifically, it was discovered that the transformation did not proceed via mononuclear oxidative addition, but rather by a dinickel intermediate that could be characterized and isolated in pure form (Scheme 2.10, *bottom*). In depth mechanistic studies, kinetic experiments and theoretical calculations allowed to rationalize the intricacies of the reaction, indicating that Cu salts can be replaced by Cs salts, with a C–Si bond-formation occurring via transmetalation of the putative oxidative addition species with silyl pronucleophiles followed by reductive elimination.



Scheme 2.11. Ni-catalyzed Phosphorylation of aryl pivalates via C–O/P–H cross-coupling

Han, Chen and co-workers demonstrated that phosphorus-based nucleophiles are also viable coupling partners in the nickel-catalyzed cross-coupling of aryl pivalates (Scheme 2.11).⁵³ Diphenylphosphines, diphenylphosphine oxides, and phosphonate reagents can all be successfully cross-coupled to form the corresponding aryl phosphine derivatives, which are used extensively in catalysis, materials science, coordination chemistry, and medicinal chemistry.⁵⁴ This discovery offered an alternative method for the construction of C–P bonds to those based on organolithium, Grignard reagents or toxic phosphorus halides. By tuning the reaction conditions, the phosphorylation of benzyl and allylic pivalates and non π -extended system was also achieved.⁵⁵ In line with Itami's studies with Ni/dcype regimes, a catalytic cycle based on an oxidative addition followed by ligand exchange aided by base and C–P bond-reductive elimination was proposed, resulting in the targeted phosphorylation event with regeneration of the catalytically competent Ni(0)/dcype species.



Scheme 2.12. Ni-catalyzed stereospecific borylation of secondary benzyl pivalates

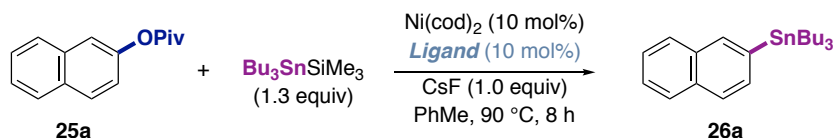
Following up our interest on C–O cleavage, we recently developed a Ni-catalyzed stereospecific borylation of enantioenriched benzyl pivalates in which C–B bond formation was catalyzed by Ni(cod)₂/PCy₃ aided by copper salts and CsF (Scheme 2.12).⁵⁶ Unfortunately, both yields and enantioselectivities were eroded when larger alkyl side chains were employed. This was tentatively ascribed to a lower tendency for transmetalation, leaving ample room for parasitic β-hydride elimination. Attempts to expand the substrate scope to regular aryl pivalates were unsuccessful as well, due to the lack of strong η² interaction of non-π extended systems with the low-valent Ni complexes that precede C–O bond cleavage. Interestingly, it was found that the reaction occurred via neat stereoretention. As both transmetalation and reductive elimination should occur with stereoretention, these results suggested a scenario consisting of a pivalate-assisted S_N2' type oxidative addition taking place with retention of configuration.

As judged by the wealth of literature data, it is evident that considerable progress has been made in the area of Ni-catalyzed cross-coupling reactions of aryl esters.^{8,9} Unlike the corresponding C–C bond-forming reactions, however, there exists a paucity on C–heteroatom bond-forming reactions, probably due to the intrinsically lower reactivity of the corresponding nucleophilic congeners and the low proclivity to trigger C–heteroatom bond-reductive elimination. In addition, a non-negligible number of C–O bond-functionalization reactions are still confined to the utilization of π-extended systems and relatively high temperatures, offering new opportunities to improve upon existing cross-coupling reactions and to understand how these reactions operate at the molecular level.

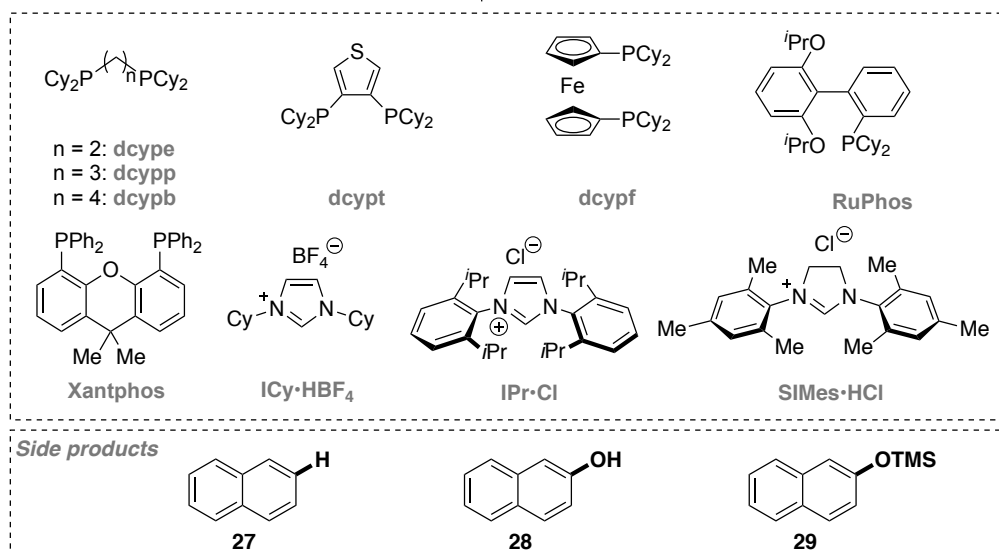
2.4. Ni-Catalyzed Stannylation of Aryl Pivalates

2.4.1. Optimization of the reaction conditions

We began our optimization by selecting the appropriate aryl pivalate and suitable stannyl reagent for our targeted C–O cleavage. Based on previous studies carried out in our group on C–O bond activation,^{42,47,51} we choose 2-naphthyl pivalate **25a** as the model starting material and Bu₃SnSiMe₃ (**18a**) reagent as a bench-stable stannyl source. Indeed, Bu₃SnSiMe₃ can be easily prepared on a large scale from easily prepared Bu₃Sn-Li reagent with Me₃SiMeCl.⁵⁷ During the screening of the optimized reaction conditions, naphthalene (**27**), naphthol (**28**), and silyl ether (**29**) were observed as the side products. The formation of these compounds can be explained by competitive hydrogenolysis, attack to acyl *sp*² C–O bond and silyl transfer to the oxygen atom.



Entry	Ligand	Yield of 26a (%) ^a	Entry	Ligand	Yield of 26a (%) ^a
1	PPh ₃ ^b	0	10	dcy pb	7
2	PMe ₃ ^b	0	11	dcy pt	33
3	P ^t Bu ₃ ^b	0	12	dcy pf	25
4	PCp ₃ ^b	0	13	Ruphos ^b	5
5	PCy ₃ ^b	0	14	Xantphos	trace
6	dppe	23	15	rac-BINAP	34
7	dppp	12	16	ICy·HBF ₄ ^c	trace
8	dcy pe	93	17	IPr·HCl ^c	0
9	dcy pp	46(49 ^{c,d})	18	SIMes·HCl ^c	0



Reaction conditions: **25a** (0.20 mmol), Bu₃SnSiMe₃ (0.26 mmol), Ni(cod)₂ (10 mol %), ligand (10 mol%), CsF (0.2 mmol), Toluene (1.0 mL) at 90 °C, 8 h. ^a GC yields using decane as internal standard. ^b Ligand 20 mol %. ^c+NaO^tBu (20 mol%).

Table 2.1. Screening of supporting ligands

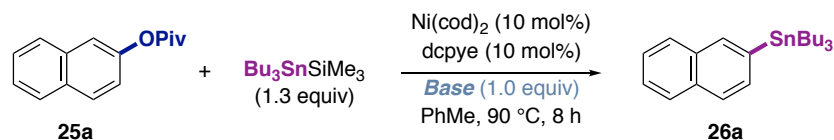
As judged by the knowledge acquired in the field, electron-rich, bulky phosphines or NHC ligands are typically needed to effect C–O bond-cleavage. This could be due to an increase of electron-density at nickel that may facilitate C–O scission, while the steric bulk exerted by these ligands might speed up reductive elimination. As evident from the results compiled in Table 2.1, the nature of the ligand played a crucial role on the targeted stannylation event. Specifically, we found that stannylation was particularly effective when dcype was used as ligand (entry 8). The use of other bidentate phosphine ligands bearing different bite angle and electronic properties led to lower yields (entries 6-7, 9-15), whereas some classical monodentate NHC and phosphine ligands gave no desired product (entries 1-5, 17-18).

Entry	[Ni]	Conv. (%) of 25a	Yield of 26a (%) ^a
1	Ni(cod)₂	99	96(69^b)
2	NiCl ₂	10	trace
3	Ni(acac) ₂	33	23
4	NiCl ₂ (dppf)	31	27
5	NiCl ₂ (dppe)	50	36
6	NiCl ₂ (dcype)	41	28
7	NiCl ₂ (PMe ₃) ₂	54	41
8	NiCl ₂ (PCy ₃) ₂	62	54
9	NiCl ₂ •glyme	19	13

Reaction conditions: **25a** (0.2 mmol), Bu₃SnSiMe₃ (0.26 mmol), Ni catalyst (0.02 mmol), dcype (0.02 mmol), CsF (0.2 mmol), toluene (1 mL). ^a Determined by GC analysis using decane as internal standard. ^b Using Ni(cod)₂ (5 mol %), dcype (5 mol %).

Table 2.2. Screening of Ni source utilized

With dcype as the optimal ligand, we examined the effect of Ni sources (Table 2.2). The reaction worked better with Ni(cod)₂ instead of Ni(II) precatalysts. Although the Ni(II) precatalysts can be reduced to the active Ni(0) species by double transmetalation with Bu₃SnSiMe₃, these results likely indicate the non-innocent character of cod as an ancillary ligand, stabilizing the propagating Ni(0) species within the catalytic cycle while preventing decomposition pathways.⁶³



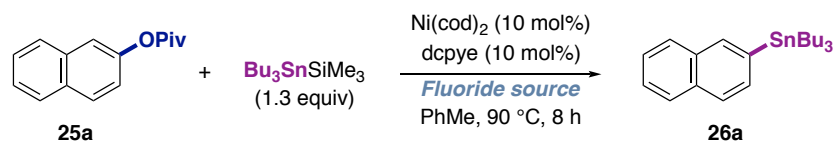
Entry	Base	Conv. (%) of 25a	Yield of 26a (%) ^a
1	KO ^t Bu	86	0
2	K ₃ PO ₄	21	0
3	KHMDS	79	19
4	KHF ₂	28	17
5	PhONa	65	46
6	NaOMe	73	0
7	KOMe	11	trace
8	LiOMe	37	15
9	PhCO ₂ Na	33	34
10	HCO ₂ Na	31	28
11	NaOAc	40	21
12	Na ₂ CO ₃	36	23
13	CsF	100	92
14	Cs ₂ CO ₃	82	61
15	CsHCO ₃	26	16
16	CsOPiv	15	trace
17	CsOAc	67	55

Reaction conditions: **25a** (0.2 mmol), Bu₃SnSiMe₃ (0.26 mmol), Ni(cod)₂ (0.02 mmol), dcype (0.02 mmol), base (0.2 mmol), toluene (1 mL). ^a Determined by GC analysis using decane as internal standard.

Table 2.3. Screening of bases

In line with our group's knowledge on Si–B interelement bonds,⁵¹ the use of a base was expected to have a profound impact for delivering the stannyl motif. As shown in Table 2.3, this turned out to be the case, with CsF providing the best yields with full conversion to products (Table 2.3, entry 13). If strong bases such as KO^tBu and KHMDS were employed, we found considerable amounts of naphthalene was detected. This is probably due to hydride generation from decomposition of the ligand via C–P bond cleavage.⁵⁸ With these results in hand, we questioned whether the escorting counteranion could also have an effect on the formation of **26a**. As shown in entries 14-17, it is evident that a significant erosion in yield was found for anions other than fluorides. This is probably due to the formation of a rather strong Si–F bond that brings the reaction forward on thermodynamic grounds. In addition, the role of Cs can be explained by its greater solubility in aprotic solvents when compared to other cations on the fluoride series (Table 2.4), as well as for the formation of a strong Cs–O bond that can facilitate Sn–Si cleavage. The cesium effect can also be attributed to its large cationic radius, low charge density and large polarizability, thus making the cesium ion the one with the lowest degree of solvation and ion-pairing as compared to the ions of analogous alkali metal salts.⁵⁹

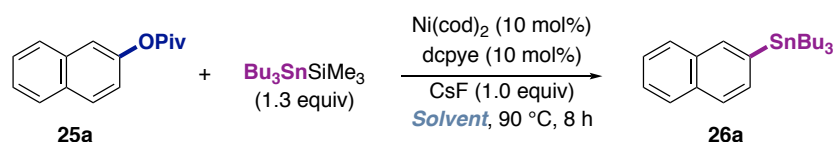
Ni-Catalyzed Stannylation of Aryl Ester via C-O Bond Cleavage



Entry	Fluoride source	Conv. (%) of 25a	Yield of 26a (%) ^a
1	CuF ₂	49	34
2	LiF	34	23
3	NaF	22	15
4	KF	14	0
5	CsF	98	94
6	FeF ₂	16	7
7	FeF ₃	11	trace
8	AgF	9	trace
9	AgF ₂	12	0
10	TiF ₄	8	0
11	ZrF ₄	7	trace
12	TBAF	37	29

Reaction conditions: 25a (0.2 mmol), Bu₃SnSiMe₃ (0.26 mmol), Ni(cod)₂ (0.02 mmol), dcype (0.02 mmol), fluoride source (0.2 mmol), toluene (1 mL). ^a Determined by GC analysis using decane as internal standard.

Table 2.4. Effect of fluoride source utilized



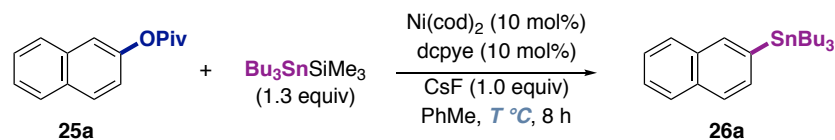
Entry	Solvent	Conv. (%) of 25a	Yield of 26a (%) ^a
1	Toluene	97	90
2	Anisole	83	75
3	<i>o</i> -xylene	77	64
4	THF	39	32
5	Dioxane	62	54
6	Cyclohexane	18	8
7	<i>n</i> -hexane	11	6
8	DMF	25	12

Reaction conditions: 25a (0.2 mmol), Bu₃SnSiMe₃ (0.26 mmol), Ni(cod)₂ (0.02 mmol), dcype (0.02 mmol), fluoride additive (0.2 mmol), solvent (1 mL). ^a Determined by GC using decane as internal standard.

Table 2.5. Screening of solvents

As shown in Table 2.5, the solvent also had an influence on productive stannylation. In particular, the best results were accomplished with benzene-based non-polar solvents (entries

1-3), with toluene giving the highest yield. Notably, moderate yields were observed in the presence of coordinating ethereal solvents (entries 4-5), which might be able to compete with binding at the nickel(II) center after oxidative addition. Likewise, a significant erosion in yield was observed with non-coordinating or polar aprotic solvents (entries 6-8).

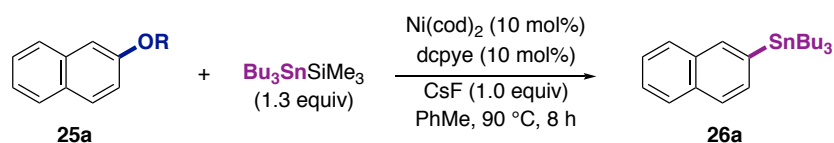


Entry	T (°C)	Conv. (%) of 25a	Yield of 26a (%) ^a
1	rt	6	trace
2	80	48	43
3	90	97	92
4	100	98	82
5	110	100	78
6	120	100	76

Reaction conditions: **25a** (0.2 mmol), Bu₃SnSiMe₃ (0.26 mmol), Ni(cod)₂ (0.02 mmol), dcype (0.02 mmol), CsF (0.2 mmol), toluene (1 mL). ^aGC yields using decane as internal standard.

Table 2.6. Effect of temperatures

Having established a Ni(cod)₂/dcype regime as the most promising results, we next evaluated the effect of the temperature on the C–Sn bond-forming reaction (Table 2.6). The best conditions were found when conducting the stannylation event at 90 °C, obtaining **26a** in 92% GC yield. At higher temperatures, significant amounts of side-products **27** or **28** were observed (entries 4-6). The formation of **28** is likely due to competitive C_{acyl}–O bond cleavage. Unfortunately, the reaction does not work at room temperature (entry 1), as the oxidative addition of **25a** to Ni(0) might require an input of energy.

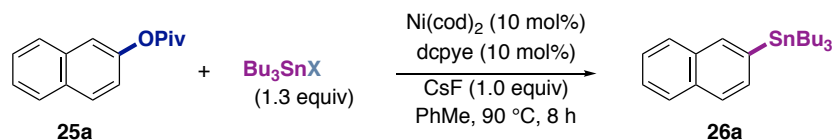


Entry	OR	Conv. (%) of 25a	Yield of 28 (%) ^a	Yield of 26a (%) ^a
1	OPiv	100	0	92
2	OAc	34	22	trace
3	OCOMs	57	14	46
4	OCOMe ₂	62	10	50
5	OBn	8	trace	0
6	OMe	15	9	0
7	OH	4	—	0

Reaction conditions: C–O electrophile (0.2 mmol), Bu₃SnSiMe₃ (0.26 mmol), Ni(cod)₂ (0.02 mmol), dcype (0.02 mmol), CsF (0.2 mmol), toluene (1 mL). ^aDetermined by GC analysis using decane as internal standard.

Table 2.7. Effect of the nature of C–O electrophiles

Ni-Catalyzed Stannylation of Aryl Ester via C–O Bond Cleavage

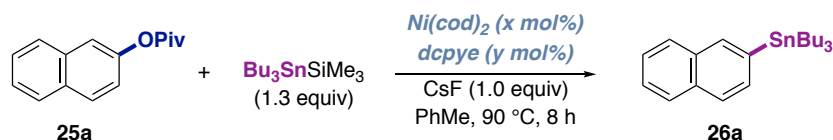


Entry	X	Conv. (%) of 25a	Yield of 26a (%) ^a
1	SiMe₃	100	91
2	SiEt ₃	56	31
3	Si ^{<i>i</i>} Pr ₃	17	0
4	SiBuMe ₂	11	trace
5	SiPh ₂ Me	45	35
6	SiPh ₃	9	trace
7	SnBu ₃	12	0
8	OMe	8	0
9	Li	53	30

Reaction conditions: **25a** (0.2 mmol), organotin (0.26 mmol), Ni(cod)₂ (0.02 mmol), dcype (0.02 mmol), CsF (0.2 mmol), toluene (1 mL). ^aGC yields using decane as internal standard.

Table 2.8. Screening of organotin reagent

Other parameters such as the nature of the C–O electrophile or the stannyl interelement group were investigated. If less-sterically encumbered 2-naphthyl acetate was used as substrate, traces amounts of **26a** were observed (Table 2.7, entry 2). This is due to a competitive cleavage of the most accessible *sp*² acyl C–O bond. An otherwise identical outcome was observed for aryl mesylates or carbamates, obtaining 2-naphthol (**28**) as the main byproduct (Table 2.7, entries 3-4). Unfortunately, aryl methyl ethers or naphthol cannot be employed as C–O electrophiles, resulting in low conversion of the starting material (entries 5-7). Influence of the nucleophilic entity was further assessed by synthesizing a series of stannyl interelement compounds (Table 2.8). Among all reagents employed, it was evident that Bu₃SnSiMe₃ (**18a**) turned out to be the most efficient transmetallating reagent. No improvement was found when using more bulky or electronically-biased silyl groups (entries 2-6). In contrast to the Sn–Si bond, the cleavage of Sn–Sn or Sn–O bonds was found to be more difficult and no product was observed in these cases (entries 7-8). Alternatively, an air-sensitive Bu₃SnLi reagent could also be employed in moderate yields, but at the expense of using a non-bench stable nucleophile (entry 8).

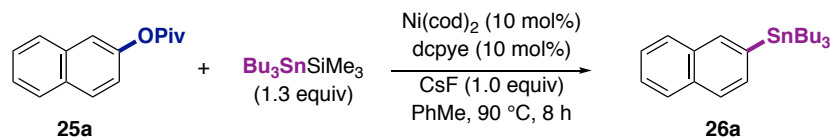


Entry	[Ni]:L (x:y)	Conv. (%) of 25a	Yield of 26a (%) ^a
1	5:5	79	68
2	5:10	65	43
3	10:10	100	93
4	10:20	68	55

Reaction conditions: **25a** (0.2 mmol), Bu₃SnSiMe₃ (0.26 mmol), Ni(cod)₂ (x mol%), dcype (y mol%), CsF (0.2 mmol), toluene (1 mL). ^a Determined by GC analysis using decane as internal standard.

Table 2.9. Effect of Ni(cod)₂/ligand ratio

We next assessed whether the ratio of Ni/ligand played an influence on both reactivity and chemoselectivity (Table 2.9). Specifically, the best results were found at 10% loading with a Ni/ligand ratio of 1:1. Indeed, lower yields were found either by reducing the catalyst loading to 5% or by increasing the amount of ligand. The latter results suggest the formation of rather stable 18-electron Ni(0)L₂ species, thus making the whole system kinetically less-accessible, thus lowering down the rate for the initial oxidative addition due to the difficulty for accessing the 14-electron Ni(0)L₁ species. Finally, blank experiments were carried out in order to ensure that all the reaction parameters were necessary for the stannylation to take place. Indeed, Table 2.10 tacitly shows that no product was formed in the absence of nickel catalyst, ligand and CsF (entries 2-5).



Entry	Bu ₃ SnSiMe ₃	Ni(cod) ₂	dcype	CsF	Yield of 26a (%) ^a
1	✓	✓	✓	✓	91
2	✓	×	✓	✓	0
3	✓	✓	×	✓	0
4	✓	×	×	✓	0
5	✓	✓	✓	×	trace

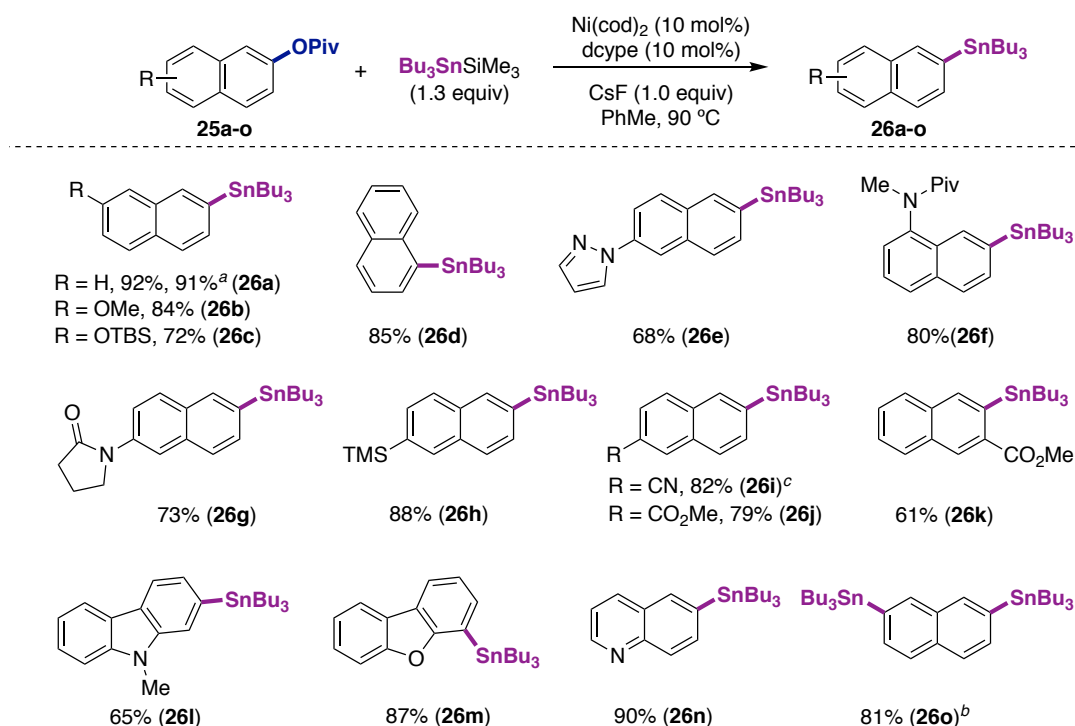
Reaction conditions: **25a** (0.2 mmol), Bu₃SnSiMe₃ (0.26 mmol), Ni(cod)₂ (0.02 mmol), dcype (0.02 mmol), CsF (0.2 mmol), Toluene (1 mL), 90 °C, 8 h. ^a Determined by GC analysis using decane as internal standard. X indicates that no reagent was added; ✓ indicates that the reagent was added.

Table 2.10. Blank experiments

2.4.2. Preparative substrate scope

2.4.2.1 Scope of naphthyl pivalates

With the best conditions in hand, the scope of our stannylation reaction was investigated by evaluating a wide range of π -extended aryl pivalates. As shown in Scheme 2.14, the electronic nature of the aromatic ring does not interfere with productive C–Sn bond formation. Our protocol turned out to be highly chemoselective, as amides (**26f** and **26g**), silyl ethers (**26c**), aryl silanes (**26h**), nitriles (**26i**), esters (**26j** and **26k**), carbazoles (**26l**), and benzofurans (**26m**) were all accommodated quite well with satisfactory yields. Notably, stannylation of sterically hindered **26k** bearing an ortho-substituent – typically a problematic substitution pattern in multiple C–O bond-functionalization techniques⁶⁰ – was achieved with a slightly lower yield. Generally, the presence of nitrogen-containing heterocycles is problematic in C–O functionalization due to competitive binding to the nickel center, leading to low catalytic turnovers. Fortunately, this was not the case, and **26e** and **26n** were both prepared in good yields following our optimized protocol. In addition, the stannylation of **25a** could be easily scaled up to 5 mmol without significant erosion in yield. Likewise, a double stannylation was within reach in high yields (**26o**), indicating the robustness and potential applicability to prepare multiple organometallic reagents via C–O bond-functionalization.

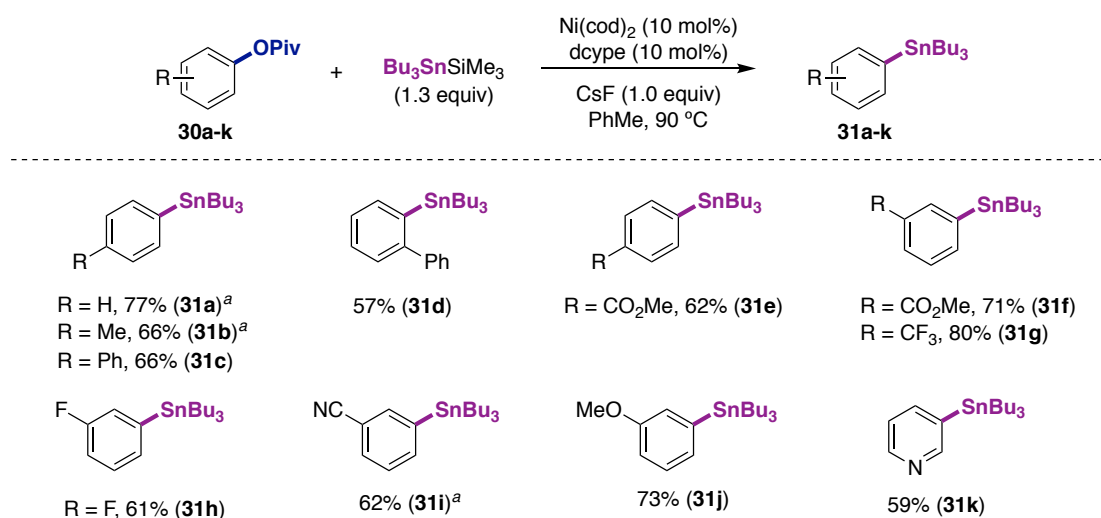


Reaction conditions: As Table 2.10, entry 1; yield of isolated product, average of at least two independent runs. ^a **25a** (5.0 mmol). ^b $\text{Bu}_3\text{SnSiMe}_3$ (2.3 equiv). ^c 6 h.

Scheme 2.14. Scope of π -extended aryl pivalates

2.4.2.2. Scope of phenyl pivalates

Encouraged by the wide functional group tolerance observed with naphthyl pivalates, we next wondered whether our protocol could be extended to non-activated phenyl pivalates, as these are typically less reactive than their π -extended congeners.^{26-29, 61} As shown in Scheme 2.15, substrates possessing either electron-withdrawing or electron-donating groups at para, meta or ortho position all afforded the targeted stannylated products in good yields (**31a** to **31k**). Likewise, the presence of esters (**31e** and **31f**), trifluoromethyl (**31g**), nitriles (**31i**) or even unbiased pyridyl backbone (**31k**) could equally be tolerated. Surprisingly, a fluoride-containing substrate (**31h**) could also undergo the C–Sn bond formation at the C–O site. This is somewhat surprising if we take into consideration the ease for promoting an oxidative addition into the sp^2 C–F bond by using Ni(0)(PCy₃)₂ species in related borylation events.⁶²



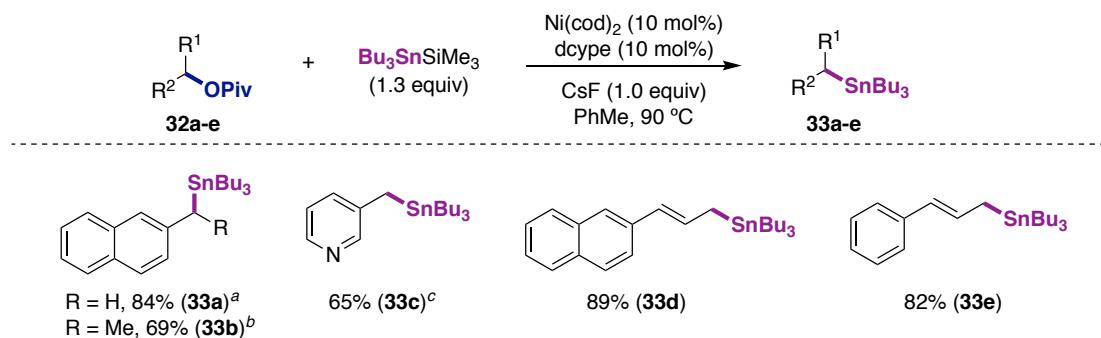
Reaction conditions: As Table 2.10, entry 1; yield of isolated product, average of at least two independent runs. ^a $\text{Bu}_3\text{SnSiMe}_3$ (2.0 equiv).

Scheme 2.15. Scope of none π -extended aryl pivalates

2.4.2.3. Scope of benzyl and allyl pivalates

Next, we decided to test whether our stannylation protocol could be implemented with benzylic or allylic pivalates (Scheme 2.16). Indeed, we found that not only primary (**32a** and **32c**), but also secondary benzyl pivalates (**33b**) with pendant β -hydrogen atoms and nitrogen donors could be stannylated in high yields under our optimal conditions. Likewise, allyl pivalates (**32d** and **31e**) could also be used as substrates, obtaining the corresponding compounds with the double bond conjugated to the arene backbone.

Ni-Catalyzed Stannylation of Aryl Ester via C–O Bond Cleavage

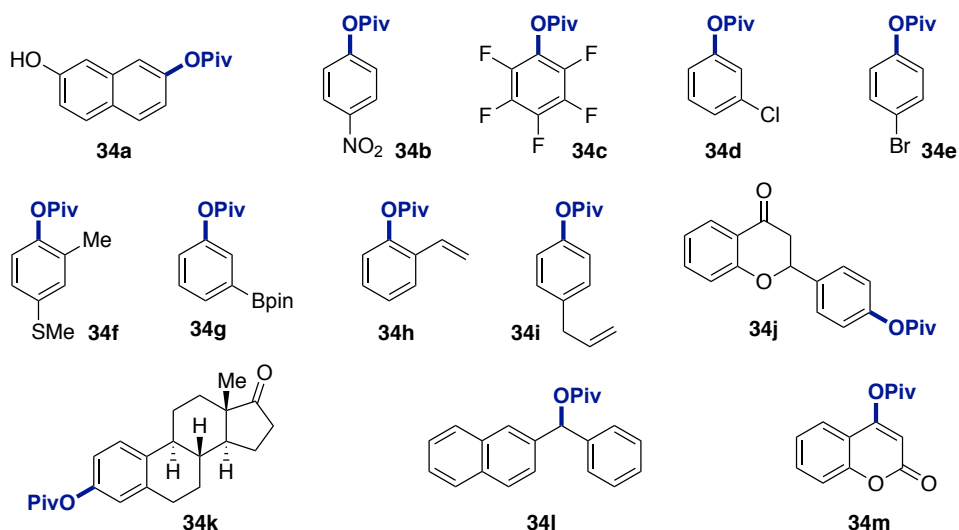


Reaction conditions: As Table 2.10, entry 1; yield of isolated product, average of at least two independent runs. ^a 6 h. ^b at 110 °C. ^c $\text{Bu}_3\text{SnSiMe}_3$ (2.0 equiv).

Scheme 2.16. Scope of benzyl and allyl pivalates

2.4.2.4. Unsuccessful substrates

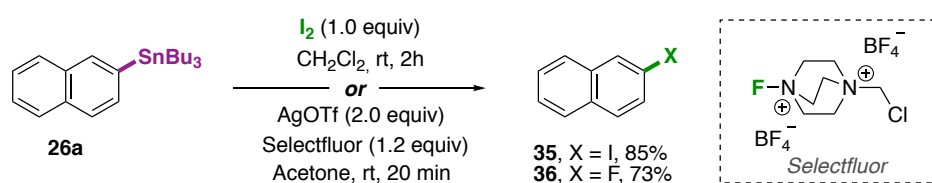
Although we demonstrated that the stannylation of aryl pivalates occurred with a wide substrate scope, a non-negligible number of examples failed to provide the targeted C–Sn bond. For instance, substrates bearing unprotected phenol (**34a**), nitro group (**34b**), and a double bond (**34h** and **34i**) resulted in no conversion. Strikingly, no conversion was observed in the presence of aryl chloride and aryl bromide. Unfortunately, we do not have a rational explanation, as a priori one might argue that a stannylation event should occur more rapidly at the C–halide bond due to their much higher tendency to promote oxidative addition to Ni(0) centers. Sterically crowded benzylic pivalate (**34l**) was met with little success (<5% yield), whereas particularly electron-poor pivalate (**34c**) failed to provide the targeted product, even at higher temperature or higher loadings. In this particular case, the presence of multiple C–F bonds might result in the formation of rather stable oxidative addition species. The presence of C–S or other C–O bonds was equally incompatible, due to the strong binding to Ni centers in the former and competitive oxidative addition in the latter.⁶³ Unfortunately, **34j** and **34k** possessing enolizable aromatic or aliphatic ketones failed to provide even traces of the targeted products, probably due to the presence of acidic α -hydrogens (no product formation was even observed with >2 equivalents of base). Moreover, Bpin-substituted pivalate (**34g**) gave low yields of the organotin compound due to problems in the isolation of the final product.



Scheme 2.17. Unsuccessful substrates of aryl pivalates

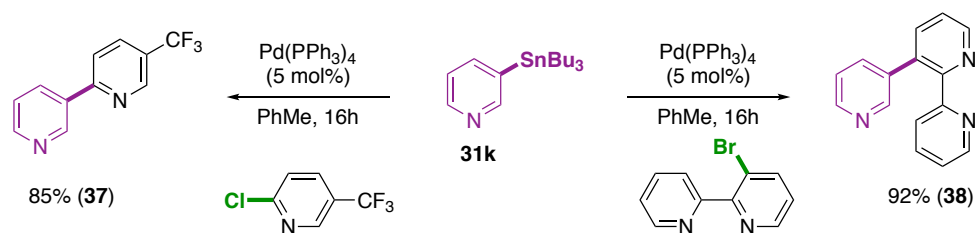
2.4.3. Synthetic applicability and orthogonal strategy

Putting our results into perspective, we conclude that our protocol provides a rapid entry for the formation of organotin reagents from readily available C–O electrophiles. In order to show the potential applicability of our method, we decided to show a range of transformations available that derive from C–Sn cleavage. Indeed, the polarized C–Sn bond can be easily transformed into the corresponding C–halide or C–C bonds.⁶⁴ Taking into consideration that aryl halides are typically used as conventional coupling partners in a myriad of transformations, we decided to show the viability for converting our organotin reagents into their corresponding aryl halide congeners. As shown in Scheme 2.18, these transformations could be easily executed by reacting **26a** with I₂ or Selectfluor,^{65,66} ending up in the corresponding halogenated compounds **35** and **36**. In a formal sense, this transformation can be visualized as a means to transform a C–O electrophile into the corresponding aryl halide. Likewise, Migita-Kosugi-Stille (MKS) cross-coupling reactions were within reach by means of Pd catalysis. In order to show the potential of these technologies, we decided to show the applicability of the method with challenging heteroaryl halides that typically fail in classical Suzuki-Miyaura or Negishi couplings where the basic nitrogen atom might interfere with binding at the metal center. As shown for **37** and **38**, the targeted C–C bond-formation occurred rather smoothly, even in the absence of base with a regular Pd(PPh₃)₄ catalyst, resulting in the formation of the bipyridine or tripyridine motifs in excellent yields.



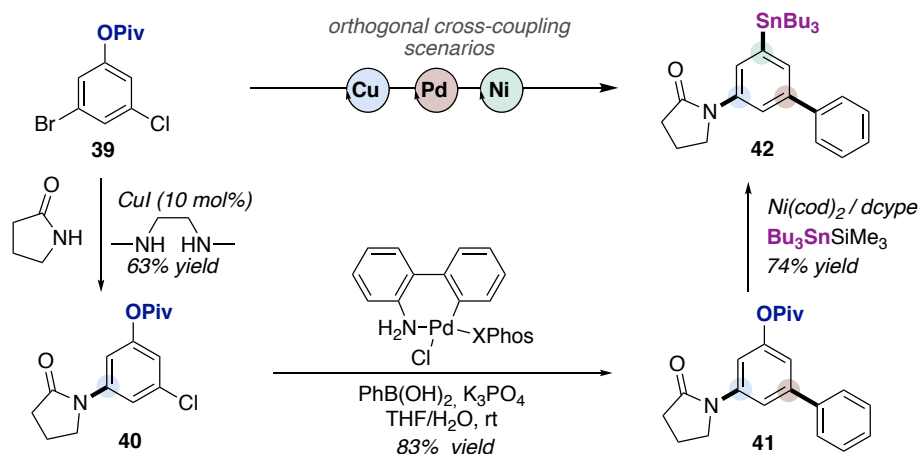
Scheme 2.18. Halogenation of 26a with I₂ and selectfluor

Ni-Catalyzed Stannylation of Aryl Ester via C-O Bond Cleavage



Scheme 2.19. Migita-Kosugi-Stille cross-coupling reactions of **31k** with azines

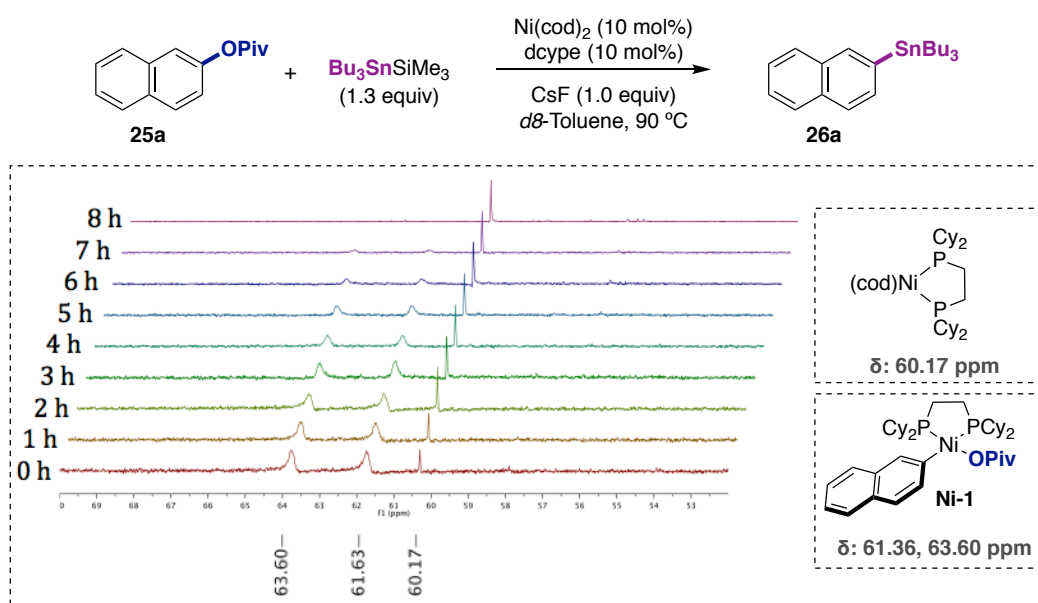
Recognizing that the functionalization of the C–O bonds is more difficult than the corresponding C–halide bonds, we wondered whether we could implement orthogonal strategies for C–C and C–heteroatom bond-formation with polyhalogenated arenes containing aryl ester motifs. As shown in Scheme 2.20, this turned out to be the case, and sequential cross-coupling reactions could be implemented by using Cu, Pd and Ni catalysts. First, a Cu-catalyzed C–N bond formation reaction rapidly occurred at the aryl bromide terminus to give compound **40** by using *N,N'*-dimethylethylenediamine as ligand. This was followed by a Pd-catalyzed Suzuki–Miyaura reaction with PhB(OH)₂ with a Pd(II)XPhos precatalyst to construct the biaryl motif (**41**) in high yields.^{67,68} Finally, the corresponding organotin reagent was within reach by exposing **41** under our optimized reaction conditions.



Scheme 2.20. Orthogonal cross-coupling reactions of compound **39**

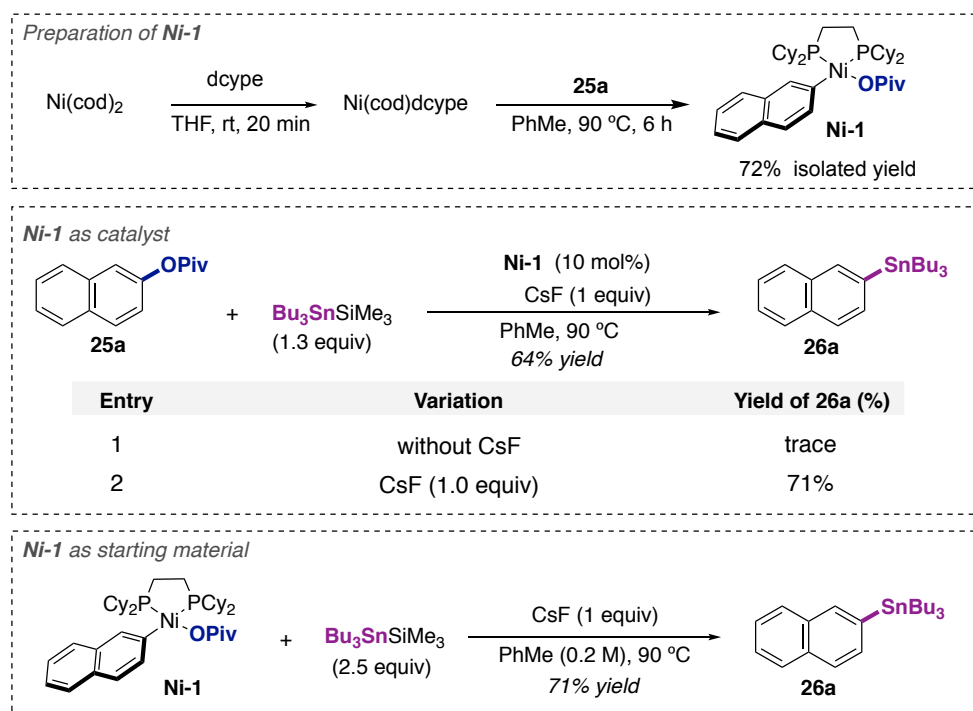
2.5. Mechanistic Considerations: Catalytic Cycle and Discussions

With the preparative results of our stannylation in hand, we next focused our attention to elucidate the mechanism of our protocol. In order to do so, we started by monitoring the stannylation reaction by ^{31}P NMR (Scheme 2.21). Interestingly, the signal of the plausible reaction intermediates could be detected, as two new downfield peaks (63.60 and 61.63 ppm) appeared alongside the signal of the Ni(cod)dcype (60.17 ppm).⁴¹ Such downfield peaks are consistent with the formation of an oxidative addition species with two phosphorus atoms in different chemical environments, as one might initially expect from a bidentate phosphine bound in a cis-fashion. After 8h, the two peaks disappeared indicating the full conversion of **25a** to **26a** with concomitant formation of the propagating Ni(cod)dcype species.



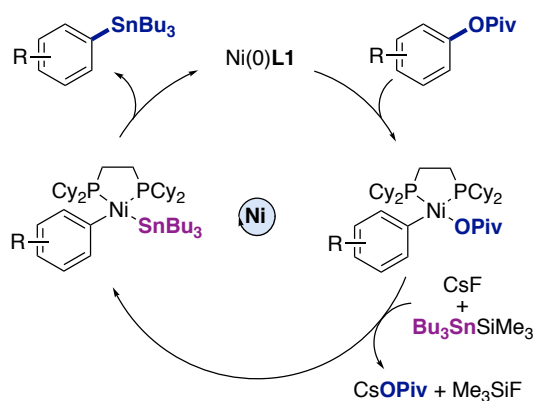
Scheme 2.21. ^{31}P NMR monitoring reaction of **25a**

To further elucidate the mechanism, we decided to isolate the putative oxidative addition species. In order to do so, we prepared **Ni-1** by exposing naphthyl pivalate **25a** to Ni(cod)dcype in PhMe at 90 °C. Under these conditions, we could isolate **Ni-1** in pure form and in high yield. As expected, ^{31}P NMR revealed an identical set of signals to that shown in the *in situ* monitoring experiment shown in Scheme 2.21. This is consistent with a Ni atom in a square-planar geometry surrounded by two phosphorus donor atoms in a cis-configuration with a $\kappa^1\text{-O-pivalate}$ ligand.



Scheme 2.22. Catalytic and stoichiometric experiments with Ni-1 oxidative complex

As expected, **Ni-1** was found to be catalytically competent as reaction intermediate, and **26a** was invariably formed in good yields regardless of whether **Ni-1** was used in a stoichiometric or catalytic manner. Notably, the reactions only provided trace of the desired product in the absence of CsF, indicating the critical role exerted by CsF for activating the Sn–Si interelement bond and facilitate the subsequent transmetalation between **Ni-1** and $\text{Bu}_3\text{SnSiMe}_3$.



Scheme 2.23. Plausible mechanism via Ni-1 intermediate

At present, we believe that the superior reactivity of dcype vs its monodentate analogue PCy_3 is attributed to the ease for oxidative addition with dcype when compared to PCy_3 , the more rigid coordination of bidentate ligands, the formation of stable long-lived entities with dcype, the low tendency for rapid ligand dissociation and avoiding unproductive disproportionation events.^{41,52} Although we were not able to observe the aryl-Ni(II)- SnBu_3 intermediate, the formation of Me_3SiF was confirmed by ^{19}F NMR and ^{29}Si NMR spectroscopy. Likewise, ^{113}Cs and

^1H NMR spectroscopy supported the formation of CsOPiv as byproduct. Based on the preliminary results presented above, at present we proposed a mechanistic rationale consisting of a canonical oxidative addition of the aryl pivalate to Ni(0)dcppe followed by transmetalation aided by CsF and a final C–Sn bond reductive elimination, thus delivering the targeted organotin reagent while recovering back the corresponding Ni(0)dcppe catalyst (Scheme 2.23).

2.6. Conclusions

This chapter summarizes our efforts towards the development of a Ni-catalyzed stannylation of aryl pivalates via C–O bond scission. The key to achieve this transformation was to find an efficient Ni/ligand catalyst system based on a suitable stannyl reagent. The mild reaction conditions utilized and the broad functional group tolerance makes these transformation an useful entry for the preparation of organotin reagents, and a complementary alternative to existing protocols based on organometallic reagents. In contrast to the known reluctance of non π -extended C–O electrophiles to react with Ni catalyst in other C–C or C–heteroatom bond-formations not involving organometallic reagents, our protocol can be applied to these motifs without much problems under relatively mild conditions. In addition, this technique can be extended to both benzyl and allyl pivalates, even in the presence of nitrogen-containing heterocycles containing donor sites that might cause competitive binding at the Ni center. These findings have been applied in the context of Migita-Kosugi-Stille couplings as well as in the design of orthogonal strategies in the presence of polyhalogenated aryl esters. The study of the mechanism indicates that the reaction occurs via a canonical oxidative addition species that can be isolated and characterized in pure form, followed by a transmetalation aided by base and a final reductive elimination to deliver the targeted organotin reagent.

2.7. References

1. Diederich, F.; Stang, P. J. *Metal-Catalyzed Cross-Coupling Reactions*; Wiley-VCH: New York, **1998**. (b) de Meijere, A.; Braš, S.; Oestreich, M. *Metal Catalyzed Cross-Coupling Reactions and More*; Wiley, **2013**; Vol. 3.
2. King, A. O.; Yasuda, N. *Palladium-Catalyzed Cross-Coupling Reactions in the Synthesis of Pharmaceuticals*. In *Organometallics in Process Chemistry*; Larsen, R. D., Ed.; Springer: Berlin, Heidelberg, **2004**; pp 205.
3. Lightowler, S.; Hird, M. *Palladium-Catalyzed Cross-Coupling Reactions in the Synthesis of Novel Aromatic Polymers*. *Chem. Mater.* **2004**, *16*, 3963.
4. Baker, M. A.; Tsai, C.-H.; Noonan, K. J. T. *Diversifying Cross-Coupling Strategies, Catalysts and Monomers for the Controlled Synthesis of Conjugated Polymers*. *Chem. - Eur. J.* **2018**, *24*, 13078.
5. (a) Diederich F.; Stang, P. J. *Metal-Catalyzed Cross-Coupling Reactions*. Wiley-VCH, New York, **1998**; (b) Nicolaou, K. C.; Bulger, P. G.; Sarlah, D. *Palladium-Catalyzed Cross-Coupling Reactions In Total Synthesis*. *Angew. Chem. Int. Ed.* **2005**, *44*, 4442.
6. (a) Wenkert, E.; Michelotti, E. L.; Swindell, C. S. *Nickel-Induced Conversion Of Carbon-Oxygen Into Carbon-Carbon Bonds. One-Step Transformations Of Enol Ethers Into Olefins And Aryl Ethers Into Biaryls*. *J. Am. Chem. Soc.* **1979**, *101*, 2246; (b) Wenkert, E.; Michelotti, E. L.; Swindell, C. S.; Tingoli, M. *Transformation Of Carbon-Oxygen Into Carbon-Carbon Bonds Mediated By Low-Valent Nickel Species*. *J. Org. Chem.* **1984**, *49*, 4894.
7. Dankwardt, J. W. *Nickel-Catalyzed Cross-Coupling Of Aryl Grignard Reagents With Aromatic Alkyl Ethers: An Efficient Synthesis Of Unsymmetrical Biaryls*. *Angew. Chem. Int. Ed.* **2004**, *43*, 2428.
8. *Selected Review on C-O bond cleavage*: (a) Tobisu, M.; Chatani, N. *Nickel-Catalyzed Cross-Coupling Reactions of Unreactive Phenolic Electrophiles via C-O Bond Activation*. *Top. Curr. Chem.* **2016**, *374*, 41. (b) Tollefson, E. J.; Hanna, L. E.; Jarvo, E. R. *Stereospecific Nickel-Catalyzed Cross-Coupling Reactions Of Benzylic Ethers And Esters*. *Acc. Chem. Res.* **2015**, *48*, 2344. (c) Cornella, J.; Zarate, C.; Martin, R. *Metal-Catalyzed Activation Of Ethers Via C-O Bond Cleavage: A New Strategy For Molecular Diversity*. *Chem. Soc. Rev.* **2014**, *43*, 8081. (d) Su, B.; Cao, Z. - C.; Shi, Z. -J. *Exploration Of Earth-Abundant Transition Metals (Fe, Co, And Ni) As Catalysts In Unreactive Chemical Bond Activations*. *Acc. Chem. Res.* **2015**, *48*, 886. (e) Yamaguchi, J.; Muto, K.; Itami, K. *Recent Progress In Nickel-Catalyzed Biaryl Coupling*. *Eur. J. Org. Chem.* **2013**, *19*. (f) Mesganaw, T.; Garg, N. K. *Ni- and Fe-Catalyzed Cross-Coupling Reactions of Phenol Derivatives*. *Org. Process Res. Dev.* **2013**, *17*, 29. (g) Rosen, B. M.; Quasdorf, K. W.; Wilson, D. A.; Zhang, N.; Resmerita, A. -M.; Garg, N. K.; Percec, V. *Nickel-Catalyzed Cross-Couplings Involving Carbon-Oxygen Bonds*. *Chem. Rev.* **2011**, *111*, 1346.
9. (a) Tobisu, M.; Chatani, N. *Metal-Catalyzed Aromatic C-O Bond Activation/Transformation*. In: Dixneuf P.; Soulé JF. (eds) *Organometallics for Green Catalysis. Topics in Organometallic Chemistry*, **2018**, vol 63. Springer, Cham. (b) Zarate, C.; van Gemmeren, M.; Somerville, R. J.; Martin, R. *Phenol Derivatives: Modern Electrophiles in Cross-Coupling*. In *Advances in Organometallic Chemistry*, vol. 66, pp. 143; Pérez, P. J. Ed.; Elsevier: Cambridge, **2016**.
10. (a) Tyman, J. H. P. *Synthetic and natural phenols*. Elsevier, Amsterdam, **1996**. (b) Rappoport, Z. *The Chemistry Of Phenols*. Wiley, Chichester, **2003**. (c) Sun, Z.; Fridrich B.; de Santi, A; Elangovan, S.; Barta, K.; *Bright Side Of Lignin Depolymerization: Toward New Platform Chemicals*. *Chem. Rev.* **2018**, *118*, 614.
11. Tasker S. Z.; Standley E. A.; Jamison T. F. *Recent Advances In Homogeneous Nickel Catalysis*. *Nature* **2014**, *509*, 299.
12. Diederich, F., Meijere, A., Eds. *Metal-Catalyzed Cross-Coupling Reactions*; Wiley-VCH: Weinheim, **2004**.
13. (a) Luo, Y.-R. *Handbook Of Bond Dissociation Energies In Organic Compound*. CRC Press: FL, **2007**. (b) Grushin, V. V.; Alper, H.; Mrrai, S. *Activation of Unreactive Bond and Organic Synthesis* Springer: Berlin, **1999**, 203.

14. For computational studies on the C–O cleavage of aryl carboxylates: (a) Theresa Sperger, Italo A. Sanhueza, Indrek Kalvet, and Franziska Schoenebeck. Computational Studies of Synthetically Relevant Homogeneous Organometallic Catalysis Involving Ni, Pd, Ir, and Rh: An Overview of Commonly Employed DFT Methods and Mechanistic Insights. *Chem. Rev.* **2015**, *115*, 9532. (b) Xu, H.; Muto, K.; Yamaguchi, J.; Zhao, C.; Itami, K.; Musaev, D. G. Key Mechanistic Features of Ni-Catalyzed C–H/C–O Biaryl Coupling of Azoles and Naphthalen-2-yl Pivalates. *J. Am. Chem. Soc.* **2014**, *136*, 14834. (c) Lu, Q.; Yu, H.; Fu, Y. Mechanistic Study of Chemoselectivity in Ni-Catalyzed Coupling Reactions between Azoles and Aryl Carboxylates. *J. Am. Chem. Soc.* **2014**, *136*, 8252.
15. Li, Z.; Zhang S.-L.; Fu, Y.; Guo, Q.-X.; Liu, L. Mechanism of Ni-Catalyzed Selective C–O Bond Activation in Cross-Coupling of Aryl Esters. *J. Am. Chem. Soc.* **2009**, *131*, 815.
16. Bauer, D. J.; Krueger, C. Bonding Of Aromatic Hydrocarbons To Nickel(0). Structure Of Bis(Tricyclohexylphosphine)(1,2-Eta.2-Anthracene)Nickel(0)-Toluene. *Inorg. Chem.* **1977**, *16*, 884.
17. Tamaru, Y. *Modern Organonickel Chemistry*. Wiley-VCH Verlag GmbH & Co. KGaA, **2005**.
18. Ananikov, V. P. Nickel: The ‘Spirited Horse’ of Transition Metal Catalysis. *ACS Catal.* **2015**, *5*, 1964.
19. Hazari, N.; Melvin, P. R.; Beromi, M. M. Well-defined Nickel and Palladium Precatalysts for Cross-Coupling. *Nat. Rev. Chem.* **2017**, *1*, 0025.
20. Ahrens, T.; Kohlmann, J.; Ahrens, M.; Braun, T. Functionalization of Fluorinated Molecules by Transition-Metal-Mediated C–F Bond Activation To Access Fluorinated Building Blocks. *Chem. Rev.* **2015**, *115*, 931.
21. Dander, J. E.; Garg, N. K. Breaking Amides using Nickel Catalysis. *ACS Catal.* **2017**, *7*, 1413.
22. Hu, X. Nickel-Catalyzed Cross Coupling of Non-Activated Alkyl Halides: A Mechanistic Perspective. *Chem. Sci.* **2011**, *2*, 1867.
23. (a) Ge, S. & Hartwig, J. F. Highly Reactive, Single-Component Nickel Catalyst Precursor for Suzuki–Miyaura Cross-Coupling of Heteroaryl Boronic Acids with Heteroaryl Halides. *Angew. Chem. Int. Ed.* **2012**, *51*, 12837. (b) Han, F.-S. Transition-metal-catalyzed Suzuki–Miyaura Cross-Coupling Reactions: a Remarkable Advance from Palladium to Nickel Catalysts. *Chem. Soc. Rev.* **2013**, *42*, 5270.
24. Li, B.-J.; Xu, L.; Wu, Z.-H.; Guan, B.-T.; Sun, C.-L.; Wang, B.-Q.; Shi, Z.-J. Cross-Coupling of Alkenyl/Aryl Carboxylates with Grignard Reagent via Fe-Catalyzed C–O Bond Activation. *J. Am. Chem. Soc.* **2009**, *131*, 14656.
25. Gärtner, D.; Stein A. L.; Grupe, S.; Arp, J.; von Wangelin, J. A Iron-Catalyzed Cross-Coupling of Alkenyl Acetates. *Angew. Chem. Int. Ed.* **2015**, *54*, 10545.
26. Li, B.-J.; Li, Y.-Z.; Lu, X.-Y.; Liu, J.; Guan, B.-T.; Shi, Z.-J. Cross-Coupling Of Aryl/Alkenyl Pivalates With Organozinc Reagents Through Nickel-Catalyzed C–O Bond Activation Under Mild Reaction Conditions. *Angew. Chem. Int. Ed.* **2008**, *47*, 10124.
27. Wisniewska, H. M.; Swift, E. C.; Jarvo, E. R. Functional Group Tolerant, Nickel-Catalyzed Cross-Coupling Reaction for Enantioselective Construction of Tertiary Methyl-Bearing Stereocenters. *J. Am. Chem. Soc.* **2013**, *135*, 9083.
28. Tobisu, M.; Shimasaki, T.; Chatani, N. Nickel-Catalyzed Cross-Coupling of Aryl Methyl Ethers with Aryl Boronic Esters. *Angew. Chem., Int. Ed.* **2008**, *47*, 4866.
29. Zhou, Q.; Srinivas, H. D.; Dasgupta, S.; Watson, M. P. Nickel-Catalyzed Cross-Couplings of Benzylic Pivalates with Arylboroxines: Stereospecific Formation of Diarylalkanes and Triarylmethanes. *J. Am. Chem. Soc.* **2013**, *135*, 3307.
30. Liu, X.; Jia, J.; Rueping M. Nickel-Catalyzed C–O Bond-Cleaving Alkylation of Esters: Direct Replacement of the Ester Moiety by Functionalized Alkyl Chains. *ACS Catal.* **2017**, *7*, 4491.
31. Guan, B.-T.; Wang, Y.; Li, B.-J.; Yu, D.-G.; Shi, Z.-J. Biaryl Construction via Ni-Catalyzed C–O Activation Of Phenolic Carboxylates. *J. Am. Chem. Soc.* **2008**, *130*, 14468.
32. Quasdorf, K. W.; Tian, X.; Garg N. K. Cross-Coupling Reactions of Aryl Pivalates with Boronic Acids. *J. Am. Chem. Soc.* **2008**, *130*, 14422.
33. Molander, G. A.; Beaumard, F. Nickel-Catalyzed C–O Activation of Phenol Derivatives with Potassium Heteroaryltrifluoroborates. *Org. Lett.* **2010**, *12*, 4022.

34. Malineni, J.; Jezorek, R. L.; Zhang, N.; Percec, V. Ni^{II}Cl(1-Naphthyl)(PCy₃)₂, An Air-Stable σ -Ni^{II} Precatalyst for Quantitative Cross-Coupling of Aryl C-O Electrophiles with Aryl Neopentylglycolboronates. *Synthesis* **2016**, *48*, A-H.
35. Guo, L.; Hsiao, C. C.; Yue, H.; Liu, X.; Rueping M. Nickel-Catalyzed C_{sp2}-C_{sp3} Cross-Coupling via C-O Bond Activation *ACS Catal.* **2016**, *6*, 4438.
36. Muto, K.; Yamaguchi, J.; Itami, K. Nickel-Catalyzed C-H/C-O Coupling of Azoles with Phenol Derivatives. *J. Am. Chem. Soc.* **2012**, *134*, 169.
37. Muto, K.; Yamaguchi, J.; Lei, A.; Itami, K. Isolation, Structure, and Reactivity of an Arylnickel(II) Pivalate Complex in Catalytic C-H/C-O Biaryl Coupling. *J. Am. Chem. Soc.* **2013**, *135*, 16384.
38. (a) Hong, X.; Liang, Y.; Houk, K. N. Mechanisms and Origins of Switchable Chemoselectivity of Ni-Catalyzed C(aryl)-O and C(acyl)-O Activation of Aryl Esters with Phosphine Ligands. *J. Am. Chem. Soc.* **2014**, *136*, 2017. (b) H. Xu, K. Muto, J. Yamaguchi, C. Zhao, K. Itami, D. G. Musaev, Key Mechanistic Features of Ni-catalyzed C-H/C-O Biaryl Coupling of Azoles and Naphthalen-2-yl Pivalates. *J. Am. Chem. Soc.* **2014**, *136*, 14834.
39. Ehle, A. R.; Zhou, Q.; Watson, M. P. Nickel(0)-Catalyzed Heck Cross-Coupling via Activation of Aryl C-OPiv Bonds. *Org. Lett.* **2012**, *14*, 1202.
40. For Watson-type Heck couplings with benzylic and allylic ethers, see: (a) Harris, M. R.; Konev, M. O.; Jarvo, E. R. Enantiospecific Intramolecular Heck Reactions of Secondary Benzylic Ethers. *J. Am. Chem. Soc.* **2014**, *136*, 7825. (b) Matsubara, R.; Jamison, T. F. Nickel-catalyzed Allylic Substitution of Simple Alkenes. *J. Am. Chem. Soc.* **2010**, *132*, 6880.
41. (a) Takise, R.; Muto, K.; Yamaguchi, J.; Itami, K. Nickel-Catalyzed α -Arylation of Ketones with Phenol Derivatives. *Angew. Chem. Int. Ed.* **2014**, *53*, 6791. (b) Koch, E.; Takise, R.; Studer, A.; Yamaguchi, J.; Itami, K. Ni-Catalyzed α -Arylation of Esters and Amides with Phenol Derivatives. *Chem. Commun.* **2015**, *51*, 855.
42. Cornella, J.; Jackson, E. P.; Martin, R. Nickel-Catalyzed Enantioselective C-C bond Formation Through C(sp²)-O Cleavage In Aryl Esters. *Angew. Chem. Int. Ed.* **2015**, *54*, 4075.
43. Takise, R.; Itami, K.; Yamaguchi, J. Cyanation of Phenol Derivatives with Aminoacetonitriles by Nickel Catalysis. *Org. Lett.* **2016**, *18*, 4428.
44. Cao, Z.-C.; Luo, Q.-Y.; Shi, Z.-J. Practical Cross-Coupling between O-Based Electrophiles and Aryl Bromides via Ni Catalysis. *Org. Lett.* **2016**, *18*, 5978.
45. Tortajada, A.; Juliá-Hernández, F.; Börjesson, M.; Moragas, T.; Martin, R. Transition Metal-Catalyzed Carboxylation Reactions with Carbon Dioxide. *Angew. Chem. Int. Ed.* **2018**, *49*, 15948.
46. Correa, A.; León, T.; Martin, R. Ni-Catalyzed Carboxylation of C(sp²)- and C(sp³)-O Bonds with CO₂. *J. Am. Chem. Soc.* **2014**, *136*, 1062.
47. Correa, A.; Martin, R. Ni-Catalyzed Direct Reductive Amidation via C-O Bond Cleavage. *J. Am. Chem. Soc.* **2014**, *136*, 7253.
48. For selected reviews: (a) Surry, D. S.; Buchwald, S. L. Biaryl Phosphane Ligands In Palladium-Catalyzed Amination. *Angew. Chem. Int. Ed.* **2008**, *47*, 6338. (b) Hartwig, J. F. Evolution Of A Fourth Generation Catalyst For The Amination And Thioetherification Of Aryl Halides. *Acc. Chem. Res.* **2008**, *41*, 1534.
49. Shimasaki, T.; Tobisu, M.; Chatani, N. Nickel-Catalyzed Amination of Aryl Pivalates by the Cleavage of Aryl C-O Bonds. *Angew. Chem. Int. Ed.* **2010**, *49*, 2929.
50. Yue, H.; Guo, L.; Liu, X.; Rueping M. Nickel-Catalyzed Synthesis of Primary Aryl and Heteroaryl Amines via C-O Bond Cleavage. *Org. Lett.* **2017**, *19*, 1788.
51. Zarate, C.; Martin, R. A Mild Ni/Cu- Catalyzed Silylation via C-O Cleavage. *J. Am. Chem. Soc.* **2014**, *136*, 2236.
52. Somerville, R.; Hale, L.; Gomez-Bengoia, E.; Bures, J.; Martin, R. Intermediacy of Ni-Ni Species in sp² C-O Bond Cleavage of Aryl Esters: Relevance in Catalytic C-Si Bond Formation. *J. Am. Chem. Soc.* **2018**, *140*, 8771.
53. Yang, J.; Chen, T.; Han, L.-B.; C-P Bond-Forming Reactions via C-O/P-H Cross-Coupling Catalyzed by Nickel. *J. Am. Chem. Soc.* **2015**, *137*, 1782.
54. Quin, L. D. A Guide to Organophosphorus Chemistry; Wiley Interscience: New York, **2000**. (b) New Aspects in Phosphorus Chemistry; Majoral, J.-P., Ed.; Springer: Berlin; Vol.s 1-5.

55. Yang, J.; Xiao, J.; Chen, T.; Han, L.-B. Nickel-Catalyzed Phosphorylation of Phenol Derivatives via C–O/P–H Cross-Coupling. *J. Org. Chem.* **2016**, *81*, 3911.
56. Martin-Montero, R. T. Krolkowski, Zárata, C.; Manzano, R.; Martin, R. Stereospecific Nickel-Catalyzed Borylation of Secondary Benzyl Pivalates. *Synlett* **2017**, *28*, 2604.
57. Wang, D.-Y.; Wang, C.; Uchiyama, M. Stannyll-Lithium: A Facile and Efficient Synthesis Facilitating Further Applications. *J. Am. Chem. Soc.* **2015**, *137*, 10488.
58. Sergeev, A. G.; Hartwig, J. F. Selective, Nickel-Catalyzed Hydrogenolysis of Aryl Ethers. *Science* **2011**, *332*, 439.
59. Data table taken from: (a) Lide, D. R., Handbook of Chemistry and Physics, 83. ed., CRC Press LLC **2002-2003**. (b) Cella, J. R.; Bacon, S. W. Preparation of Dialkyl Carbonates via the Phase-Transfer-Catalyzed Alkylation of Alkali Metal Carbonate and Bicarbonate Salts. *J. Org. Chem.* **1984**, *49*, 1122.
60. Guo, L.; Chatupheeraphat, A.; Rueping, M. Decarbonylative Silylation of Esters by Combined Nickel and Copper Catalysis for the Synthesis of Arylsilanes and Heteroarylsilanes. *Angew. Chem. Int. Ed.* **2016**, *55*, 11810.
61. For selected C–O cleavage protocols mainly limited to π -extended backbones: (a) Yu, D.-G.; Shi, Z.-J. Mutual Activation: Suzuki-Miyaura Coupling through Direct Cleavage of the sp^2 C–O Bond of Naphtholate. *Angew. Chem. Int. Ed.* **2011**, *50*, 7097. (b) Taylor, B. L.; Harris, M. R.; Jarvo, E. R. Synthesis of Enantioenriched Triarylmethanes by Stereospecific Cross-Coupling Reactions. *Angew. Chem. Int. Ed.* **2012**, *51*, 7790.
62. Liu, X.-W.; Zarate, C.; Martin, R. Base-Mediated Defluorosilylation of C(sp^2)–F and C(sp^3)–F Bonds. *Angew. Chem. Int. Ed.* **2019**, *58*, 2064.
63. Dürr, A. B.; Yin, G.; Kalvet, I.; Napoly, F.; Schoenebeck, F. Nickel-catalyzed Trifluoromethylthiolation of Csp²–O Bonds. *Chem. Sci.* **2016**, *7*, 1076.
64. (a) Cordovilla, C.; Bartolomé, C.; Martínez-Ilduya, J. M.; Espinet, P. The Stille Reaction, 38 Years Later. *ACS Catal.* **2015**, *5*, 3040. (b) Korch, K.M.; Watson, D. A. Cross-Coupling of Heteroatomic Electrophiles. *Chem. Rev.* **2019**, *119*, 8192.
65. Pati, K.; dos Passos Gomes, G.; Harris, T.; Hughes, A.; Phan, H.; Banerjee, T.; Hanson, K.; Alabugin, I. V. Traceless Directing Groups in Radical Cascades: From Oligoalkynes to Fused Helicenes without Tethered Initiators. *J. Am. Chem. Soc.* **2015**, *137*, 1165.
66. Furuya, T.; Strom, A. E.; Ritter, T. Silver-Mediated Fluorination of Functionalized Aryl Stannanes. *J. Am. Chem. Soc.* **2009**, *131*, 1662.
67. Klapars, A.; Huang, X.; Buchwald, S. L. A General and Efficient Copper Catalyst for the Amidation of Aryl Halides. *J. Am. Chem. Soc.* **2002**, *124*, 7421.
68. Kinzel, T.; Zhang, Y.; Buchwald, S. L. A New Palladium Precatalyst Allows for the Fast Suzuki–Miyaura Coupling Reactions of Unstable Polyfluorophenyl and 2-Heteroaryl Boronic Acids. *J. Am. Chem. Soc.* **2010**, *132*, 14073.

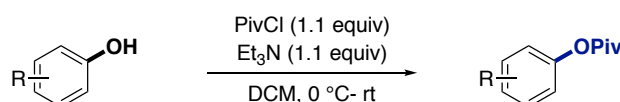
2.8. Experimental Section

2.8.1. General considerations

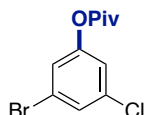
Reagents: Commercially available materials were used without further purification. Ni(COD)₂ and dcype were purchased from Strem Chemicals. Anhydrous toluene was purchased from Alfa Aesar. CsF was purchased from Aldrich. Silylstanane **18a** was prepared according to a known literature procedure.⁵¹ All the other reagents were purchased from commercial sources and used as received. Flash chromatography was performed with EM Science silica gel 60 (230-400 mesh). Thin layer chromatography was carried out using Merck TLC Silica gel 60 F₂₅₄.

Analytical Methods. ¹H NMR, ¹³C NMR, ¹⁹F NMR and ¹¹⁹Sn-NMR spectra are included for all compounds. ¹H NMR, ¹³C NMR, ¹⁹F NMR, ³¹P-NMR and ¹¹⁹Sn-NMR spectra were recorded on a Bruker 300 MHz, a Bruker 400 MHz or a Bruker 500 MHz at 20 °C. All ¹H NMR spectra are reported in parts per million (ppm) downfield of TMS and were measured relative to the signals for CHCl₃ (7.26 ppm). All ¹³C NMR spectra were reported in ppm relative to residual CHCl₃ (77.16 ppm) and were obtained with ¹H decoupling. Coupling constants, *J*, are reported in hertz (Hz). Melting points were measured using open glass capillaries in a Büchi B540 apparatus. Infrared spectra were recorded on a Bruker Tensor 27. Mass spectra were recorded on a Waters LCT Premier spectrometer. Gas chromatographic analyses were performed on HewlettPackard 6890 gas chromatography instrument with a FID detector using 25m x 0.20 mm capillary column with cross-linked methyl siloxane as the stationary phase. Flash chromatography was performed with EM Science silica gel 60 (230-400 mesh) and using KMnO₄ TLC stain. The procedures described in this section are representative. Thus, the yields may differ slightly from those given in the mentioned Schemes.

2.8.2. Synthesis of the starting materials



General procedure for the synthesis of pivalates. A round bottom flask was charged with the corresponding phenol (1.0 equiv) and dissolved with CH₂Cl₂ (3 mL/mmol). Triethylamine (1.1 equiv) and acetyl chloride derivative (1.1 equiv) were subsequently added dropwise to the reaction vessel at 0 °C. The mixture was then allowed to warm to room temperature, and stirred for 3-4 h. The mixture was then quenched with NH₄Cl(aq) and extracted three times with CH₂Cl₂. The combined organic layers were washed with brine, dried over MgSO₄, and concentrated under reduced pressure. The crude residue was purified by flash chromatography (Hex/EtOAc) to afford corresponding products.

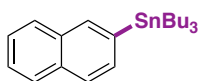


3-bromo-5-chlorophenyl pivalate (39). Following the general procedure, using 3-bromo-5-chlorophenol (2g, 10 mmol) provided the corresponding pivalate as a colorless oil in 85% yield (2.50 g). ¹H NMR (400 MHz, CDCl₃): δ 7.38 (t, *J* = 1.7 Hz, 1H), 7.17 (t, *J* = 1.8 Hz, 1H), 7.06 (t, *J* = 1.9 Hz, 1H), 1.34 (s, 9H) ppm. ¹³C NMR (101 MHz, CDCl₃) δ 176.4, 152.0, 135.5, 128.9, 123.7, 122.6, 121.4, 39.3, 27.1 ppm. IR (neat, cm⁻¹):

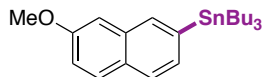
1756, 1573, 1423, 1212, 1396, 1088, 771, 667. HRMS (APCI) [C₁₁H₁₂BrClNaO₂] (M+Na) *calcd.* 312.9601, *found* 312.9592.

2.8.3. General procedure for Ni-catalyzed stannylation of aryl esters via C–O cleavage

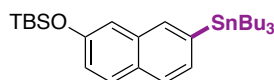
An oven-dried 5 mL screw-capped test tube containing a stirring bar was charged with the aryl pivalate (0.20 mmol). The test tube was introduced in an argon-filled glovebox where Ni(cod)₂ (5.4 mg, 10.0 mol %), dcype (**L1**, 8.4 mg, 10.0 mol %), CsF (30.2 mg, 1.0 equiv), anhydrous toluene (1 mL) were added. The mixture was stirred at room temperature for 1 minute and then **18a** (94.4 mg, 1.30 equiv) was added. The reaction tube was taken out of the glovebox and stirred at 90 °C for 8 h. The mixture was then allowed to cool to room temperature, diluted with EtOAc (5 mL) and filtered through a Celite® plug, eluting with additional EtOAc (10 mL). The filtrate was concentrated and the products were purified by flash chromatography to afford the targeted stannyl derivative.



Tributyl(naphthalen-2-yl)stannane (26a). Following the general procedure A, using **25a** (45.6 mg, 0.20 mmol). Purification by column chromatography on silica gel (Hexane) afforded the title compound as a colorless oil in 91% yield (75.8 mg). ¹H NMR (300 MHz, CDCl₃): δ 8.03 (s, 1H), 7.91-7.85 (m, 3H), 7.65 (d, *J* = 8.7 Hz, 1H), 7.56-7.51 (m, 2H), 1.73-1.63 (m, 6H), 1.51-1.39 (m, 6H), 1.25-1.20 (m, *J*_{H-Sn} = 49.9 Hz, 6H), 0.99 (t, *J* = 7.2 Hz, 9H) ppm. ¹³C NMR (75 MHz, CDCl₃) δ 139.7, 136.7, 133.4, 133.4, 133.3, 127.9, 127.7, 126.9, 125.9, 125.8, 29.3, 27.6, 13.9, 9.8 ppm. ¹¹⁹Sn NMR (149 MHz, CDCl₃) δ -40.80 ppm. Spectroscopic data for **26a** match those previously reported in the literature.¹

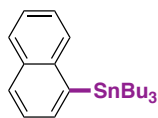


Tributyl(7-methoxynaphthalen-2-yl)stannane (26b). Following the general procedure A, using **25b** (51.5 mg, 0.20 mmol). Purification by column chromatography on silica gel (Hexane) afforded the title compound as a colorless oil in 85% yield (75.9 mg). ¹H NMR (300 MHz, CDCl₃): δ 7.85 (s, 1H), 7.34-7.70 (m, 2H), 7.43 (dd, *J* = 7.9, 0.7 Hz, 1H), 7.15-7.12 (m, 2H), 3.94 (s, 3H), 1.65-1.55 (m, 6H), 1.43-1.31 (m, 6H), 1.16-1.11 (m, *J*_{H-Sn} = 50.0 Hz, 6H), 0.91 (t, *J* = 7.2 Hz, 9H) ppm. ¹³C NMR (75 MHz, CDCl₃) δ 157.6, 140.3, 135.5, 134.4, 131.1, 129.4, 128.9, 126.7, 118.7, 105.5, 55.4, 29.3, 27.6, 13.9, 9.8 ppm. ¹¹⁹Sn NMR (149 MHz, CDCl₃) δ -40.82 ppm. IR (neat, cm⁻¹): 2954, 2923, 2870, 2850, 1624, 1457, 1212, 836. HRMS (ESI) [C₂₃H₃₆NaOSn] (M+Na) *calcd.* 471.1680, *found* 471.1660.

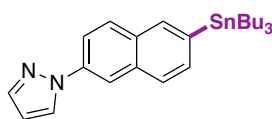


Tert-butyldimethyl((7-(tributylstannyl)naphthalen-2-yl)oxy)silane(26c). Following the general procedure A, using **25c** (71.6 mg, 0.20 mmol). Purification by column chromatography on silica gel (Hexane) afforded the title compound as a colorless oil in 70% yield (76.6 mg). ¹H NMR (500 MHz, CDCl₃): δ 7.89-7.80 (m, 1H), 7.69 (d, *J* = 8.8 Hz, 1H), 7.64 (d, *J* = 8.1 Hz, 1H), 7.49 (d, *J* = 8.0 Hz, 1H), 7.15 (d, *J* = 2.0 Hz, 1H), 7.06 (dd, *J* = 8.5, 2.5 Hz, 1H), 1.64-1.54 (m, 6H), 1.39-1.31 (m, 6H), 1.12-1.09 (m, *J*_{H-Sn} = 66.4 Hz, 6H), 1.02 (s, 9H), 0.89 (t, *J* = 10.0 HZ, 9H), 0.24 (s, 6H) ppm. ¹³C NMR (126 MHz, CDCl₃) δ 153.6, 136.8, 136.4, 134.6, 133.6, 129.5, 129.2, 125.9, 122.1, 114.9, 29.3, 27.6, 25.9, 18.4, 13.8, 9.8, -4.2 ppm. ¹¹⁹Sn

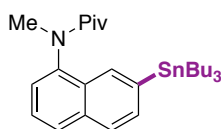
NMR (149 MHz, CDCl₃) δ -40.77 ppm. IR (neat, cm⁻¹): 2956, 2927, 2856, 1624, 1467, 1258, 932. HRMS (APCI) [C₂₈H₄₉OSiSn] (M+H) *calcd.* 549.2569, *found* 549.2574.



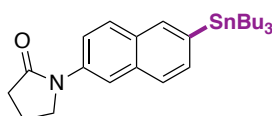
Tributyl(naphthalen-1-yl)stannane (26d). Following the general procedure A, using **25d** (45.6 mg, 0.20 mmol). Purification by column chromatography on silica gel (Hexane) afforded the title compound as a colorless oil in 86% yield (71.7 mg). ¹H NMR (300 MHz, CDCl₃): δ 7.87-7.77 (m, 3H), 7.65 (dd, *J* = 6.6, 1.2 Hz, 1H), 7.53-7.42 (m, 3H), 1.64-1.54 (m, 6H), 1.42-1.30 (m, 6H), 1.25-1.90 (m, *J*_{H-Sn} = 50.5 Hz, 6H), 0.89 (t, *J* = 7.2 Hz, 9H) ppm. ¹³C NMR (75 MHz, CDCl₃) δ 143.07, 139.14, 135.24, 133.80, 130.31, 129.03, 128.56, 125.76, 125.46, 29.34, 27.52, 13.81, 10.55 ppm. ¹¹⁹Sn NMR (149 MHz, CDCl₃) δ -39.71 ppm. Spectroscopic data for **26d** match those previously reported in the literature.¹



1-(6-(tributylstannyl)naphthalen-2-yl)-1H-pyrazole (26e). Following the general procedure A, using **25e** (58.9 mg, 0.20 mmol) and **18a** (145.2 mg, 0.40 mmol). After 6 hours, purification by column chromatography on silica gel (Hex:EtOAc 5:1) afforded the title compound as a colorless oil in 66% yield (63.8 mg). ¹H NMR (300 MHz, CDCl₃): δ 8.08-8.06 (m, 2H), 7.96-7.78 (m, 5H), 7.62-7.57 (m, 1H), 6.53-6.51 (m, 1H), 1.65-1.55 (m, 6H), 1.43-1.33 (m, 6H), 1.17-1.12 (m, *J*_{H-Sn} = 50.3 Hz, 6H), 0.91 (t, *J* = 7.2 Hz, 9H) ppm. ¹³C NMR (75 MHz, CDCl₃) δ 141.3, 140.1, 137.6, 136.5, 134.4, 133.5, 131.8, 129.4, 127.1, 126.7, 118.5, 116.4, 107.9, 29.3, 27.5, 13.8, 9.8 ppm. ¹¹⁹Sn NMR (149 MHz, CDCl₃) δ -40.56 ppm. IR (neat, cm⁻¹): 2955, 2921, 2870, 2851, 1686, 1579, 1375, 861. HRMS (ESI) [C₂₅H₃₆N₂NaSn] (M+Na) *calcd.* 507.1792, *found* 507.1786.

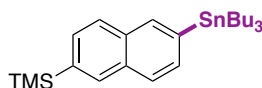


N-methyl-N-(7-(tributylstannyl)naphthalen-1-yl)pivalamide (26f). Following the general procedure A, using **25f** (68.2 mg, 0.20 mmol). Purification by column chromatography on silica gel (Hex:EtOAc 5:2) afforded the title compound as a colorless oil in 80% yield (84.9 mg). ¹H NMR (500 MHz, CDCl₃): δ 7.94 (s, 1H), 7.82 (t, *J* = 10.0 Hz, 2H), 7.63-7.61 (m, 1H), 7.43-7.40 (m, 1H), 7.33-7.32 (m, 1H), 3.31 (s, 3H), 1.59-1.53 (m, 6H), 1.36-1.31 (m, 6H), 1.13-1.10 (m, *J*_{H-Sn} = 67.1 Hz, 6H), 0.97 (s, 9H), 0.87 (t, *J* = 8.0 Hz, 9H) ppm. ¹³C NMR (126 MHz, CDCl₃) δ 179.1, 141.9, 141.2, 134.52, 133.9, 131.9, 130.3, 128.6, 127.3, 126.2, 125.2, 77.2, 41.1, 40.8, 29.4, 29.3, 27.5, 13.8, 9.9 ppm. ¹¹⁹Sn NMR (149 MHz, CDCl₃) δ -38.98 ppm. IR (neat, cm⁻¹): 2955, 2923, 2870, 2852, 1639, 1480, 1364, 1083, 829. HRMS (ESI) [C₂₈H₄₆NOSn] (M+H) *calcd.* 523.2596, *found* 523.2607.

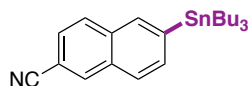


1-(6-(tributylstannyl)naphthalen-2-yl)pyrrolidin-2-one (26g). Following the general procedure A, using **25g** (62.3 mg, 0.20 mmol). Purification by column chromatography on silica gel (Hex:EtOAc 1:1) afforded

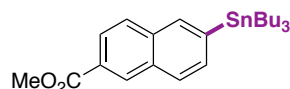
the title compound as a colorless oil in 73% yield (72.9 mg). ^1H NMR (300 MHz, CDCl_3): δ 7.98 (dd, $J = 9.0$, 2.1 Hz, 1H), 7.90-7.74 (m, 4H), 7.55 (dd, $J = 8.0$, 1.0 Hz, 1H), 3.97 (t, $J = 7.2$ Hz, 2H), 2.66 (t, $J = 7.8$ Hz, 2H), 2.25-2.15 (m, 2H), 1.68-1.53 (m, 6H), 1.42-1.30 (m, 6H), 1.15-1.10 (m, $J_{\text{H-Sn}} = 66.6$ Hz, 6H), 0.90 (t, $J = 7.2$ Hz, 9H) ppm. ^{13}C NMR (75 MHz, CDCl_3) δ 174.5, 139.0, 137.2, 136.2, 133.8, 133.4, 130.7, 128.4, 126.7, 119.8, 116.7, 49.2, 33.0, 29.3, 27.5, 18.2, 13.8, 9.8 ppm. ^{119}Sn NMR (149 MHz, CDCl_3) δ -40.55 ppm. IR (neat, cm^{-1}): 2955, 2922, 2870, 2851, 1686, 1407, 1299, 861. HRMS (APCI) [$\text{C}_{26}\text{H}_{40}\text{NOSn}$] (M+H) *calcd.* 502.2126, *found* 502.2132.



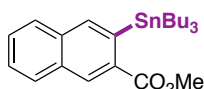
Trimethyl(6-(tributylstannyl)naphthalen-2-yl)silane (26h). Following the general procedure A, using **25h** (60.0 mg, 0.20 mmol). Purification by column chromatography on silica gel (Hexane) afforded the title compound as a colorless oil in 89% yield (87.1 mg). ^1H NMR (300 MHz, CDCl_3): δ 8.00-7.94 (m, 2H), 7.82 (d, $J = 8.0$ Hz, 2H), 7.60 (t, $J = 8.6$ Hz, 2H), 1.66-1.53 (m, 6H), 1.42-1.35 (m, 6H), 1.18-1.13 (m, $J_{\text{H-Sn}} = 66.9$ Hz, 6H), 0.92 (t, $J = 7.2$ Hz, 9H), 0.37 (s, 9H) ppm. ^{13}C NMR (75 MHz, CDCl_3) δ 140.3, 137.9, 136.5, 133.8, 133.5, 133.4, 132.9, 129.8, 127.0, 126.7, 29.3, 27.5, 13.9, 9.8, -0.9 ppm. ^{119}Sn NMR (149 MHz, CDCl_3) δ -40.55 ppm. IR (neat, cm^{-1}): 2955, 2924, 2871, 2851, 1246, 1086, 833, 815. HRMS (ESI) [$\text{C}_{21}\text{H}_{33}\text{SiSn}$] (M-Bu) *calcd.* 433.1368, *found* 433.1354.



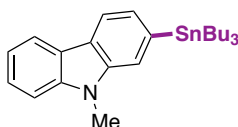
6-(tributylstannyl)-2-naphthonitrile (26i). Following the general procedure A, using **25i** (50.6 mg, 0.20 mmol). After 6 hours, purification by column chromatography on silica gel (Hexane) afforded the title compound as a colorless oil in 80% yield (70.7 mg). ^1H NMR (500 MHz, CDCl_3): δ 8.20 (s, 1H), 7.99 (s, 1H), 7.88 (d, $J = 8.5$ Hz, 1H), 7.82 (d, $J = 8.0$ Hz, 1H), 7.70 (d, $J = 8.0$ Hz, 1H), 7.60 (dd, $J = 8.5$, 1.5 Hz, 1H), 1.64-1.56 (m, 6H), 1.40-1.33 (m, 6H), 1.18-1.15 (m, $J_{\text{H-Sn}} = 68.4$ Hz, 6H), 0.91 (t, $J = 7.2$ Hz, 9H) ppm. ^{13}C NMR (126 MHz, CDCl_3) δ 145.2, 136.6, 135.3, 134.2, 134.2, 132.2, 128.9, 127.0, 126.3, 119.5, 109.2, 29.2, 27.5, 13.8, 9.9 ppm. ^{119}Sn NMR (149 MHz, CDCl_3) δ -38.81 ppm. IR (neat, cm^{-1}): 2955, 2922, 2870, 2851, 2226, 1462, 892, 816. HRMS (ESI) [$\text{C}_{23}\text{H}_{33}\text{NNaSn}$] (M+Na) *calcd.* 466.1527, *found* 466.1522.



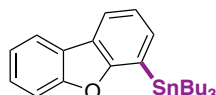
Methyl 6-(tributylstannyl)-2-naphthoate (26j). Following the general procedure A, using **25j** (57.2 mg, 0.20 mmol). Purification by column chromatography on silica gel (Hex:EtOAc 20:1) afforded the title compound as a colorless oil in 80% yield (76.1 mg). ^1H NMR (300 MHz, CDCl_3): δ 8.58 (s, 1H), 8.06 (dd, $J = 8.6$, 1.7 Hz, 2H), 7.90-7.83 (m, 2H), 7.63 (d, $J = 8.0$ Hz, 1H), 3.98 (s, 3H), 1.64-1.53 (m, 6H), 1.42-1.30 (m, 6H), 1.17-1.12 (m, $J_{\text{H-Sn}} = 51.6$ Hz, 6H), 0.90 (t, $J = 7.2$ Hz, 9H) ppm. ^{13}C NMR (75 MHz, CDCl_3) δ 167.5, 143.8, 136.4, 135.2, 134.1, 132.4, 131.2, 128.1, 127.9, 127.3, 125.3, 52.3, 29.3, 27.5, 13.8, 9.9 ppm. ^{119}Sn NMR (149 MHz, CDCl_3) δ -39.93 ppm. IR (neat, cm^{-1}): 2954, 2924, 2870, 2850, 1719, 1280, 1225, 747. HRMS (ESI) [$\text{C}_{24}\text{H}_{36}\text{NaO}_2\text{Sn}$] (M+Na) *calcd.* 499.1629, *found* 499.1621.



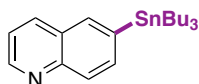
Methyl 3-(tributylstannyl)-2-naphthoate (26k). Following the general procedure A, using **25k** (57.3 mg, 0.20 mmol). Purification by column chromatography on silica gel (Hex:EtOAc 20:1) afforded the title compound as a colorless oil in 61% yield (57.9 mg). ^1H NMR (300 MHz, CDCl_3): δ 8.66 (t, $J = 6.0$ Hz, 1H), 8.15-7.99 (m, 1H), 7.89 (dd, $J = 14.7, 8.0$ Hz, 2H), 7.62-7.49 (m, 2H), 3.98 (s, 3H), 1.59-1.48 (m, 6H), 1.38-1.27 (m, 6H), 1.16-1.10 (m, $J_{\text{H-Sn}} = 66.3$ Hz, 6H), 0.86 (t, $J = 7.2$ Hz, 9H) ppm. ^{13}C NMR (75 MHz, CDCl_3) δ 169.3, 141.3, 137.6, 135.0, 132.6, 132.4, 130.8, 129.2, 128.3, 127.7, 126.6, 52.5, 29.4, 27.6, 13.9, 11.4 ppm. ^{119}Sn NMR (149 MHz, CDCl_3) δ -38.33 ppm. IR (neat, cm^{-1}): 2954, 2920, 2870, 2853, 1709, 1446, 1282, 742. HRMS (ESI) [$\text{C}_{24}\text{H}_{36}\text{NaO}_2\text{Sn}$] ($\text{M}+\text{Na}$) *calcd.* 499.1629, *found* 499.1621.



9-methyl-2-(tributylstannyl)-9H-carbazole (26l). Following the general procedure A, using **25l** (56.2 mg, 0.20 mmol) and **2a** (166.9 mg, 0.46 mol). Purification by column chromatography on silica gel (Hex:EtOAc 20:1) afforded the title compound as a colorless oil in 63% yield (60.1 mg). ^1H NMR (500 MHz, CDCl_3): δ 8.07 (t, $J = 10.0$ Hz, 2H), 7.49-7.37 (m, 3H), 7.31 (d, $J = 7.5$ Hz, 1H), 7.24-7.19 (m, 1H), 3.86 (s, 3H), 1.66-1.56 (m, 6H), 1.41-1.32 (m, 6H), 1.15-1.11 (m, $J_{\text{H-Sn}} = 53.6$ Hz, 6H), 0.90 (t, $J = 7.2$ Hz, 9H) ppm. ^{13}C NMR (101 MHz, CDCl_3) δ 141.0, 140.8, 139.2, 126.6, 125.8, 123.0, 122.9, 120.4, 119.8, 118.8, 116.1, 108.5, 29.3, 29.1, 27.6, 13.8, 10.0 ppm. ^{119}Sn NMR (149 MHz, CDCl_3) δ -37.58 ppm. IR (neat, cm^{-1}): 2954, 2922, 2870, 2850, 1590, 1318, 1246, 743, 724. HRMS (ESI) [$\text{C}_{25}\text{H}_{37}\text{NNaSn}$] ($\text{M}+\text{Na}$) *calcd.* 494.1844, *found* 494.1845.

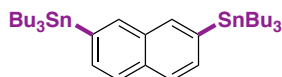


Tributyl(dibenzo[*b,d*]furan-4-yl)stannane (26m). Following the general procedure A, using **25m** (53.6 mg, 0.20 mmol) and purification by column chromatography on silica gel (Hexane) afforded the title compound as a colorless oil in 87% yield (79.5 mg). ^1H NMR (400 MHz, CDCl_3): δ 7.97 (d, $J = 8.0$ Hz, 1H), 7.94 (dd, $J = 7.6, 1.2$ Hz, 1H), 7.58-7.54 (m, 2H), 7.48-7.44 (m, 1H), 7.35 (dt, $J = 7.4, 2.5$ Hz, 2H), 1.71-1.59 (m, 6H), 1.45-1.39 (m, 6H), 1.32-1.25 (m, $J_{\text{H-Sn}} = 52.9$ Hz, 6H), 0.93 (t, $J = 8.0$ Hz, 9H) ppm. ^{13}C NMR (101 MHz, CDCl_3) δ 162.3, 156.1, 135.0, 126.8, 124.9, 123.6, 122.8, 122.5, 122.1, 120.8, 120.6, 111.7, 29.3, 27.5, 13.8, 10.1 ppm. ^{119}Sn NMR (149 MHz, CDCl_3) δ -39.79 ppm. Spectroscopic data for **26m** match those previously reported in the literature.³

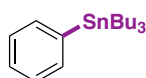


6-(tributylstannyl)quinoline (26n). Following the general procedure A, using **25n** (45.8 mg, 0.20 mmol) and purification by column chromatography on silica gel (Hex:EtOAc 4:1) afforded the title compound as a colorless oil in 88% yield (73.9 mg). ^1H NMR (400 MHz, CDCl_3): δ 8.88 (dd, $J = 4.2, 1.7$ Hz, 1H), 8.12 (d, $J = 8.0$ Hz, 1H), 8.05 (dd, $J = 8.2, 4.1$ Hz, 1H), 7.90 (s, 1H), 7.81 (dd, $J = 8.2, 1.1$ Hz, 1H), 7.38 (dd, $J = 8.3, 4.2$ Hz, 1H), 1.64-1.55 (m, 6H), 1.40-1.31 (m, 6H), 1.16-1.12 (m, $J_{\text{H-Sn}} = 67.3$ Hz, 6H), 0.89 (t, $J = 8.0$ Hz, 9H) ppm. ^{13}C NMR (101 MHz, CDCl_3) δ 150.4, 148.4, 141.4, 136.9, 136.4, 135.8, 128.3, 128.2, 121.1, 29.2, 27.5, 13.8,

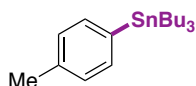
9.9 ppm. ^{119}Sn NMR (149 MHz, CDCl_3) δ -39.38 ppm. Spectroscopic data for **26n** match those previously reported in the literature.⁴



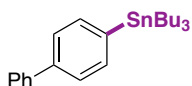
2,7-bis(tributylstannyl)naphthalene (26o). Following the general procedure A, using **25o** (65.7 mg, 0.20 mmol) and **18a** (166.9 mg, 0.46 mmol). Purification by column chromatography on silica gel (Hexane) afforded the title compound as a colorless oil in 81% yield (114.3 mg). ^1H NMR (500 MHz, CDCl_3): δ 7.95-7.86 (m, 2H), 7.83-7.75 (m, 2H), 7.55-7.44 (m, 2H), 1.63-1.56 (m, 12H), 1.41-1.34 (m, 12H), 1.16-1.13 (m, $J_{\text{H-Sn}} = 68.0$ Hz, 12H), 0.91 (t, $J = 7.0$ Hz, 18H) ppm. ^{13}C NMR (101 MHz, CDCl_3) δ 139.8, 139.6, 136.7, 136.4, 133.2, 127.9, 127.7, 126.9, 126.8, 125.8, 29.3, 27.6, 13.8, 9.8 ppm. ^{119}Sn NMR (149 MHz, CDCl_3) δ -40.93 ppm. IR (neat, cm^{-1}): 2955, 2922, 2870, 2851, 1462, 1376, 1061, 835. HRMS (APCI) [$\text{C}_{30}\text{H}_{51}\text{Sn}_2$] (M-Bu) *calcd.* 651.2029, *found* 651.2058.



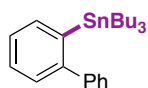
Tributyl(phenyl)stannane (31a). Following the general procedure A, using **30a** (35.6 mg, 0.20 mmol) and **18a** (145.2 mg, 0.40 mmol). Purification by column chromatography on silica gel (Hexane) afforded the title compound as a colorless oil in 77% yield (56.5 mg). ^1H NMR (300 MHz, CDCl_3): δ 7.49-7.46 (m, 2H), 7.35-7.30 (m, 3H), 1.61-1.51 (m, 6H), 1.41-1.29 (m, 6H), 1.09-1.04 (m, $J_{\text{H-Sn}} = 59.3$ Hz, 6H), 0.90 (t, $J = 7.2$ Hz, 9H) ppm. ^{13}C NMR (126 MHz, CDCl_3) δ 142.2, 136.6, 128.1, 128.0, 29.3, 27.5, 13.8, 9.7 ppm. ^{119}Sn NMR (149 MHz, CDCl_3) δ -43.23 ppm. Spectroscopic data for **31a** match those previously reported in the literature.¹



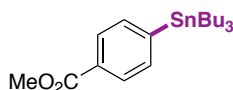
Tributyl(p-tolyl)stannane (31b). Following the general procedure A, using **30b** (38.4 mg, 0.20 mmol) and **18a** (145.2 mg, 0.40 mmol). Purification by column chromatography on silica gel (Hexane) afforded the title compound as a colorless oil in 68% yield (52.3 mg). ^1H NMR (300 MHz, CDCl_3): δ 7.35 (d, $J = 4.0$ Hz, 2H), 7.15 (d, $J = 4.0$ Hz, 2H), 2.33 (s, 3H), 1.57-1.49 (m, 6H), 1.35-1.26 (m, 6H), 1.05-1.01 (m, $J_{\text{H-Sn}} = 59.3$ Hz, 6H), 0.88 (t, $J = 7.2$ Hz, 9H) ppm. ^{13}C NMR (101 MHz, CDCl_3) δ 138.0, 137.8, 136.6, 129.0, 29.3, 27.5, 21.6, 13.8, 9.7 ppm. ^{119}Sn NMR (149 MHz, CDCl_3) δ -42.73 ppm. Spectroscopic data for **31b** match those previously reported in the literature.¹



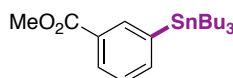
[1,1'-biphenyl]-4-yltributylstannane (31c). Following the general procedure A, using **30c** (50.9 mg, 0.20 mmol). Purification by column chromatography on silica gel (Hexane) afforded the title compound as a colorless oil in 64% yield (56.8 mg). ^1H NMR (400 MHz, CDCl_3): δ 7.62-7.56 (m, 6H), 7.46-7.42 (m, 2H), 7.36-7.32 (m, 1H), 1.62-1.54 (m, 6H), 1.41-1.32 (m, 6H), 1.18-1.01 (m, $J_{\text{H-Sn}} = 67.4$ Hz, 6H), 0.91 (t, $J = 7.2$ Hz, 9H) ppm. ^{13}C NMR (126 MHz, CDCl_3) δ 141.5, 141.0, 140.9, 137.0, 128.9, 127.3, 127.3, 126.8, 29.3, 27.6, 13.8, 9.8 ppm. ^{119}Sn NMR (149 MHz, CDCl_3) δ -42.16 ppm. Spectroscopic data for **31c** match those previously reported in the literature.⁵



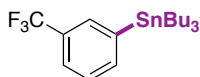
[1,1'-biphenyl]-2-yltributylstannane (31d). Following the general procedure A, using **30d** (50.9 mg, 0.20 mmol). Purification by column chromatography on silica gel (Hexane) afforded the title compound as a colorless oil in 67% yield (59.5 mg). ^1H NMR (400 MHz, CDCl_3): δ 7.54 (dt, $J = 6.9, 1.2$ Hz, 1H), 7.41-7.29 (m, 8H), 1.38-1.30 (m, 6H), 1.26-1.19 (m, 6H), 0.83 (t, $J = 7.2$ Hz, 9H), 0.74-0.70 (m, $J_{\text{H-Sn}} = 59.8$ Hz, 6H) ppm. ^{13}C NMR (126 MHz, CDCl_3) δ 150.6, 145.9, 142.1, 137.1, 128.9, 128.9, 128.3, 128.1, 127.1, 126.4, 29.2, 27.5, 13.8, 10.9 ppm. ^{119}Sn NMR (149 MHz, CDCl_3) δ -38.70 ppm. Spectroscopic data for **31d** match those previously reported in the literature.⁶



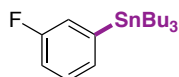
Methyl 4-(tributylstannyl)benzoate (31e). Following the general procedure A, using **30e** (47.2 mg, 0.20 mmol). Purification by column chromatography on silica gel (Hex:EtOAc 20:1) afforded the title compound as a colorless oil in 60% yield (51.1 mg). ^1H NMR (500 MHz, CDCl_3): δ 7.95 (d, $J = 8.1$ Hz, 2H), 7.55 (d, $J = 8.1$ Hz, 2H), 3.91 (s, 3H), 1.57-1.50 (m, 6H), 1.35-1.30 (m, 6H), 1.10-1.07 (m, $J_{\text{H-Sn}} = 68.5$ Hz, 6H), 0.88 (t, $J = 7.2$ Hz, 9H) ppm. ^{13}C NMR (126 MHz, CDCl_3) δ 167.7, 149.8, 136.6, 129.7, 128.5, 52.1, 29.2, 27.5, 13.8, 9.8 ppm. ^{119}Sn NMR (149 MHz, CDCl_3) δ -40.78 ppm. IR (neat, cm^{-1}): 2955, 2924, 2871, 2852, 1726, 1276, 1114, 751. HRMS (ESI) [$\text{C}_{20}\text{H}_{34}\text{NaO}_2\text{Sn}$] (M+Na) *calcd.* 449.1473, *found* 449.1474.



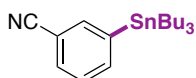
Methyl 3-(tributylstannyl)benzoate (31f). Following the general procedure A, using **30f** (47.2 mg, 0.20 mmol). Purification by column chromatography on silica gel (Hex:EtOAc 20:1) afforded the title compound as a colorless oil in 73% yield (62.5 mg). ^1H NMR (500 MHz, CDCl_3): δ 8.17-8.10 (m, 1H), 7.96 (dt, $J = 7.8, 1.6$ Hz, 1H), 7.65 (dt, $J = 7.2, 1.2$ Hz, 1H), 7.38 (t, $J = 7.8$ Hz, 1H), 3.92 (s, 3H), 1.58-1.50 (m, 6H), 1.34-1.30 (m, 6H), 1.11-1.08 (m, $J_{\text{H-Sn}} = 67.5$ Hz, 6H), 0.89 (t, $J = 7.2$ Hz, 9H) ppm. ^{13}C NMR (126 MHz, CDCl_3) δ 167.8, 142.7, 141.1, 137.4, 129.5, 129.3, 127.8, 52.1, 29.2, 27.5, 13.8, 9.8 ppm. ^{119}Sn NMR (149 MHz, CDCl_3) δ -39.80 ppm. IR (neat, cm^{-1}): 2955, 2924, 2871, 2857, 1724, 1274, 1113, 741. HRMS (ESI) [$\text{C}_{20}\text{H}_{34}\text{NaO}_2\text{Sn}$] (M+Na) *calcd.* 449.1473, *found* 449.1469.



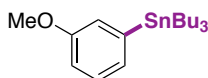
Tributyl(3-(trifluoromethyl)phenyl)stannane (31g). Following the general procedure A, using **31g** (49.3 mg, 0.20 mmol). Purification by column chromatography on silica gel (Hexane) afforded the title compound as a colorless oil in 79% yield (67.2 mg). ^1H NMR (400 MHz, CDCl_3): δ 7.77-7.71 (m, 1H), 7.66-7.64 (m, 1H), 7.57-7.54 (m, 1H), 7.43 (t, $J = 7.5$ Hz, 1H), 1.65-1.52 (m, 6H), 1.42-1.30 (m, 6H), 1.14-1.09 (m, $J_{\text{H-Sn}} = 66.5$ Hz, 6H), 0.91 (t, $J = 7.2$ Hz, 9H) ppm. ^{13}C NMR (75 MHz, CDCl_3) δ 143.6, 139.9, 132.7, 132.7, 128.0, 124.8, 124.8, 29.2, 27.5, 13.8, 9.8 ppm. ^{19}F NMR (367 MHz, CDCl_3) δ -26.7 ppm. ^{119}Sn NMR (149 MHz, CDCl_3) δ -38.71 ppm. IR (neat, cm^{-1}): 2957, 2924, 2872, 2853, 1313, 1124, 1081, 703. HRMS (APCI) [$\text{C}_{15}\text{H}_{22}\text{F}_3\text{Sn}$] (M-Bu) *calcd.* 379.0683, *found* 379.0683.



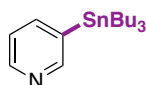
Tributyl(3-fluorophenyl)stannane (31h). Following the general procedure A, using **30h** (38.5 mg, 0.20 mmol). Purification by column chromatography on silica gel (Hexane) afforded the title compound as a colorless oil in 62% yield (47.8 mg). ^1H NMR (500 MHz, CDCl_3): δ 7.35-7.30 (m, 1H), 7.24 (dd, $J = 7.1$, 0.8 Hz, 1H), 7.19 (dd, $J = 8.1$, 2.7 Hz, 1H), 7.02-6.98 (m, 1H), 1.60-1.54 (m, 6H), 1.40-1.33 (m, 6H), 1.12-1.08 (m, $J_{\text{H-Sn}} = 67.6$ Hz, 6H), 0.92 (t, $J = 7.2$ Hz, 9H) ppm. ^{13}C NMR (126 MHz, CDCl_3) δ 162.7 (d, $J = 125.4$ Hz), 145.1, 132.0, 129.4, 122.7, 115.0, 29.2, 27.5, 13.8, 9.8 ppm. ^{19}F NMR (376 MHz, CDCl_3) δ -113.9 ppm. ^{119}Sn NMR (149 MHz, CDCl_3) δ -39.23 ppm. IR (neat, cm^{-1}): 2956, 2923, 2871, 2852, 1571, 1467, 1408, 1206, 780. HRMS (ESI) [$\text{C}_{14}\text{H}_{222}\text{FSn}$] (M-Bu) *calcd.* 329.0722, *found* 329.0723.



3-(tributylstannyl)benzonitrile (31i). Following the general procedure A, using **30i** (40.7 mg, 0.20 mmol). Purification by column chromatography on silica gel (Hexane) afforded the title compound as a colorless oil in 60% yield (47.5 mg). ^1H NMR (400 MHz, CDCl_3): δ 7.72 (t, $J = 1.0$ Hz, 1H), 7.68-7.66 (m, 1H), 7.67 (dt, $J = 7.3$, 1.1 Hz, 1H), 7.57 (dt, $J = 7.8$, 1.5 Hz, 1H), 1.57-1.49 (m, 6H), 1.37-1.29 (m, 6H), 1.11-1.07 (m, $J_{\text{H-Sn}} = 56.7$ Hz, 6H), 0.89 (t, $J = 7.2$ Hz, 9H) ppm. ^{13}C NMR (101 MHz, CDCl_3) δ 144.3, 140.6, 139.8, 131.6, 128.2, 119.6, 112.3, 29.1, 27.4, 13.8, 9.9 ppm. ^{119}Sn NMR (149 MHz, CDCl_3) δ -36.95 ppm. Spectroscopic data for **31i** match those previously reported in the literature.⁸

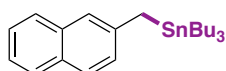


tributyl(3-methoxyphenyl)stannane (31j). Following the general procedure A, using **30j** (41.6 mg, 0.20 mmol). Purification by column chromatography on silica gel (Hexane) afforded the title compound as a colorless oil in 74% yield (58.8 mg). ^1H NMR (300 MHz, CDCl_3): δ 7.32-7.25 (m, 1H), 7.14-6.99 (m, 2H), 6.86 (dd, $J = 8.2$, 1.8 Hz, 1H), 3.84 (s, 3H), 1.63-1.52 (m, 6H), 1.42-1.30 (m, 7H), 1.11-1.05 (m, $J_{\text{H-Sn}} = 51.3$ Hz, 5H), 0.92 (t, $J = 7.2$ Hz, 9H) ppm. ^{13}C NMR (75 MHz, CDCl_3) δ 159.0, 143.6, 128.9, 128.8, 122.2, 113.1, 55.2, 29.2, 27.5, 13.8, 9.7 ppm. ^{119}Sn NMR (149 MHz, CDCl_3) δ -41.08 ppm. Spectroscopic data for **31j** match those previously reported in the literature.⁷

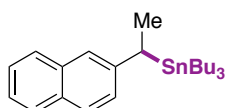


3-(tributylstannyl)pyridine (31k). Following the general procedure A, using **30k** (35.8 mg, 0.20 mmol). Purification by column chromatography on silica gel (Hex:EtOAc 10:1) afforded the title compound as a colorless oil in 60% yield (44.2 mg). Scaling up the reaction to 6.0 mmol resulted in 63% yield of **5k**. ^1H NMR (500 MHz, CDCl_3): δ 8.59 (t, $J = 9.5$ Hz, 1H), 8.50 (dd, $J = 7.8$, 1.5 Hz, 1H), 7.73 (dt, $J = 7.3$, 1.7 Hz, 1H), 7.21 (ddd, $J = 7.3$, 4.9, 1.7 Hz, 1H), 1.58-1.48 (m, 6H), 1.36-1.29 (m, 6H), 1.10-1.07 (m, $J_{\text{H-Sn}} = 68.8$ Hz, 6H), 0.88 (t, $J = 7.5$ Hz, 9H) ppm. ^{13}C NMR (126 MHz, CDCl_3) δ 156.2, 149.3, 144.2, 137.1, 124.0, 29.1, 27.4, 13.7, 9.7 ppm. ^{119}Sn NMR (149 MHz, CDCl_3) δ -40.90 ppm. Spectroscopic data for **31k** match those previously reported in the literature.⁸

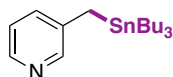
Ni-Catalyzed Stannylation of Aryl Ester via C-O Bond Cleavage



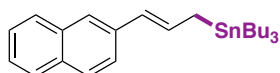
Tributyl(naphthalen-2-ylmethyl)stannane (33a). Following the general procedure A, using **32a** (48.5 mg, 0.20 mmol). After 6 hours, purification by column chromatography on silica gel (Hexane) afforded the title compound as a colorless oil in 82% yield (70.6 mg). ^1H NMR (400 MHz, CDCl_3): δ 7.78 (d, $J = 8.1$ Hz, 1H), 7.71 (d, $J = 8.2$ Hz, 2H), 7.45-7.34 (m, 3H), 7.20 (dd, $J = 8.4, 1.8$ Hz, 1H), 2.53 (s with Sn satellites, $J_{\text{H-Sn}} = 56.4$ Hz, 2H), 1.57-1.50 (m, 6H), 1.35-1.30 (m, 6H), 0.88 (m, $J_{\text{H-Sn}} = 65.1$ Hz, 15H) ppm. ^{13}C NMR (101 MHz, CDCl_3) δ 141.6, 134.2, 130.7, 127.8, 127.7, 127.4, 126.8, 125.9, 124.0, 123.6, 29.2, 27.5, 18.9, 13.8, 9.6 ppm. ^{119}Sn NMR (149 MHz, CDCl_3) δ -10.33 ppm. Spectroscopic data for **32a** match those previously reported in the literature.²



Tributyl(1-(naphthalen-2-yl)ethyl)stannane (33b). Following the general procedure A, using **32b** (51.4 mg, 0.20 mmol) at 110 °C. Purification by column chromatography on silica gel (Hexane) afforded the title compound as a colorless oil in 69% yield (61.4 mg). ^1H NMR (300 MHz, CDCl_3): δ 7.76-7.66 (m, 3H), 7.43-7.30 (m, 3H), 7.19 (dd, $J = 8.4, 1.9$ Hz, 1H), 2.95-2.81 (m, $J_{\text{H-Sn}} = 79.1$ Hz, 1H), 1.67 (d with Sn satellites, $J_{\text{H-Sn}} = 66.5$ Hz, $J = 7.5$ Hz, 3H), 1.47-1.33 (m, 6H), 1.29-1.17 (m, 6H), 0.88-0.77 (m, 15H) ppm. ^{13}C NMR (101 MHz, CDCl_3) δ 146.9, 134.2, 131.0, 127.6, 127.6, 127.1, 126.5, 125.8, 124.1, 121.9, 29.2, 27.6, 17.5, 13.8, 9.1 ppm. ^{119}Sn NMR (149 MHz, CDCl_3) δ -6.98 ppm. IR (neat, cm^{-1}): 2954, 2926, 2870, 2850, 1666, 1580, 1375, 761. HRMS (APCI) [$\text{C}_{20}\text{H}_{29}\text{Sn}$] (M-Bu) *calcd.* 389.1294, *found* 389.1286.

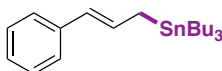


3-((tributylstannyl)methyl)pyridine (33c). Following the general procedure A, using **32c** (38.6 mg, 0.20 mmol) and **2a** (145.2 mg, 0.40 mmol). Purification by column chromatography on silica gel (Hexane) afforded the title compound as a colorless oil in 64% yield (48.7 mg). ^1H NMR (400 MHz, CDCl_3): δ 8.29 (d, $J = 2.1$ Hz, 1H), 8.22 (dd, $J = 4.7, 1.4$ Hz, 1H), 7.29-7.26 (m, 1H), 7.08 (dd, $J = 7.5, 4.5$ Hz, 1H), 2.24 (s with Sn satellites, $J_{\text{H-Sn}} = 54.6$ Hz, 2H), 1.49-1.38 (m, 6H), 1.29-1.21 (m, 6H), 0.89-0.81 (m, $J_{\text{H-Sn}} = 64.5$ Hz, 15H) ppm. ^{13}C NMR (101 MHz, CDCl_3) δ 148.6, 144.5, 139.8, 134.0, 123.2, 29.1, 27.4, 15.0, 13.8, 9.6 ppm. ^{119}Sn NMR (149 MHz, CDCl_3) δ -7.28 ppm. IR (neat, cm^{-1}): 2955, 2922, 2871, 2851, 1568, 1463, 1224, 1189, 797, 712. HRMS (ESI) [$\text{C}_{18}\text{H}_{34}\text{NSn}$] (M+H) *calcd.* 384.1708, *found* 384.1707.



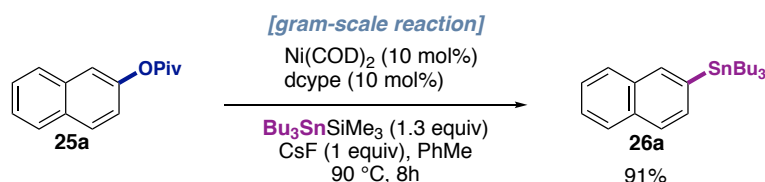
(E)-tributyl(3-(naphthalen-2-yl)allyl)stannane (33d). Following the general procedure A, using **32d** (53.7 mg, 0.20 mmol). Purification by column chromatography on silica gel (Hexane) afforded the title compound as a colorless oil in 90% yield (82.3 mg). ^1H NMR (400 MHz, CDCl_3): δ 7.77-7.72 (m, 3H), 7.57 (s, 1H), 7.52 (dd, $J = 8.5, 1.6$ Hz, 1H), 7.46-7.35 (m, 2H), 6.56 (dt, $J = 15.5, 8.7$ Hz, 1H), 6.36 (dt, $J = 15.7, 1.4$ Hz, 1H), 2.09 (dd, $J_{\text{H-Sn}} = 71.0$ Hz, $J = 8.7, 1.0$ Hz, 2H), 1.58-1.46 (m, 6H), 1.37-1.27 (m, 6H), 0.97-0.89 (m, $J_{\text{H-Sn}} = 68.7$ Hz, 15H) ppm. ^{13}C NMR (101 MHz, CDCl_3) δ 136.5, 134.1, 132.3, 132.0, 128.0, 127.7, 126.1, 125.2, 125.0, 124.0, 123.6, 29.3, 27.5, 16.5, 13.9, 9.8 ppm. ^{119}Sn NMR (149 MHz, CDCl_3) δ -11.35 ppm. IR (neat,

cm⁻¹): 2954, 2924, 2854, 1586, 1463, 1374, 744, 671. HRMS (APCI) [C₂₅H₃₈Sn] (M+H) *calcd.* 458.1984, *found* 458.1965.

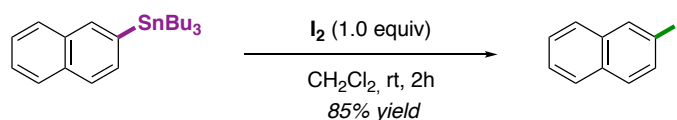


Tributyl(cinnamyl)stannane (33e). Following the general procedure A, using **32e** (43.7 mg, 0.20 mmol). Purification by column chromatography on silica gel (Hexane) afforded the title compound as a colorless oil in 84% yield (68.6 mg). ¹H NMR (500 MHz, CDCl₃): δ 7.25-7.23 (m, 4H), 7.13-7.09 (m, 1H), 6.40 (dt, *J* = 15.5, 8.8 Hz, 1H), 6.19 (m, *J* = 15.5, 1.2 Hz, 1H), 1.95 (dd with Sn satellites, *J*_{H-Sn} = 72.2 Hz, *J* = 8.2, 1.1 Hz, 2H), 1.54-1.46 (m, 6H), 1.34-1.26 (m, 6H), 0.98-0.87 (m, 15H) ppm. ¹³C NMR (126 MHz, CDCl₃) δ 139.0, 131.3, 128.5, 125.8, 125.3, 125.1, 29.3, 27.5, 16.2, 13.9, 9.7 ppm. ¹¹⁹Sn NMR (149 MHz, CDCl₃) δ -11.78 ppm. Spectroscopic data for **33e** match those previously reported in the literature.⁹

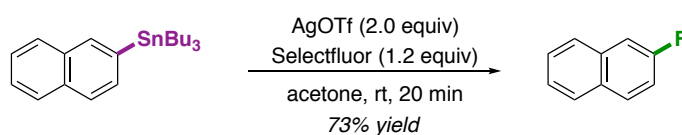
2.8.4. Gram scale reaction and synthetic applicability



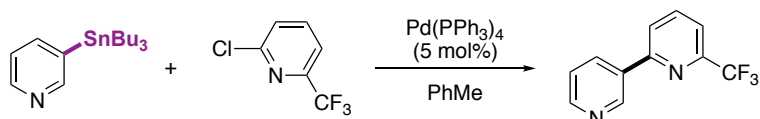
A 100 mL Schlenk was charged with **25a** (1.14 g, 5 mmol), Ni(COD)₂ (137 mg, 10 mol %), dcype (211 mg, 10 mol %) and CsF (760 mg, 5 mmol) and 20 mL of anhydrous toluene. The mixture was stirred for 2 minutes at room temperature. Then, Me₃SiSnBu₃ (2.3 g, 6.5 mmol) was added dropwise. The flask was taken out of the glovebox, and the mixture was stirred for 8 h at 90 °C. The flask was then cooled to room temperature and diluted with 60 mL hexane. The organic layer was washed with H₂O (3x) and brine, dried over anhydrous MgSO₄, and concentrated under reduced pressure. The crude material was purified by silica gel column chromatography (pentane) to yield **26a** (1.9 g, 91%) as colorless oil.



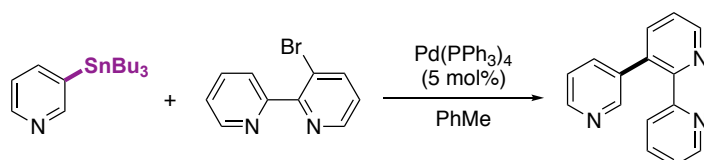
2-iodonaphthalene (35). An oven-dried 10 mL screw-capped test tube containing a stirring bar was charged with **26a** (208.5 mg, 0.50 mmol), I₂ (126.5 mg, 0.50 mmol) and CH₂Cl₂ (5.0 mL). The resulting solution was stirred at room temperature for 2 h.¹⁴ Then the mixture was concentrated and purified by column chromatography in silica gel (Hexane) to yield the title compound as a white solid in 85% yield (108 mg). ¹H NMR (300 MHz, CDCl₃): δ 8.26 (s, 1H), 7.82-7.79 (m, 1H), 7.74-7.71 (m, 2H), 7.58-7.55 (m, 1H), 7.51-7.49 (m, 2H) ppm. ¹³C NMR (126 MHz, CDCl₃) δ 136.7, 135.1, 134.5, 132.2, 129.6, 128.0, 126.9, 126.8, 126.6, 91.7 ppm. Mp 53.2-54.6 °C, (Lit. 54.0-54.5 °C). Spectroscopic data for **35** match those previously reported in the literature.¹⁵



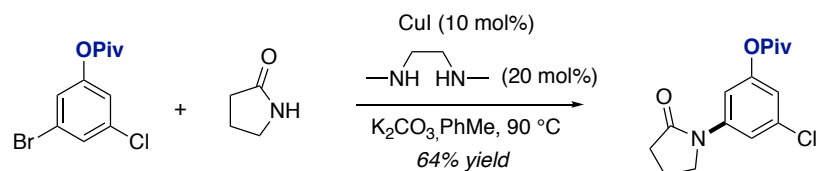
2-fluoronaphthalene (36). A 25 mL round bottom flask containing a stirring bar was charged with **26a** (208.5 mg, 0.50 mmol) and acetone (5.0 mL). Subsequently, AgOTf (256.9 mg, 1.0 mmol) and Selectfluor (212.4 mg, 0.6 mmol) were sequentially added at room temperature. The reaction mixture was stirred for 20 min at 25 °C and then concentrated under vacuum.¹² The residue was purified by chromatography (hexane:EA 50:1) to yield the title compound as white solid in 73% isolated yield (54 mg). ¹H NMR (300 MHz, CDCl₃): δ 8.18 (s, 1H), 7.98-7.88 (m, 4H), 7.56-7.48 (m, 2H) ppm. ¹³C NMR (101 MHz, CDCl₃) δ 138.6, 133.9, 132.8, 128.7, 128.4, 127.8, 126.5, 126.3, 126.2, 125.9 ppm. ¹⁹F NMR (376 MHz, CDCl₃) δ -128.1 ppm. Mp 59.4-60.3 °C, (Lit. 59.0-60.0 °C). Spectroscopic data for **36** match those previously reported in the literature.¹³



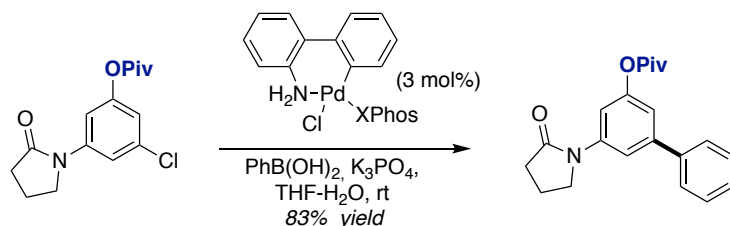
6-(trifluoromethyl)-2,3'-bipyridine(37). An oven-dried 10 mL screw-capped test tube containing a stirring bar was charged with **31k** (184 mg, 0.50 mmol), 2-chloro-5-fluoropyridine (90 mg, 0.5 mmol) and Pd(PPh₃)₄ (10.4 mg, 0.025 mmol). Anhydrous toluene (3 mL) was then added by syringe and the mixture was stirred for 16 h at 110 °C. The reaction was then cooled to room temperature and filtered through a short silica gel column eluting with dichloromethane. The solution was concentrated under reduced pressure to give a crude residue, which was purified by silica gel flash column chromatography (Hex:EtOAc:DCM 1:3:1) to yield the title product as a white solid in 85% yield (95.2 mg). ¹H NMR (500 MHz, CDCl₃): δ 9.20 (d, *J* = 2.0 Hz, 1H), 8.92 (s, 1H), 8.65 (dd, *J* = 4.8, 1.6 Hz, 1H), 8.31 (dt, *J* = 8.0, 1.8 Hz, 1H), 7.97 (dt, *J* = 8.3, 2.3 Hz, 1H), 7.84-7.82 (m, 1H), 7.38 (ddd, *J* = 8.0, 4.8, 0.8 Hz, 1H) ppm. ¹³C NMR (101 MHz, CDCl₃) δ 158.1, 150.9, 148.5, 146.9, 134.7, 134.2, 133.5, 127.6, 125.6 (*J* = 49.5 Hz, 17.2 Hz), 123.7, 123.6 (*J* = 409.6 Hz, 135.3 Hz), 120.0 ppm. ¹⁹F NMR (376 MHz, CDCl₃) δ -62.5 ppm. Mp 61.4-63.1 °C. IR (neat, cm⁻¹): 1601, 1582, 1326, 1302, 1109, 1082, 812, 701, 432. HRMS (ESI) [C₁₁H₈F₃N₂] (M+H) *calcd.* 225.0634, *found* 225.0635.



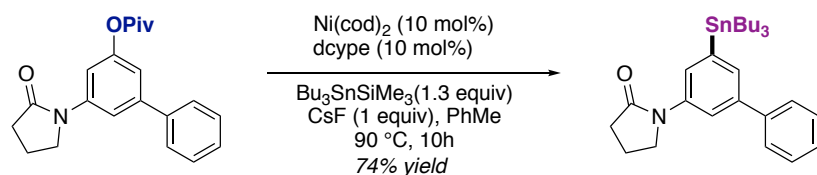
2,2',3',3''-terpyridine(38). An oven-dried 10 mL screw-capped test tube containing a stirring bar was charged with **31k** (184 mg, 0.5 mmol), 2-bromo-5-fluoropyridine (117 mg, 0.5 mmol) and Pd(PPh₃)₄ (10.4 mg, 0.025 mmol). Anhydrous toluene (3 mL) was then added by syringe and the mixture was stirred for 16 h at 110 °C. The reaction was then cooled to room temperature and filtered through a short silica gel column eluting with dichloromethane. The solution was concentrated under reduced pressure to give a crude residue, which was purified by silica gel flash column chromatography (Hex:EtOAc:DCM 2:4:1) to yield the title product as a white solid in 92% yield (107.2 mg). ¹H NMR (500 MHz, d₈-Toulene): δ 9.42 (s, 1H), 8.60-8.56 (m, 3H), 8.52 (d, *J* = 8.6 Hz, 1H), 8.09 (dt, *J* = 7.9, 2.0 Hz, 1H), 7.30-7.20 (m, 2H), 7.13-7.11 (m, 1H), 6.89 (dd, *J* = 7.9, 2.0 Hz, 1H), 6.76 (ddd, *J* = 7.4, 4.7, 1.1 Hz, 1H) ppm. ¹³C NMR (126 MHz, CDCl₃) δ 156.3, 156.1, 154.0, 150.1, 149.3, 148.6, 138.10, 137.1, 134.9, 134.4, 124.1, 123.7, 121.4, 120.4, 120.2 ppm. Mp 99.5-101.8 °C. IR (neat, cm⁻¹): 1582, 1561, 1470, 1421, 1391, 767, 742, 701, 618. HRMS (ESI) [C₁₅H₁₂N₃] (M+H) *calcd.* 234.1026, *found* 234.1030.



3-chloro-5-(2-oxopyrrolidin-1-yl)phenyl pivalate (40). A Schlenk tube was charged with CuI (19 mg, 0.1 mmol, 10 mol%), K₂CO₃ (277 mg, 2 mmol, 2.0 equiv), and was evacuated and backfilled with argon three times. Subsequently, N,N'-Dimethylethylenediamine (17.6 mg, 0.2 mmol, 20 mol%), 2-Pyrrolidinone (85 mg, 1 mmol, 1.0 equiv) and a solution of **39** (291 mg, 1 mmol, 1.0 equiv) in 5 mL anhydrous PhMe were added under argon. The Schlenk tube was sealed with a Teflon valve and the reaction mixture was stirred at 90 °C for 10 h.¹⁰ The resulting suspension was allowed to reach room temperature and filtered through silica gel eluting with ethyl acetate (10 mL). The filtrate was concentrated and the residue was purified by flash chromatography in silica gel (Hex:EtOAc 1:1) to afford the title compound as a pale yellow oil in 64% yield (188.8 mg). ¹H NMR (300 MHz, CDCl₃): δ 7.47 (t, *J* = 3.0 Hz, 1H), 7.39 (t, *J* = 3.0 Hz, 1H), 6.86 (t, *J* = 3.0 Hz, 1H), 3.81 (t, *J* = 6.0 Hz, 2H), 2.60 (t, *J* = 6.0 Hz, 2H), 2.19-2.09 (m, 2H), 1.33 (s, 9H) ppm. ¹³C NMR (75 MHz, CDCl₃) δ 176.6, 174.4, 151.7, 141.0, 134.6, 117.8, 116.5, 111.3, 48.6, 39.1, 32.8, 27.1, 17.7 ppm. IR (neat, cm⁻¹): 2975, 1751, 1702, 1598, 1457, 1325, 1219, 1188, 1176, 730. HRMS (ESI) [C₁₅H₁₃ClNO₃] (M+H) *calcd.* 296.1048, *found* 296.1051.



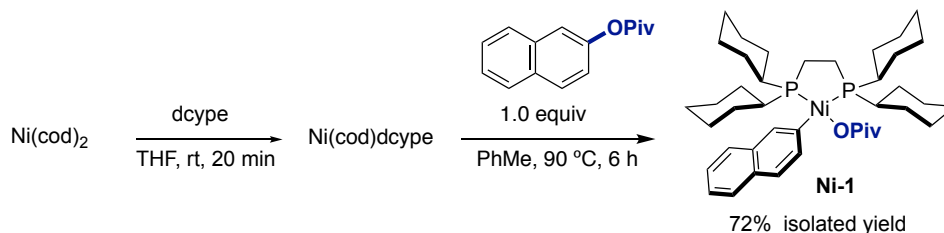
5-(2-oxopyrrolidin-1-yl)-[1,1'-biphenyl]-3-yl pivalate (41). An oven-dried schlenk tube containing a stirring bar was charged with XPhos Pd G2 (11.8 mg, 0.015 mmol, 3mol%), and phenylboronic acid (90 mg, 0.75 mmol, 1.50 equiv). The schlenk tube was evacuated and back-filled under Ar (this procedure was repeated two times). A solution of **40** (147 mg, 0.5 mmol, 1.0 equiv) in degassed THF (1.0 mL) and a 0.5 M solution of K₃PO₄ in degassed H₂O (2.0 mL) were then added. The schlenk tube was next closed and stirred at rt for 12 h.¹¹ Water and EtOAc were then added to the mixture and extracted twice with EtOAc. The combined organic layers were dried over MgSO₄ and concentrated under reduced pressure. Purification by flash column chromatography in silica gel (Hex:EtOAc 1:1) provided the title compound as a pale yellow oil in 83% yield (139.8 mg). ¹H NMR (300 MHz, CDCl₃): δ 7.64 (t, *J* = 3.0 Hz, 1H), 7.59-7.56 (m, 2H), 7.48 (t, *J* = 3.0 Hz, 1H), 7.45-7.34 (m, 3H), 7.70 (t, *J* = 3.0 Hz, 1H), 3.88 (t, *J* = 6.0 Hz, 2H), 2.60 (t, *J* = 6.0 Hz, 2H), 2.18-2.08 (m, 2H), 1.38 (s, 9H) ppm. ¹³C NMR (75 MHz, CDCl₃) δ 177.0, 174.4, 151.7, 142.9, 140.7, 140.2, 128.8, 127.8, 127.3, 116.4, 115.5, 112.1, 48.7, 39.2, 32.8, 27.2, 17.9 ppm. IR (neat, cm⁻¹): 3026, 2980, 2950, 1739, 1705, 1239, 729, 694. HRMS (ESI) [C₂₁H₂₄NO₃] (M+H) *calcd.* 338.1751, *found* 338.1754.



1-(5-(tributylstannyl)-[1,1'-biphenyl]-3-yl)pyrrolidin-2-one (42). Following the general procedure A using **41** (67.4 mg, 0.2 mmol) at 90 °C. After 10 h, purification by column chromatography in silica gel (Hex: 2:1)

afforded the title compound as a pale yellow oil in 74% yield (77.8 mg). ^1H NMR (300 MHz, CDCl_3): δ 7.79 (t, $J = 3.0$ Hz, 1H), 7.64-7.59 (m, 3H), 7.48-7.42 (m, 3H), 7.38-7.33 (m, 1H), 3.93 (t, $J = 6.0$ Hz, 2H), 2.64 (t, $J = 6.0$ Hz, 2H), 2.24-2.21 (m, 2H), 1.70-1.53 (m, 6H), 1.40-1.30 (m, 6H), 1.14-1.08 (m, $J_{\text{H-Sn}} = 66.8$ Hz, 6H), 0.91 (t, $J = 9.0$ Hz, 9H) ppm. ^{13}C NMR (75 MHz, CDCl_3) δ 174.4, 143.5, 141.5, 141.3, 139.4, 131.5, 128.8, 127.5, 127.4, 126.6, 119.3, 49.2, 32.9, 29.21, 27.5, 18.3, 13.8, 9.9 ppm. ^{119}Sn NMR (149 MHz, CDCl_3) δ -38.94 ppm. IR (neat, cm^{-1}): 2955, 2923, 2870, 2851, 1696, 1411, 1378, 732, 698. HRMS (ESI) $[\text{C}_{28}\text{H}_{42}\text{NOSn}]$ (M+H) *calcd.* 528.2283, *found* 528.2293.

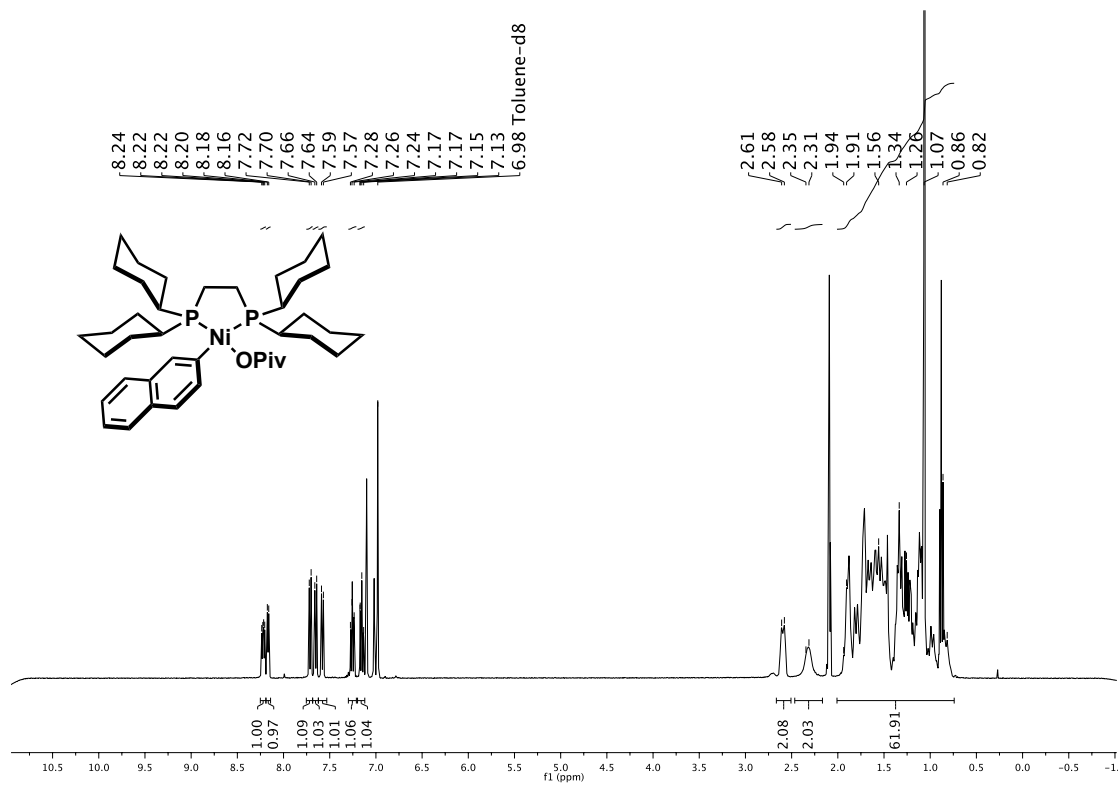
2.8.5. Synthesis of oxidative addition complex Ni-1



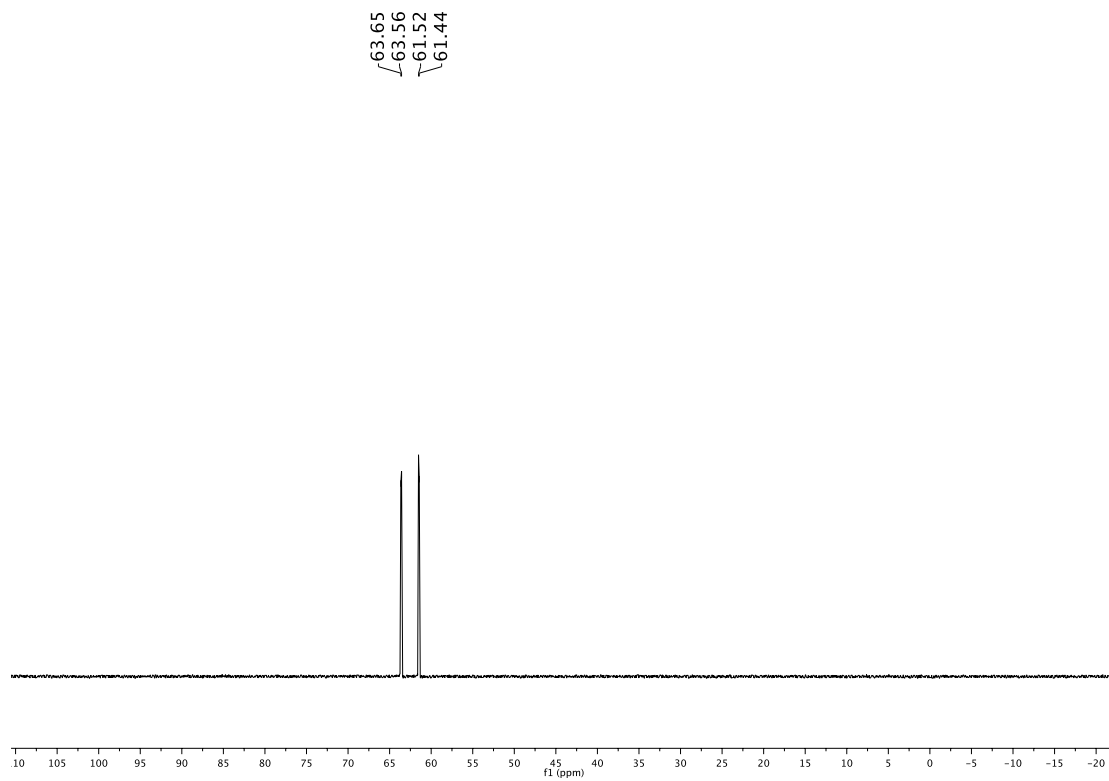
Synthesis of Ni(cod)dcype. An oven-dried 20 mL vial containing a stirring bar was introduced in a nitrogen-filled glovebox and charged with the $\text{Ni}(\text{COD})_2$ and dcype (1:1) in THF (1 M). After stirring the mixture for 20 min, it was cooled to 0 °C and the title compound cleanly precipitated from the solution as a yellow solid in 83% yield. Spectroscopic data for Ni(cod)dcype match those previously reported in the literature.¹⁷

Synthesis of Ni-1. An oven-dried 5 mL screw-capped test tube containing a stirring bar was introduced in a nitrogen-filled glovebox and charged with Ni(cod)dcype (236 mg, 0.4 mmol, 1.0 equiv), **25a** (1.0 equiv) and anhydrous toluene (8 mL). The tube was then taken out of the glovebox and stirred at 90 °C for 8 h. The mixture was then allowed to cool to room temperature, and the liquids were removed under vacuum. The residue was recrystallized from toluene:Hex (1:20) at 0 °C to afford complex **Ni-1** as an orange crystalline solid (204 mg, 72% yield). ^1H NMR (400 MHz, d_8 -toluene): δ 8.24-8.20 (m, 1H), 8.17 (d, $J = 8.0$ Hz, 1H), 7.71 (d, $J = 8.0$ Hz, 1H), 7.65 (d, $J = 8.0$ Hz, 1H), 7.58 (d, $J = 8.0$ Hz, 1H), 7.26 (t, $J = 8.8$ Hz, 1H), 7.15 (t, $J = 8.8$ Hz, 1H), 2.61-2.58 (m, 2H), 2.40-2.20 (m, 2H), 1.94-0.82 (m, 53H) ppm. ^{31}P NMR (162 MHz, d_8 -toluene): δ 63.6 (d, $J_{\text{PP}} = 13.9$ Hz, 1P), 61.5 (d, $J_{\text{PP}} = 13.9$ Hz, 1P) ppm. Spectroscopic data for complex **I** match those previously reported in the literature.¹⁷

¹H NMR of complex Ni-1



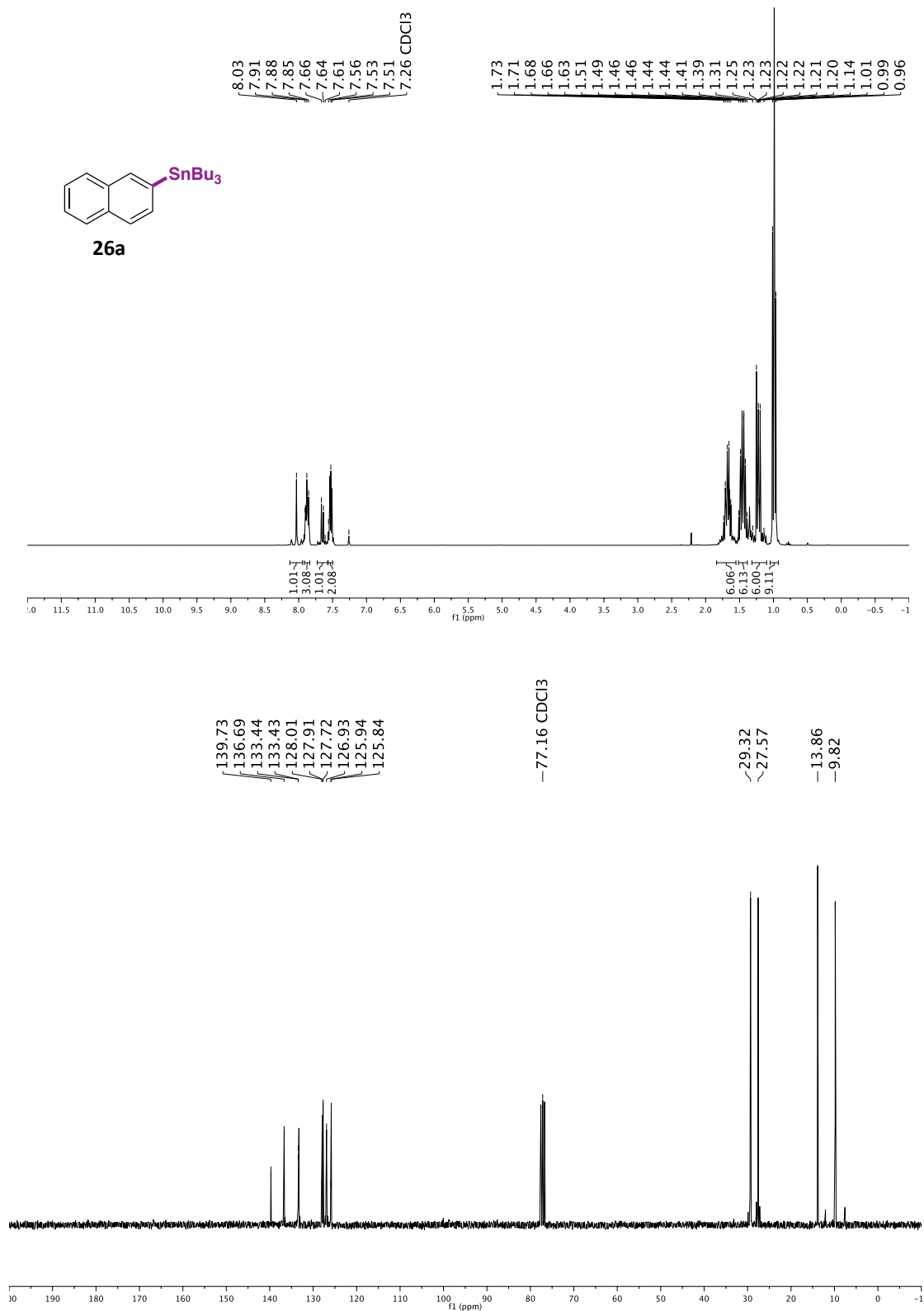
³¹P NMR of complex Ni-1



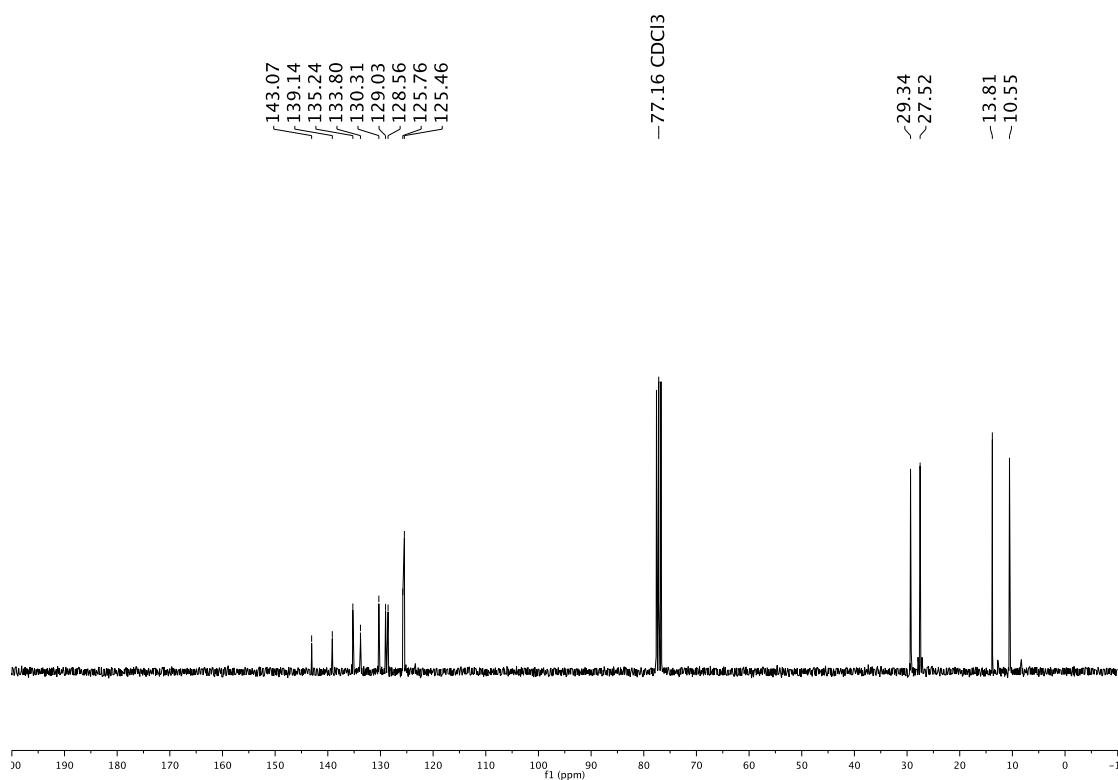
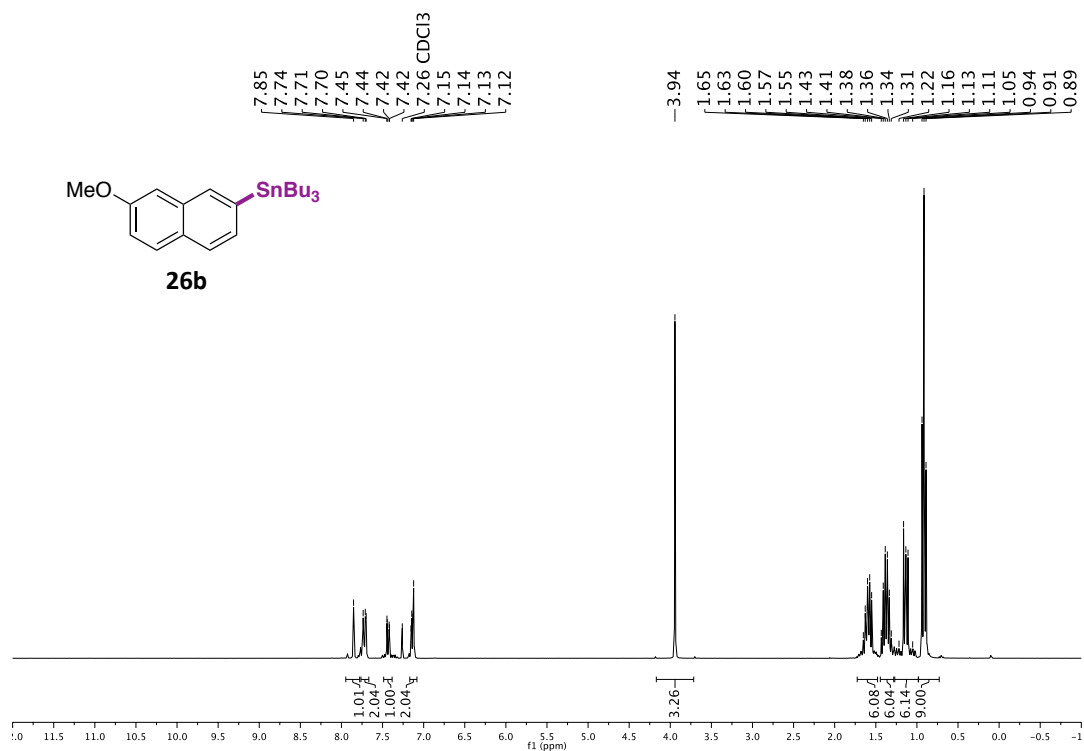
2.8.6. Bibliography of known compounds

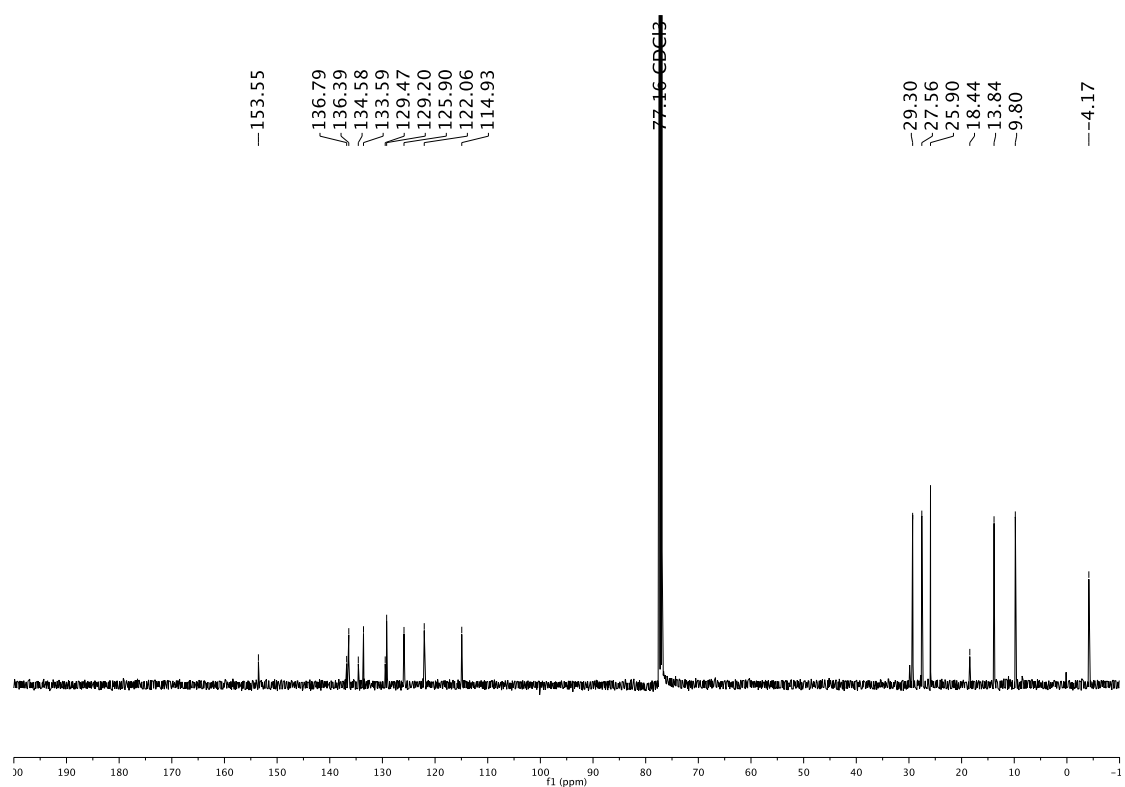
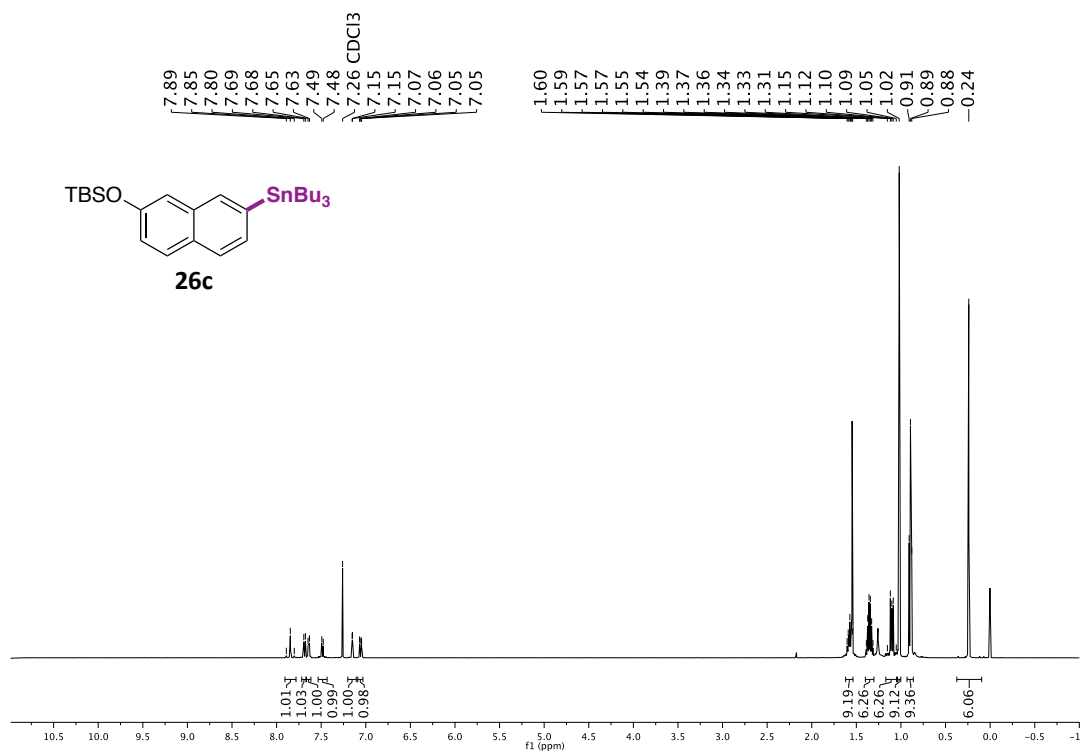
1. Oikawa, A.; Kindaichi, G.; Shimotori, Y.; Okimoto, M.; Hoshi, M. *Tetrahedron* **2015**, *71*, 1705.
2. Tius, M. A.; Gomez-Galeno, J. *Tetrahedron Letters* **1986**, *27*, 2571.
3. Aboutayab, K.; Caddick, S.; Jenkins, K.; Joshi, S.; Khan, S. *Tetrahedron* **1996**, *52*, 11329.
4. Czakó, B.; Kürti, L.; Mammoto, A.; Ingber, D. E.; Corey, E. J. *J. Am. Chem. Soc.* **2009**, *131*, 9014.
5. Komeyama, K.; Asakura, R.; Takaki, K. *Org. Biomol. Chem.* **2015**, *13*, 8713.
6. Lakshmi, B. V.; Wefelscheid, U. K.; Kazmaier, U. *Synlett* **2011**, *3*, 345.
7. Chun, J.-H.; Lu, S.; Pike V. W. *Eur. J. Org. Chem.* **2011**, *23*, 4439.
8. Fargeas, V.; Favresse, F.; Mathieu, D.; Beaudet, I.; Charrue, P.; Lebret, B.; Piteau, M.; Quintard, P.-Q. *Eur. J. Org. Chem.* **2003**, *9*, 1711.
9. Wallner, O. A.; Szabo, K. *J. Org. Lett.* **2004**, *6*, 1829.
10. Klapars, A.; Huang, X.; Buchwald, S. L. *J. Am. Chem. Soc.* **2002**, *124*, 7421.
11. Kinzel, T.; Zhang, Y.; Buchwald, S. L. *J. Am. Chem. Soc.* **2010**, *132*, 14073.
12. Furuya, T.; Strom, A. E.; Ritter, T. *J. Am. Chem. Soc.* **2009**, *131*, 1662.
13. Ichiishi, N.; Canty, A. J.; Yates, B. F.; Sanford, M. S. *Org. Lett.* **2013**, *15*, 5134.
14. Pati, K.; dos Passos Gomes, G.; Harris, T.; Hughes, A.; Phan, H.; Banerjee, T.; Hanson, K.; Alabugin, I. V. *J. Am. Chem. Soc.* **2015**, *137*, 1165.
15. Shen, H.-C.; Pal, S.; Lian, J.-J.; Liu, R.-S. *J. Am. Chem. Soc.* **2003**, *125*, 15762.
16. Freund, R. R. A.; Görls, H.; Langer, J. *Dalton Trans.* **2014**, *43*, 13988.
17. Muto, K.; Yamaguchi, J.; Lei, A.; Itami, K. *J. Am. Chem. Soc.* **2013**, *135*, 16384.

2.8.7. NMR spectra

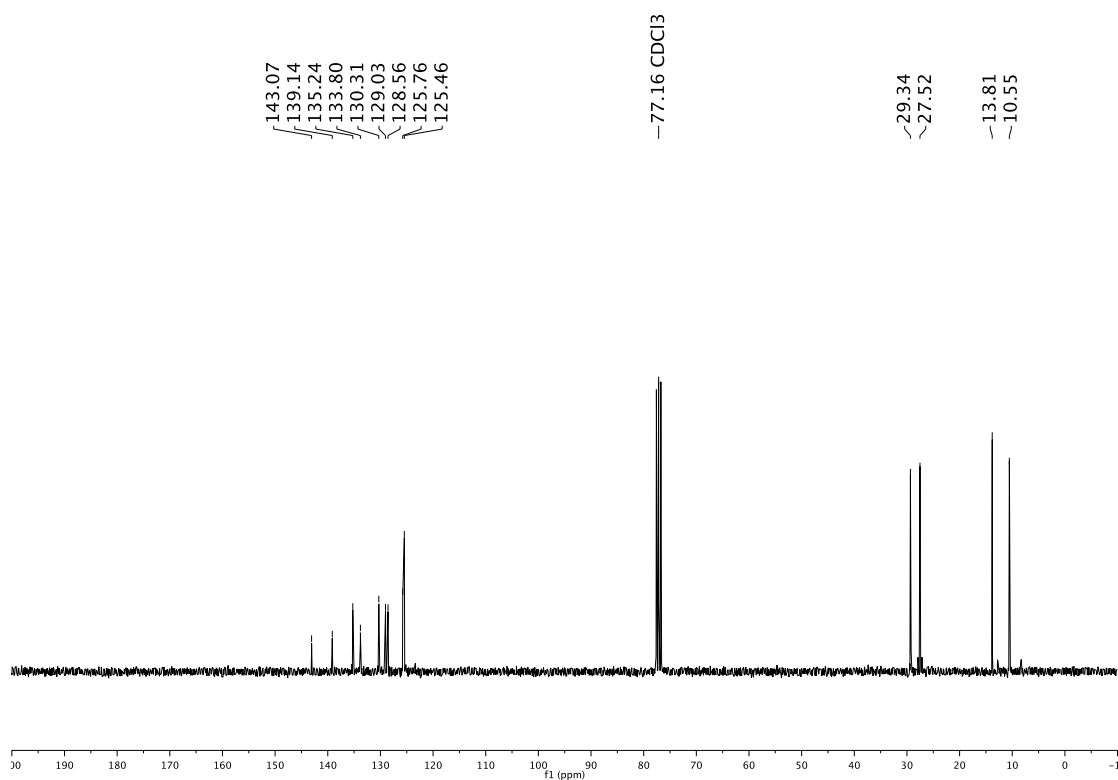
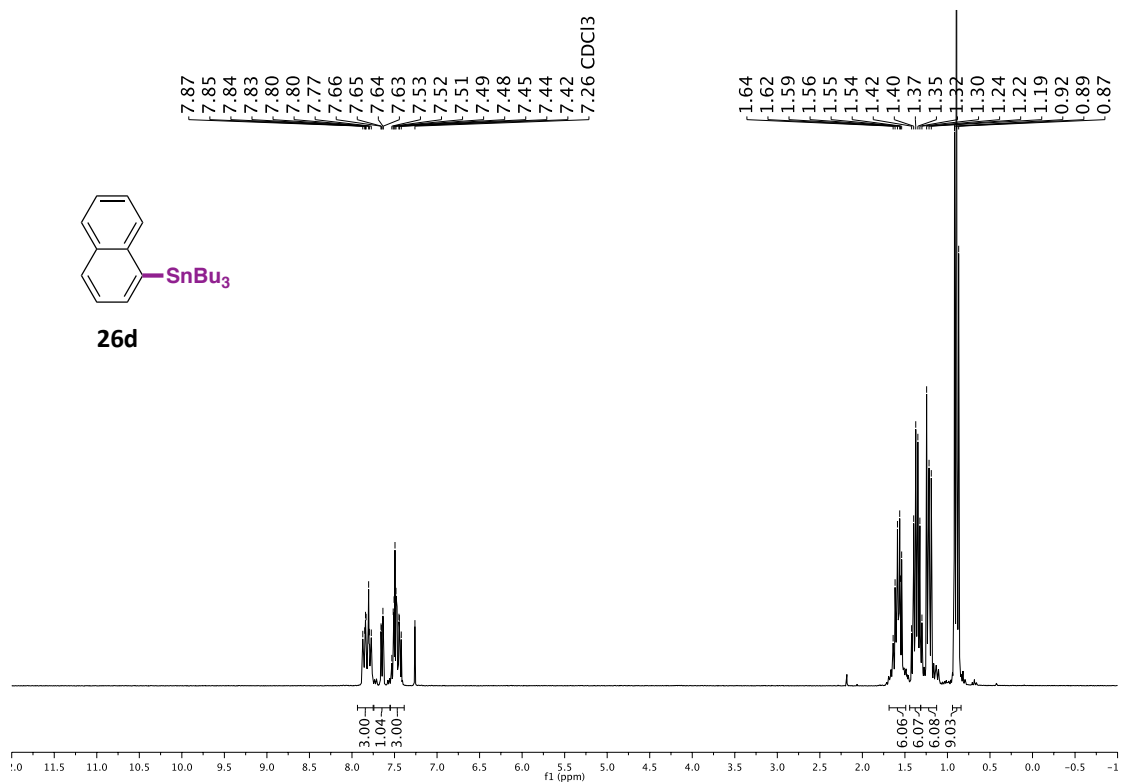


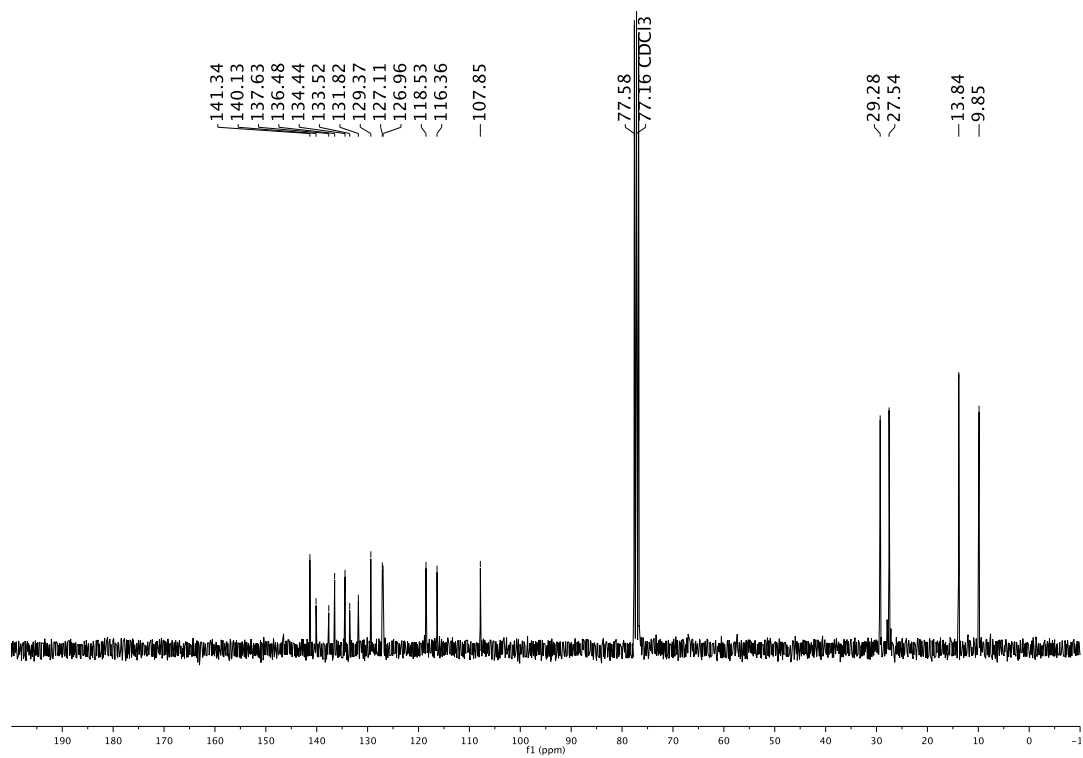
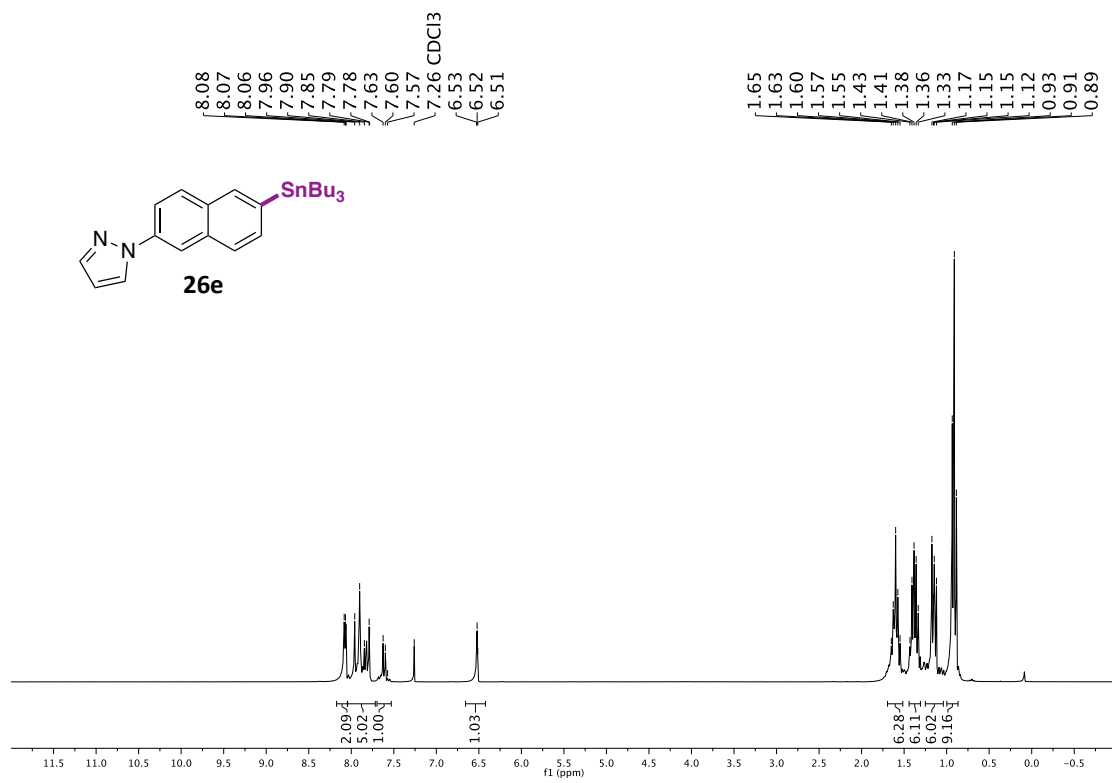
Ni-Catalyzed Stannylation of Aryl Ester via C-O Bond Cleavage



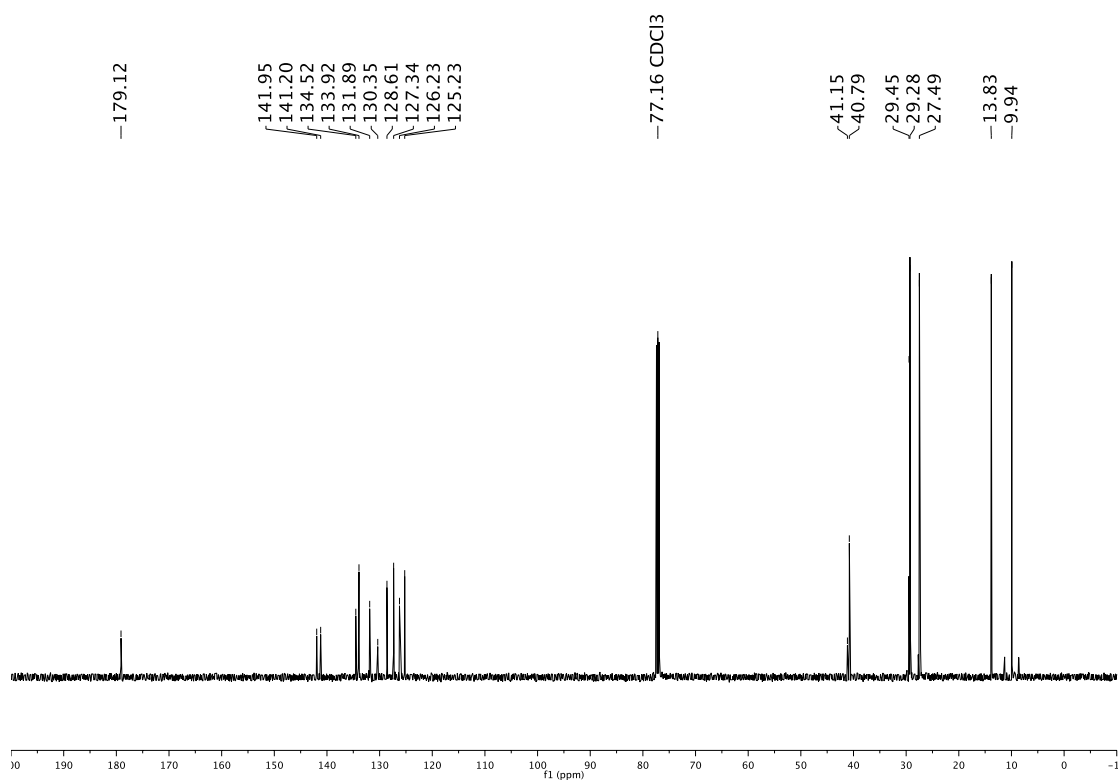
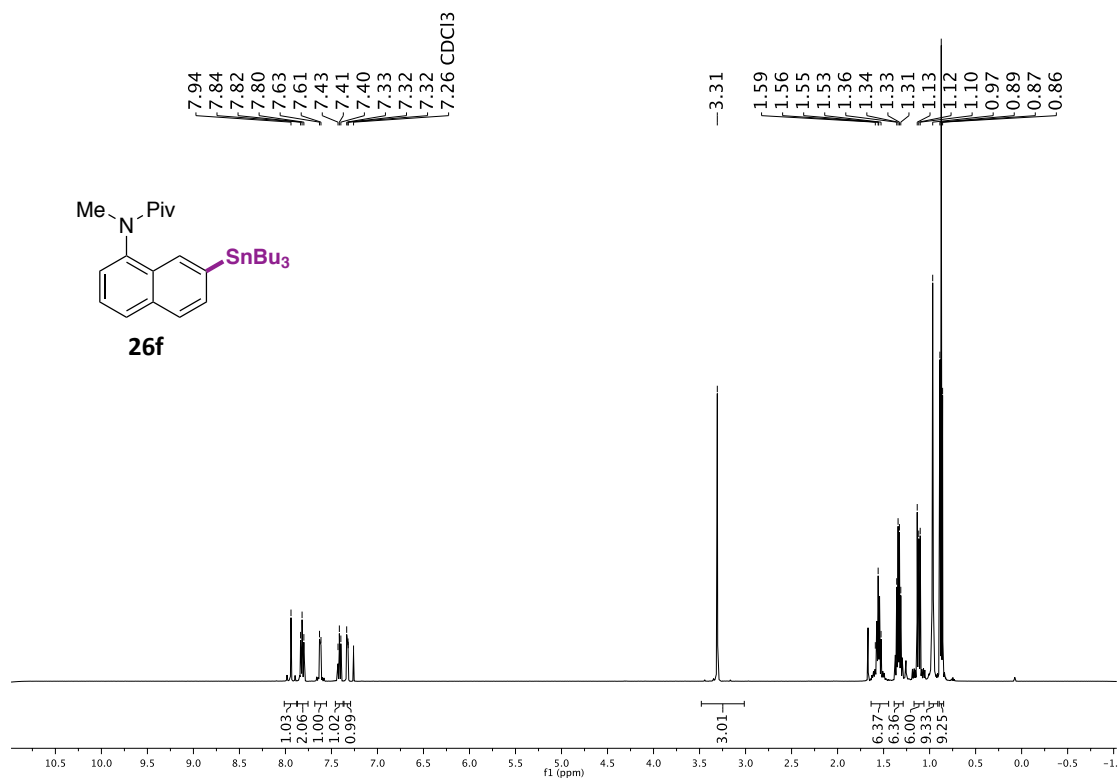


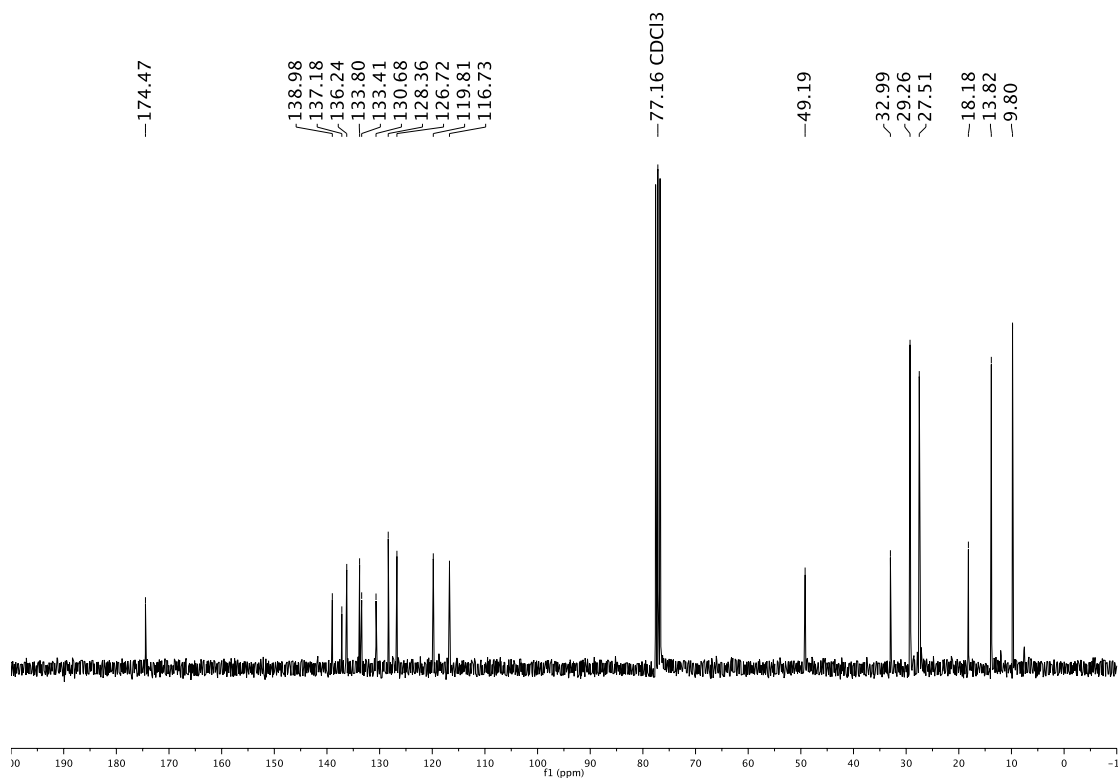
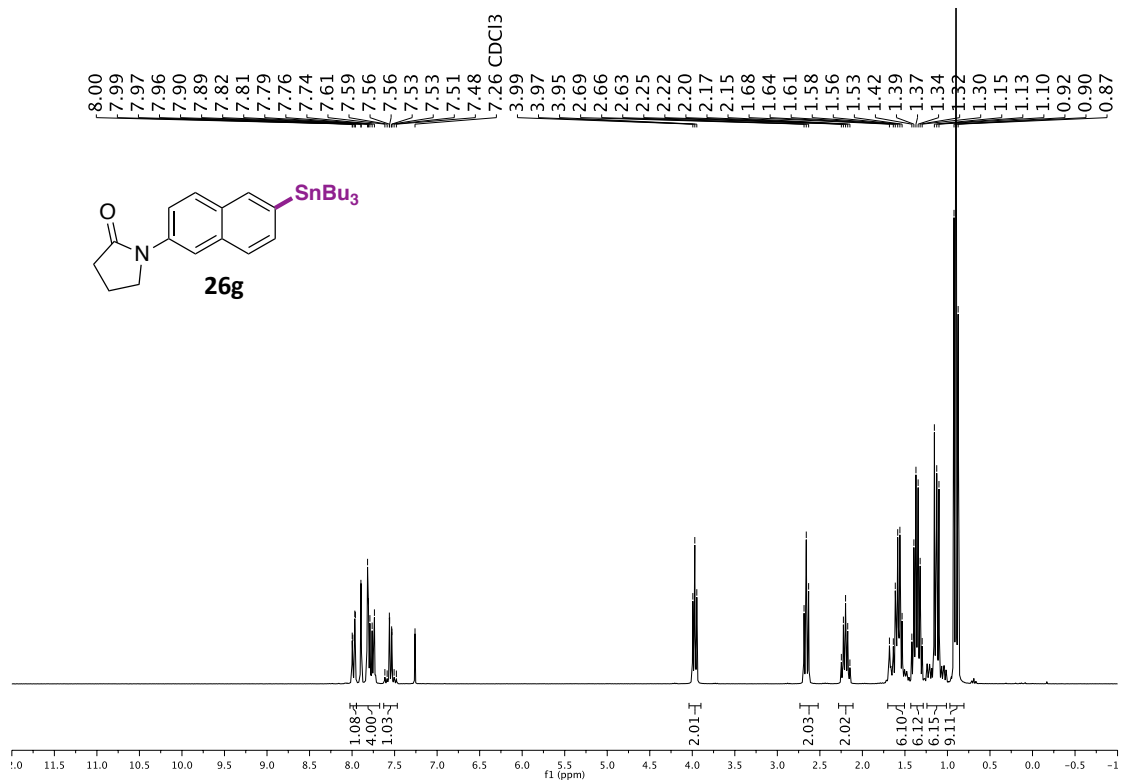
Ni-Catalyzed Stannylation of Aryl Ester via C-O Bond Cleavage



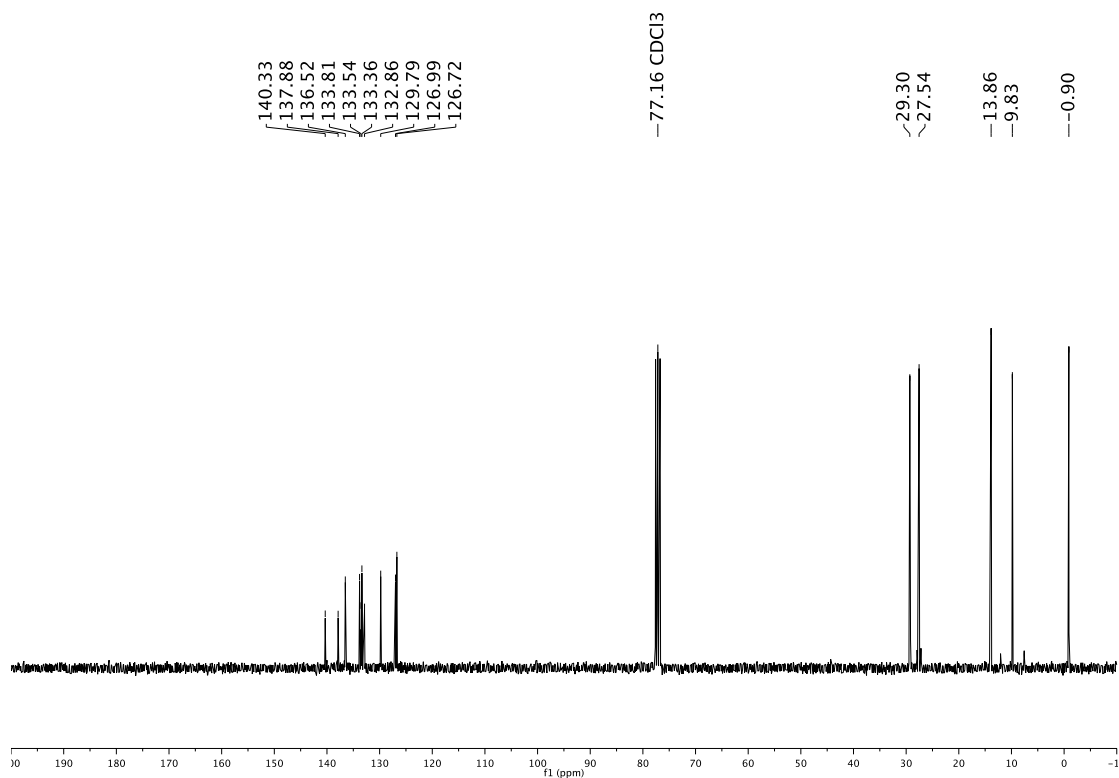
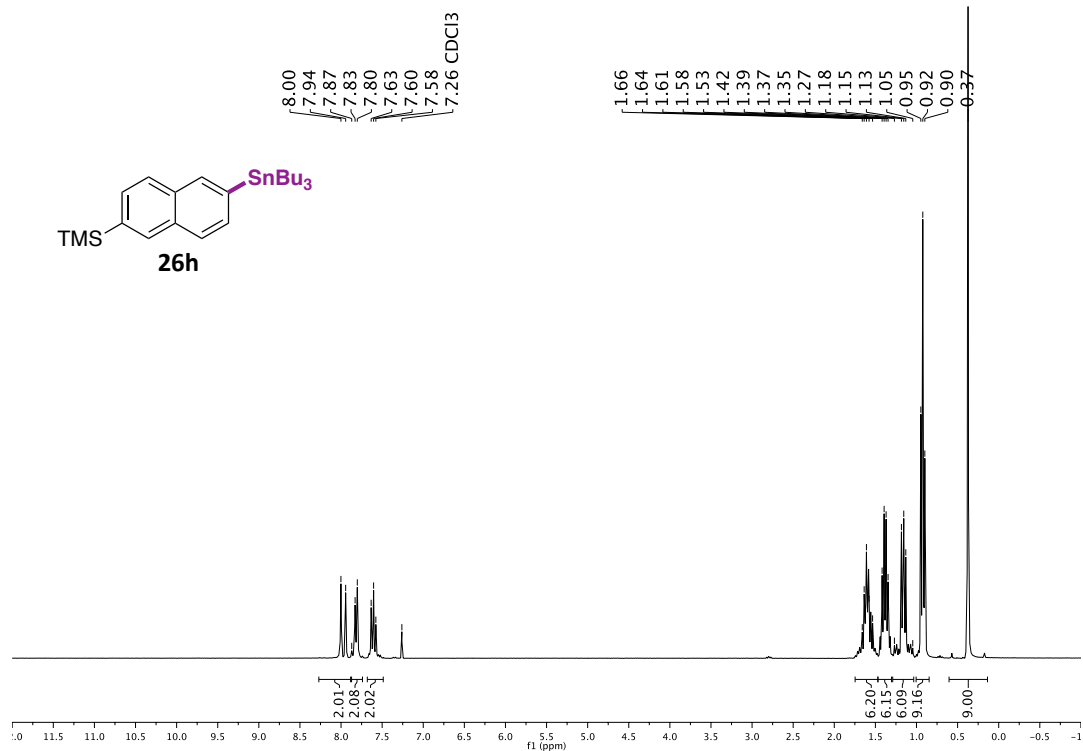


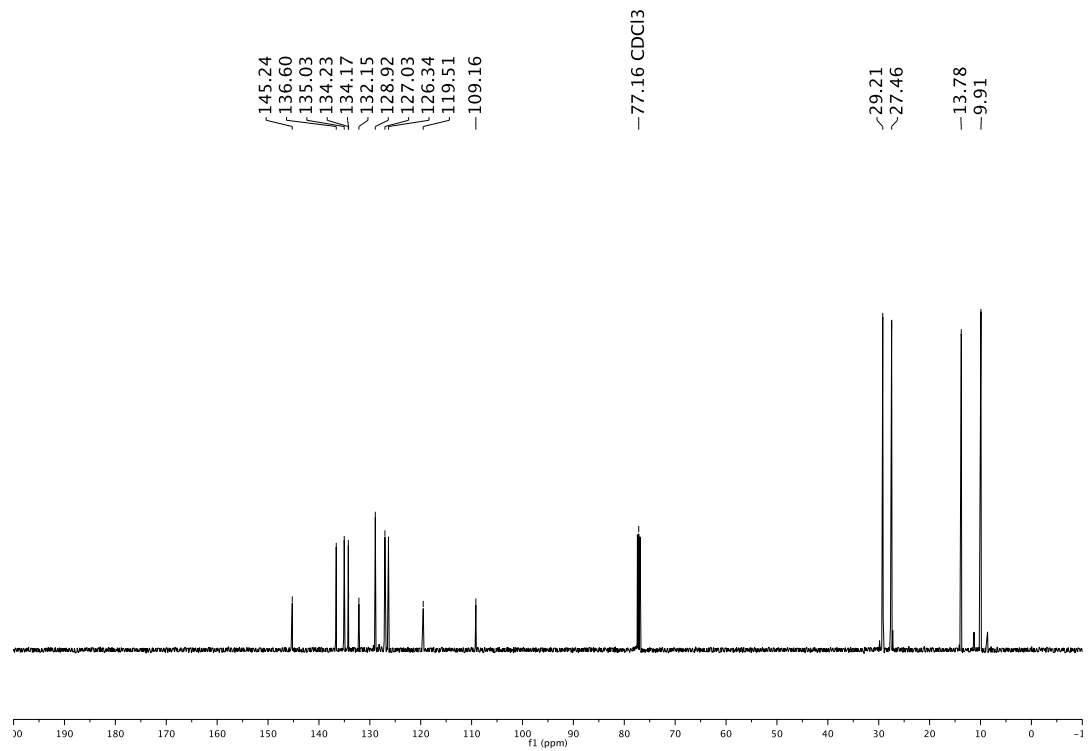
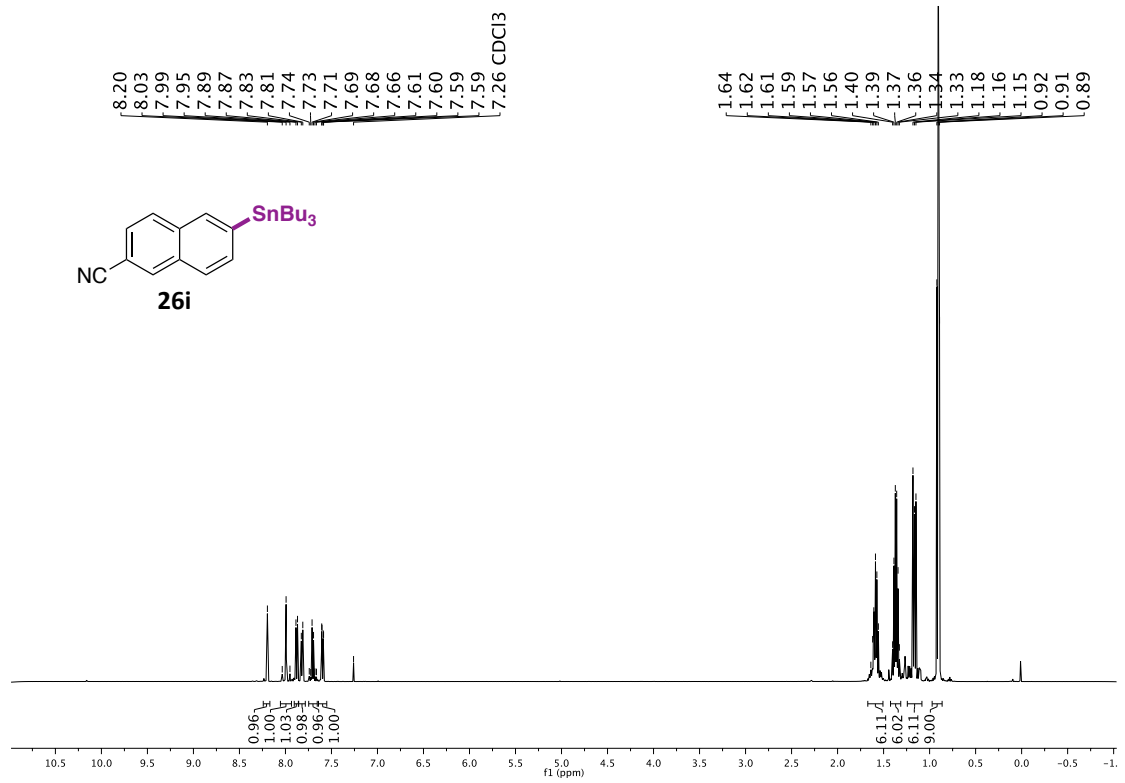
Ni-Catalyzed Stannylation of Aryl Ester via C-O Bond Cleavage



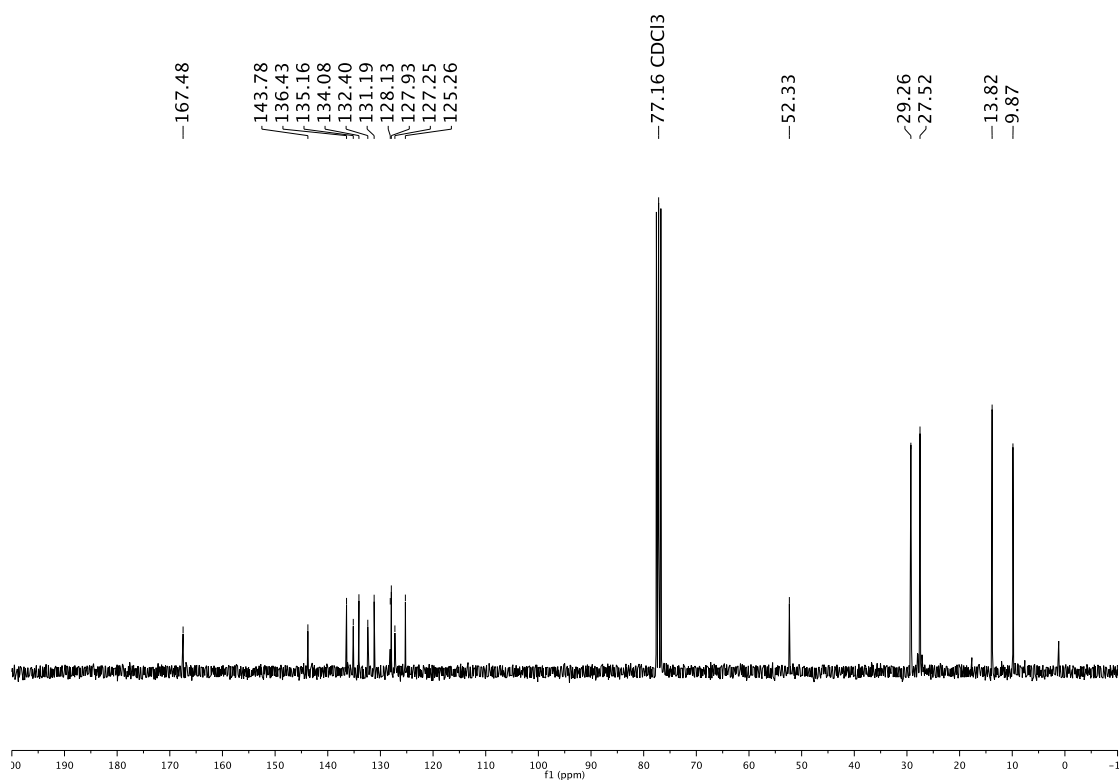
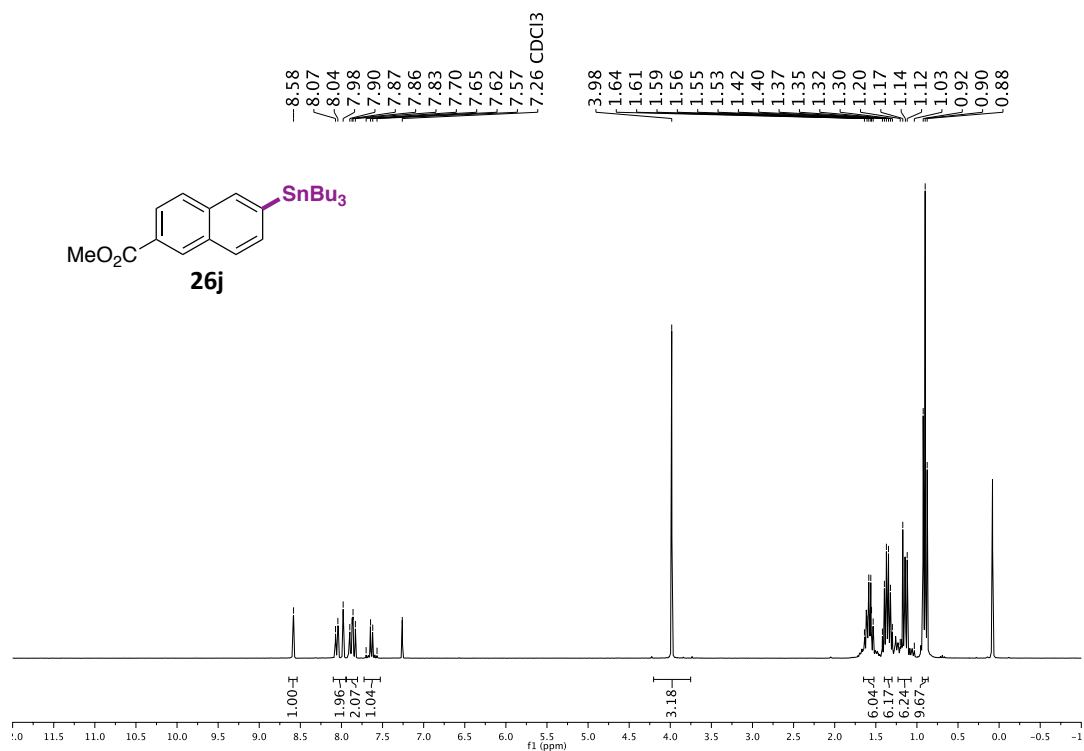


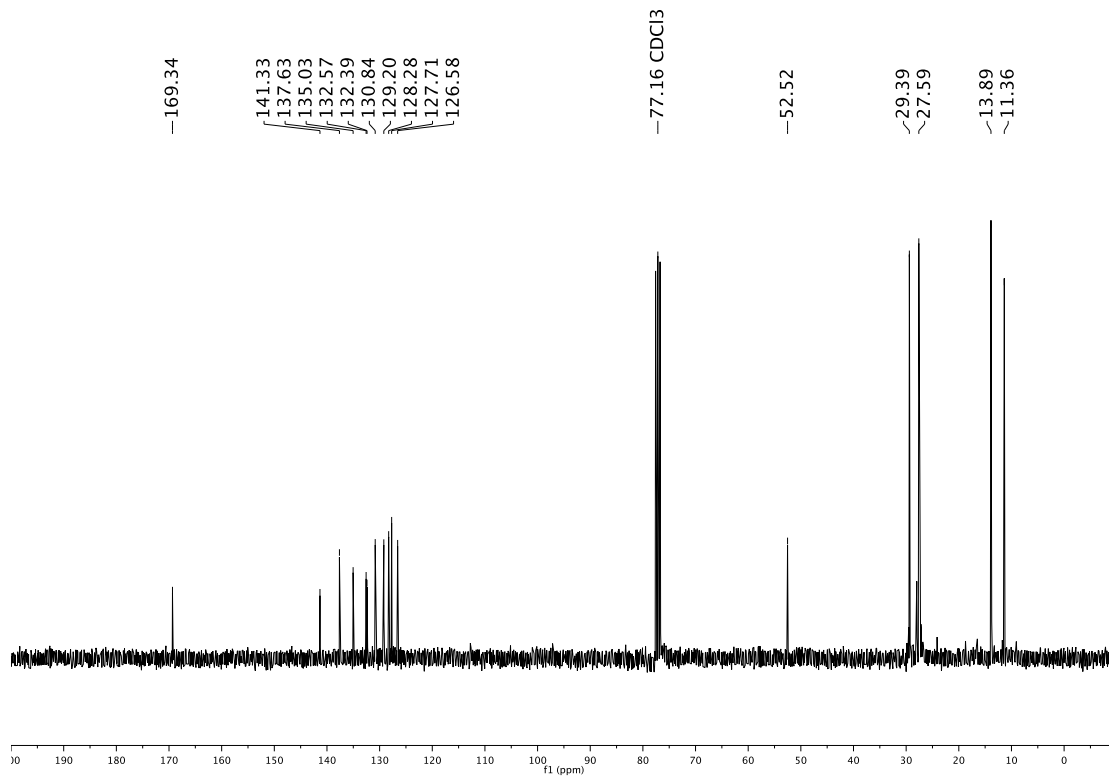
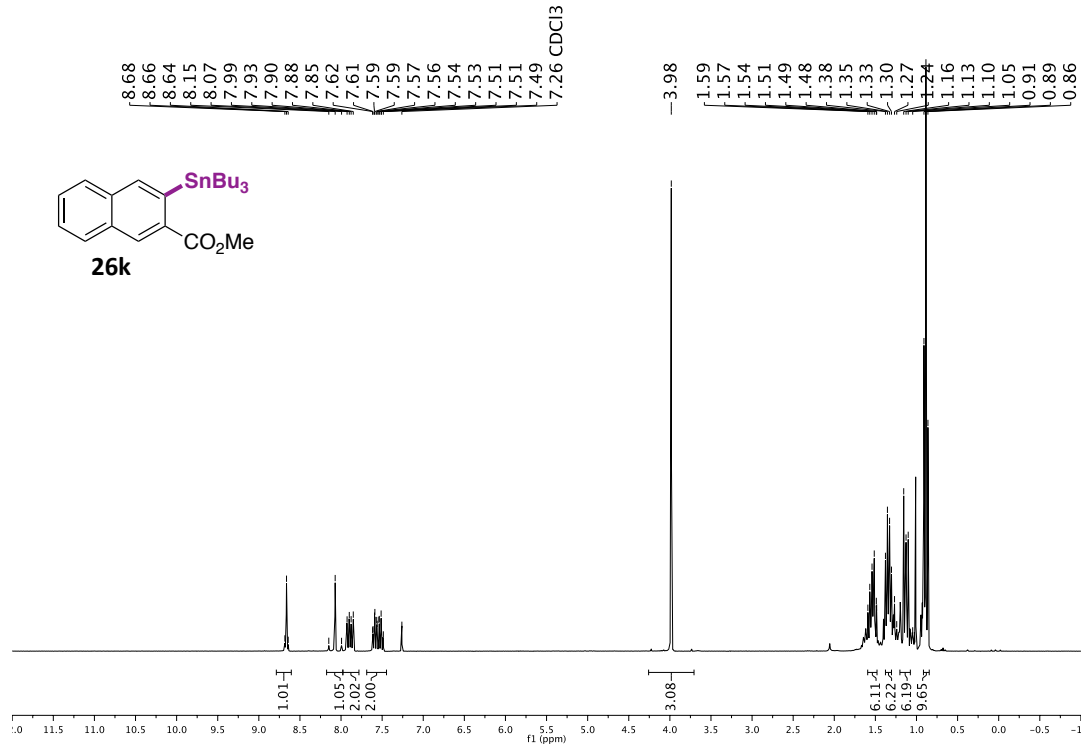
Ni-Catalyzed Stannylation of Aryl Ester via C-O Bond Cleavage



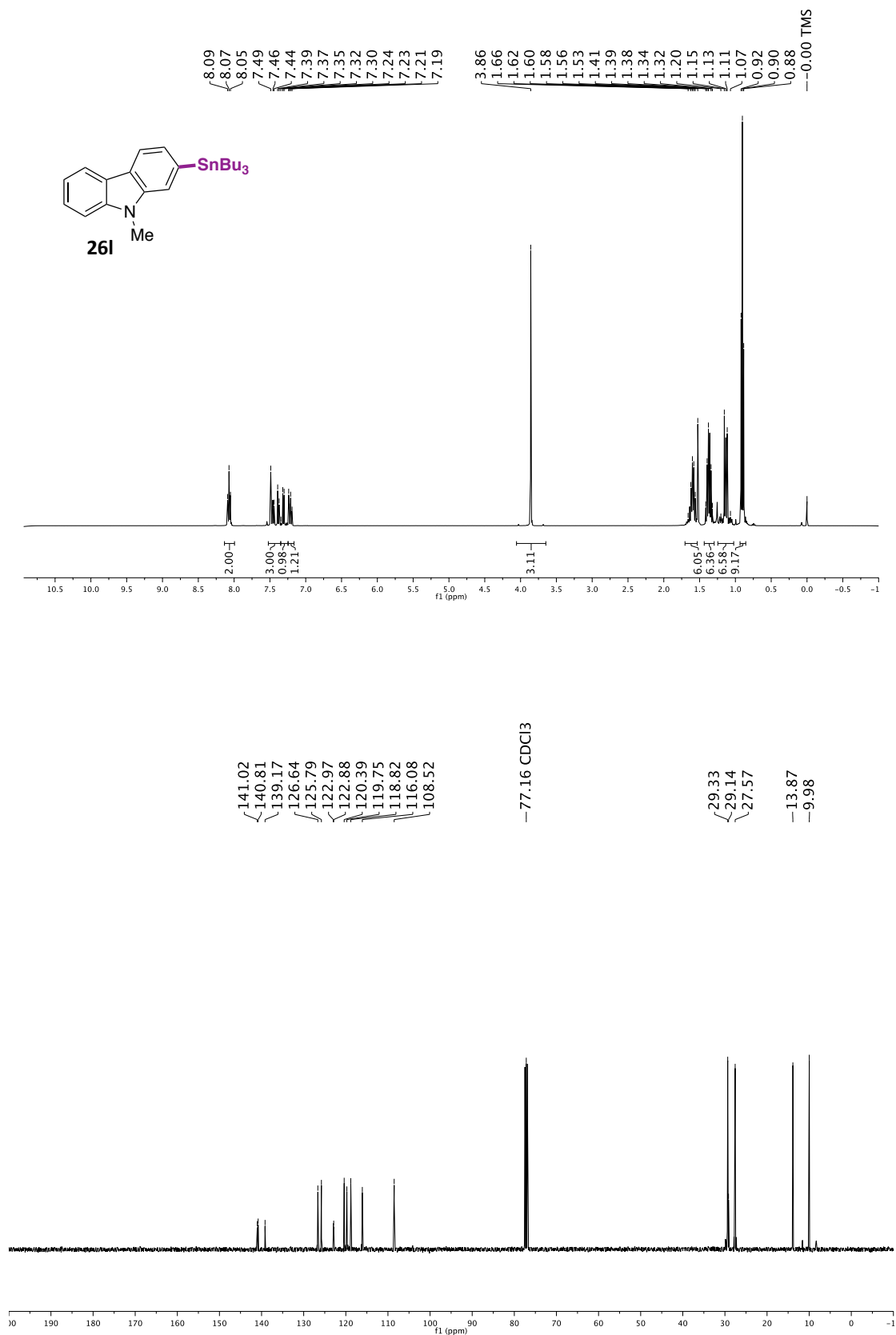


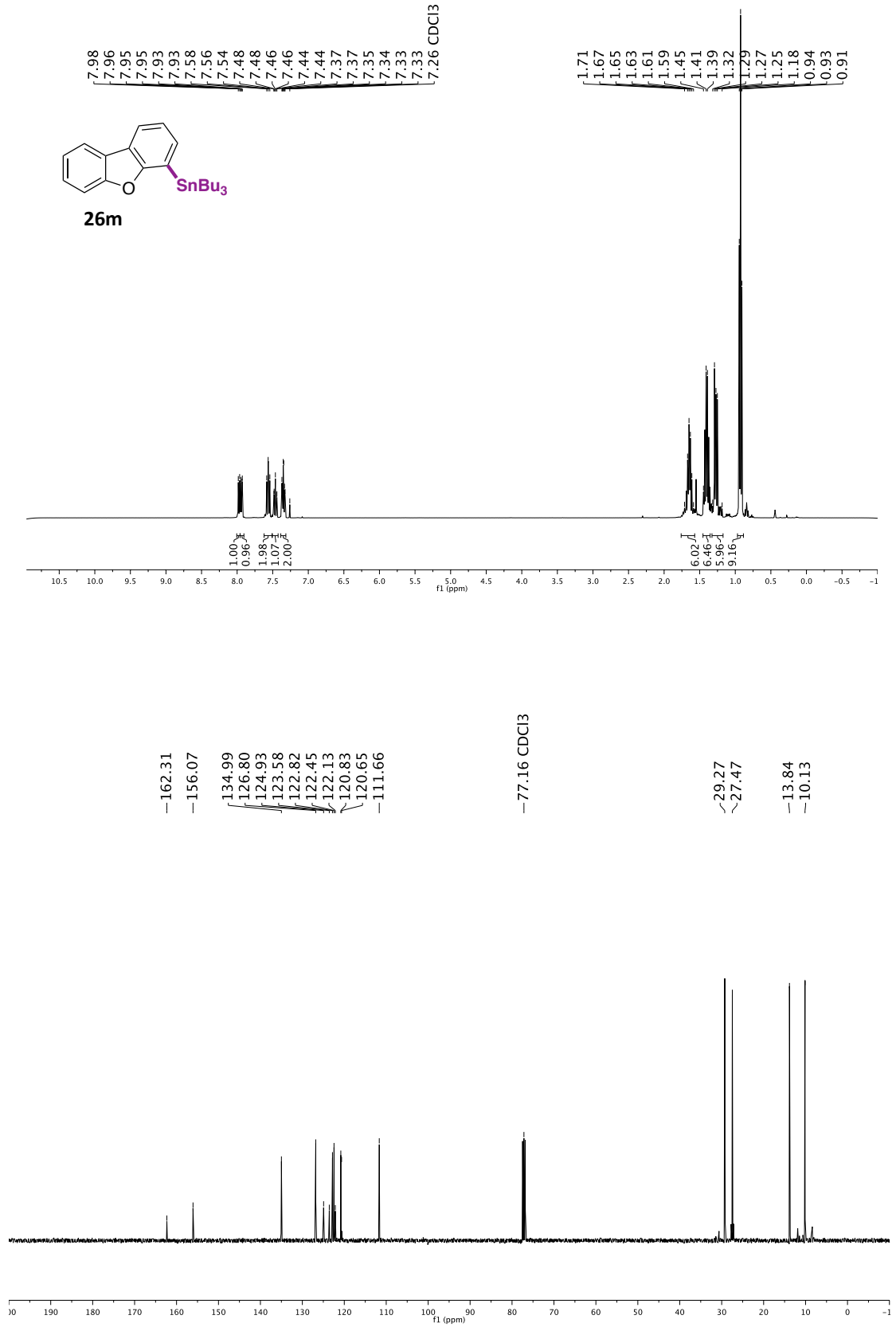
Ni-Catalyzed Stannylation of Aryl Ester via C-O Bond Cleavage



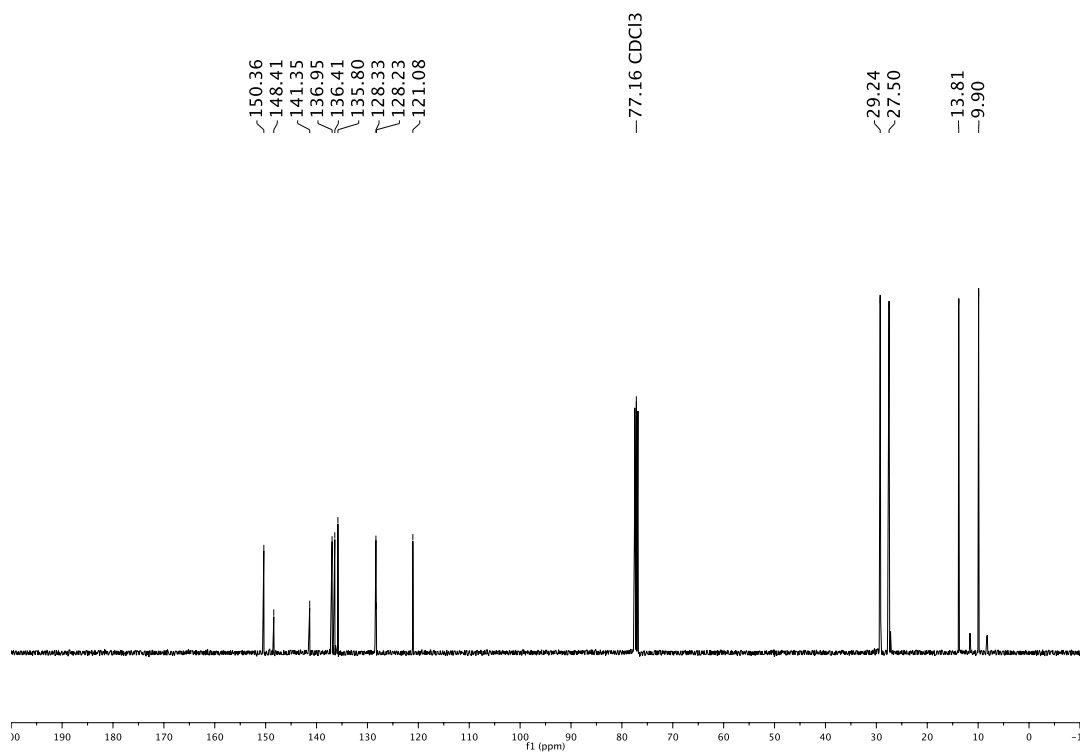
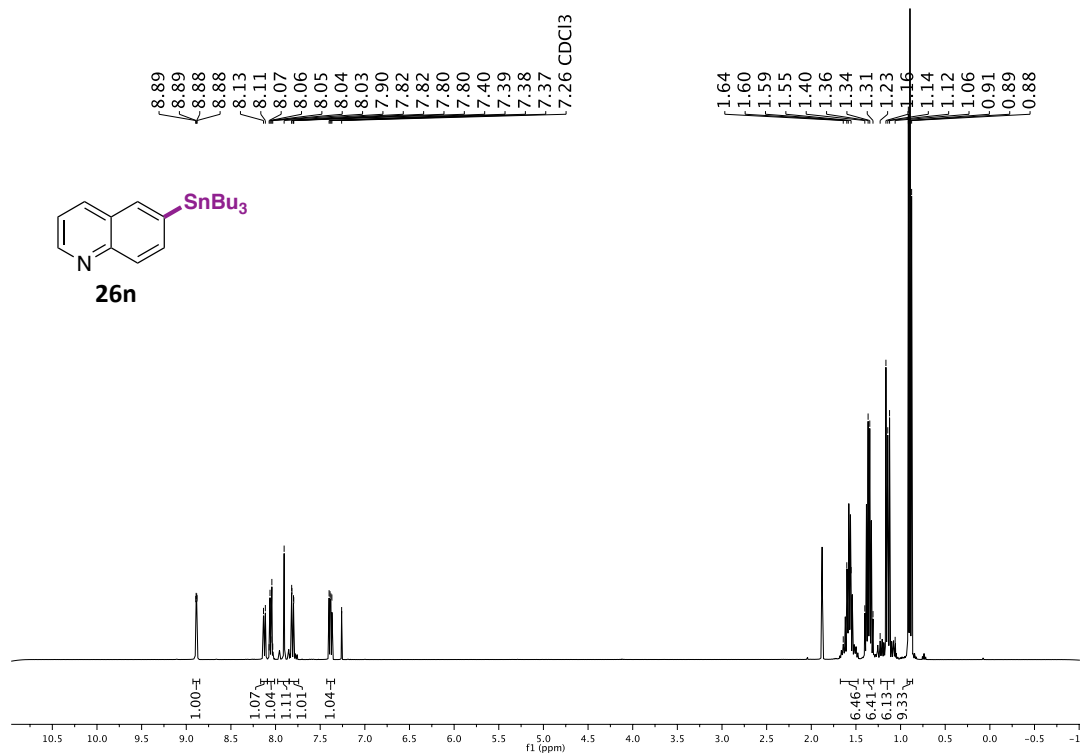


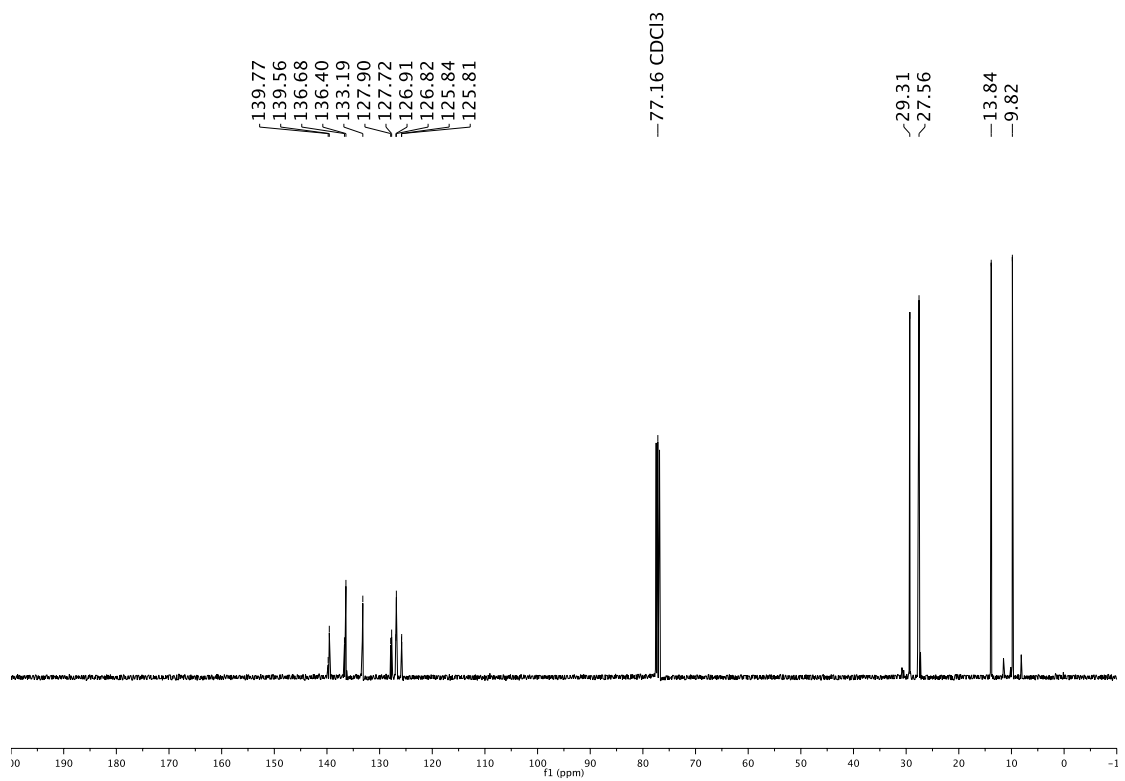
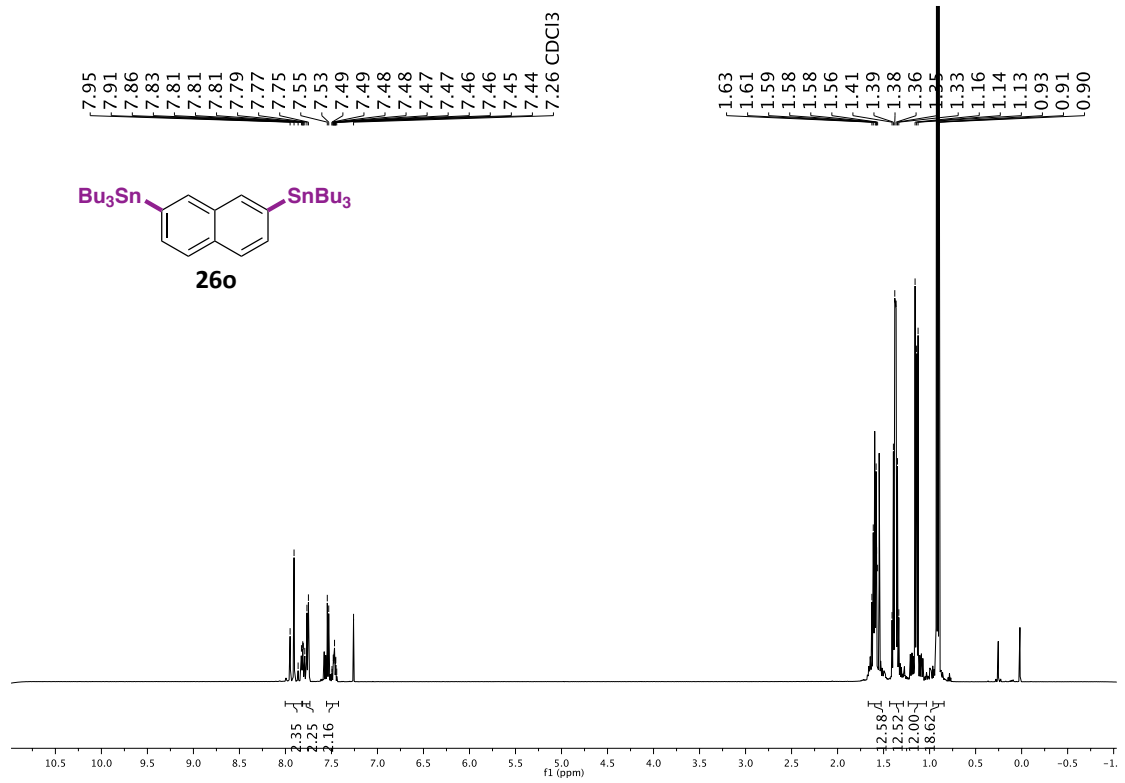
Ni-Catalyzed Stannylation of Aryl Ester via C-O Bond Cleavage



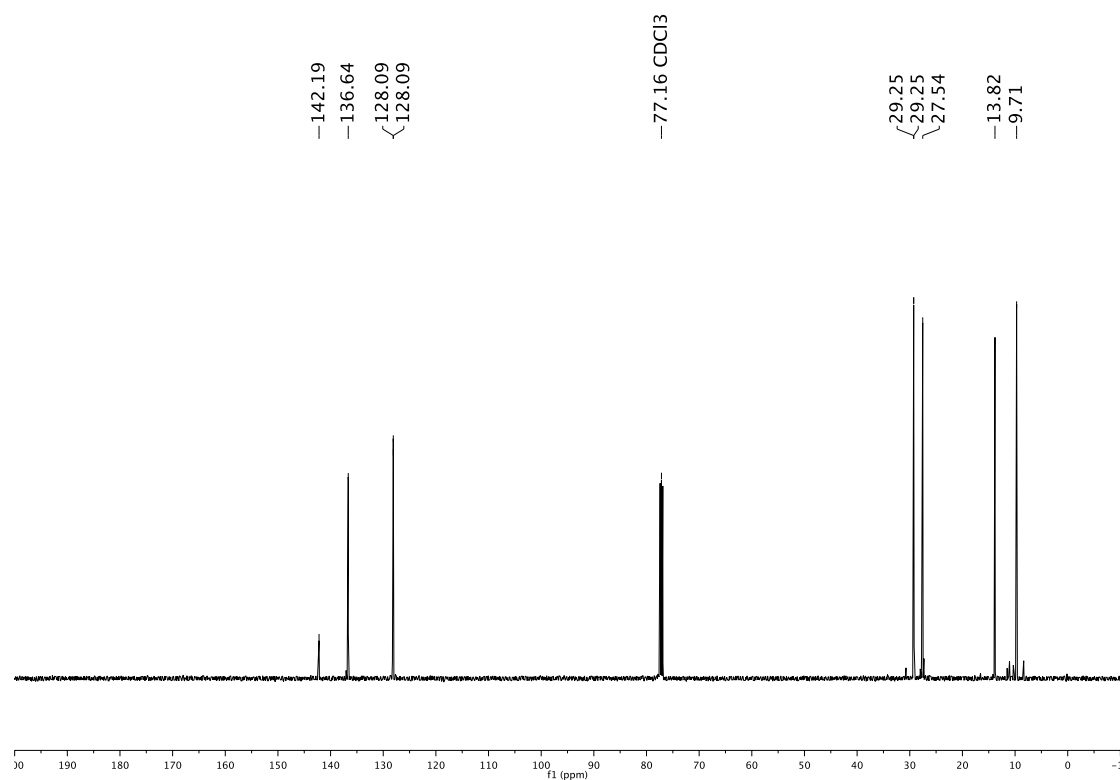
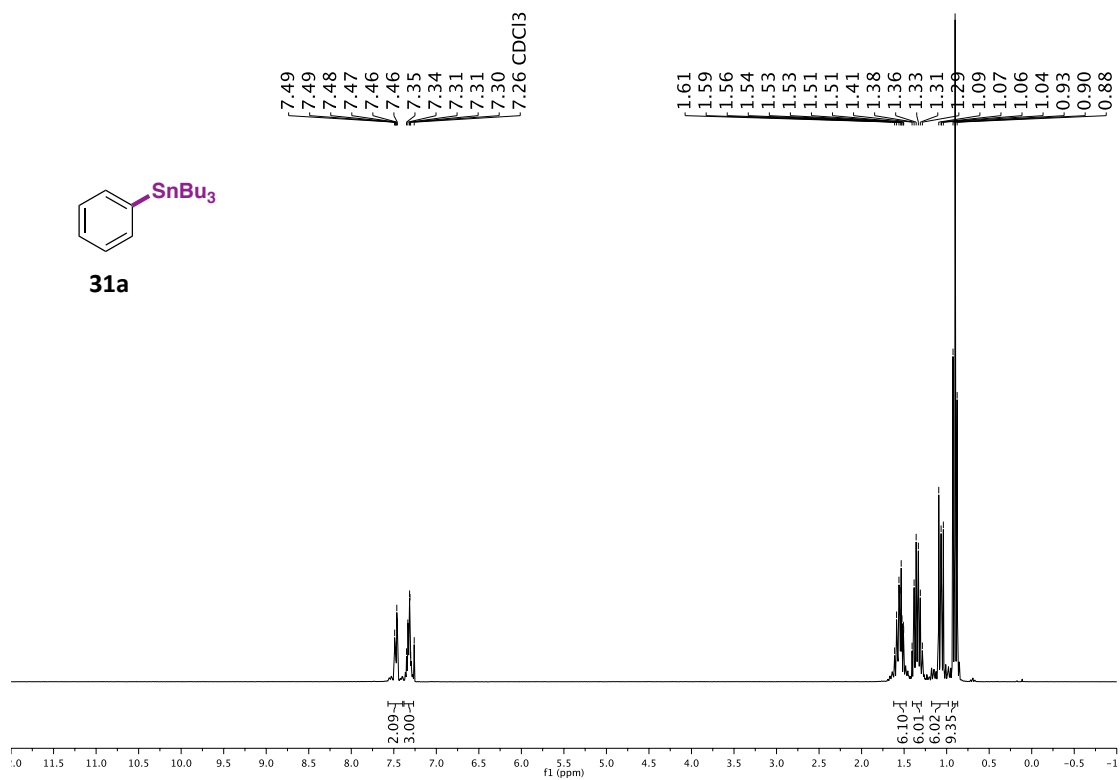


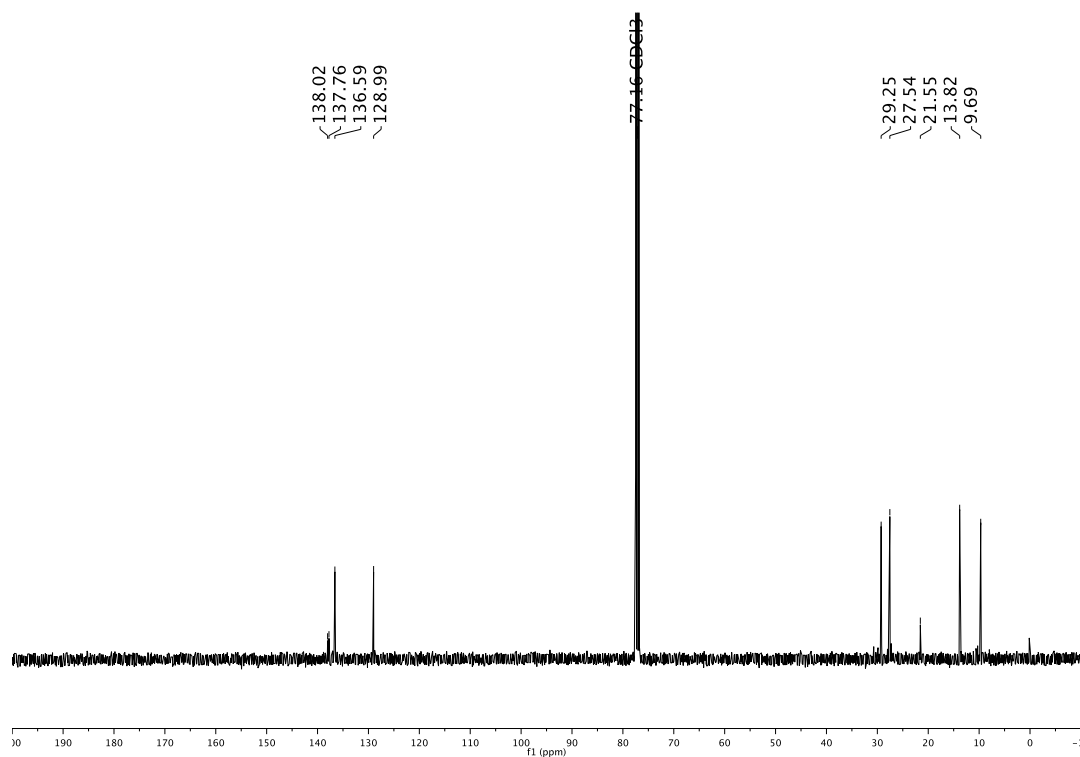
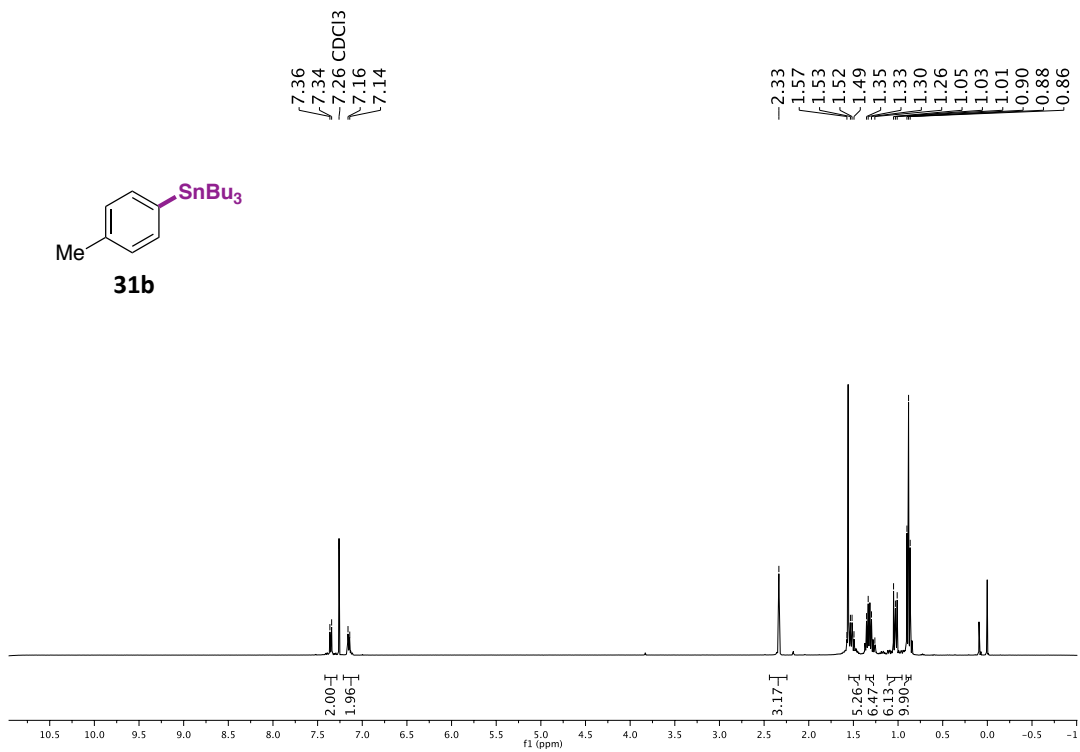
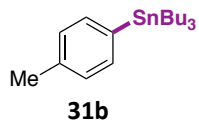
Ni-Catalyzed Stannylation of Aryl Ester via C-O Bond Cleavage



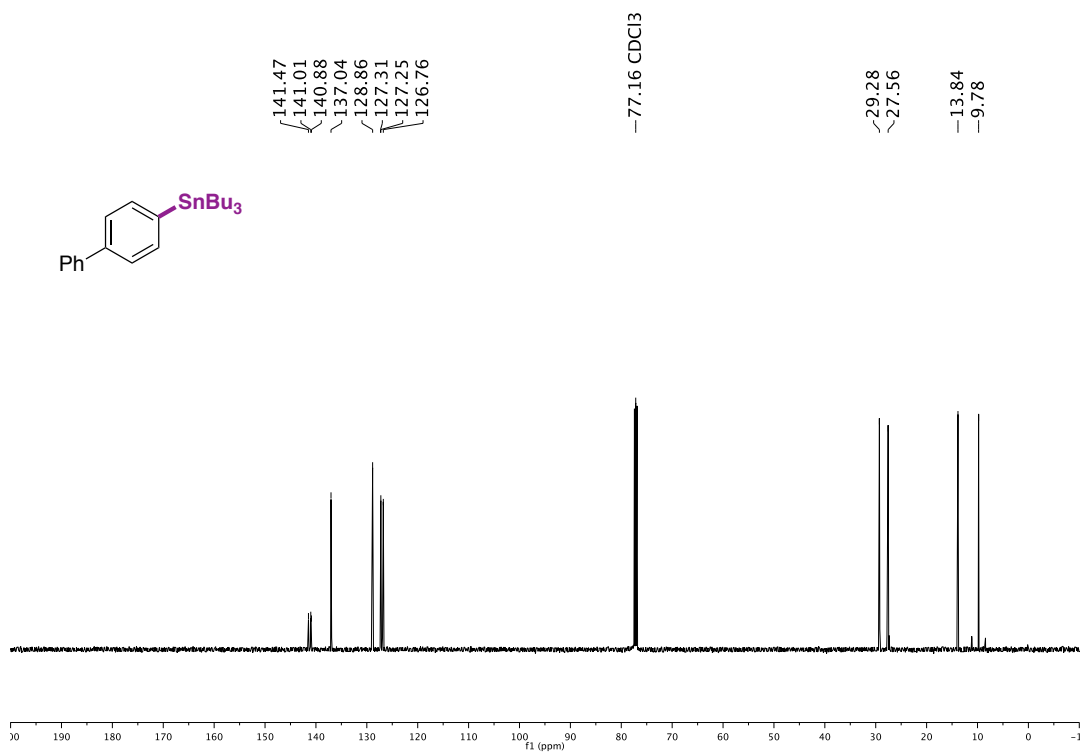
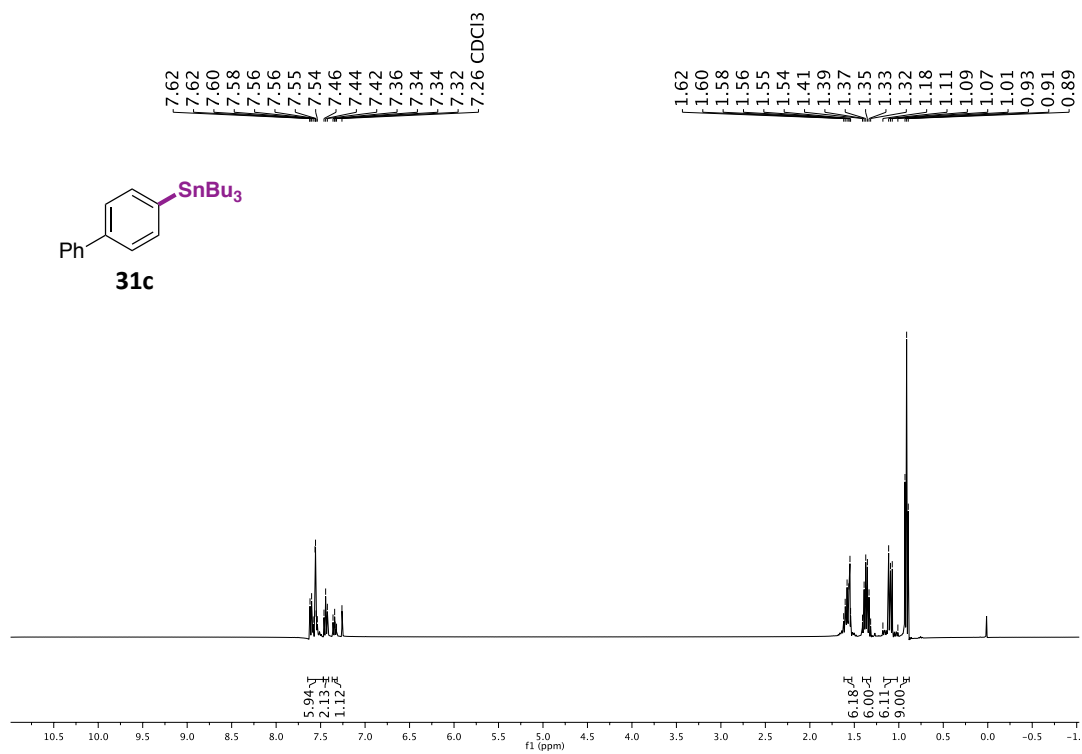


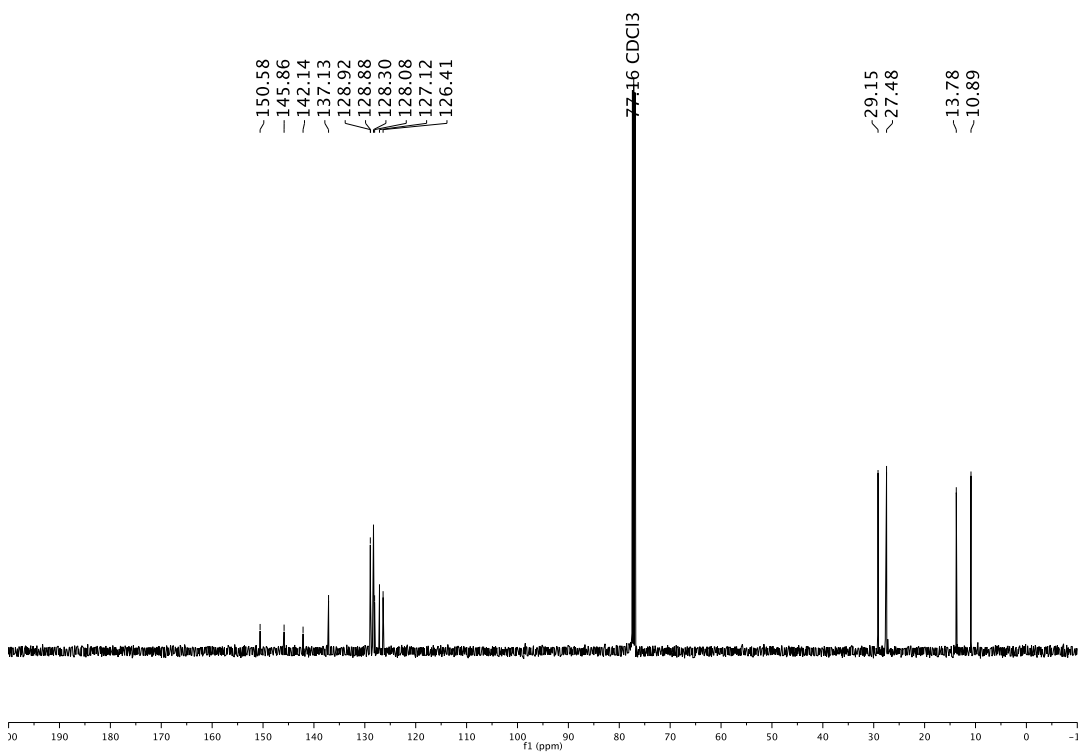
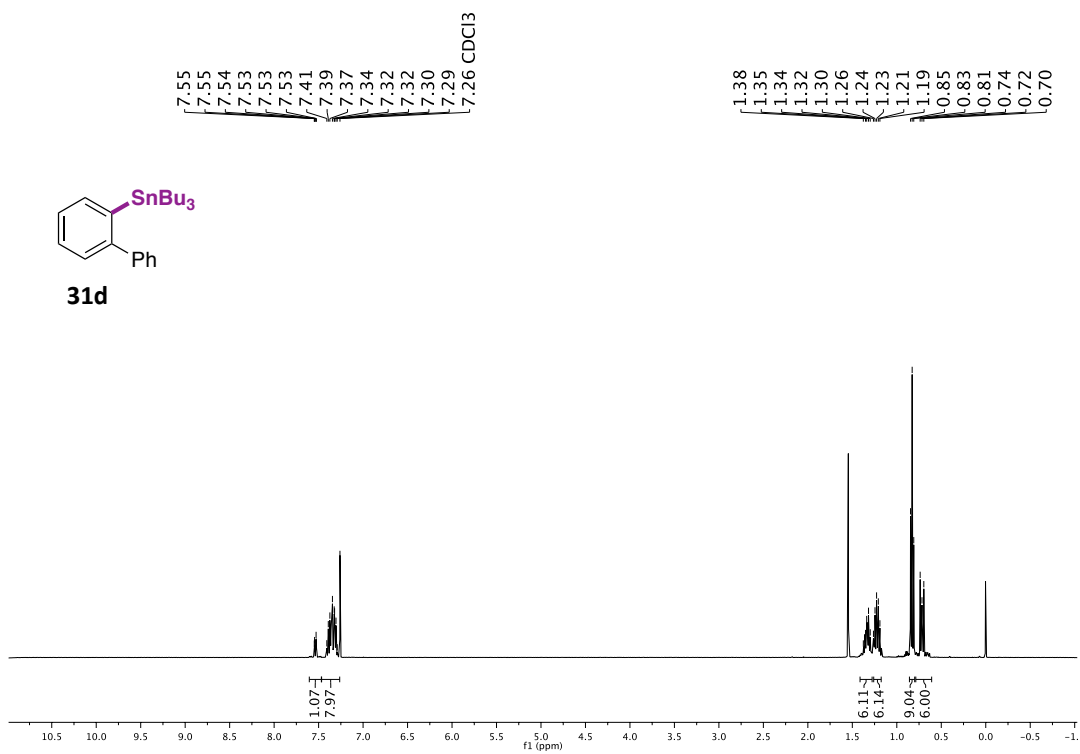
Ni-Catalyzed Stannylation of Aryl Ester via C-O Bond Cleavage



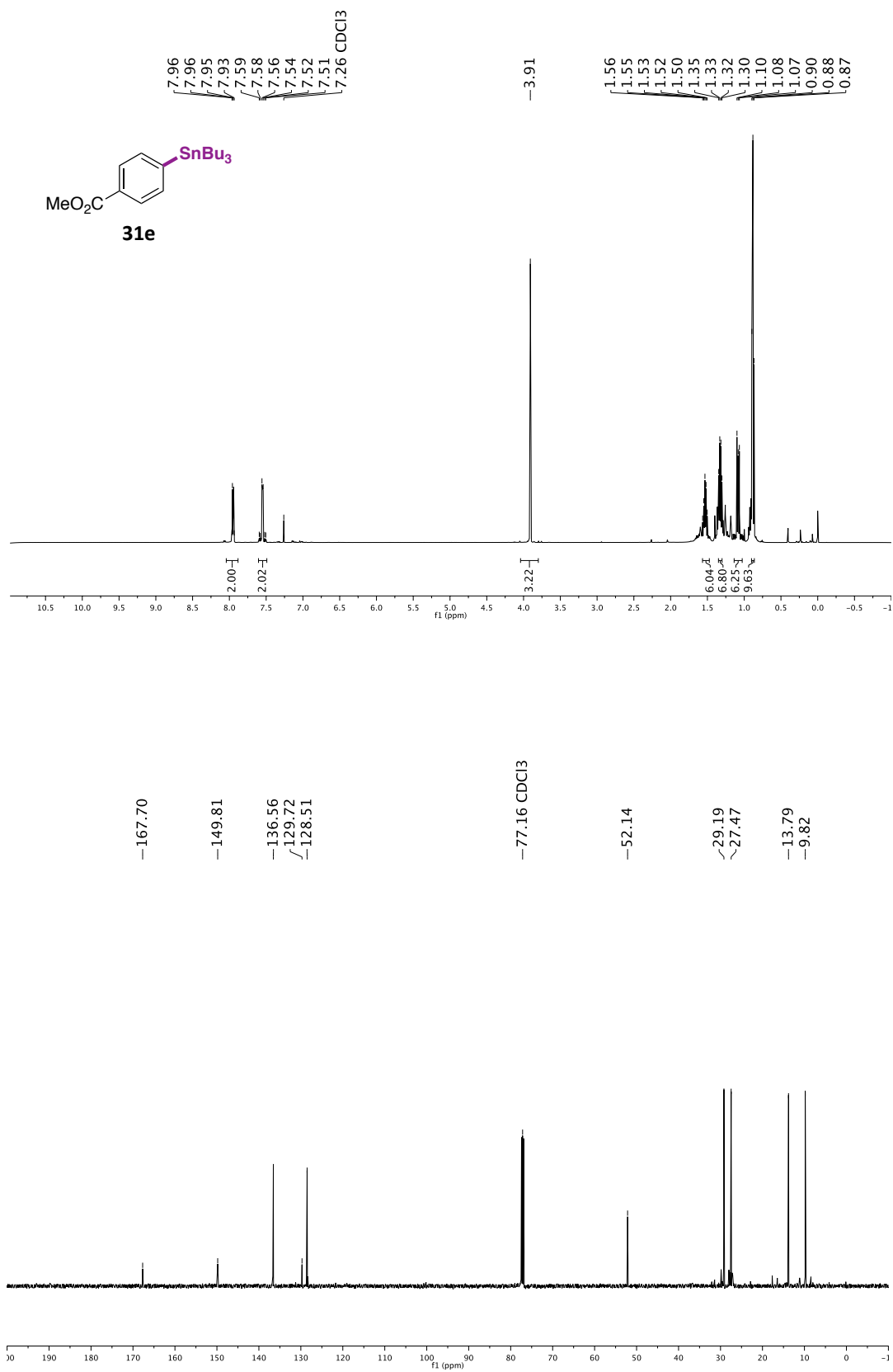


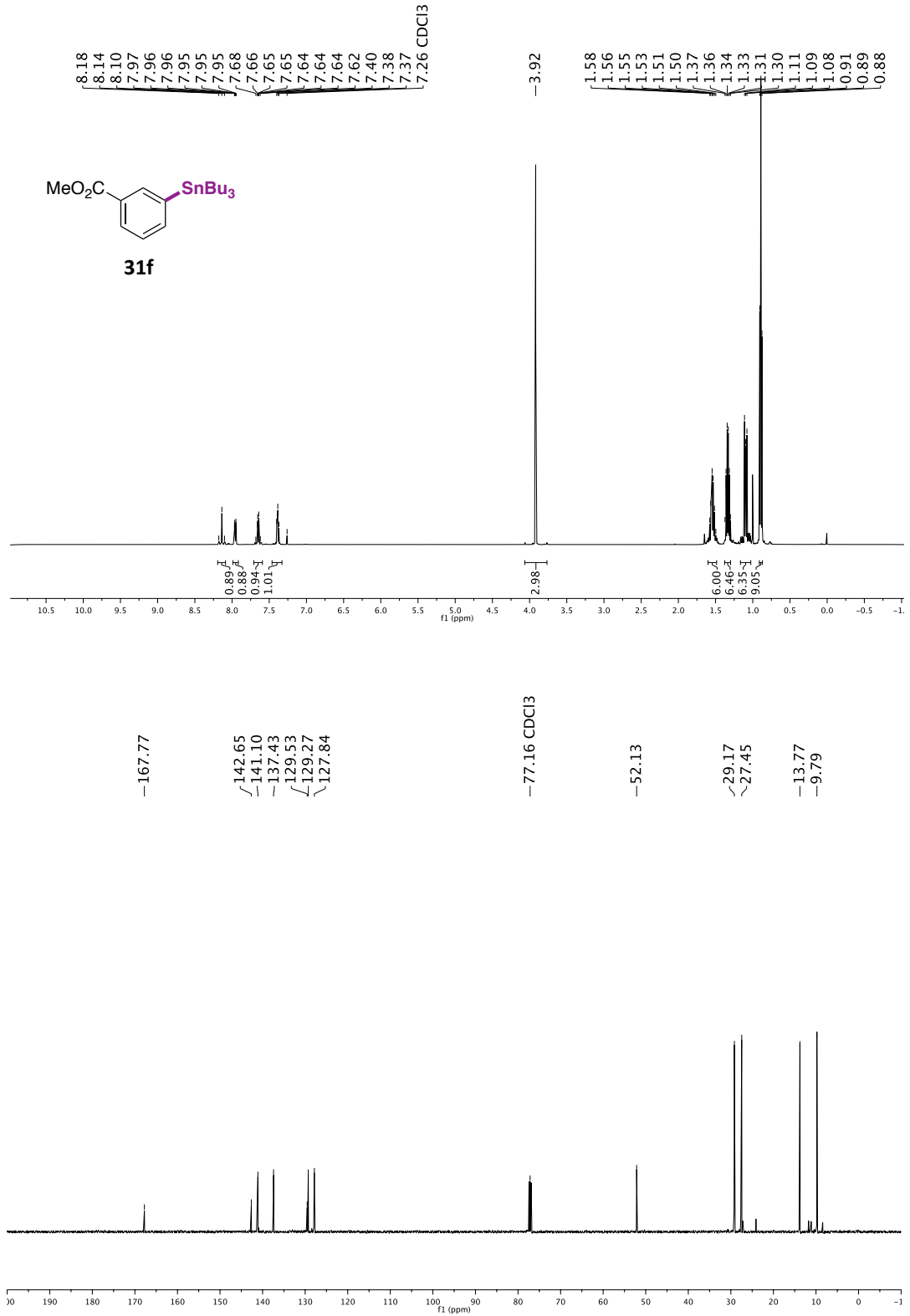
Ni-Catalyzed Stannylation of Aryl Ester via C-O Bond Cleavage



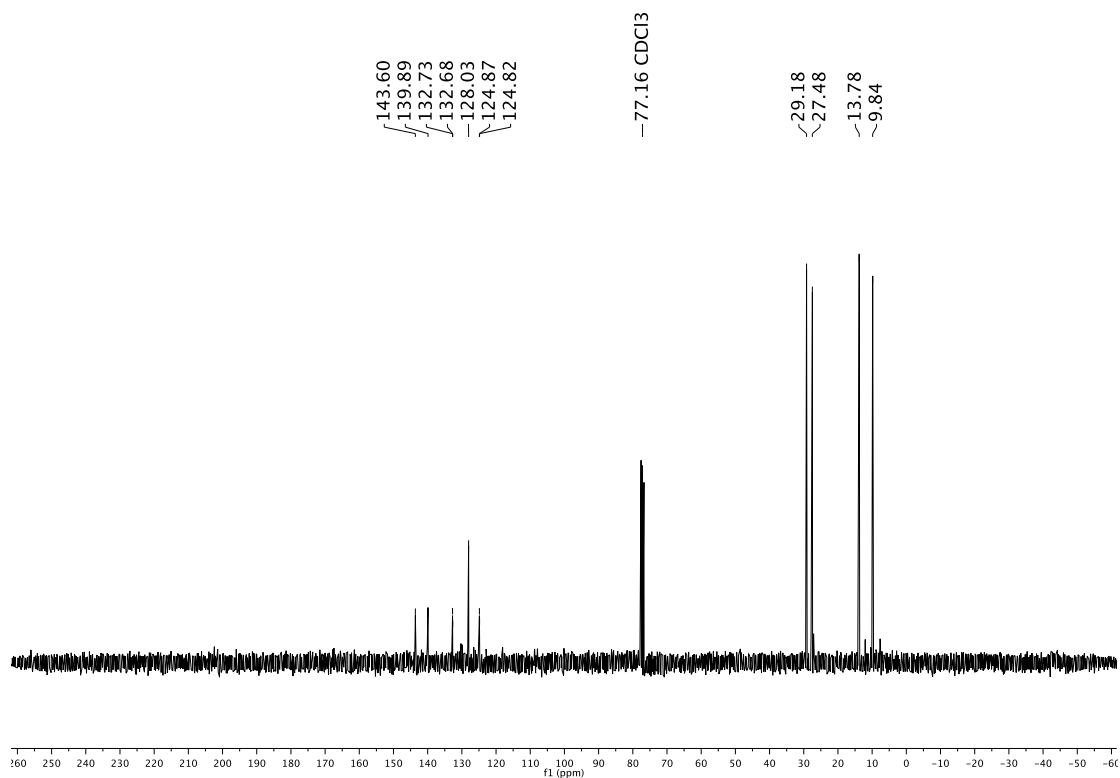
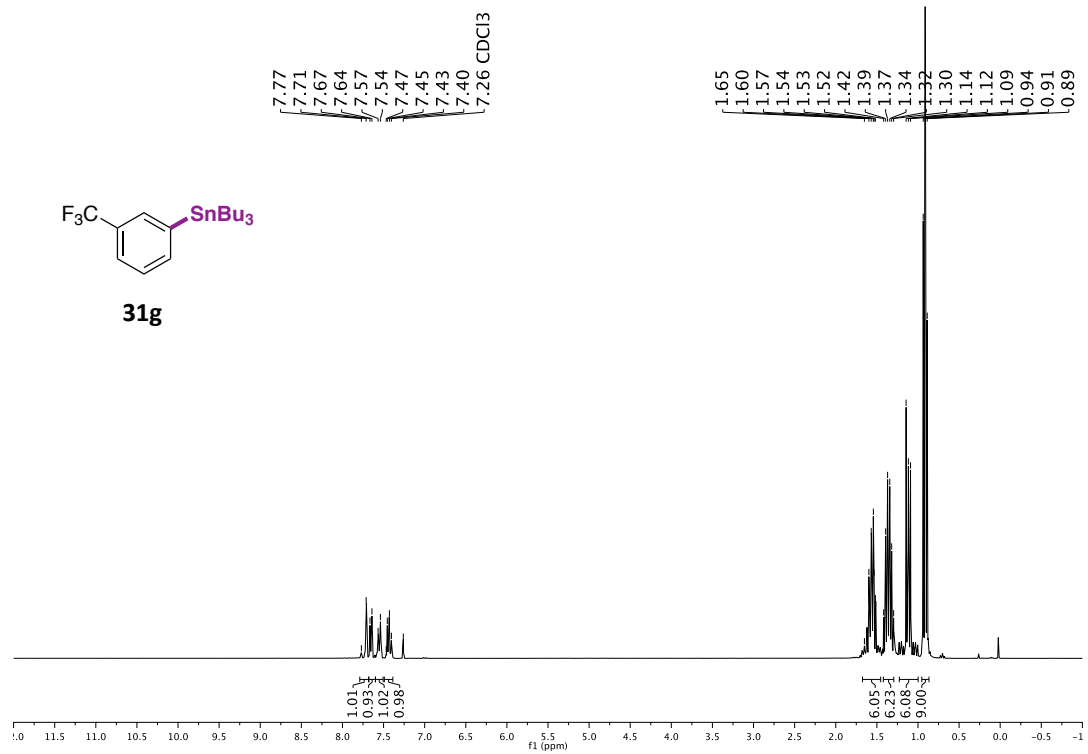


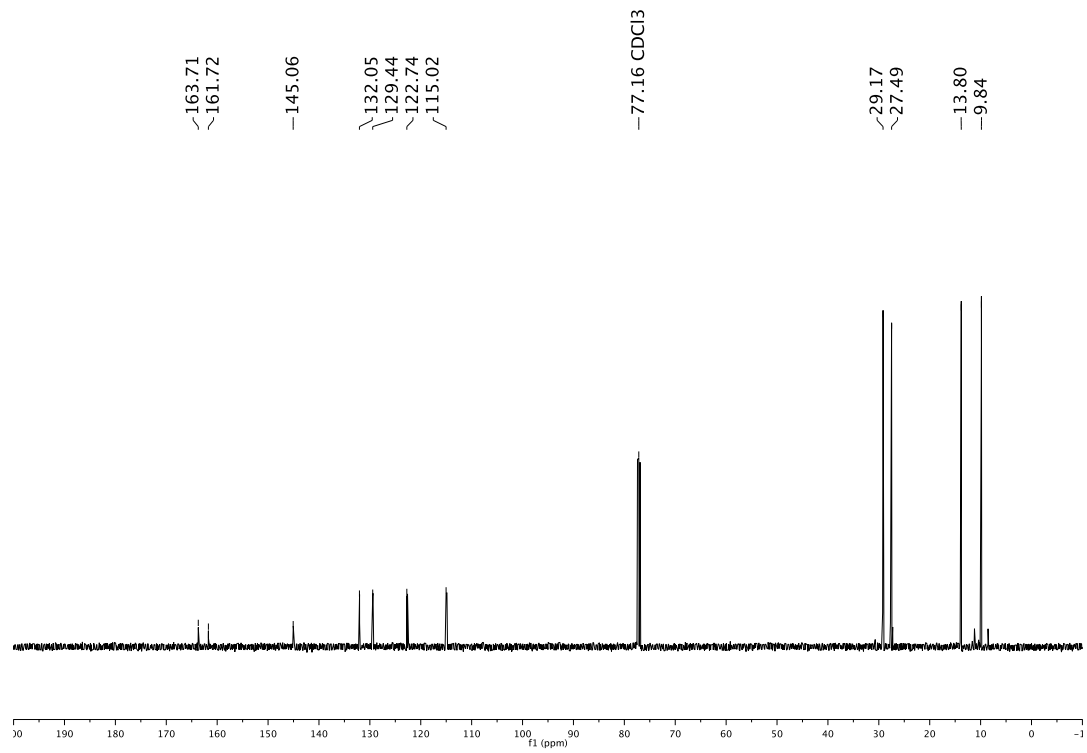
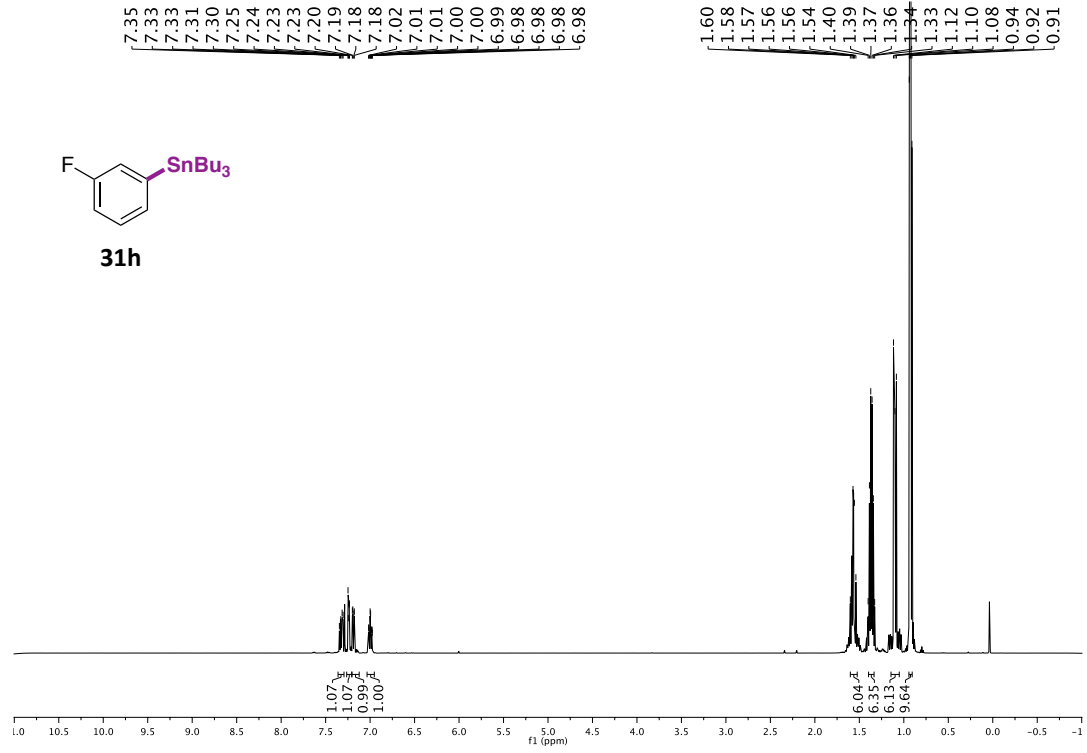
Ni-Catalyzed Stannylation of Aryl Ester via C-O Bond Cleavage



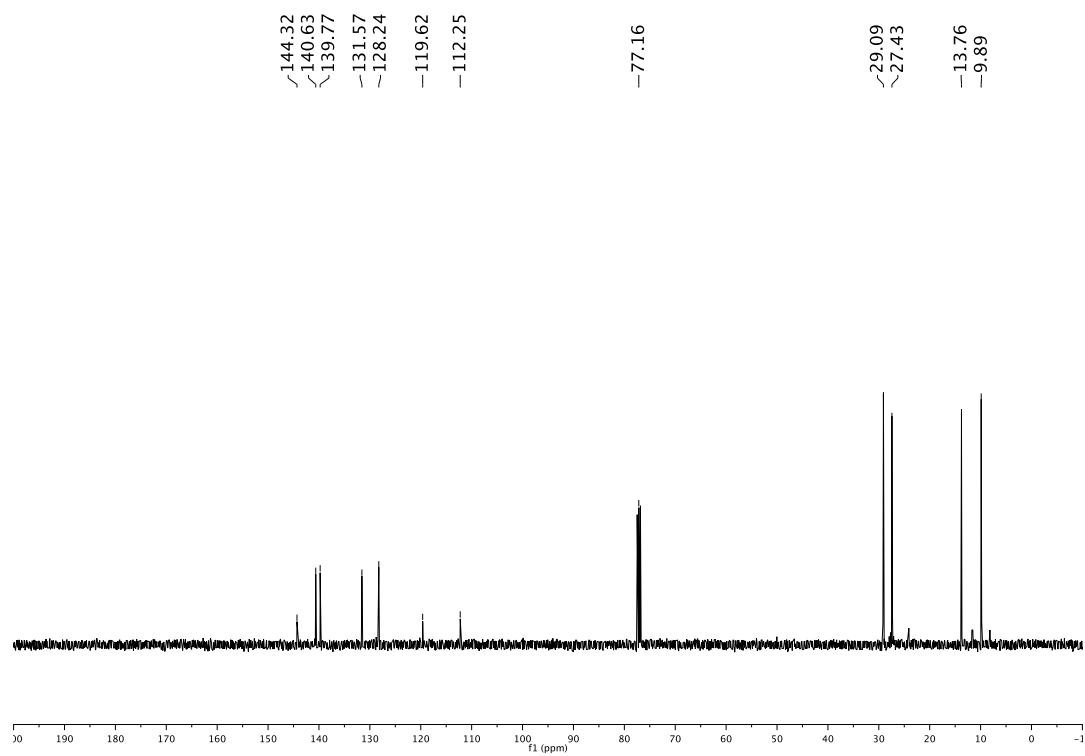
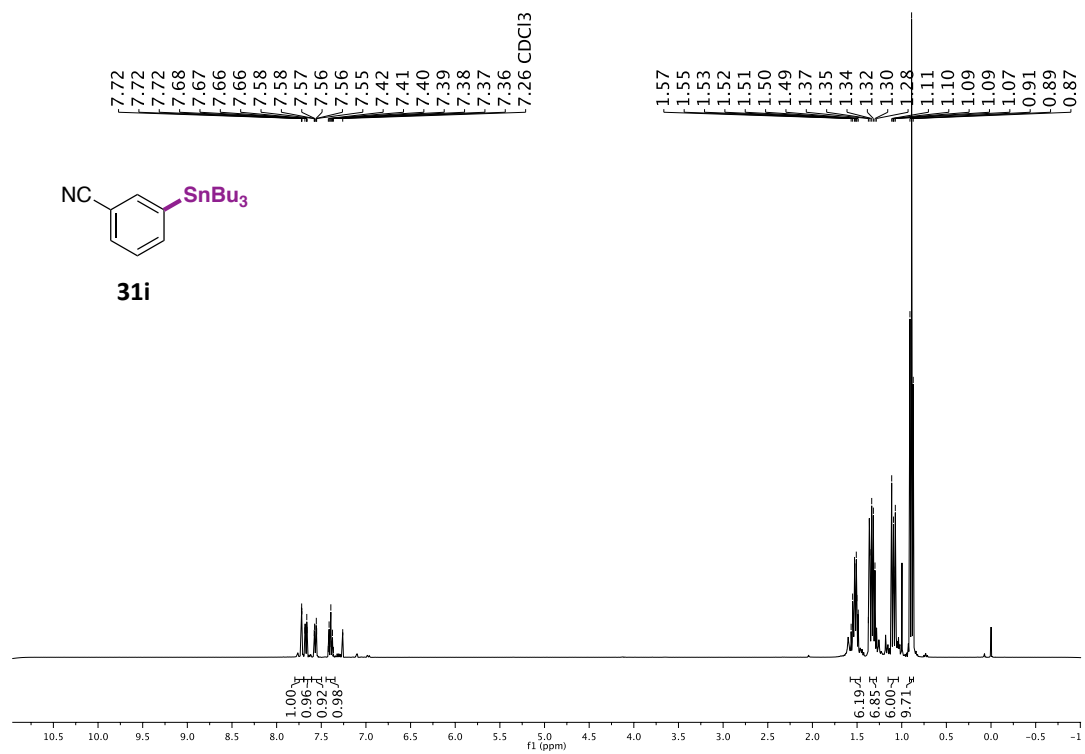


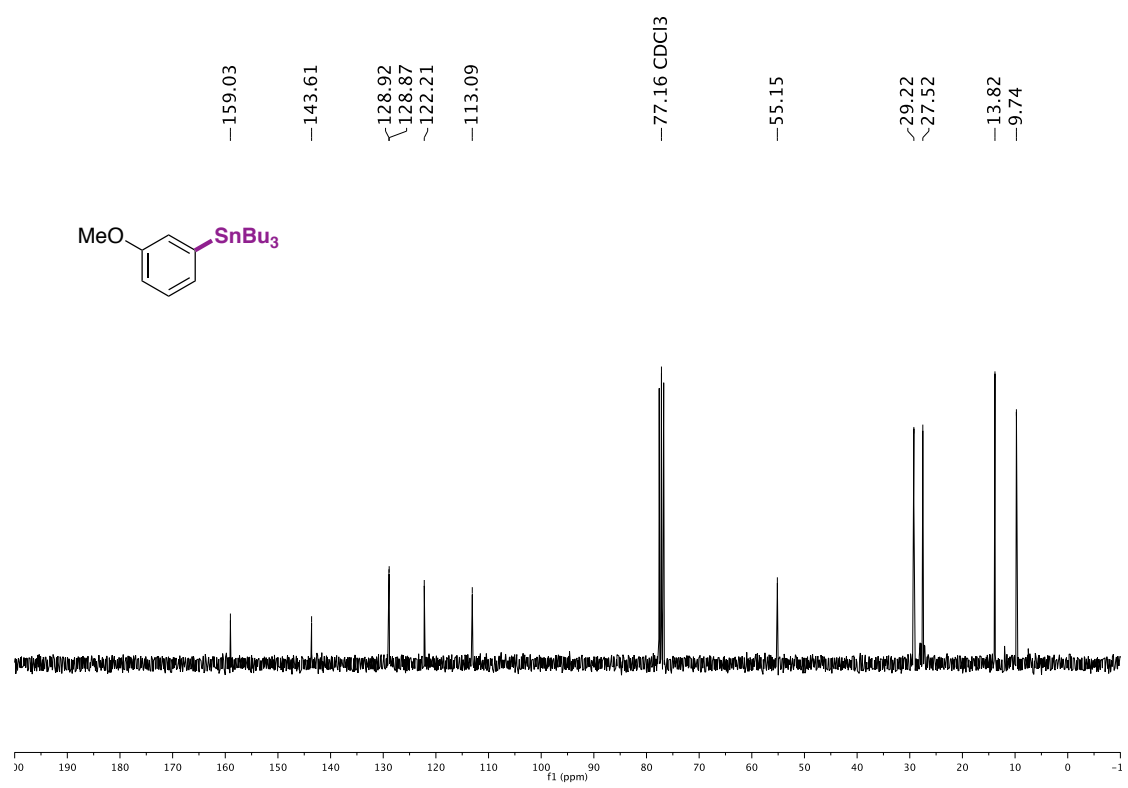
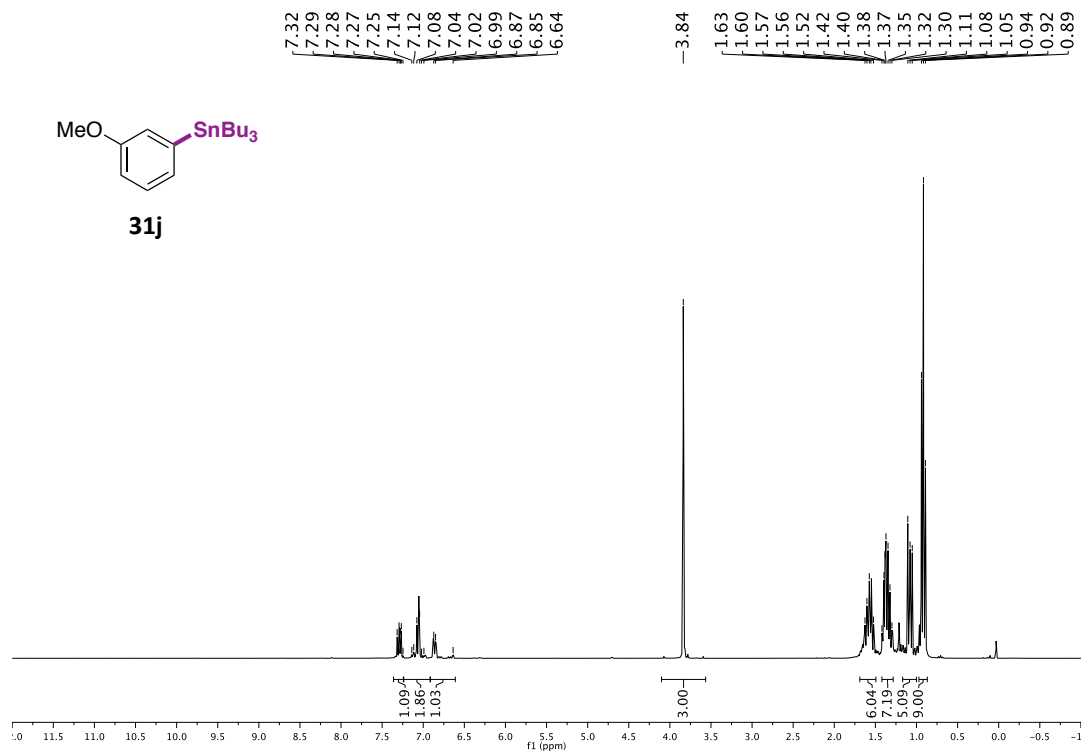
Ni-Catalyzed Stannylation of Aryl Ester via C-O Bond Cleavage



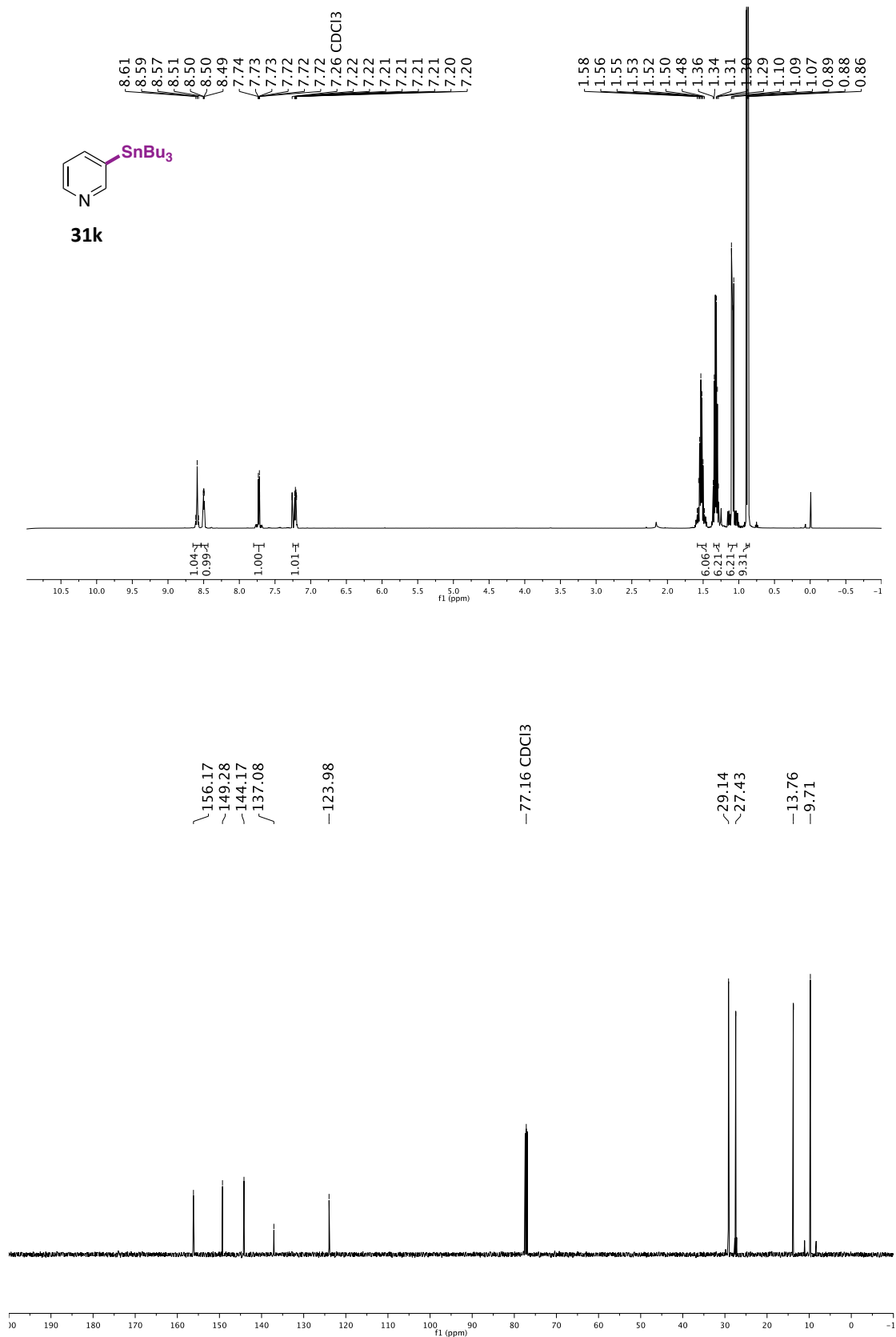


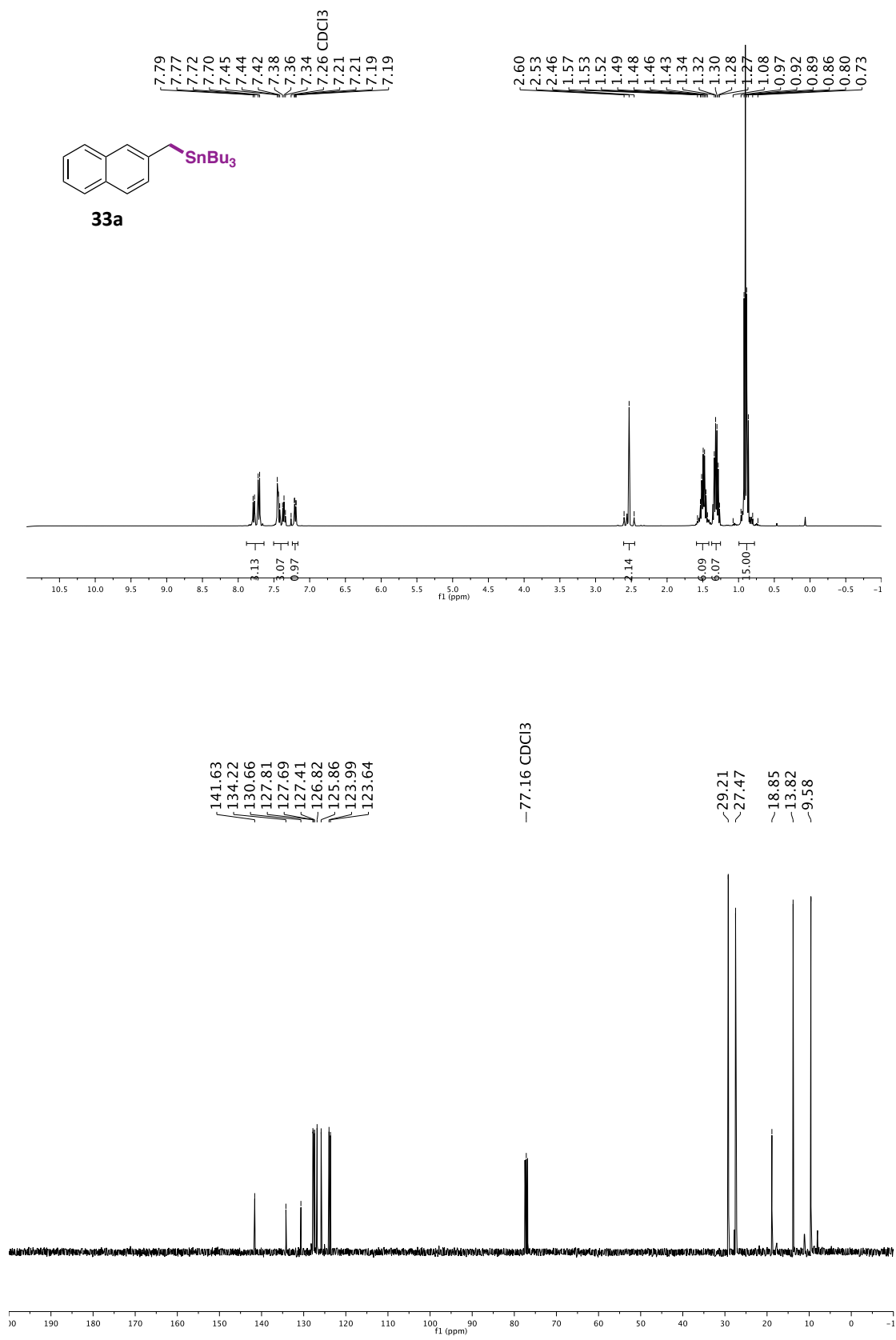
Ni-Catalyzed Stannylation of Aryl Ester via C-O Bond Cleavage



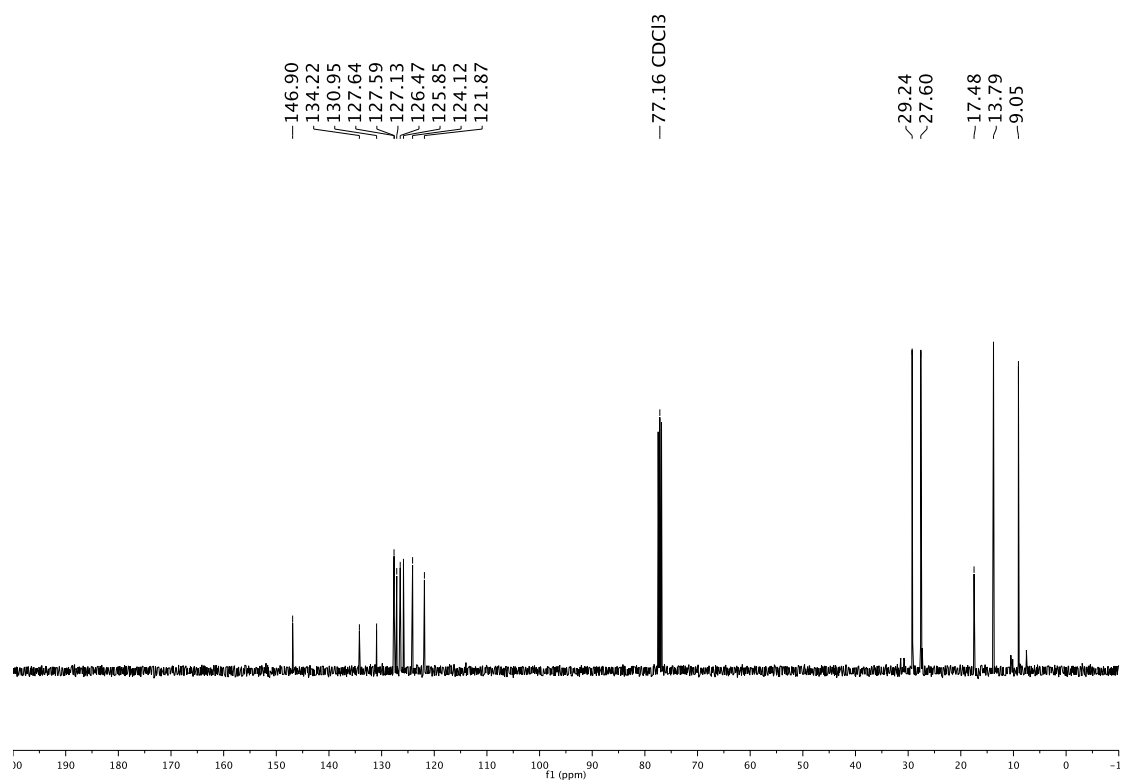
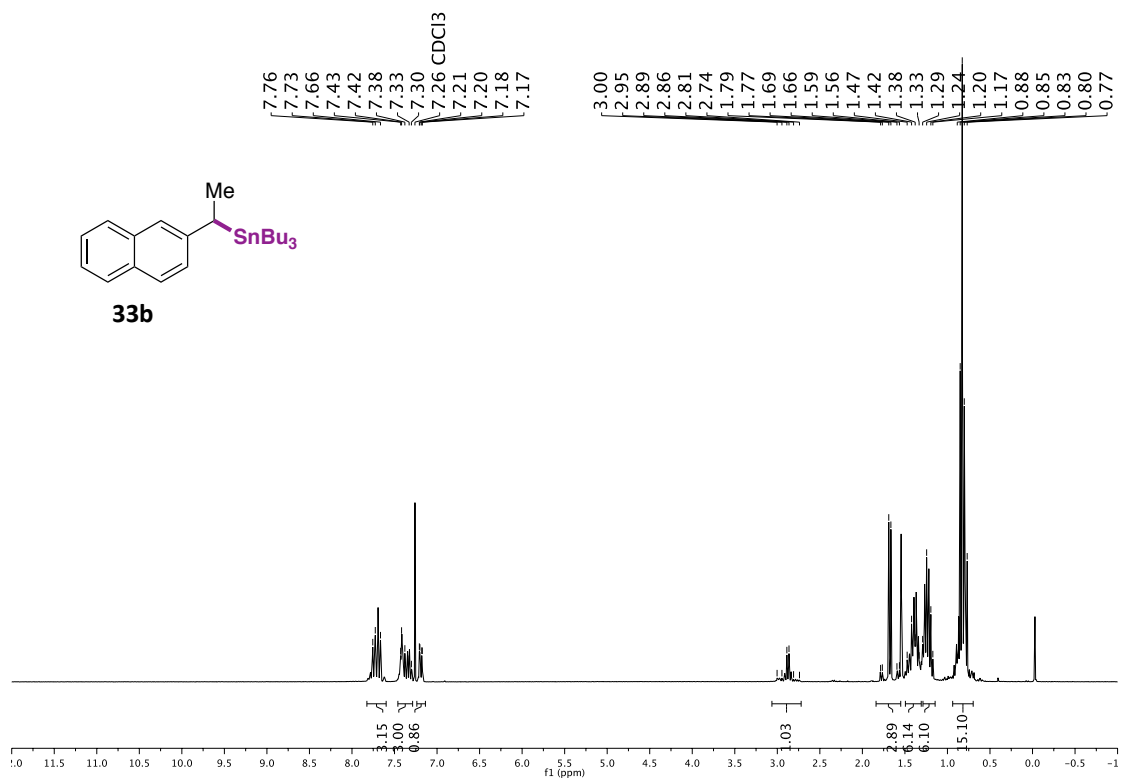


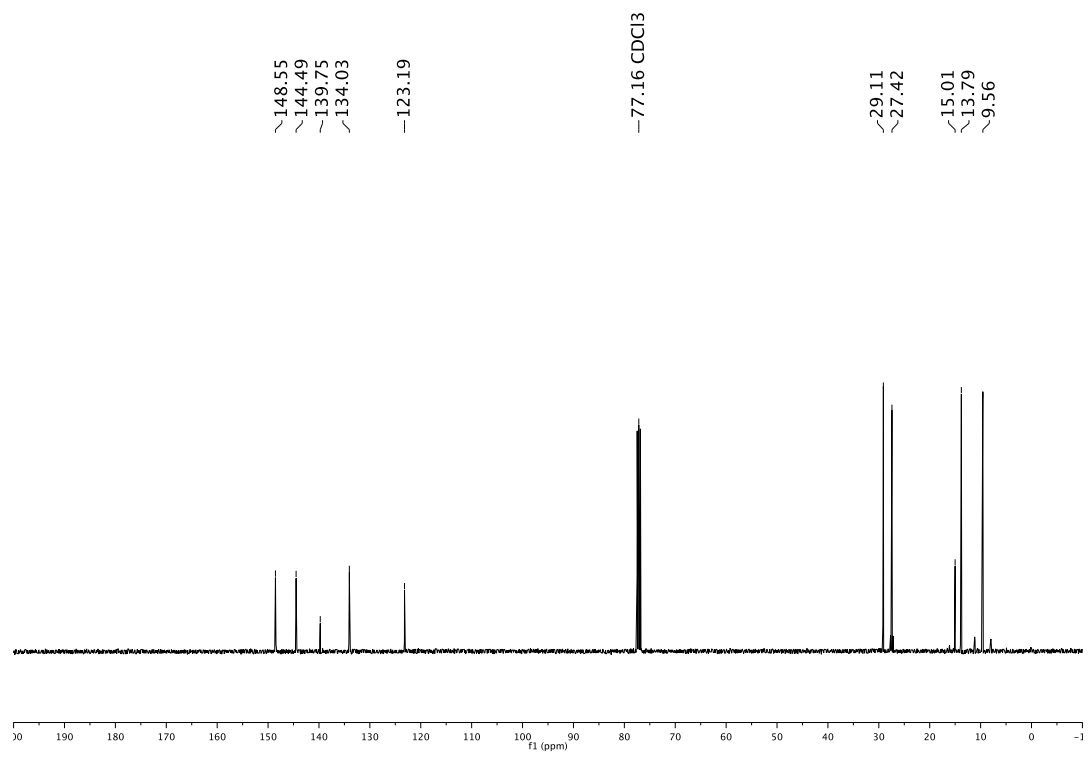
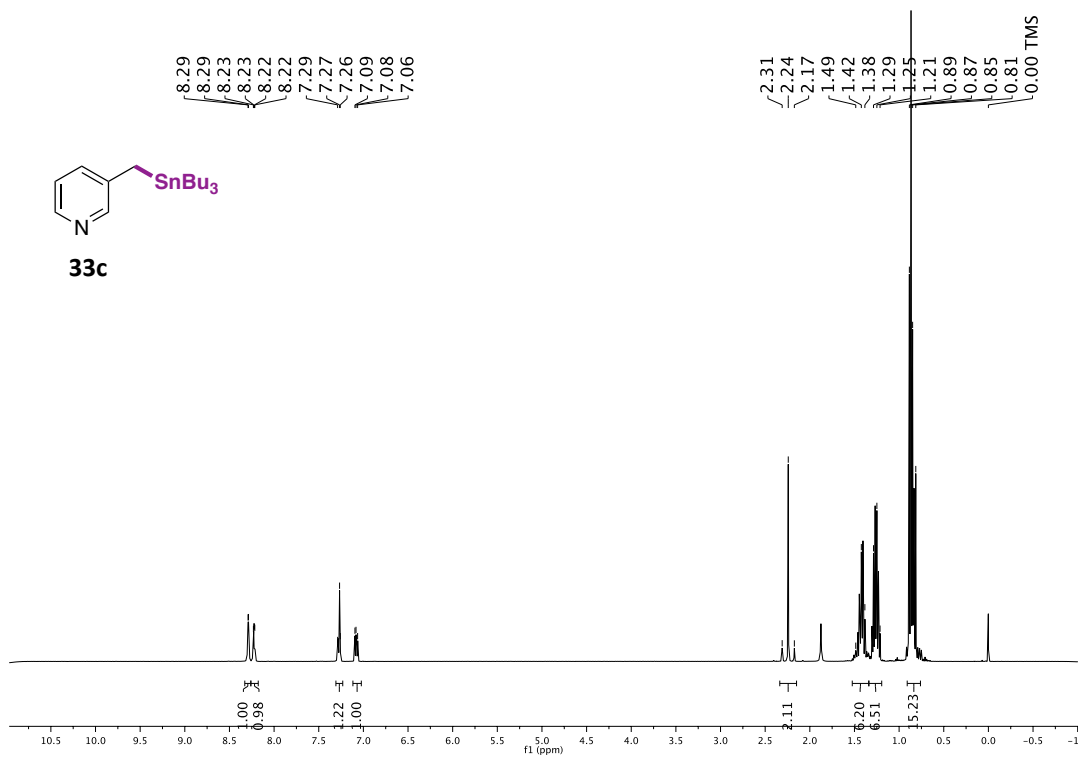
Ni-Catalyzed Stannylation of Aryl Ester via C-O Bond Cleavage



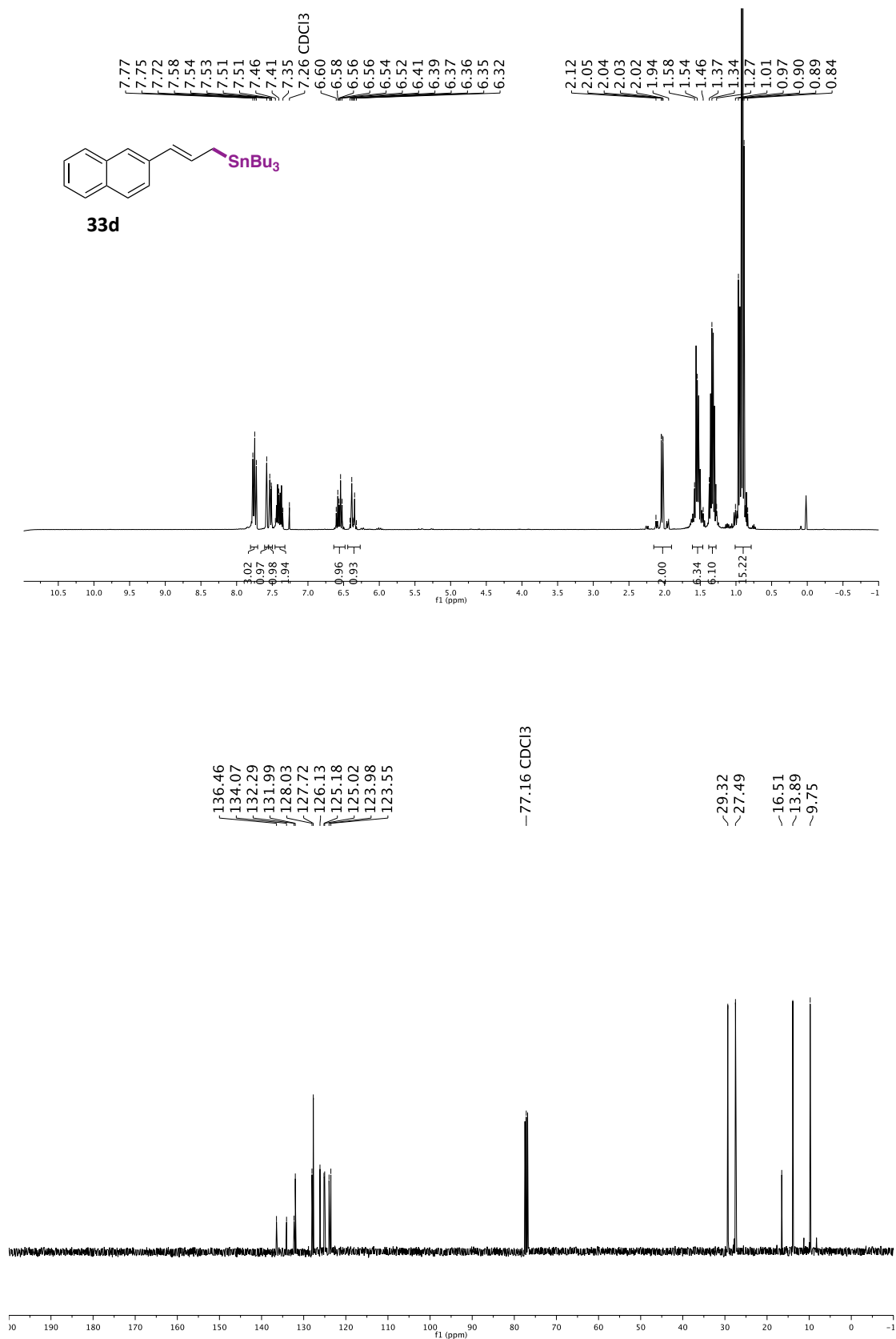


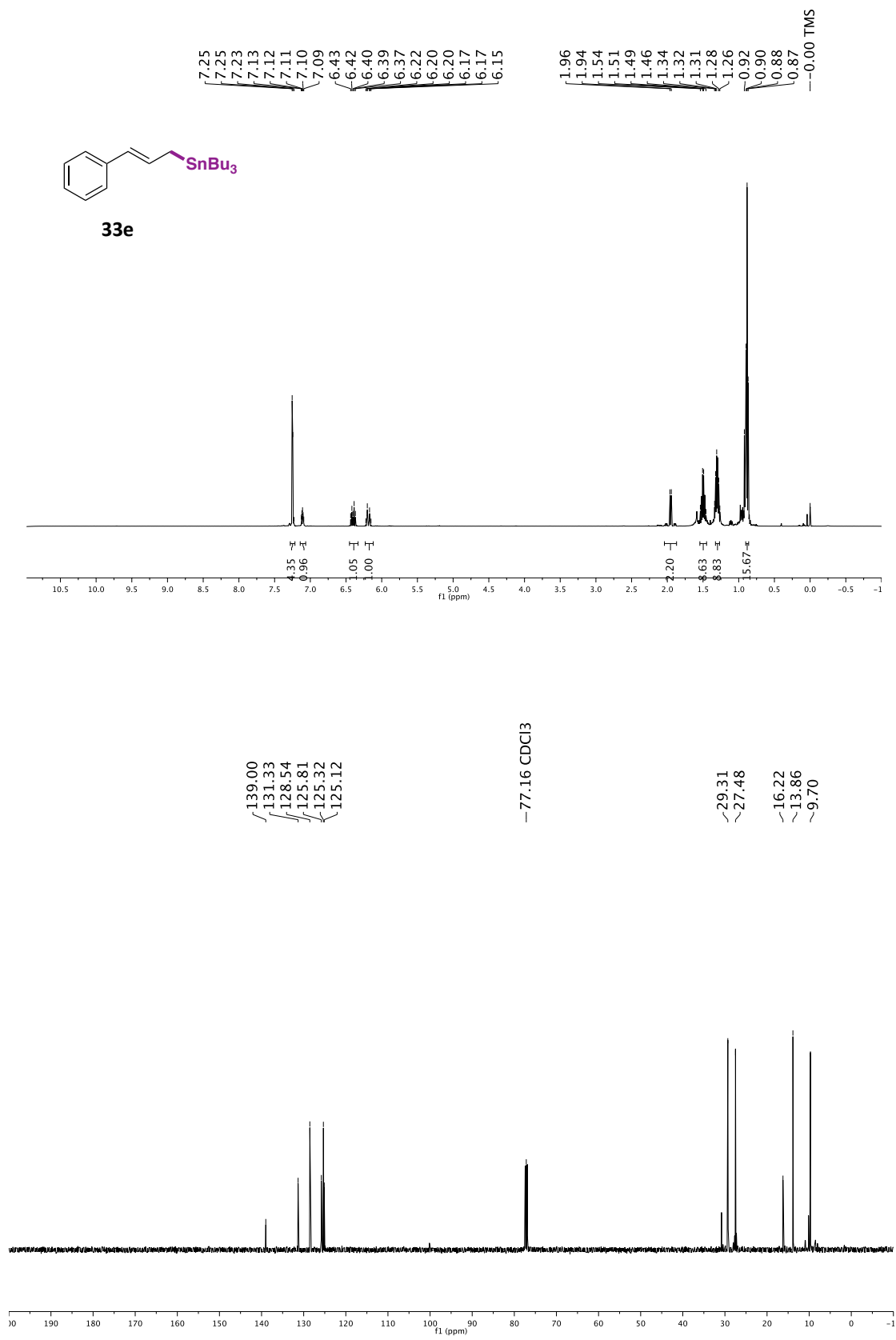
Ni-Catalyzed Stannylation of Aryl Ester via C-O Bond Cleavage



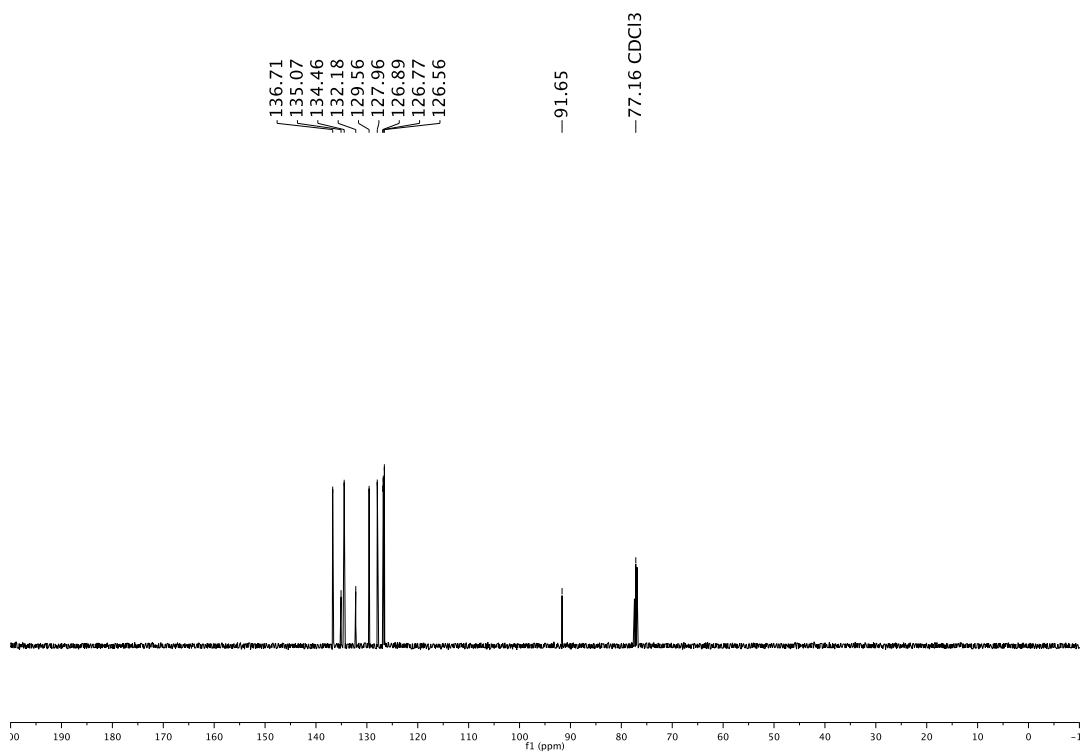
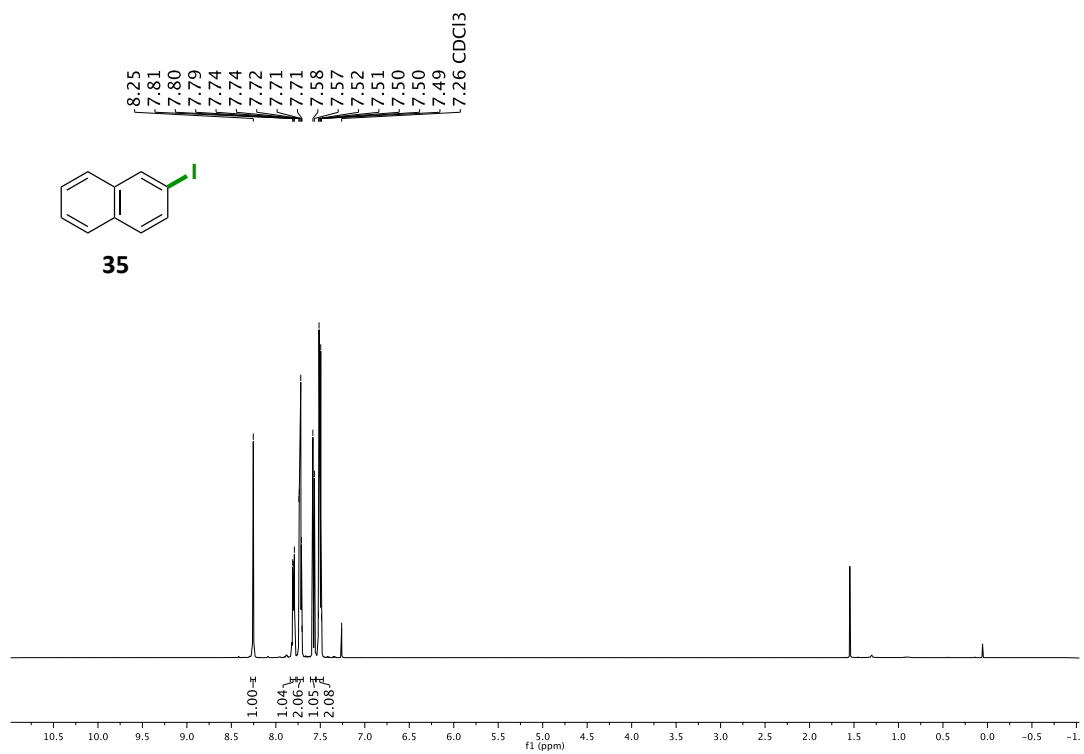


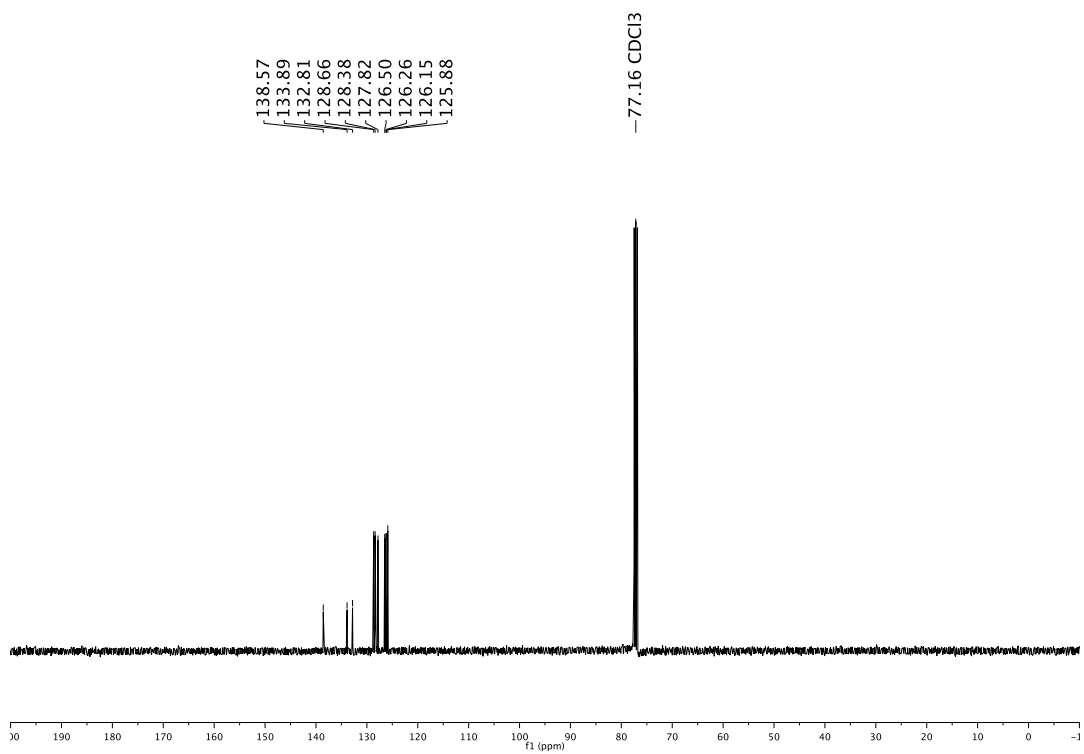
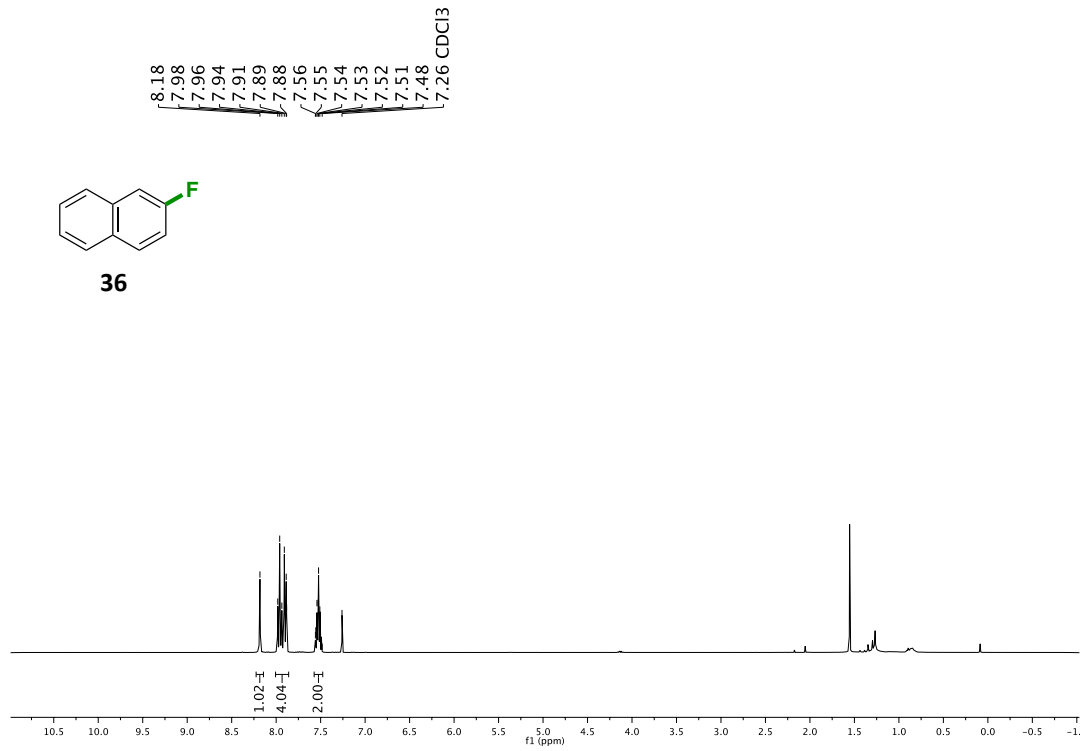
Ni-Catalyzed Stannylation of Aryl Ester via C-O Bond Cleavage



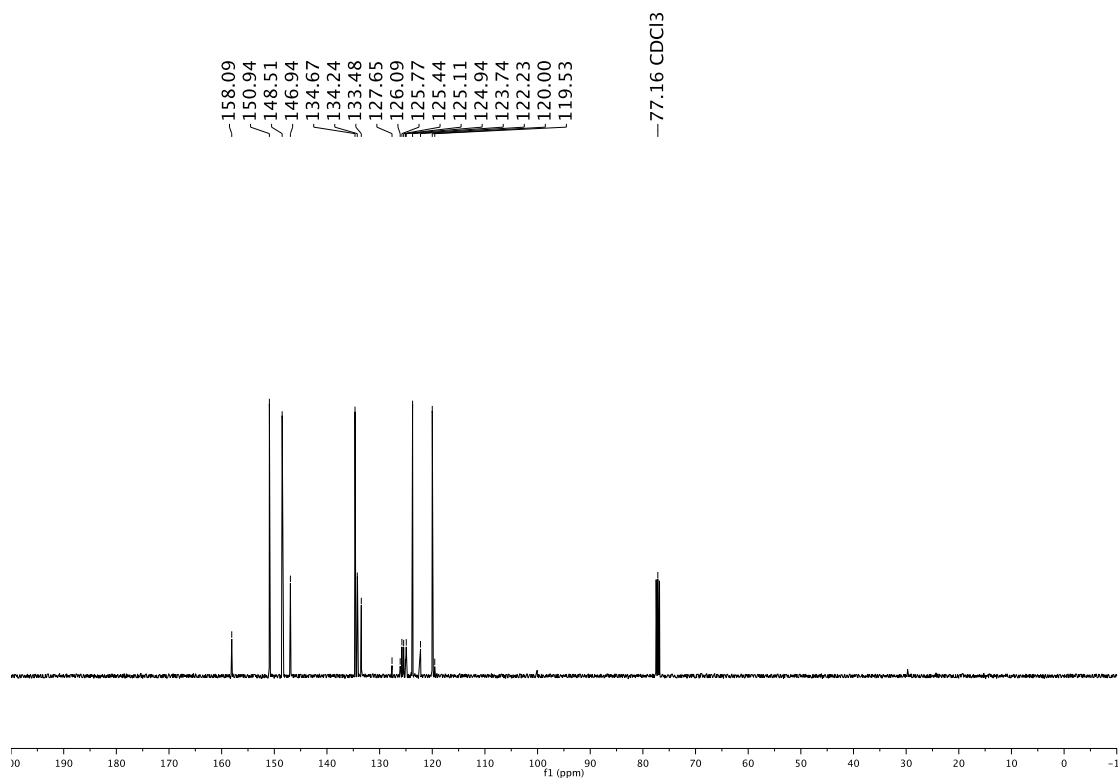
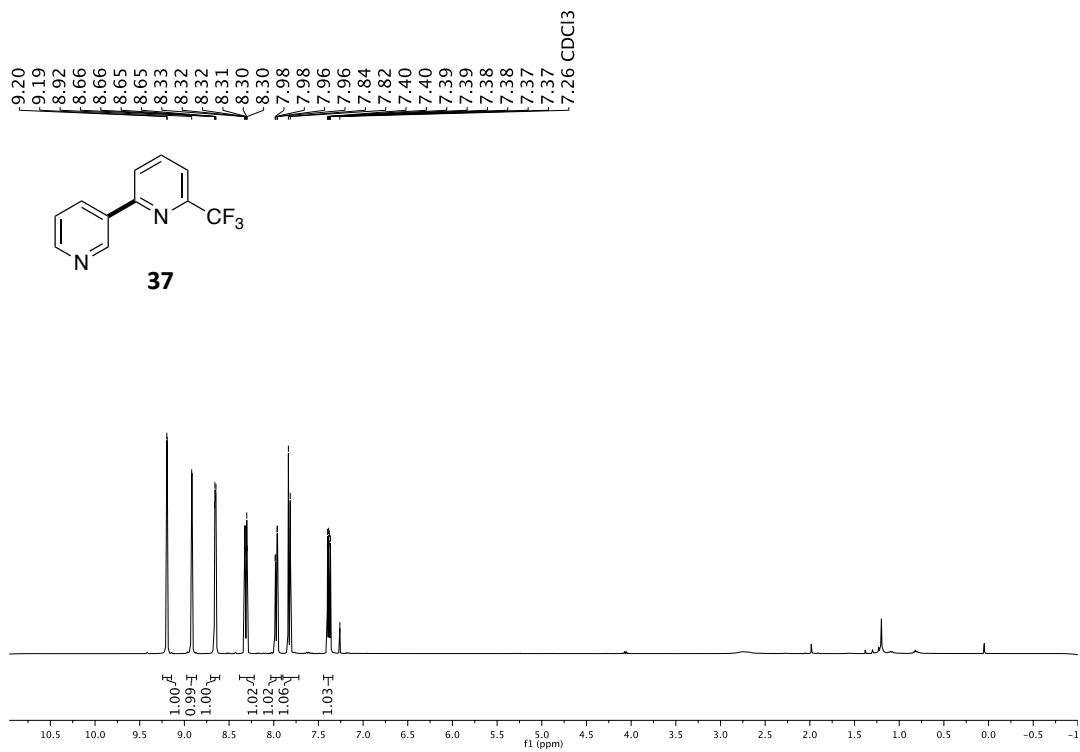


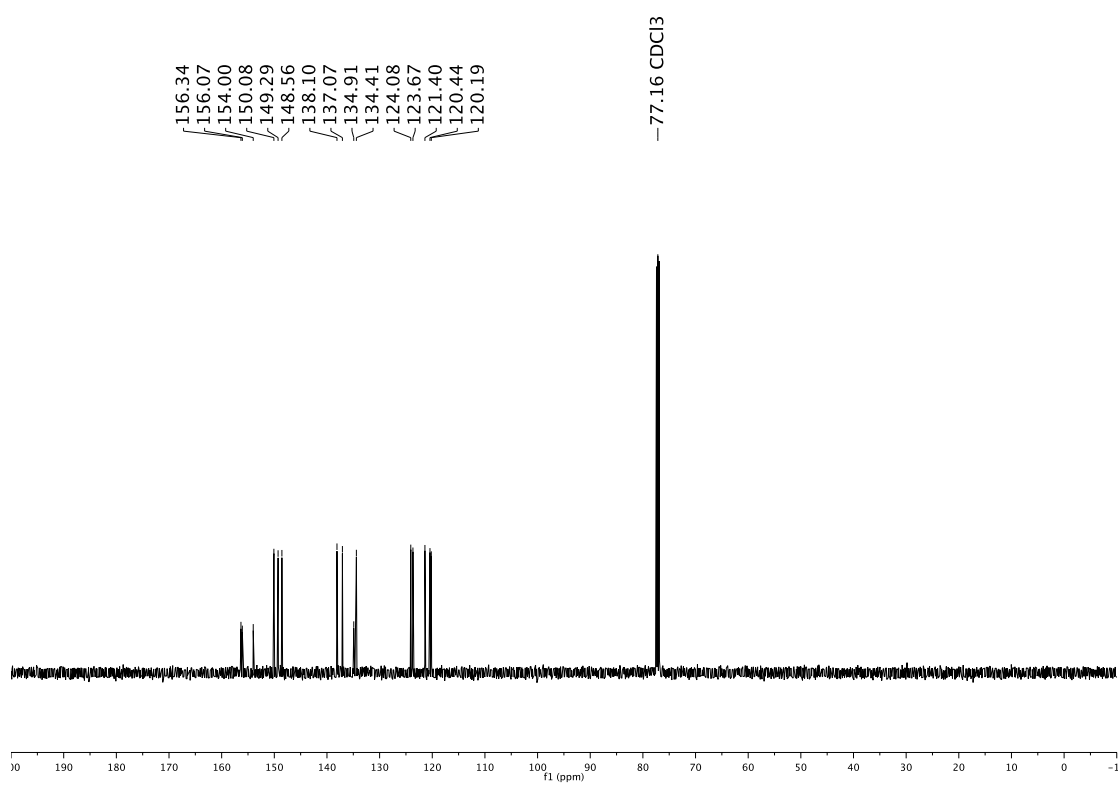
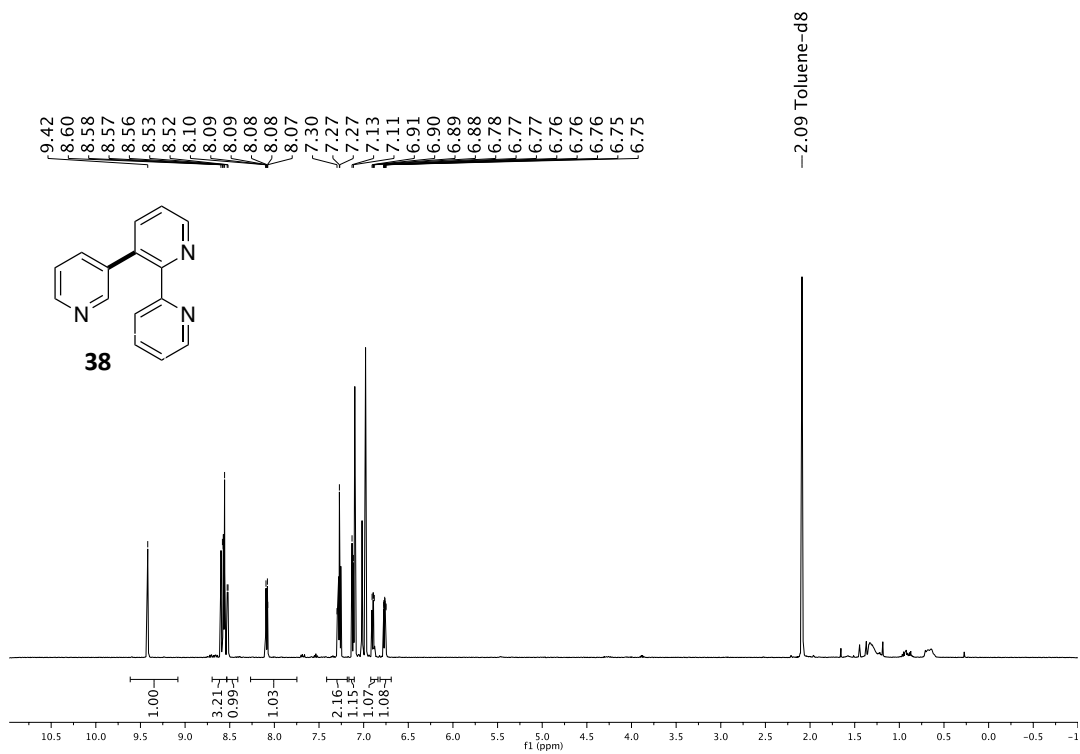
Ni-Catalyzed Stannylation of Aryl Ester via C-O Bond Cleavage



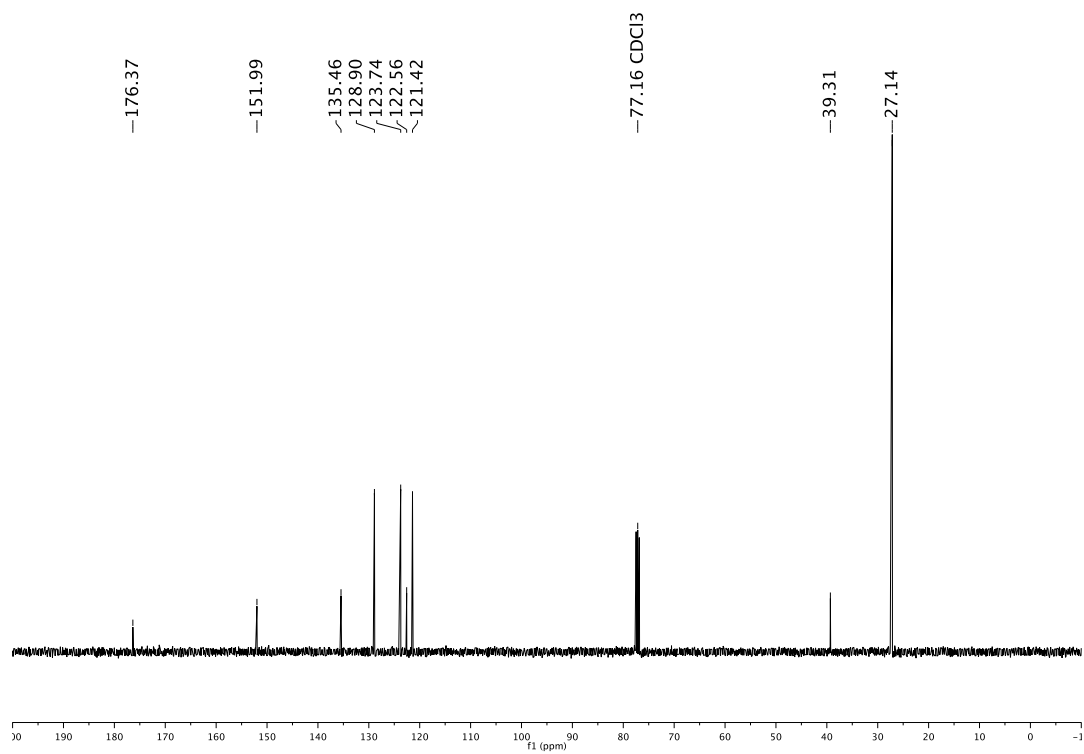
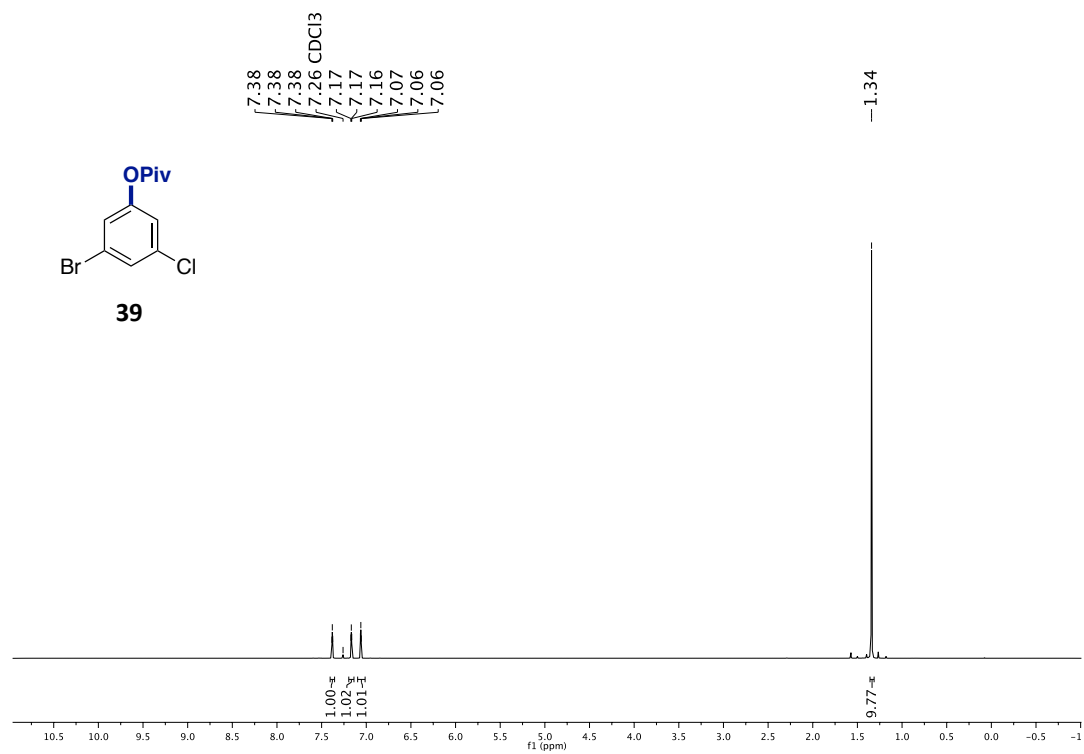


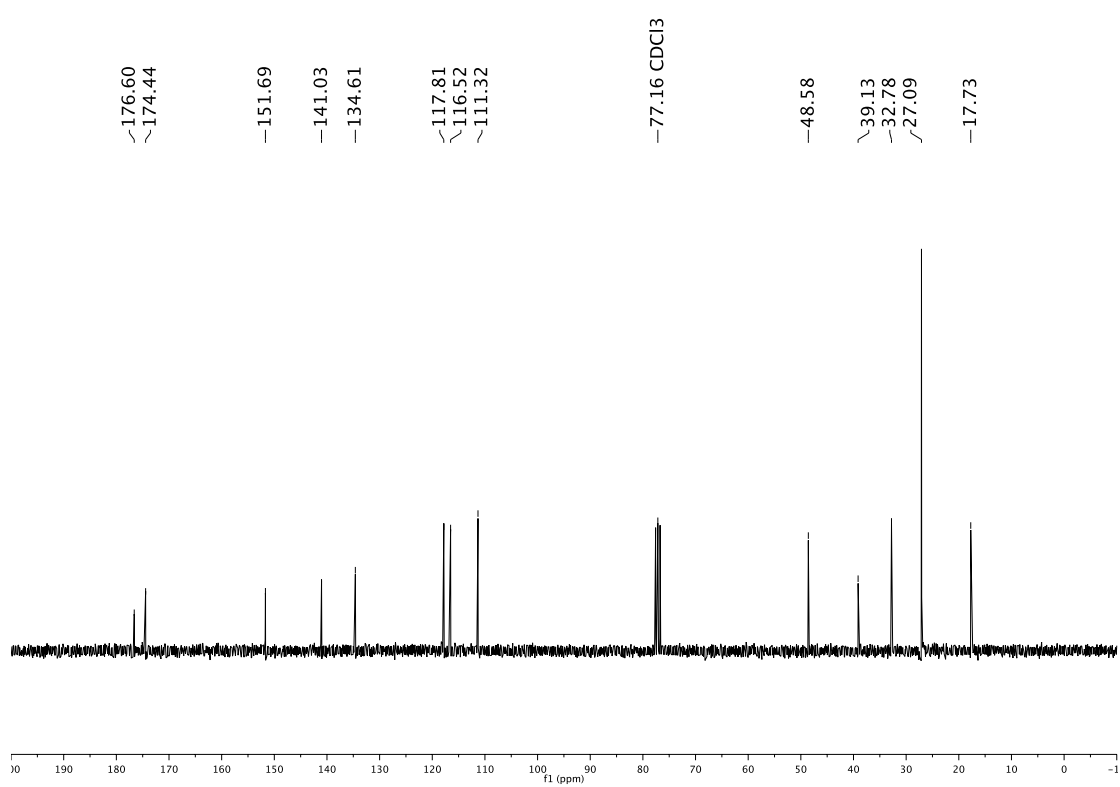
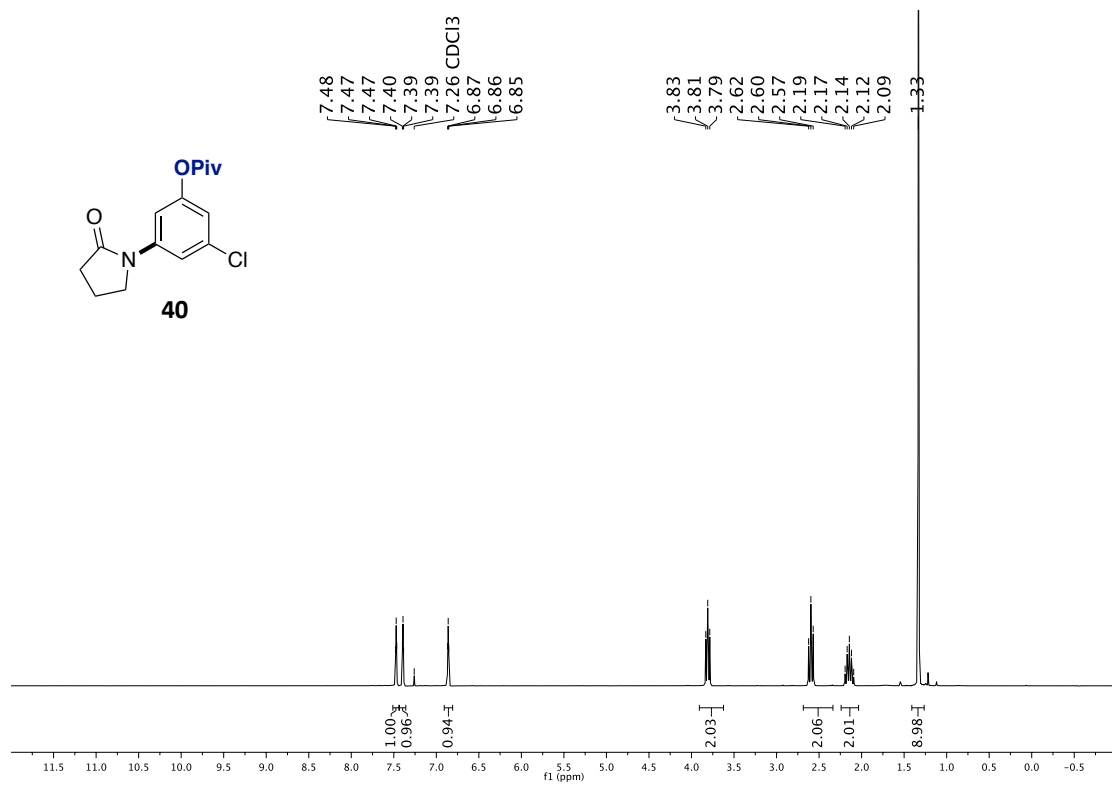
Ni-Catalyzed Stannylation of Aryl Ester via C-O Bond Cleavage



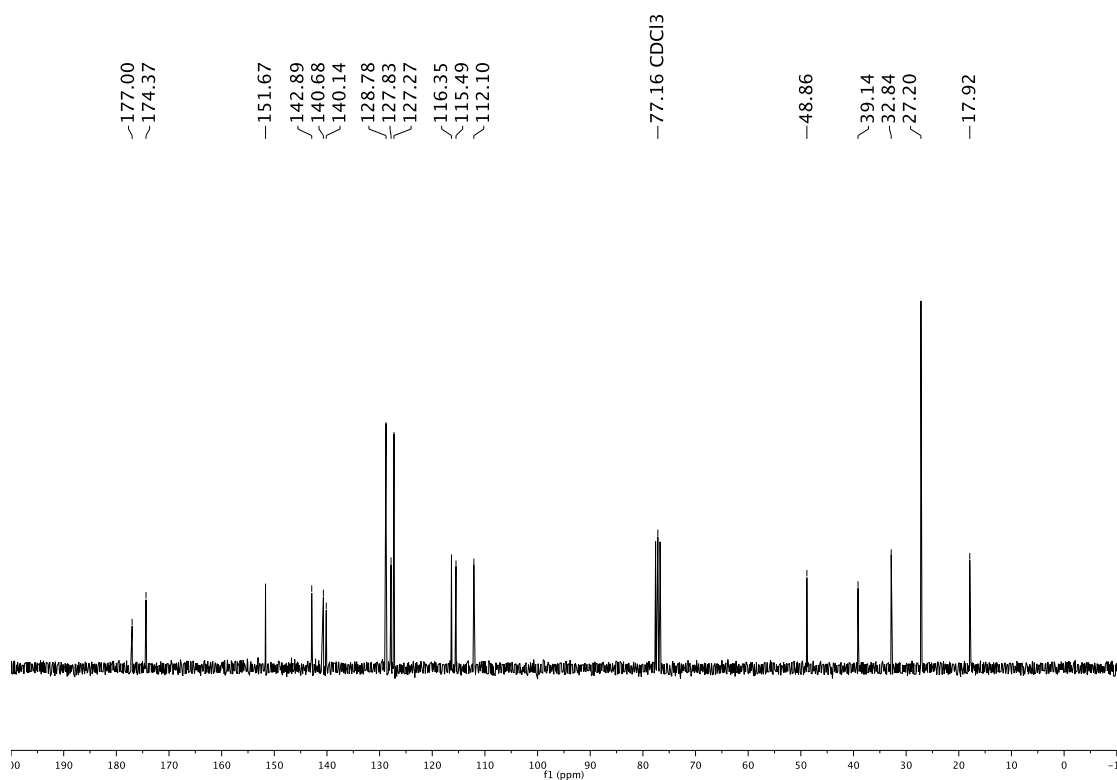
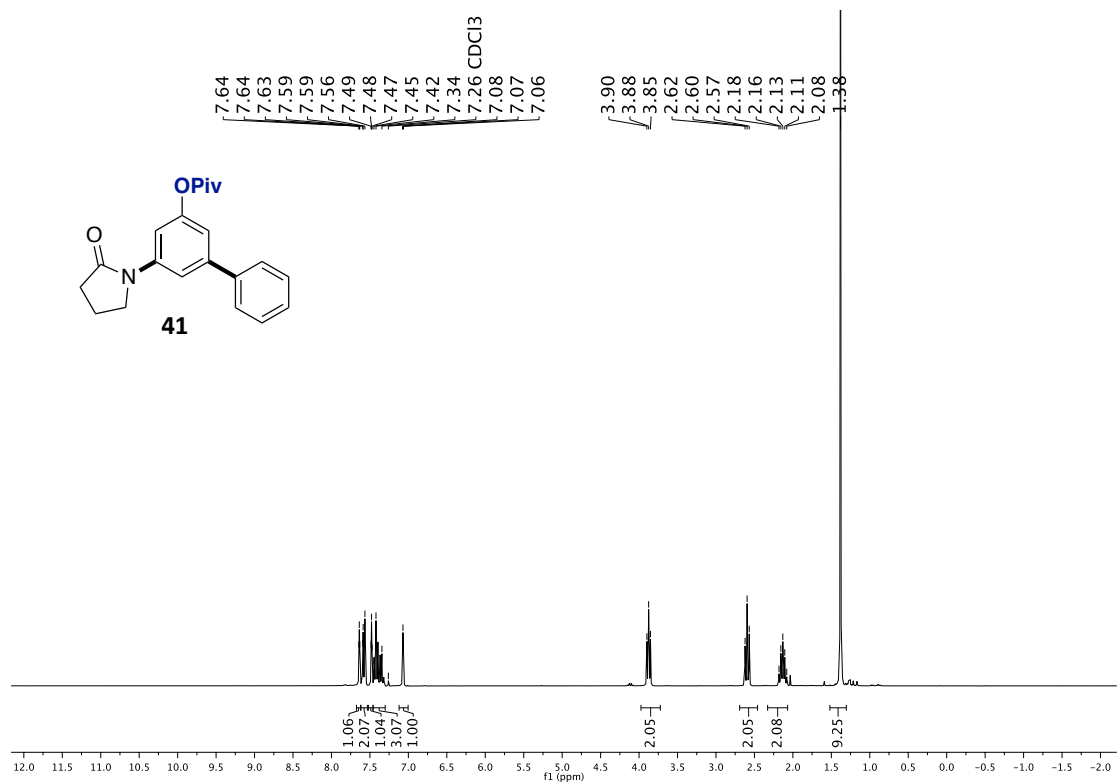


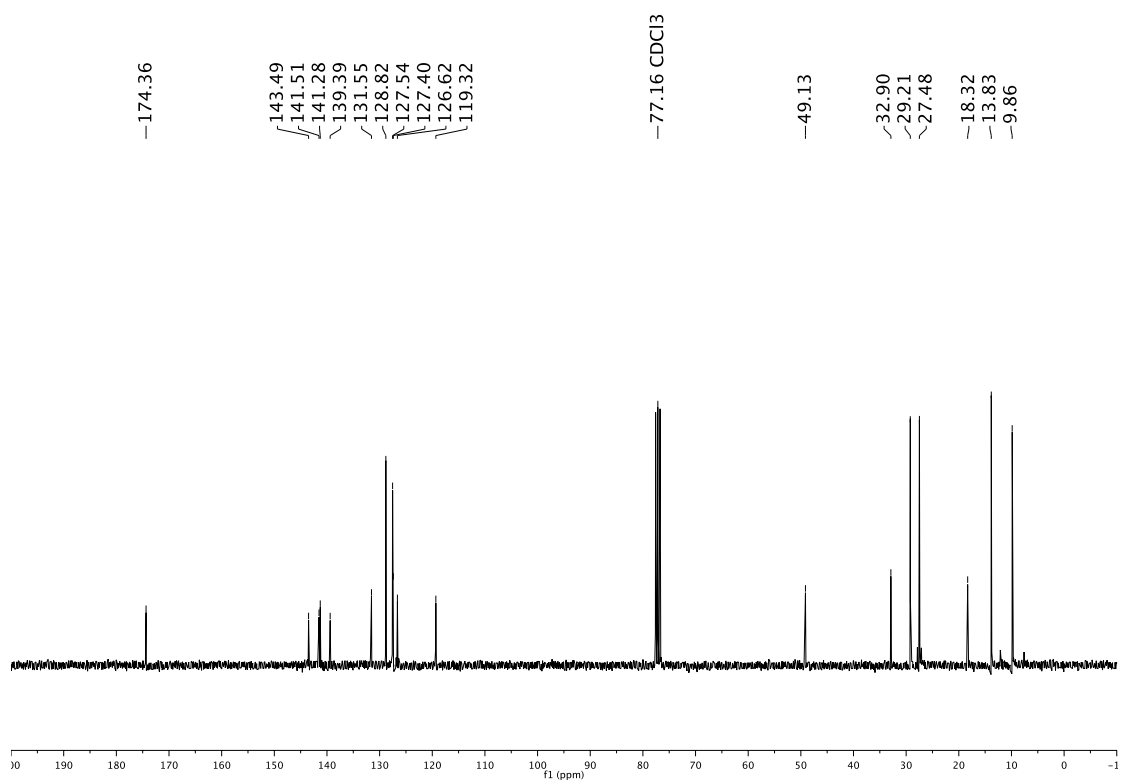
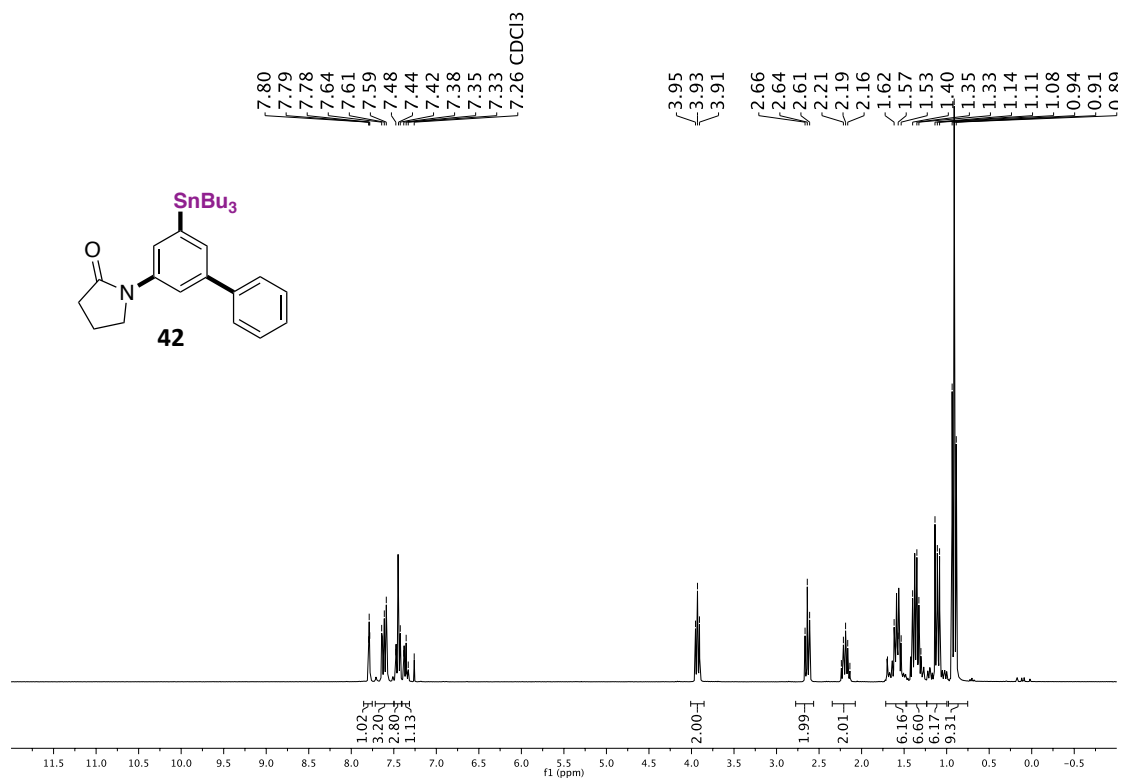
Ni-Catalyzed Stannylation of Aryl Ester via C-O Bond Cleavage





Ni-Catalyzed Stannylation of Aryl Ester via C-O Bond Cleavage



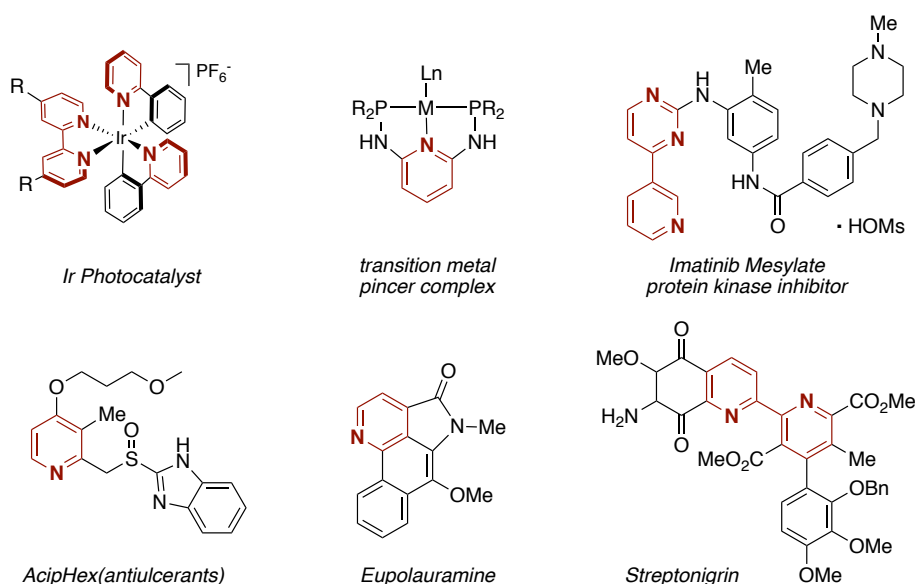


Chapter 3.

A Mild and Direct Site-Selective sp^2 C-H Silylation of (Poly)Azines

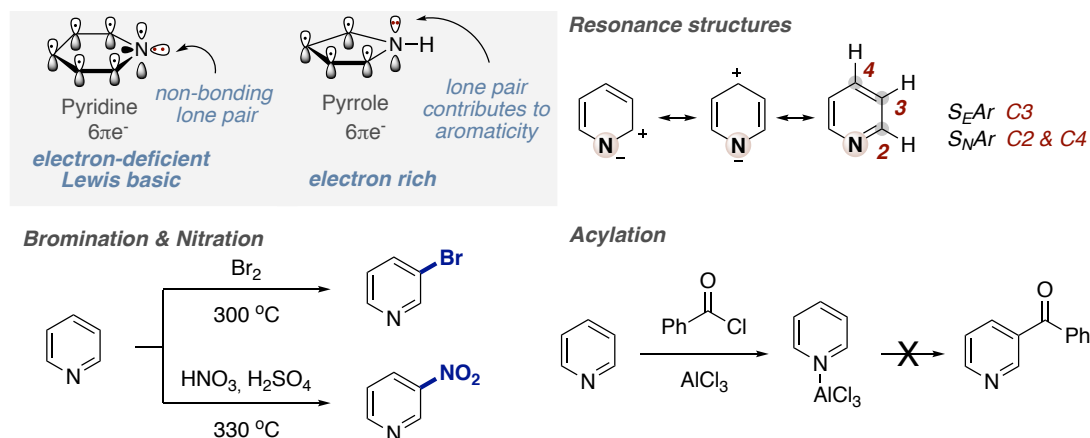
3.1. General Characteristics of (Poly)Azines

(Poly)azines are six-membered heteroaromatic rings that contain one or more nitrogen atoms. Due to their electron-withdrawing nature when compared to other nitrogen-containing heterocycles, (poly)azines have been frequently employed in S_NAr reactions and as versatile building blocks to build up molecular complexity. In addition, it is worth noting that (poly)azines rank among the most prevalent motifs in a myriad of drug-type molecules (Scheme 3.1).¹⁻⁶ These observations have prompted chemists to develop new efficient protocols to selectively modify (poly)azines in a rapid and reliable manner with exquisite control of the site-selectivity.



Scheme 3.1. Selected examples containing (poly)azines

(Poly)azines are structurally related to benzene, but have different properties. Owing to the presence of the electronegative nitrogen atom, the electron density of an azine is not distributed equally well over the aromatic ring. For example, pyridine possesses its free electron pair and it has conjugated system of six π electrons that are delocalized over the sp^2 -hybridized ring. The nitrogen atom involved in the π -bonding aromatic system use a non-hybridized p orbital. The lone pair is in an sp^2 orbital, projecting outward from the ring in the same plane. As a result, pyridine is inherently electron-deficient and Lewis basic (Scheme 3.2).

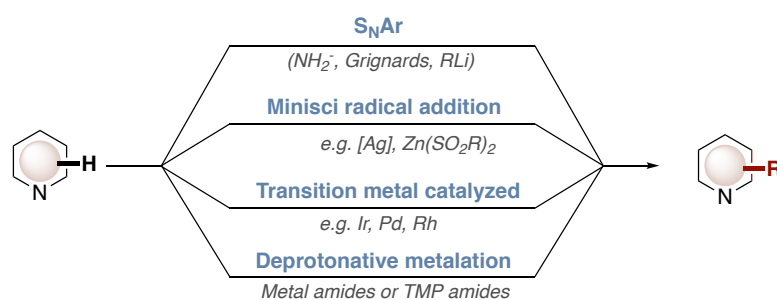


Scheme 3.2.. Electron deficient property and resonance structure of pyridine

Unlike electron-rich 5-membered nitrogen-containing heterocycles such as pyrroles, indoles, furans or thiophenes, (poly)azines are considerably less reactive and therefore significantly more difficult to functionalize under mild reaction conditions with high selectivity profile. For example, classical aromatic electrophilic substitution (S_EAr) reactions on pyridine such as halogenation and nitration require harsh reaction conditions (>300 °C), typically eroding the regioselectivity pattern. In addition, the presence of a Lewis basic nitrogen atom prevents the possibility of conducting Friedel-Craft-type reactions. Indeed, the resonance structure of pyridine indicates that nucleophilic aromatic substitution (S_NAr) takes place relatively easily at C2 and C4 position.

3.2. C-H Functionalization of Pyridine

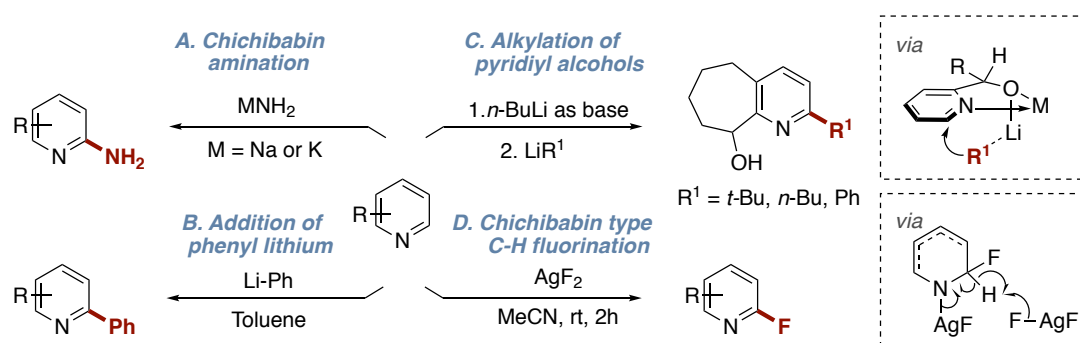
3.2.1. Overview on C-H bond functionalization of pyridine



Scheme 3.3.. C-H functionalization of electron-deficient heterocycles

A wide variety of protocols have been reported for the direct C-H functionalization of pyridine and other electron-poor azines via nucleophilic substitution, radical addition, deprotonative metalation, and transition metal-catalyzed C-H functionalization, among others (Scheme 3.3).³⁴ Due to the electron-poor nature of the pyridine π system, most of the current protocols for the functionalization of pyridine and related azines involve nucleophilic

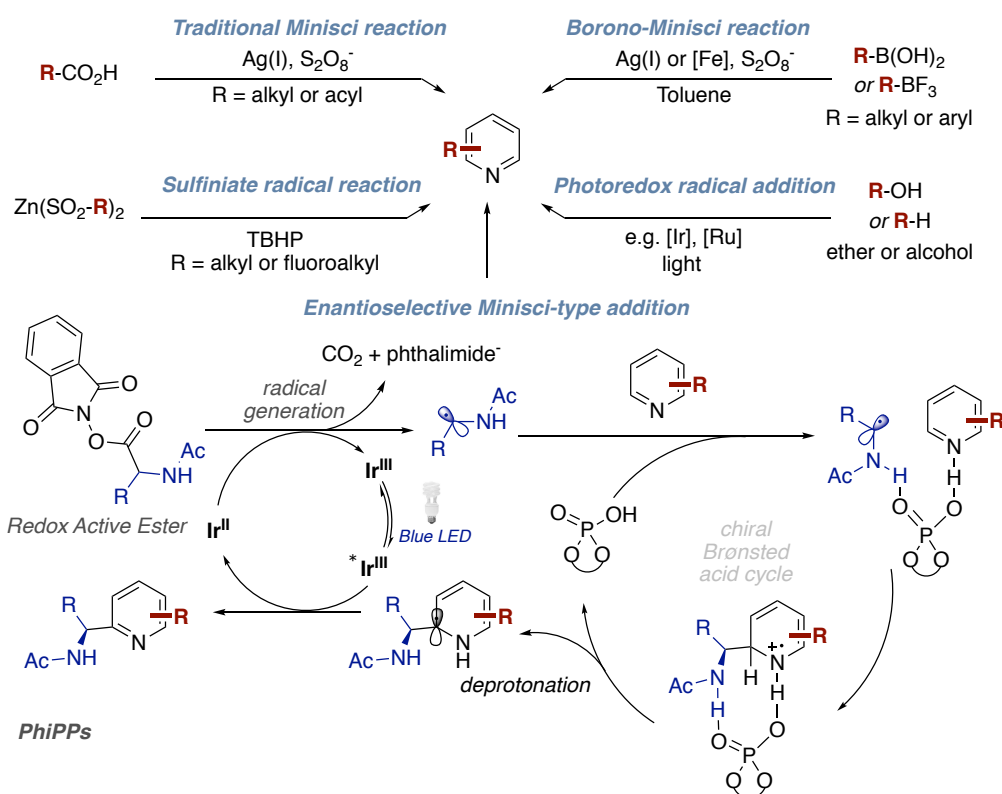
addition to the π system, followed by oxidation in order to obtain the formal C-H functionalization product. Initial studies aimed at this goal were reported by Chichibabin and co-workers, allowing to convert pyridines into the corresponding 2-aminopyridines using sodium or potassium amides as pronucleophiles (Scheme 3.4, **A**).^{7,8} Later on, it was found that pyridine could directly react with PhLi to afford the corresponding 2-arylpyridine at high temperature upon oxidation under air (Scheme 3.4, **B**).⁹



Scheme 3.4. S_NAr reaction of pyridine

The Chichibabin-type alkylation of pyridyl alcohols using alkyl lithium reagents has been accomplished by Sarpong and co-workers (Scheme 3.4, **C**).¹⁰ The reaction is thought to proceed via the intermediacy of a lithium alkoxide intermediate. Interaction between the alkoxide counteranion (M) and the pyridine nitrogen enhances the electrophilicity at C6 position, while simultaneously increasing the basicity of the alkoxide lone pairs. The increased basicity of the alkoxide would enhance interactions with the incoming organometallic reagent. In 2013, Hartwig group reported a Chichibabin-type sp^2 C-H fluorination of pyridines and diazines by using commercially available and easy-to-handle silver(II) fluoride as fluorinating reagent (Scheme 3.4, **D**).¹¹ The reaction occurs at ambient temperature with exclusively selectivity for fluorination adjacent to nitrogen atom. A tandem sequence of sp^2 C-H fluorination followed by S_NAr allowed to obtain a series of alkoxy-, amino- and thio-substituted pyridines that can be difficult to access through traditional methods.¹² A different, yet equally powerful, strategy to functionalize pyridines includes the utilization of carbon radical intermediates (Scheme 3.5).¹³ This technology was first employed in 1971 by Minisci and co-workers, demonstrating the viability to trigger C2-alkylation of pyridines with alkyl carboxylic acids and Ag(I) salts via the intermediacy of transient open-shell intermediates.¹⁴ This transformation is limited to alkyl or acyl radicals and often requires higher temperatures (greater than 70 °C), transition-metal additives and strongly oxidizing conditions. Regioisomeric mixtures are inevitably observed, but the innate regioselectivity can be influenced by the presence of acids,¹⁵ solvents,¹⁶ the nature of the substituents on the azine ring¹⁷ and the nature of the carbon radical.¹⁸ Inspired by Minisci's work, aryl boronic acids can be used as aryl radical precursors en route to C2-arylated azines.^{19,20} The reaction of Ag(I) with S₂O₈²⁻ affords reactive SO₄^{•-} that can easily generate the aryl radical by formal SET oxidation

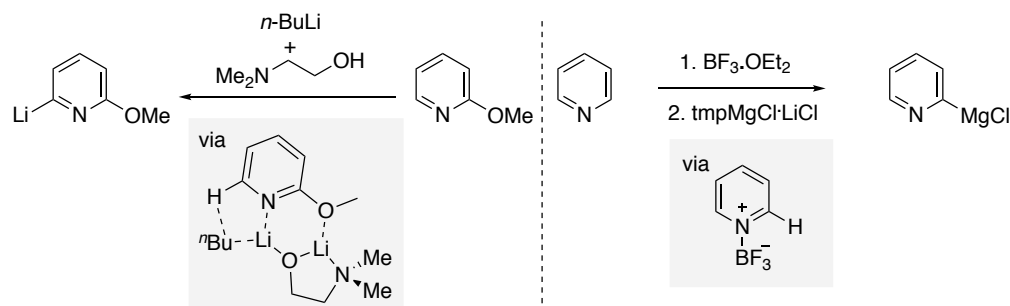
upon addition to the corresponding arylboronic acid. Few years later it was shown that alkyl trifluoroborate salts can also serve as radical precursors via SET oxidation in the presence of appropriate electron donors,²¹ including the utilization of iron.²² In 2012, zinc bis(alkanesulphinat) salts have been utilized as bench stable reagents that generate alkyl radicals in situ.²³ Notably, this platform was later on extended to accommodate a large family of alkylating (R-SO₂)₂Zn reagents [R = CF₃, CF₂H, CF₃CH₂, CH₂F, CH(CH₃)₂, CH₃(CH₂CH₂O)₃]. These reagents were found to be applied in a myriad of different (poly)azines, resulting in the innate C-H functionalization at either C2 or C4, with a reactivity trend that could be predicted on the basis of the substitution pattern.²⁴



Scheme 3.5. Minisci-type radical addition to pyridine rings.

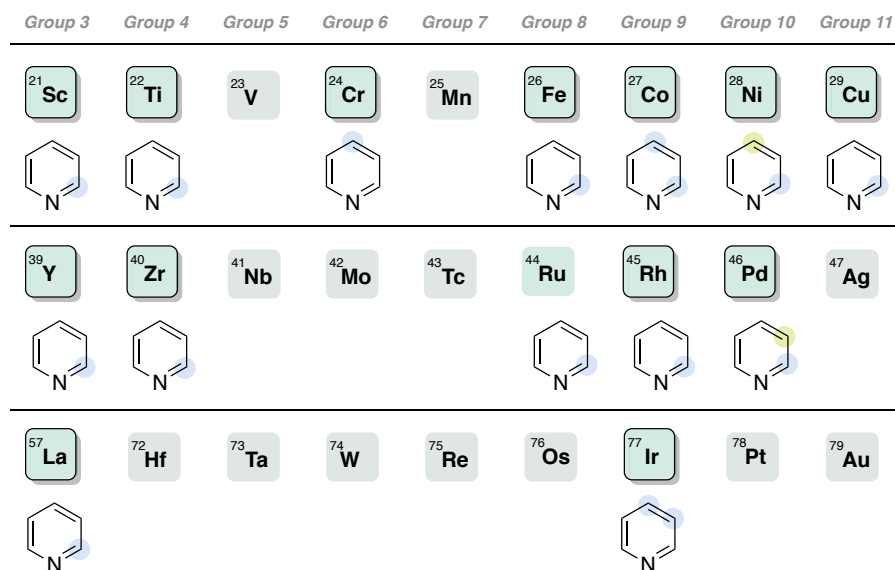
Driven by the unique ability of visible light photoredox catalysis to generate fleeting reaction intermediates under mild conditions, it comes as no surprise that photochemical techniques have been applied within the realm of Minisci-type reactions.²⁵ A particularly attractive methodology was reported by MacMillan, who demonstrated the implementation of an alkylation of azine with alcohols under visible light irradiation.²⁶ The reaction initiates from the addition of α -oxy radicals to azines to form α -amino radicals, which are dehydrated to give pyridyl-alkyl radicals via spin center shift. A single-electron transfer from the catalyst affords the corresponding products while recovering back the ground state of the photocatalyst. Very recently, Phipps disclose the direct addition of α -amino alkyl radicals to the C2-position of pyridine by a combination of chiral Brønsted acid catalyst and photoredox

catalysis.²⁷ Upon generation of amino radical from the amino acid redox active ester, the chiral phosphoric acid dictates the enantioselective radical attack to the protonated pyridine via hydrogen bonding. A fast deprotonation occurred, forming readily oxidized α -amino radicals, followed by the single electron transfer to the photocatalyst (Scheme 3.5, *bottom*).



Scheme 3.6. Deprotonative metalation of Pyridine

Traditionally, strong bases such as n -butyllithium and/or lithium amides have been used for the direct metalation of pyridine. However, these bases often lead to undesirable side reactions as a result of their high reactivity and their strong nucleophilicity (Chichibabin-type additions for example). Alternatives have been developed using a combination of $n\text{-BuLi}$ with TMEDA, which could disrupt the organolithium aggregates into much more reactive dimeric complexes.^{28, 29} Caubère and co-workers reported a new class of unimetallic superbases combining an alkyl lithium and a lithium aminoalkoxide (BuLi-LiDMAE), which could change the regioselectivity of lithiation of the 6-position of 2-alkoxy pyridine (Scheme 3.6, left).³⁰ However, the functional group tolerance is limited due to the high nucleophilicity of the organolithium reagent, making it difficult to be applied in the late stages of synthesis. Knochel and co-workers developed a series of LiCl -complexed 2,2,6,6-tetramethylpiperidyl (tmp) metal amide bases, such as $\text{tmpMgCl}\cdot\text{LiCl}$, $\text{tmpZnCl}\cdot\text{LiCl}$, $\text{TMPMgCl}\cdot\text{LiCl}$ as efficient deprotonation reagents, allowing to effect a site-selective metalation of sensitive aromatic compounds and azines, with deprotonation typically occurring at the most acidic C–H site (Scheme 3.6, right).^{31, 32} However, attempts to access otherwise related pyridines bearing a C–Mg, C–Zn or C–Al bonds proved to be unsuccessful. An interesting solution could be performed upon complexation of the pyridine with BF_3 prior to metalation with hindered Mg/Zn/Li bases or using BF_3 -based frustrated Lewis Pair ($\text{tmpMgCl}\cdot\text{BF}_3\cdot\text{LiCl}$), which allows an efficient, regioselective metalation of various N-containing heterocycles to occur.³³ Importantly, these metalation techniques enables the implementation of a complementary regioselective functionalization to generate a range of new polyfunctional pyridines.

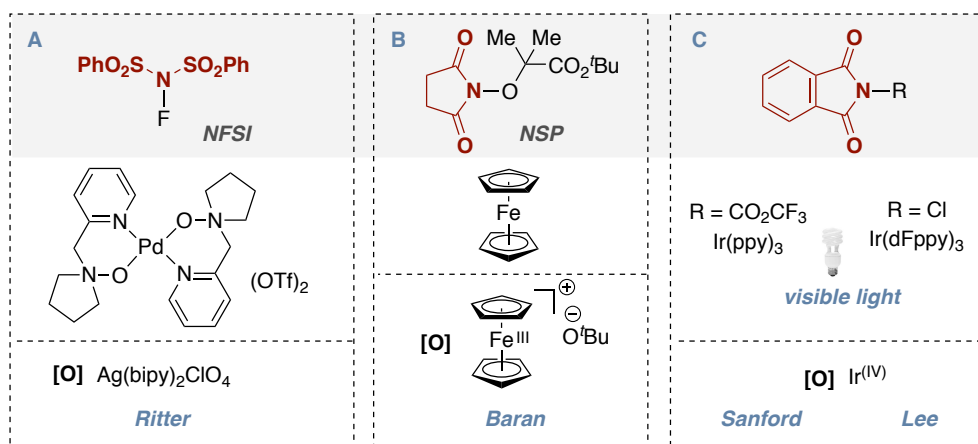


Scheme 3.7. Regioselectivity of Transition metal-catalyzed pyridine C–H functionalization.

The last decades have witnessed the rapid development of transition-metal-catalyzed direct C–H functionalization techniques. However, few examples are available regarding the direct C–H functionalization of unactivated pyridines and the scope of these methods is inherently limited due to low reactivity of pyridine and the coordinative nature of the nitrogen atom.^{34,35} The regioselectivity in transition-metal-catalyzed C–H functionalization of pyridine through non-radical pathways is summarized in Scheme 3.7. Most transition metals have their inherent reactivities toward specific positions of the pyridyl core. Notably, the fine-tuning of the catalyst or reaction conditions allowed for a modulation of the regioselectivity pattern.³⁶ Given the prevalence of (poly)azines in a myriad of pharmaceuticals, a mild, site-selective and tunable pyridine C–H functionalization that operates with a broad scope and chemoselectivity pattern will have important implications at the community.

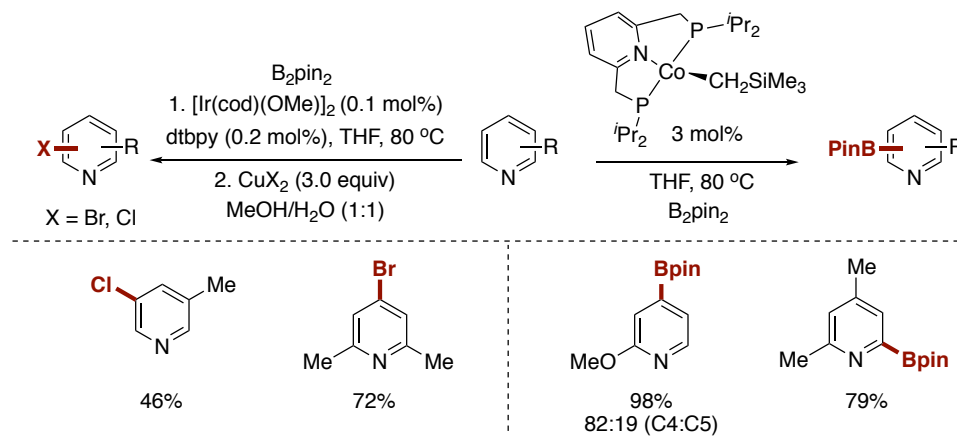
3.2.2. C–heteroatom bond-formation via C–H functionalization with transition metal

Ritter and co-workers reported an elegant work on the direct C–H imidation of pyridine with NFSI in the presence of N-oxide-ligated palladium catalyst and Ag(bipy)₂ClO₄ as co-catalyst (Scheme 3.8, A).³⁷ This transformation involved a Pd/Ag-mediated sulfonimidyl radical transfer from NFSI to pyridine substrates at C3 and C5 followed by silver-mediated single electron transfer. The reaction is believed to proceed via Pd(IV) complexes, with C–N bond formation occurring without the involvement of a canonical C–H palladation event. In 2014, a ferrocene-catalyzed C–H imidation of (hetero)arenes has been developed by Baran with an imidyl radical *N*-succinimidyl perester precursor (NSP) (Scheme 3.8 B).³⁸ The succinimidyl group was installed at the electron-rich position of the (hetero)arenes. The reaction showed broad scope in the presence of multiple functional groups. On the basis of these experiments, it was anticipated that ferrocene acts as an electron shuttle, generating an imidyl radical through an outer-sphere single electron transfer (SET).



Scheme 3.8. Metal-catalyzed regioselectivity of pyridine

The Sanford group developed a rather intriguing visible light-induced C3-amination of pyridines with *N*-acyloxyphthalimide with Ir-based photocatalysts at room temperature (Scheme 3.8, C).³⁹ Key for the success was the formation of PhthN• radicals with PhthNCO₂R compounds possessing electron-withdrawing CF₃ groups, likely due to improving the leaving group ability of the carboxylate anion, thereby favoring fragmentation to release RCO₂⁻ and PhthN•. A similar work by Lee described a visible light induced, Ir- catalyzed amination of pyridines by using *N*-chlorophthalimide as amination reagent.⁴⁰



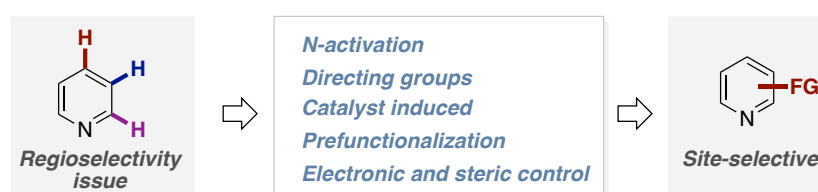
Scheme 3.9. Regioselective metal-catalyzed borylation of pyridine

Ishiyama and Miyaura described a highly active catalyst for arene borylation generated from the combination of [Ir(cod)(OMe)]₂ and 4,4'-di-*t*-butylbipyridine (dtbpy).⁴¹ Notably, Ir-catalyzed C-H borylation preferentially occurred at the C3-position of unsubstituted pyridine. Subsequently, Hartwig reported a one-pot method for the synthesis of bromoarenes and chloroarenes using the combination of a [Ir(cod)(OMe)]₂/dtbpy catalyzed borylation of arenes followed by a halogenation event with CuBr₂ or CuCl₂ (Scheme 3.9).⁴² The regioselectivity of the corresponding products can be explained by steric effects. In 2014, Chirik and co-workers reported a Co-catalyzed borylation of pyridines at C2 and C4 by using pincer-type ligands

possessing σ -donating phosphines.⁴³ As expected, C4-borylation took place if C2-substituted pyridines are employed as substrates, whereas C4-selectivity is observed for C2-substituted analogues.

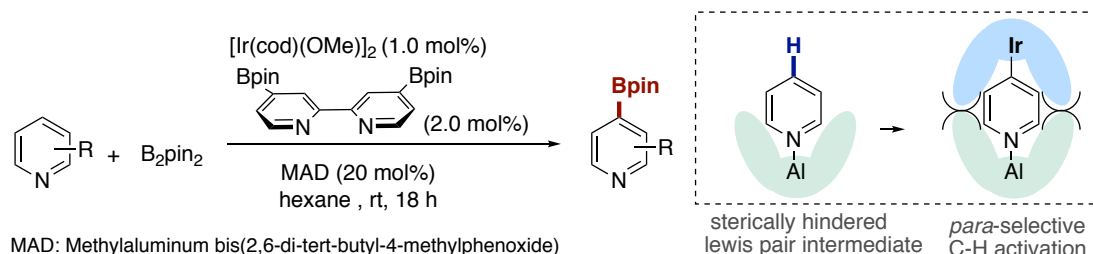
3.2.3. Selectivity control in C-H functionalization of pyridine

Since azines contain several C-H bonds with different innate reactivities, the development of new synthetic methods that allows for discriminating at will these moieties has become an important problem to be overcome in synthetic organic endeavors. As shown in scheme 3.10, such challenge has been tackled by a number of different approaches. The following section summarizes recent advances to control the site-selectivity in the direct C-H functionalization of pyridine or related azines.

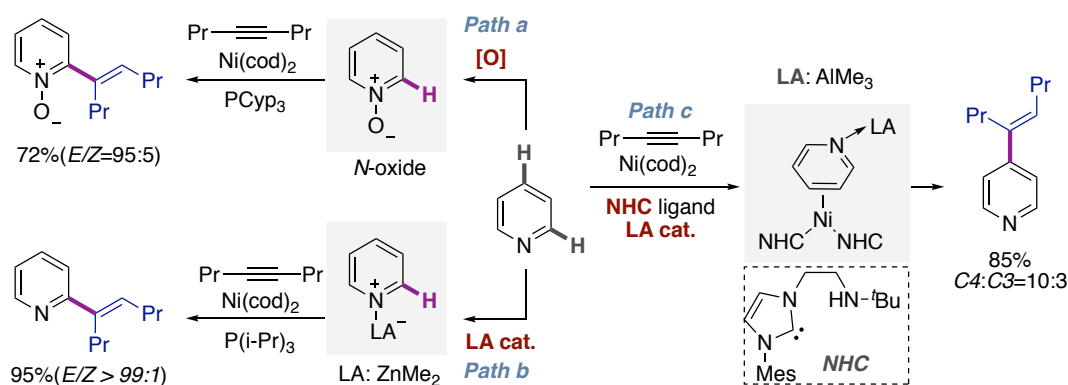


Scheme 3.10. Metal-catalyzed regioselectivity of pyridine

Steric control allows to functionalize the less sterically encumbered C-H bond. An unprecedented strategy for controlling the regioselectivity of C-H borylation of pyridines has been successfully developed by Nakao (Scheme 3.11).⁴⁴ The authors employed cooperative bulky aluminum-based Lewis acid and Iridium catalysts to furnish para-selective C-H borylation. The efficiency of this Ir/Al regime could be rationalized by the following: (a) the pyridine core coordinates a Lewis acid (MAD), resulting in a charge transfer while making the pyridine moiety considerably more electron-deficient, (b) steric repulsion between dtbpy on iridium and Lewis acid blocks the C2- and C3-positions, thus directing the C-H borylation at C4 instead. In a formal sense, this work shows the potential of cooperative iridium/aluminum catalysis as a powerful tool to control the regioselectivity of otherwise difficult C-H functionalization reactions.

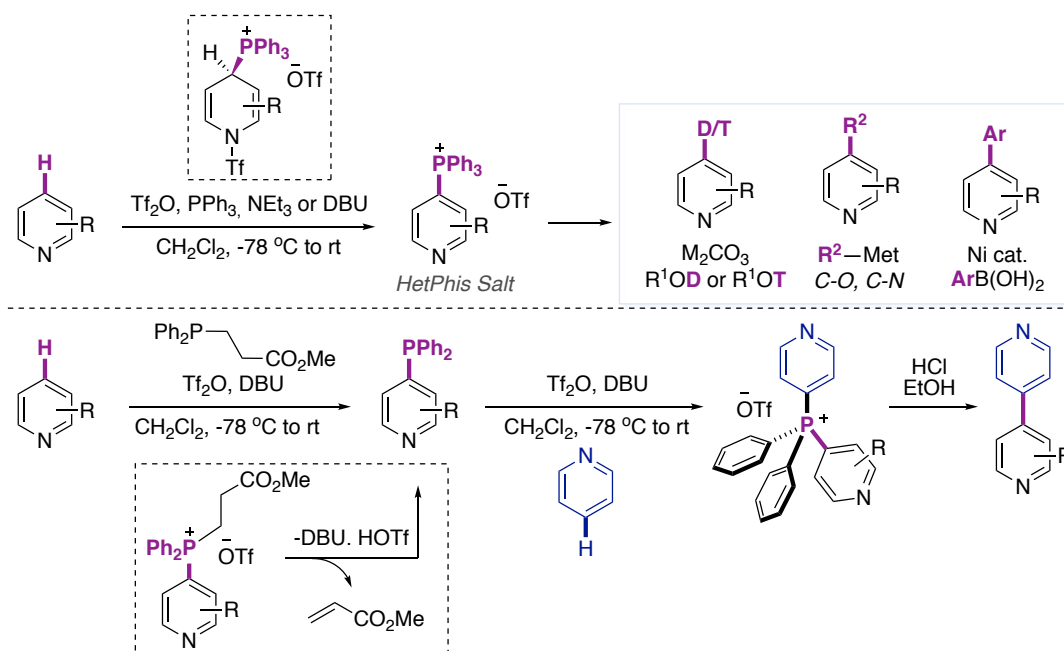


Scheme 3.11. *para*-Selective C-H borylation by cooperative Ir/Al catalysis



Scheme 3.12. Nickel-catalyzed C-H alkenylation of pyridine

Scheme 3.12 shows different strategies used in Ni-catalyzed direct C-H alkenylation with 4-octyne to control the site-selectivity and overcome the inherent low reactivity of pyridine via the intermediacy of pyridine-*N*-oxides. The reactivity of the latter is enhanced compared with that of parent pyridines, probably due to an increase in acidity at the proximal C2 C-H bond. The presence of a *N*-oxide does not hamper the application profile, as this motif can be easily deprotected by using classical reduction events with Pd/C or Zn dust. In all cases analyzed, this technology results in (*E*)-2-alkenylpyridine-*N*-oxides.⁴⁵ The reaction proceeds via initial activation of pyridine by a Lewis acid, setting the basis for an oxidative addition of the C2 C-H bond to Ni(0). Coordination with the alkyne moiety followed by migratory insertion and reductive elimination affords the corresponding vinyl moiety. Recent work by Hiyama and Nakao utilizes bifunctional catalysts consisting of nickel and a Lewis acid to derivatize the C2-H bond of pyridines.⁴⁶ Specifically, it was found that the combination of zinc and aluminum catalysts with mild Lewis acidity was critical for success. Thus, C2-alkenylation could be obtained in the presence of ZnMe₂ obtaining the targeted compound in 95% yield with high stereoselectivity. The regioselectivity can be altered to induce C4-selectivity when amino-linked NHC are utilized as ligands.⁴⁷ The hard donor amino side arm may act as a hemilabile group, stabilizing the reactive nickel center before being displaced by small molecule substrates. Owing to the steric bulk, oxidative addition to Ni(0)L_n occurs at C4 instead.



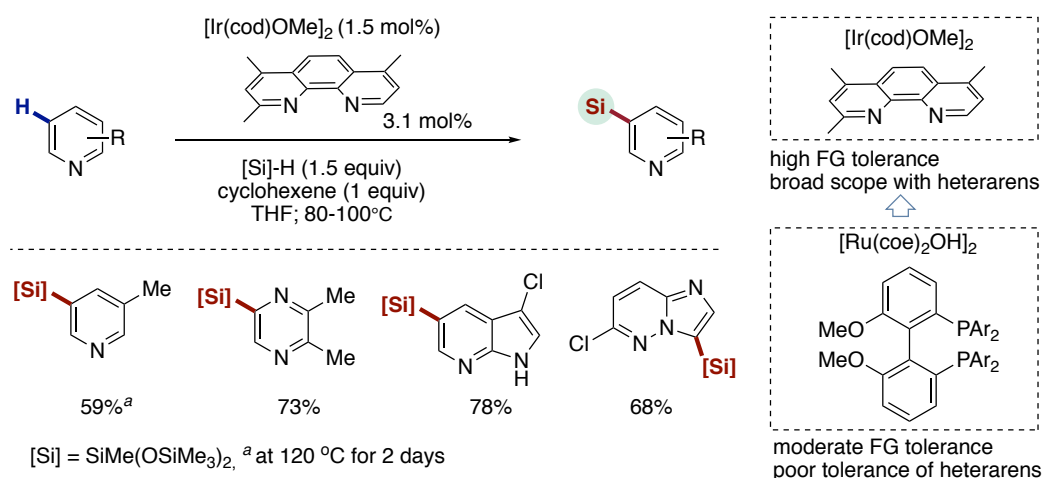
Scheme 3.13. Metal-catalyzed regioselectivity of pyridine

Site-selective functionalization of pyridines can also be achieved through functional group interconversions by pre-functionalizing the initial reaction site. Very recently, McNally and co-workers reported a new approach for the two-step C4-functionalization of pyridine (Scheme 3.13).⁴⁸ Heterocyclic phosphonium salts, which can be prepared via reactions of azines with triphenylphosphine in the presence of trifluoromethanesulfonic anhydride undergo S_NAr reactions with various nucleophiles such as alkoxides, thiolates, azides, or organolithium reagents.^{49, 50} As expected, the reaction of C4-substituted azines result in exclusive C2-functionalization. Subsequently, the same group described a Ni-catalyzed cross-coupling reaction of heteroaryl phosphonium salt with boronic acid to prepare heterobiaryls.⁵¹ Interestingly, deuterium and tritium atoms could also be incorporated into pyridine, diazine and pharmaceuticals using the same strategy, thus providing new ways to labelled *N*-containing heterocycles that are critical for absorption, distribution, metabolism and excretion (ADME) studies.⁵² More recently, a transition metal free C-C bond-forming reaction of pyridines was discovered via P(V) intermediates by reacting 4-phosphino azines with a different azine in combination with TfOH en route to a bis-heteroaryl phosphonium salt.⁵³ The targeted C-C bond-formation was then triggered upon exposure to acidic conditions, delivering the densely functionalized heterobiaryl compound in good yields.

3.2.3. sp^2 C-H silylation of pyridine

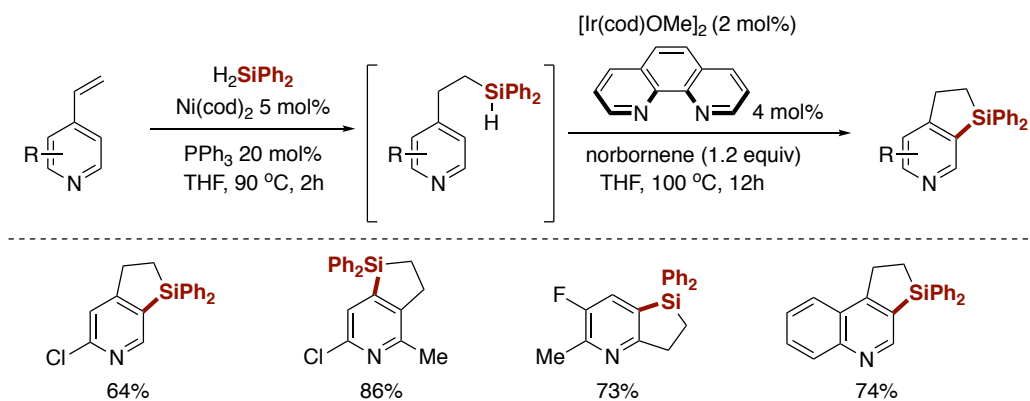
Traditional C-Si bond formation often relies on prefunctionalized substrates and typically employs stoichiometric amount of organometallic reagents such as organolithium, Grignard reagents, silicon halides or silicon alkoxides as electrophiles. Therefore, the development of a direct silylation of sp^2 C-H bonds would be a much more desirable endeavor, as it might allow

to access heteroaryl organic silanes, versatile building blocks with promising therapeutic agents with interesting biological properties.⁵⁴⁻⁵⁸ Over the last years, a handful of studies have been described to enable a sp^2 C–H silylation of electron-deficient (poly)azines.



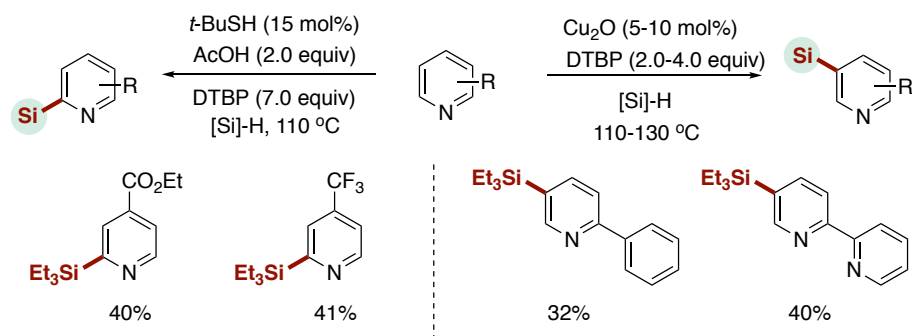
Scheme 3.14. Iridium-catalyzed silylation of sp^2 C–H bonds in (poly)azines.

Unlike the corresponding metal-boryl complexes, metal-silyl complexes are much less reactive towards C–H bond functionalization, and the vast majority of methods for the catalytic intermolecular silylation of aryl C–H bonds often require high temperatures, a large excess of the arene,⁵⁹ or ortho-directing groups.⁶⁰ Recent approaches have overcome these limitations, affording electron-deficient heteroarylsilanes under mild reaction conditions. For example, Cheng and Hartwig have developed a series of steric-controlled Rh- or Ir-catalyzed C–H silylation of pyridines (Scheme 3.14). The use of [Rh(cod)OH]₂ and a chiral biaryl phosphine allowed for a mild intermolecular silylation using arenes as limiting reagent. However, the applicability of this protocol is compromised by the high cost of the ligand as well as the poor functional group tolerance and the absence of reactivity in the presence of azines. Subsequently, the authors discovered a combination of [Ir(cod)(OMe)]₂ and phenanthroline as ligand that enabled the C–H silylation of various heteroarenes with high functional group compatibility.⁶¹ Nevertheless, high temperatures with prolonged reaction time are still required and poor regioselectivity is obtained with 1,2-disubstituted substrates.⁶²



Scheme 3.15. Nickel/Iridium catalyzed one-pot synthesis of dihydrosiloles

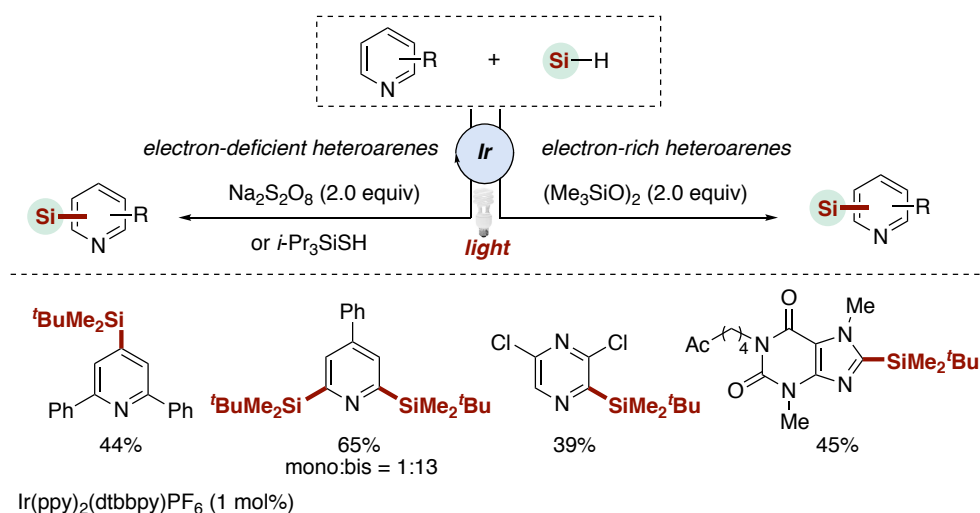
The development of intramolecular C–H silylation is comparatively easier than the intermolecular C–H silylation event due to the innate control of the regioselectivity while preventing undesirable two-fold C–H silylation. To such end, Gevorgyan described an interesting nickel-catalyzed intramolecular hydrosilylation followed by Iridium-catalyzed dehydrogenative coupling (Scheme 3.15).⁶³ Higher yields are usually obtained when a sacrificial H_2 acceptor (norbornene) is added to the reaction mixture as hydrogen is released as byproduct. It was found that both electron-donating and electron-withdrawing groups were tolerated leading to a dehydrogenative Si–H/C–H coupling at the less hindered site.



Scheme 3.16. Copper or thiol-catalyzed C–H silylation of azines

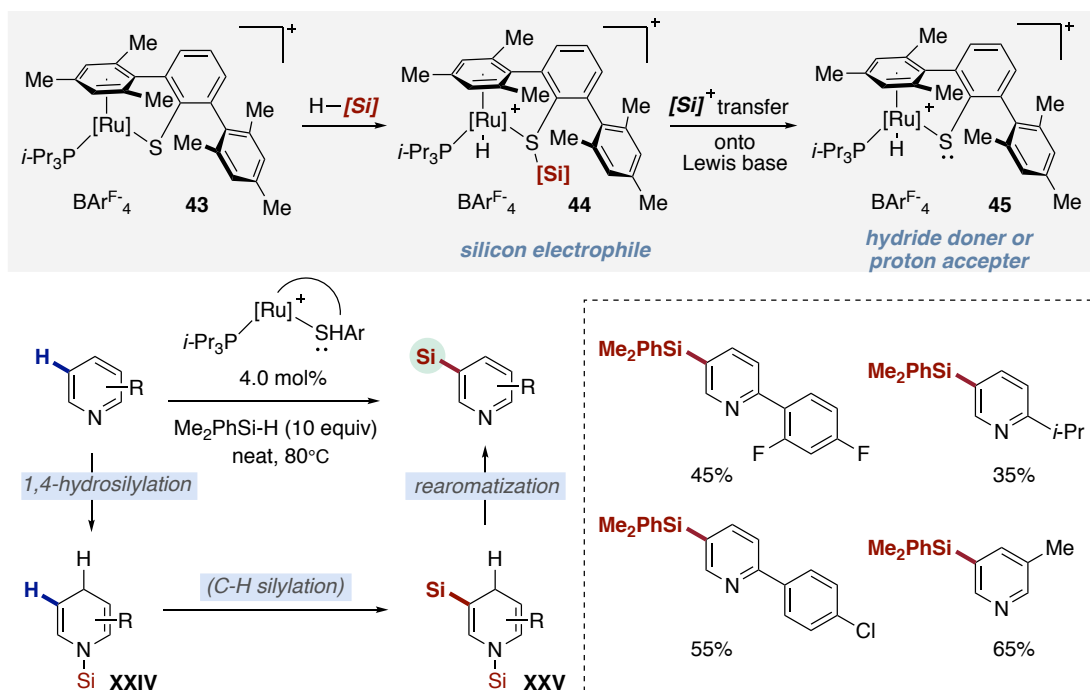
Maruoka and coworkers disclosed an interesting thiol-catalyzed approach for the C–H silylation of electron-deficient heteroarenes such as pyridines, pyrazines and quinoxalines.⁶⁴ The reaction gives rise to mono-silylation at the ortho-position in low yields (4 - 53%) accompanied with the formation of a significant amount of bis-silylation products (Scheme 3.16). Furthermore, this process is carried out at high reaction temperature (110 °C) with a large excess amount of non-particularly friendly DTBP, thus causing a significant safety concern. In 2017, the Liu group reported a Cu_2O catalyzed site-selective approach enabling the introduction of trialkylsilyl groups into pyridine rings at high temperatures.⁶⁵ The observed site-selectivity presumably arises from the better resonance stabilization of the radical σ -complex through conjugation with the para substituent. Although C2-silylation would benefit

from the same stabilizing effect, steric hindrance prevents functionalization of this position. It is worth noting that electron-deficient heteroarenes display lower efficiency and only two pyridine examples were shown. Taking all these observations into consideration, the development of a mild, efficient and tunable site-selective silylation of electron-deficient azines still represents a problematic endeavor, and an opportunity for method development.



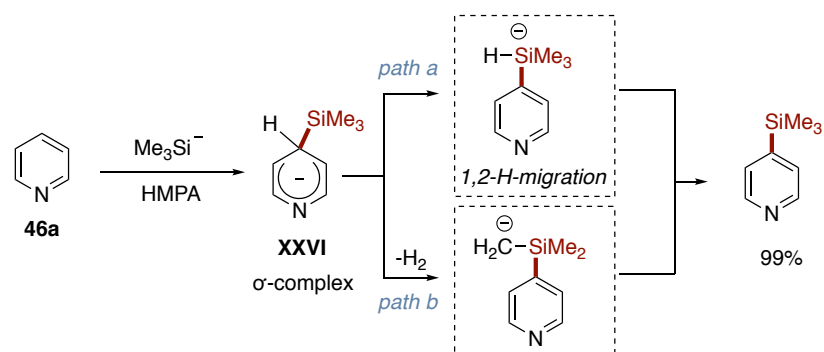
Scheme 3.17. Photocatalytic C–H silylation of heteroarenes

Recently, a photoredox C–H silylation of heteroarenes under visible light irradiation has been reported by Zhang (Scheme 3.17).⁶⁶ The significant advantage of this approach is that the reaction employed safe and readily available oxidants under very mild temperatures (30°C) and open to air. With the right choice of oxidant [$\text{Na}_2\text{S}_2\text{O}_8$ or $(\text{Me}_3\text{SiO})_2$], silylation of electron-deficient isoquinolines and benzonitriles as well as electron-rich heterocyclic systems could be achieved. However, stoichiometric amounts of peroxides were necessary for this reaction.



Scheme 3.18. Ru-catalyzed electrophilic C–H silylation of pyridine

Apart from the above examples that describe the means to effect a radical or a transition metal-catalyzed C–H silylation, the preparation of heteroarylsilanes can also be effected by electrophilic aromatic substitution reactions (S_EAr). However, this technology is particularly challenging due to parasitic protodesilylation, as the Wheland intermediate is substantially stabilized by the β-silicon effect. Therefore, proton capture at the *ipso* position of the arylsilane is more likely, which will lead to release of the silicon electrophile and regeneration of the defunctionalized arene. As a result, protons have to be effectively removed from the reaction mixture to suppress the backward reaction. Oestreich and coworkers have developed a counterintuitive Ru-catalyzed dehydrogenative aromatic C–H silylation reaction using hydrosilanes as counterparts (Scheme 3.18).⁶⁷ The polar ruthenium thiolate complex **43** is capable of generating silicon electrophiles in a catalytic manner through cooperative Si–H bond activation. In this manner, the sulfur-stabilized silicon cation species **44** could promote the S_EAr reaction. The reaction shows perfect regioselectivity at the more nucleophilic *meta* (C3) position. This unusual reaction takes place via a S_EAr mechanism which involves formation of cationic low-energy σ-complex followed by deprotonation in the presence of the basic sulfur atom in **45** with the release of hydrogen. In fact, the ruthenium thiolate complex **45** serves as both hydride donor and proton acceptor and the reaction proceeds through a sequence of dearomatization, silylation, and rearomatization over the pyridine motif.^{68, 69} Unfortunately, the reactivity is limited to mainly 2-substituted pyridines.



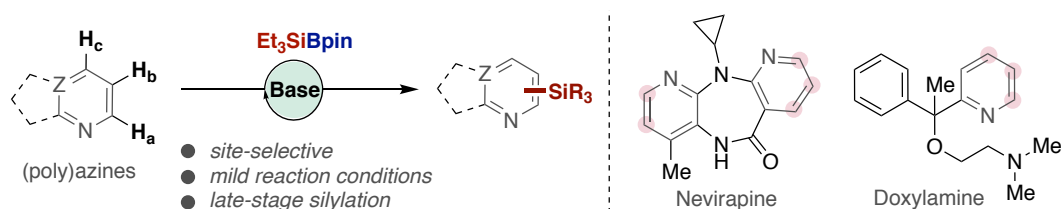
Scheme 3.19. Nucleophilic substitution with trimethylsilyl anion

Rossi and coworkers found that fluorobenzene smoothly undergoes para and ortho silylation instead of displacement of the fluoride group when treated with silyl anions in HMPA (Scheme 3.19).⁷⁰⁻⁷² Even electron-deficient pyridine can be silylated as well. The authors rationalized these observations via an anionic σ -complex **XXVI** (Meisenheimer intermediate) arising from the attack of silyl anion at the *para* position of pyridine. This adduct could produce the silylated product through deprotonation of the methyl group from the trimethylsilyl substituent to furnish silylated pyridine (path b). Alternatively, a 1,2-H shift from carbon to silicon could take place (path a). A pentacoordinate silicon species would thus be formed, which can persist in an anionic form until aqueous workup, delivering the targeted compound.

3.3. General Aim of the Project

The general interest of our research group is primarily focused on the activation of strong σ -bonds with the aim of producing synthetically relevant molecules. Azines containing C–Si bonds are of great contemporary interest in drug discovery, material science, organic synthesis and complex molecule synthesis.⁵⁴⁻⁵⁸ Among the many strategies that have been investigated, direct C–H functionalization of azines would allow to access azine-cores, useful building blocks that can be easily transformed into other congeners via C–Si bond-cleavage. In this chapter, we will tackle the challenge of promoting a switchable site-selective C–H silylation of azines under mild conditions and in the absence of transition metal complexes.

□ A mild and direct site-selective C–H silylation of (Poly)azines (**this chapter**)



Scheme 3.4. Base-mediated C–H silylation of azines.

3.4. KHMDS Mediated Direct Site-Selected C-H Silylation of (Poly)Azines

3.4.1. Optimization of the reaction conditions

Our study began by using simple pyridine as substrate with Et₃SiBpin (**47**) as the silicon source. The choice of the latter was not arbitrary due to its ease of synthesis in bulk from simple precursors,⁷³ its effectiveness in related silylation events from our group⁷⁴⁻⁷⁷ and more importantly, the ability to functionalize the C-Si bond at later stages without site-selectivity problems that typically arise if using otherwise related Me₂PhSiBpin (**3**). After some experimentation, we found that a transition metal-free protocol simply consisting of a base and Et₃SiBpin in DME could afford the targeted C-H silylated pyridine. As shown in Table 3.1, the role of the base was found to be crucial for success. Only strong, non-nucleophilic bases resulted in high conversions to **48a/48a'**. Likewise, the escorting counterion had a non-obvious influence on reactivity and site-selectivity (entries 1-3), with KHMDS giving the best reactivity and the highest ratio (1:5.6) of C4 to C2 silylation. Other bases with higher nucleophilicity such as KOMe, that are known to efficiently activate Si-B compounds, didn't afford **48a** or **48a'**. Similarly, milder bases were found to have a deleterious effect on reactivity (entries 8-18).

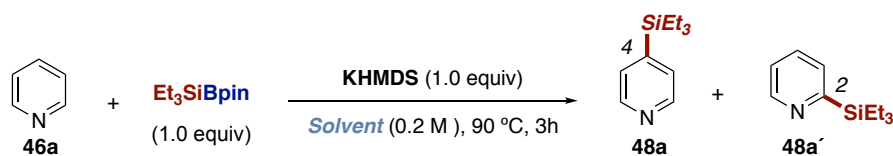
Entry	Base	Yield (%) ^a	48a/48a'	Entry	Base	Yield (%) ^a
1	LiHMDS	27	2:1	10	KOAc	0
2	NaHMDS	59	3.3:1	11	KOH	0
3	KHMDS	61	5.6:1	12	Zn(HMDS) ₂	0
4	LiOt-Bu	0	—	13	Mg(HMDS) ₂	0
5	NaOt-Bu	0	—	14	Cs ₂ CO ₃	0
6	KOt-Bu	51	1.7:1	15	CsF	0
7	NaH	0	—	16	KF	0
8	KOMe	0	—	17	NaOPh	0
9	KOTMS	0	—	18	DABCO	0

Reaction conditions: Conditions: **46a** (0.40 mmol), Et₃SiBpin (0.4 mmol), KHMDS (0.4 mmol), DME (1.0 mL) at 90 °C, 8h. ^a Yield of **48a** and **48a'** detected by GC, using decane as internal standard.

Table 3.1. Screening of bases

We decided to evaluate the direct C4-silylation of pyridine with Et₃SiBpin by changing the solvent of the reaction (Table 3.2). Interestingly, a strong solvent effect was noticed. Non-polar solvents such as hexane and toluene provided silylated product in moderate yields, but the ratio of **48a** and **48a'** was found to be 1:1 (entries 1, 2). An otherwise similar result was

observed when the reaction was conducted without solvent (entry 3). Notably, ethereal solvents such as Et₂O, *t*-BuOMe or THP provided the C2-silylated **48a** as major product (entries 4-10). Specifically, C2 silylation was predominantly observed with dioxane (entry 10), whereas the use of bidentate DME and diglyme gave the opposite selectivity, predominantly forming C4-silylation instead (entry 11, 12). Particularly noteworthy was the observation that highly polar aprotic solvents such as DMF or MeCN shut down the reactivity profile (entries 13, 14).



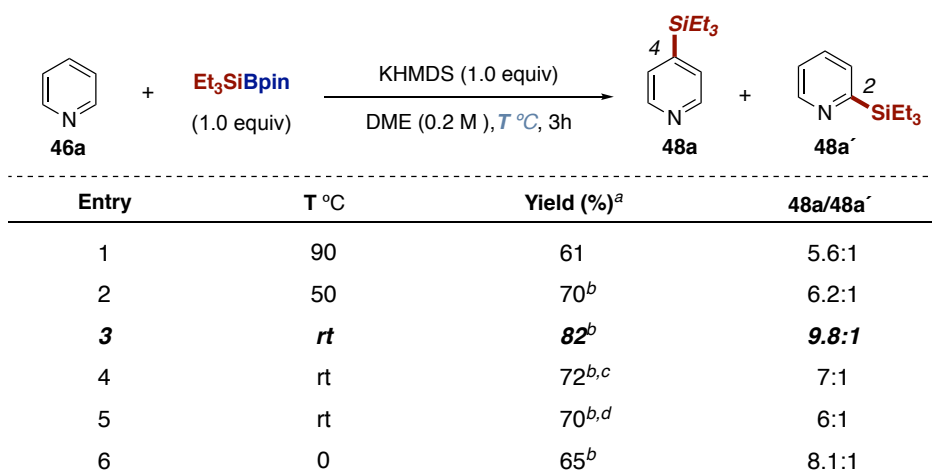
Entry	Solvent	Yield (%) ^a	48a/48a'
1	<i>n</i> -hexane	54	1.1:1
2	Toluene	59	1.3:1
3	None	58	1.5:1
4	Et ₂ O	56	1:1.8
5	<i>t</i> -Bu ₂ O	46	1:2.4
6	<i>i</i> -Pr ₂ O	48	1:2.4
7	<i>t</i> -BuOMe	43	1:2.7
8	THF	58	1.7:1
9	THP	49	1:2.9
10	Dioxane	55	1:3.2
11	DME	59	5.5:1
12	Diglyme	49	12:1
13	DMF	0	—
14	AcCN	0	—

Reaction conditions: Conditions: **46a** (0.40 mmol), Et₃SiBpin (0.4 mmol), KHMDS (0.4 mmol), Toluene (1.0 mL) at 90 °C, 8h. ^aYield of **48a** and **48a'** detected by GC, using decane as internal standard.

Table 3.2. Screening of solvent

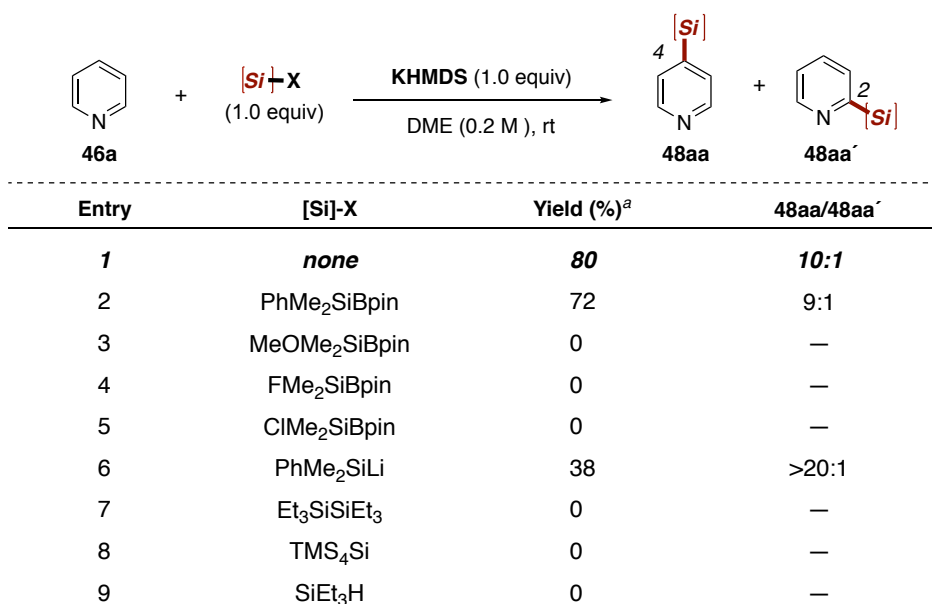
With these results in hand, we then focused our attention on studying the effect of the temperature. As shown in Table 3.3, the ratio of C4 silylated product **48a** was improved as the temperature decreased from 90 °C to rt (entries 1-3). The best results were found at room temperature providing 82% of silylated product (C4:C2 = 9.8:1 ratio). Notably, this transition-metal free C-H silylation was equally effective at temperatures as low as 0 °C (entry 6). In line with the strong solvent effect, the use of commercially available KHMDS (2M in toluene) had a deleterious impact on site-selectivity (entries 4, 5).

A Mild and Site-Selective sp^2 C-H Silylation of (Poly)Azines



Reaction conditions: Conditions: **46a** (0.40 mmol), Et₃SiBpin (0.4 mmol), KHMDS (0.4 mmol), Toluene (1.0 mL) at 90 °C, 8h. ^aYield of **48a** and **48a'** detected by GC, using decane as internal standard. ^bReaction time 18h. ^cKHMDS solution (2M in toluene) was used. ^dKHMDS solution (1M in toluene) was used.

Table 3.3. Screening of reaction temperature



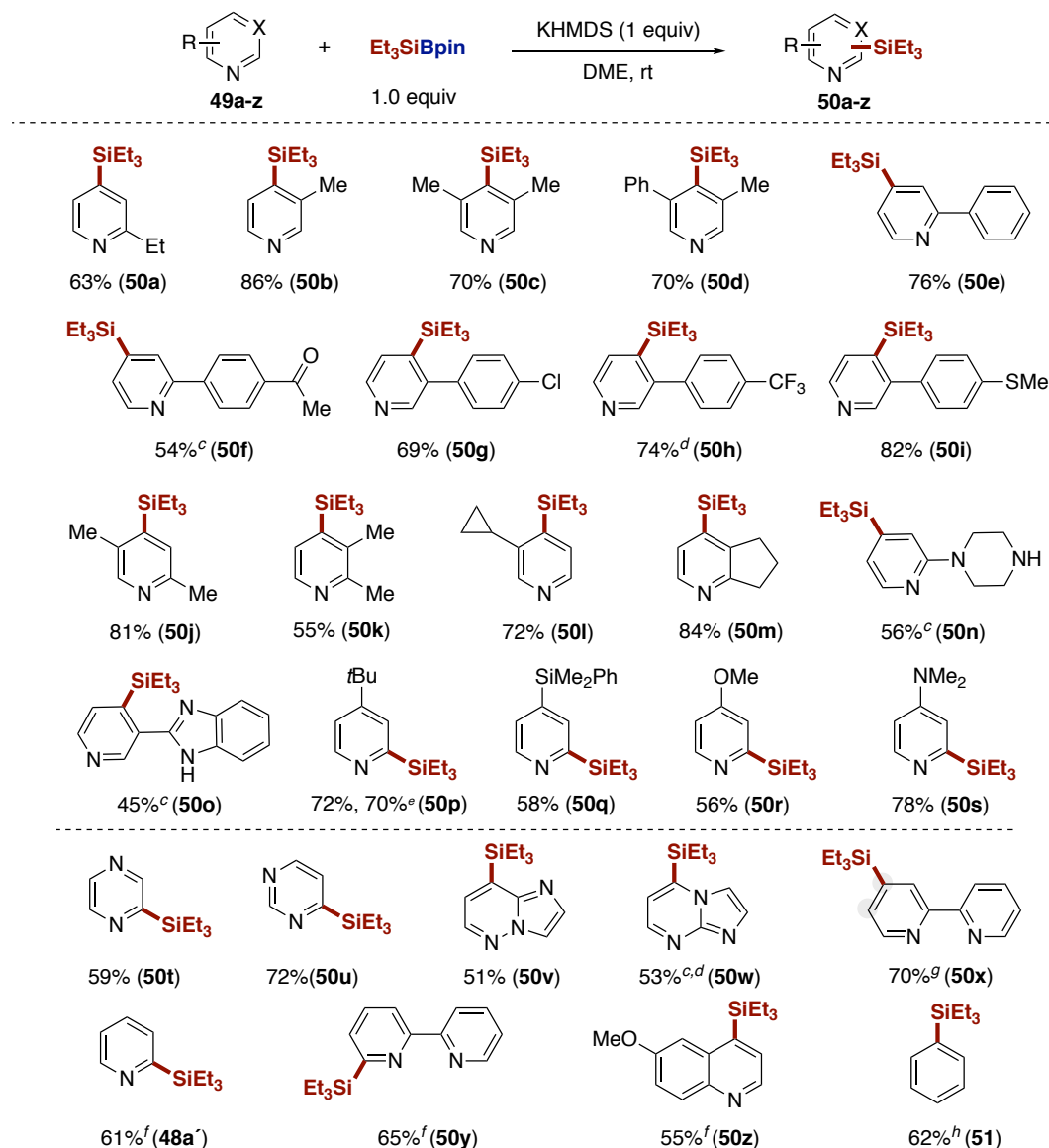
Reaction conditions: Conditions: **46a** (0.40 mmol), Et₃SiBpin (0.4 mmol), KHMDS (0.4 mmol), Toluene (1.0 mL) at 90 °C, 8h. ^aYield of **48aa** and **48aa'** detected by GC, using decane as internal standard.

Table 3.4. Screening of the silicon source

Next, we decided to explore the effect of the silicon source (Table 3.4). As shown in entries 2-5, among all silylboranes utilized, only PhMe₂SiBpin gave moderate yields in a high C4:C2 ratio. Unfortunately, we do not have any rationale for such striking behavior and the role of the substituents at the silicon atom on the targeted reactivity. Intriguingly, hexaethyldisilane, TMS₄Si or Et₃SiH failed to provide desired product (entry 7-9). Driven by the perception that in situ generated silyl metal species were generated under the reaction conditions, we found

that freshly prepared PhMe₂SiLi (2M in THF) led to **48** in lower yields, but with a high C4:C2 ratio (entry 6).

3.4.2. Substrate scope and late-stage silylation of functional azines

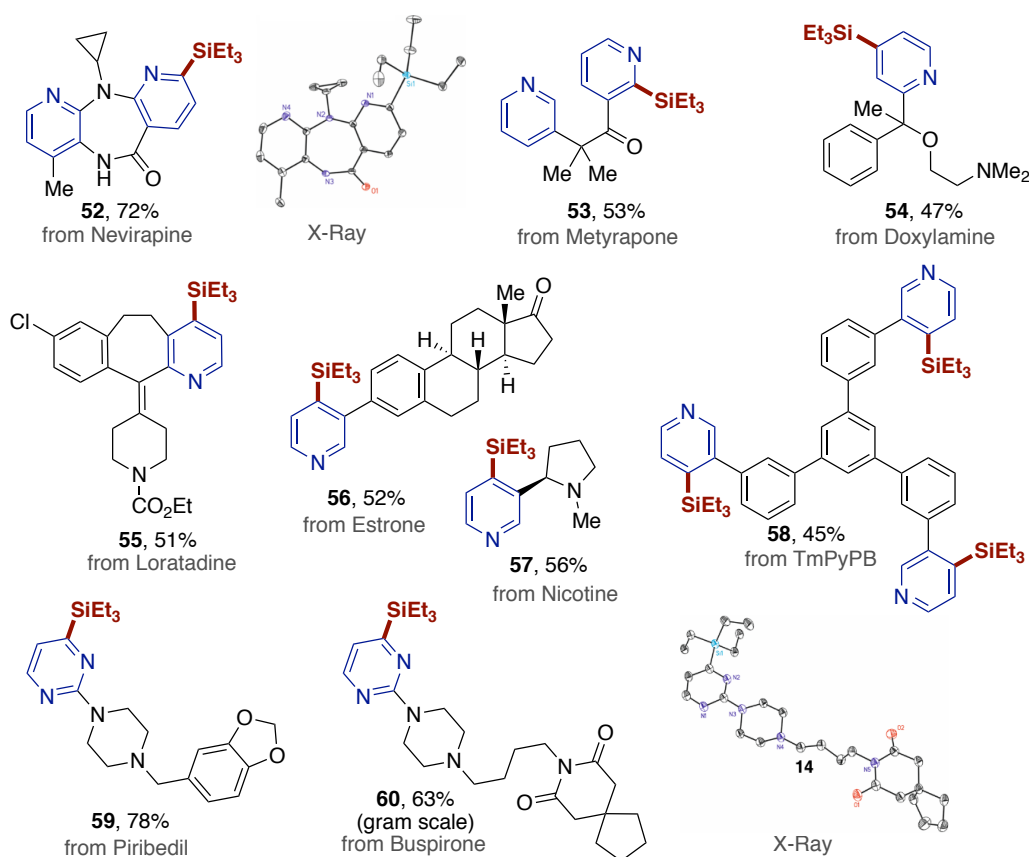


^aAs Table 3.3 (entry 3). ^bIsolated yields, average of two independent runs. ^cKHMDS (2 equiv). ^d0 °C. ^e5 mmol scale. ^fFrom N-oxide derivative. ^gC4:C5 = 2.7:1. ^hmono:bis = 8:1 from PhH.

Scheme 3.20. Scope of site-selective silylation of azines

With a robust set of reaction conditions in hand, we decided to study the generality of our site-selective C–H silylation. As shown in Scheme 3.20., a wide variety of azines underwent the targeted site-selective C–H silylation. Notably, aliphatic or aromatic substituents at either C2 or C3 position did not interfere with C4-silylation, even for bulky substrates (**50a-50o**). Substituents at C4 gave rise to C2-silylated compounds (**50p-50s**). Our C–H silylation displayed an excellent chemoselectivity profile, and ethers (**50l**), chlorides (**50g**) or free amines (**50n**)

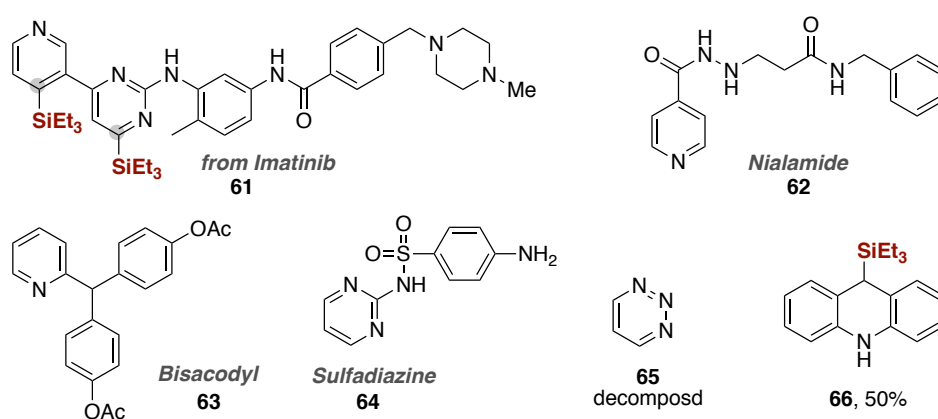
were well-tolerated. Surprisingly, ketone (**50f**) did not undergo silicon attack across the C=O bond under our optimized reaction conditions. Furthermore, other azines such as pyrazine (**50t**), pyrimidine (**50u**, **50w**), imidazo[1,2-b]pyridazines (**50v**), bipyridine (**50x**) were also accommodated with high selectivity. Interestingly, the reaction utilizing *N*-oxide derivatives proceeded in a highly regioselective manner, leading to C2-silylation exclusively due to its ability to coordinate the potassium cation (**48a'** and **50y**). Even unactivated benzene can be silylated in moderate yield (**51**). This finding showcases the complementarity between our transition-metal-free technique and classical methods based on Rh/Ir/Ru catalysts that typically require high temperatures and only provide low site-selectivity.



Scheme 3.21. Late-stage silylation of azine drugs

Prompted by the broad generality of our C-H silylation, we anticipated that our protocol might streamline the synthesis of complex molecules within the context of late-stage functionalization. To this end, we found that a wide variety of pharmaceuticals with C2 or C3 substitution underwent late-stage C4-silylation, giving rise to silylated drugs in high yields and excellent site-selectivities (**52-60**). Substrates containing two pyridine motifs could be selectively silylated on the more electron-poor pyridyl backbone. C2-selectivity was observed with antiretroviral Nevirapine and Metyrapone (**52** and **53**), which was confirmed by NMR spectroscopy and X-ray crystallography of **52**. The amide group in **52** activates *ortho* and *para*

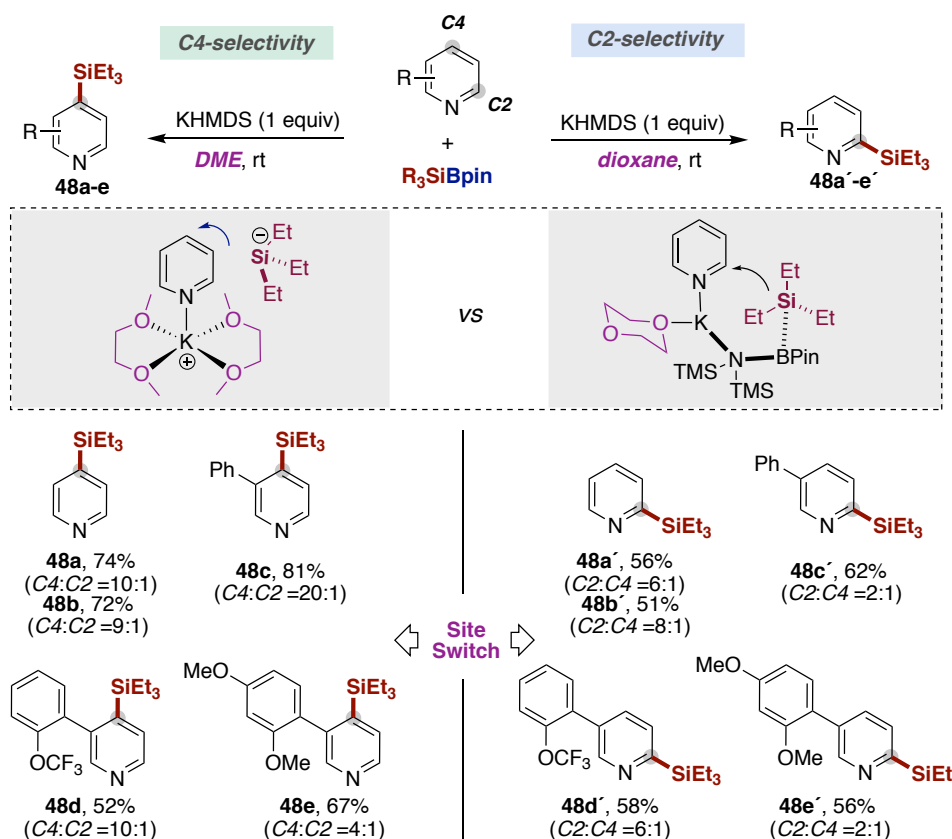
position because of its π -conjugation to induce δ^+ charge at the *ortho* and *para* sites, which are correspondingly activated to attack by nucleophiles.²⁴ And the amine group functions as *meta*-deactivators with the effect being particularly strong at the pyridine β and γ positions. The reason for this is unclear but may be due to the π -donor capability. Although it is elusive about the selectivity in **53**, one explanation is that the carbonyl group at *meta* position might act as directing group. Notably, we also found that a three-fold C4- silylation protocol was applicable to crystal material TmPyPB (**58**). Other pyrimidine-containing drugs such as piribedil and buspirone worked equally well, and the latter reaction could be easily scaled up to a gram-scale (**59** and **60**). The results in Scheme 3.21 highlight the impact of our protocol on rapidly generating structural diversity in drug discovery as the prevalence of diazines in pharmaceuticals.



Scheme 3.22. Unsuccessful substrates

As shown in Scheme 3.22, our system currently has some limitations with advanced intermediates substrates possessing particularly activated benzylic C–H bonds. Indeed, Imatinib underwent mono- and bis-silylation, giving inseparable mixture of silylated products. Preparative HPLC was investigated as a method of separating the silylated Imatinib products, but unfortunately we failed to isolate the corresponding products. While the basic and nucleophilic NH functionality in nialamide may compromise the stability of the Et_3SiBpin reagent, the presence of a particularly activated benzylic C–H bond in bisacodyl (**63**) led to the formation of the benzylic anion instead. The inability of using sulfadiazine (**64**) under our silylation procedure can be explained by deprotonation of the acidic NH bond, deactivating the azine for nucleophilic attack. Although we initially assumed that silylation of triazines should occur with similar ease, no desired silylated products were observed when using **65**, leading to rapid decomposition. Interestingly, the utilization of π -extended acridine as substrate resulted in dearomatized product **66**, which might arise from a silaboration of acridine followed by deborylation during the subsequent quenching process.

3.4.3. Regiodivergent C-H silylation

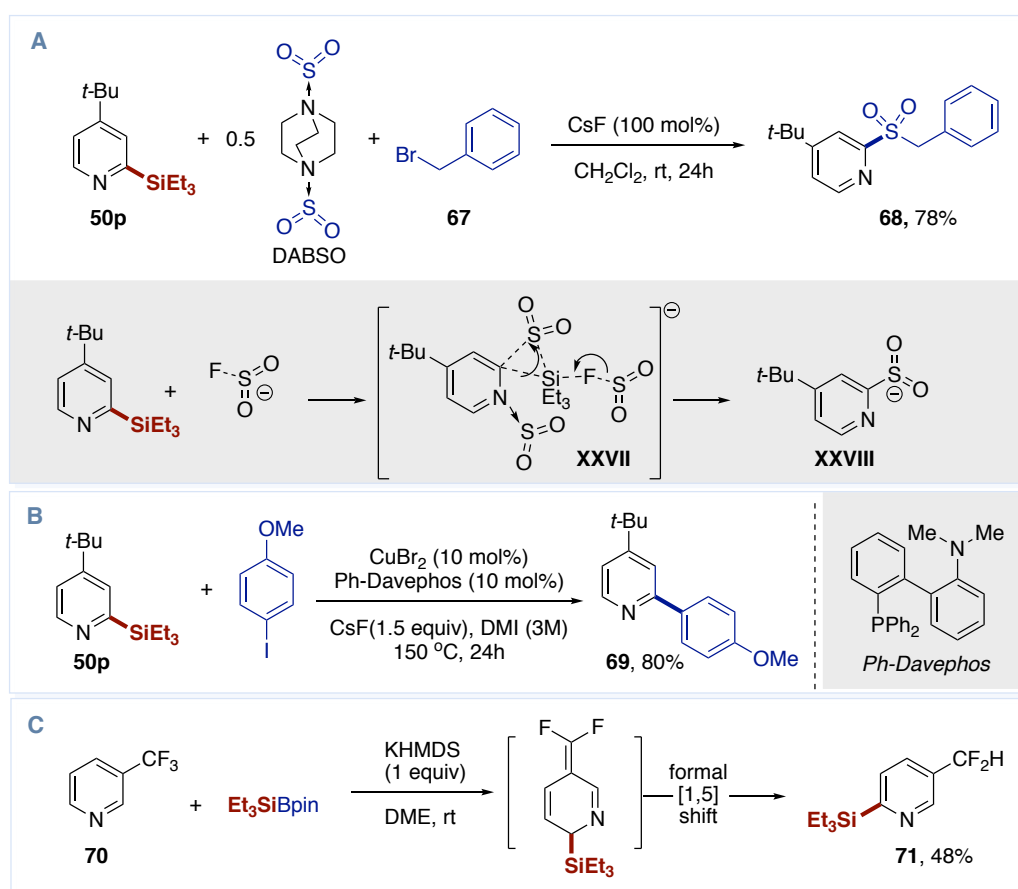


Scheme 3.23. Regiodivergent silylation of pyridine

During the screening of the reaction conditions, we noticed a different C2/C4 ratio depending on the nature of the ethereal solvent (Table 3.2). These results prompted us to investigate whether the C2-selective silylation could be further improved. Interestingly, the selectivity could be easily switched by simply changing the solvent to dioxane. As depicted in Scheme 3.23, silylation of simple pyridine in DME showed highly C4 selectivity, while a completely reversed selectivity was observed in dioxane (**48a'**–**48b'**). The same trend also applied to C3-substituted pyridines (**48c'**–**48e'**). It is known that ethereal ligands such as THF, THP, and dioxane are able to coordinate to alkali metal salts of HMDS (1,1,1,3,3,3-hexamethyldisilazide). Although the aggregation, solvation and stability of KHMDs in a variety of coordinating solvents is largely unexplored compared to that of LiHMDS and NaHMDS, we propose that a solvent-separated ion pair comes into play in DME, thus explaining the C4-selectivity profile. In this model, two DME ligands are coordinated to the potassium cation, making the approach to the C2 position more difficult due to steric effects. In contrast, the utilization of dioxane might lead to a contacted ion pair, resulting in a C2-silylation instead. We cannot certainly rule out that site-selectivity might also be influenced by the different solubility and aggregation of KHMDs in DME when compared to that in dioxane.

3.4.4. Application of silylated pyridines

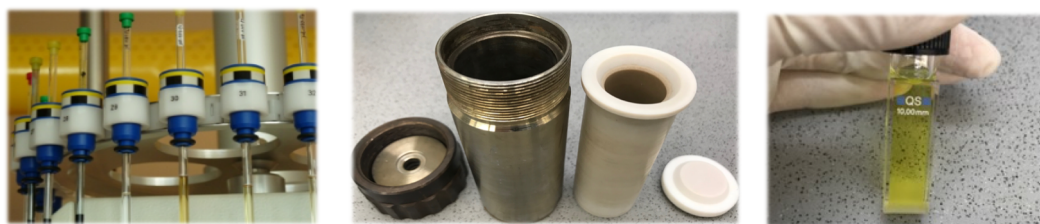
In view of the application profile of our protocol, we decided to explore the synthetic applicability of our method by transforming the corresponding silylated azines into valuable heterocyclic building blocks by promoting the functionalization of the new C–Si bond (Scheme 3.24). As shown, **50p** could easily be converted to the corresponding arylsulfone upon treatment with DABSO and alkylbromide **67** in the presence of a fluoride source.⁷⁸ A copper catalyzed Hiyama cross-coupling reaction also occurred smoothly with **50p** as stable and easy-handling organometallic reagent to afford biaryl compound **69** in high yield.⁷⁹ Intriguingly, we found that **70** could successfully undergo defluorinative C–H silylation via nucleophilic attack followed by two consecutive [1,3]-H shifts giving rise to **71** in 48%.



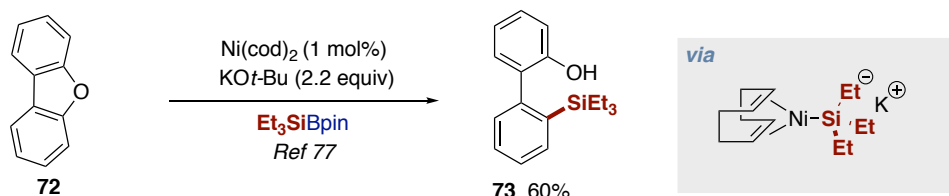
Scheme 3.24. Synthetic applications

3. 5. Mechanistic Studies and Proposal

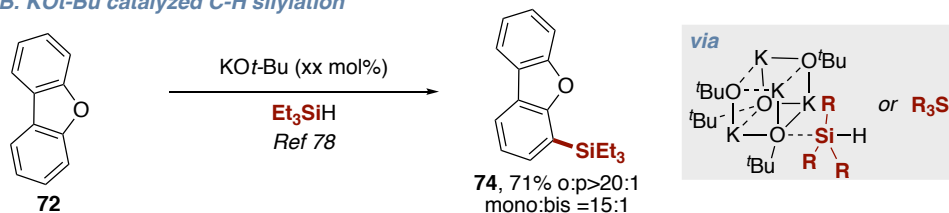
In order to shed light onto the mechanism, an orthogonal strategy was designed to study the course of the reaction (Scheme 3.25). Recently, our group reported that dibenzofuran (**72**) could be smoothly converted into **73** by Ni catalyzed C–O bond cleavage via Ni(0)-silyl ate complexes (Scheme 3.25, A).⁷⁵ Alternatively, *o*-, *p*-Silylated dibenzofuran could also be formed using Grubbs' KO^t-Bu/Et₃SiH-promoted protocol (Scheme 3.25, B).⁸⁰ However, when **72** was subjected to our silylation system, dearomatization of dibenzofuran (**75** and **76**) was found upon quenching with D₂O or Me₃SiCl. Subsequently, treatment with an oxidant led to rearomatization forming **77** and **78** (Scheme 3.25, C). In line with this notion, it is fairly apparent that a different mechanism to that depicted in Scheme 3.25 A-B takes place under our protocol. Although tentative, we suggest that silyl anion species are involved in the sp^2 C–H silylation reaction, thus indicating that our transition metal-free silylation protocol constitutes a new reactivity mode complementary to “classical” ortho-metalation or modern catalytic C–H silylation techniques.



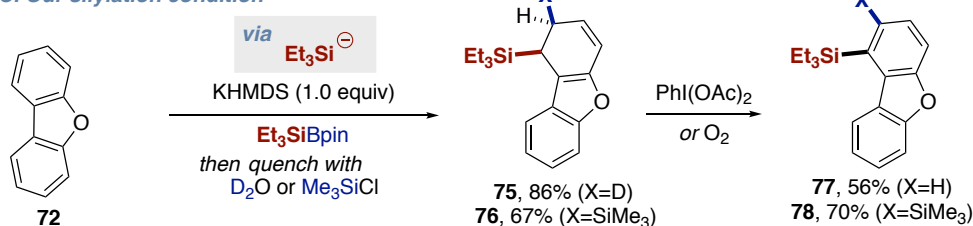
A. Ni-catalyzed silylation via C-OMe cleavage



B. KO^t-Bu catalyzed C-H silylation

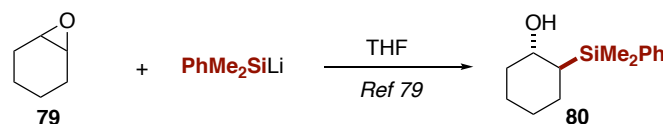


C. Our silylation condition

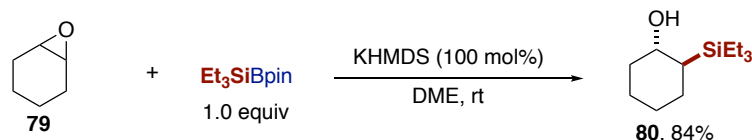


Scheme 3.25. Unraveling the nature of the silyl anionic species

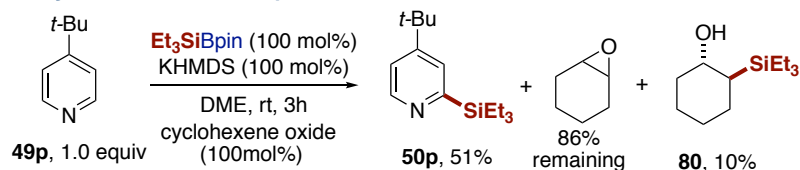
A. Ring opening reaction of epoxide by silyl anion



B. Ring opening reaction of epoxide by KHMDS and Et₃SiBpin

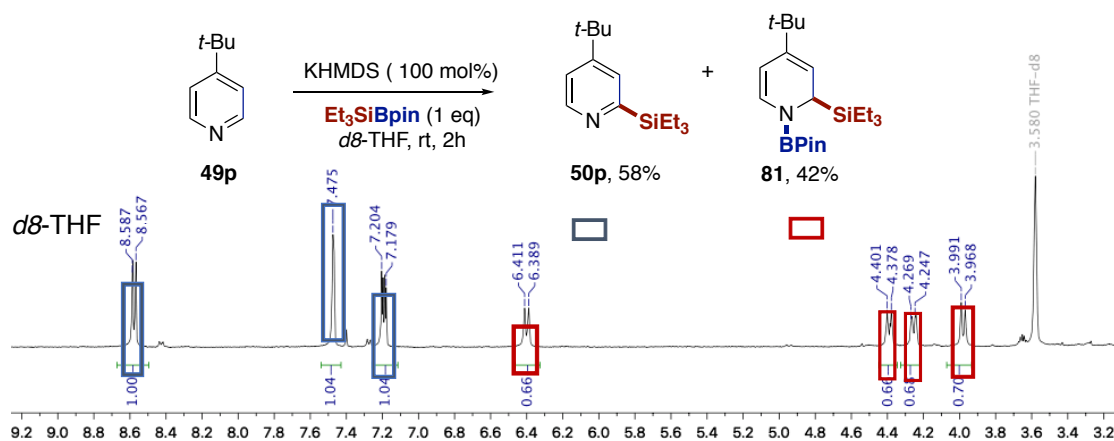


C. C-H silylation of azine with epoxide as additive



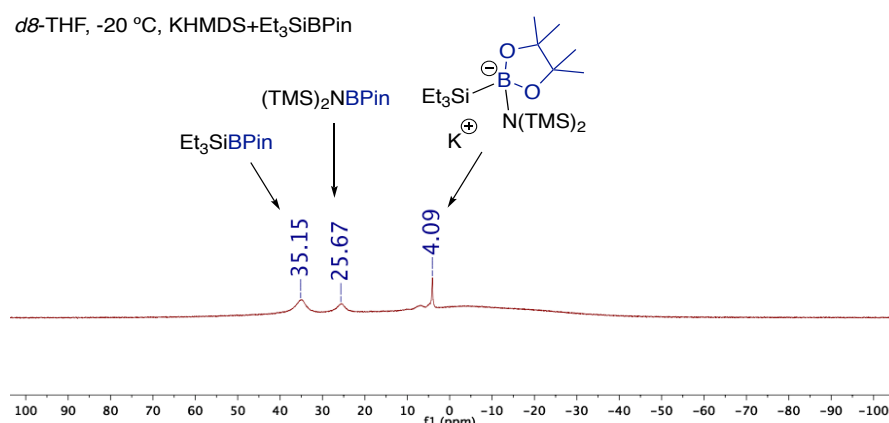
Scheme 3.26. Control experiment with ring opening reaction of epoxide

Next, we turned our attention to study the nature of the nucleophilic silylated species. As shown in Table 3.4 (entry 6), we found that PhMe₂SiLi can be employed as silyl reagent, suggesting that silyl anions might be the responsible for the targeted C–Si bond-formation. To such end, we turned our attention to the reaction of cyclohexene oxide, as it is known that such substrate undergoes nucleophilic ring opening by silyl anions (Scheme 3.26, A).⁸¹ As expected, we indeed obtained the ring opening product in high yield (Scheme 3.26, B). To lend support for silyl anion intermediates, we decided to conduct our KHMDS-mediated reaction with 4-*t*-Bu-pyridine (**49p**) as substrate in the presence of cyclohexene oxide (**79**) as an additive (Scheme 3.26, C). Intriguingly 86% of the cyclohexene epoxide was recovered after the reaction, with moderate yield of the targeted C2-silylation product **50p** being observed in the crude mixtures, suggesting that the silyl anion obtained upon reacting Et₃SiBpin/KHMDS preferentially attacks the azine moiety, probably by the polarization of the azine upon coordination to the escorting counter cation.



Scheme 3.27. NMR experiments to detect possible reaction intermediates

Next, we attempted to detect reaction intermediates using NMR spectroscopy. Silylation of 4-*t*Bu-pyridine in *d*8-THF under optimized condition was carried out at room temperature. After stirring for 2 hours, the reaction mixture was transferred to a J-Young NMR tube and analyzed by ^1H NMR. The results summarized in Scheme 3.27 show a 58% yield of silylated pyridine together with a new species with a new set of signals at 6.39, 4.39, 4.25 and 3.97 ppm in ^1H NMR. We tentatively assigned these signals to *N*-Bpin-2-triethylsilyl-4-*t*Bu-1,2-dihydropyridine (**81**). Interestingly, upon extending the reaction time or by adding additional KHMDS under standard condition, we could obtain the corresponding silylated pyridine in almost quantitative yield, thus suggesting that the dearomatized pyridine seems the most plausible avenue to explain our observations.

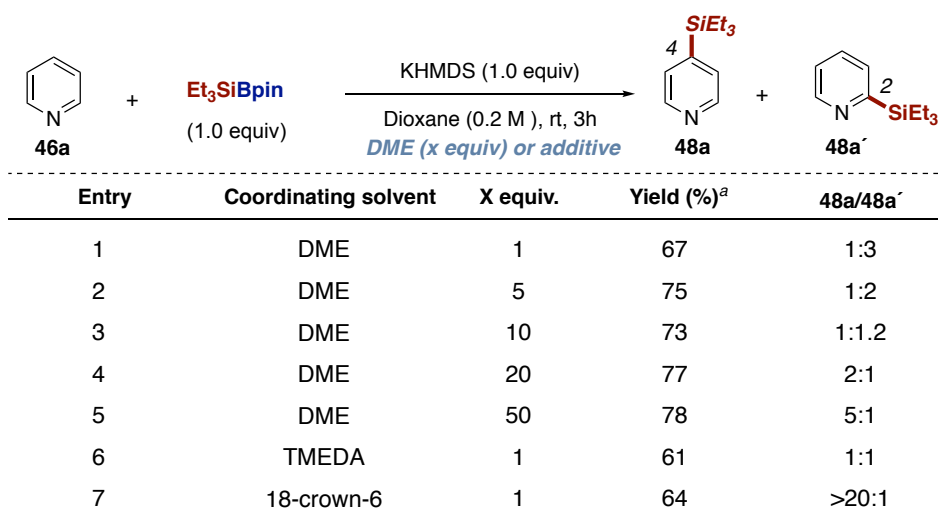


We also monitored a mixture of Et_3SiBpin (23.2 mg, 1.25 eq, 0.10 mmol) and KHMDS (15.9 mg, 1.0 eq, 0.08 mmol) in *d*8-THF by ^{11}B NMR spectroscopy at -20°C . As a result, three peaks at $\delta = 4.1$, 25.7 and 35.1 ppm were observed. These peaks could be assigned as tetracoordinated anionic boron species, Et_3SiBpin and $(\text{TMS})_2\text{NBpin}$,^{82,83} the formation of which and likely suggests the in situ generation of triethylsilyl potassium.⁸⁴⁻⁸⁵

Sample	Fe	Cu	Ni	Mn	Co	Ti	Pd	Ir	Rh
KHMDS	<DL	<DL	<DL	<DL	<DL	<DL	0.028	0.093	0.018
Et_3SiBpin	0.025	0.016	<DL	<DL	<DL	<DL	0.019	<DL	<DL
Reaction in Dioxane	<DL	<DL	<DL	<DL	0.414	<DL	0.016	0.002	<DL
Reaction in DME	0,034	0,005	<DL	<DL	<DL	<DL	0.017	<DL	<DL
Blank	<DL	<DL	<DL	<DL	<DL	<DL	0.016	0.141	<DL

Scheme 3.28. ICP-OES analysis

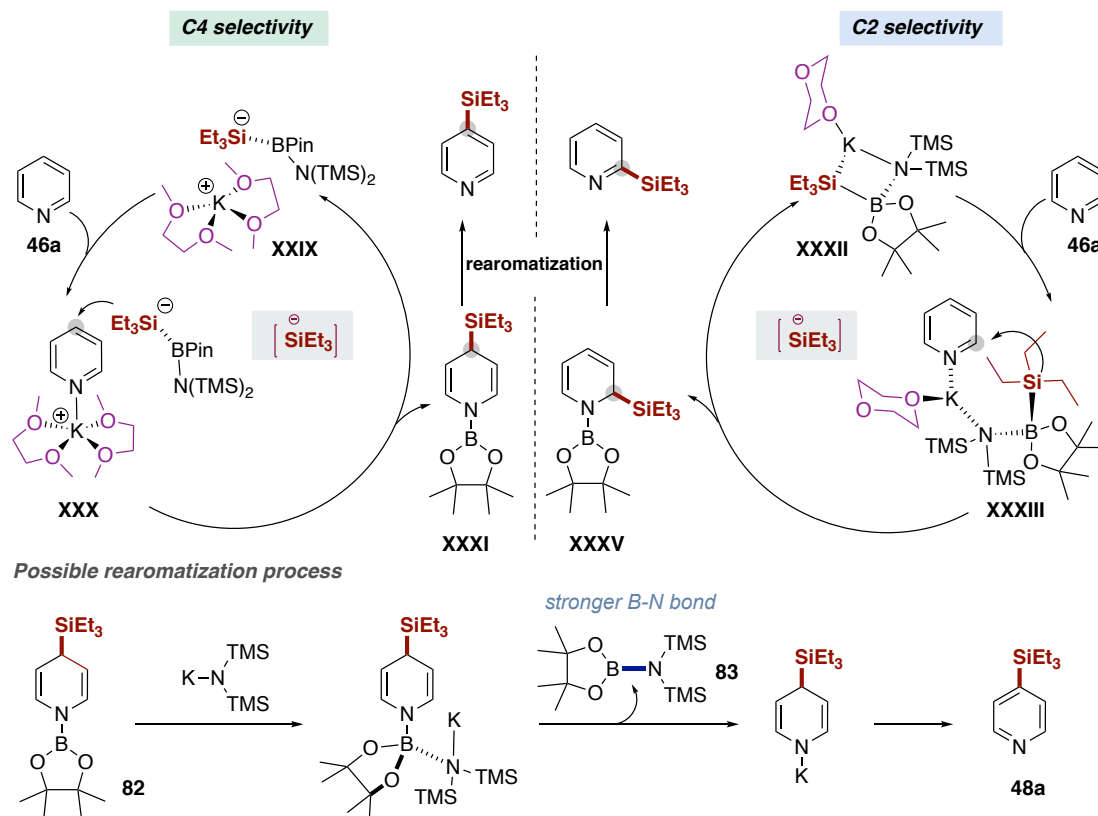
ICP-OES (Inductively coupled plasma atomic emission spectroscopy) trace metal analysis of all the reaction components ruled out the possibility that adventitious trace metal species would be enabling a C–H functionalization (Scheme 3.28). The results from quantitative analysis revealed that most metal contaminants were present below the instrument’s lowest limit of detection. The DL (Detection limit, in mg/l) for the different elements measured are: Fe 0.0006 ppm, Cu 0.0014 ppm, Ni 0.0002 ppm, Mn 0.0006 ppm, Co 0.0004 ppm, Ti 0.0003 ppm, Pd 0.0033 ppm, Ir 0.0033 ppm, Rh 0.0029 ppm.



^a Yield of 48a and 48a' detected by GC, using decane as internal standard.

Scheme 3.29. Effect of DME and additives

In order to gain some insight into the solvent dependent site-selectivity, the effect of DME was studied by varying the amount of solvent utilized (Scheme 3.29). Surprisingly, the more DME added to the reaction mixture, the higher C4-silylated product **48a**, an observation that is consistent with the ability of bidentate ethereal motifs to coordinate potassium cations.⁸⁶ If 50 equiv DME were added, the site-selectivity was totally switched from C2 to C4 (entries 1-5). In line with this notion, the utilization of TMEDA or 18-crown-6 as additive led to an improved C4-silylation due to its proclivity to act as bidentate ligand that might sequester the potassium cation (entries 6 and 7).

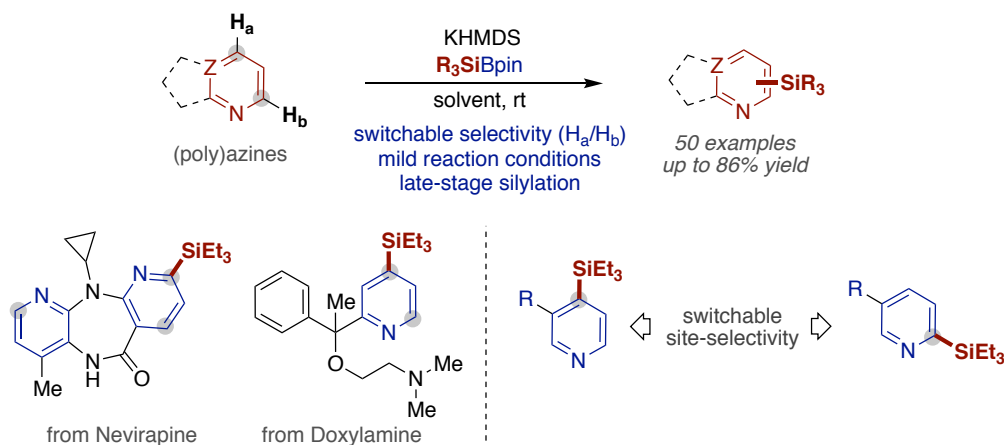


Scheme 3.30. Mechanistic proposal

Based on the above experiments, we propose that our C-H silylation involves the intermediacy of silyl anion and dearomatized intermediates, with site-selectivity being particularly sensitive to the denticity of the solvent (Scheme 3.30). We believe that the reaction is initiated by *in situ* generation of silyl anion species in the presence of KHMDS and Et_3SiBpin . If DME is utilized, we propose that a separated ion pair **XXIX** is generated due to the bidentate nature of the solvent,^{87,88} leading to a preferential attack of the silicon anion at C4 due to steric effects. In dioxane, however, a different denticity comes into play, and the corresponding contacted ion pair **XXXII** leads to a silicon anion attack at C2 (**XXXIII**). The higher solubility of KHMDS in DME vs dioxane does not allow us to completely rule out whether kinetics come into play for determining C2/C4-selectivity. Careful monitoring of the reaction mixtures by GC allowed to observe quantitative formation of $(\text{TMS})_2\text{N-Bpin}$, suggesting that the activation of Et_3SiBpin by KHMDS, likely via the initial formation of discrete $[(\text{Me}_3\text{Si})_2\text{N}(\text{Bpin})\text{SiEt}_3]\text{K}$ species and a dearomatized product is a reaction intermediate en route to the corresponding silylated arene. At present, we are not entirely sure on how the rearomatization takes place; although one might argue that oxidation might take place in the presence of advantageous oxygen, we observed the final aromatized silylated azine in the exclusion of oxygen. Although further experiments should be conducted, we cannot rule out that rearomatization might also be promoted with KHMDS by forming a strong N-B bond.^{89,90}

3.6. Conclusions

We have discovered a KHMDS-mediated direct C–H silylation of (poly)azines using Et_3SiBpin . The substrate scope of this reaction includes challenging substrate combinations with multiple (poly)azines, which would be of potential value in both pharmaceutical and academic laboratories. This methodology displays excellent regioselectivity and broad substrate scope. Importantly, regioselectivity could be switched by tuning the denticity and aggregation of ethereal solvents. Moreover, its simplicity and mild reaction conditions make our method applicable to late stage silylation events, thus showcasing the potential value for medicinal chemists. In addition, we have presented a mechanistic discussion based on experimental evidence and literature precedent, although more experiments should be conducted to unravel the intricacies of this reaction.



Scheme 3.31. KHMDS-mediated site-selective silylation of (poly)azines

3.7. References

1. Blakemore, D. C.; Castro, L.; Churcher, I.; Rees, D. C.; Thomas, A. W.; Wilson, D. M.; Wood, A. Organic Synthesis Provides Opportunities to Transform Drug Discovery. *Nat. Chem.* **2018**, *10*, 383.
2. St. Jean, D. J., Jr.; Fotsch, C. Mitigating Heterocycle Metabolism in Drug Discovery. *J. Med. Chem.* **2012**, *55*, 6002.
3. Vitaku, E.; Smith, D. T.; Njardarson, J. T. Analysis of the Structural Diversity, Substitution Patterns, and Frequency of Nitrogen Heterocycles among U.S. FDA Approved Pharmaceuticals. *J. Med. Chem.* **2014**, *57*, 10257.
4. Campeau, L.-C.; Fagnou, K. Applications of and Alternatives to π -Electron-Deficient Azine Organometallics in Metal-Catalyzed Cross-Coupling Reactions. *Chem. Soc. Rev.* **2007**, *36*, 1058.
5. Leclerc, N.; Sanaur, S.; Galmiche, L.; Mathevet, F.; Attias, A.-J.; Fave, J.-L.; Roussel, J.; Hapiot, P.; Lemaître, N.; Geffroy, B. 6-(Arylvinyleno)-3-bromopyridine Derivatives as Lego Building Blocks for Liquid Crystal, Nonlinear Optical, and Blue Light Emitting Chromophores. *Chem. Mater.* **2005**, *17*, 502.
6. Kaes, C.; Katz, A.; Hosseini, M. W. Bipyridine: The Most Widely Used Ligand. A Review of Molecules Comprising at Least Two 2,2'-Bipyridine Units *Chem. Rev.* **2000**, *100*, 3553.
7. Chichibabin, A. E.; Zeide, O. A. New Reaction for Compounds Containing the Pyridine Nucleus. *J. Russ. Phys. Chem. Soc.* **1914**, *46*, 1216.
8. Lewis, D. E. Aleksei Yevgen'evich Chichibabin (1871–1945): A Century of Pyridine Chemistry *Angew. Chem. Int. Ed.* **2017**, *56*, 2.
9. Evans, J. C. W.; Allen, C. F. H. 2-Phenylpyridine. *Org. Synth.* **1938**, *18*, 70.
10. Jeffrey, J. L.; Sarpong, R. Chichibabin-Type Direct Alkylation of Pyridyl Alcohols with Alkyl Lithium Reagents. *Org. Lett.* **2012**, *14*, 5400.
11. Fier, P. S.; Hartwig, J. F. Selective C–H Fluorination of Pyridines and Diazines Inspired by a Classic Amination Reaction. *Science* **2013**, *342*, 956.
12. Fier, P. S.; Hartwig, J. F. Synthesis and Late-Stage Functionalization of Complex Molecules through C–H Fluorination and Nucleophilic Aromatic Substitution. *J. Am. Chem. Soc.* **2014**, *136*, 10139.
13. Bowman, W. R.; Storey, J. M. D. Synthesis Using Aromatic Homolytic Substitution—Recent Advances. *Chem. Soc. Rev.* **2007**, *36*, 1803.
14. Minisci, F.; Bernardi, R.; Bertini, F.; Galli, R.; Perchinummo, M. Nucleophilic Character of Alkyl Radicals VI: A New Convenient Selective Alkylation of Heteroaromatic Bases. *Tetrahedron* **1971**, *27*, 3575.
15. Lynch, B. M.; Chang, H. S. *Tetrahedron Lett.* **1964**, *5*, 2965.
16. Minisci, F.; Vismara, E.; Fontana, F.; Morini, G.; Serravalle, M.; Giordano, C. *J. Org. Chem.* **1987**, *52*, 730.
17. Minisci, F.; Mondelli, R.; Gardini, G. P.; Porta, O. *Tetrahedron* **1972**, *28*, 2403.
18. For a study of substituent effect on the rate of radical phenylation of C4-substituted pyridines, see: Minisci, F.; Vismara, E.; Fontana, F.; Morini, G.; Serravalle, M.; Giordano, C. *J. Org. Chem.* **1986**, *51*, 4411.
19. Seiple, I. B.; Su, S.; Rodriguez, R. A.; Gianatassio, R.; Fujiwara, Y.; Sobel, A. L.; Baran, P. S. Direct C–H Arylation of Electron-Deficient Heterocycles with Arylboronic Acids. *J. Am. Chem. Soc.* **2010**, *132*, 13194.
20. Patel, N.; Flowers, R. Uncovering the Mechanism of the Ag(I)/Persulfate-Catalyzed Cross-Coupling Reaction of Arylboronic Acids and Heteroarenes. *J. Am. Chem. Soc.* **2013**, *135*, 4672.
21. Molander, G. A.; Colombel, V.; Braz, V. A. Direct Alkylation of Heteroaryls Using Potassium Alkyl- and Alkoxyethyltrifluoroborates. *Org. Lett.* **2011**, *13*, 1852.
22. Wang, J.; Wang, S.; Wang, G.; Zhang, J.; Yu, X.-Q. Iron-Mediated Direct Arylation with Arylboronic Acids through an Aryl Radical Transfer Pathway. *Chem. Commun.* **2012**, *48*, 11769.

23. Fujiwara, Y.; Dixon, J. A.; O'Hara, F.; Funder, E. D.; Dixon, D. D.; Rodriguez, R. A.; Baxter, R. D.; Herlé, B.; Sach, N.; Collins, M. R.; Ishihara, Y.; Baran, P. Practical and Innate Carbon-Hydrogen Functionalization of Heterocycles. *Nature* **2012**, *492*, 95.
24. O'Hara, F.; Blackmond, D. G.; Baran, P. S. Radical-Based Regioselective C-H Functionalization of Electron-Deficient Hetero-arenes: Scope, Tunability, and Predictability. *J. Am. Chem. Soc.* **2013**, *135*, 12122.
25. DiRocco, D. A.; Dykstra, K.; Krska, S.; Vachal, P.; Conway, D. V.; Tudge, M. Late-Stage Functionalization of Biologically Active Heterocycles Through Photoredox Catalysis. *Angew. Chem., Int. Ed.* **2014**, *53*, 4802.
26. Jin, J.; MacMillan, D. W. C. Direct α -Arylation of Ethers through the Combination of Photoredox-Mediated C-H Functionalization and the Minisci Reaction. *Angew. Chem., Int. Ed.* **2015**, *54*, 1565.
27. Proctor, R. S. J.; Davis, H. J.; Phipps, R. J. Catalytic Enantioselective Minisci-type Addition to Heteroarenes. *Science* **2018**, *360*, 419.
28. Rennels, R. A.; Rutherford, J. L.; Collum, D. B. Are *n*-BuLi/TMEDA-Mediated Arene Ortholithiations Directed? Substituent-Dependent Rates, Substituent-Independent Mechanisms *J. Am. Chem. Soc.* **2000**, *122*, 8640.
29. Schlosser, M.; Faigl, F.; Franzini, L.; Geneste, H.; Katsoulos, G.; Zhong, G.-F. Site Selective Hydrogen/Metal Exchange: Competition and Cooperation between Superbases and Neighboring Group *Pure Appl. Chem.* **1994**, *66*, 1439.
30. Khartabil, H. K.; Gros, P. C.; Fort, Y.; Ruiz-López, M. F. Metalation of Pyridines with *n*BuLi-Li-Aminoalkoxide Mixed Aggregates: The Origin of Chemoselectivity. *J. Am. Chem. Soc.* **2010**, *132*, 2410.
31. Krasovskiy, A.; Krasovskaya, V.; Knochel, P. Mixed Mg/Li Amides of the Type $R_2NMgCl \cdot LiCl$ as Highly Efficient Bases for the Regioselective Generation of Functionalized Aryl and Heteroaryl Magnesium Compounds. *Angew. Chem., Int. Ed.* **2006**, *45*, 2958.
32. Klatt, T.; Werner, V.; Maximova, M. G.; Didier, D.; Apeloig, Y.; Knochel, P. Preparation and Regioselective Magnesiation or Lithiation of Bis(trimethylsilyl)methyl-Substituted Heteroaryls for the Generation of Highly Functionalized Heterocycles. *Chem. - Eur. J.* **2015**, *21*, 7830.
33. Jaric, M.; Haag, B. A.; Unsinn, A.; Karaghiosoff, K.; Knochel, P. Highly Selective Metalations of Pyridines and Related Heterocycles Using New Frustrated Lewis Pairs or tmp-Zincandtmp-Magnesium Bases with $BF_3 \cdot OEt_2$. *Angew. Chem., Int. Ed.* **2010**, *49*, 5451.
34. Murakami, K.; Yamada, S.; Kaneda, T.; Itami, K. C-H Functionalization of Azines. *Chem. Rev.* **2017**, *117*, 9302.
35. Nakao, Y. Transition Metal-Catalyzed C-H Functionalization for the Synthesis of Substituted Pyridines. *Synthesis* **2011**, *2011*, 3209.
36. Yamada, S.; Murakami, K.; Itami, K. Regiodivergent Cross-Dehydrogenative Coupling of Pyridines and Benzoxazoles: Discovery of Organic Halides as Regio-Switching Oxidants. *Org. Lett.* **2016**, *18*, 2415.
37. Boursalian, G. B.; Ham, W. S.; Mazzotti, A. R.; Ritter, T. Charge-Transfer-Directed Radical Substitution Enables para-Selective C-H Functionalization. *Nat. Chem.* **2016**, *8*, 810.
38. Foo, K.; Sella, E.; Thomé, I.; Eastgate, M. D.; Baran, P. S. A Mild, Ferrocene-Catalyzed C-H Imidation of (Hetero)Arenes. *J. Am. Chem. Soc.* **2014**, *136*, 5279.
39. Allen, L. J.; Cabrera, P. J.; Lee, M.; Sanford, M. S. N- Acyloxyphthalimides as Nitrogen Radical Precursors in the Visible Light Photocatalyzed Room Temperature C-H Amination of Arenes and Heteroarenes. *J. Am. Chem. Soc.* **2014**, *136*, 5607.
40. Kim, H.; Kim, T.; Lee, D. G.; Roh, S. W.; Lee, C. Nitrogen-Centered Radical-Mediated C-H Imidation of Arenes and Hetero-arenes via Visible Light Induced Photocatalysis. *Chem. Commun.* **2014**, *50*, 9273.
41. Takagi, J.; Sato, K.; Hartwig, J. F.; Ishiyama, T.; Miyaura, N. Iridium-Catalyzed C-H Coupling Reaction of Heteroaromatic Compounds with Bis(pinacolato)diboron: Regioselective Synthesis of Heteroarylboronates. *Tetrahedron Lett.* **2002**, *43*, 5649.

42. Murphy, J. M.; Liao, X.; Hartwig, J. F. Meta Halogenation of 1,3-Disubstituted Arenes via Iridium-Catalyzed Arene Borylation. *J. Am. Chem. Soc.* **2007**, *129*, 15434.
43. Obligacion, J. V.; Semproni, S. P.; Chirik, P. J. Cobalt-Catalyzed C-H Borylation. *J. Am. Chem. Soc.* **2014**, *136*, 4133.
44. Yang, L.; Semba, K.; Nakao, Y. Para-Selective C-H Borylation of (Hetero)Arenes by Cooperative Iridium/Aluminum Catalysis. *Angew. Chem., Int. Ed.* **2017**, *56*, 4853.
45. Kanyiva, K. S.; Nakao, Y.; Hiyama, T. Nickel-Catalyzed Addition of Pyridine-N-oxides across Alkynes. *Angew. Chem. Int. Ed.* **2007**, *46*, 8872.
46. Nakao, Y.; Kanyiva, K. S.; Hiyama, T. A Strategy for C-H Activation of Pyridines: Direct C-2 Selective Alkenylation of Pyridines by Nickel/Lewis Acid Catalysis. *J. Am. Chem. Soc.* **2008**, *130*, 2448.
47. Tsai, C.-C.; Shih, W.-C.; Fang, C.-H.; Li, C.-Y.; Ong, T.-G.; Yap, G. P. A. Bimetallic Nickel Aluminum Mediated Para-Selective Alkenylation of Pyridine: Direct Observation of η^2, η^1 -Pyridine Ni(0)-Al(III) Intermediates Prior to C-H Bond Activation. *J. Am. Chem. Soc.* **2010**, *132*, 11887.
48. Hilton, M. C.; Dolewski, R. D.; McNally, A. Selective Functionalization of Pyridines via Heterocyclic Phosphonium Salts. *J. Am. Chem. Soc.* **2016**, *138*, 13806.
49. Haase, M.; Goerls, H.; Anders, E. Synthesis of PO(OR)⁻ and PR₃⁺-Disubstituted Pyridines via N-(Trifluoromethylsulfonyl)-pyridinium Triflates. *Synthesis* **1998**, *1998*, 195.
50. Patel, C.; Moheike, M.; Hilton, M.C.; McNally, A. A Strategy to Aminate pyridines, Diazines, and Pharmaceuticals via Heterocyclic Phosphonium Salts. *Org. Lett.* **2018**, *20*, 2607.
51. Zhang, X.; McNally, A. Phosphonium Salts as Pseudohalides: Regioselective Nickel-Catalyzed Cross-Coupling of Complex Pyridines and Diazines. *Angew. Chem. Int. Ed.* **2017**, *56*, 9833.
52. Koniarczyk, J.; Hesk, D.; Overgard, A.; Davies, L. W.; McNally, A. A General Strategy for Site-Selective Incorporation of Deuterium and Tritium into Pyridines, Diazines and Pharmaceuticals *J. Am. Chem. Soc.* **2018**, *140*, 1990.
53. Hilton, M. C.; Zhang, X.; Boyle, B. T.; Alegre-Requena, J. V.; Paton, R. S.; McNally, A. Heterobiaryl synthesis by contractive C-C coupling via P(V) intermediates. *Science* **2018**, *362*, 799.
54. Ramesh, R.; Reddy, D. S. Organosilicon Molecules with Medicinal Applications *J. Med. Chem.* **2018**, *61*, 3779.
55. Du, W.; Kaskar, B.; Blumbergs, P.; Subramanian, P. K.; Curran, D. P. Emisynthesis of DB-67 and Other Silatecans from Camptothecin by Thiol-Promoted Addition of Silyl Radicals *Bioorg. Med. Chem.* **2003**, *11*, 451.
56. Nakao, Y.; Hiyama, T. Silicon-based Cross-Coupling Reaction: an Environmentally Benign Version *Chem. Soc. Rev.* **2011**, *40*, 4893.
57. Sore, H. F.; Galloway, J. D.; Spring, D. R. Palladium-catalysed Cross-Coupling of Organosilicon Reagents. *Chem. Soc. Rev.* **2012**, *41*, 1845.
58. Minami, Y.; Hiyama, T. Designing for Cross-coupling Reactions Using Aryl(trialkyl)silanes. *Chem. Eur. J.* **2019**, *25*, 391.
59. Ishiyama, T.; Sato, K.; Nishio, Y.; Miyaura, N. Direct Synthesis of Aryl Halosilanes through Iridium(I)-Catalyzed Aromatic C-H Silylation by Disilanes. *Angew. Chem. Int. Ed.* **2003**, *42*, 5346.
60. Oyamada, J.; Nishiura, M.; Hou, Z. Scandium-Catalyzed Silylation of Aromatic C-H Bonds. *Angew. Chem. Int. Ed.* **2011**, *50*, 10720.
61. Cheng, C.; Hartwig, J. F. Iridium-catalyzed Silylation of Aryl C-H Bonds. *J. Am. Chem. Soc.* **2015**, *137*, 592.
62. Karmel, C.; Chen, Z.; Hartwig, J. F. Iridium-catalyzed Silylation of C-H Bonds in Unactivated Arenes: a Sterically Encumbered Phenanthroline Ligand Accelerates Catalysis. *J. Am. Chem. Soc.* **2019**, *141*, 7063.
63. Kuznetsov, A.; Onishi, Y.; Inamoto, Y.; Gevorgan, V. Fused Heteroaromatic Dihydrosiloles: Synthesis and Double-Fold Modification. *Org. Lett.* **2013**, *15*, 2498.
64. Sakamoto, R.; Nguyen, B.-N.; Maruoka, K. Transition-metal-free direct C-H silylation of electron-deficient heteroarenes with hydrosilanes via a radical mechanism. *Asian J. Org. Chem.* **2018**, *7*, 1085.
65. Xu, Z.; Chai, L.; Liu, Z.-Q. Free-Radical-Promoted Site-Selective C-H Silylation of Arenes by Using Hydrosilanes. *Org. Lett.* **2017**, *19*, 5573.

66. Liu, S.; Pan, P.; Fan, H.; Li, H.; Wang, W.; Zhang, Y. Photocatalytic C–H Silylation of Heteroarenes by Using Trialkylhydrosilanes. *Chem. Sci.* **2019**, *10*, 3817.
67. Wübbolt, S.; Oestreich, M. Catalytic Electrophilic C–H Silylation of Pyridines Enabled by Temporary Dearomatization. *Angew. Chem. Int. Ed.* **2015**, *54*, 15876.
68. Königs, C. D. F.; Klare, H. F. T.; Oestreich, M. Catalytic Dehydrogenative Si–N Coupling of Pyrroles, Indoles, Carbazoles as well as Anilines with Hydrosilanes without Added Base. *Chem. Commun.* **2013**, *49*, 1506.
69. Hermeke, J.; Klare, H.F.T.; Oestreich, M. Direct Catalytic Access to N-Silylated Enamines from Enolizable Imines and Hydrosilanes by Base-Free Dehydrogenative Si–N Coupling *Chem. Eur. J.* **2014**, *20*, 9250.
70. Postigo, A.; Rossi, R.A. A Novel Type of Nucleophilic Substitution Reactions on Nonactivated Aromatic Compounds and Benzene Itself with Trimethylsiliconide Anions. *Org. Lett.* **2001**, *3*, 1197.
71. Postigo, A. Reactions of Trimethylstannide and Trimethylsiliconide Anions with Aromatic and Heteroaromatic Substrates. *J. Phys. Org. Chem.* **2002**, *15*, 889.
72. Postigo, A.; Mechanistic Studies on the Reactions of Trimethylsilanide and Trimethylstannylide Ions with Haloarenes in Hexamethylphosphoramide. *J. Organomet. Chem.* **2002**, *656*, 108.
73. Boebel, T. A.; Hartwig, J. F. Iridium-Catalyzed Preparation of Silylboranes by Silane Borylation and Their Use in the Catalytic Borylation of Arenes. *Organometallics* **2008**, *27*, 6013.
74. Zarate, C.; Martin, R. A Mild Ni/Cu- Catalyzed Silylation via C–O Cleavage. *J. Am. Chem. Soc.* **2014**, *136*, 2236.
75. Zarate, C.; Nakajima, M.; Martin, R. A Mild and Ligand-Free Ni-Catalyzed Silylation via C–OME Cleavage. *J. Am. Chem. Soc.* **2017**, *139*, 1191.
76. Liu, X.-W.; Zarate, C.; Martin, R. Base-Mediated Defluorosilylation of C(sp²)–F and C(sp³)–F Bonds. *Angew. Chem. Int. Ed.* **2019**, *58*, 2064.
77. Somerville, R.; Hale, L.; Gomez-Bengoia, E.; Bureś, J.; Martin, R. Intermediacy of Ni–Ni Species in sp² C–O Bond Cleavage of Aryl Esters: Relevance in Catalytic C–Si Bond Formation. *J. Am. Chem. Soc.* **2018**, *140*, 8771.
78. von Wolff, N.; Char, J.; Frogneux, X.; Cantat, T. Synthesis of Aromatic Sulfones from SO₂ and Organosilanes Under Metal-Free Conditions. *Angew. Chem. Int. Ed.* **2017**, *56*, 5616.
79. Komiyama, T.; Minami, Y.; Hiyama, T. Aryl(triethyl)silanes for Biaryl and Teraryl Synthesis by Copper(II)-Catalyzed Cross-Coupling Reaction. *Angew. Chem. Int. Ed.* **2016**, *55*, 15787.
80. Toutov, A. A.; Liu, W.-B.; Betz, K. N.; Fedorov, A.; Stoltz, B. M.; Grubbs, R. H. Silylation of C–H Bonds in Aromatic Heterocycles by an Earth-Abundant Metal Catalyst. *Nature.* **2015**, *518*, 80.
81. Gilman, H. ; Aoki, D.; Wittenberg, D. Some Reactions of Silyllithium Compounds with Epoxides. *J. Am. Chem. Soc.* **1959**, *81*, 1107.
82. Ito, H.; Horita Y.; Yamamoto, E Potassium tert-butoxide-mediated regioselective silaboration of aromatic alkenes. *Chem. Commun.*, **2012**, *48*, 8006.
83. Cui, Y.; Li, W.; Sato, T.; Yamashita, Y.; Kobayashi, S. Catalytic Use of Zinc Amide for Transmetalation with Allylboronates: General and Efficient Catalytic Allylation of Carbonyl Compounds, Imines, and Hydrazones. *Adv. Synth. Catal.* **2013**, *355*, 1193.
84. Yamamoto, E.; Ukigai, S.; Ito, H. Formal Nucleophilic Silyl Substitution of Aryl Halides with Silyllithium Reagents via Halogenophilic Attack of Silyl Nucleophiles. *Synlett* **2017**, *28*, 2460.
85. Holmes, R. R. Comparison of Phosphorus and Silicon: Hypervalency, Stereochemistry, and Reactivity. *Chem. Rev.* **1996**, *3*, 927.
86. Algera, R. F.; Ma, Y.; Collum, D. B. Sodium Diisopropylamide: Aggregation, Solvation, and Stability. *J. Am. Chem. Soc.* **2017**, *139*, 7921.
87. Lucht, B. L.; Collum, D. B. Lithium Ion Solvation: Amine and Unsaturated Hydrocarbon Solvates of Lithium Hexamethyldisilazide (LiHMDS). *J. Am. Chem. Soc.* **1996**, *118*, 2217.
88. Lucht, B. L.; Collum, D. B. Ethereal Solvation of Lithium Hexamethyldisilazide: Unexpected Relationships of Solvation Number, Solvation Energy, and Aggregation State. *J. Am. Chem. Soc.* **1995**, *117*, 9863.

89. Morimasa, Y.; Kabasawa, K.; Ohmura T.; and Suginome, M. Pyridine-Based Organocatalysts for Regioselective syn-1,2-Silaboration of Terminal Alkynes and Allenes. *Asian J. Org. Chem.* **2019**, *8*, 1092.
90. Wang, G.; Zhang, H.; Zhao, J.; Li, W.; Cao, J.; Zhu, C.; Li, S. Homolytic Cleavage of a B-B Bond by the Cooperative Catalysis of Two Lewis Bases: Computational Design and Experimental Verification. *Angew. Chem. Int. Ed.* **2016**, *55*, 5985.

3.8. Experimental Section

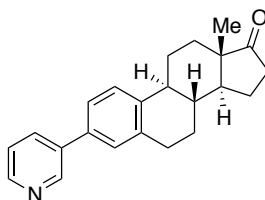
3.8.1. General considerations

Reagents. Commercially available materials were used without further purification. KHMDS was purchased from Strem Chemicals. Anhydrous DME and Dioxane were purchased from Alfa Aesar. Silylborane Et₃SiBpin was prepared in bulk quantities in one-step from Et₃SiH and B₂pin₂ according to a known literature procedure.¹ All the other reagents were purchased from commercial sources and used as received. Flash chromatography was performed with EM Science silica gel 60 (230-400 mesh). Thin layer chromatography was carried out using Merck TLC Silica gel 60 F₂₅₄.

Analytical methods: ¹H-NMR, ¹³C-NMR, and ¹⁹F-NMR spectra and melting points (where applicable) are included for all new compounds. ¹H-NMR, ¹³C-NMR, and ¹⁹F-NMR spectra were recorded on a Bruker 300 MHz, a Bruker 400 MHz or Bruker 500 MHz. All ¹H-NMR spectra are reported in parts per million (ppm) downfield of TMS and were measured relative to the signals for CHCl₃ (7.26 ppm). All ¹³C-NMR spectra were reported in ppm relative to residual CHCl₃ (77.2 ppm) and were obtained with ¹H decoupling. Coupling constants, *J*, are reported in hertz (Hz). Melting points were measured using open glass capillaries in a Büchi B540 apparatus. Infrared spectra were recorded on a Bruker Tensor 27. Specific optical rotation measurements were carried out on a Jasco P-1030 model polarimeter equipped with a PMT detector using the Sodium line at 589 nm. Mass spectra were recorded on a Waters LCT Premier spectrometer. Gas chromatographic analyses were performed on HewlettPackard 6890 gas chromatography instrument with a FID detector using 25m x 0.20 mm capillary column with cross-linked methyl siloxane as the stationary phase. Atomic absorption analysis was measured in a ICP-OES Spectro Arcos at the "Servei de Recursos Científics i Tècnics de la URV" in Tarragona, Spain. The yields reported refer to isolated yields and represent an average of at least two independent runs. The procedures described in this section are representative. Thus, the yields may differ slightly from those given in the tables and Schemes of the manuscript.

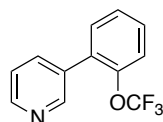
3.8.2 Synthesis of starting materials

General conditions for Suzuki cross-coupling: In a 4.0 mL Schlenk tube, PdCl₂(PPh₃)₂ (35 mg, 5 mmol%), Aryl halide (1.0 mmol), 3-pyridinylboronic acid (146.4 mg, 1.2 mmol) and K₂CO₃ (441.6 mg, 3.2 mmol) were weight out. Then, DME (10 mL) and water (4 ml) were added. The reaction mixture was stirred at 120 °C for 16 h. After cooling to room temperature, the reaction mixture was diluted with ether (15 ml), washed with water (10 ml), the organic phase was dried over MgSO₄, filtered and concentrated. The product was isolated by column chromatography to give the corresponding substituted pyridine.



(8R,9S,13S,14S)-13-methyl-3-(pyridin-3-yl)-6,7,8,9,11,12,13,14,15,16-decahydro-17H-cyclopenta[*a*]phenanthren-17-one. Following the general procedure, using (8R,9S,13S,14S)-3-bromo-13-methyl-6,7,8,9,11,12,13,14,15,16-decahydro-17H-cyclopenta[*a*]phenanthren-17-one (333.2 mg,

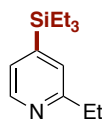
0.4 mmol), the title compound was obtained in 82% yield (271.5 mg) as white solid. R_f 0.65 (Hex: EtOAc 2:1). ^1H NMR (300 MHz, CDCl_3) δ 8.84 (s, 1H), 8.57 (d, $J = 4.1$ Hz, 1H), 7.92 (d, $J = 7.9$ Hz, 1H), 7.45- 7.35 (m, 3H), 7.33 (s, 1H), 3.12-2.91 (m, 2H), 2.62-2.42 (m, 2H), 2.37 (dt, $J = 14.6, 7.0$ Hz, 1H), 2.25-2.03 (m, 3H), 2.00 (dd, $J = 9.2, 2.5$ Hz, 1H), 1.80-1.40 (m, 6H), 0.93 (s, 3H) ppm. ^{13}C NMR (75 MHz, CDCl_3) δ 220.8, 147.3, 140.3, 137.6, 137.0, 135.1, 134.9, 127.8, 126.4, 124.6, 124.0, 50.6, 48.1, 44.5, 38.2, 35.9, 31.7, 29.6, 26.5, 25.8, 21.7, 14.0 ppm. Mp 172.1-173.5 °C. $[\alpha]_D^{26} = 268.8$ ($c = 0.1053$, CH_2Cl_2). IR (neat, cm^{-1}): 2925, 2853, 1733, 1471, 1422, 1005, 806, 711. HRMS (ESI) $[\text{C}_{23}\text{H}_{26}\text{NO}]$ (M+H) *calcd.* 332.2004, *found* 332.2009.



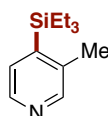
3-(2-(trifluoromethoxy)phenyl)pyridine (46d). Following the general procedure, using 1-bromo-2-(trifluoromethoxy)benzene (241.0 mg, 0.4 mmol), the title compound was obtained in 88% yield (210.4 mg) as colorless oil. R_f 0.45 (Hex: EtOAc 4:1). ^1H NMR (400 MHz, CDCl_3) δ 8.70 (dd, $J = 2.3, 0.9$ Hz, 1H), 8.61 (dd, $J = 4.9, 1.7$ Hz, 1H), 7.79 (dt, $J = 7.9, 1.8$ Hz, 1H), 7.50-7.26 (m, 5H) ppm. ^{13}C NMR (101 MHz, CDCl_3) δ 149.9, 149.0, 146.5 (d, $J = 1.8$ Hz), 136.7, 132.8, 131.8, 131.4, 129.7, 127.4, 123.2, 121.6 (d, $J_{C-F} = 1.5$ Hz), 120.46 (q, $J_{C-F} = 258.3$ Hz) ppm. ^{19}F NMR (376 MHz, CDCl_3) δ -57.36 ppm. IR (neat, cm^{-1}): 2958, 2875, 1677, 1580, 1301, 1265, 1024, 709. HRMS (ESI) $[\text{C}_{12}\text{H}_9\text{F}_3\text{NO}]$ (M+H) *calcd.* 240.0631, *found* 240.0626.

3.8.3 General procedure for site-selective sp^2 C-H silylation of (poly)azines

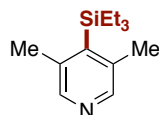
An oven-dried 10 mL screw-capped test tube containing a stirring bar was charged with corresponding azine (1.0 eq, 0.4 mmol). The test tube was transferred to a nitrogen-filled glove-box where KHMDS (79.8 mg, 0.4 mmol), Et_3SiBpin (96.9 mg, 0.4 mmol) and dry ethylene glycol dimethyl ether (DME, 0.2 M, 2mL) were added. Then, the reaction mixture was stirred for 1 minute and taken out of the glovebox. The reaction was rigorously stirred for 3 h and diluted with EtOAc (8 mL). After filtered through a Celite® plug, the desired product was directly purified by flash column chromatography in silica gel.



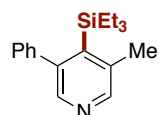
2-ethyl-4-(triethylsilyl)pyridine (50a). Following the general procedure, using 2-ethylpyridine (42.8 mg, 0.4 mmol), the title compound was obtained in 64% yield (56.6 mg) as colorless oil. R_f 0.40 (Hex: EtOAc 10:1). ^1H NMR (300 MHz, CDCl_3) δ 8.45 (dd, $J = 4.8, 1.0$ Hz, 1H), 7.20 (s, 1H), 7.14 (dd, $J = 4.8, 1.1$ Hz, 1H), 2.79 (q, $J = 7.6$ Hz, 2H), 1.29 (t, $J = 7.6$ Hz, 3H), 1.08-0.86 (m, 9H), 0.85-0.62 (m, 6H) ppm. ^{13}C NMR (75 MHz, CDCl_3) δ 162.1, 148.0, 127.5, 126.3, 31.5, 14.2, 7.3, 3.0 ppm. IR (neat, cm^{-1}): 2955, 2875, 1587, 1458, 1382, 1110, 1009, 718. HRMS (ESI) $[\text{C}_{13}\text{H}_{24}\text{NSi}]$ (M+H) *calcd.* 222.1673, *found* 222.1665.



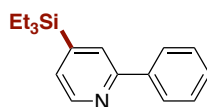
3-methyl-4-(triethylsilyl)pyridine(50b). Following the general procedure, using 3-methylpyridine (37.2 mg, 0.4 mmol), the title compound was obtained in 85% yield (70.4 mg) as colorless oil. R_f 0.52 (Hex: EtOAc 5:1). ^1H NMR (300 MHz, CDCl_3) δ 8.36 (br, 2H), 7.27 (d, $J = 4.8$ Hz, 1H), 2.38 (s, 3H), 1.05-0.80 (m, 15H) ppm. ^{13}C NMR (75 MHz, CDCl_3) δ 149.9, 146.0, 145.6, 138.6, 129.6, 19.9, 7.4, 3.4 ppm. IR (neat, cm^{-1}): 2954, 2875, 1457, 1398, 1095, 1002, 714, 671. HRMS (ESI) [$\text{C}_{12}\text{H}_{22}\text{NSi}$] (M+H) *calcd.* 208.1516, *found* 208.1515.



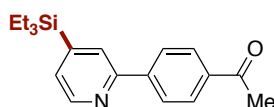
3,5-dimethyl-4-(triethylsilyl)pyridine (50c). Following the general procedure, using 3,5-dimethylpyridine (42.8 mg, 0.4 mmol), the title compound was obtained in 69% yield (61.1 mg) as colorless oil. R_f 0.55 (Hex: EtOAc 10:1). ^1H NMR (300 MHz, CDCl_3) δ 8.13 (s, 2H), 2.37 (s, 6H), 0.96-0.88 (m, 15H) ppm. ^{13}C NMR (75 MHz, CDCl_3) δ 148.4, 144.5, 138.6, 21.3, 7.8, 5.7 ppm. IR (neat, cm^{-1}): 2954, 2874, 1457, 1410, 1182, 1082, 999, 725. HRMS (ESI) [$\text{C}_{13}\text{H}_{24}\text{NSi}$] (M+H) *calcd.* 222.1673, *found* 226.1667.



3-methyl-5-phenyl-4-(triethylsilyl)pyridine (50d). Following the general procedure, using 3-methyl-5-phenylpyridine (67.6 mg, 0.4 mmol), the title compound was obtained in 71% yield (80.4 mg) as colorless oil. R_f 0.65 (Hex: EtOAc 10:1). ^1H NMR (300 MHz, CDCl_3) δ 8.34 (s, 1H), 8.20 (s, 1H), 7.39-7.34 (m, 3H), 7.26-7.20 (m, 2H), 2.50 (s, 3H), 0.79 (t, $J = 7.8$ Hz, 9H), 0.48 (q, $J = 7.8$ Hz, 6H) ppm. ^{13}C NMR (75 MHz, CDCl_3) δ 149.2, 147.8, 145.0, 144.0, 142.0, 138.8, 129.8, 127.9, 127.7, 21.1, 7.9, 4.8 ppm. IR (neat, cm^{-1}): 2953, 2874, 1459, 1404, 1076, 999, 726, 699. HRMS (ESI) [$\text{C}_{18}\text{H}_{26}\text{NSi}$] (M+H) *calcd.* 284.1829, *found* 284.1835.

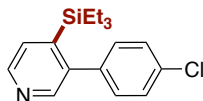


2-phenyl-4-(triethylsilyl)pyridine (50e). Following the general procedure, using 2-phenylpyridine (62.1 mg, 0.4 mmol), the title compound was obtained in 77% yield (82.9 mg) as colorless oil. R_f 0.63 (Hex: EtOAc 5:1). ^1H NMR (400 MHz, CDCl_3) δ 8.65 (dd, $J = 4.7, 0.9$ Hz, 1H), 7.98 (dd, $J = 8.3, 1.2$ Hz, 2H), 7.80 (t, $J = 0.9$ Hz, 1H), 7.48 (t, $J = 7.4$ Hz, 2H), 7.45-7.38 (m, 1H), 7.31 (dd, $J = 4.7, 1.0$ Hz, 1H), 1.00 (t, $J = 7.7$ Hz, 9H), 0.91-0.80 (m, 6H) ppm. ^{13}C NMR (101 MHz, CDCl_3) δ 156.3, 148.6, 148.5, 140.0, 128.9, 128.8, 127.6, 127.2, 126.1, 7.4, 3.0 ppm. Spectroscopic data for **50e** match those previously reported in the literature.²

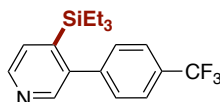


1-(4-(4-(triethylsilyl)pyridin-2-yl)phenyl)ethan-1-one (50f). Following the general procedure, using 1-(4-(pyridin-2-yl)phenyl)ethan-1-one (78.9 mg, 0.4 mmol) and 2 equivalent of KHMDS, the title compound was obtained in 53% yield (66.1 mg) as colorless oil. R_f 0.45 (Hex: EtOAc 4:1). ^1H NMR (300 MHz, CDCl_3) δ 8.67 (dd, $J = 4.7, 1.0$ Hz, 1H), 8.12-8.02 (m, 4H), 7.83 (t, $J = 1.1$ Hz, 1H), 7.36 (dd, $J = 4.7,$

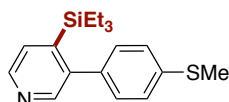
1.0 Hz, 1H), 2.64 (s, 3H), 1.02-0.96 (m, 9H), 0.92-0.80 (m, 6H) ppm. ^{13}C NMR (75 MHz, CDCl_3) δ 197.9, 154.9, 149.0, 148.8, 144.2, 137.1, 128.9, 128.5, 127.3, 126.38, 26.85, 7.37, 2.99 ppm. IR (neat, cm^{-1}): 2954, 2875, 1682, 1585, 1359, 1264, 1014, 701. HRMS (ESI) [$\text{C}_{19}\text{H}_{26}\text{NOSi}$] (M+H) *calcd.* 312.1778, *found* 312.1778.



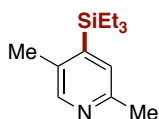
3-(4-chlorophenyl)-4-(triethylsilyl)pyridine (50g). Following the general procedure, using 3-(4-chlorophenyl)pyridine (75.8 mg, 0.4 mmol), the title compound was obtained in 70% yield (85.1 mg) as colorless oil. R_f 0.48 (Hex: EtOAc 4:1). ^1H NMR (400 MHz, CDCl_3) δ 8.54 (d, J = 4.9 Hz, 1H), 8.39 (d, J = 0.9 Hz, 1H), 7.42 (dd, J = 4.9, 0.9 Hz, 1H), 7.42-7.35 (m, 2H), 7.24-7.17 (m, 2H), 0.81 (t, J = 7.9 Hz, 9H), 0.51 (q, J = 8.3, 7.9 Hz, 6H) ppm. ^{13}C NMR (101 MHz, CDCl_3) δ 149.5, 147.5, 145.5, 143.3, 139.4, 134.2, 130.8, 129.9, 128.3, 7.4, 3.9 ppm. IR (neat, cm^{-1}): 2954, 2870, 1470, 1350, 1074, 1051, 998, 710. HRMS (ESI) [$\text{C}_{17}\text{H}_{23}\text{ClNSi}$] (M+H) *calcd.* 304.1283, *found* 304.1281.



4-(triethylsilyl)-3-(4-(trifluoromethyl)phenyl)pyridine (50h). Following the general procedure, 3-(4-(trifluoromethyl)phenyl)pyridine (89.2 mg, 0.4 mmol) was used. The reaction was conducted at 0 $^\circ\text{C}$ and the title compound was obtained in 75% yield (101.2 mg) as colorless oil. R_f 0.51 (Hex: EtOAc 4:1). ^1H NMR (300 MHz, CDCl_3) δ 8.58 (d, J = 4.9 Hz, 1H), 8.41 (s, 1H), 7.68 (d, J = 8.1 Hz, 2H), 7.46 (d, J = 4.1 Hz, 1H), 7.40 (d, J = 8.5 Hz, 2H), 0.81 (t, J = 7.8 Hz, 9H), 0.50 (q, J = 8.4, 7.8 Hz, 6H) ppm. ^{13}C NMR (101 MHz, CDCl_3) δ 149.1, 148.6, 145.7, 144.6, 144.6, 143.2, 130.4 (q, $J_{\text{C-F}}$ = 32.7 Hz), 130.1, 129.9, 125.1 (q, $J_{\text{C-F}}$ = 3.7 Hz), 124.2 (q, $J_{\text{C-F}}$ = 272.2 Hz), 7.6, 3.9 ppm. ^{19}F NMR (376 MHz, CDCl_3) δ -62.57 ppm. IR (neat, cm^{-1}): 2955, 2877, 1322, 1125, 1066, 1002, 721, 663. HRMS (ESI) [$\text{C}_{18}\text{H}_{23}\text{F}_3\text{NSi}$] (M+H) *calcd.* 338.1546, *found* 338.1556.

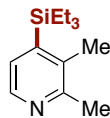


3-(4-(methylthio)phenyl)-4-(triethylsilyl)pyridine (50i). Following the general procedure, using 3-(4-(methylthio)phenyl)pyridine (80.4 mg, 0.4 mmol), the title compound was obtained in 80% yield (100.9 mg) as colorless oil. R_f 0.46 (Hex: EtOAc 4:1). ^1H NMR (400 MHz, CDCl_3) δ 8.52 (d, J = 4.9 Hz, 1H), 8.40 (d, J = 0.8 Hz, 1H), 7.40 (dd, J = 4.9, 0.8 Hz, 1H), 7.30-7.25 (m, 2H), 7.20-7.16 (m, 2H), 2.53 (s, 3H), 0.81 (t, J = 7.9 Hz, 9H), 0.52 (q, J = 7.9 Hz, 6H) ppm. ^{13}C NMR (101 MHz, CDCl_3) δ 149.7, 147.1, 145.4, 144.0, 138.5, 137.7, 129.9, 129.8, 125.9, 15.9, 7.4, 3.9 ppm. IR (neat, cm^{-1}): 2952, 2873, 1461, 1391, 1101, 1090, 1000, 718. HRMS (ESI) [$\text{C}_{18}\text{H}_{26}\text{NSSi}$] (M+H) *calcd.* 316.1550, *found* 316.1550.

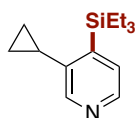


2,5-dimethyl-4-(triethylsilyl)pyridine (50j). Following the general procedure, using 2,5-dimethylpyridine (42.8 mg, 0.4 mmol), the title compound was obtained in 80% yield (70.8 mg) as

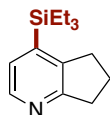
colorless oil. R_f 0.62 (Hex: EtOAc 4:1). ^1H NMR (300 MHz, CDCl_3) δ 8.21 (s, 1H), 7.10 (s, 1H), 2.47 (s, 3H), 2.31 (s, 3H), 0.95-0.78 (m, 15H) ppm. ^{13}C NMR (75 MHz, CDCl_3) δ 154.2, 149.3, 145.7, 135.1, 129.1, 24.0, 19.4, 7.4, 3.4 ppm. IR (neat, cm^{-1}): 2954, 2875, 1584, 1458, 1330, 1082, 1002, 717. HRMS (ESI) [$\text{C}_{13}\text{H}_{24}\text{NSi}$] (M+H) *calcd.* 222.1673, *found* 226.1672.



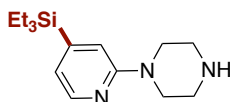
2,3-dimethyl-4-(triethylsilyl)pyridine (50k). Following the general procedure, using 2,3-dimethylpyridine (42.8 mg, 0.4 mmol), the title compound was obtained in 55% yield (48.7 mg) as colorless oil. R_f 0.48 (Hex: EtOAc 10:1). ^1H NMR (300 MHz, CDCl_3) δ 8.27 (d, $J = 4.8$ Hz, 1H), 7.13 (d, $J = 4.8$ Hz, 1H), 2.51 (s, 3H), 2.33 (s, 3H), 0.97-0.81 (m, 15H) ppm. ^{13}C NMR (75 MHz, CDCl_3) δ 156.2, 145.6, 145.3, 136.9, 127.9, 23.4, 19.4, 7.6, 3.9 ppm. IR (neat, cm^{-1}): 2953, 2875, 1458, 1400, 1381, 1175, 1005, 722. HRMS (ESI) [$\text{C}_{13}\text{H}_{24}\text{NSi}$] (M+H) *calcd.* 222.1673, *found* 226.1671.



3-cyclopropyl-4-(triethylsilyl)pyridine (50l). Following the general procedure, using 3-cyclopropylpyridine (47.6 mg, 0.4 mmol), the title compound was obtained in 72% yield (67.2 mg) as colorless oil. R_f 0.54 (Hex: Et₂O 3:1). ^1H NMR (300 MHz, CDCl_3) δ 8.35 (d, $J = 4.8$ Hz, 1H), 8.13 (s, 1H), 7.27 (dd, $J = 4.4, 1.1$ Hz, 1H), 1.97 (tt, $J = 8.4, 5.3$ Hz, 1H), 1.02-0.89 (m, 17H), 0.88-0.82 (m, 2H) ppm. ^{13}C NMR (75 MHz, CDCl_3) δ 146.4, 145.8, 145.0, 143.7, 129.4, 14.3, 9.1, 7.5, 3.8 ppm. IR (neat, cm^{-1}): 2954, 2874, 1457, 1404, 1089, 1002, 712, 671. HRMS (ESI) [$\text{C}_{14}\text{H}_{24}\text{NSi}$] (M+H) *calcd.* 234.1673, *found* 234.1670.

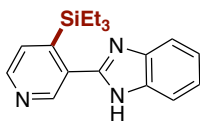


4-(triethylsilyl)-6,7-dihydro-5H-cyclopenta[b]pyridine (50m). Following the general procedure, using 6,7-dihydro-5H-cyclopenta[b]pyridine (47.6 mg, 0.4 mmol), the title compound was obtained in 85% yield (79.3 mg) as colorless oil. R_f 0.54 (Hex: EtOAc 5:1). ^1H NMR (300 MHz, CDCl_3) δ 8.27 (d, $J = 4.9$ Hz, 1H), 7.07 (d, $J = 4.9$ Hz, 1H), 3.01-2.91 (m, 4H), 2.08 (p, $J = 7.7$ Hz, 2H), 0.91 (d, $J = 6.5$ Hz, 9H), 0.86-0.75 (m, 6H) ppm. ^{13}C NMR (75 MHz, CDCl_3) δ 163.9, 146.3, 142.6, 142.4, 126.9, 34.0, 32.3, 23.0, 7.4, 3.1 ppm. IR (neat, cm^{-1}): 2953, 2874, 1573, 1459, 1369, 1003, 829, 720. HRMS (ESI) [$\text{C}_{14}\text{H}_{24}\text{NSi}$] (M+H) *calcd.* 234.1673, *found* 234.1679.

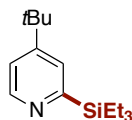


2-(piperazin-1-yl)-4-(triethylsilyl)pyrimidine (50n). Following the general procedure, using 1-(pyridin-2-yl)piperazine (65.3 mg, 0.4 mmol) and 2 equivalent of KHMDS, the title compound was obtained in 55% yield (61.1 mg) as colorless oil. R_f 0.33 (Hex: EtOAc 2:1). ^1H NMR (300 MHz, CDCl_3) δ 8.15 (dd, $J = 4.8, 1.0$ Hz, 1H), 6.74 (s, 1H), 6.71 (dd, $J = 4.8, 0.8$ Hz, 1H), 3.52 (t, $J = 6.8$ Hz, 4H), 3.02 (t, $J = 6.8$ Hz, 4H),

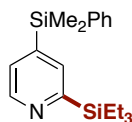
2.32 (br, 1H), 0.96 (t, $J = 7.8$ Hz, 9H), 0.77 (q, $J = 8.9$ Hz, 6H) ppm. ^{13}C NMR (75 MHz, CDCl_3) δ 159.0, 148.9, 146.8, 118.9, 112.7, 46.4, 45.9, 7.4, 3.1 ppm. IR (neat, cm^{-1}): 2952, 2874, 1583, 1522, 1413, 1243, 985, 720. HRMS (ESI) [$\text{C}_{15}\text{H}_{28}\text{N}_3\text{Si}$] (M+H) *calcd.* 278.2052, *found* 278.2056.



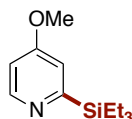
2-(4-(triethylsilyl)pyridin-3-yl)-1H-benzo[d]imidazole (50o). Following the general procedure, using 2-(pyridin-3-yl)-1H-benzo[d]imidazole (78.1 mg, 0.4 mmol) and 2 equivalent of KHMDS, the title compound was obtained in 42% yield (51.8 mg) as colorless oil. R_f 0.68 (EtOAc). ^1H NMR (300 MHz, CDCl_3) δ 9.14 (s, 1H), 8.58 (d, $J = 5.1$ Hz, 1H), 7.73-7.70 (m, 3H), 7.32 (dd, $J = 6.1, 3.2$ Hz, 2H), 0.88-0.85 (m, 15H). ^{13}C NMR (75 MHz, CDCl_3) δ 157.3, 148.1, 138.4, 123.9, 121.4, 116.0, 7.7, 4.2. IR (neat, cm^{-1}): 2856, 2794, 1673, 1419, 1332, 1296, 1105, 786. HRMS (ESI) [$\text{C}_{18}\text{H}_{24}\text{N}_3\text{Si}$] (M+H) *calcd.* 310.1734, *found* 310.1730.



4-(tert-butyl)-2-(triethylsilyl)pyridine (50p). Following the general procedure, using 4-(tert-butyl)pyridine (54.1 mg, 0.4 mmol), the title compound was obtained in 74% yield (73.8 mg) as colorless oil. R_f 0.82 (Hex: EtOAc 10:1). ^1H NMR (500 MHz, CDCl_3) δ 8.67 (dd, $J = 5.3, 0.8$ Hz, 1H), 7.44 (dd, $J = 2.1, 0.8$ Hz, 1H), 7.16 (dd, $J = 5.3, 2.2$ Hz, 1H), 1.29 (s, 9H), 0.98 (t, $J = 7.8$ Hz, 9H), 0.89-0.82 (m, 6H) ppm. ^{13}C NMR (126 MHz, CDCl_3) δ 165.7, 157.1, 150.2, 126.9, 119.7, 34.6, 30.7, 7.5, 3.2 ppm. IR (neat, cm^{-1}): 2954, 2875, 1603, 1414, 1005, 842, 822, 720. HRMS (ESI) [$\text{C}_{15}\text{H}_{28}\text{NSi}$] (M+H) *calcd.* 250.1986, *found* 250.1984.

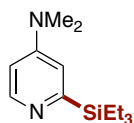


4-(dimethyl(phenyl)silyl)-2-(triethylsilyl)pyridine (50q). Following the general procedure, using 4-(dimethyl(phenyl)silyl)pyridine (85.2 mg, 0.4 mmol), the title compound was obtained in 59% yield (77.3 mg) as colorless oil. R_f 0.82 (Hex: EtOAc 5:1). ^1H NMR (300 MHz, CDCl_3) δ 8.73 (dd, $J = 4.8, 1.0$ Hz, 1H), 7.55 (t, $J = 1.2$ Hz, 1H), 7.54-7.45 (m, 2H), 7.42-7.33 (m, 3H), 7.27 (dd, $J = 4.8, 1.3$ Hz, 1H), 0.97 (t, $J = 7.5$ Hz, 9H), 0.90-0.81 (m, 6H), 0.57 (s, 6H) ppm. ^{13}C NMR (75 MHz, CDCl_3) δ 164.9, 149.2, 145.1, 136.7, 134.9, 134.3, 129.7, 128.1, 127.9, 7.5, 3.1, -2.9 ppm. IR (neat, cm^{-1}): 2955, 1875, 1737, 1406, 1250, 1113, 818, 730. HRMS (ESI) [$\text{C}_{19}\text{H}_{30}\text{NSi}_2$] (M+H) *calcd.* 328.1911, *found* 328.1915.

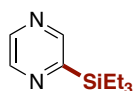


4-methoxy-2-(triethylsilyl)pyridine (50r). Following the general procedure, using 4-methoxypyridine (43.7 mg, 0.4 mmol), the title compound was obtained in 55% yield (49.2 mg) as colorless oil. R_f 0.54 (Hex: EtOAc 4:1). ^1H NMR (300 MHz, CDCl_3) δ 8.60 (d, $J = 5.7$ Hz, 1H), 7.00 (d, $J = 2.7$ Hz, 1H), 6.70 (dd, $J = 5.7, 2.7$ Hz, 1H), 3.82 (s, 3H), 0.97 (t, $J = 7.5$ Hz, 9H), 0.89-0.79 (m, 6H) ppm. ^{13}C NMR (75 MHz, CDCl_3)

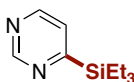
δ 167.7, 164.0, 151.6, 116.9, 108.1, 54.8, 7.5, 3.0 ppm. IR (neat, cm^{-1}): 2953, 2875, 1600, 1460, 1290, 1211, 1015, 722. HRMS (ESI) [$\text{C}_{12}\text{H}_{22}\text{NOSi}$] (M+H) *calcd.* 224.1465, *found* 224.1459.



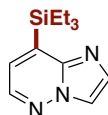
N,N-dimethyl-2-(triethylsilyl)pyridin-4-amine (50s). Following the general procedure, using *N,N*-dimethylpyridin-4-amine (48.9 mg, 0.4 mmol), the title compound was obtained in 79% yield (74.7 mg) as colorless oil. R_f 0.43 (Methanol: EtOAc 1:1). ^1H NMR (500 MHz, CDCl_3) δ 8.39 (d, $J = 6.3$ Hz, 1H), 6.70 (d, $J = 2.9$ Hz, 1H), 6.46 (dd, $J = 6.3, 2.9$ Hz, 1H), 3.03 (s, 6H), 0.97 (t, $J = 7.6$ Hz, 9H), 0.88 (q, $J = 6.9$ Hz, 6H) ppm. ^{13}C NMR (126 MHz, CDCl_3) δ 153.3, 148.2, 113.3, 105.8, 39.3, 7.5, 3.0 ppm. IR (neat, cm^{-1}): 2927, 1736, 1604, 1525, 1446, 1375, 1229, 1043. HRMS (ESI) [$\text{C}_{13}\text{H}_{25}\text{N}_2\text{Si}$] (M+H) *calcd.* 237.1782, *found* 237.1781.



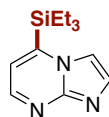
2-(triethylsilyl)pyrazine (50t). Following the general procedure, using pyrazine (32 mg, 0.4 mmol), the title compound was obtained in 61% yield (47.4 mg) as colorless oil. R_f 0.71 (Hex: EtOAc 5:1). ^1H NMR (300 MHz, CDCl_3) δ 8.73 (t, $J = 2.4$ Hz, 1H), 8.62 (s, 1H), 8.44 (d, $J = 2.5$ Hz, 1H), 0.99 (t, $J = 7.5$ Hz, 9H), 0.93-0.82 (m, 6H) ppm. ^{13}C NMR (75 MHz, CDCl_3) δ 149.8, 146.1, 143.8, 7.4, 2.9 ppm. IR (neat, cm^{-1}): 2964, 2874, 1506, 1350, 1103, 823, 795, 701. HRMS (ESI) [$\text{C}_{10}\text{H}_{19}\text{N}_2\text{Si}$] (M+H) *calcd.* 195.1312, *found* 195.1306.



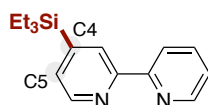
4-(triethylsilyl)pyrimidine (50u). Following the general procedure, using pyrimidine (32 mg, 0.4 mmol), the title compound was obtained in 70% yield (54.4 mg) as colorless oil. R_f 0.69 (Hex: EtOAc 10:1). ^1H NMR (300 MHz, CDCl_3) δ 9.23 (d, $J = 1.6$ Hz, 1H), 8.52 (d, $J = 4.9$ Hz, 1H), 7.37 (dd, $J = 4.9, 1.6$ Hz, 1H), 0.95-0.87 (m, 9H), 0.83-0.74 (m, 6H) ppm. ^{13}C NMR (75 MHz, CDCl_3) δ 176.5, 158.2, 154.4, 127.5, 7.2, 2.5 ppm. IR (neat, cm^{-1}): 2954, 2876, 1565, 1520, 1380, 1006, 719, 690. HRMS (ESI) [$\text{C}_{10}\text{H}_{19}\text{N}_2\text{Si}$] (M+H) *calcd.* 195.1312, *found* 195.1309.



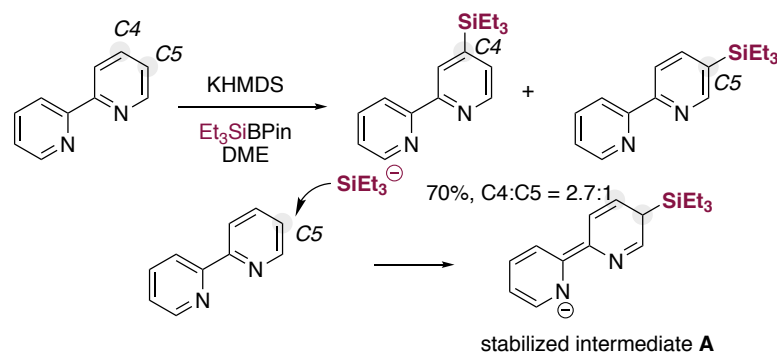
8-(triethylsilyl)imidazo[1,2-*b*]pyridazine (50v). Following the general procedure, using imidazo[1,2-*b*]pyridazine (47.6 mg, 0.4 mmol), the title compound was obtained in 49% yield (45.7 mg) as colorless oil. R_f 0.44 (Hex: EtOAc 5:1). ^1H NMR (300 MHz, CDCl_3) δ 8.21 (d, $J = 4.3$ Hz, 1H), 7.92 (d, $J = 1.3$ Hz, 1H), 7.77 (d, $J = 1.3$ Hz, 1H), 7.04 (d, $J = 4.3$ Hz, 1H), 1.17-0.90 (m, 15H) ppm. ^{13}C NMR (75 MHz, CDCl_3) δ 142.2, 141.9, 138.3, 133.0, 123.3, 116.0, 7.4, 2.9 ppm. IR (neat, cm^{-1}): 2953, 2874, 1456, 1319, 1249, 1198, 1005, 722. HRMS (ESI) [$\text{C}_{12}\text{H}_{20}\text{N}_3\text{Si}$] (M+H) *calcd.* 234.1421, *found* 234.1416.



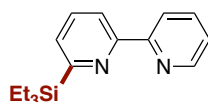
5-(triethylsilyl)imidazo[1,2-*a*]pyrimidine (50w). Following the general procedure, using imidazo[1,2-*a*]pyrimidine (47.6 mg, 0.4 mmol) and 2 equivalent of KHMDS, the reaction was conducted at 0 °C. The title compound was obtained in 44% yield (41.1 mg) as colorless oil. R_f 0.34 (Hex: EtOAc 5:1). ^1H NMR (300 MHz, CDCl_3) δ 8.46 (d, J = 4.0 Hz, 1H), 7.82 (d, J = 1.4 Hz, 1H), 7.60 (d, J = 1.4 Hz, 1H), 6.89 (d, J = 4.0 Hz, 1H), 1.05-0.90 (m, 15H) ppm. ^{13}C NMR (75 MHz, CDCl_3) δ 148.5, 148.4, 135.2, 116.9, 111.5, 7.2, 2.3 ppm. IR (neat, cm^{-1}): 2962, 2860, 1532, 1239, 1218, 1181, 1006, 723. HRMS (ESI) [$\text{C}_{12}\text{H}_{20}\text{N}_3\text{Si}$] (M+H) *calcd.* 234.1436, *found* 234.1438.



4-(triethylsilyl)-2,2'-bipyridine (50x). Following the general procedure, using 2,2'-bipyridine (68.8 mg, 0.4 mmol), the product was obtained in 70% yield (75.6 mg) in a mixture (C4:C5=2.7:1) as pale yellow oil. R_f 0.32 (Hex: Methanol 10:1). [C4]: ^1H NMR (300 MHz, CDCl_3) δ 8.75 (s, 1H), 8.69-8.68 (m, 2H), 8.44-8.35 (m, 2H), 7.91 (dd, J = 7.8, 1.7 Hz, 1H), 7.84-7.77 (m, 1H), 1.02-0.95 (m, 9H), 0.90-0.83 (m, 6H) ppm. [C5]: ^1H NMR (300 MHz, CDCl_3) δ 8.69-8.62 (m, 1H), 8.63 (d, J = 4.8 Hz, 1H), 8.50 (s, 1H), 8.40-8.48 (m, 1H), 7.81 (t, J = 7.8 Hz, 1H), 7.44 (d, J = 4.8 Hz, 1H), 7.27-7.32 (m, 1H), 1.02-0.95 (m, 9H), 0.90-0.83 (m, 6H) ppm. ^{13}C NMR (75 MHz, CDCl_3) δ 156.5, 156.0, 155.9, 154.5, 153.87, 149.3, 149.3, 147.8, 143.5, 137.1, 137.1, 132.9, 129.4, 126.5, 124.0, 123.7, 121.5, 121.3, 120.6, 7.4, 7.4, 3.3, 2.9 ppm. IR (neat, cm^{-1}): 2874, 2868, 1612, 1503, 1436, 1276, 1098, 1011. HRMS (ESI) [$\text{C}_{19}\text{H}_{28}\text{NO}_2\text{Si}$] (M+H) *calcd.* 330.1884, *found* 330.1872.

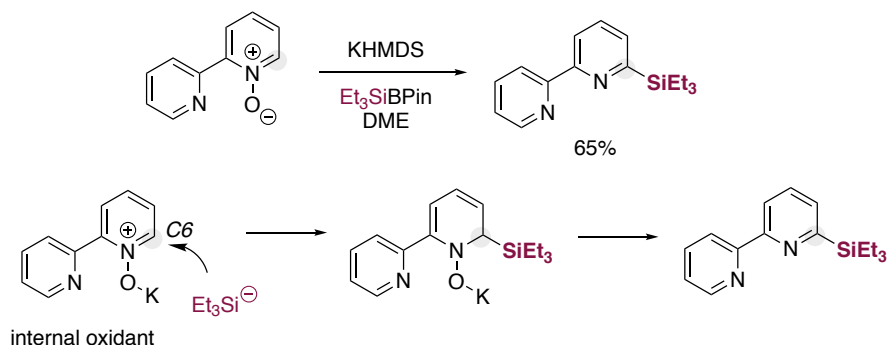


The reaction with 2,2'-bipyridine deliver a mixture of regioisomers (C4:C5 = 2.7 :1). This result is interpreted on the basis of the electron-withdrawing ability of the nitrogen atom, making the C5-position particularly electron-poor.

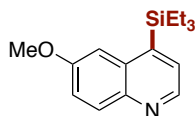


6-(triethylsilyl)-2,2'-bipyridine (50y). Following the general procedure, using [2,2'-bipyridine] 1-oxide (68.8 mg, 0.4 mmol), the title compound was obtained in 64% yield (68 mg) as colorless oil. R_f 0.39 (Hex: EtOAc 4:1). ^1H NMR (300 MHz, CDCl_3) δ 8.66 (ddd, J = 4.8, 1.6, 0.8 Hz, 1H), 8.55 (d, J = 8.0 Hz, 1H), 8.31

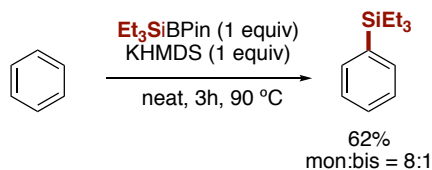
(dd, $J = 8.0, 1.1$ Hz, 1H), 7.81 (td, $J = 7.8, 1.8$ Hz, 1H), 7.73-7.65 (m, 1H), 7.46 (dd, $J = 7.4, 1.2$ Hz, 1H), 7.34-7.26 (m, 1H), 1.10-1.01 (m, 9H), 0.95-0.86 (m, 6H) ppm. ^{13}C NMR (75 MHz, CDCl_3) δ 165.9, 157.1, 155.8, 149.0, 136.9, 134.6, 129.8, 123.6, 121.4, 119.8, 7.6, 3.3 ppm. IR (neat, cm^{-1}): 2954, 2865, 1614, 1570, 1453, 1241, 1203, 1110, 998. HRMS (ESI) [$\text{C}_{16}\text{H}_{23}\text{N}_2\text{Si}$] (M+H) *calcd.* 271.1625, *found* 271.1623.



The reactivity of pyridine-*N*-oxides could be explained by activating the adjacent motif upon coordination of the potassium ion, thus setting the stage for triggering the corresponding C2-attack. In this case, the *N*-oxides could also act as an internal oxidant, thus facilitating the rearomatization process.

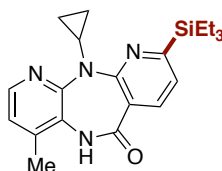


6-methoxy-4-(triethylsilyl)quinolone (50z). Following the general procedure, using 6-methoxyquinoline 1-oxide (70.1 mg, 0.4 mmol), the title compound was obtained in 58% yield (63.4 mg) as yellow oil. R_f 0.41 (Hex: EtOAc 2:1). ^1H NMR (300 MHz, CDCl_3) δ 8.71 (d, $J = 4.2$ Hz, 1H), 8.02 (d, $J = 9.0$ Hz, 1H), 7.46 (d, $J = 4.2$ Hz, 1H), 7.41-7.31 (m, 3H), 3.93 (s, 3H), 1.08-0.93 (m, 15H) ppm. ^{13}C NMR (75 MHz, CDCl_3) δ 157.4, 147.0, 144.5, 143.6, 133.5, 131.9, 129.1, 121.1, 106.3, 55.6, 7.7, 4.2 ppm. IR (neat, cm^{-1}): 2953, 2874, 1619, 1503, 1464, 1231, 826, 720. HRMS (ESI) [$\text{C}_{16}\text{H}_{24}\text{NOSi}$] (M+H) *calcd.* 274.1622, *found* 274.1619.

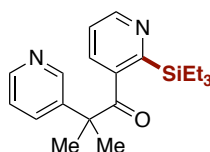


An oven-dried 10 mL screw-capped test tube containing a stirring bar was transferred to a nitrogen-filled glove-box, where KHMDS (79.8 mg, 0.4 mmol), Et_3SiBPIn (96.9 mg, 0.4 mmol) and Benzene (0.4 mmol) were added. The reaction was rigorously stirred for 3 hours at 90 °C and diluted with Et_2O . The desired product **51** was directly purified by flash column chromatography in silica gel. R_f 0.88 (Hexanes). ^1H NMR (300 MHz, CDCl_3) δ 7.60-7.50 (m, 2H), 7.46-7.36 (m, 3H), 1.03 (t, $J = 7.6$ Hz, 9H), 0.85 (q, $J = 8.6, 7.6$ Hz, 6H) ppm. ^{13}C NMR (75 MHz, CDCl_3) δ 137.6, 134.3, 128.8, 127.8, 7.5, 3.5 ppm. Spectroscopic data match those previously reported in the literature.⁶

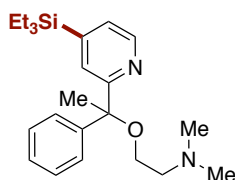
General procedure_Late-stage silylation of (poly)azine drugs: An oven-dried 10 mL screw-capped test tube containing a stirring bar was charged with corresponding azine (1.0 eq, 0.4 mmol). The test tube was transferred to a nitrogen-filled glove-box where the KHMDS (100 mol%, 79.8 mg, 0.4 mmol), Et_3SiBpin (100 mol%, 96.9 mg, 0.4 mmol) and dry ethylene glycol dimethyl ether (DME, 0.2 M, 2mL) were added. Then the reaction mixture was stirred for 1 minute and taken out of the glovebox. The reaction was rigorously stirred for 3 h and diluted with EtOAc (8 mL). After filtered through a Celite® plug, the desired product was directly purified by flash column chromatography in silica gel.



11-cyclopropyl-4-methyl-9-(triethylsilyl)-5,11-dihydro-6H-dipyrido[3,2-b:2',3'-e][1,4]diazepin-6-one (52). Following the general procedure, using Nevirapine (106.5 mg, 0.4 mmol), 2.0 eq. of KHMDS and 2.0 eq. of Et_3SiBpin , the title compound was obtained in 74% yield (112.7 mg) as white solid. R_f 0.81 (Hex: EtOAc 2:1). ^1H NMR (300 MHz, CDCl_3) δ 8.69 (s, 1H), 8.14 (d, $J = 4.9$ Hz, 1H), 7.96 (d, $J = 7.5$ Hz, 1H), 7.21 (d, $J = 4.9$ Hz, 1H), 6.89 (d, $J = 4.9$ Hz, 1H), 3.77 (tt, $J = 6.6, 3.9$ Hz, 1H), 2.39 (s, 3H), 1.02-0.78 (m, 17H), 0.45 (m, 2H) ppm. ^{13}C NMR (75 MHz, CDCl_3) δ 171.6, 169.7, 159.7, 154.5, 144.3, 139.3, 137.4, 125.0, 125.0, 121.8, 118.6, 29.9, 17.9, 9.3, 8.8, 7.5, 3.1 ppm. Mp 208.1-209.3 °C. IR (neat, cm^{-1}): 2956, 2872, 1653, 1575, 1405, 1334, 1285, 711. HRMS (ESI) [$\text{C}_{21}\text{H}_{29}\text{N}_4\text{OSi}$] (M+H) *calcd.* 381.2105, *found* 381.2104.

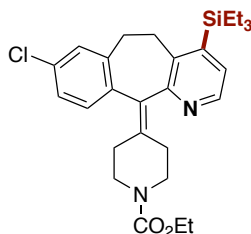


2-methyl-2-(pyridin-3-yl)-1-(2-(triethylsilyl)pyridin-3-yl)propan-1-one (53). Following the general procedure, using Metyrapone (90.5 mg, 0.4 mmol), the title compound was obtained in 54% yield (73.5 mg) as colorless oil. In this case, 36% of the starting material could be recovered. R_f 0.61 (Hex: EtOAc 4:1). ^1H NMR (300 MHz, CDCl_3) δ 8.81 (dd, $J = 2.2, 1.0$ Hz, 1H), 8.60 (dd, $J = 2.6, 0.9$ Hz, 1H), 8.55 (dd, $J = 4.8, 1.6$ Hz, 1H), 7.71 (dd, $J = 8.0, 2.2$ Hz, 1H), 7.63 (ddd, $J = 8.1, 2.5, 1.6$ Hz, 1H), 7.42 (dd, $J = 7.9, 1.0$ Hz, 1H), 7.31 (ddd, $J = 8.0, 4.8, 0.9$ Hz, 1H), 1.66 (s, 6H), 0.96-0.90 (m, 9H), 0.86-0.79 (m, 6H) ppm. ^{13}C NMR (75 MHz, CDCl_3) δ 201.7, 171.5, 150.3, 148.6, 147.5, 140.2, 134.7, 133.7, 129.8, 129.6, 124.2, 50.4, 27.5, 7.4, 2.9 ppm. IR (neat, cm^{-1}): 2954, 2875, 1681, 1577, 1465, 1416, 1256, 970. HRMS (ESI) [$\text{C}_{20}\text{H}_{29}\text{N}_2\text{OSi}$] (M+H) *calcd.* 341.2041, *found* 341.2044.

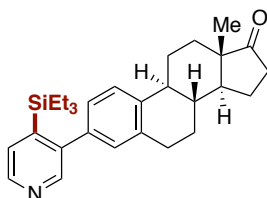


***N,N*-dimethyl-2-(1-phenyl-1-(4-(triethylsilyl)pyridin-2-yl)ethoxy)ethan-1-amine (54).** Following the general procedure, using Doxylamine (108.1 mg, 0.4 mmol), the title compound was obtained in 45% yield (69.2 mg) as colorless oil. R_f 0.54 (Hex: EtOAc 3:1). ^1H NMR (300 MHz, CDCl_3) δ 8.49 (dd, $J = 4.7,$

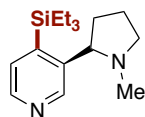
1.0 Hz, 1H), 7.69 (t, $J = 1.1$ Hz, 1H), 7.41-7.38 (m, 2H), 7.31-7.25 (m, 2H), 7.23-7.16 (m, 2H), 3.68-3.26 (m, 2H), 2.66 (td, $J = 6.1, 2.0$ Hz, 2H), 2.34 (s, 6H), 2.00 (s, 3H), 0.94 (t, $J = 7.7$ Hz, 9H), 0.85-0.66 (m, 6H) ppm. ^{13}C NMR (75 MHz, CDCl_3) δ 163.3, 147.9, 147.4, 146.0, 128.1, 127.2, 126.9, 126.5, 126.3, 82.4, 61.4, 59.5, 46.1, 24.2, 7.4, 3.0 ppm. IR (neat, cm^{-1}): 2952, 2875, 2768, 1583, 1458, 1367, 1141, 1100. HRMS (ESI) [$\text{C}_{23}\text{H}_{37}\text{N}_2\text{OSi}$] (M+H) *calcd.* 385.2689, *found* 385.2670.



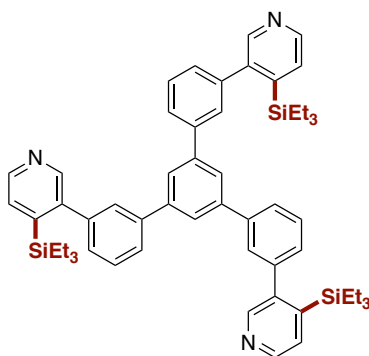
ethyl 4-(8-chloro-4-(triethylsilyl)-5,6-dihydro-11H-benzo[5,6]cyclohepta[1,2-b]pyridin-11-ylidene)piperidine-1-carboxylate (55). Following the general procedure, using Loratadine (153.1 mg, 0.4 mmol), the title compound was obtained in 51% yield (107.3 mg) as colorless oil. In this case, 30% of the starting material could be recovered. R_f 0.36 (Hex: EtOAc 2:1). ^1H NMR (500 MHz, CDCl_3) δ 8.34 (d, $J = 4.9$ Hz, 1H), 7.22 (d, $J = 4.9$ Hz, 1H), 7.16-7.05 (m, 3H), 4.12 (q, $J = 7.1$ Hz, 2H), 3.85-3.70 (m, 2H), 3.43 (td, $J = 13.5, 4.3$ Hz, 1H), 3.35 (dt, $J = 17.2, 4.5$ Hz, 1H), 3.21 (dt, $J = 13.1, 6.5$ Hz, 1H), 3.10 (ddd, $J = 13.1, 9.3, 3.8$ Hz, 1H), 2.93 (dt, $J = 14.1, 4.4$ Hz, 1H), 2.83 (ddd, $J = 17.3, 12.9, 4.3$ Hz, 1H), 2.45 (t, $J = 5.8$ Hz, 2H), 2.31 (ddd, $J = 13.7, 9.1, 4.4$ Hz, 1H), 2.12 – 1.99 (m, 1H), 1.23 (t, $J = 7.1$ Hz, 3H), 0.95 (t, $J = 7.4$ Hz, 9H), 0.95-0.83 (m, 6H) ppm. ^{13}C NMR (126 MHz, CDCl_3) δ 159.2, 155.6, 145.7, 139.2, 138.6, 136.3, 135.1, 134.7, 133.0, 131.8, 130.3, 129.2, 126.0, 61.4, 44.9, 44.6, 32.8, 30.8, 30.5, 29.78, 14.8, 7.6, 4.1 ppm. IR (neat, cm^{-1}): 2963, 2861, 1664, 1570, 1398, 1325, 1165, 701. HRMS (ESI) [$\text{C}_{28}\text{H}_{38}\text{ClN}_2\text{O}_2\text{Si}$] (M+H) *calcd.* 497.2379, *found* 497.2386.



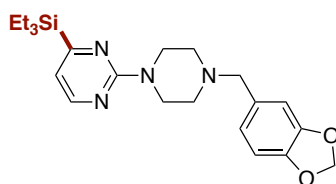
(8R,9S,13S,14S)-13-methyl-3-(4-(triethylsilyl)pyridin-3-yl)-6,7,8,9,11,12,13,14,15,16-decahydro-17H-cyclopenta[a]phenanthren-17-one (56). Following the general procedure, using (8R,9S,13S,14S)-13-methyl-3-(pyridin-3-yl)-6,7,8,9,11,12,13,14,15,16-decahydro-17H-cyclopenta[a]phenanthren-17-one (132.6 mg, 0.4 mmol), the title compound was obtained in 48% yield (85.6 mg) as colorless oil. In this case, 28% of the starting material could be recovered. R_f 0.74 (Hex: EtOAc 2:1). ^1H NMR (500 MHz, CDCl_3) δ 8.51 (d, $J = 4.8$ Hz, 1H), 8.43 (s, 1H), 7.43 (d, $J = 4.8$ Hz, 1H), 7.32 (d, $J = 8.0$ Hz, 1H), 7.05 (d, $J = 6.7$ Hz, 1H), 6.99 (s, 1H), 3.00-2.85 (m, 2H), 2.59-2.44 (m, 2H), 2.39 (td, $J = 10.9, 4.2$ Hz, 1H), 2.21-2.13 (m, 1H), 2.12-2.03 (m, 2H), 2.00 (dd, $J = 12.5, 3.2$ Hz, 1H), 1.71-1.60 (m, 2H), 1.60-1.46 (m, 4H), 0.95 (s, 3H), 0.81 (t, $J = 7.9$ Hz, 9H), 0.51 (q, $J = 7.9$ Hz, 6H) ppm. ^{13}C NMR (126 MHz, CDCl_3) δ 220.9, 149.0, 146.3, 146.2, 144.7, 139.6, 138.1, 136.1, 130.1, 130.0, 126.8, 125.0, 50.7, 48.1, 44.5, 38.3, 36.0, 31.8, 29.5, 26.6, 25.9, 21.7, 14.1, 7.4, 3.9 ppm. $[\alpha]_D^{26} = 146.8$ ($c = 0.1053$, CH_2Cl_2). IR (neat, cm^{-1}): 2932, 2873, 1738, 1463, 1373, 1238, 1007, 731. HRMS (ESI) [$\text{C}_{29}\text{H}_{40}\text{NOSi}$] (M+H) *calcd.* 446.2874, *found* 446.2868.



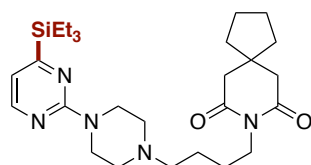
(S)-3-(1-methylpyrrolidin-2-yl)-4-(triethylsilyl)pyridine (57). Following the general procedure, using Nicotine (64.9 mg, 0.4 mmol), the title compound was obtained in 55% yield (60.8 mg) as colorless oil. In this case, 33% of the starting material could be recovered. R_f 0.36 (Methanol: EtOAc 1:4). ^1H NMR (300 MHz, CDCl_3) δ 8.84 (s, 1H), 8.38 (d, $J = 4.9$ Hz, 1H), 7.22 (d, $J = 4.9$ Hz, 1H), 3.33-3.10 (m, 2H), 2.33-2.20 (m, 1H), 2.15 (s, 3H), 2.10-1.50 (m, 4H), 0.96-0.80 (m, 15H) ppm. ^{13}C NMR (75 MHz, CDCl_3) δ 149.2, 146.8, 145.2, 145.1, 129.1, 68.8, 57.0, 40.4, 36.5, 22.9, 7.4, 4.3 ppm. $[\alpha]_D^{26} = -76.9$ ($c = 0.1000$, CH_2Cl_2). IR (neat, cm^{-1}): 2953, 2875, 2776, 1458, 1399, 1001, 720, 674. HRMS (ESI) $[\text{C}_{16}\text{H}_{29}\text{N}_2\text{Si}]$ (M+H) *calcd.* 277.2095, *found* 277.2089.



3,3'-(5'-(3-(4-(triethylsilyl)pyridin-3-yl)phenyl)-[1,1':3',1''-terphenyl]-3,3''-diyl)bis(4-(triethylsilyl)pyridine) (58). Following the general procedure, using TmPyPB (215.0 mg, 0.4 mmol), 3.0 eq. of KHMDS and 3.0 eq. of Et_3SiBpin in this case, and the title compound was obtained in 45% yield (158.4 mg) as colorless oil. R_f 0.28 (EtOAc). ^1H NMR (300 MHz, CDCl_3) δ 8.56 (d, $J = 4.9$ Hz, 3H), 8.51 (s, 1H), 7.87 (s, 3H), 7.77 (dt, $J = 7.9, 1.4$ Hz, 3H), 7.62 (t, $J = 1.8$ Hz, 3H), 7.53 (t, $J = 7.7$ Hz, 3H), 7.46 (dd, $J = 4.9, 0.8$ Hz, 3H), 7.31 (dt, $J = 7.6, 1.4$ Hz, 3H), 0.80 (t, $J = 7.8$ Hz, 27H), 0.54 (q, $J = 8.5, 7.9$ Hz, 18H) ppm. ^{13}C NMR (75 MHz, CDCl_3) δ 149.1, 146.9, 146.1, 144.4, 142.1, 141.4, 140.5, 130.1, 128.8, 128.3, 126.9, 125.2, 7.4, 3.9 ppm. IR (neat, cm^{-1}): 2953, 2874, 1594, 1463, 1379, 1238, 1102, 1003. HRMS (ESI) $[\text{C}_{57}\text{H}_{70}\text{N}_3\text{Si}_3]$ (M+H) *calcd.* 880.4872, *found* 880.4847.



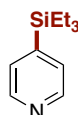
2-(4-(benzo[d][1,3]dioxol-5-ylmethyl)piperazin-1-yl)-4-(triethylsilyl)pyrimidine (59). Following the general procedure, using Piribedil (119.3 mg, 0.4 mmol), the title compound was obtained in 79% yield (130.2 mg) as colorless oil. R_f 0.54 (Hex: EtOAc 1:1). ^1H NMR (300 MHz, CDCl_3) δ 8.18 (d, $J = 4.7$ Hz, 1H), 6.90 (s, 1H), 6.80-6.72 (m, 2H), 6.62 (d, $J = 4.7$ Hz, 1H), 5.95 (s, 2H), 4.02-3.76 (m, 4H), 3.46 (s, 2H), 2.70-2.35 (m, 4H), 0.98 (t, $J = 7.8$ Hz, 9H), 0.86-0.69 (m, 6H) ppm. ^{13}C NMR (75 MHz, CDCl_3) δ 176.9, 161.0, 155.2, 147.8, 146.8, 132.1, 122.4, 116.3, 109.7, 108.0, 101.0, 63.1, 53.0, 43.8, 7.5, 2.8 ppm. IR (neat, cm^{-1}): 2943, 2845, 1730, 1557, 1530, 1438, 1130, 722. HRMS (ESI) $[\text{C}_{22}\text{H}_{33}\text{N}_4\text{O}_2\text{Si}]$ (M+H) *calcd.* 413.2367, *found* 413.2369.



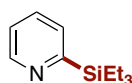
8-(4-(4-(4-(triethylsilyl)pyrimidin-2-yl)piperazin-1-yl)butyl)-8-azaspiro[4.5]decane-7,9-dione (60).

Following the general procedure, using Buspirone (154.2 mg, 0.4 mmol), the title compound was obtained in 64% yield (127.5 mg) as colorless oil. In this case, 29% of the starting material could be recovered. R_f 0.42 (EtOAc). ^1H NMR (400 MHz, CDCl_3) δ 8.17 (d, $J = 4.7$ Hz, 1H), 6.63 (d, $J = 4.7$ Hz, 1H), 3.86 (t, $J = 5.6$ Hz, 4H), 3.77 (t, $J = 6.9$ Hz, 2H), 2.57 (s, 4H), 2.54 (t, $J = 5.1$ Hz, 4H), 2.46-2.42 (m, 2H), 1.74-1.66 (m, 4H), 1.56-1.54 (m, 4H), 1.48 (t, $J = 7.1$ Hz, 4H), 0.97 (t, $J = 7.8$ Hz, 9H), 0.77 (q, $J = 8.3$ Hz, 6H) ppm. ^{13}C NMR (101 MHz, CDCl_3) δ 177.0, 172.4, 160.9, 155.2, 116.5, 58.3, 53.1, 45.0, 43.4, 39.6, 39.3, 37.7, 26.1, 24.3, 23.9, 7.5, 2.8 ppm. IR (neat, cm^{-1}): 3450, 2949, 2875, 1665, 1556, 1438, 1359, 1133. HRMS (ESI) [$\text{C}_{27}\text{H}_{46}\text{N}_5\text{O}_2\text{Si}$] (M+H) *calcd.* 500.3415, *found* 500.3419.

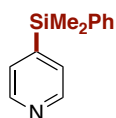
General procedure for regiodivergent silylation conditions: An oven-dried 10 mL screw-capped test tube containing a stirring bar was charged with pyridine derivative (0.4 mmol). The test tube was transferred to a nitrogen-filled glove-box where the KHMDS (79.8 mg, 0.4 mmol), Et_3SiBpin (96.9 mg, 0.4 mmol) and dry solvent (0.2 M, 2mL) were added. Then the reaction mixture was stirred for 1 minute and taken out of the glovebox. The reaction was rigorously stirred for 3 h and diluted with EtOAc (8 mL). After filtered through a Celite® plug, the filtrate was evaporated and dried in vacuum. The ratio of regioisomers was detect by crude NMR. Then the desired product was purified by flash chromatography in silica gel.



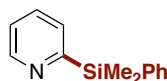
4-(triethylsilyl)pyridine (48a). Following the general procedure, using pyridine (31.6 mg, 0.4 mmol), 2 mL DME as solvent, the title compound was obtained in 67% yield (51.8 mg) as colorless oil. R_f 0.50 (Hex: EtOAc 10:1). ^1H NMR (300 MHz, CDCl_3) δ 8.53 (d, $J = 5.7$ Hz, 2H), 7.34 (d, $J = 5.7$ Hz, 2H), 0.94 (t, $J = 7.6$ Hz, 9H), 0.84-0.74 (m, 6H) ppm. ^{13}C NMR (75 MHz, CDCl_3) δ 148.7, 147.8, 129.2, 7.3, 2.9 ppm. IR (neat, cm^{-1}): 2954, 2875, 1583, 1458, 1402, 1120, 718, 672. HRMS (ESI) [$\text{C}_{11}\text{H}_{20}\text{NSi}$] (M+H) *calcd.* 194.1360, *found* 194.1361.



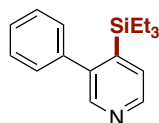
2-(triethylsilyl)pyridine (48a'). Following the general procedure, using pyridine (31.6 mg, 0.4 mmol), 2 mL Dioxane as solvent, the title compound was obtained in 48% yield (37.1 mg) as colorless oil. R_f 0.82 (Hex: EtOAc 10:1). ^1H NMR (300 MHz, CDCl_3) δ 8.75 (d, $J = 4.9$ Hz, 1H), 7.53 (t, $J = 7.6$ Hz, 1H), 7.43 (d, $J = 7.5$ Hz, 1H), 7.16-7.12 (m, 1H), 0.96 (t, $J = 7.5$ Hz, 9H), 0.90-0.80 (m, 6H) ppm. ^{13}C NMR (75 MHz, CDCl_3) δ 166.5, 150.3, 133.7, 129.9, 122.6, 7.5, 3.0 ppm. Spectroscopic data for **48a'** match those previously reported in the literature.³



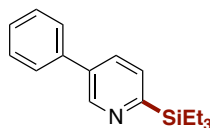
4-(dimethyl(phenyl)silyl)pyridine (48b). Following the general procedure, using pyridine (31.6 mg, 0.4 mmol), PhMe₂SiBpin (104.8 mg, 0.4 mmol), 2 mL DME as solvent, the title compound was obtained in 64% yield (54.6 mg) as colorless oil. ¹H NMR (300 MHz, CDCl₃) δ 8.60-8.51 (m, 2H), 7.54-7.46 (m, 2H), 7.42-7.33 (m, 5H), 0.58 (s, 6H) ppm. R_f 0.56 (Hex: EtOAc 10:1). ¹³C NMR (75 MHz, CDCl₃) δ 148.9, 148.5, 136.3, 134.2, 129.7, 128.9, 128.2, -3.0 ppm. Spectroscopic data for **48b** match those previously reported in the literature.⁴



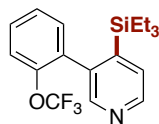
2-(dimethyl(phenyl)silyl)pyridine (48b'). Following the general procedure, using pyridine (31.6 mg, 0.4 mmol), PhMe₂SiBpin (104.8 mg, 0.4 mmol), 2 mL Dioxane as solvent, the title compound was obtained in 46% yield (39.1 mg) as colorless oil. R_f 0.68 (Hex: EtOAc 5:1). ¹H NMR (300 MHz, CDCl₃) δ 8.80 (ddd, *J* = 4.9, 1.7, 1.1 Hz, 1H), 7.63-7.55 (m, 2H), 7.54 (dd, *J* = 7.6, 1.8 Hz, 1H), 7.44 (dt, *J* = 7.6, 1.3 Hz, 1H), 7.40-7.38 (m, 3H), 7.19 (ddd, *J* = 7.6, 4.9, 1.5 Hz, 1H), 0.62 (s, 3H) ppm. ¹³C NMR (75 MHz, CDCl₃) δ 166.6, 150.2, 137.3, 134.4, 130.0, 129.5, 128.1, 128.0, 123.1, -3.0 ppm. Spectroscopic data for **48b'** match those previously reported in the literature.⁵



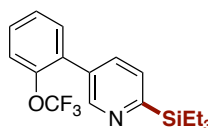
3-phenyl-4-(triethylsilyl)pyridine (48c). Following the general procedure, using 3-phenylpyridine (62.1 mg, 0.4 mmol), 2 mL DME as solvent, the title compound was obtained in 76% yield (81.5 mg) as colorless oil. R_f 0.81 (Hex: EtOAc 10:1). ¹H NMR (300 MHz, CDCl₃) δ 8.55 (d, *J* = 4.9 Hz, 1H), 8.45 (s, 1H), 7.45-7.40 (m, 4H), 7.29 (dd, *J* = 5.5, 2.0 Hz, 2H), 0.82 (t, *J* = 7.8 Hz, 9H), 0.51 (q, *J* = 8.4, 7.9 Hz, 6H) ppm. ¹³C NMR (75 MHz, CDCl₃) δ 149.6, 147.2, 145.3, 144.6, 141.0, 129.9, 129.5, 128.0, 128.0, 7.4, 3.8 ppm. IR (neat, cm⁻¹): 2953, 2874, 1462, 1442, 1393, 1174, 1097, 1003. HRMS (ESI) [C₁₇H₂₄NSi] (M+H) *calcd.* 270.1673, *found* 270.1681.



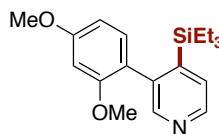
3-phenyl-2-(triethylsilyl)pyridine (48c'). Following the general procedure, using 3-phenylpyridine (62.1 mg, 0.4 mmol), 2 mL Dioxane as solvent, the title compound was obtained in 46% yield (49.4 mg) as colorless oil. R_f 0.62 (Hex: EtOAc 10:1). ¹H NMR (300 MHz, CDCl₃) δ 9.04 (dd, *J* = 2.3, 0.8 Hz, 1H), 7.77 (dd, *J* = 7.8, 2.3 Hz, 1H), 7.60 (dd, *J* = 8.3, 1.3 Hz, 2H), 7.55 (dd, *J* = 7.8, 0.8 Hz, 1H), 7.48 (t, *J* = 7.3 Hz, 2H), 7.43-7.36 (m, 1H), 1.02 (t, *J* = 7.5 Hz, 9H), 0.96-0.86 (m, 6H) ppm. ¹³C NMR (75 MHz, CDCl₃) δ 165.0, 148.9, 138.4, 135.3, 132.0, 129.9, 129.2, 128.1, 127.2, 7.6, 3.2 ppm. IR (neat, cm⁻¹): 2952, 2874, 1457, 1412, 1237, 1003, 840, 695. HRMS (ESI) [C₁₇H₂₄NSi] (M+H) *calcd.* 270.1673, *found* 270.1674.



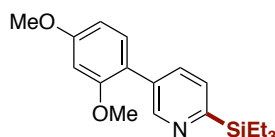
4-(triethylsilyl)-3-(2-(trifluoromethoxy)phenyl)pyridine (48d). Following the general procedure, using 3-(2-(trifluoromethoxy)phenyl)pyridine (95.6 mg, 0.4 mmol), 2 mL DME as solvent, the title compound was obtained in 47% yield (66.2 mg) as colorless oil. R_f 0.53 (Hex: EtOAc 4:1). ^1H NMR (400 MHz, CDCl_3) δ 8.58 (d, $J = 4.9$ Hz, 1H), 8.40 (s, 1H), 7.56-7.42 (m, 2H), 7.40-7.31 (m, 2H), 7.31-7.24 (m, 1H), 0.82 (t, $J = 7.9$ Hz, 9H), 0.58-0.37 (m, 6H) ppm. ^{13}C NMR (75 MHz, CDCl_3) δ 149.9, 147.5, 147.3 (q, $J_{\text{C-F}} = 1.5$ Hz), 146.7, 138.6, 133.6, 132.4, 129.9, 129.7, 126.2, 120.4 (q, $J_{\text{C-F}} = 258.3$ Hz), 120.1 (q, $J_{\text{C-F}} = 1.8$ Hz), 7.2, 3.2 ppm. ^{19}F NMR (376 MHz, CDCl_3) δ -56.93 ppm. IR (neat, cm^{-1}): 2986, 2877, 1248, 1216, 1160, 1094, 1002, 720. HRMS (ESI) [$\text{C}_{18}\text{H}_{23}\text{F}_3\text{NOSi}$] (M+H) *calcd.* 354.1496, *found* 354.1492.



2-(triethylsilyl)-5-(2-(trifluoromethoxy)phenyl)pyridine (48d'). Following the general procedure, using 3-(2-(trifluoromethoxy)phenyl)pyridine (95.6 mg, 0.4 mmol), 2 mL Dioxane as solvent, the title compound was obtained in 50% yield (70.6 mg) as colorless oil. R_f 0.25 (Hex: EtOAc 4:1). ^1H NMR (300 MHz, CDCl_3) δ 8.87 (dd, $J = 2.3, 1.0$ Hz, 1H), 7.70 (dd, $J = 7.8, 2.3$ Hz, 1H), 7.55 (dd, $J = 7.8, 1.0$ Hz, 1H), 7.48-7.35 (m, 4H), 1.05-0.99 (m, 9H), 0.95-0.89 (m, 6H) ppm. ^{13}C NMR (75 MHz, CDCl_3) δ 150.1, 146.6, 134.3, 131.5, 129.6, 129.4, 127.4, 127.3, 121.4 (q, $J_{\text{C-F}} = 1.8$ Hz), 7.5, 3.1 ppm. ^{19}F NMR (376 MHz, CDCl_3) δ -57.22 ppm. IR (neat, cm^{-1}): 1984, 1956, 1731, 1484, 1373, 1234, 1044, 847. HRMS (ESI) [$\text{C}_{18}\text{H}_{23}\text{F}_3\text{NOSi}$] (M+H) *calcd.* 354.1496, *found* 354.1489.



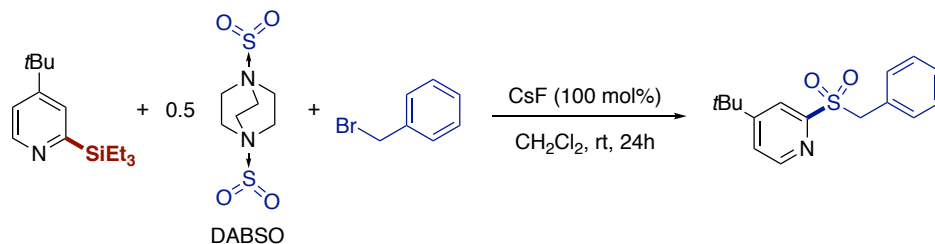
3-(2,4-dimethoxyphenyl)-4-(triethylsilyl)pyridine (48e). Following the general procedure, using 3-(2,4-dimethoxyphenyl)pyridine (86.1 mg, 0.4 mmol), 2 mL DME as solvent, the title compound was obtained in 53% yield (69.8 mg) as colorless oil. R_f 0.72 (Hex: EtOAc 3:1). ^1H NMR (500 MHz, CDCl_3) δ 8.49 (d, $J = 4.9$ Hz, 1H), 8.34 (s, 1H), 7.42 (dd, $J = 4.9, 0.9$ Hz, 1H), 6.99 (d, $J = 8.3$ Hz, 1H), 6.53-6.40 (m, 2H), 3.87 (s, 3H), 3.68 (s, 3H), 0.81 (t, $J = 7.9$ Hz, 9H), 0.50 (q, $J = 7.9$ Hz, 6H) ppm. ^{13}C NMR (75 MHz, CDCl_3) δ 161.1, 158.3, 150.8, 147.0, 146.6, 140.7, 131.9, 129.8, 122.3, 103.5, 98.3, 55.6, 55.1, 7.3, 3.4 ppm. IR (neat, cm^{-1}): 2952, 2874, 1610, 1461, 1393, 1279, 1207, 1158. HRMS (ESI) [$\text{C}_{19}\text{H}_{28}\text{NO}_2\text{Si}$] (M+H) *calcd.* 330.1884, *found* 330.1872.



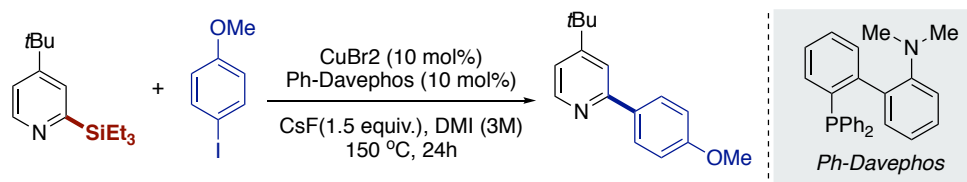
5-(2,4-dimethoxyphenyl)-2-(triethylsilyl)pyridine (48e'). Following the general procedure, using 3-(2,4-dimethoxyphenyl)pyridine (86.1 mg, 0.4 mmol), 2 mL Dioxane as solvent, the title compound was obtained in 38% yield (50.1 mg) as colorless oil. R_f 0.48 (Hex: EtOAc 3:1). ^1H NMR (300 MHz, CDCl_3) δ

8.94 (d, $J = 1.4$ Hz, 1H), 7.73 (dd, $J = 7.8, 2.2$ Hz, 1H), 7.49 (dd, $J = 7.8, 1.0$ Hz, 1H), 7.26 (dd, $J = 8.0, 0.6$ Hz, 1H), 6.61-6.50 (m, 2H), 3.85 (s, 3H), 3.81 (s, 3H), 1.02 (t, $J = 7.5$ Hz, 9H), 0.95-0.83 (m, 6H) ppm. ^{13}C NMR (75 MHz, CDCl_3) δ 163.5, 161.0, 157.8, 150.7, 134.2, 132.8, 131.2, 129.3, 120.3, 105.0, 99.1, 55.6, 55.5, 7.6, 3.2 ppm. IR (neat, cm^{-1}): 2952, 2874, 1610, 1580, 1457, 1301, 1208, 1160, 1032. HRMS (ESI) [$\text{C}_{19}\text{H}_{28}\text{NO}_2\text{Si}$] (M+H) *calcd.* 330.1884, *found* 330.1882.

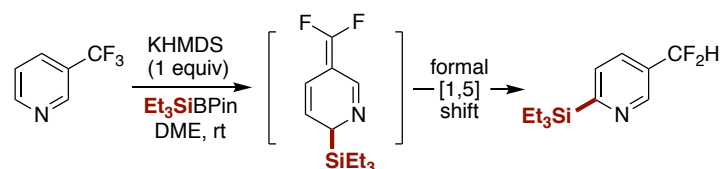
3.8.4. Synthetic application profile



2-sulfonylbenzyl pyridine-4-tertbutyl (68). A general procedure for synthesis pyridylsulfones from SO_2 and 4-(tert-butyl)-2-(triethylsilyl)pyridine.⁸ A mixture of 4-(tert-butyl)-2-(triethylsilyl)pyridine **50p** (74.7 mg, 0.3 mmol), DABSO (36 mg, 0.15 mmol), CsF (45.3 mg, 0.3 mmol) and benzyl bromide (36 μL , 0.3 mmol) in dichloromethane (0.6 mL) was stirred 24 h at room temperature. The reaction mixture was then quenched with 15 mL H_2O . The aqueous phase was extracted with Et_2O (3 x 10 mL) and the combined organic phases were dried under reduced pressure. The concentrated residue was purified by column chromatography over silica gel to afford **2-(benzylsulfonyl)-4-(tert-butyl)pyridine (68)** as a yellow oil in 80% yield (69.1 mg). R_f 0.53 (Hex: EtOAc 2:1). ^1H NMR (300 MHz, CDCl_3) δ 8.69 (d, $J = 5.1$ Hz, 1H), 7.71 (dd, $J = 1.9, 0.7$ Hz, 1H), 7.47 (dd, $J = 5.1, 1.9$ Hz, 1H), 7.28-7.20 (m, 3H), 7.18-7.14 (m, 2H), 4.60 (s, 2H), 1.23 (s, 9H) ppm. ^{13}C NMR (75 MHz, CDCl_3) δ 163.0, 156.2, 150.3, 131.1, 129.1, 128.8, 128.7, 127.8, 124.4, 120.8, 58.8, 35.5, 30.4 ppm. HRMS (ESI) [$\text{C}_{16}\text{H}_{19}\text{NO}_2\text{SiNa}$] (M+Na) *calcd.* 312.1029, *found* 312.1035.

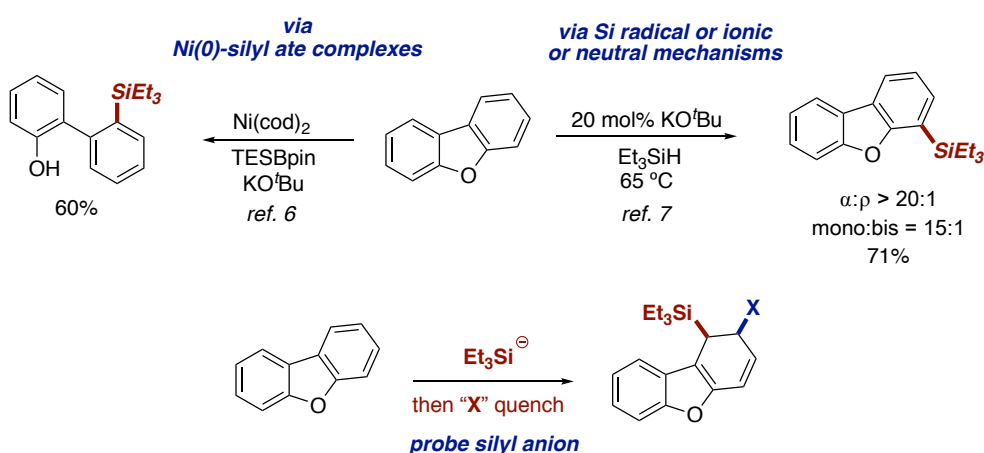


4-(tert-butyl)-2-(4-methoxyphenyl)pyridine (69). A general procedure for Copper(II) catalyzed cross-coupling of 4-(tert-butyl)-2-(triethylsilyl)pyridine with 1-iodo-4-methoxybenzene.³ In a glove box, **50p** (74.7 mg, 0.3 mmol) was added to a solution of CuBr_2 (6.7 mg, 30 μmol), Ph-Davephos (11.5 mg, 30 μmol), CsF (68 mg, 0.45 mmol), and Et_3SiBpin (105.3 mg, 0.45 mmol) in DMI (0.1 mL) prepared in a 4.0 mL Schlenk tube. The resultant mixture was heated at 150 $^\circ\text{C}$ for 24 h. Then the resulting suspension was allowed to reach room temperature and was diluted with dichloromethane. After filtrated with glass filter, the filtrate was evaporated and dried in vacuum. The residue was purified by flash chromatography in silica gel to afford the desired product **69** as a pale yellow oil in 78% yield (56.3 mg). R_f 0.36 (Hex: EtOAc 5:1). ^1H NMR (300 MHz, CDCl_3) δ 8.56 (d, $J = 5.3$ Hz, 1H), 7.95 (d, $J = 8.8$ Hz, 2H), 7.66 (d, $J = 1.5$ Hz, 1H), 7.21 (dd, $J = 5.3, 1.8$ Hz, 1H), 7.00 (d, $J = 8.9$ Hz, 2H), 3.86 (s, 3H), 1.36 (s, 9H) ppm. ^{13}C NMR (75 MHz, CDCl_3) δ 161.5, 160.6, 156.9, 149.0, 132.1, 128.5, 119.0, 117.3, 114.3, 55.5, 35.1, 30.7 ppm. Spectroscopic data for **69** match those previously reported in the literature.³

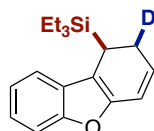


5-(difluoromethyl)-2-(triethylsilyl)pyridine (71). Following the general procedure, using 3-trifluoromethyl pyridene (58.8 mg, 0.4 mmol), the title compound was obtained in 47% yield (45.7 mg) as colorless oil. R_f 0.46 (Hex: EtOAc 10:1). ^1H NMR (500 MHz CDCl_3) δ 8.89 (s, 1H), 7.72 (dd, $J = 7.5, 2.2$ Hz, 1H), 7.57 (d, $J = 7.8$ Hz, 1H), 6.68 (t, $J_{\text{H-F}} = 55.9$ Hz, 1H), 0.98 (t, $J = 7.7$ Hz, 13H), 0.88 (q, $J = 7.0$ Hz, 8H) ppm. ^{13}C NMR (101 MHz, CDCl_3) δ 170.4, 147.3 (t, $J_{\text{C-F}} = 6.6$ Hz), 130.9 (t, $J_{\text{C-F}} = 5.5$ Hz), 129.6, 128.8 (t, $J_{\text{C-F}} = 22.9$ Hz), 113.9 (t, $J_{\text{C-F}} = 239.2$ Hz), 7.4, 3.0 ppm. ^{19}F NMR (376 MHz, CDCl_3) δ -112.51 ppm. IR (neat, cm^{-1}): 2955, 2912, 2876, 1349, 1235, 1076, 1020, 719. HRMS (ESI) $[\text{C}_{12}\text{H}_{20}\text{F}_2\text{NSi}]$ (M+H) *calcd.* 244.1328, *found* 244.1319.

3.8.5 Orthogonal strategies and intermediacy of silyl anion species

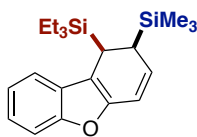


General procedure: An oven-dried 10 mL screw-capped test tube containing a stirring bar was charged with dibenzo[*b,d*]furan (67.2 mg, 0.4 mmol). The test tube was transferred to a nitrogen-filled glovebox where the KHMDS (79.8 mg, 0.4 mmol), Et_3SiBPin (96.9 mg, 0.4 mmol) and DME (0.2 M, 2mL) were added. Then the reaction mixture was stirred for 10 minutes at room temperature, and taken out of the glovebox. The reaction was quenched with D_2O or Me_3SiCl (10 eq). Stirring for another 10 mins, the reaction mixture was diluted with EA (6mL) and filtered through a Celite® plug. The filtrate was evaporated and dried in vacuum. Then the desired product was purified by flash chromatography in silica gel.

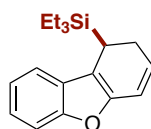


(3,4-dihydrodibenzo[*b,d*]furan-3-yl-4-*d*)triethylsilane (75). Following the general procedure, using D_2O (80.0 mg, 10eq) to quench the reaction, the title compound was obtained in 87% yield (99.3 mg, dr = 3: 2) as colorless oil. R_f 0.80 (Hex: EtOAc 30:1). ^1H NMR (500 MHz, CDCl_3) δ 7.47-7.39 (m, 2H), 7.31-7.14 (m, 2H), 6.00 (ddd, $J = 9.8, 4.4, 2.4$ Hz, 1H), 5.87-5.75 (m, 1H), 3.57-3.37 (m, 1H), 3.22 (t, $J = 5.1$ Hz, 1H),

0.97 (t, $J = 8.0$ Hz, 9H), 0.75-0.60 (m, 6H) ppm. ^{13}C NMR (126 MHz, CDCl_3) δ 154.7, 149.6, 128.2, 127.9, 123.0, 122.0, 120.0, 119.4, 113.03, 111.0, 25.8 ($J = 23.9$ Hz), 25.6 ($J = 20.2$ Hz), 25.4, 7.6, 2.9 ppm. IR (neat, cm^{-1}): 2951, 2909, 1450, 1250, 1127, 1008, 739, 698. HRMS (ESI) [$\text{C}_{18}\text{H}_{23}\text{DOSi}$] (M) *calcd.* 285.1659, *found* 285.1651.

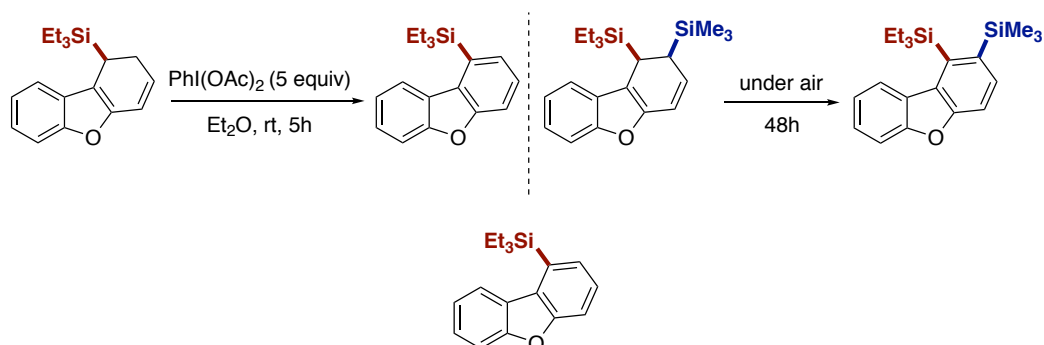


triethyl(2-(trimethylsilyl)-1,2-dihydrodibenzo[*b,d*]furan-1-yl)silane (76). Following the general procedure, using Me_3SiCl (432.0 mg, 10 eq) to quench the reaction, the title compound was obtained in 66% yield (94.1 mg, dr = 3: 2) as colorless oil. R_f 0.85 (Hex: EtOAc 30:1). ^1H NMR (300 MHz, CDCl_3) δ 7.40-7.36 (m, 2H), 7.19-7.15 (m, 2H), 5.82 (ddd, $J = 9.9, 4.2, 2.6$ Hz, 1H), 5.62 (ddd, $J = 9.9, 2.7, 1.4$ Hz, 1H), 3.21 (ddd, $J = 7.0, 4.2, 1.4$ Hz, 1H), 3.07 (dt, $J = 7.0, 2.6$ Hz, 1H), 0.95 (t, $J = 7.9$ Hz, 9H), 0.74-0.50 (m, 6H), 0.12 (s, 9H) ppm. ^{13}C NMR (75 MHz, CDCl_3) δ 154.3, 152.8, 128.2, 126.2, 122.4, 121.8, 121.7, 119.1, 111.3, 110.6, 29.7, 25.0, 7.7, 3.1, -2.3 ppm. IR (neat, cm^{-1}): 2953, 1874, 1450, 1247, 1195, 838, 730, 701. HRMS (ESI) [$\text{C}_{21}\text{H}_{32}\text{OSi}_2$] (M+H) *calcd.* 357.2064, *found* 357.2064.



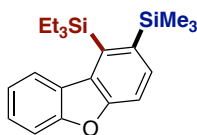
(3,4-dihydrodibenzo[*b,d*]furan-3-yl)triethylsilane (75'). Following the general procedure, using H_2O (72.0 mg, 10 eq) to quench the reaction, the title compound was obtained in 92% yield (104.3 mg) as colorless oil. R_f 0.83 (Hex: EtOAc 30:1). ^1H NMR (300 MHz, CDCl_3) δ 7.52-7.40 (m, 2H), 7.32-7.18 (m, 2H), 6.10-6.95 (m, 1H), 5.88-5.75 (m, 1H), 3.65-3.40 (m, 2H), 3.30-3.18 (m, 1H), 0.98 (t, $J = 7.8$ Hz, 9H), 0.74-0.60 (m, 6H) ppm. ^{13}C NMR (75 MHz, CDCl_3) δ 154.7, 149.6, 128.1, 127.9, 122.0, 120.0, 119.4, 113.0, 111.0, 25.9, 25.3, 7.6, 2.9 ppm. IR (neat, cm^{-1}): 2965, 2883, 1596, 1439, 1235, 786, 748, 714, 654. HRMS (ESI) [$\text{C}_{18}\text{H}_{24}\text{OSi}$] (M) *calcd.* 284.1596, *found* 284.1604.

Rearomatization

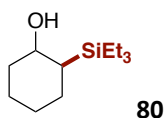


dibenzo[*b,d*]furan-1-yltriethylsilane (77). An oven-dried 10 mL screw-capped test tube containing a stirring bar was charged with **75'** (56.7 mg, 0.2 mmol), $\text{PhI}(\text{OAc})_2$ (5 equiv, 322.1mg), and 2mL Et_2O was added. Then the reaction mixture was stirred for 5 hours at room temperature before diluted with EA (10mL). The mixture was filtered through a Celite® plug, then the filtrate was evaporated and dried in

vacuum. The desired product was purified by flash chromatography in silica gel, and **20** was obtained in 56% (31.5 mg) as colorless oil. R_f 0.78 (Hexanes). ^1H NMR (500 MHz, CDCl_3) δ 8.09 (d, $J = 7.4$ Hz, 1H), 7.60 (t, $J = 7.5$ Hz, 2H), 7.51-7.39 (m, 3H), 7.36 (t, $J = 7.6$ Hz, 1H), 1.09 (t, $J = 7.4$ Hz, 6H), 1.03-0.99 (m, 9H) ppm. ^{13}C NMR (75 MHz, CDCl_3) δ 156.4, 156.0, 132.3, 130.2, 127.3, 126.8, 126.4, 123.2, 122.4, 120.8, 112.7, 111.9, 7.8, 3.5 ppm. IR (neat, cm^{-1}): 2963, 2855, 1560, 1362, 1113, 845, 720, 702, 642. HRMS (ESI) [$\text{C}_{16}\text{H}_{17}\text{OSi}$] (M-Et) *calcd.* 253.1043, *found* 253.1044.



triethyl(2-(trimethylsilyl)dibenzo[*b,d*]furan-1-yl)silane (78). 0.2 mmol (mg) **19** was exposure to the air for 48 hours. Then the desired product was purified by flash chromatography in silica gel. The titled compound was obtained in 70% (99.2 mg) as colorless oil. R_f 0.85 (Hexanes). ^1H NMR (300 MHz, CDCl_3) δ 8.09 (d, $J = 7.9$ Hz, 1H), 7.62 (d, $J = 8.1$ Hz, 1H), 7.56-7.41 (m, 3H), 7.35 (t, $J = 8.1$ Hz, 1H), 1.13-1.08 (m, 6H), 1.05-1.00 (m, 9H), 0.48 (s, 9H) ppm. ^{13}C NMR (75 MHz, CDCl_3) δ 156.2, 133.2, 131.7, 129.8, 126.5, 125.2, 123.8, 123.1, 122.1, 111.9, 7.9, 3.5, -0.9 ppm. IR (neat, cm^{-1}): 2953, 2874, 1450, 1342, 1195, 838, 729, 701, 630. HRMS (APCI) [$\text{C}_{21}\text{H}_{30}\text{OSi}_2$] (M) *calcd.* 354.1830, *found* 354.1827.



R_f 0.68 (Hex: EtOAc 5:1). ^1H NMR (300 MHz CDCl_3) δ 3.52 (td, $J = 10.3, 3.8$ Hz, 1H), 2.01-1.94 (m, 1H), 1.79-1.71 (m, 2H), 1.66-1.60 (m, 1H), 1.31-1.07 (m, 5H), 0.96 (t, $J = 7.9$ Hz, 9H), 0.79-0.70 (m, 1H), 0.61 (q, $J = 7.9$ Hz, 6H) ppm. ^{13}C NMR (75 MHz, CDCl_3) δ 73.3, 38.6, 32.5, 27.4, 27.0, 25.4, 7.9, 3.2 ppm. IR (neat, cm^{-1}): 2873, 1446, 1418, 1236, 1084, 1007, 961, 715. HRMS (APCI) [$\text{C}_{12}\text{H}_{25}\text{OSi}$] (M-H) *calcd.* 213.1669, *found* 213.1669.

3.8.6. ICP-OES trace metal analysis and ring opening reaction with epoxide

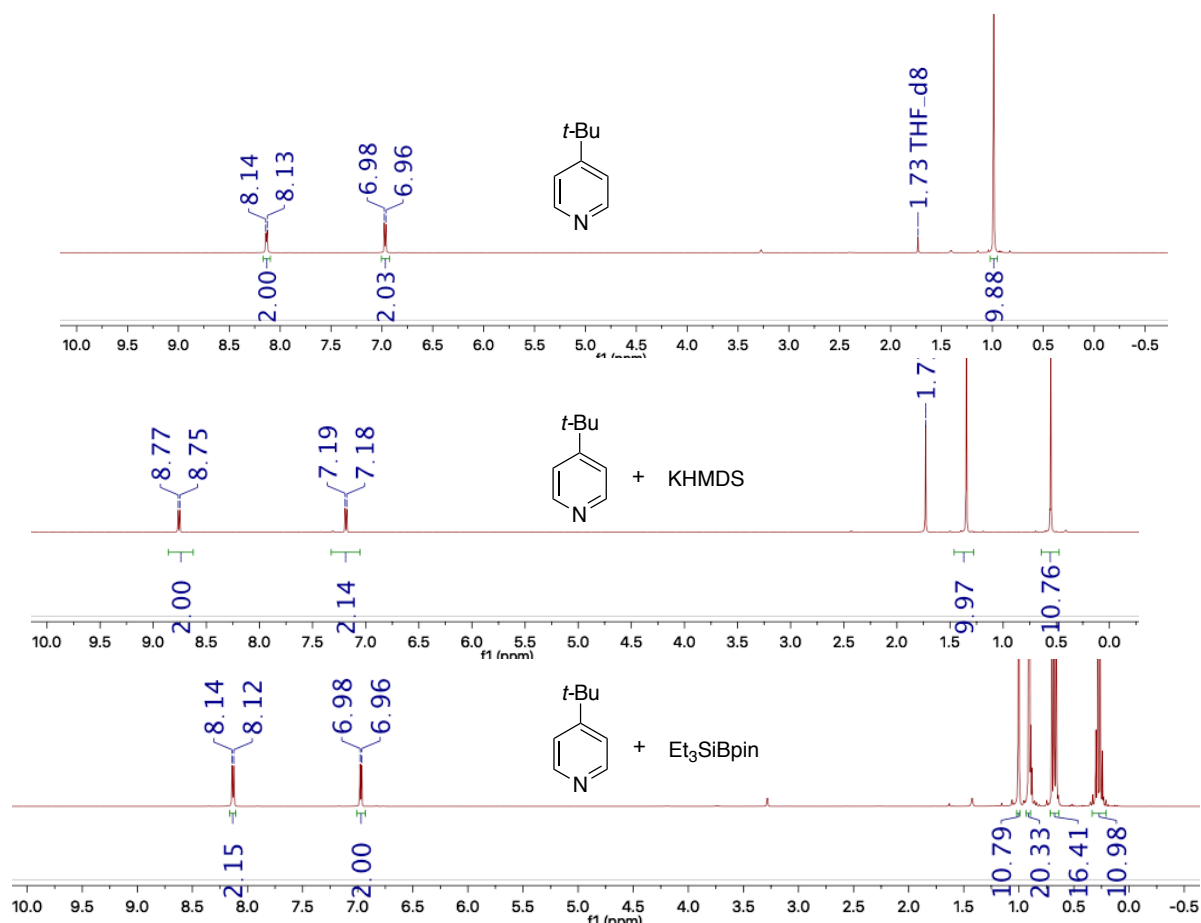
2.0 g KHMDS (from Aldrich), 700 mg Et_3SiBpin , two standard reaction mixtures (0.8 mmol scale, prepared following the general procedure with 63.2 mg of pyridine, 157.6 mg of KHMDS, 193.2 mg of Et_3SiBpin in 4 mL of DME or Dioxane, then stirred in the glovebox for 3 h.) were analyzed. Each sample was added to a 100 mL tefolon reactor followed by addition of 2.0 mL of nitric acid (scharlab, untratrace, ppb-trace analysis grade) and heating to 80 °C for 24 hours. After digestion, each sample was diluted with Milli Q water to 100 mL and sample analysis was performed on Inductively coupled plasma ICP-OES 400 PerkinElmer. Element concentration expressed in mg/l (ppm) on measured sample.



3.8.7. NMR experiments

non-innocent role of the escorting K counterion

In a nitrogen filled glove box, 0.6 mL of d^8 -THF were added to a small vial containing **4p** (13.5 mg, 0.1 mmol) and KHMDS (19.9 mg, 0.1 mmol), and the mixture was stirred at room temperature for 10 mins. Then, the solution was transferred to the NMR tube using a syringe, and analyzed by ^1H NMR. As evident from the spectra below, two new downfield peaks (8.76 and 7.18 ppm) appeared, thus suggesting the establishment of a binding mode between the pyridine and KHMDS.



3.8.8. X-ray crystallography

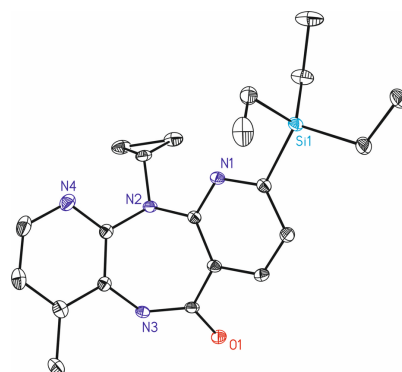


Table 1. Crystal data and structure refinement for compound **52**.

Identification code	YTG323-b	
Empirical formula	C ₂₁ H ₂₈ N ₄ O Si	
Formula weight	380.56	
Temperature	100(2) K	
Wavelength	0.71073 Å	
Crystal system	Triclinic	
Space group	P-1	
Unit cell dimensions	a = 10.3674(15)Å	a = 85.780(4)°.
b = 10.4431(15)Å	b = 85.901(4)°.	
c = 10.6187(15)Å	g = 63.710(4)°.	
Volume	1027.0(3) Å ³	
Z	2	
Density (calculated)	1.231 Mg/m ³	
Absorption coefficient	0.132 mm ⁻¹	
F(000)	408	
Crystal size	0.30 x 0.15 x 0.05 mm ³	
Theta range for data collection	1.925 to 30.564°.	
Index ranges	-14<=h<=13,-14<=k<=14,-15<=l<=10	
Reflections collected	13156	
Independent reflections	5984[R(int) = 0.0305]	

A Mild and Site-Selective sp^2 C-H Silylation of (Poly)Azines

Completeness to theta =30.564°	95.0%
Absorption correction	Multi-scan
Max. and min. transmission	0.993 and 0.861
Refinement method	Full-matrix least-squares on F^2
Data / restraints / parameters	5984/ 0/ 248
Goodness-of-fit on F^2	1.030
Final R indices [$I > 2\sigma(I)$]	R1 = 0.0447, wR2 = 0.1040
R indices (all data)	R1 = 0.0660, wR2 = 0.1140
Largest diff. peak and hole	0.491 and -0.382 e.Å ⁻³

Table 2. Bond lengths [Å] and angles [°] for **10**.

Bond lengths----

Si1-C16	1.8734(16)
Si1-C18	1.8741(17)
Si1-C20	1.8767(16)
Si1-C1	1.8980(13)
O1-C6	1.2349(17)
N1-C2	1.3380(15)
N1-C1	1.3591(17)
N2-C2	1.4189(17)
N2-C8	1.4215(18)
N2-C13	1.4462(17)
N3-C6	1.3495(18)
N3-C7	1.4137(18)
N3-H3	0.8800
N4-C8	1.3283(19)
N4-C9	1.342(2)
C1-C5	1.390(2)
C2-C3	1.4023(19)
C3-C4	1.3869(19)
C3-C6	1.4906(17)
C4-C5	1.3903(18)
C4-H4	0.9500
C5-H5	0.9500
C7-C11	1.400(2)
C7-C8	1.4039(19)
C9-C10	1.376(2)
C9-H9	0.9500
C10-C11	1.392(2)
C10-H10	0.9500
C11-C12	1.503(2)

A Mild and Site-Selective sp^2 C-H Silylation of (Poly)Azines

C12-H12A	0.9800
C12-H12B	0.9800
C12-H12C	0.9800
C13-C15	1.489(2)
C13-C14	1.491(2)
C13-H13	1.0000
C14-C15	1.510(2)
C14-H14A	0.9900
C14-H14B	0.9900
C15-H15A	0.9900
C15-H15B	0.9900
C16-C17	1.526(2)
C16-H16A	0.9900
C16-H16B	0.9900
C17-H17A	0.9800
C17-H17B	0.9800
C17-H17C	0.9800
C18-C19	1.530(2)
C18-H18A	0.9900
C18-H18B	0.9900
C19-H19A	0.9800
C19-H19B	0.9800
C19-H19C	0.9800
C20-C21	1.5387(19)
C20-H20A	0.9900
C20-H20B	0.9900
C21-H21A	0.9800
C21-H21B	0.9800
C21-H21C	0.9800
Angles-----	
C16-Si1-C18	110.82(7)

Chapter 3

C16-Si1-C20	110.46(7)
C18-Si1-C20	113.17(8)
C16-Si1-C1	108.15(6)
C18-Si1-C1	107.52(7)
C20-Si1-C1	106.45(6)
C2-N1-C1	119.10(12)
C2-N2-C8	115.06(11)
C2-N2-C13	114.78(10)
C8-N2-C13	115.23(12)
C6-N3-C7	128.96(11)
C6-N3-H3	115.5
C7-N3-H3	115.5
C8-N4-C9	116.95(13)
N1-C1-C5	121.01(12)
N1-C1-Si1	115.51(10)
C5-C1-Si1	123.47(10)
N1-C2-C3	122.88(12)
N1-C2-N2	116.70(12)
C3-C2-N2	120.36(11)
C4-C3-C2	117.83(11)
C4-C3-C6	117.29(12)
C2-C3-C6	124.69(12)
C3-C4-C5	119.48(13)
C3-C4-H4	120.3
C5-C4-H4	120.3
C1-C5-C4	119.63(13)
C1-C5-H5	120.2
C4-C5-H5	120.2
O1-C6-N3	120.90(12)
O1-C6-C3	119.45(12)
N3-C6-C3	119.62(12)
C11-C7-C8	118.67(13)

A Mild and Site-Selective sp^2 C-H Silylation of (Poly)Azines

C11-C7-N3	118.79(12)
C8-C7-N3	122.42(12)
N4-C8-C7	123.60(13)
N4-C8-N2	116.50(12)
C7-C8-N2	119.90(12)
N4-C9-C10	123.78(15)
N4-C9-H9	118.1
C10-C9-H9	118.1
C9-C10-C11	119.76(14)
C9-C10-H10	120.1
C11-C10-H10	120.1
C10-C11-C7	117.11(14)
C10-C11-C12	121.24(14)
C7-C11-C12	121.65(14)
C11-C12-H12A	109.5
C11-C12-H12B	109.5
H12A-C12-H12B	109.5
C11-C12-H12C	109.5
H12A-C12-H12C	109.5
H12B-C12-H12C	109.5
N2-C13-C15	116.33(13)
N2-C13-C14	117.03(11)
C15-C13-C14	60.87(11)
N2-C13-H13	116.9
C15-C13-H13	116.9
C14-C13-H13	116.9
C13-C14-C15	59.51(10)
C13-C14-H14A	117.8
C15-C14-H14A	117.8
C13-C14-H14B	117.8
C15-C14-H14B	117.8
H14A-C14-H14B	115.0

Chapter 3

C13-C15-C14	59.63(10)
C13-C15-H15A	117.8
C14-C15-H15A	117.8
C13-C15-H15B	117.8
C14-C15-H15B	117.8
H15A-C15-H15B	114.9
C17-C16-Si1	114.79(12)
C17-C16-H16A	108.6
Si1-C16-H16A	108.6
C17-C16-H16B	108.6
Si1-C16-H16B	108.6
H16A-C16-H16B	107.5
C16-C17-H17A	109.5
C16-C17-H17B	109.5
H17A-C17-H17B	109.5
C16-C17-H17C	109.5
H17A-C17-H17C	109.5
H17B-C17-H17C	109.5
C19-C18-Si1	117.04(12)
C19-C18-H18A	108.0
Si1-C18-H18A	108.0
C19-C18-H18B	108.0
Si1-C18-H18B	108.0
H18A-C18-H18B	107.3
C18-C19-H19A	109.5
C18-C19-H19B	109.5
H19A-C19-H19B	109.5
C18-C19-H19C	109.5
H19A-C19-H19C	109.5
H19B-C19-H19C	109.5
C21-C20-Si1	114.62(11)
C21-C20-H20A	108.6

A Mild and Site-Selective sp^2 C-H Silylation of (Poly)Azines

Si1-C20-H20A	108.6
C21-C20-H20B	108.6
Si1-C20-H20B	108.6
H20A-C20-H20B	107.6
C20-C21-H21A	109.5
C20-C21-H21B	109.5
H21A-C21-H21B	109.5
C20-C21-H21C	109.5
H21A-C21-H21C	109.5
H21B-C21-H21C	109.5

Table 3. Torsion angles [°] for **10**.

C2-N1-C1-C5	1.7(2)
C2-N1-C1-Si1	-178.09(10)
C16-Si1-C1-N1	60.33(12)
C18-Si1-C1-N1	-59.39(12)
C20-Si1-C1-N1	179.05(11)
C16-Si1-C1-C5	-119.43(13)
C18-Si1-C1-C5	120.84(13)
C20-Si1-C1-C5	-0.72(15)
C1-N1-C2-C3	-0.7(2)
C1-N1-C2-N2	-178.01(12)
C8-N2-C2-N1	-118.10(13)
C13-N2-C2-N1	19.14(18)
C8-N2-C2-C3	64.54(17)
C13-N2-C2-C3	-158.23(13)
N1-C2-C3-C4	-1.4(2)
N2-C2-C3-C4	175.76(13)
N1-C2-C3-C6	-176.31(13)
N2-C2-C3-C6	0.9(2)
C2-C3-C4-C5	2.6(2)
C6-C3-C4-C5	177.87(14)
N1-C1-C5-C4	-0.5(2)
Si1-C1-C5-C4	179.29(11)
C3-C4-C5-C1	-1.7(2)
C7-N3-C6-O1	173.84(14)
C7-N3-C6-C3	-4.1(2)
C4-C3-C6-O1	-29.6(2)
C2-C3-C6-O1	145.34(15)
C4-C3-C6-N3	148.42(14)
C2-C3-C6-N3	-36.7(2)
C6-N3-C7-C11	-138.95(15)

A Mild and Site-Selective sp^2 C-H Silylation of (Poly)Azines

C6-N3-C7-C8	45.2(2)
C9-N4-C8-C7	1.6(2)
C9-N4-C8-N2	-178.85(13)
C11-C7-C8-N4	-4.0(2)
N3-C7-C8-N4	171.82(13)
C11-C7-C8-N2	176.44(12)
N3-C7-C8-N2	-7.7(2)
C2-N2-C8-N4	120.14(13)
C13-N2-C8-N4	-16.90(17)
C2-N2-C8-C7	-60.31(16)
C13-N2-C8-C7	162.65(12)
C8-N4-C9-C10	1.8(2)
N4-C9-C10-C11	-2.6(2)
C9-C10-C11-C7	0.1(2)
C9-C10-C11-C12	-179.49(14)
C8-C7-C11-C10	3.0(2)
N3-C7-C11-C10	-173.03(12)
C8-C7-C11-C12	-177.43(13)
N3-C7-C11-C12	6.6(2)
C2-N2-C13-C15	76.31(16)
C8-N2-C13-C15	-146.52(12)
C2-N2-C13-C14	145.38(14)
C8-N2-C13-C14	-77.45(17)
N2-C13-C14-C15	-106.60(15)
N2-C13-C15-C14	107.74(13)
C18-Si1-C16-C17	-173.64(11)
C20-Si1-C16-C17	-47.39(12)
C1-Si1-C16-C17	68.74(12)
C16-Si1-C18-C19	42.05(16)
C20-Si1-C18-C19	-82.67(15)
C1-Si1-C18-C19	160.06(14)
C16-Si1-C20-C21	-59.12(13)

C18-Si1-C20-C21	65.80(14)
C1-Si1-C20-C21	-176.31(11)

A Mild and Site-Selective sp^2 C-H Silylation of (Poly)Azines

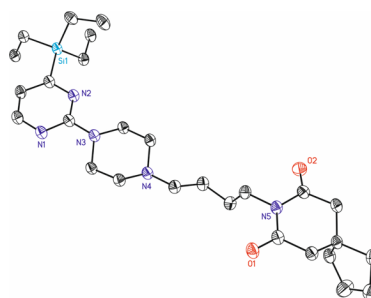


Table 1. Crystal data and structure refinement for **60**.

Identification code	mo_YGU801_0m	
Empirical formula	C ₂₇ H ₄₅ N ₅ O ₂ Si	
Formula weight	499.77	
Temperature	100(2) K	
Wavelength	0.71073 Å	
Crystal system	Triclinic	
Space group	P-1	
Unit cell dimensions	a = 7.1983(7)Å	a = 101.815(3)°.
b = 11.5830(12)Å	b = 94.813(3)°.	
c = 17.2442(18)Å	g = 99.388(3)°.	
Volume	1378.2(2) Å ³	
Z	2	
Density (calculated)	1.204 Mg/m ³	
Absorption coefficient	0.118 mm ⁻¹	
F(000)	544	
Crystal size	0.20 x 0.10 x 0.02 mm ³	
Theta range for data collection	1.828 to 30.686°.	
Index ranges	-8<=h<=10, -14<=k<=16, -23<=l<=24	
Reflections collected	14894	
Independent reflections	7821[R(int) = 0.0575]	
Completeness to theta =30.686°	91.5%	
Absorption correction	Multi-scan	
Max. and min. transmission	0.998 and 0.66	
Refinement method	Full-matrix least-squares on F ²	

Data / restraints / parameters	7821/ 0/ 319
Goodness-of-fit on F^2	1.035
Final R indices [$I > 2\sigma(I)$]	R1 = 0.0640, wR2 = 0.1654
R indices (all data)	R1 = 0.0874, wR2 = 0.1852
Largest diff. peak and hole	0.762 and -0.395 e.Å ⁻³

Table 2. Bond lengths [Å] and angles [°] for **14**.

Bond lengths----

Si1-C24	1.8653(18)
Si1-C22	1.8682(18)
Si1-C26	1.8732(19)
Si1-C1	1.8924(17)
O1-C13	1.216(2)
O2-C17	1.210(2)
N1-C3	1.324(2)
N1-C4	1.354(2)
N2-C1	1.349(2)
N2-C4	1.353(2)
N3-C4	1.372(2)
N3-C5	1.465(2)
N3-C8	1.470(2)
N4-C7	1.460(2)
N4-C6	1.466(2)
N4-C9	1.468(2)
N5-C13	1.390(2)
N5-C17	1.407(2)
N5-C12	1.473(2)
C1-C2	1.387(2)
C2-C3	1.390(2)
C2-H2	0.9500
C3-H3	0.9500
C5-C6	1.514(2)
C5-H5A	0.9900
C5-H5AB	0.9900
C6-H6A	0.9900
C6-H6AB	0.9900
C7-C8	1.520(2)

Chapter 3

C7-H7A	0.9900
C7-H7AB	0.9900
C8-H8A	0.9900
C8-H8AB	0.9900
C9-C10	1.523(2)
C9-H9A	0.9900
C9-H9AB	0.9900
C10-C11	1.529(2)
C10-H10A	0.9900
C10-H10B	0.9900
C11-C12	1.522(2)
C11-H11A	0.9900
C11-H11B	0.9900
C12-H12A	0.9900
C12-H12B	0.9900
C13-C14	1.507(2)
C14-C15	1.526(2)
C14-H14A	0.9900
C14-H14B	0.9900
C15-C16	1.517(3)
C15-C18	1.538(2)
C15-C21	1.544(2)
C16-C17	1.503(2)
C16-H16A	0.9900
C16-H16B	0.9900
C18-C19	1.522(3)
C18-H18A	0.9900
C18-H18B	0.9900
C19-C20	1.527(3)
C19-H19A	0.9900
C19-H19B	0.9900
C20-C21	1.516(3)

A Mild and Site-Selective sp^2 C-H Silylation of (Poly)Azines

C20-H20A	0.9900
C20-H20B	0.9900
C21-H21A	0.9900
C21-H21B	0.9900
C22-C23	1.537(2)
C22-H22A	0.9900
C22-H22B	0.9900
C23-H23A	0.9800
C23-H23B	0.9800
C23-H23C	0.9800
C24-C25	1.534(2)
C24-H24A	0.9900
C24-H24B	0.9900
C25-H25A	0.9800
C25-H25B	0.9800
C25-H25C	0.9800
C26-C27	1.528(3)
C26-H26A	0.9900
C26-H26B	0.9900
C27-H27A	0.9800
C27-H27B	0.9800
C27-H27C	0.9800

Angles-----

C24-Si1-C22	109.47(8)
C24-Si1-C26	111.33(9)
C22-Si1-C26	109.25(9)
C24-Si1-C1	108.26(8)
C22-Si1-C1	110.00(8)
C26-Si1-C1	108.51(8)
C3-N1-C4	115.83(14)
C1-N2-C4	116.78(14)

Chapter 3

C4-N3-C5	117.97(14)
C4-N3-C8	117.96(13)
C5-N3-C8	113.64(14)
C7-N4-C6	108.15(14)
C7-N4-C9	111.95(13)
C6-N4-C9	110.11(12)
C13-N5-C17	124.08(14)
C13-N5-C12	118.24(14)
C17-N5-C12	117.67(14)
N2-C1-C2	121.17(15)
N2-C1-Si1	115.11(12)
C2-C1-Si1	123.71(13)
C1-C2-C3	117.24(16)
C1-C2-H2	121.4
C3-C2-H2	121.4
N1-C3-C2	123.21(16)
N1-C3-H3	118.4
C2-C3-H3	118.4
N2-C4-N1	125.74(15)
N2-C4-N3	117.44(15)
N1-C4-N3	116.80(14)
N3-C5-C6	110.47(14)
N3-C5-H5A	109.6
C6-C5-H5A	109.6
N3-C5-H5AB	109.6
C6-C5-H5AB	109.6
H5A-C5-H5AB	108.1
N4-C6-C5	111.09(13)
N4-C6-H6A	109.4
C5-C6-H6A	109.4
N4-C6-H6AB	109.4
C5-C6-H6AB	109.4

A Mild and Site-Selective sp^2 C-H Silylation of (Poly)Azines

H6A-C6-H6AB	108.0
N4-C7-C8	111.34(14)
N4-C7-H7A	109.4
C8-C7-H7A	109.4
N4-C7-H7AB	109.4
C8-C7-H7AB	109.4
H7A-C7-H7AB	108.0
N3-C8-C7	110.98(12)
N3-C8-H8A	109.4
C7-C8-H8A	109.4
N3-C8-H8AB	109.4
C7-C8-H8AB	109.4
H8A-C8-H8AB	108.0
N4-C9-C10	112.95(13)
N4-C9-H9A	109.0
C10-C9-H9A	109.0
N4-C9-H9AB	109.0
C10-C9-H9AB	109.0
H9A-C9-H9AB	107.8
C9-C10-C11	113.23(13)
C9-C10-H10A	108.9
C11-C10-H10A	108.9
C9-C10-H10B	108.9
C11-C10-H10B	108.9
H10A-C10-H10B	107.7
C12-C11-C10	112.05(14)
C12-C11-H11A	109.2
C10-C11-H11A	109.2
C12-C11-H11B	109.2
C10-C11-H11B	109.2
H11A-C11-H11B	107.9
N5-C12-C11	112.76(14)

Chapter 3

N5-C12-H12A	109.0
C11-C12-H12A	109.0
N5-C12-H12B	109.0
C11-C12-H12B	109.0
H12A-C12-H12B	107.8
O1-C13-N5	120.45(16)
O1-C13-C14	121.77(16)
N5-C13-C14	117.77(15)
C13-C14-C15	114.96(13)
C13-C14-H14A	108.5
C15-C14-H14A	108.5
C13-C14-H14B	108.5
C15-C14-H14B	108.5
H14A-C14-H14B	107.5
C16-C15-C14	107.46(14)
C16-C15-C18	112.84(14)
C14-C15-C18	111.07(13)
C16-C15-C21	112.33(13)
C14-C15-C21	111.50(14)
C18-C15-C21	101.68(14)
C17-C16-C15	112.87(14)
C17-C16-H16A	109.0
C15-C16-H16A	109.0
C17-C16-H16B	109.0
C15-C16-H16B	109.0
H16A-C16-H16B	107.8
O2-C17-N5	119.98(16)
O2-C17-C16	122.93(16)
N5-C17-C16	117.06(14)
C19-C18-C15	104.54(15)
C19-C18-H18A	110.8
C15-C18-H18A	110.8

A Mild and Site-Selective sp^2 C-H Silylation of (Poly)Azines

C19-C18-H18B	110.8
C15-C18-H18B	110.8
H18A-C18-H18B	108.9
C18-C19-C20	105.43(17)
C18-C19-H19A	110.7
C20-C19-H19A	110.7
C18-C19-H19B	110.7
C20-C19-H19B	110.7
H19A-C19-H19B	108.8
C21-C20-C19	107.14(17)
C21-C20-H20A	110.3
C19-C20-H20A	110.3
C21-C20-H20B	110.3
C19-C20-H20B	110.3
H20A-C20-H20B	108.5
C20-C21-C15	105.77(15)
C20-C21-H21A	110.6
C15-C21-H21A	110.6
C20-C21-H21B	110.6
C15-C21-H21B	110.6
H21A-C21-H21B	108.7
C23-C22-Si1	114.85(13)
C23-C22-H22A	108.6
Si1-C22-H22A	108.6
C23-C22-H22B	108.6
Si1-C22-H22B	108.6
H22A-C22-H22B	107.5
C22-C23-H23A	109.5
C22-C23-H23B	109.5
H23A-C23-H23B	109.5
C22-C23-H23C	109.5
H23A-C23-H23C	109.5

Chapter 3

H23B-C23-H23C	109.5
C25-C24-Si1	112.06(13)
C25-C24-H24A	109.2
Si1-C24-H24A	109.2
C25-C24-H24B	109.2
Si1-C24-H24B	109.2
H24A-C24-H24B	107.9
C24-C25-H25A	109.5
C24-C25-H25B	109.5
H25A-C25-H25B	109.5
C24-C25-H25C	109.5
H25A-C25-H25C	109.5
H25B-C25-H25C	109.5
C27-C26-Si1	115.47(15)
C27-C26-H26A	108.4
Si1-C26-H26A	108.4
C27-C26-H26B	108.4
Si1-C26-H26B	108.4
H26A-C26-H26B	107.5
C26-C27-H27A	109.5
C26-C27-H27B	109.5
H27A-C27-H27B	109.5
C26-C27-H27C	109.5
H27A-C27-H27C	109.5
H27B-C27-H27C	109.5

Table 3. Torsion angles [°] for **14**.

C4-N2-C1-C2	-0.2(2)
C4-N2-C1-Si1	178.90(11)
C24-Si1-C1-N2	51.50(14)
C22-Si1-C1-N2	171.08(11)
C26-Si1-C1-N2	-69.46(14)
C24-Si1-C1-C2	-129.47(15)
C22-Si1-C1-C2	-9.89(17)
C26-Si1-C1-C2	109.57(15)
N2-C1-C2-C3	1.5(2)
Si1-C1-C2-C3	-177.50(12)
C4-N1-C3-C2	0.0(2)
C1-C2-C3-N1	-1.4(3)
C1-N2-C4-N1	-1.4(2)
C1-N2-C4-N3	-179.99(13)
C3-N1-C4-N2	1.5(2)
C3-N1-C4-N3	-179.93(14)
C5-N3-C4-N2	-157.65(14)
C8-N3-C4-N2	-14.9(2)
C5-N3-C4-N1	23.7(2)
C8-N3-C4-N1	166.39(14)
C4-N3-C5-C6	-164.62(13)
C8-N3-C5-C6	51.10(17)
C7-N4-C6-C5	61.68(17)
C9-N4-C6-C5	-175.70(14)
N3-C5-C6-N4	-56.99(19)
C6-N4-C7-C8	-60.48(16)
C9-N4-C7-C8	178.04(12)
C4-N3-C8-C7	165.60(14)
C5-N3-C8-C7	-50.11(18)
N4-C7-C8-N3	54.90(18)

Chapter 3

C7-N4-C9-C10	-66.60(18)
C6-N4-C9-C10	173.05(15)
N4-C9-C10-C11	-168.46(14)
C9-C10-C11-C12	-67.4(2)
C13-N5-C12-C11	-87.65(18)
C17-N5-C12-C11	91.26(18)
C10-C11-C12-N5	-168.81(14)
C17-N5-C13-O1	-178.25(15)
C12-N5-C13-O1	0.6(2)
C17-N5-C13-C14	2.8(2)
C12-N5-C13-C14	-178.33(14)
O1-C13-C14-C15	155.85(16)
N5-C13-C14-C15	-25.3(2)
C13-C14-C15-C16	50.63(18)
C13-C14-C15-C18	174.50(14)
C13-C14-C15-C21	-72.86(19)
C14-C15-C16-C17	-55.96(17)
C18-C15-C16-C17	-178.74(14)
C21-C15-C16-C17	67.02(18)
C13-N5-C17-O2	173.22(16)
C12-N5-C17-O2	-5.6(2)
C13-N5-C17-C16	-8.7(2)
C12-N5-C17-C16	172.44(14)
C15-C16-C17-O2	-145.28(17)
C15-C16-C17-N5	36.7(2)
C16-C15-C18-C19	-159.86(16)
C14-C15-C18-C19	79.40(18)
C21-C15-C18-C19	-39.33(18)
C15-C18-C19-C20	30.2(2)
C18-C19-C20-C21	-8.8(3)
C19-C20-C21-C15	-15.9(2)
C16-C15-C21-C20	154.71(17)

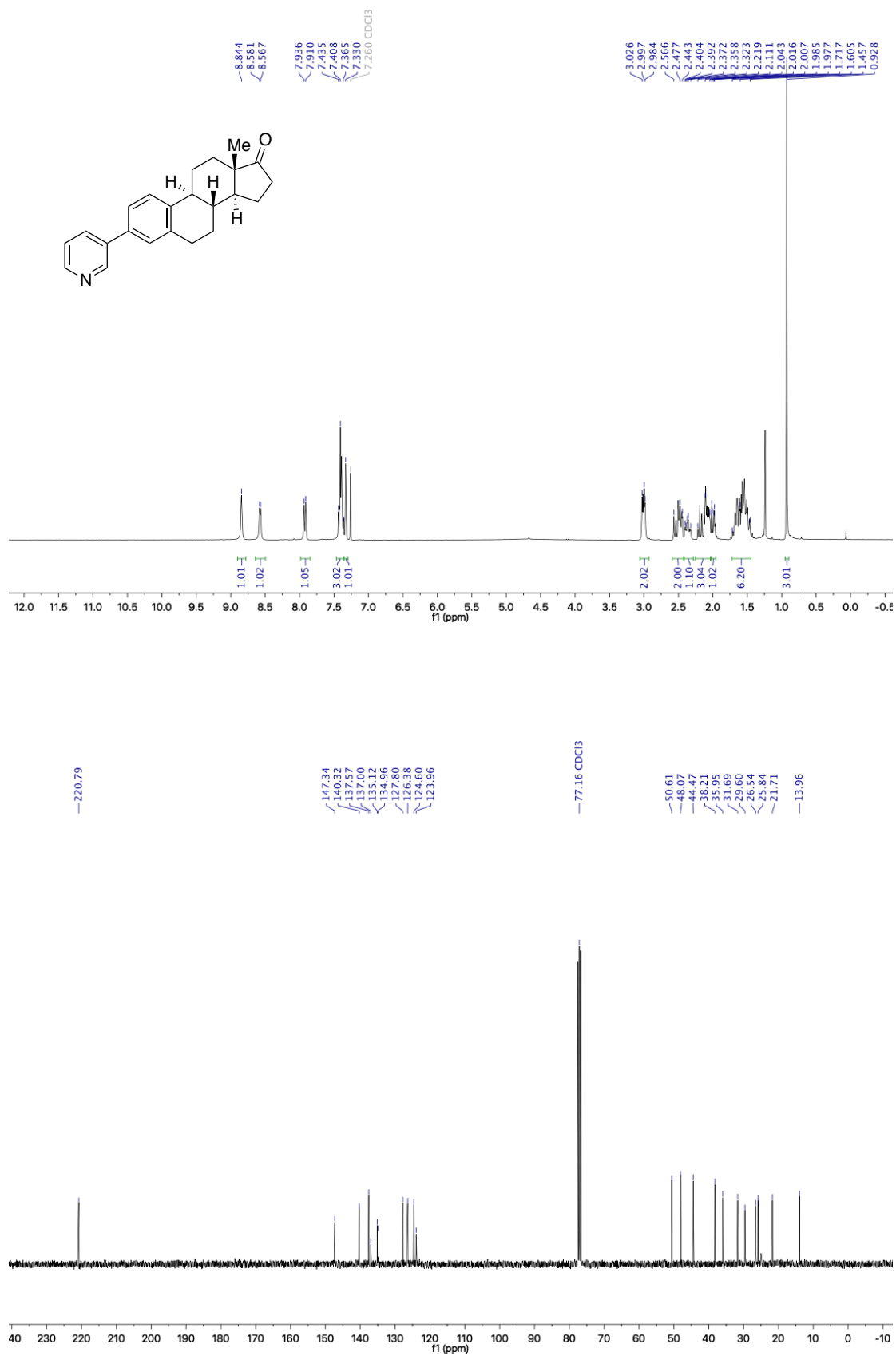
A Mild and Site-Selective sp^2 C-H Silylation of (Poly)Azines

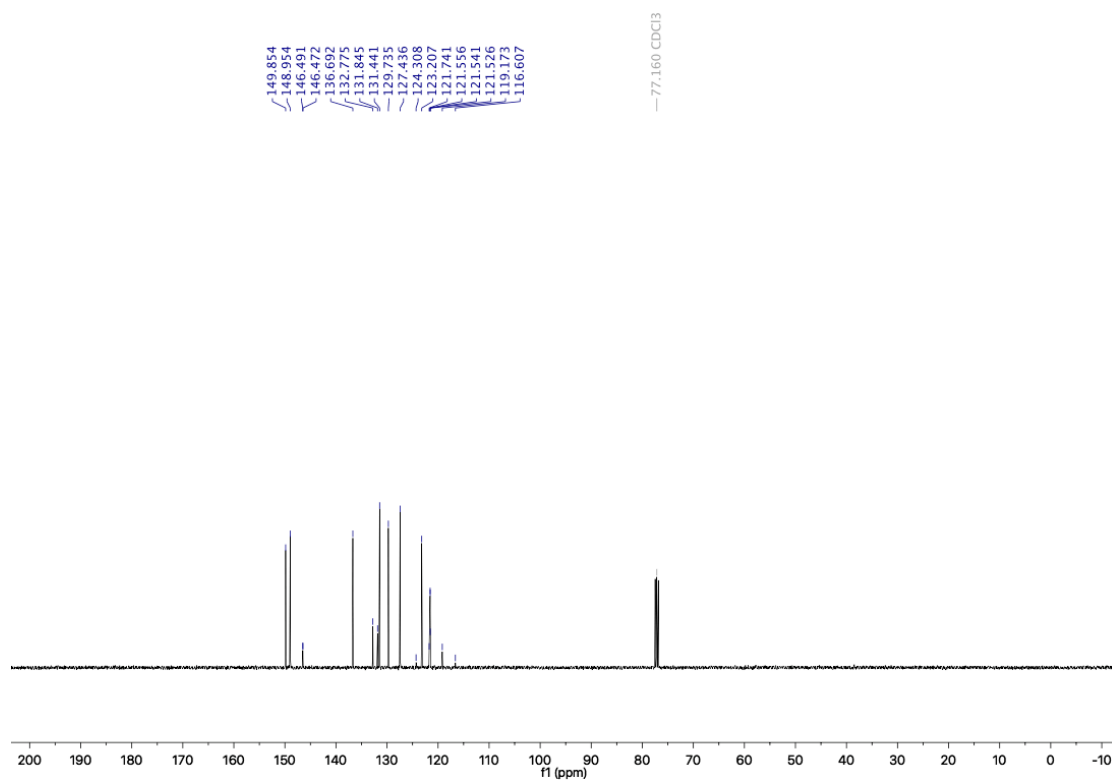
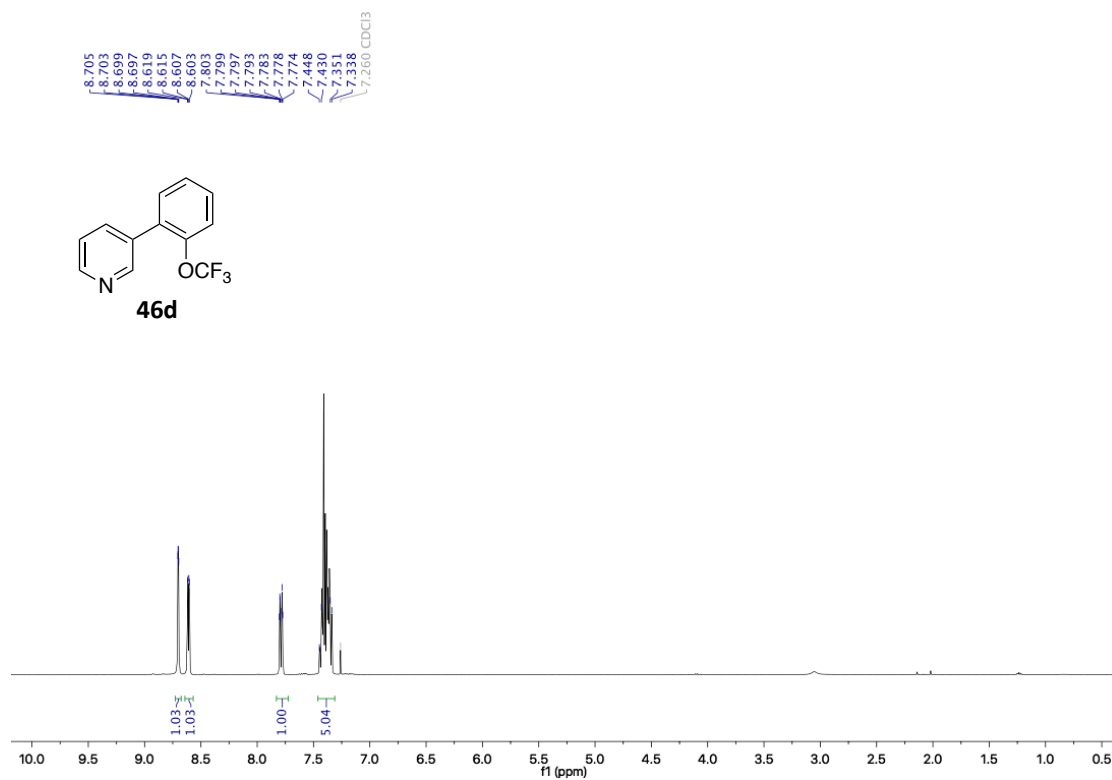
C14-C15-C21-C20	-84.6(2)
C18-C15-C21-C20	33.8(2)
C24-Si1-C22-C23	45.17(15)
C26-Si1-C22-C23	167.32(12)
C1-Si1-C22-C23	-73.67(14)
C22-Si1-C24-C25	60.55(14)
C26-Si1-C24-C25	-60.35(15)
C1-Si1-C24-C25	-179.54(12)
C24-Si1-C26-C27	-46.44(16)
C22-Si1-C26-C27	-167.46(13)
C1-Si1-C26-C27	72.61(16)

3.8.9. Bibliography of known compounds

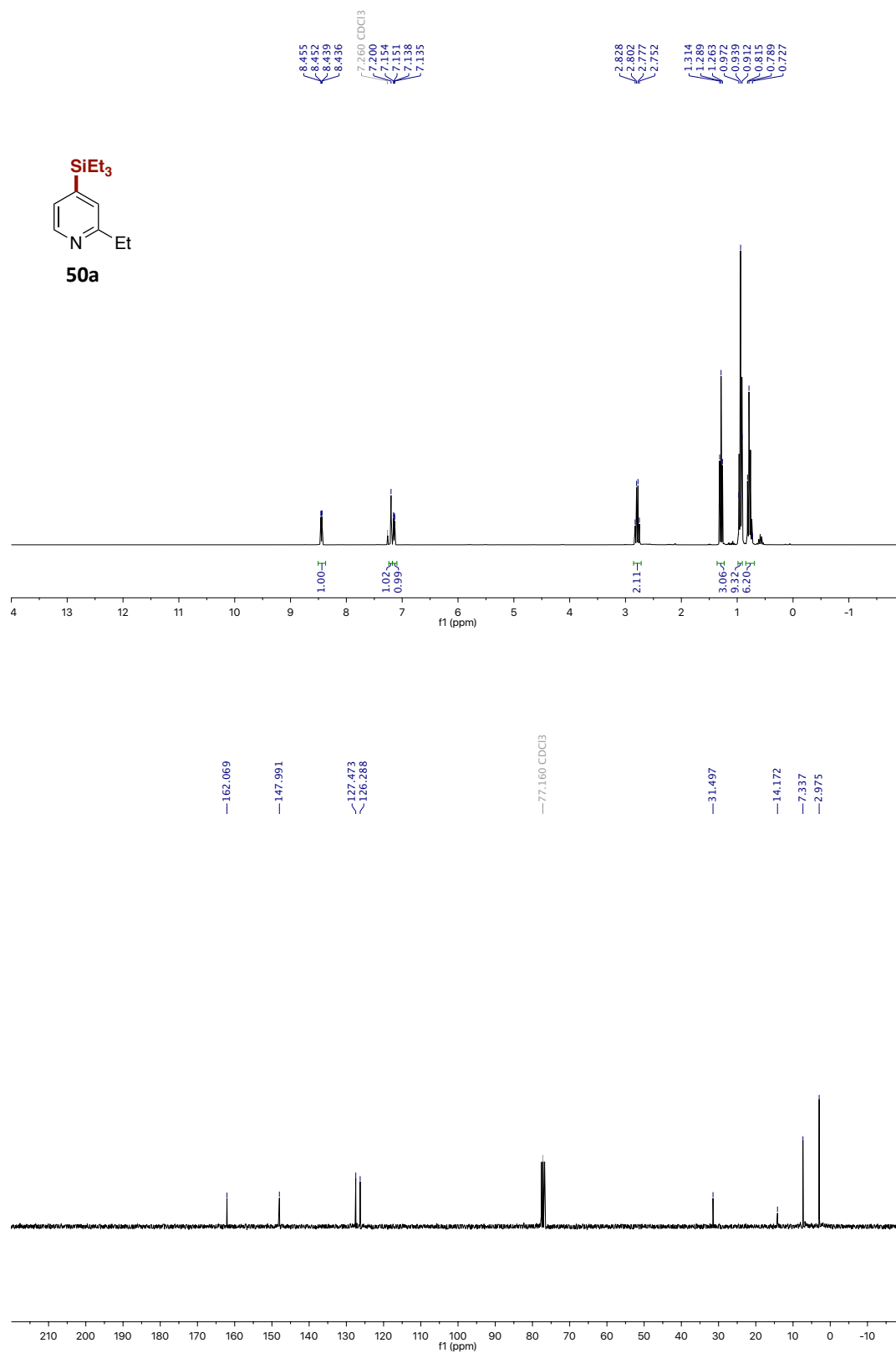
1. Boebel, A. B.; Hartwig, J. F. Iridium-Catalyzed Preparation of Silylboranes by Silane Borylation and Their Use in the Catalytic Borylation of Arenes *Organometallics* **2008**, *27*, 6013.
2. Pu, X.; Hu, J.; Zhao, Y.; Shi, Z. Nickel-Catalyzed Decarbonylative Borylation and Silylation of Esters *ACS Catal.* **2016**, *6*, 6692.
3. Komiyama, T.; Minami, Y.; Hiyama, T. Aryl(triethyl)silanes for Biaryl and Teraryl Synthesis by Copper(II)-Catalyzed Cross-Coupling Reaction. *Angew. Chem. Int. Ed.* **2016**, *55*, 15787.
4. Oshima, K.; Ohmura, T.; Suginome, M. Palladium-Catalyzed Regioselective Silaboration of Pyridines Leading to the Synthesis of Silylated Dihydropyridines. *J. Am. Chem. Soc.* **2011**, *133*, 7324.
5. Chernyak, N.; Dudnik, A. S.; Huang, C.; Gevorgyan, V. PyDipSi: A General and Easily Modifiable/Traceless Si-Tethered Directing Group for C-H Acyloxylation of Arenes. *J. Am. Chem. Soc.* **2010**, *132*, 8270.
6. Zarate, C.; Nakajima, M.; Martin, R. A Mild and Ligand-Free Ni-Catalyzed Silylation via C-OMe Cleavage. *J. Am. Chem. Soc.* **2017**, *139*, 1191.
7. Toutov, A. A.; Liu, W.-B.; Betz, K. N.; Fedorov, A.; Stoltz, B. M.; Grubbs, R. H. Silylation of C-H Bonds in Aromatic Heterocycles by an Earth-Abundant Metal Catalyst. *Nature.* **2015**, *518*, 80.
8. von Wolff, N.; Char, J.; Frogneux, X.; Cantat, T. Synthesis of Aromatic Sulfones from SO₂ and Organosilanes Under Metal-free Conditions. *Angew. Chem. Int. Ed.* **2017**, *56*, 5616.

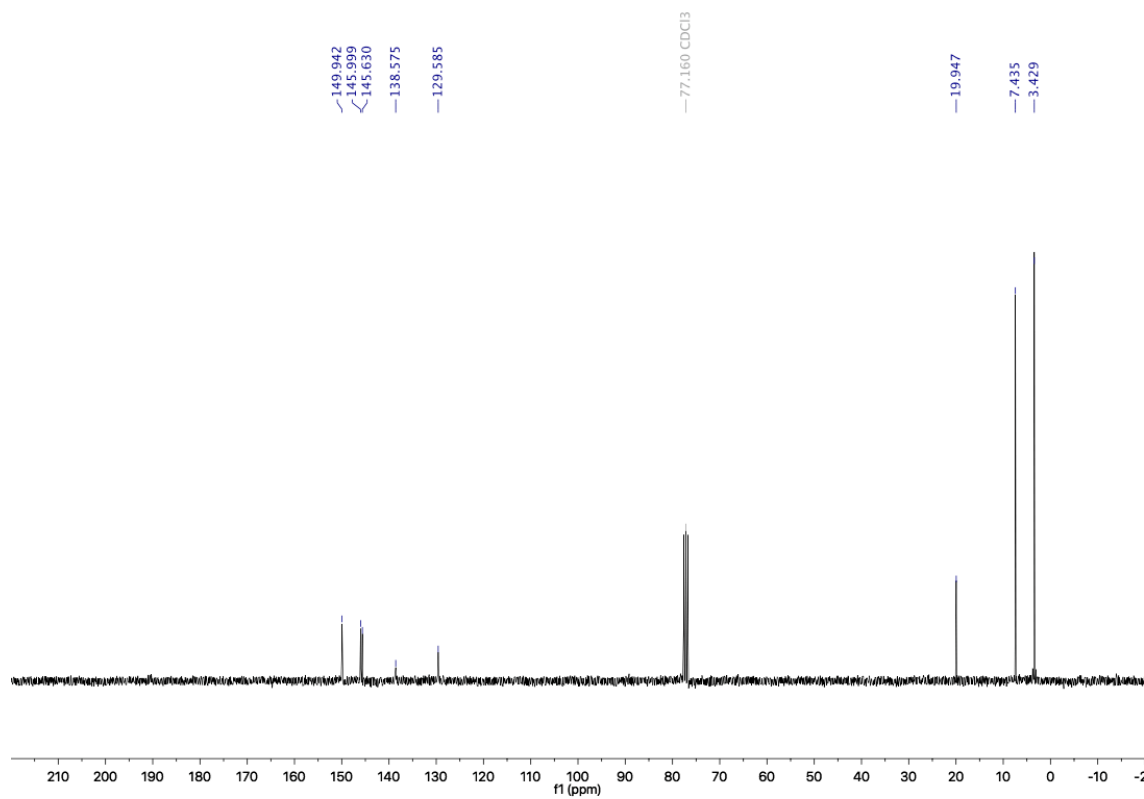
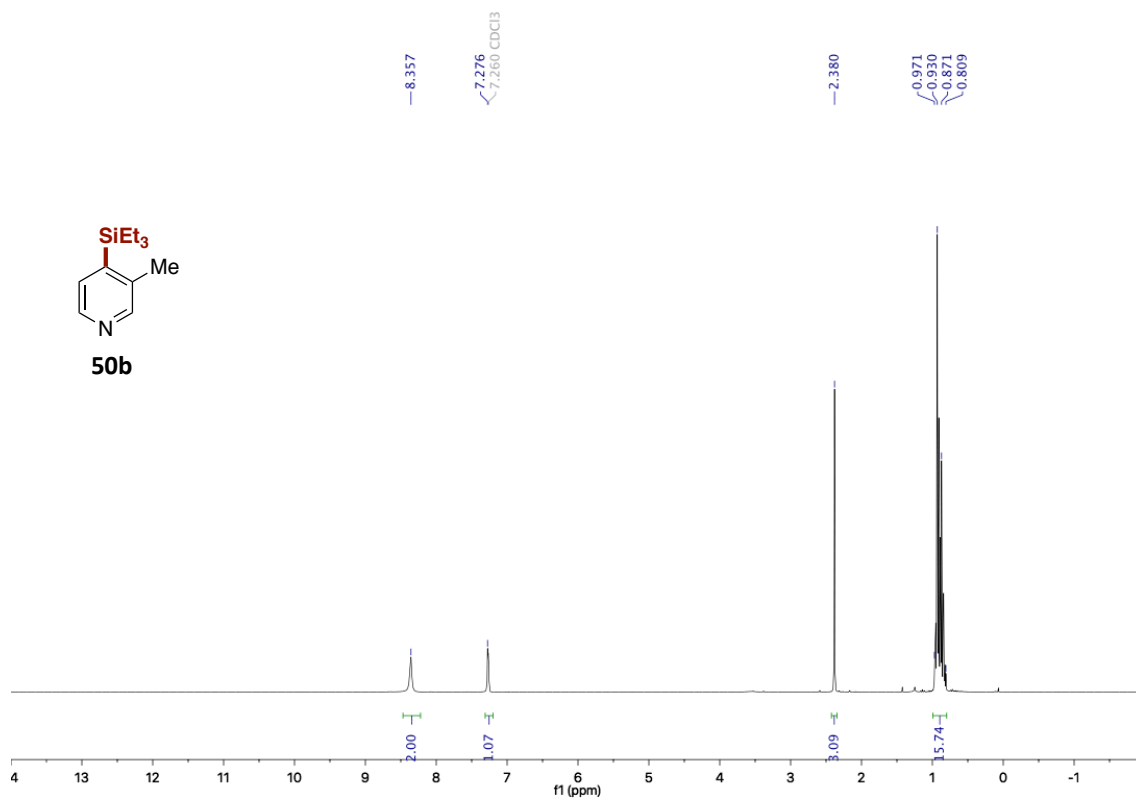
3.8.10. NMR spectra



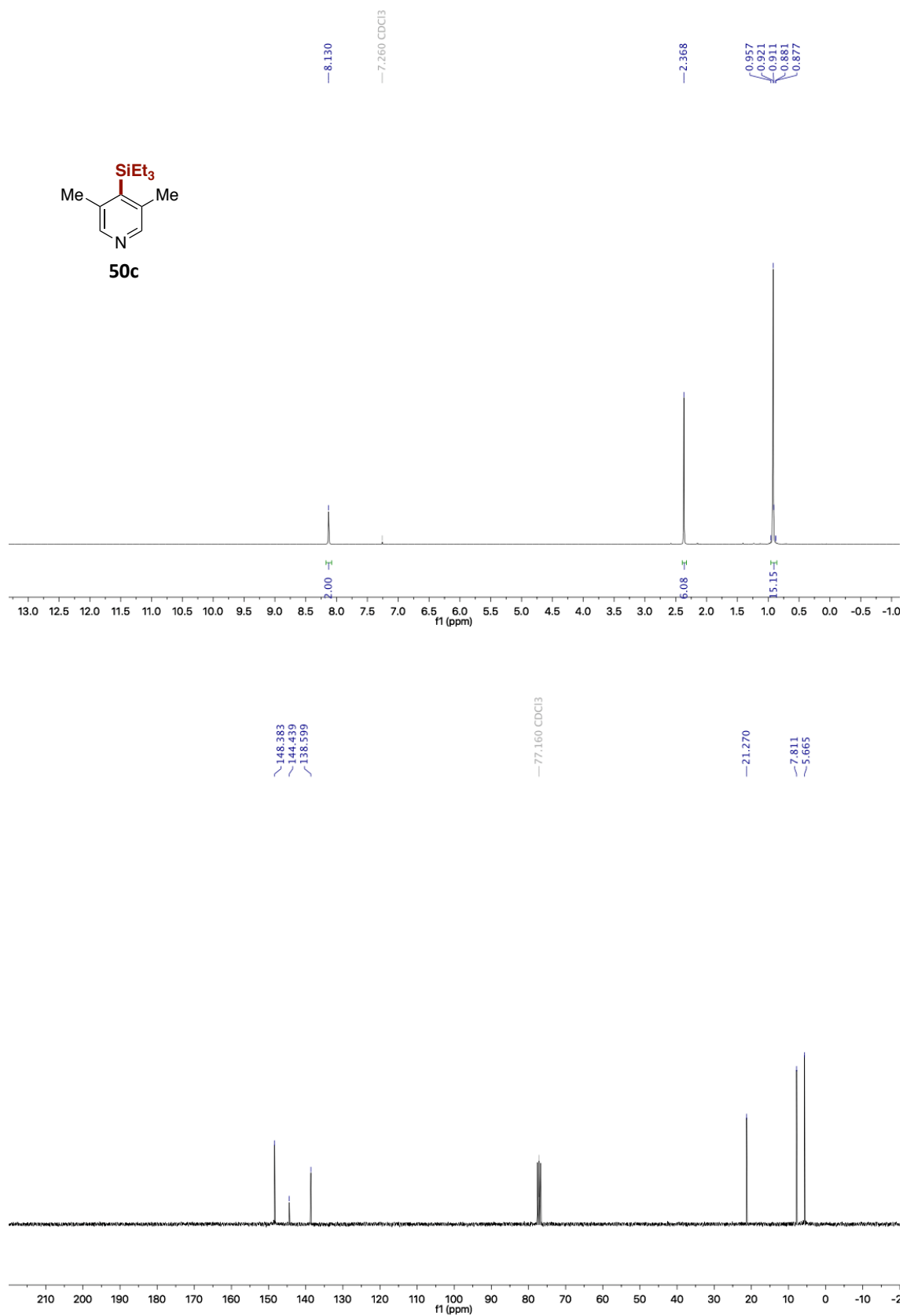


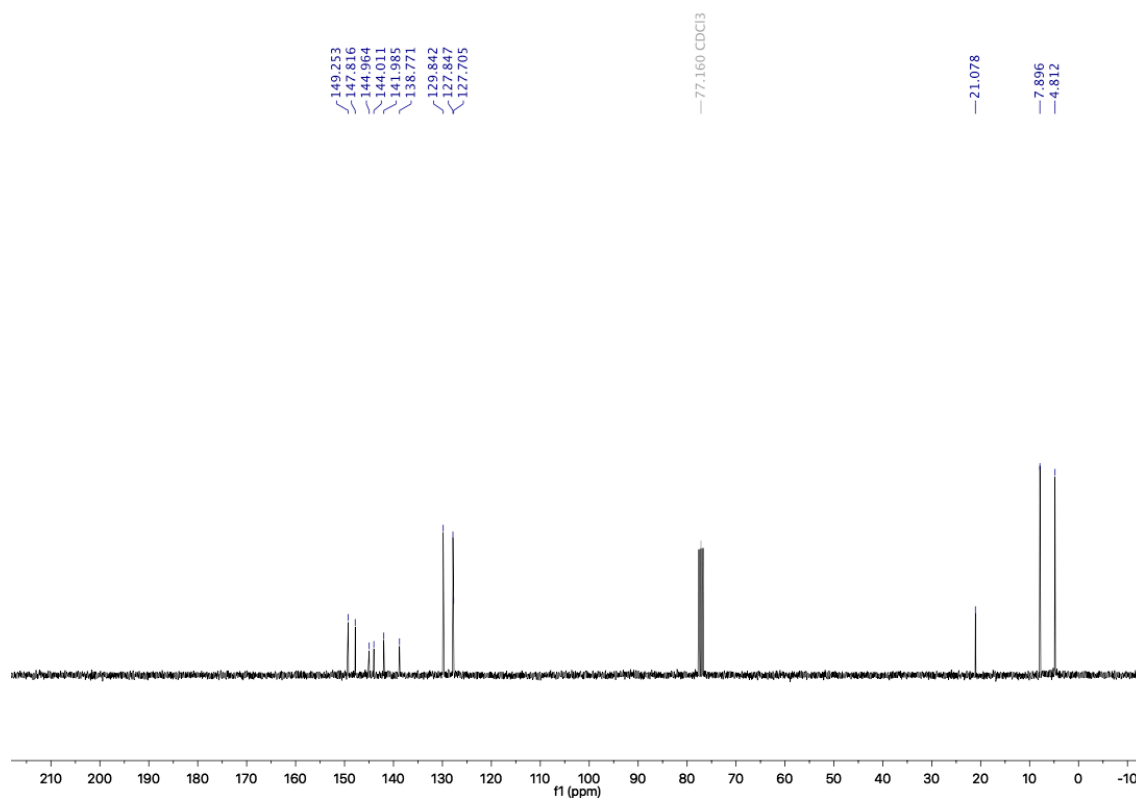
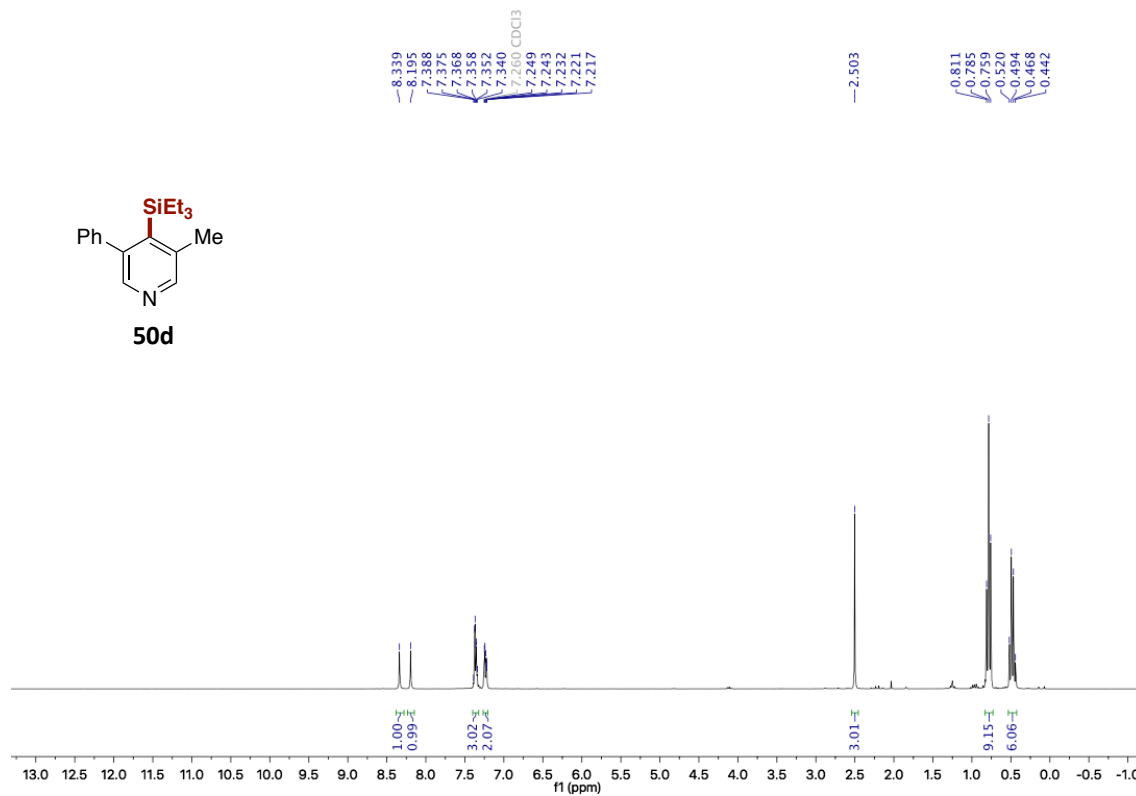
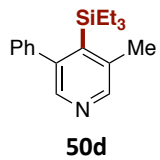
A Mild and Site-Selective sp^2 C-H Silylation of (Poly)Azines



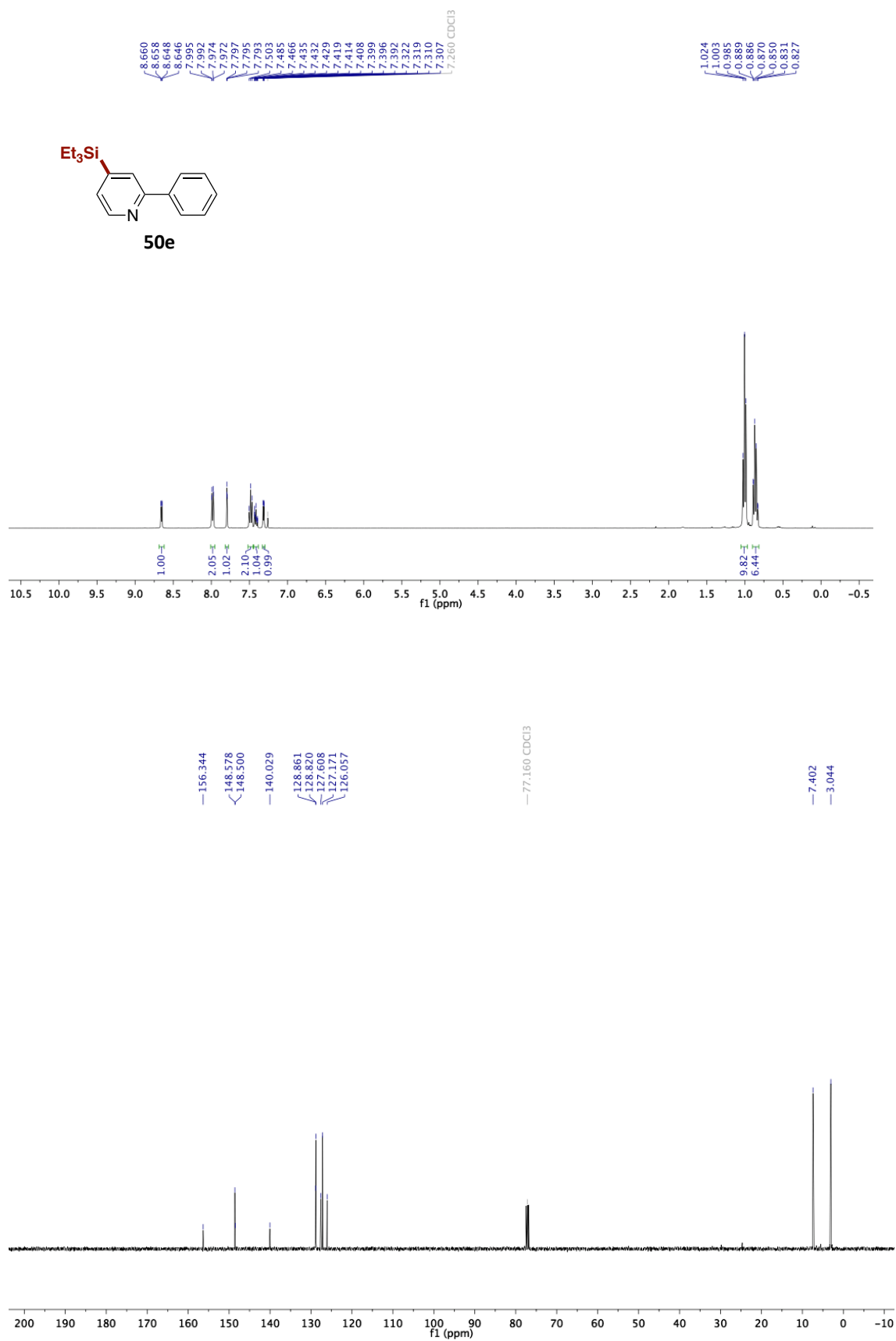


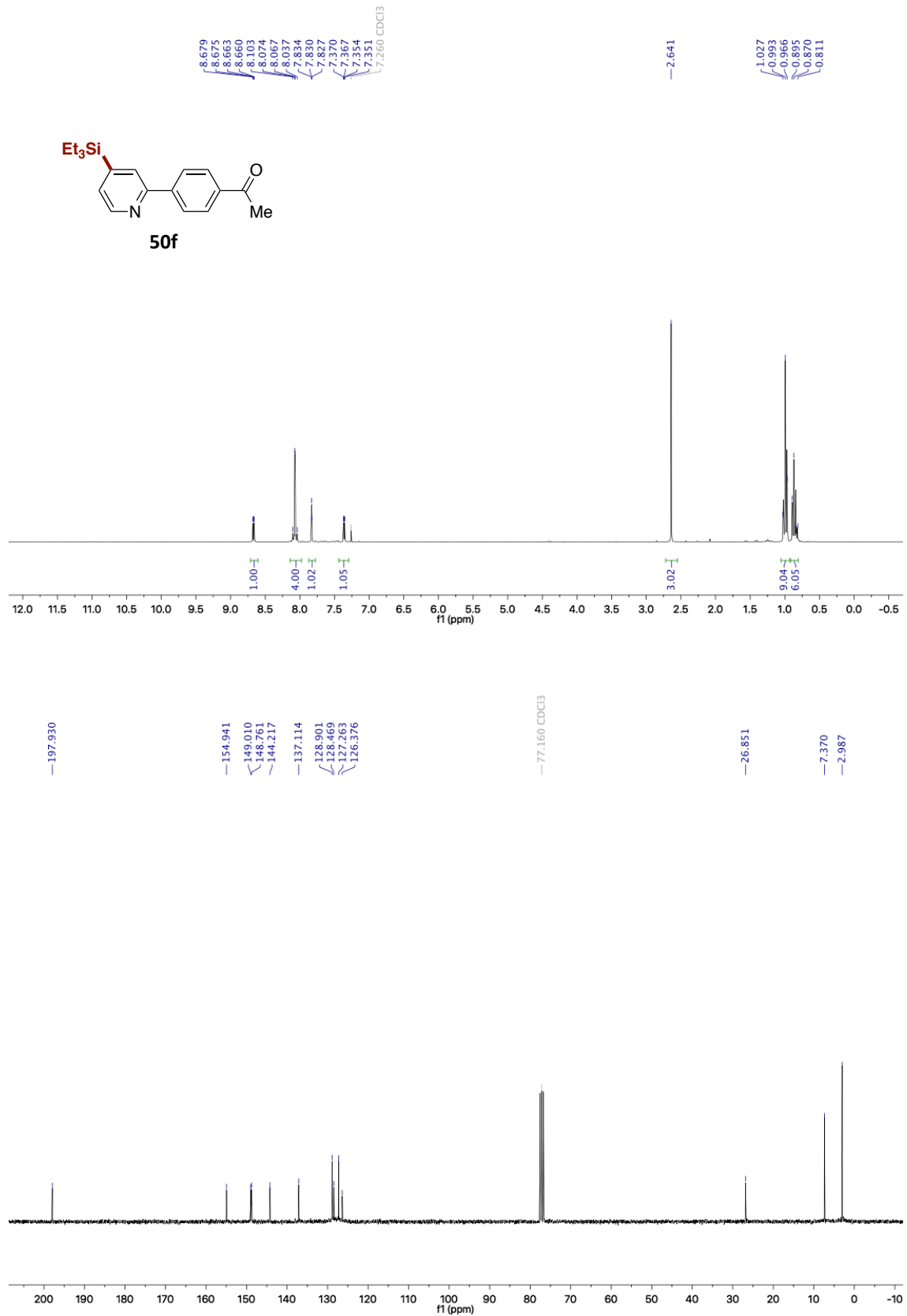
A Mild and Site-Selective sp^2 C-H Silylation of (Poly)Azines



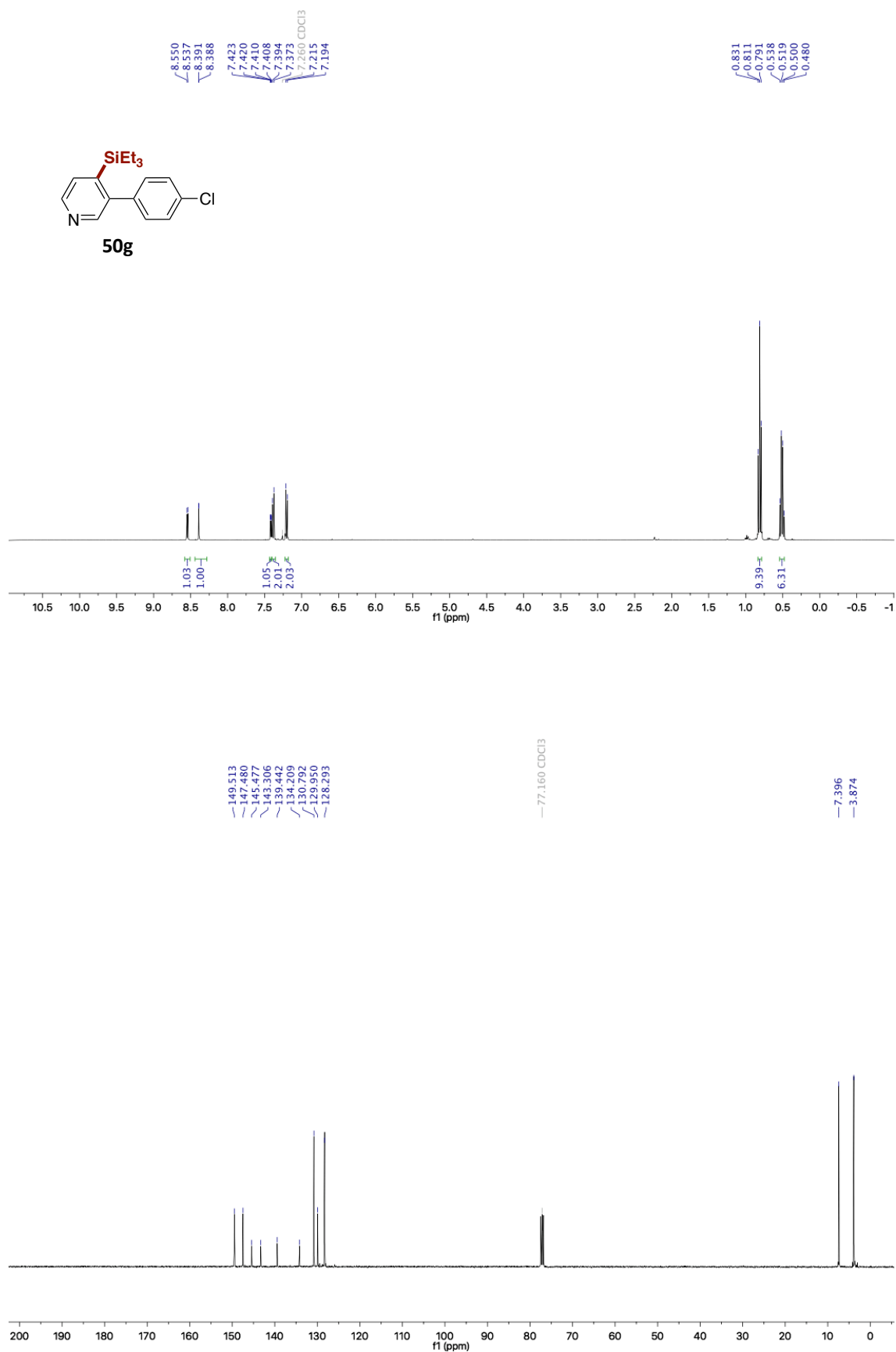


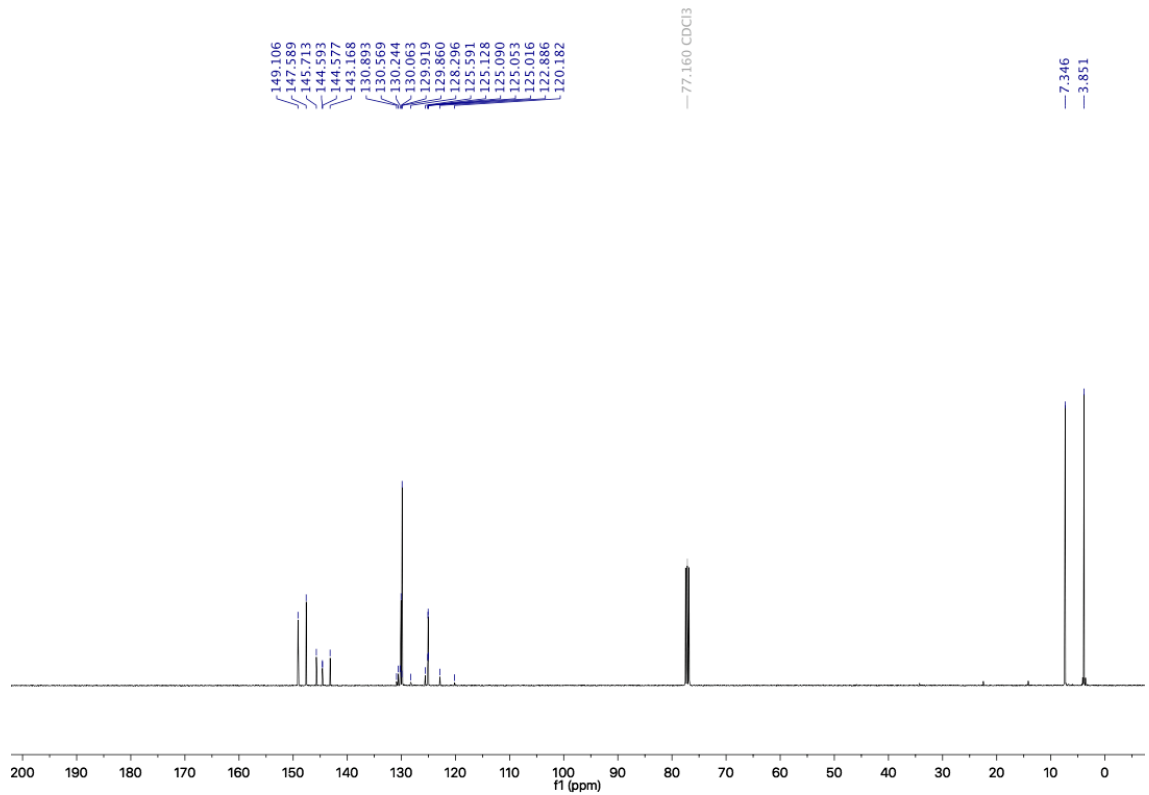
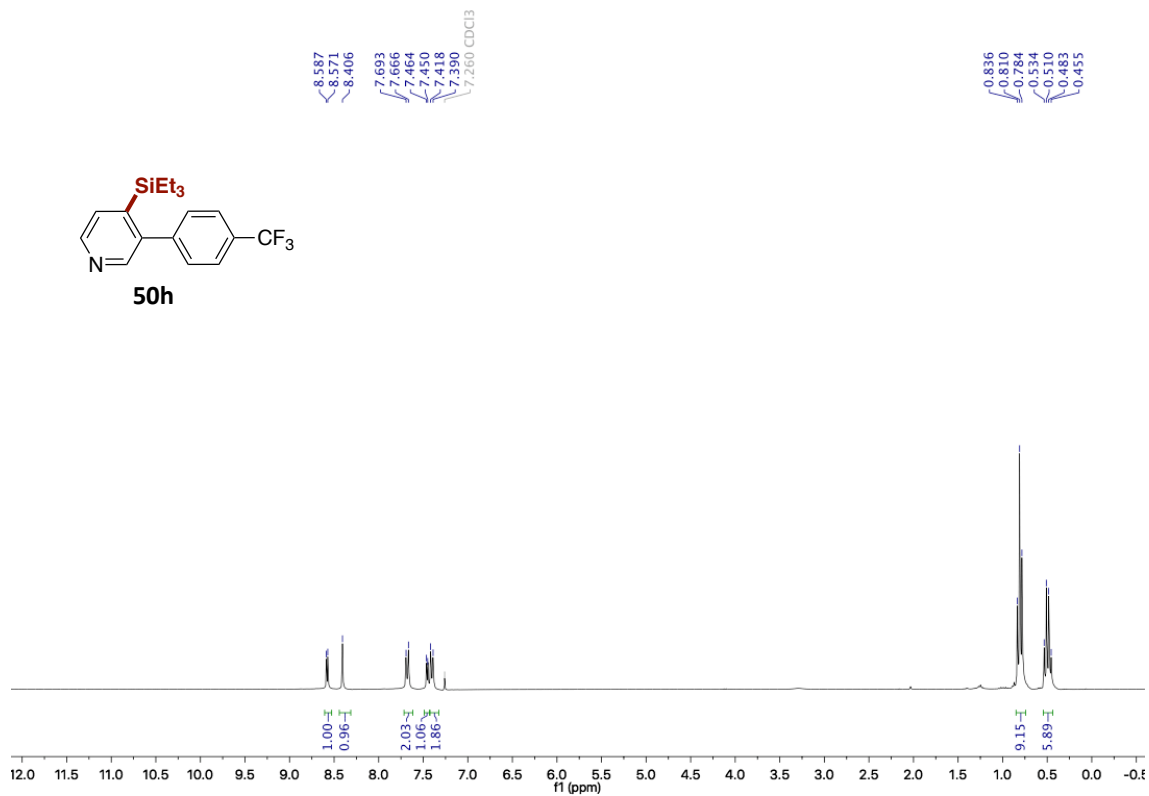
A Mild and Site-Selective sp^2 C-H Silylation of (Poly)Azines



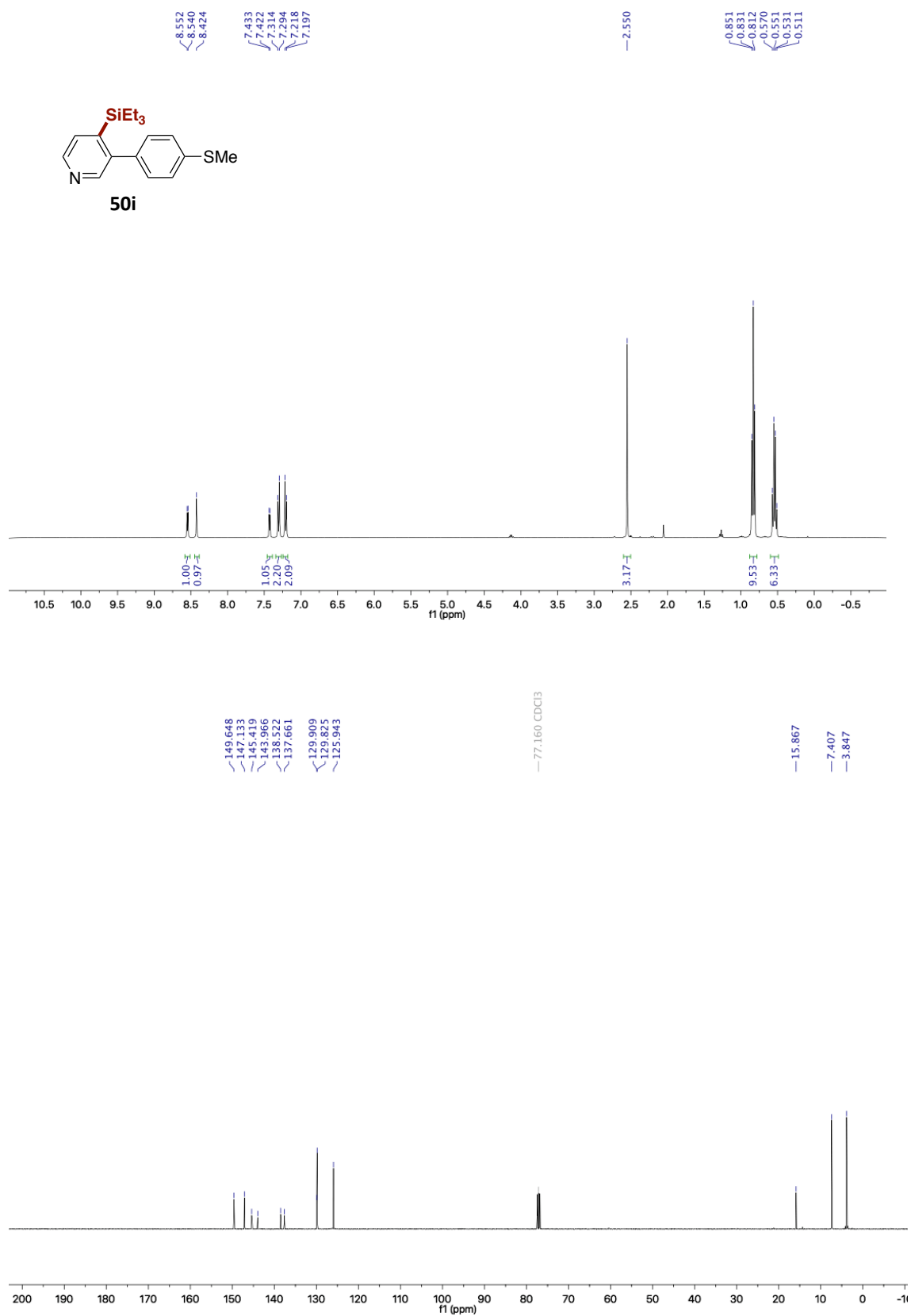


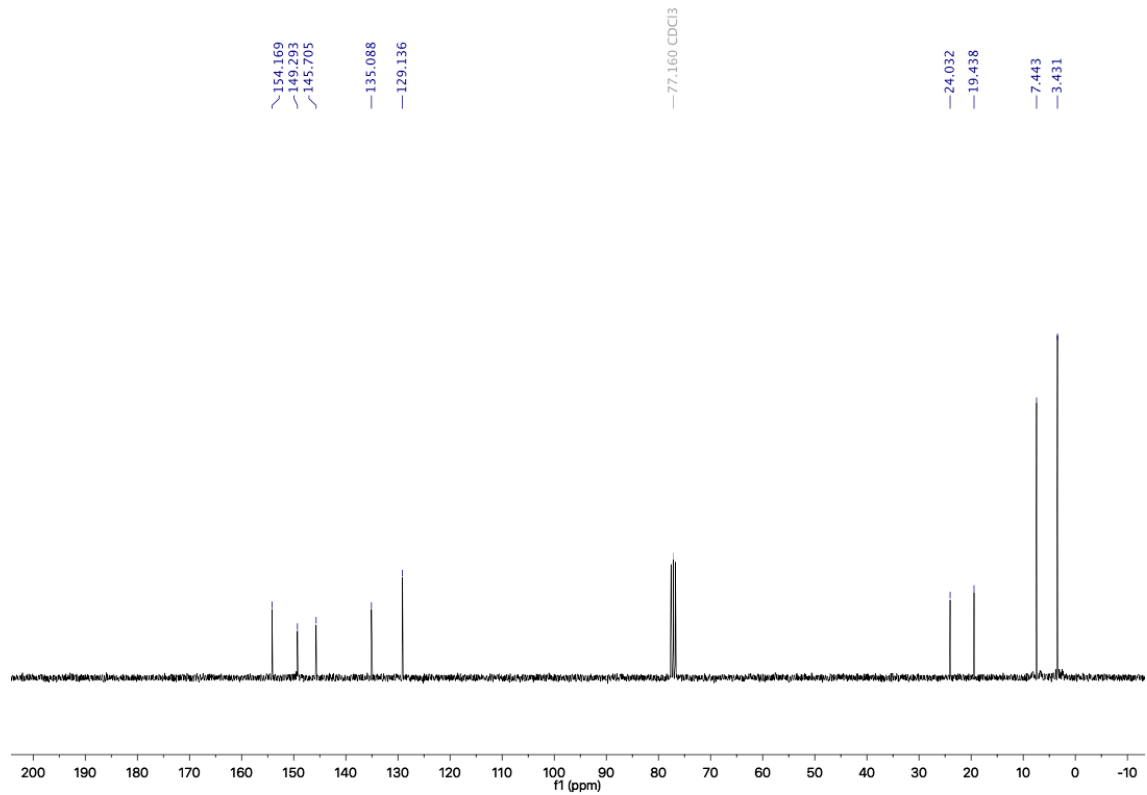
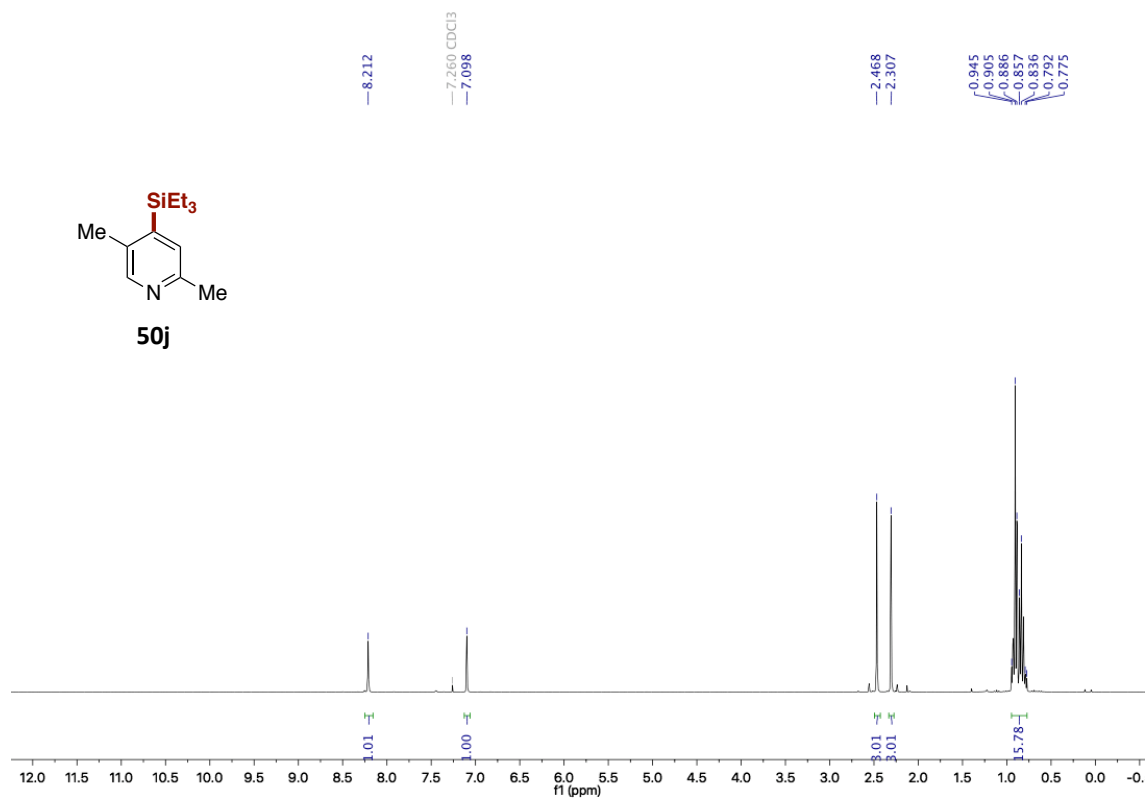
A Mild and Site-Selective sp^2 C-H Silylation of (Poly)Azines



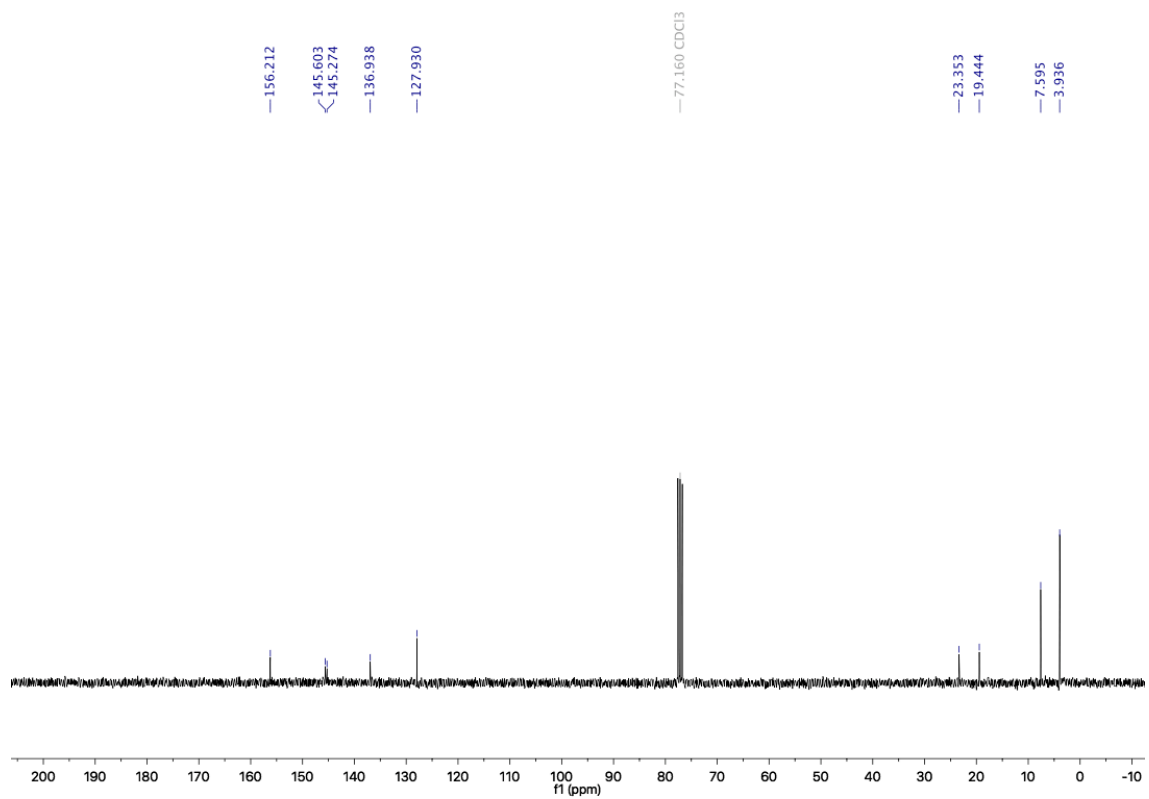
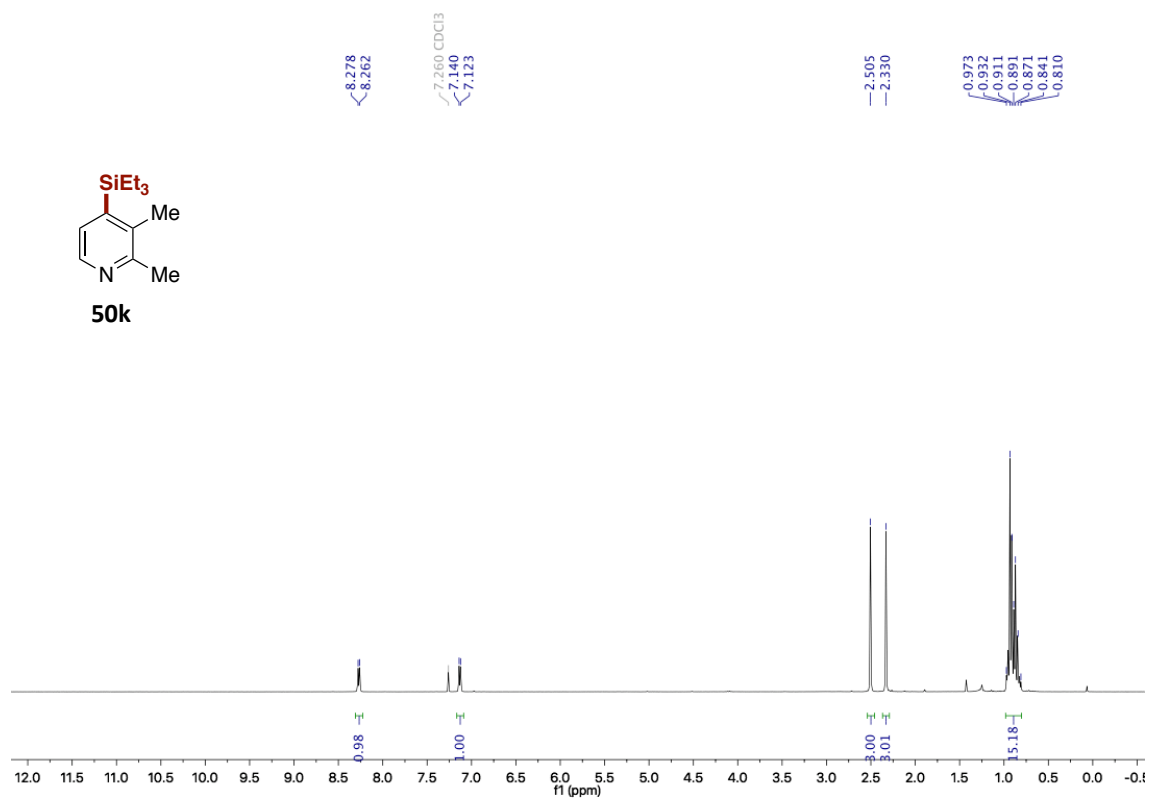


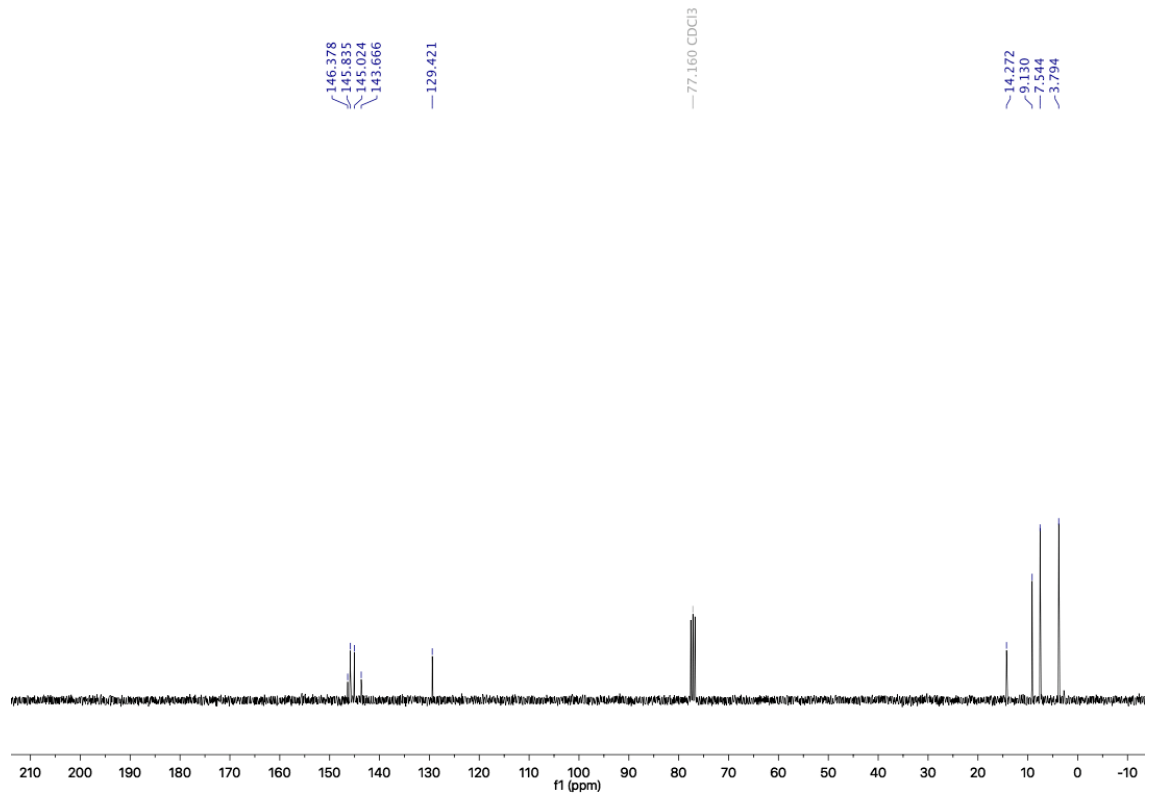
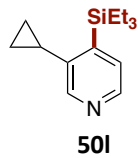
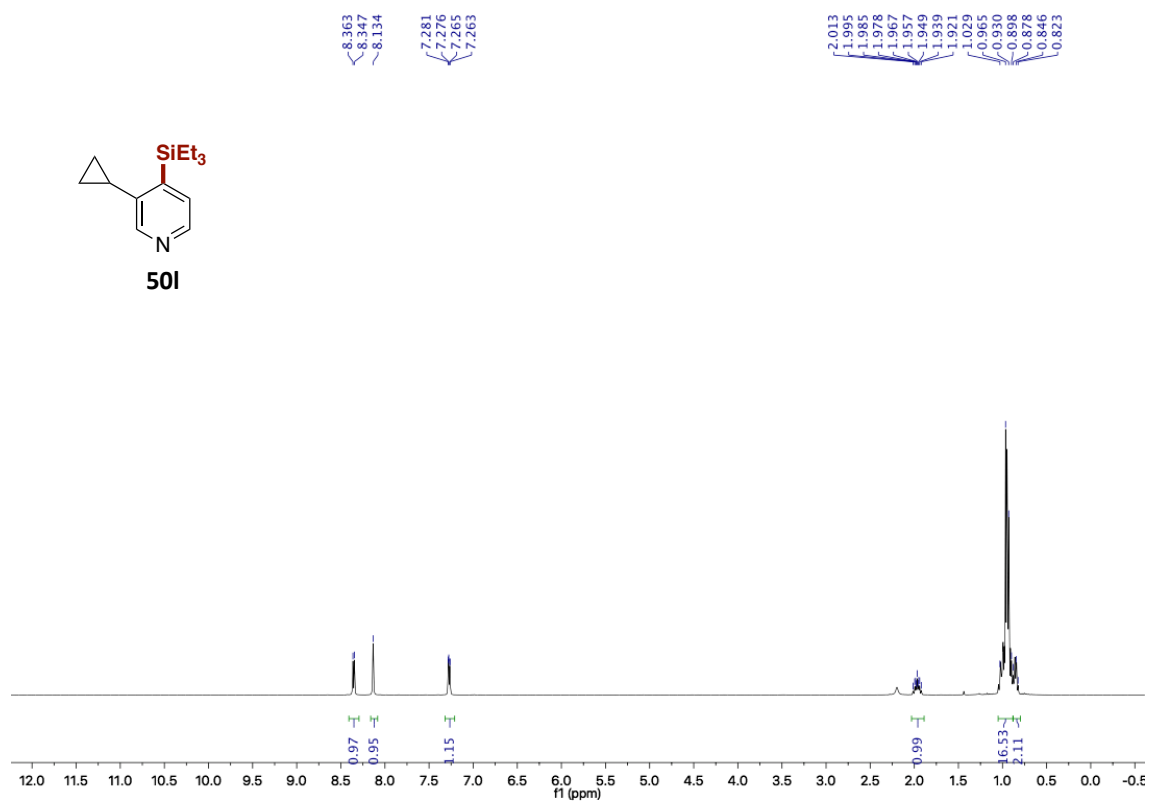
A Mild and Site-Selective sp^2 C-H Silylation of (Poly)Azines



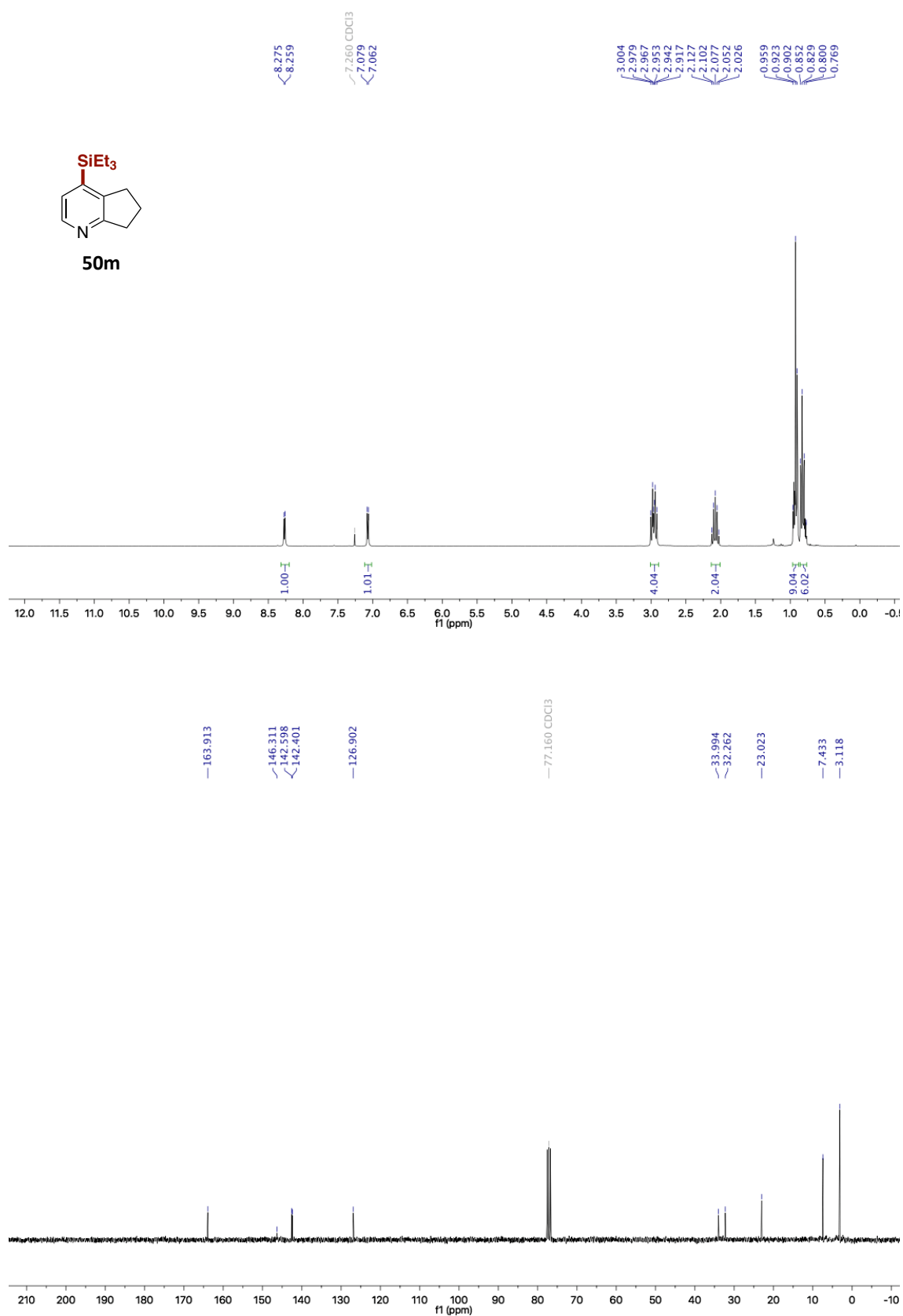


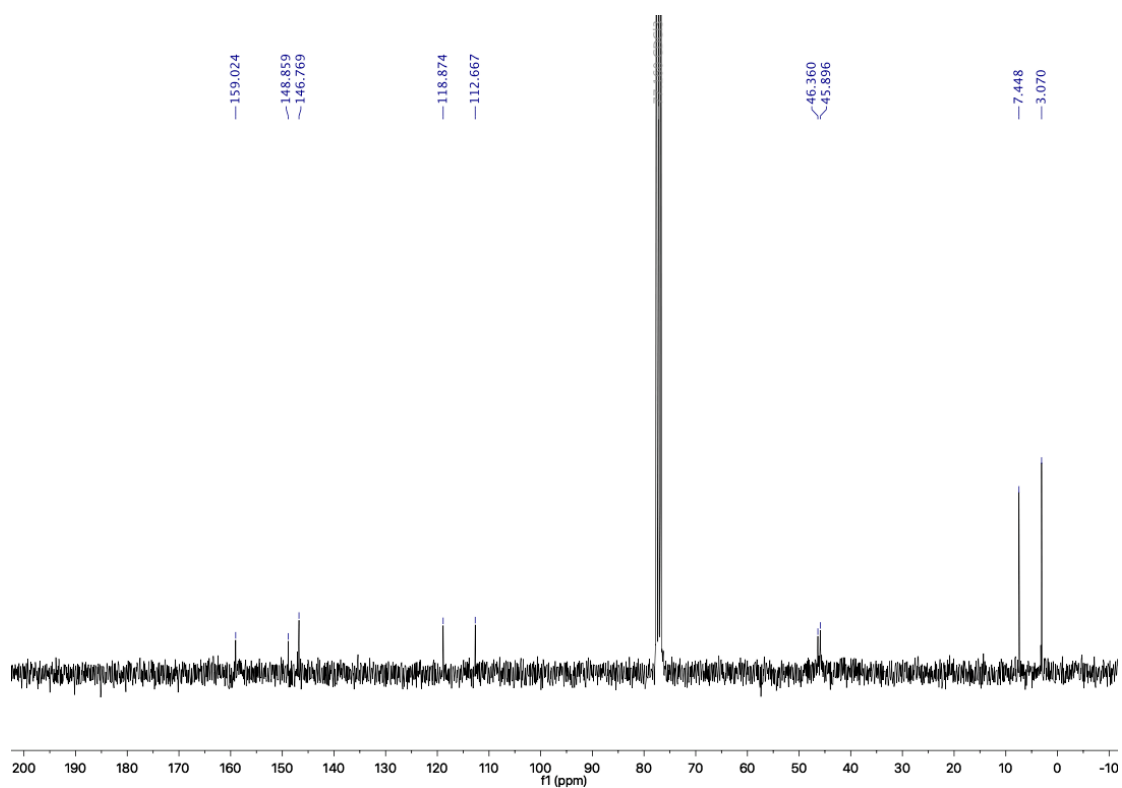
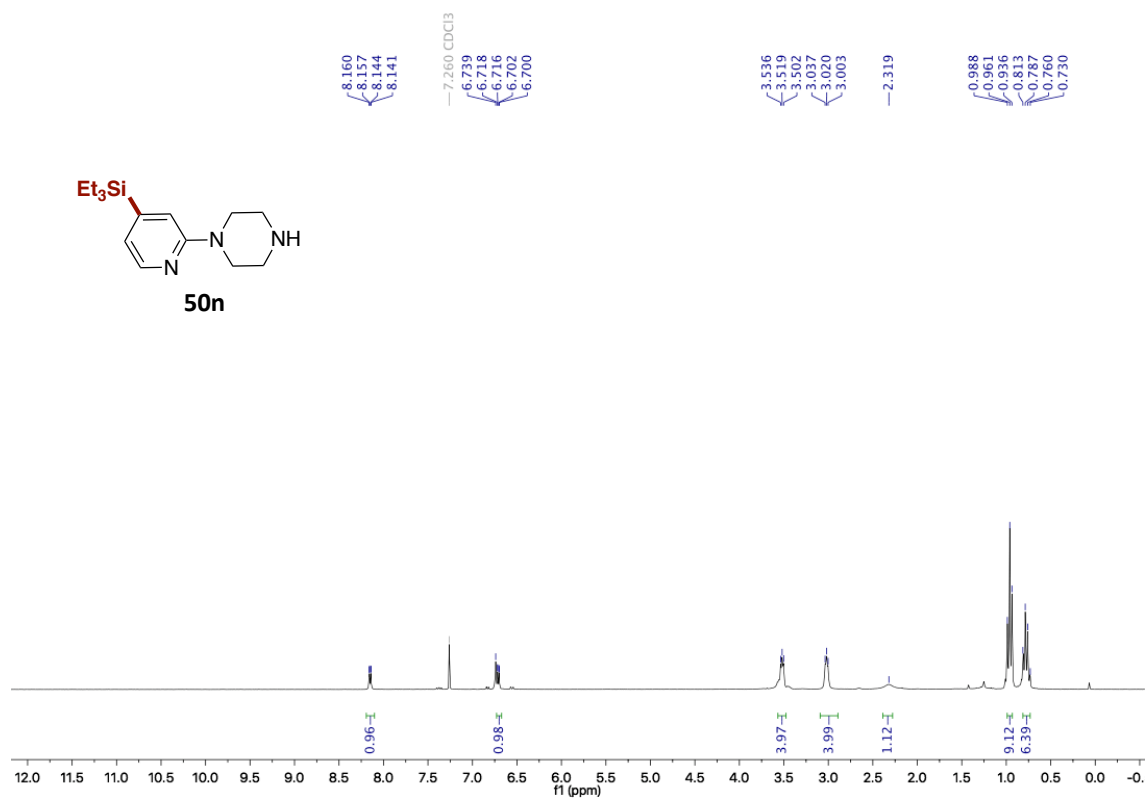
A Mild and Site-Selective sp^2 C-H Silylation of (Poly)Azines

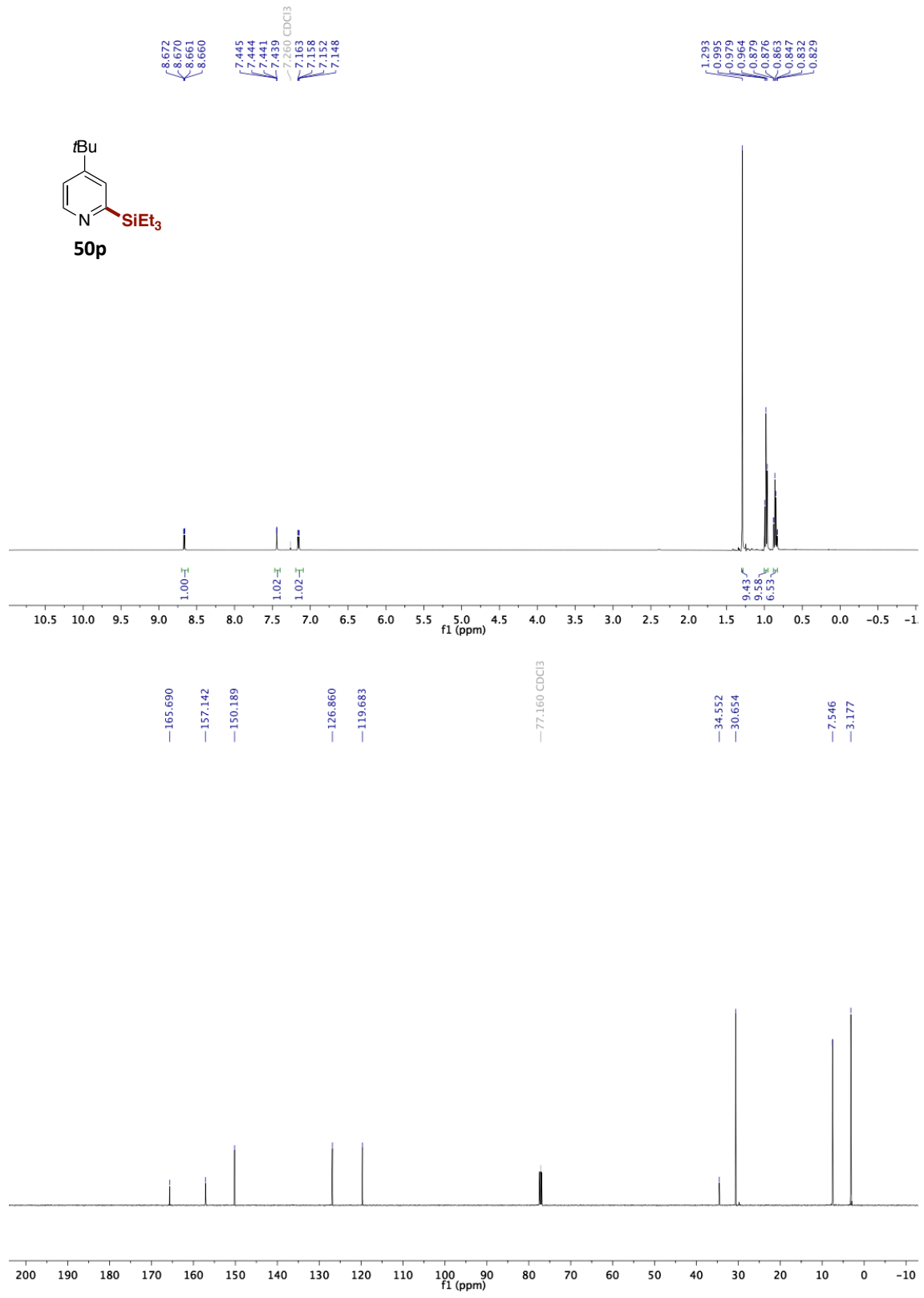




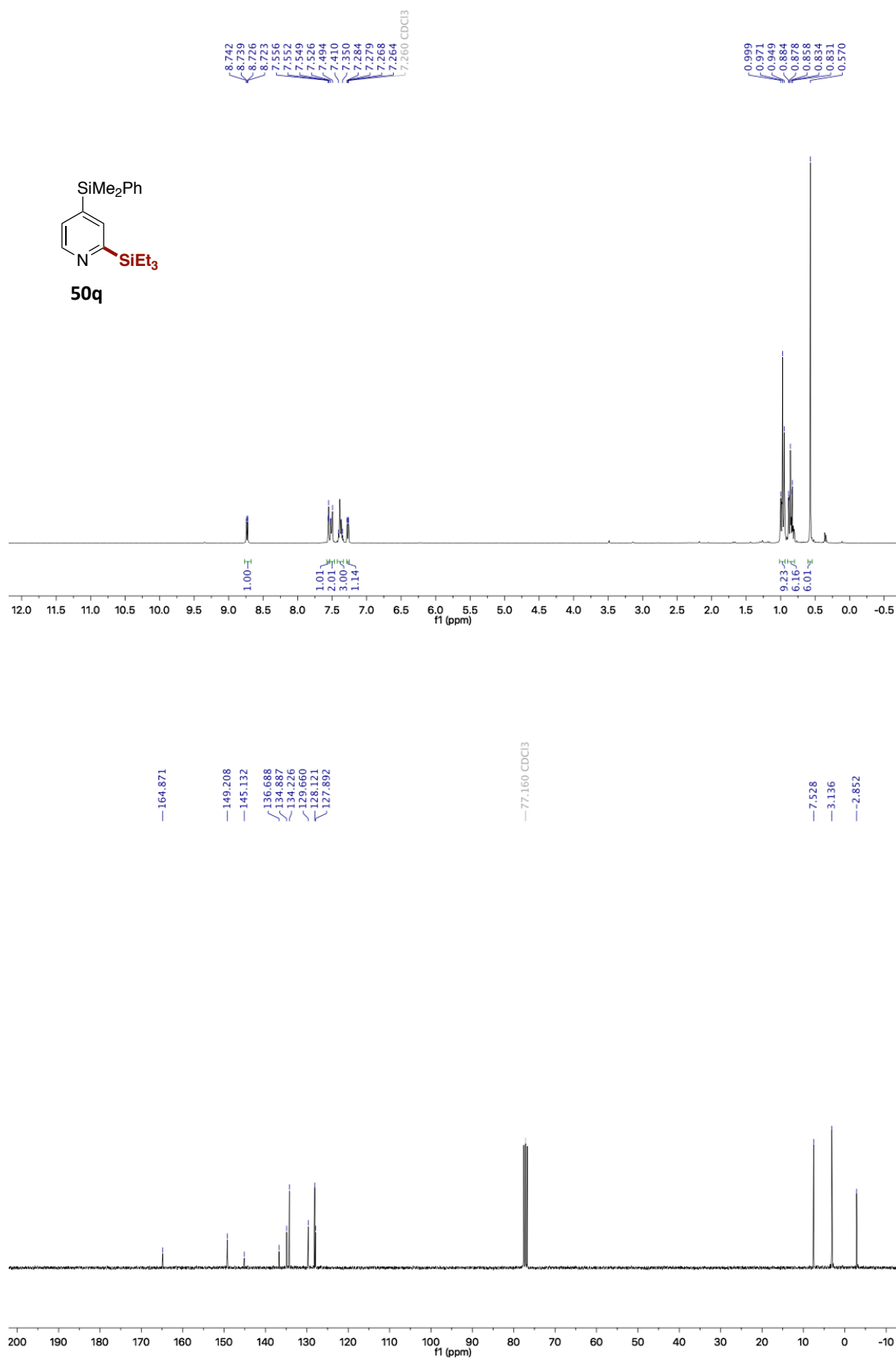
A Mild and Site-Selective sp^2 C-H Silylation of (Poly)Azines

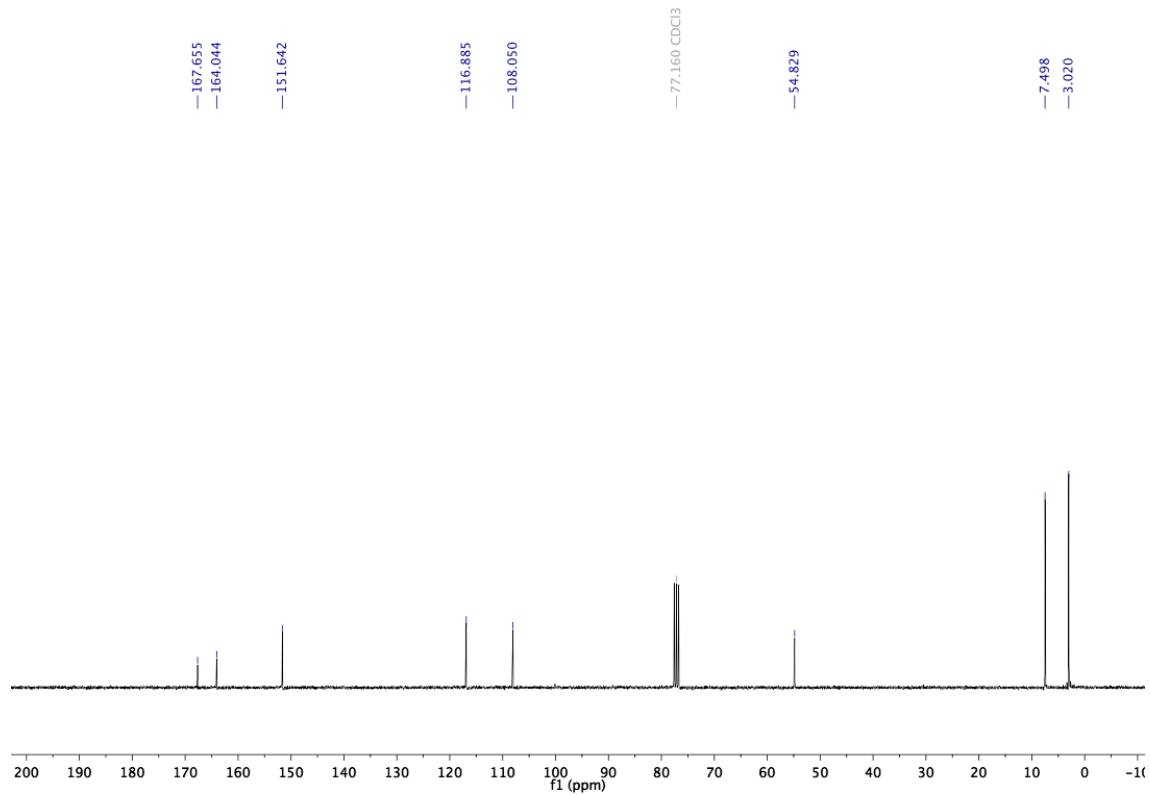
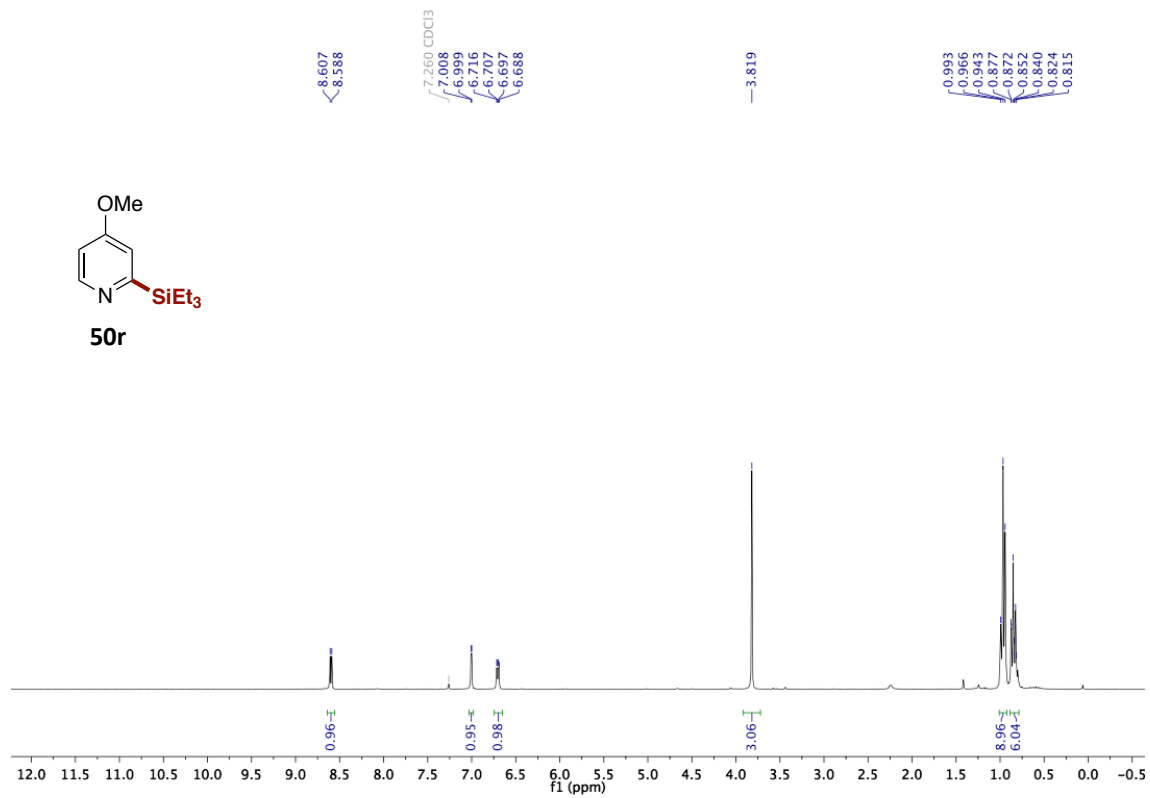




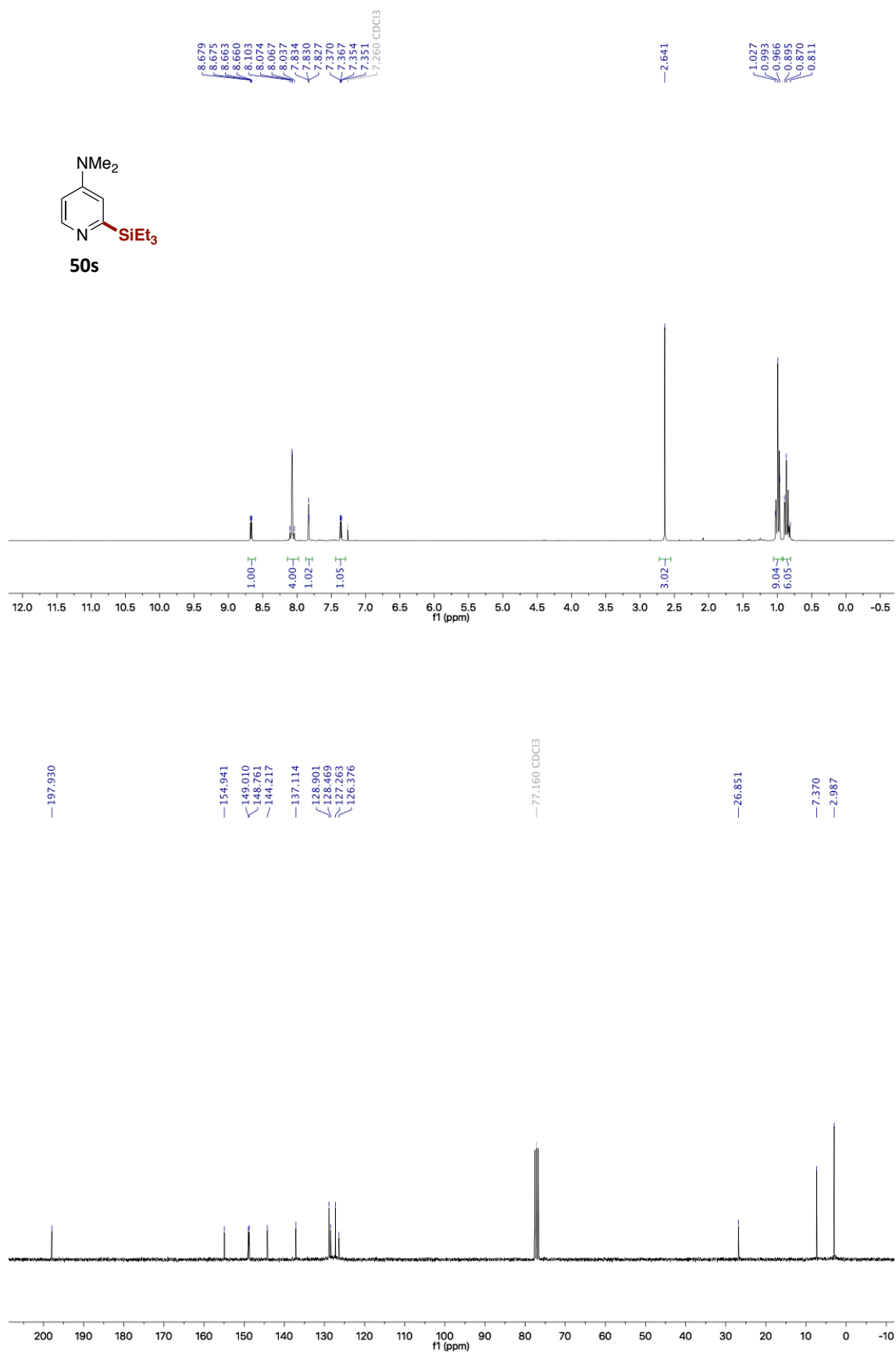


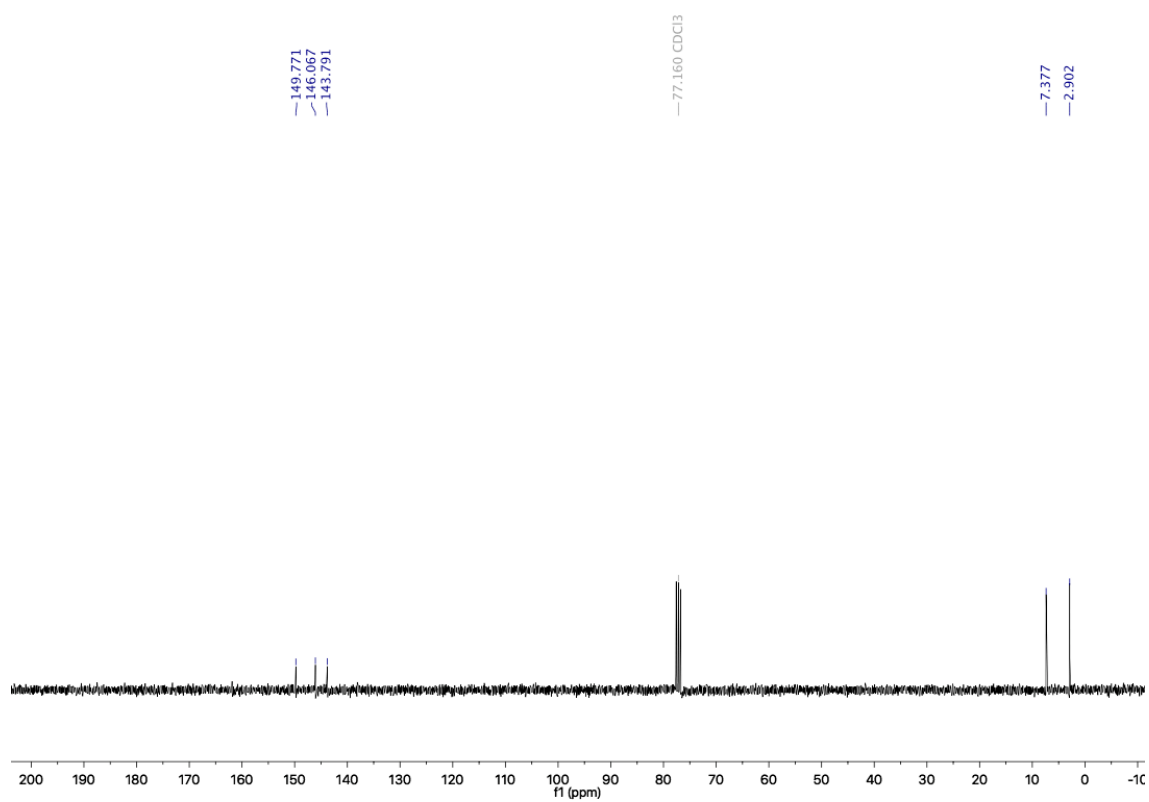
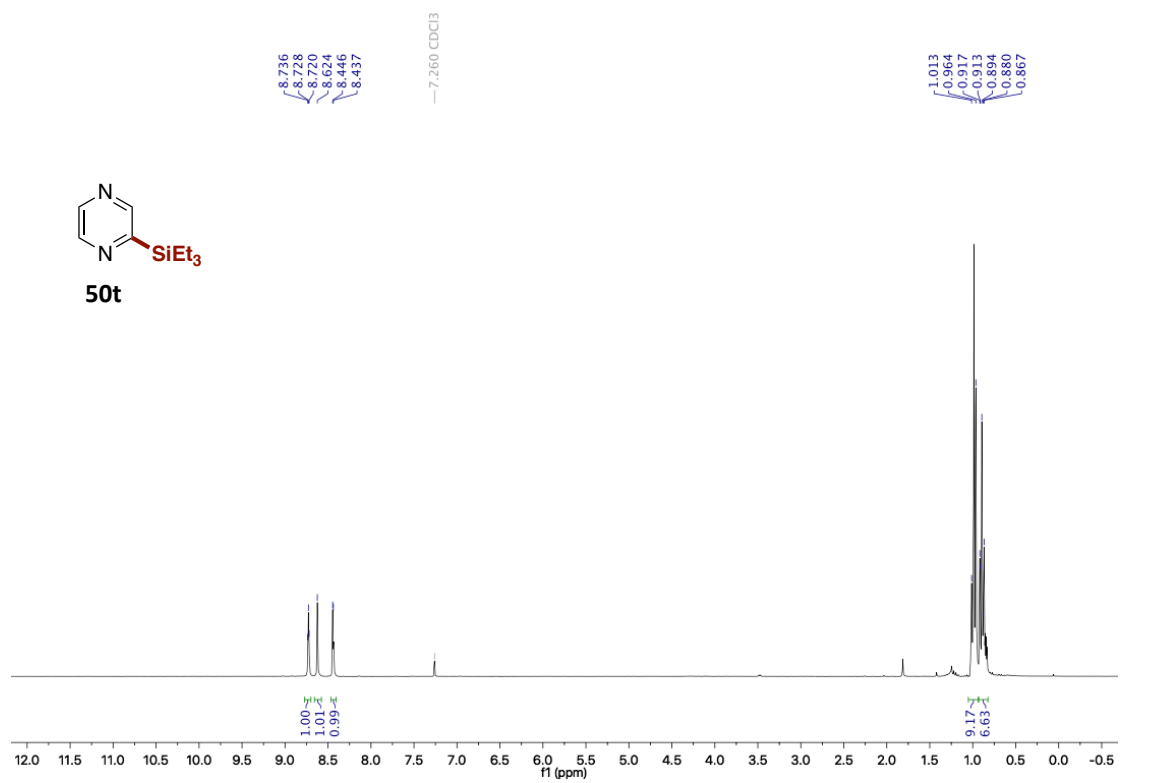
A Mild and Site-Selective sp^2 C-H Silylation of (Poly)Azines



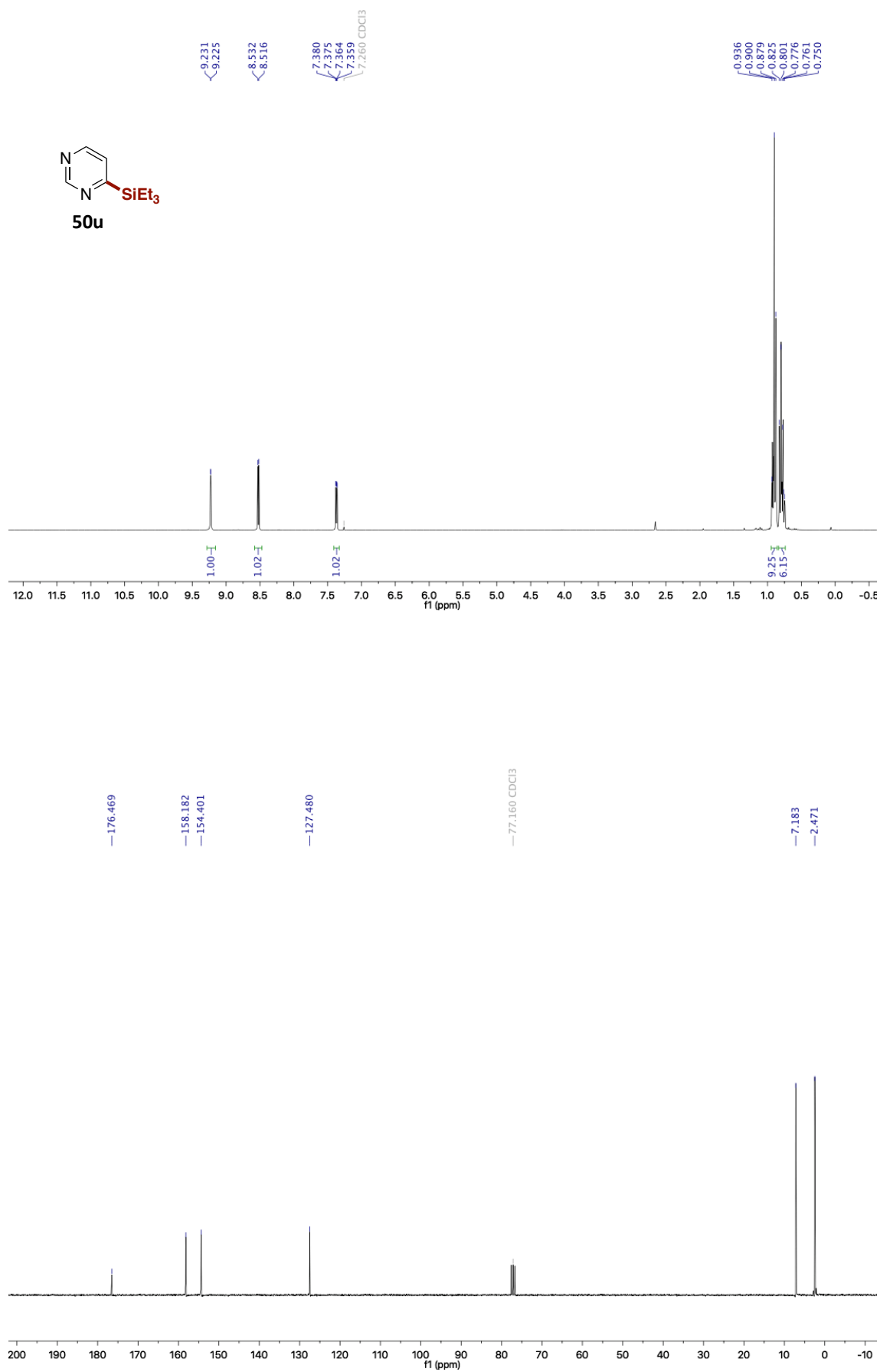


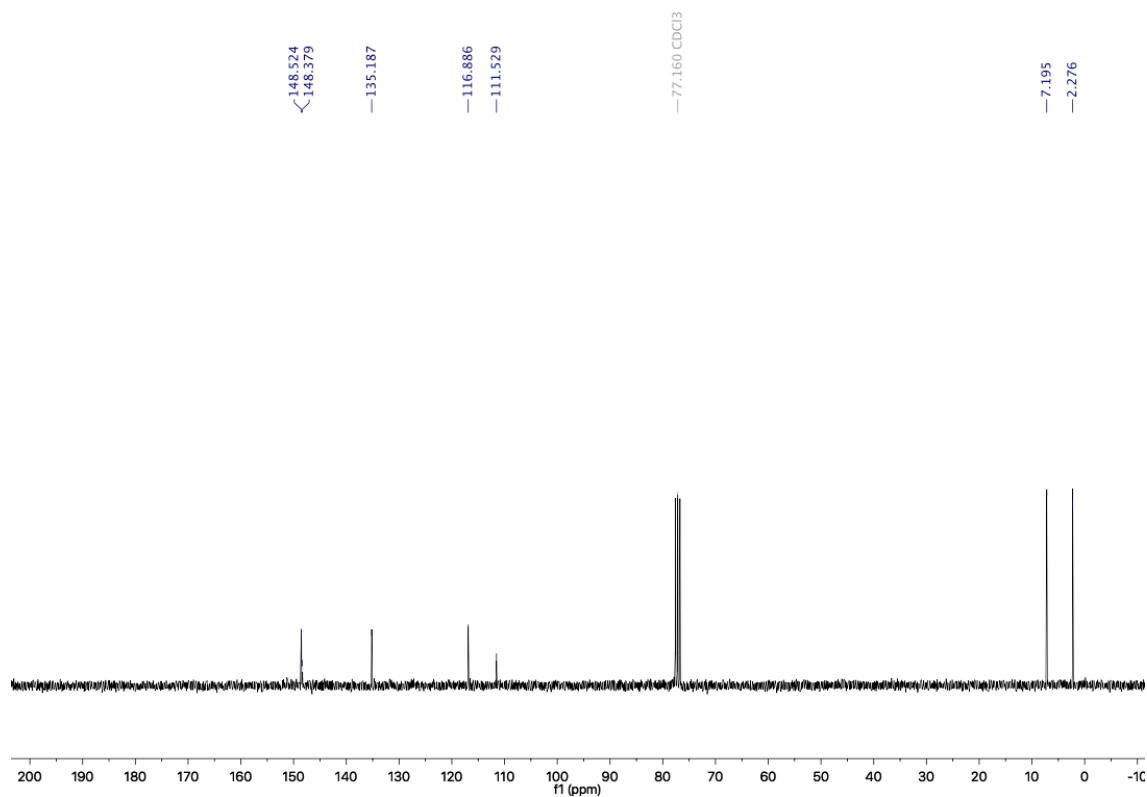
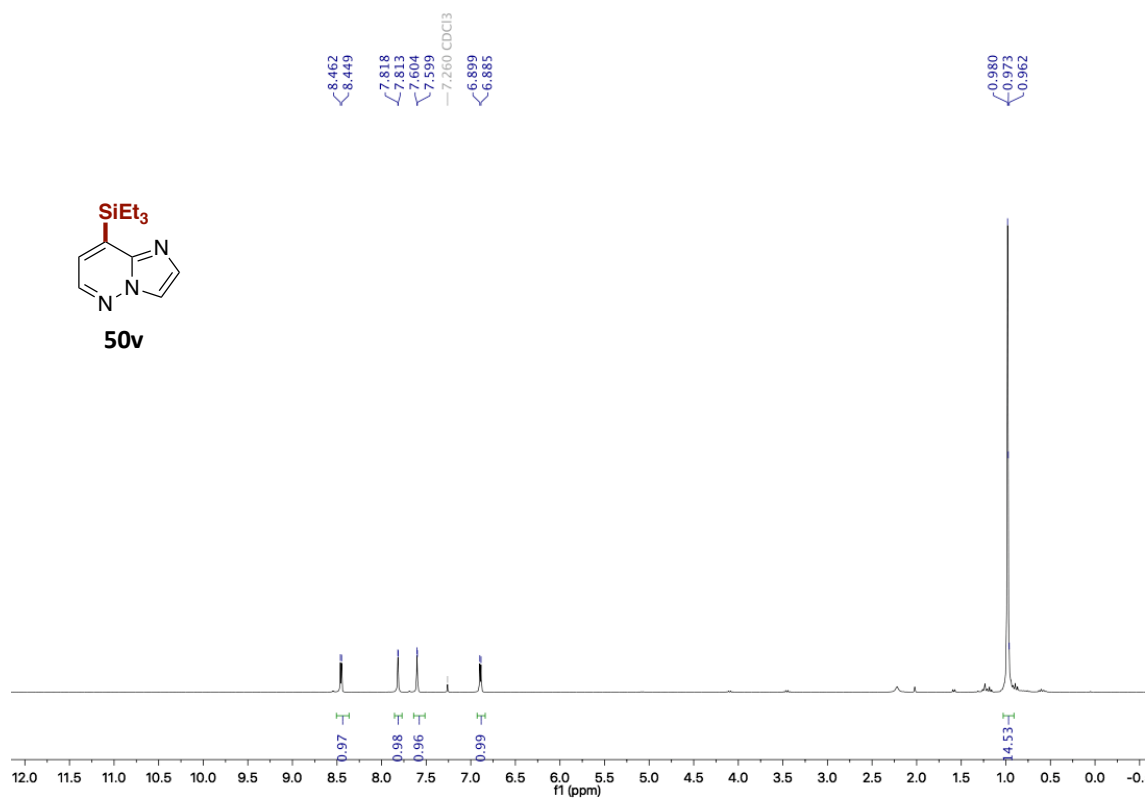
A Mild and Site-Selective sp^2 C-H Silylation of (Poly)azines



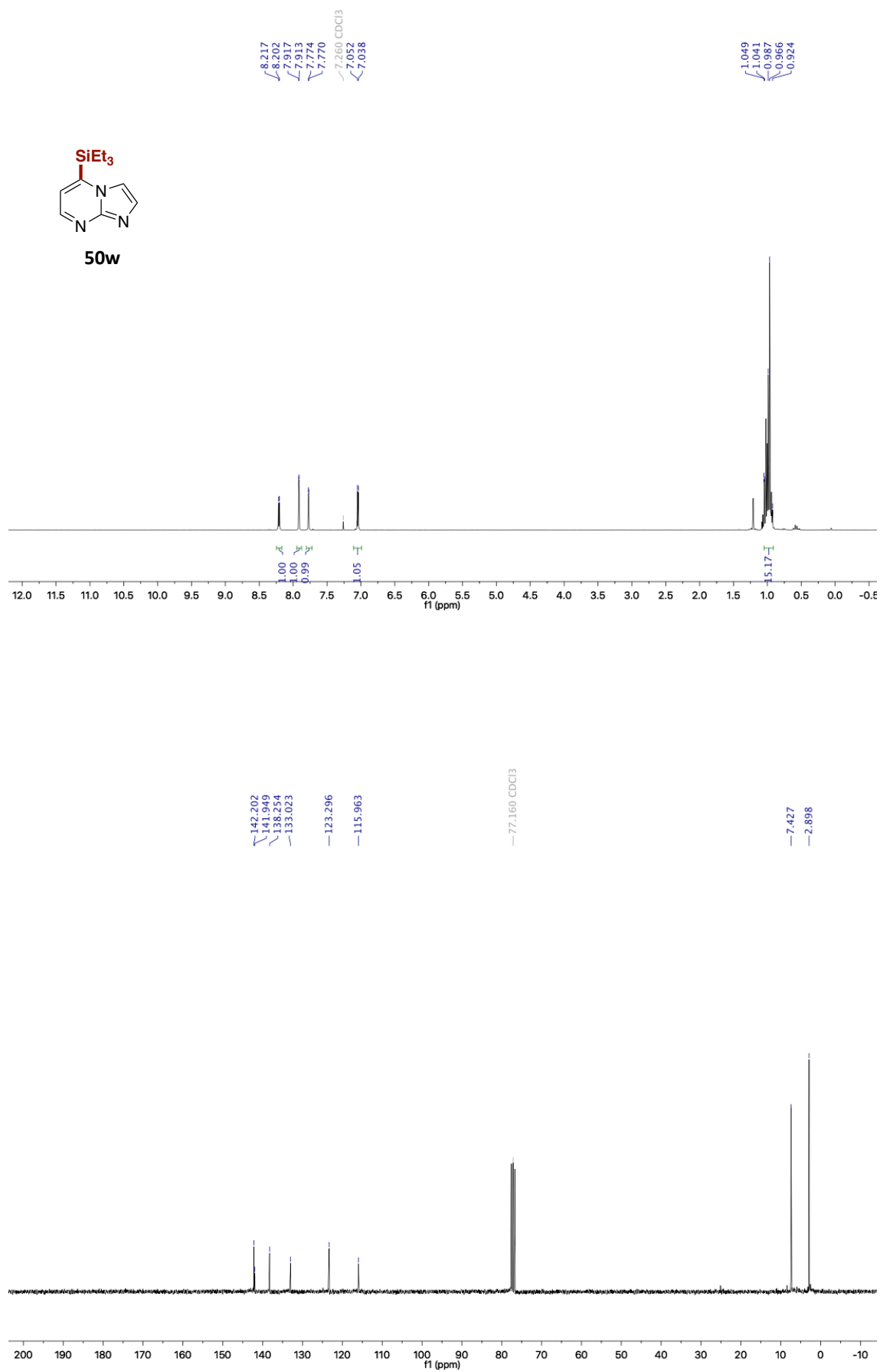


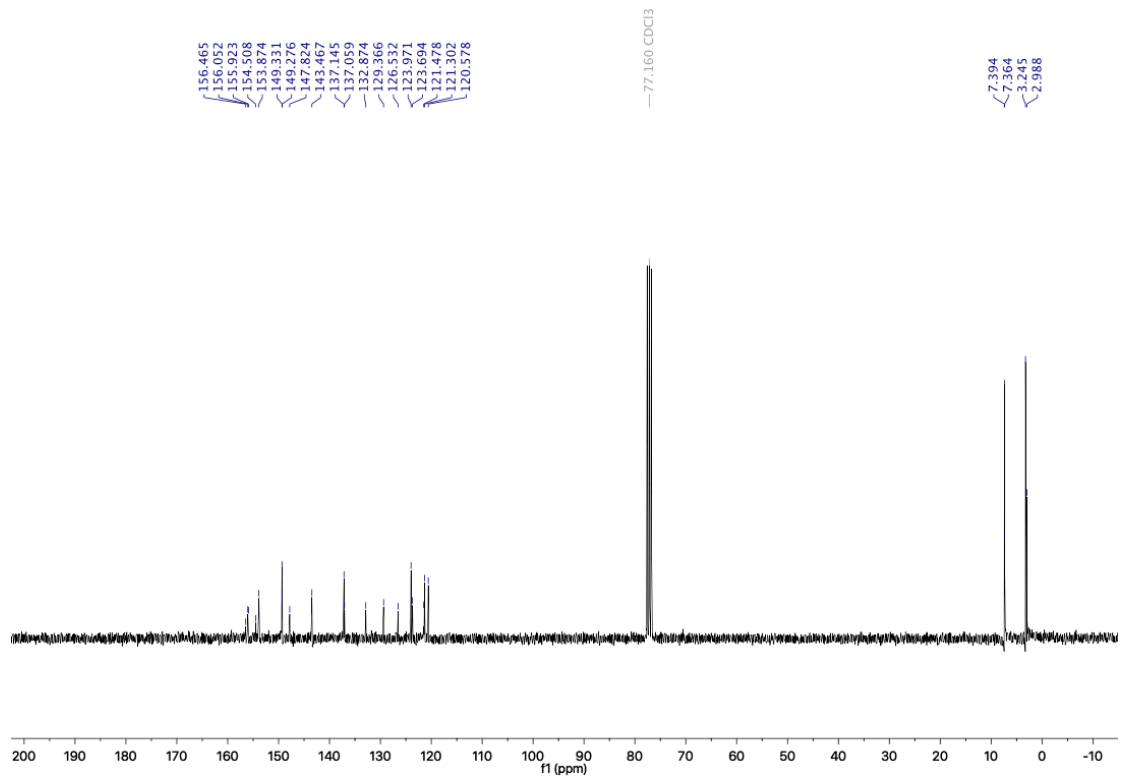
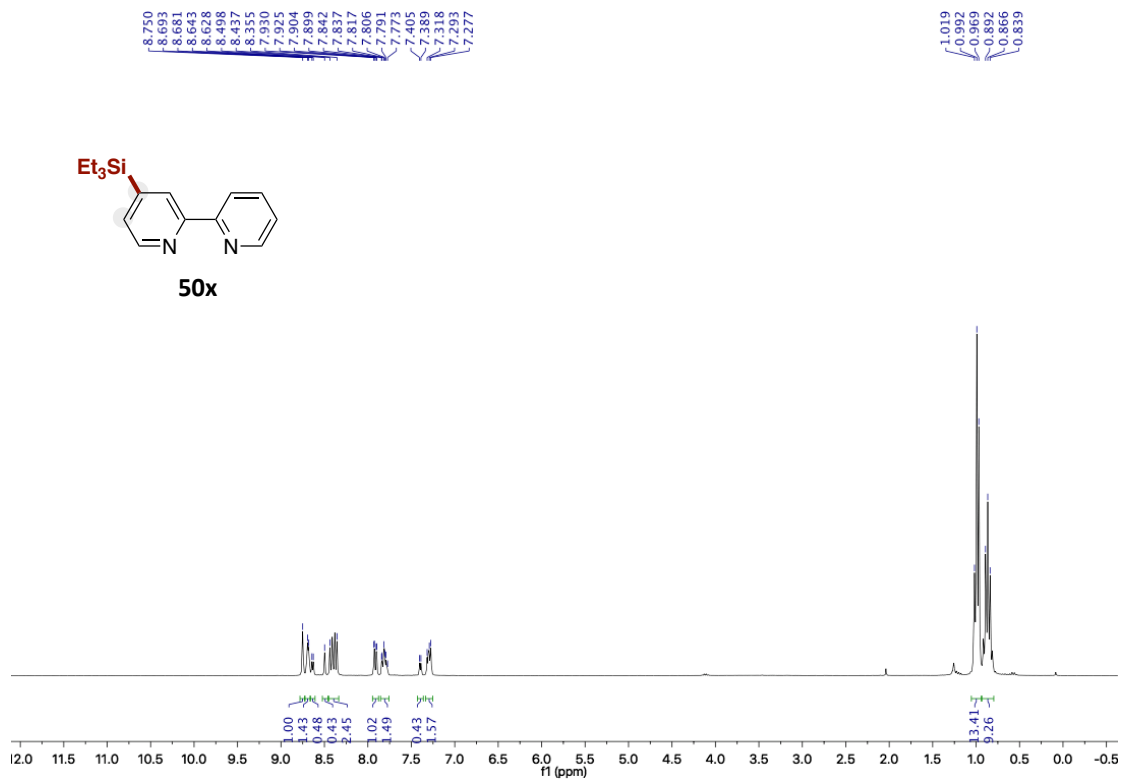
A Mild and Site-Selective sp^2 C-H Silylation of (Poly)Azines



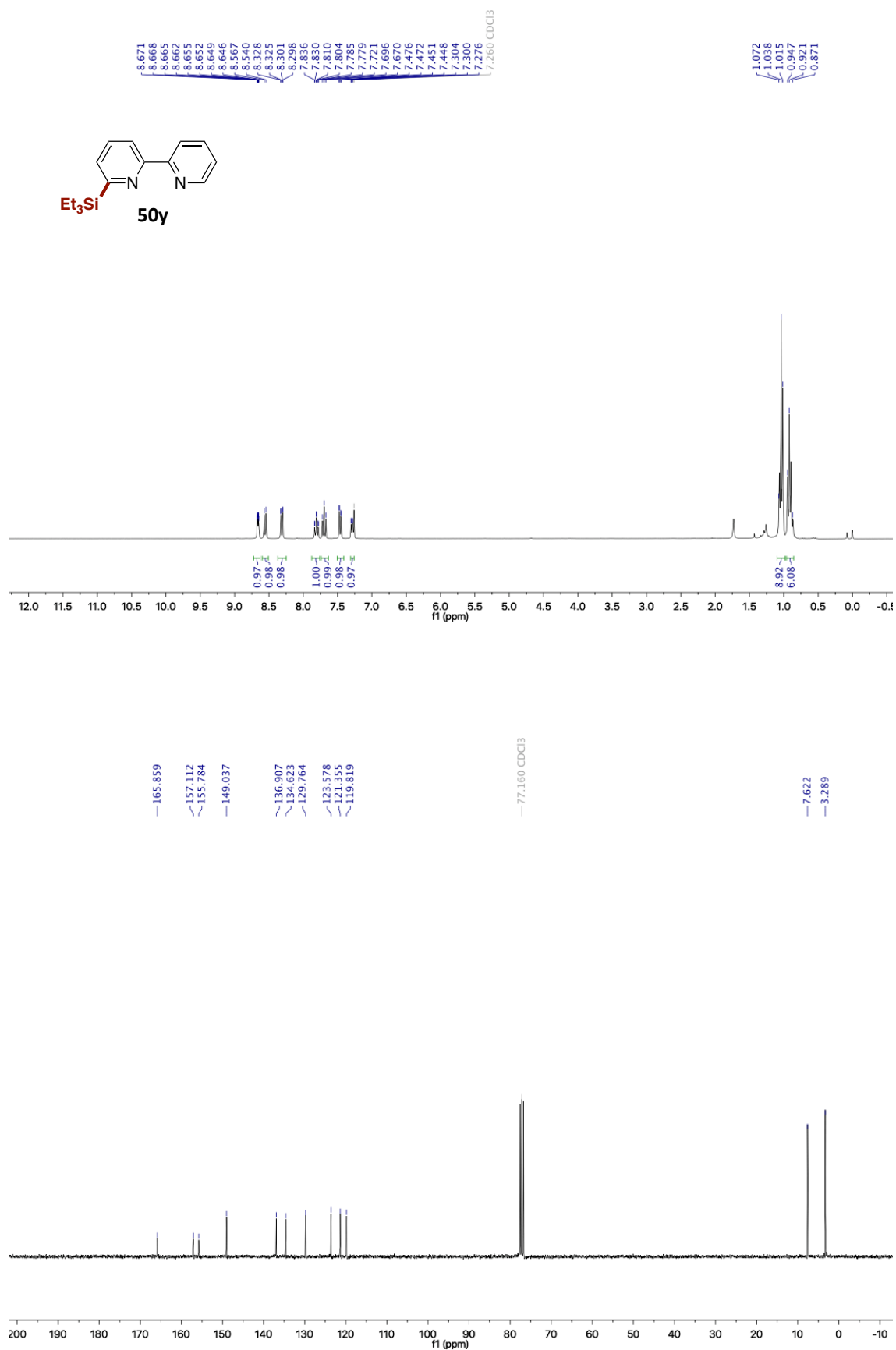


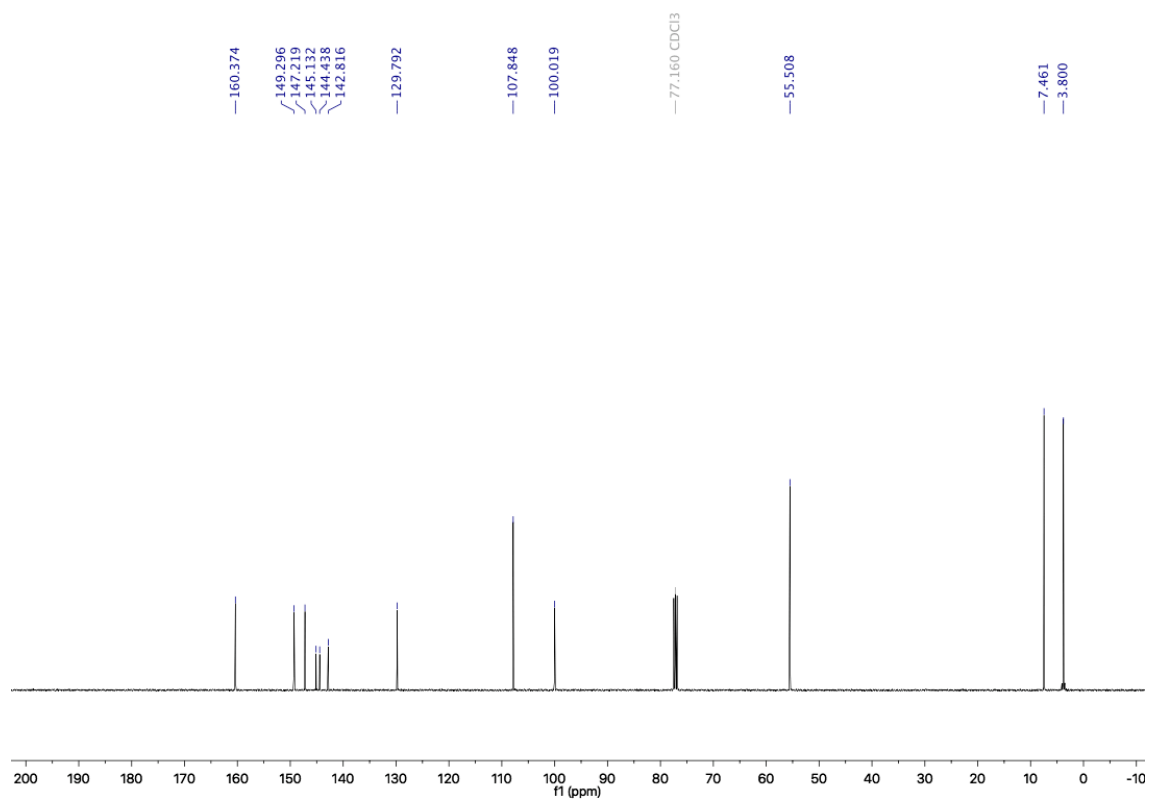
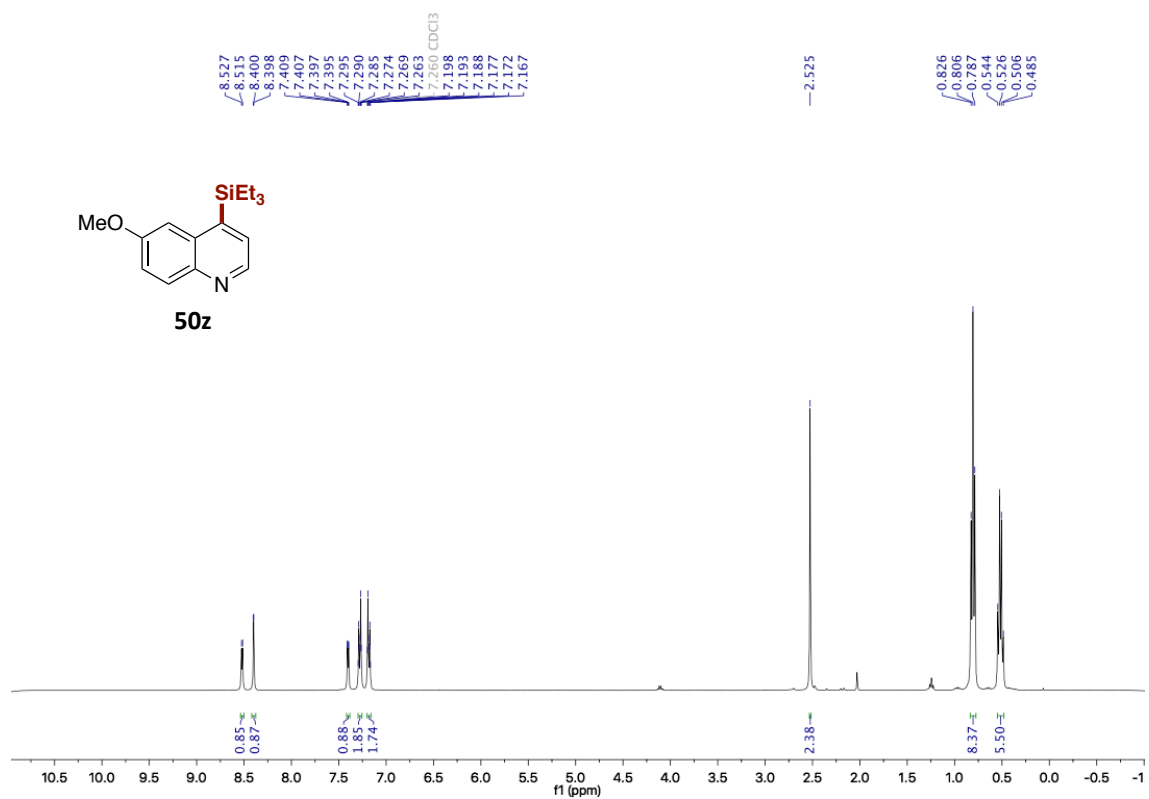
A Mild and Site-Selective sp^2 C-H Silylation of (Poly)Azines



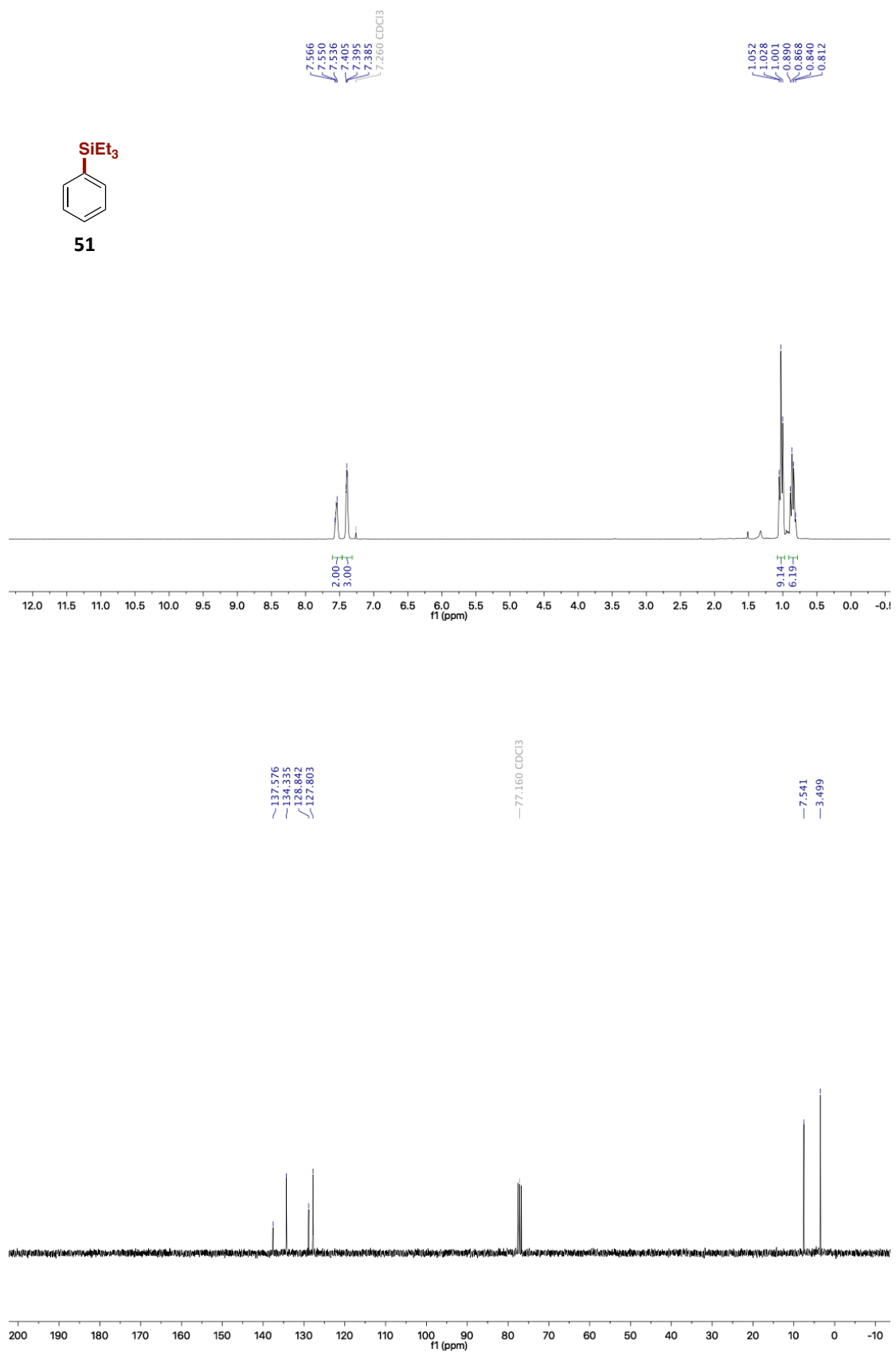


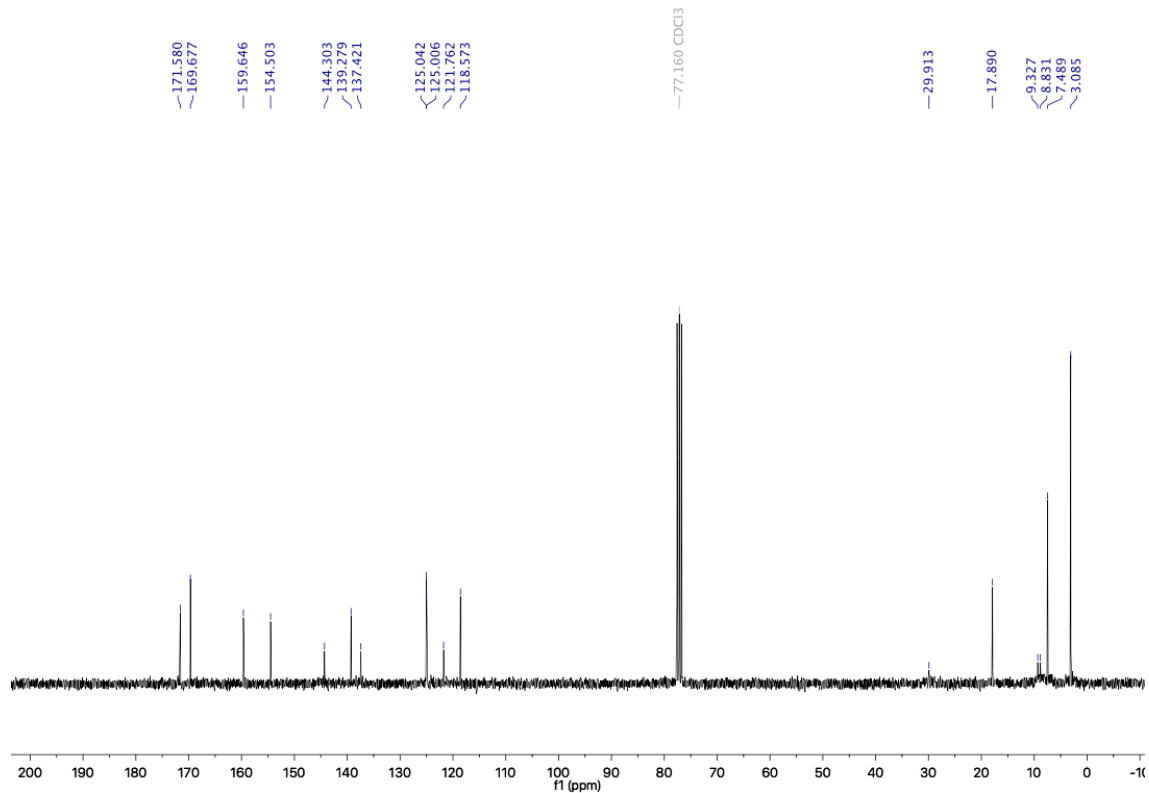
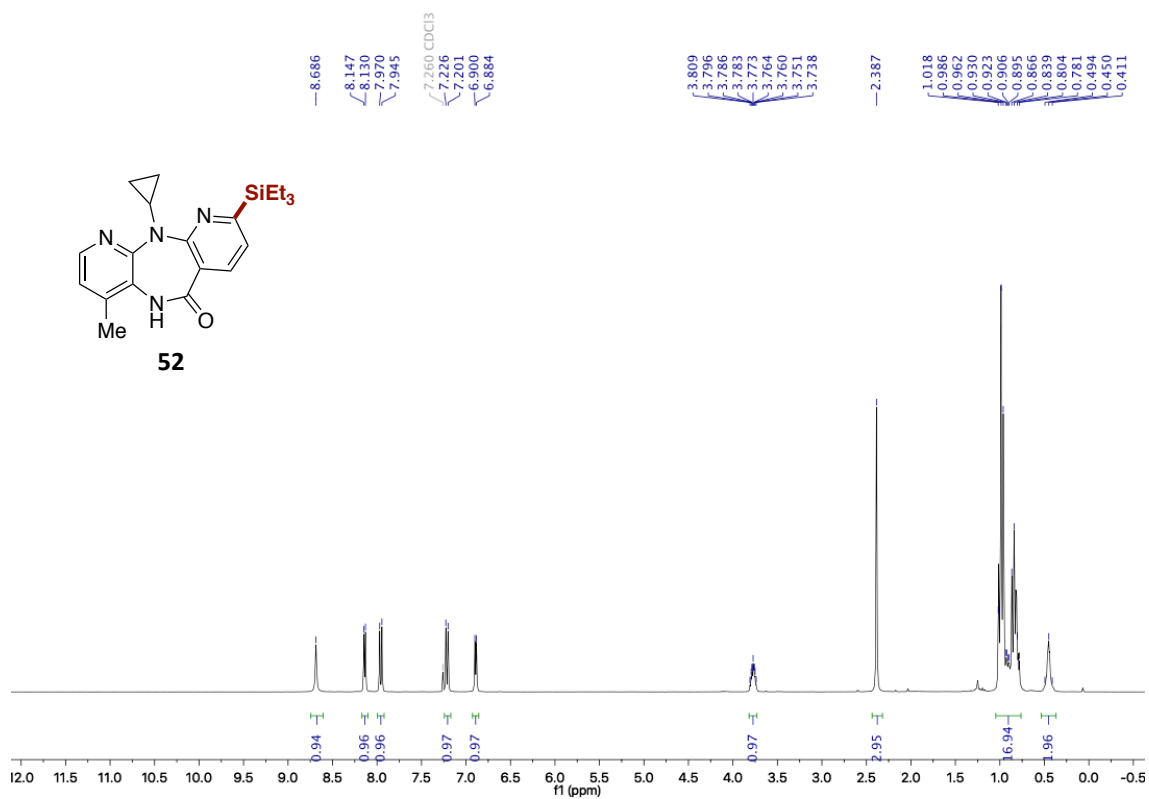
A Mild and Site-Selective sp^2 C-H Silylation of (Poly)Azines



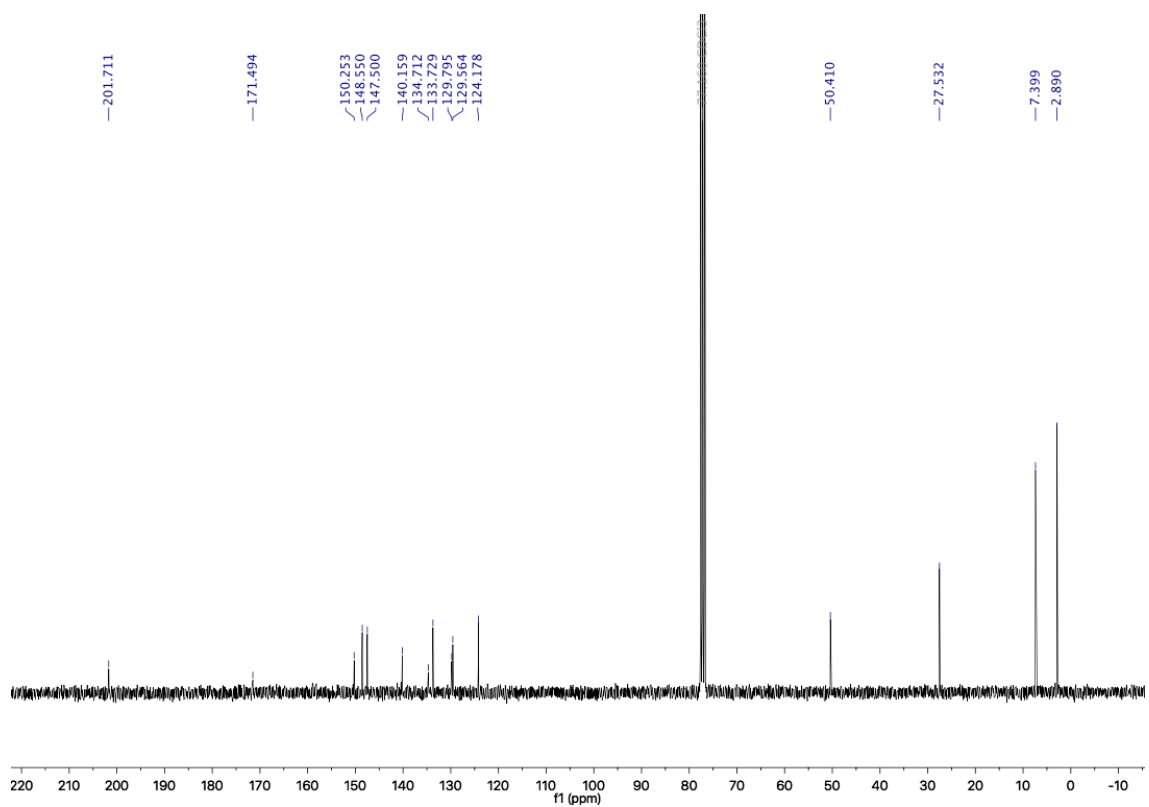
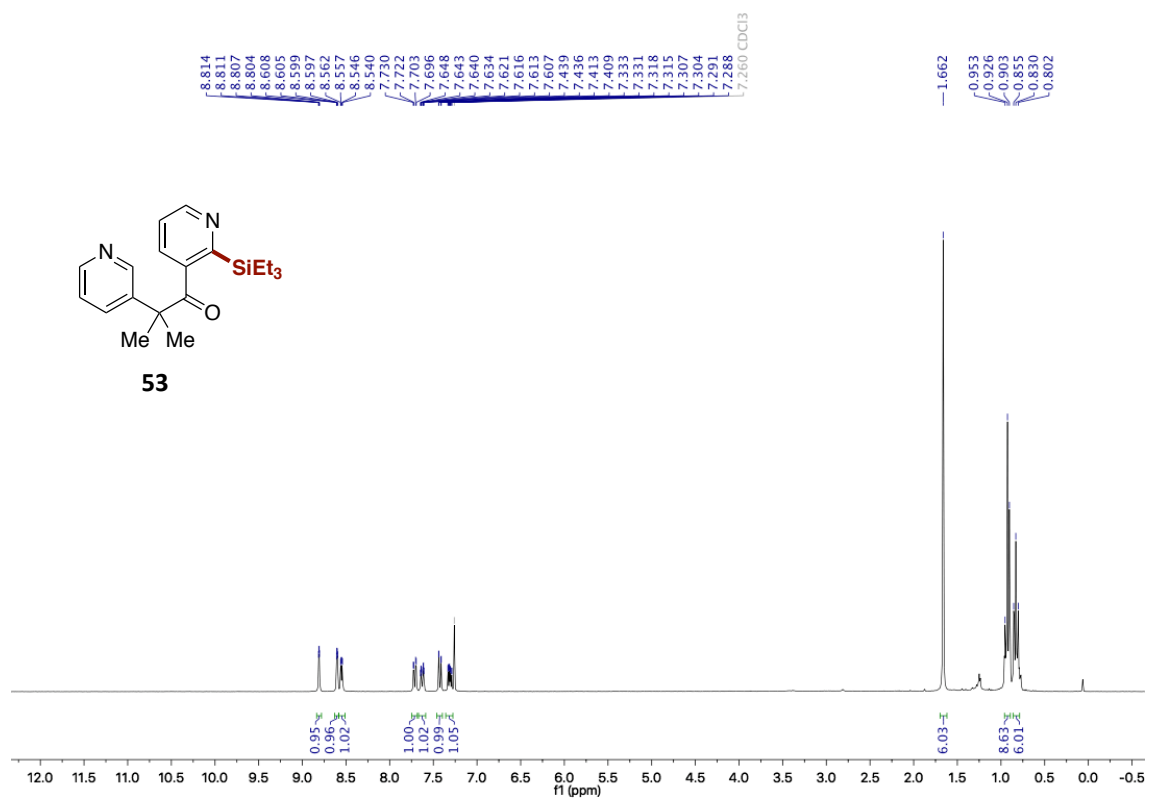


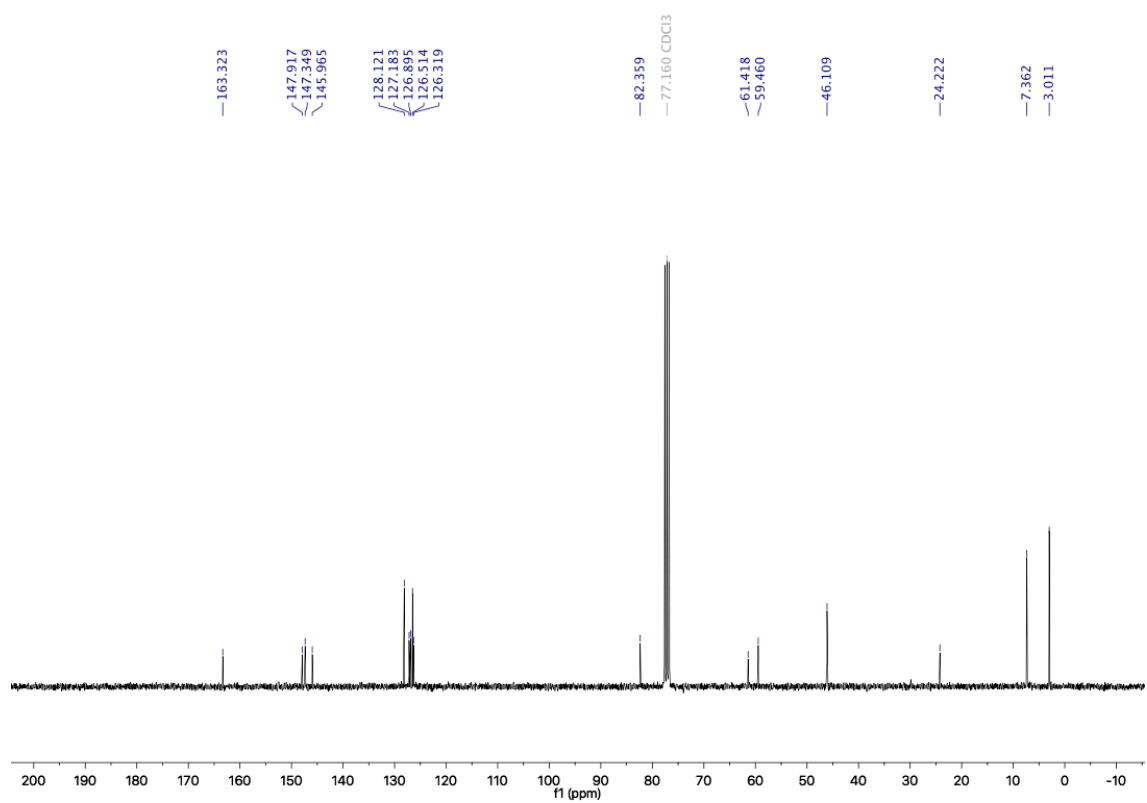
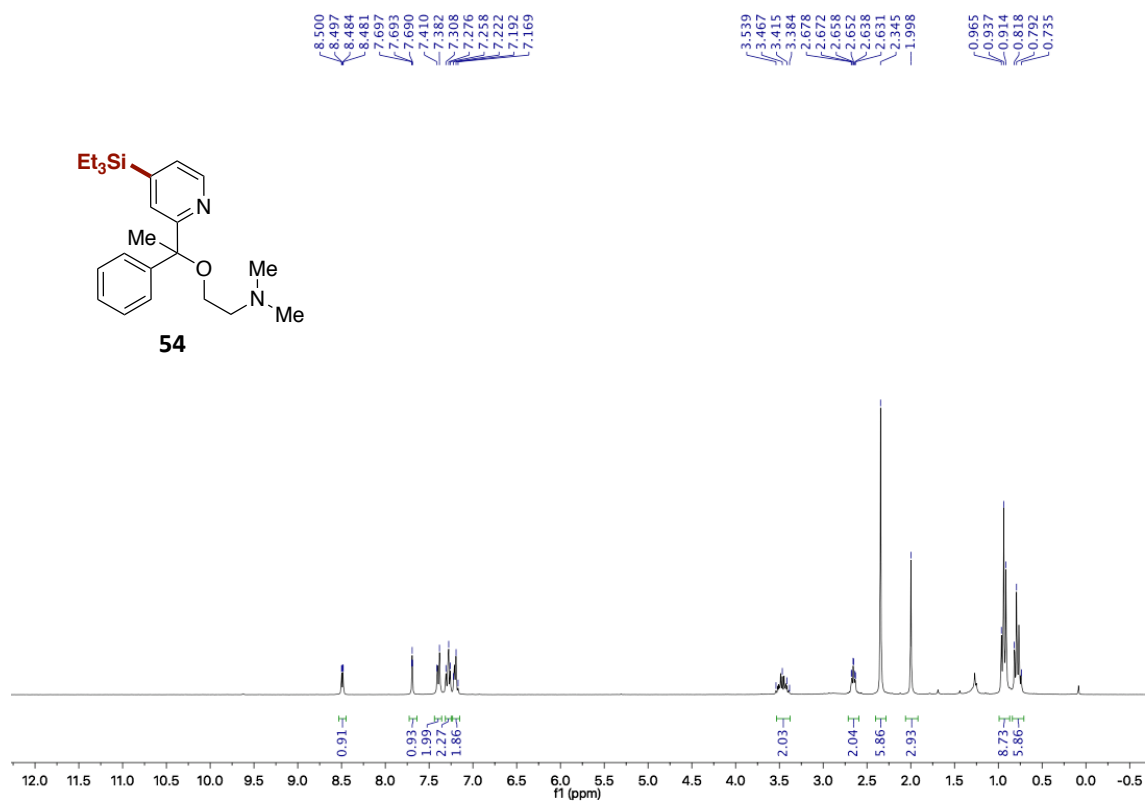
A Mild and Site-Selective sp^2 C-H Silylation of (Poly)Azines



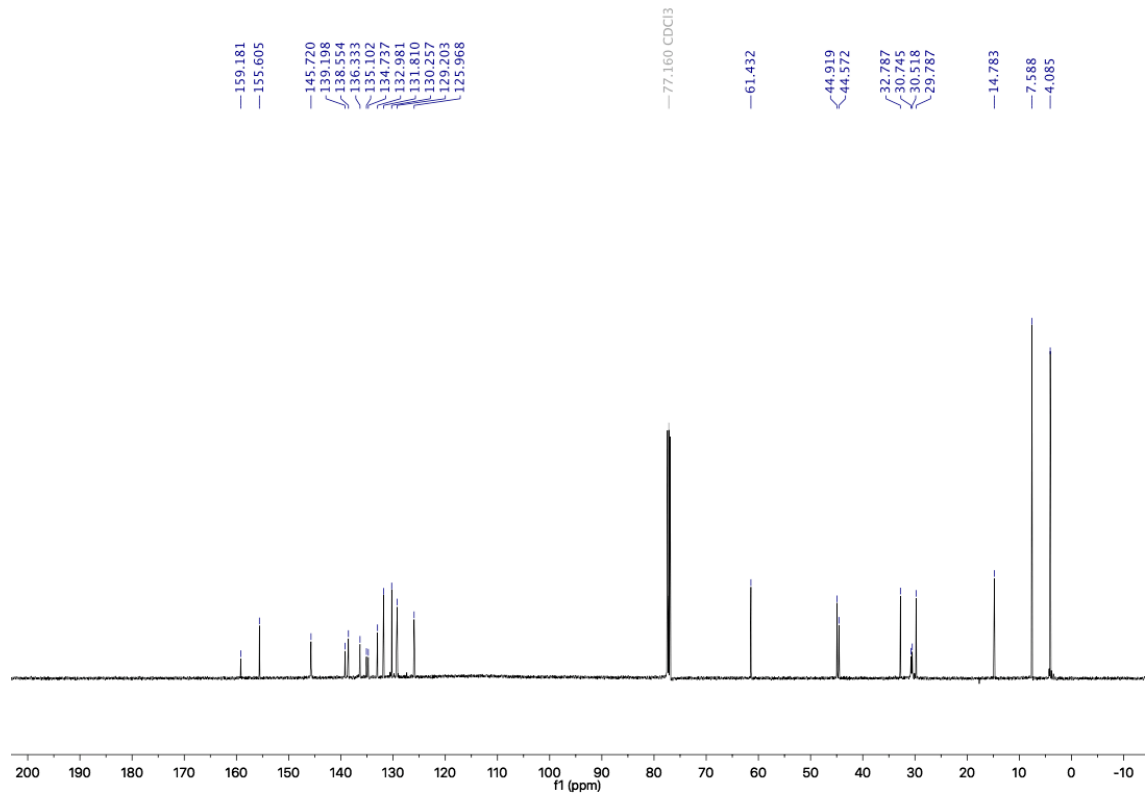
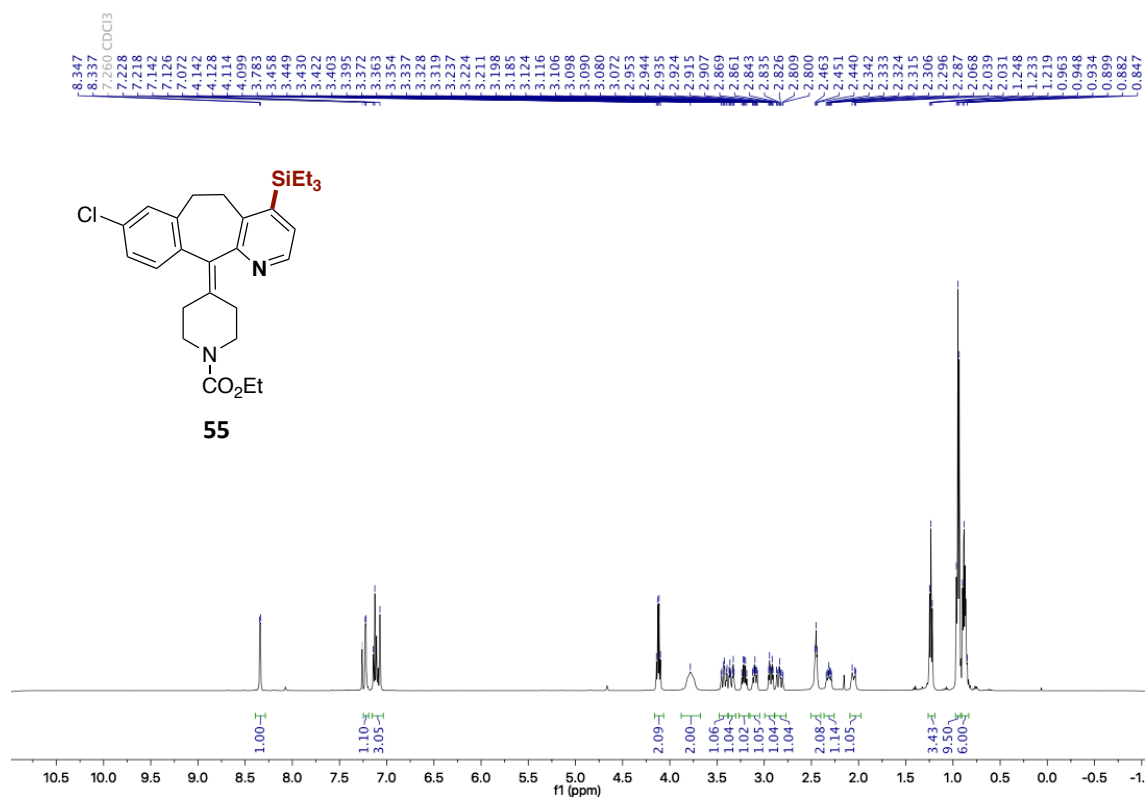


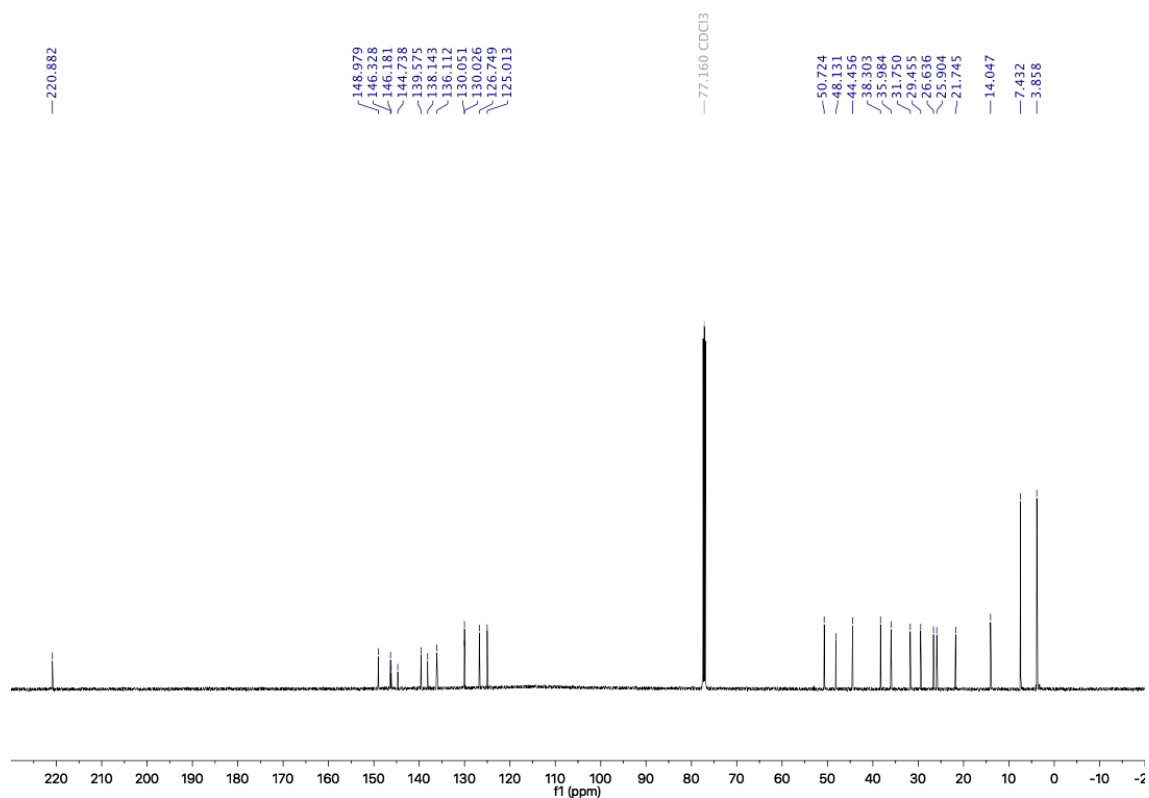
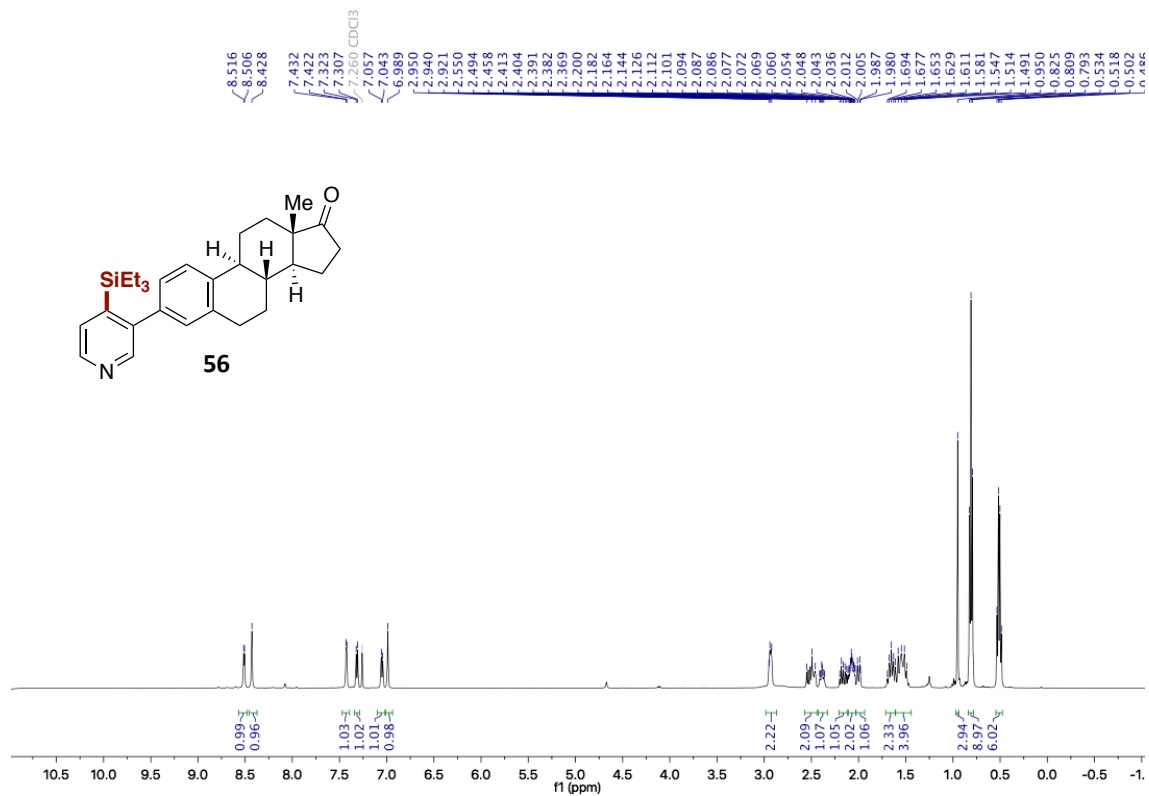
A Mild and Site-Selective sp^2 C-H Silylation of (Poly)Azines



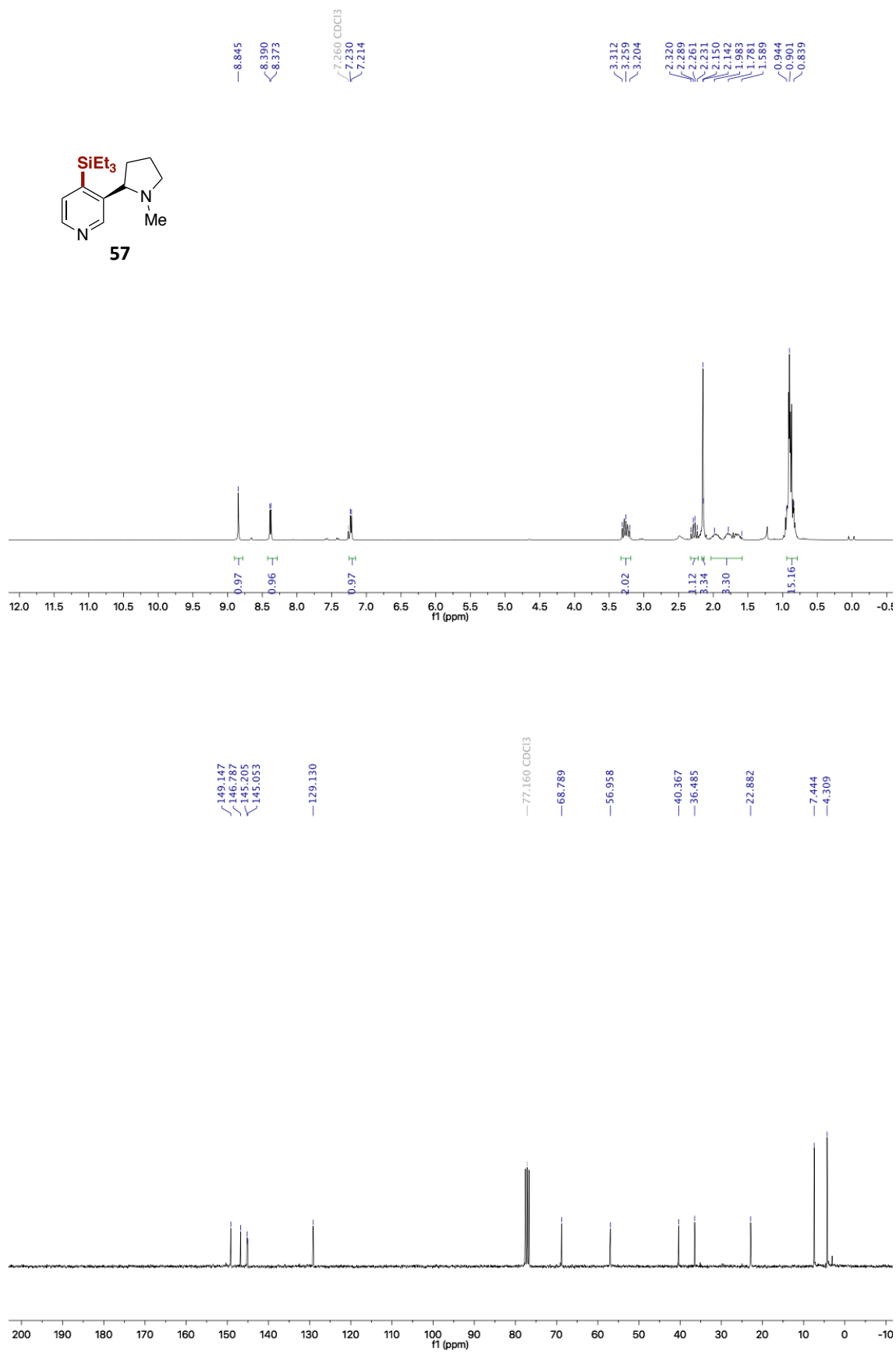


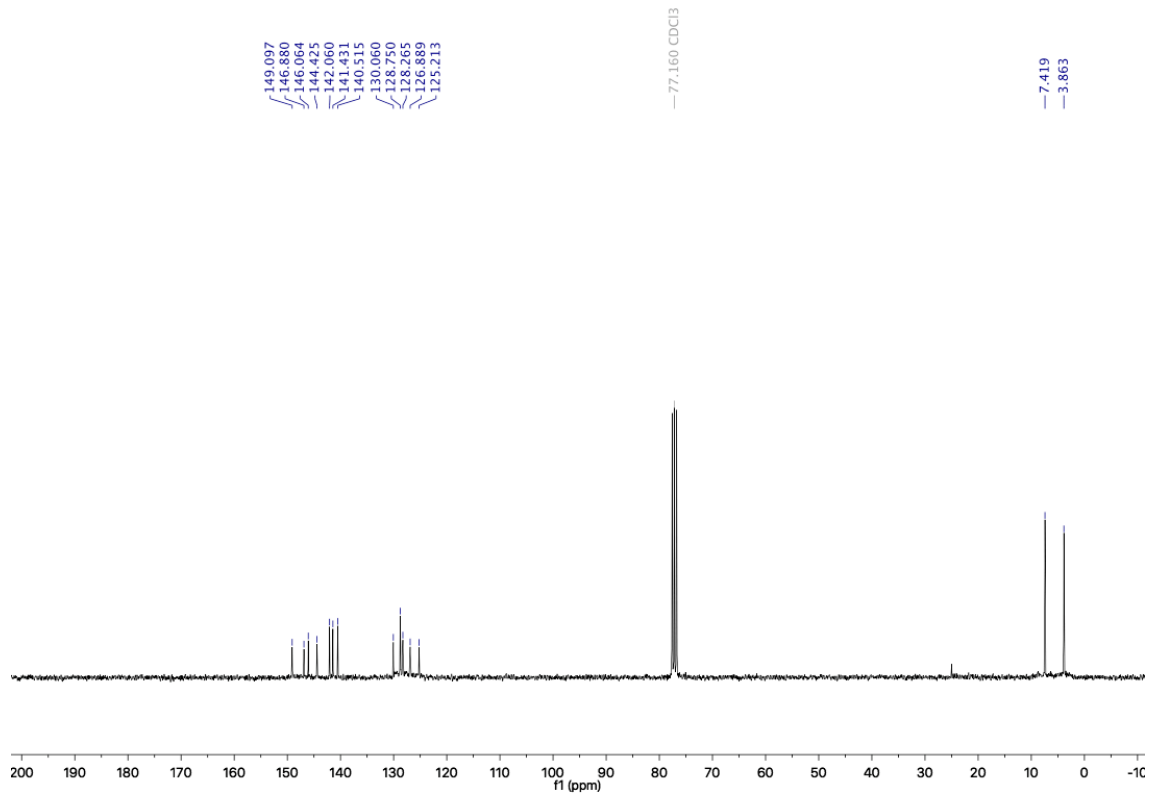
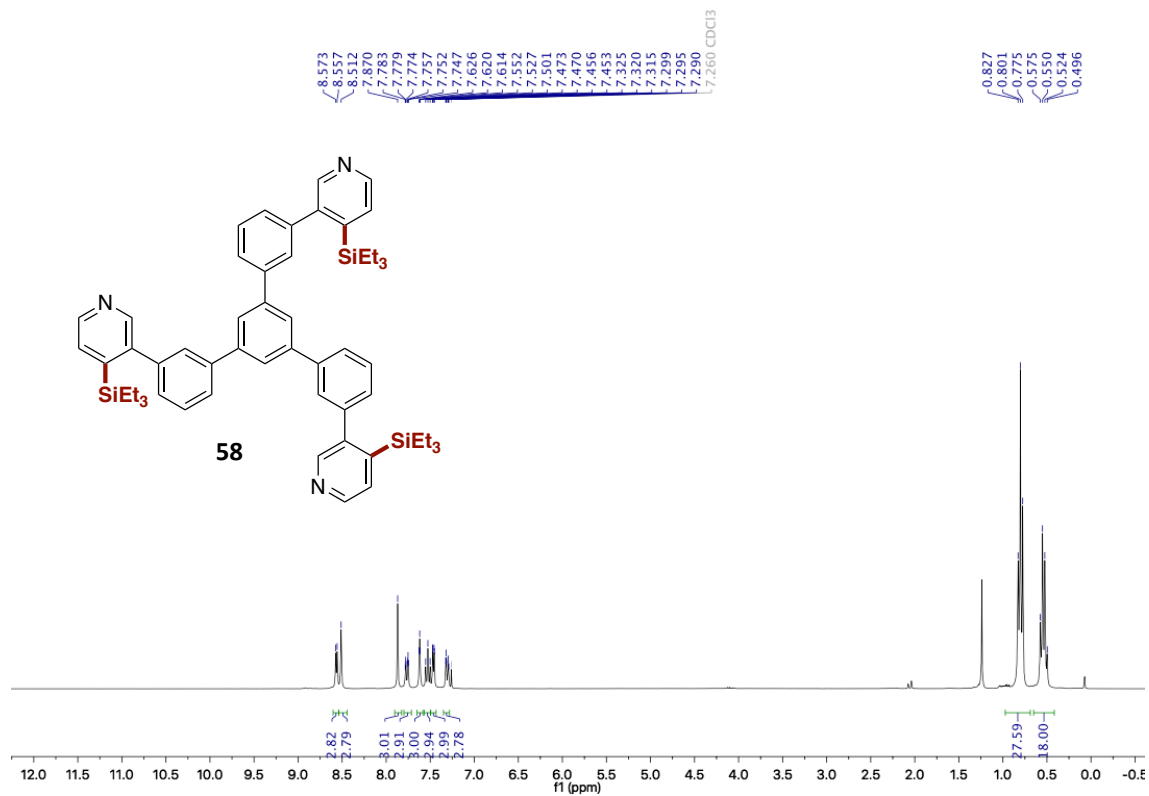
A Mild and Site-Selective sp^2 C-H Silylation of (Poly)Azines



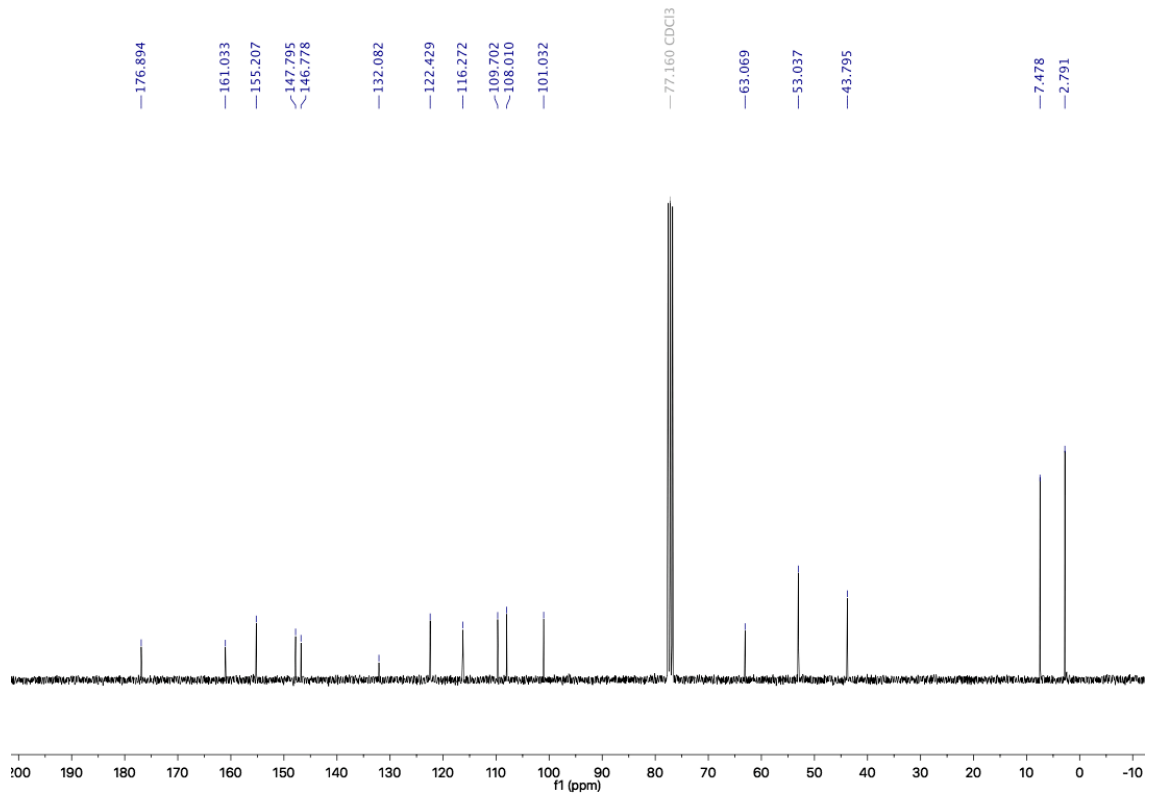
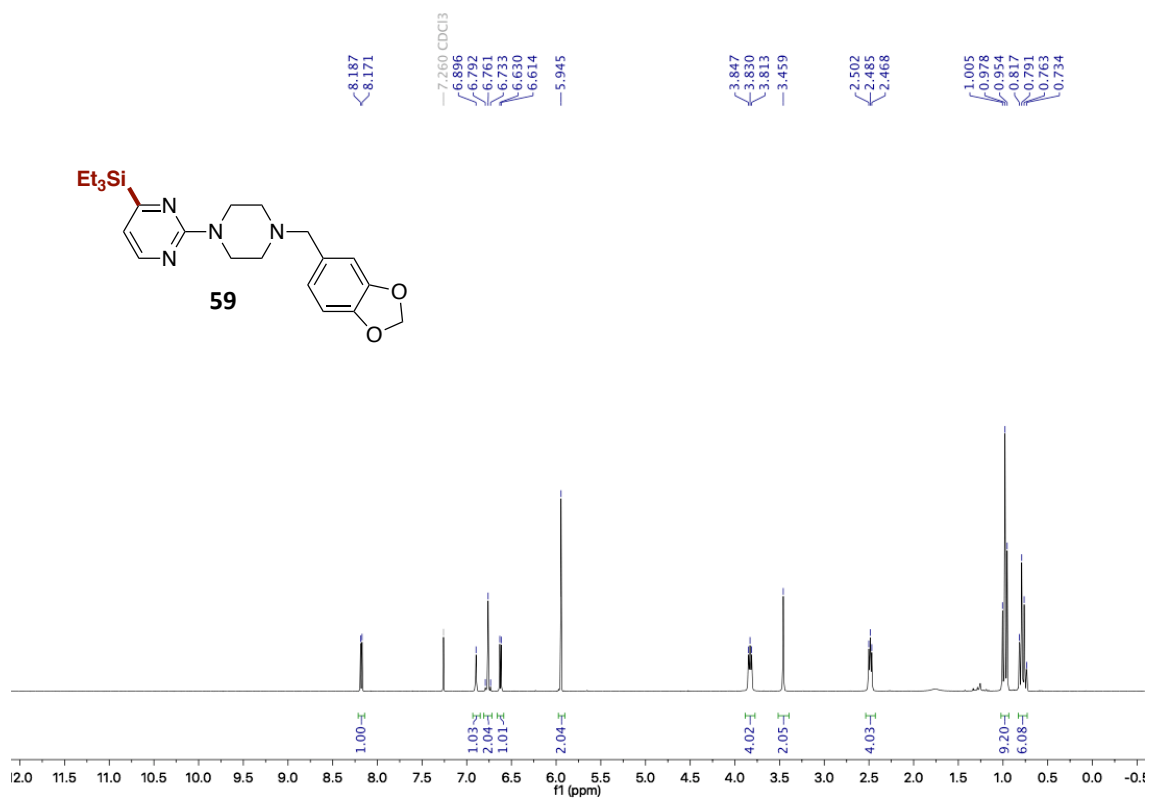


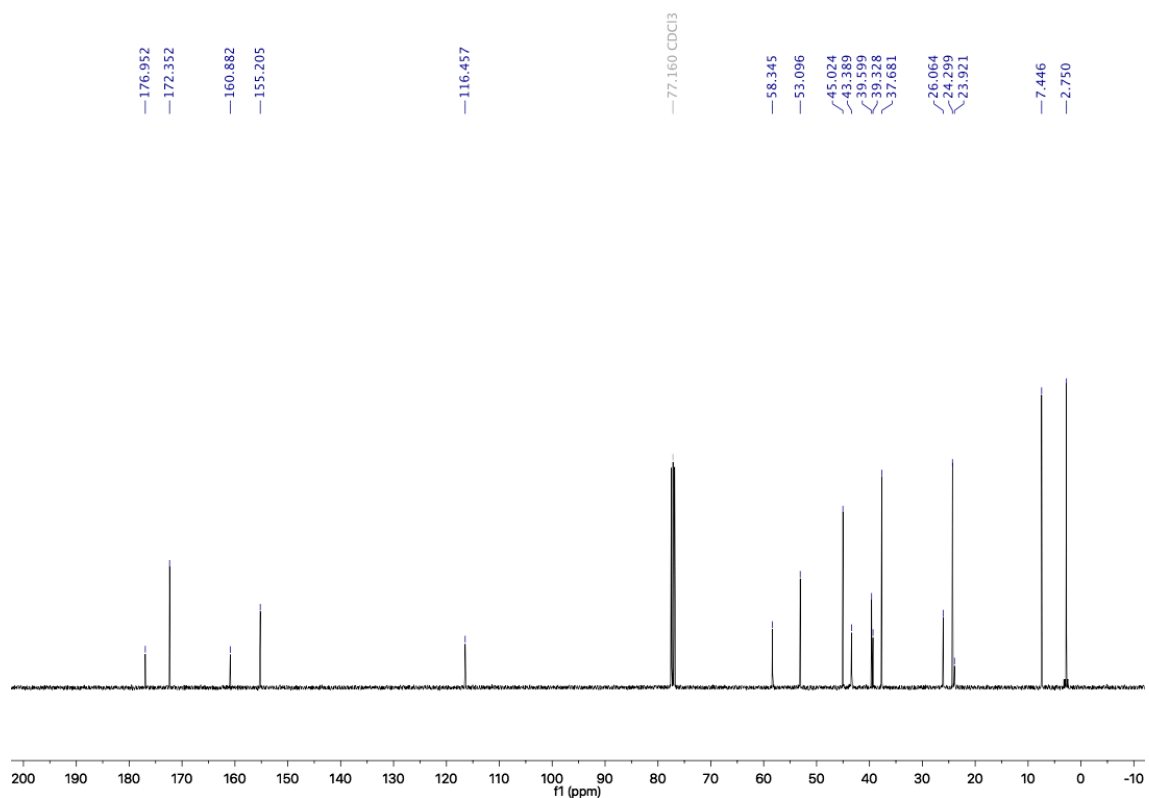
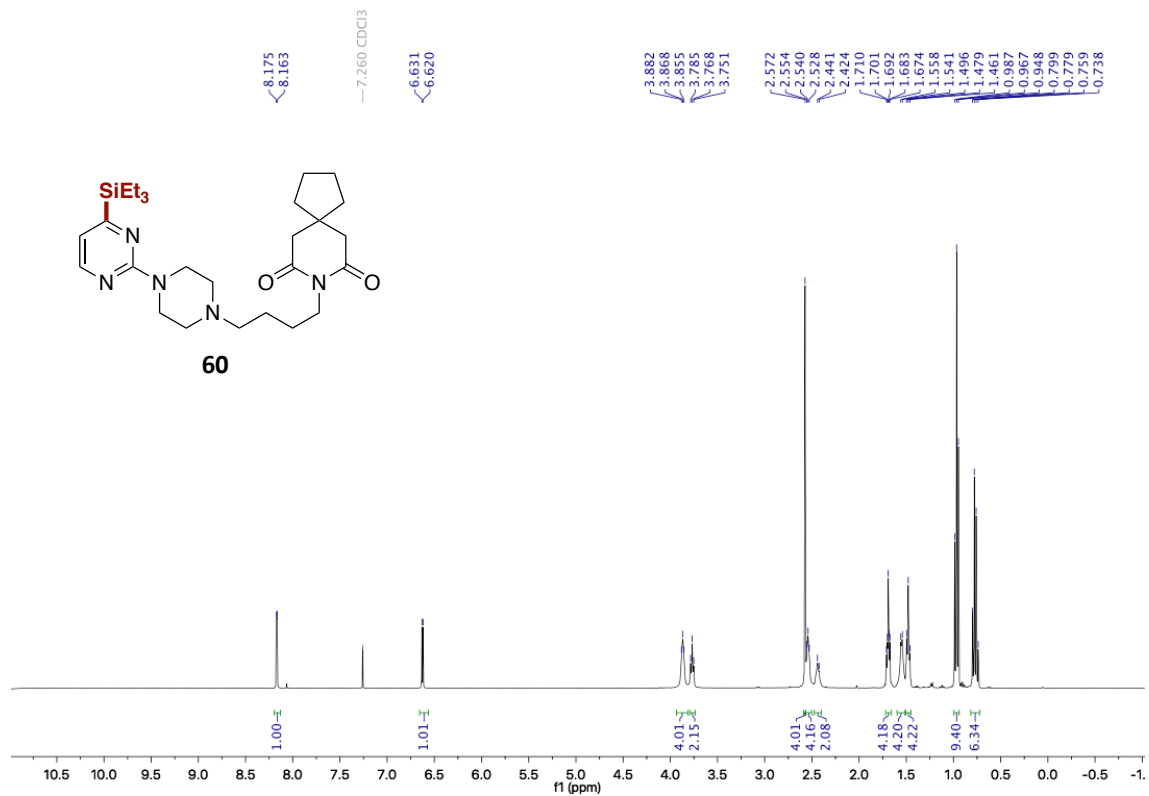
A Mild and Site-Selective sp^2 C-H Silylation of (Poly)Azines



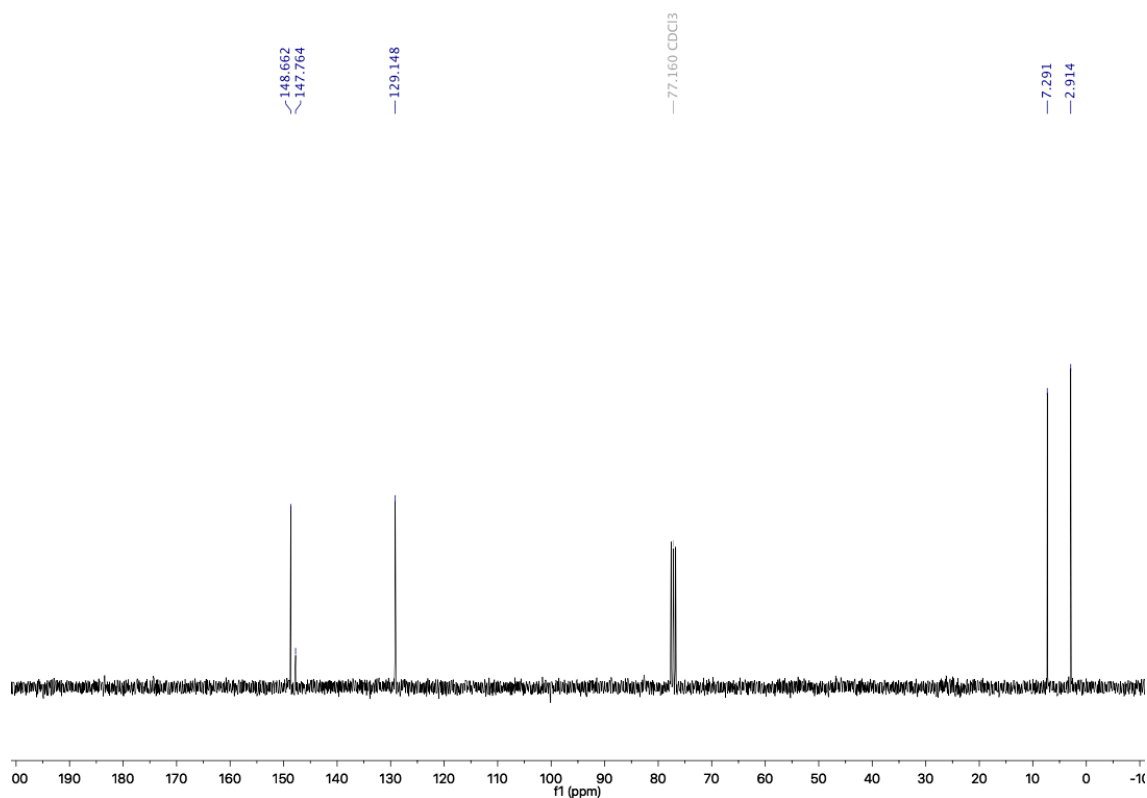
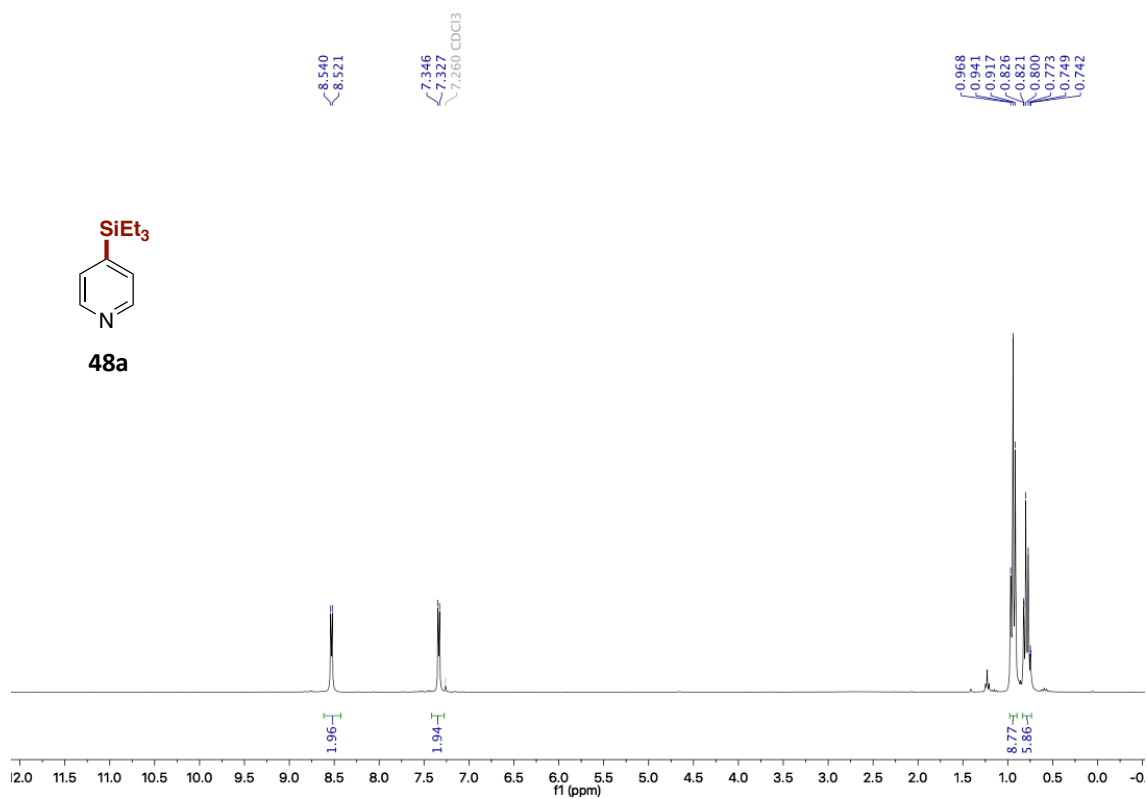


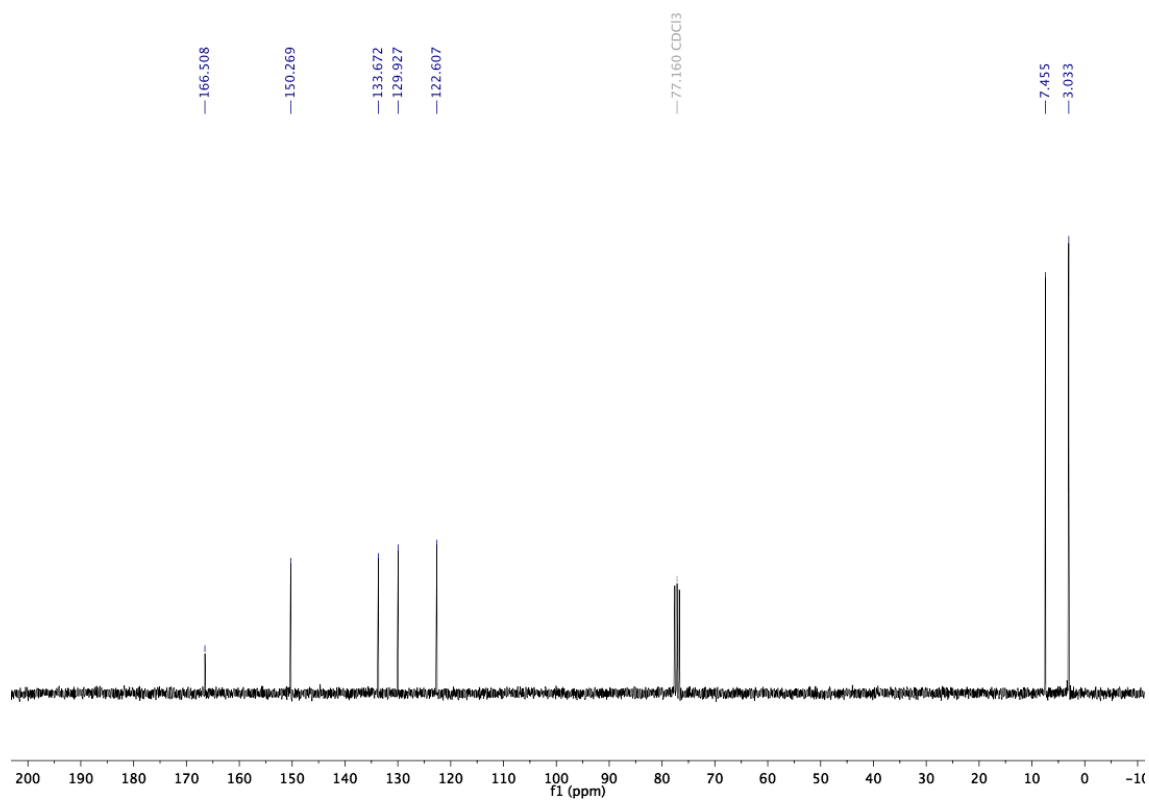
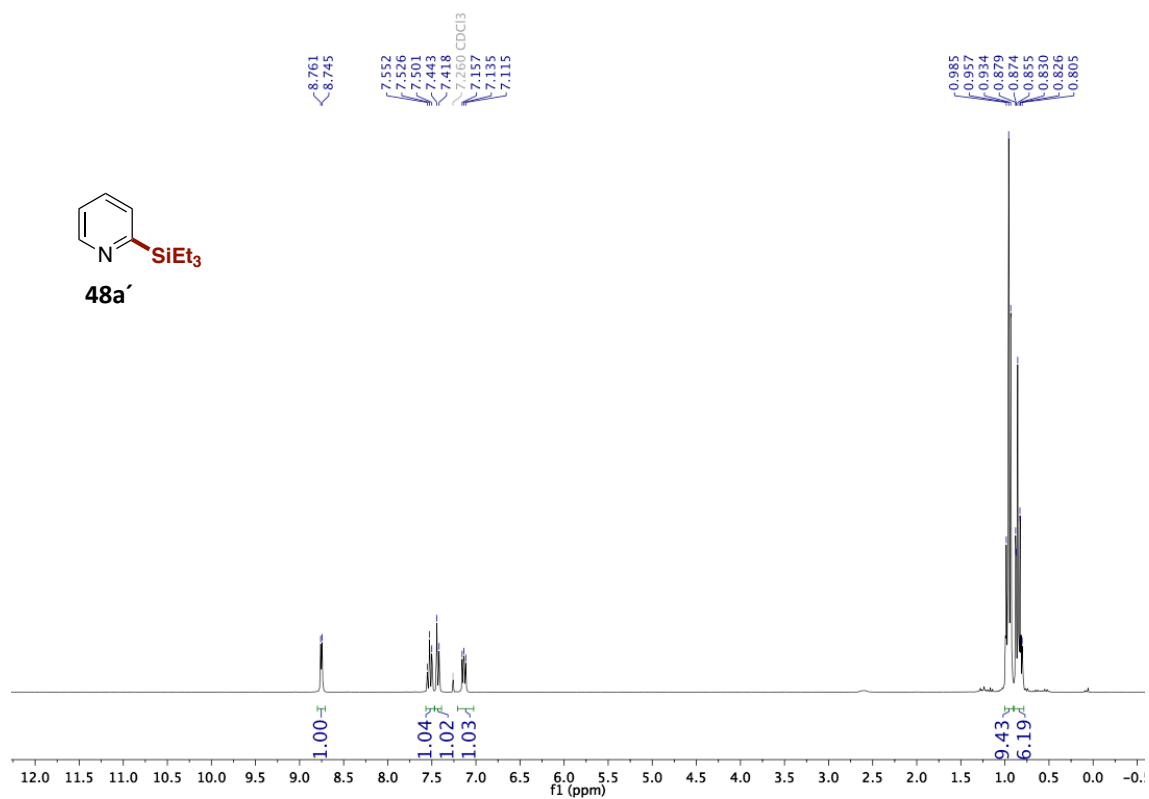
A Mild and Site-Selective sp^2 C-H Silylation of (Poly)Azines



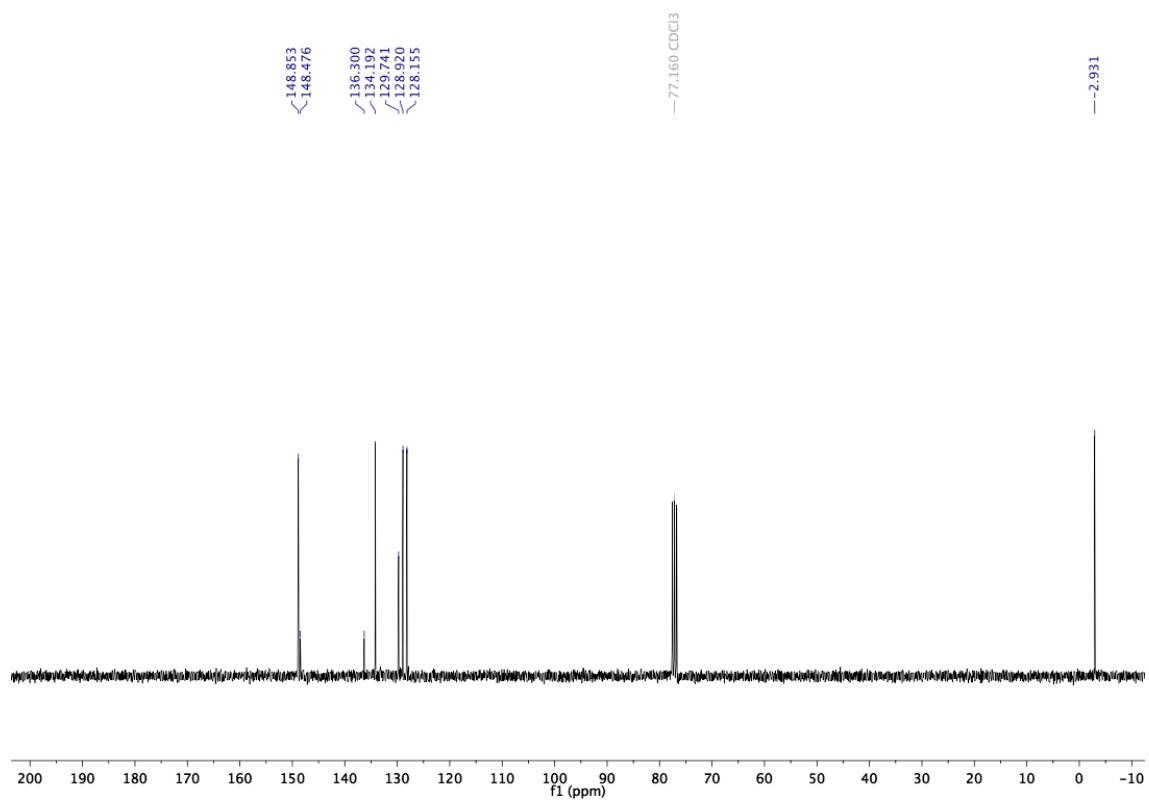
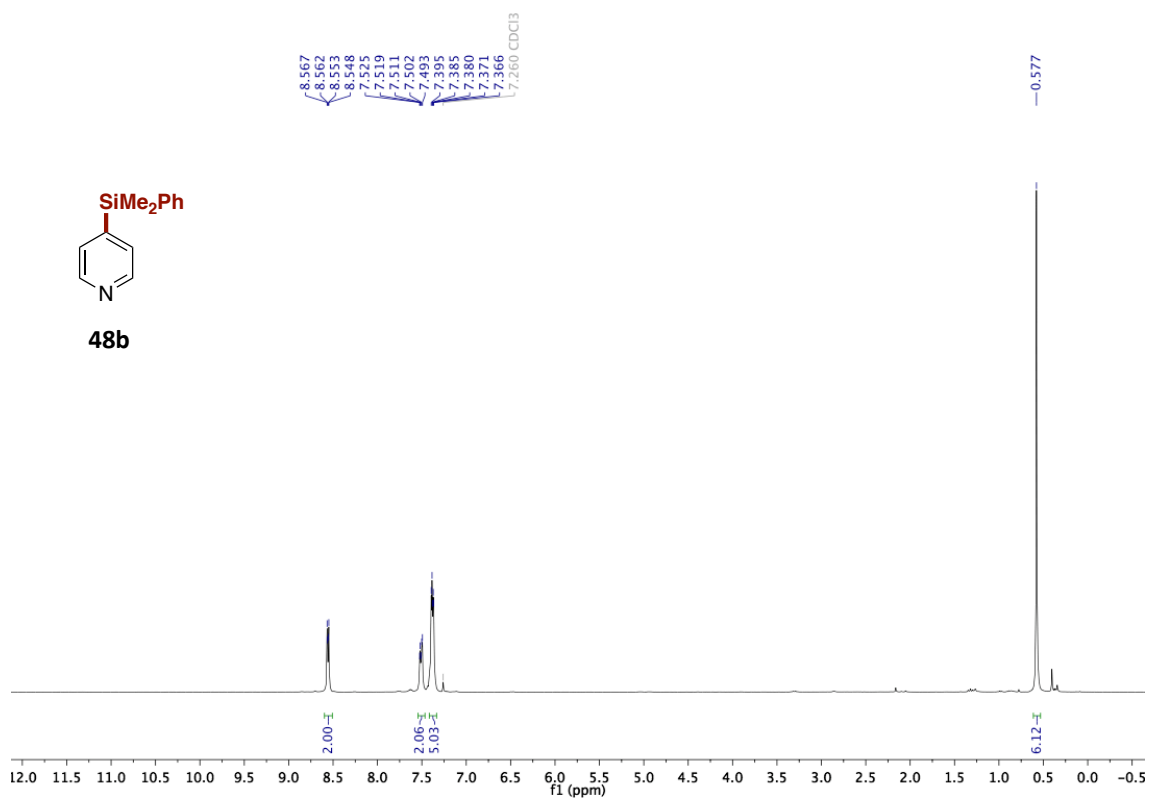


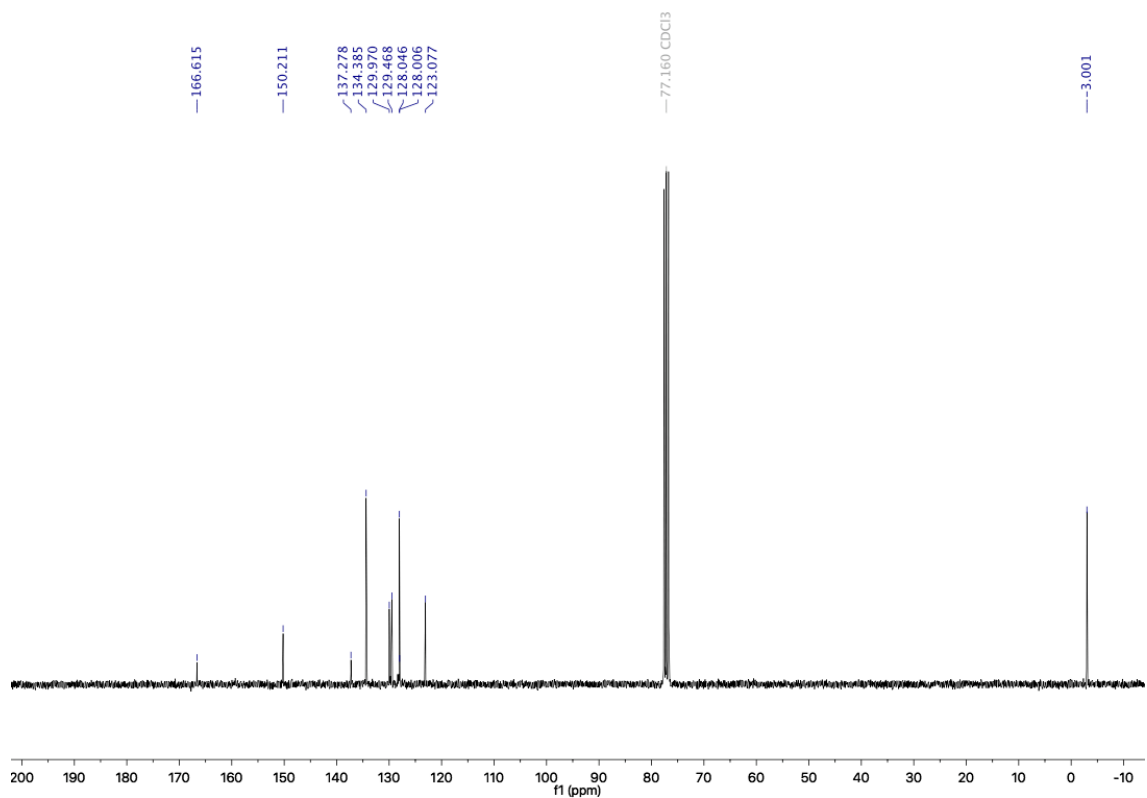
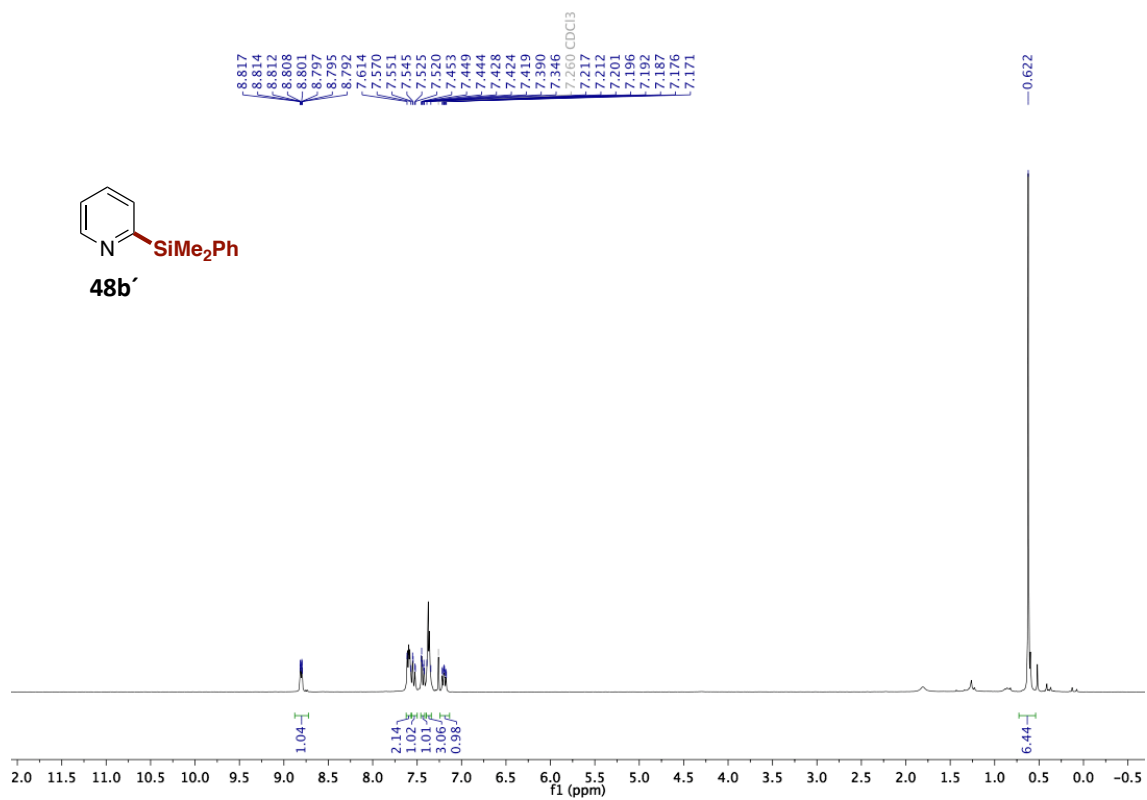
A Mild and Site-Selective sp^2 C-H Silylation of (Poly)azines



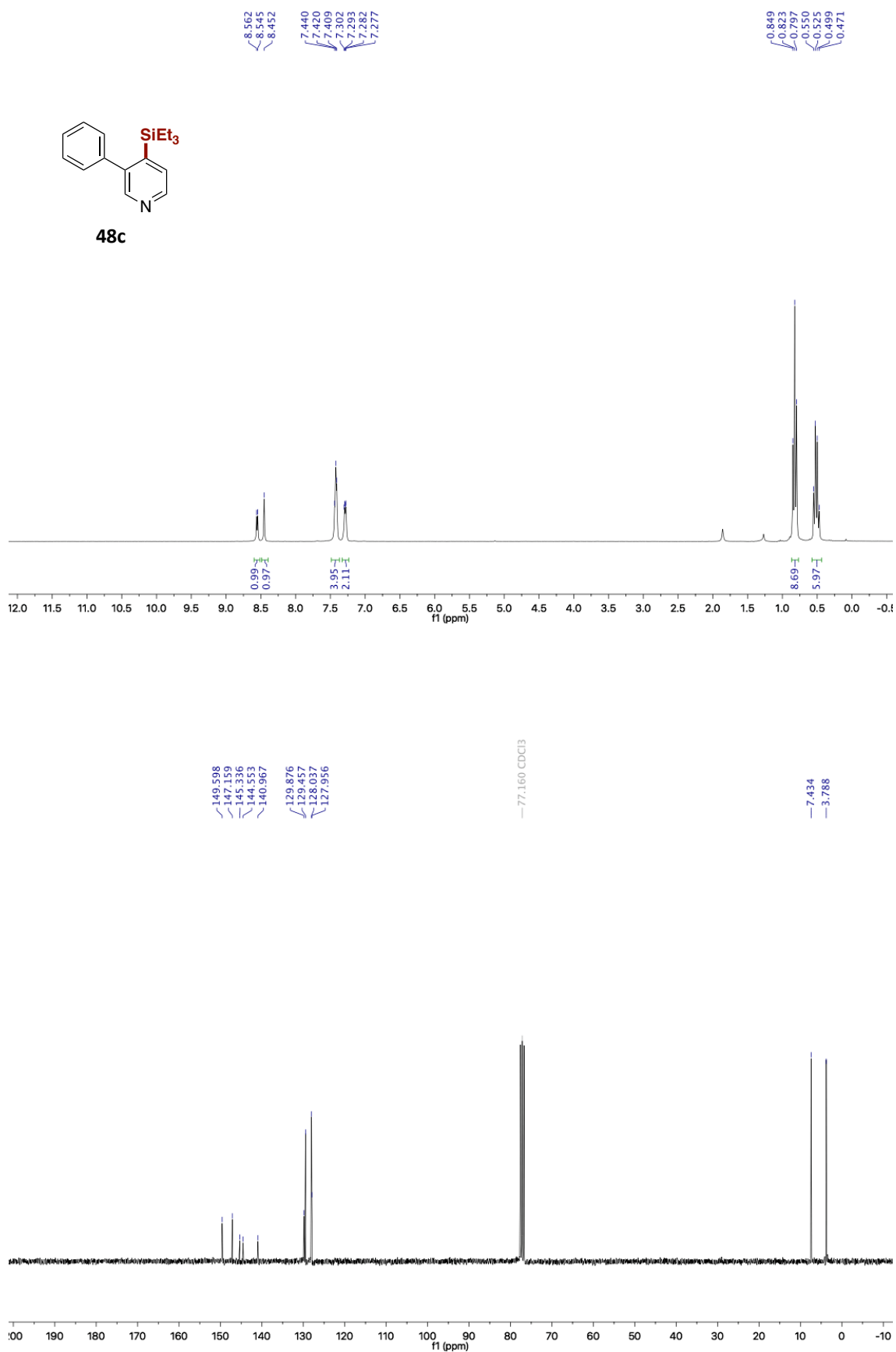


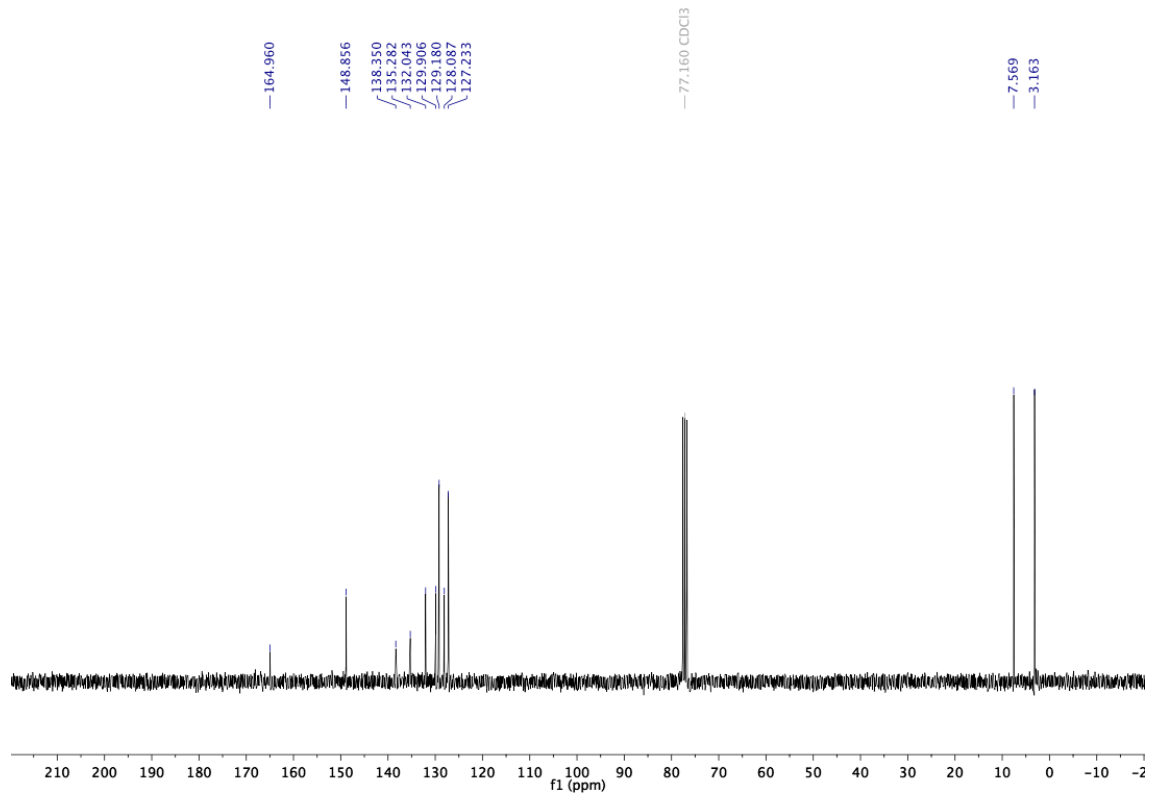
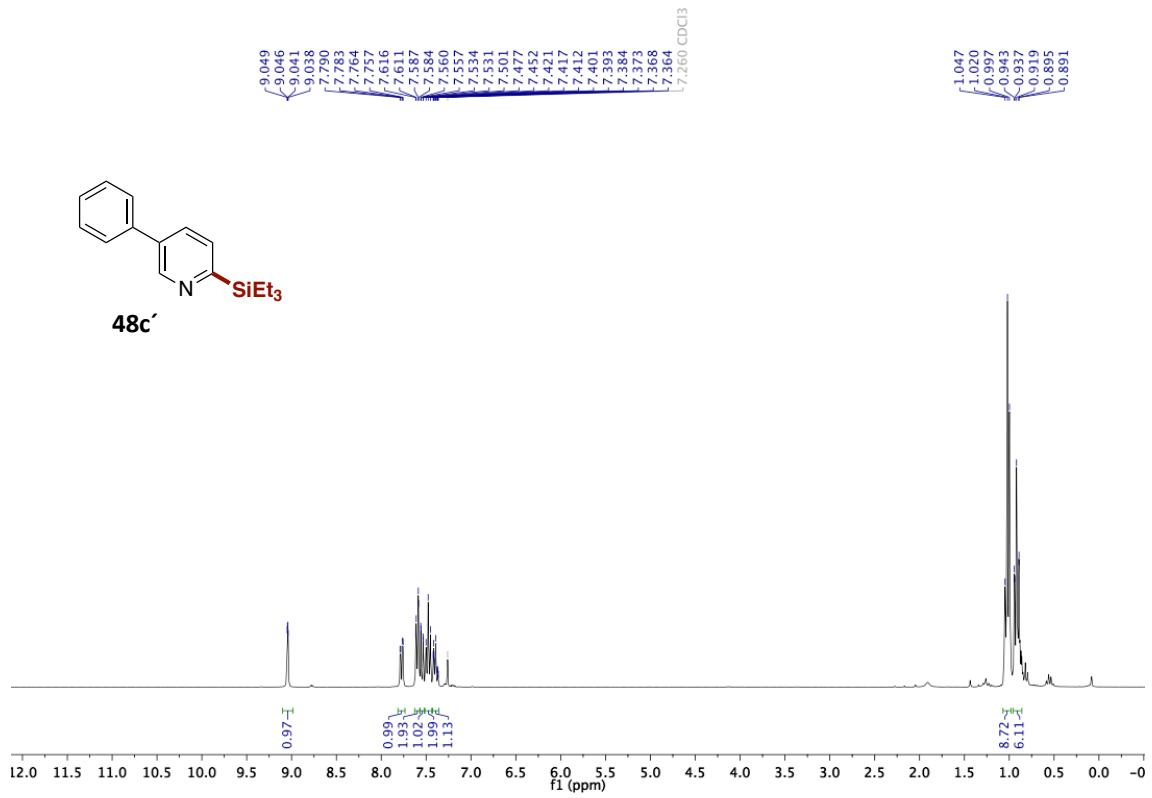
A Mild and Site-Selective sp^2 C-H Silylation of (Poly)Azines



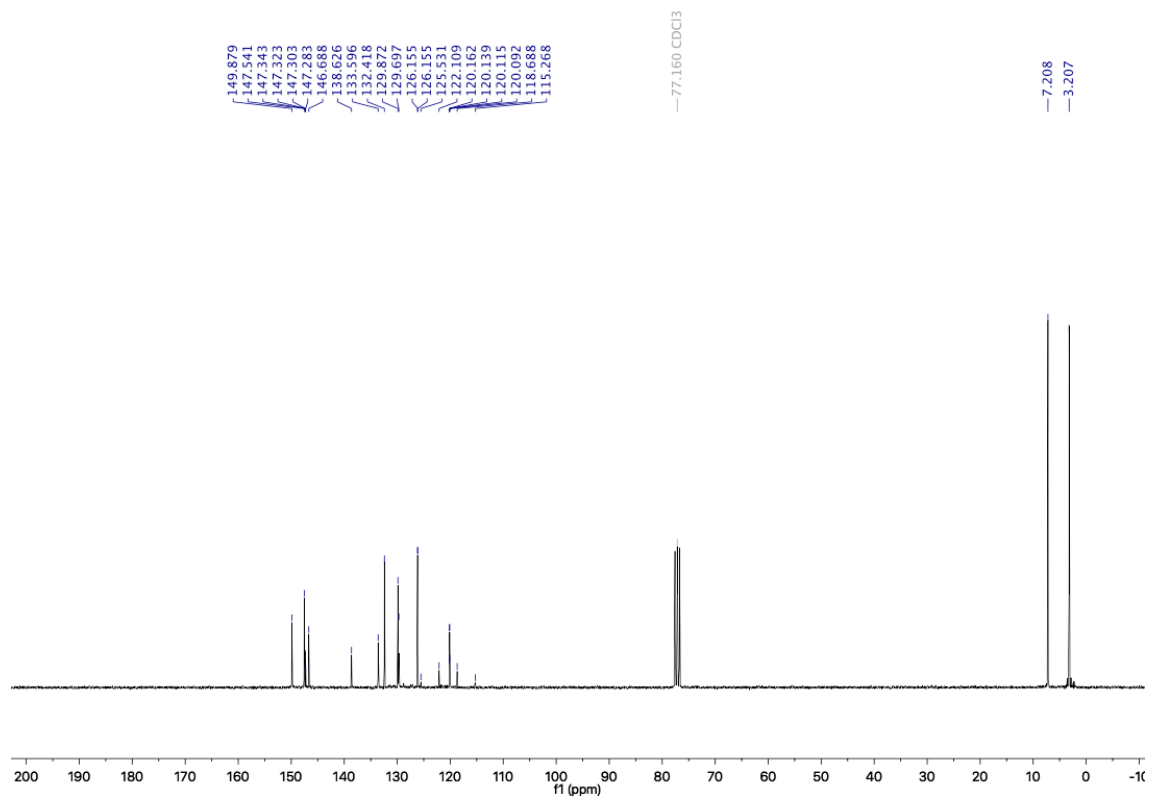
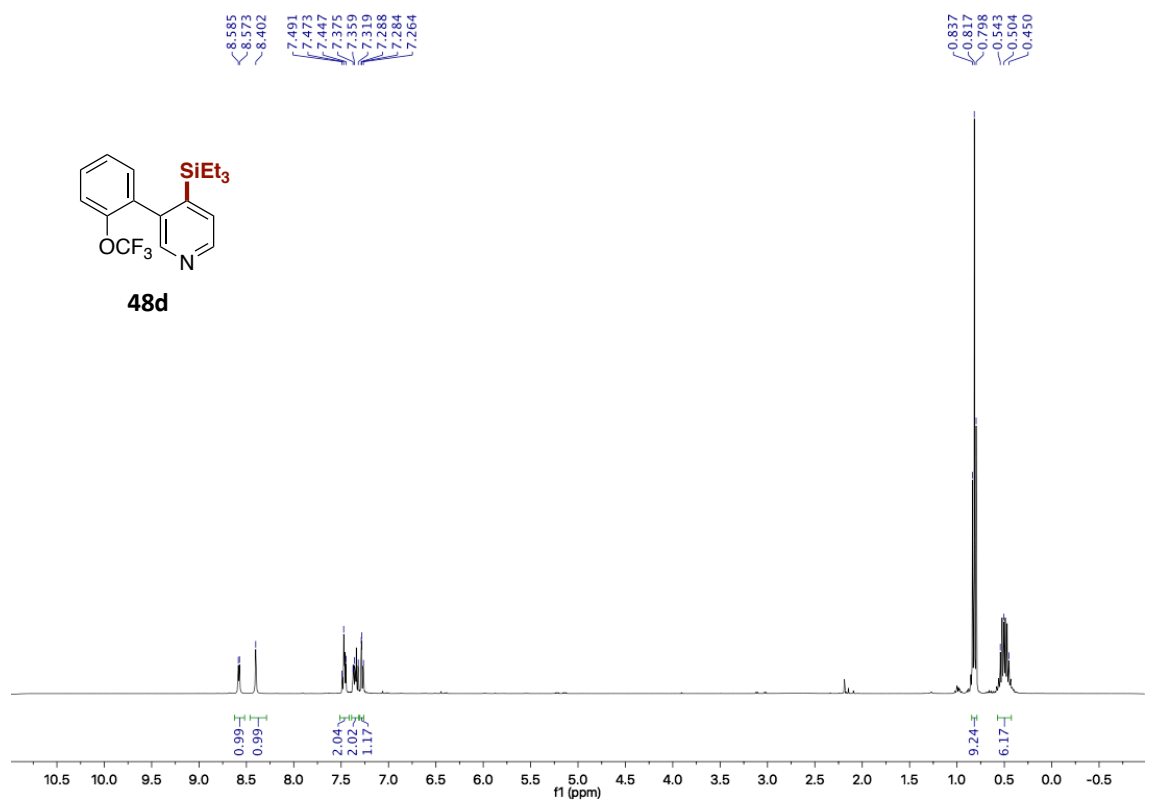


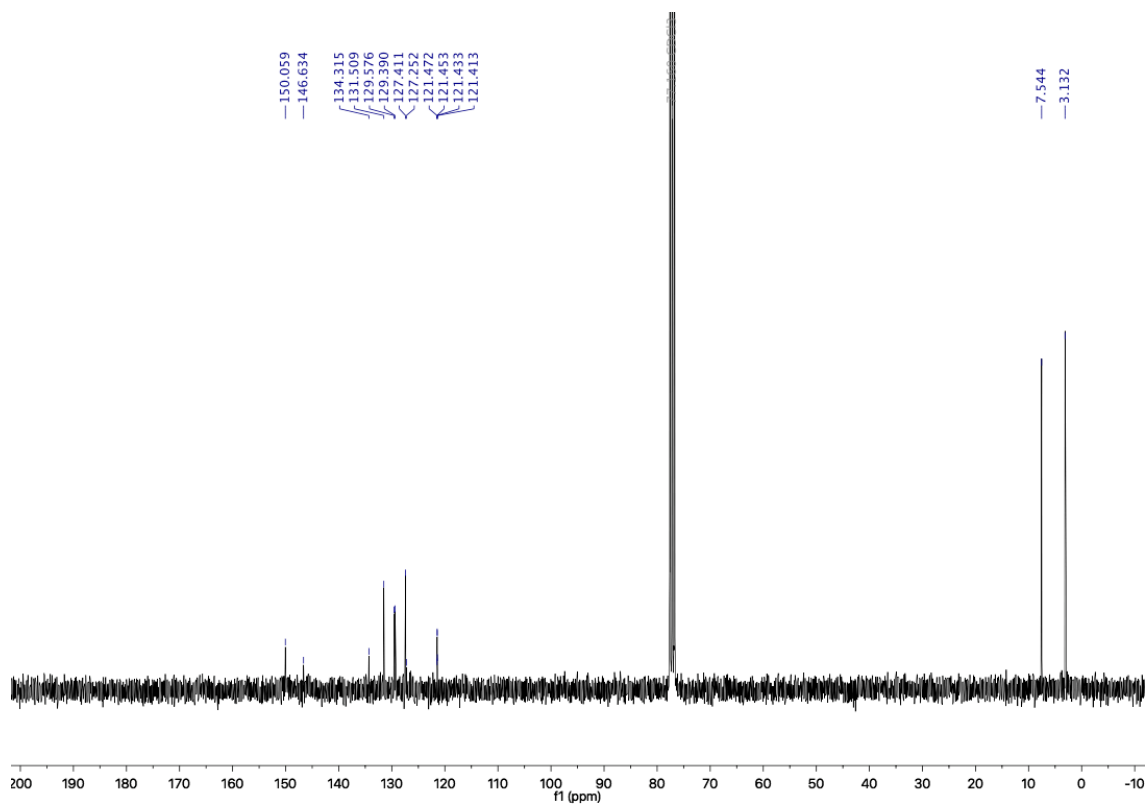
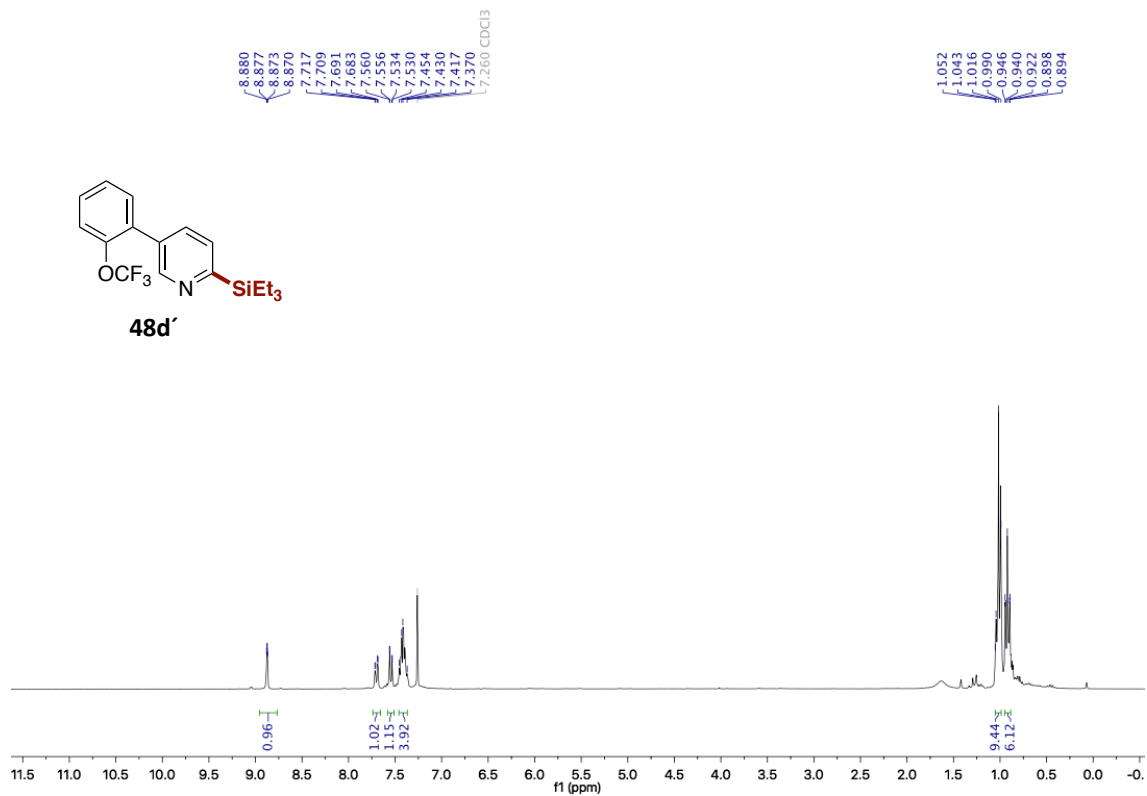
A Mild and Site-Selective sp^2 C-H Silylation of (Poly)Azines



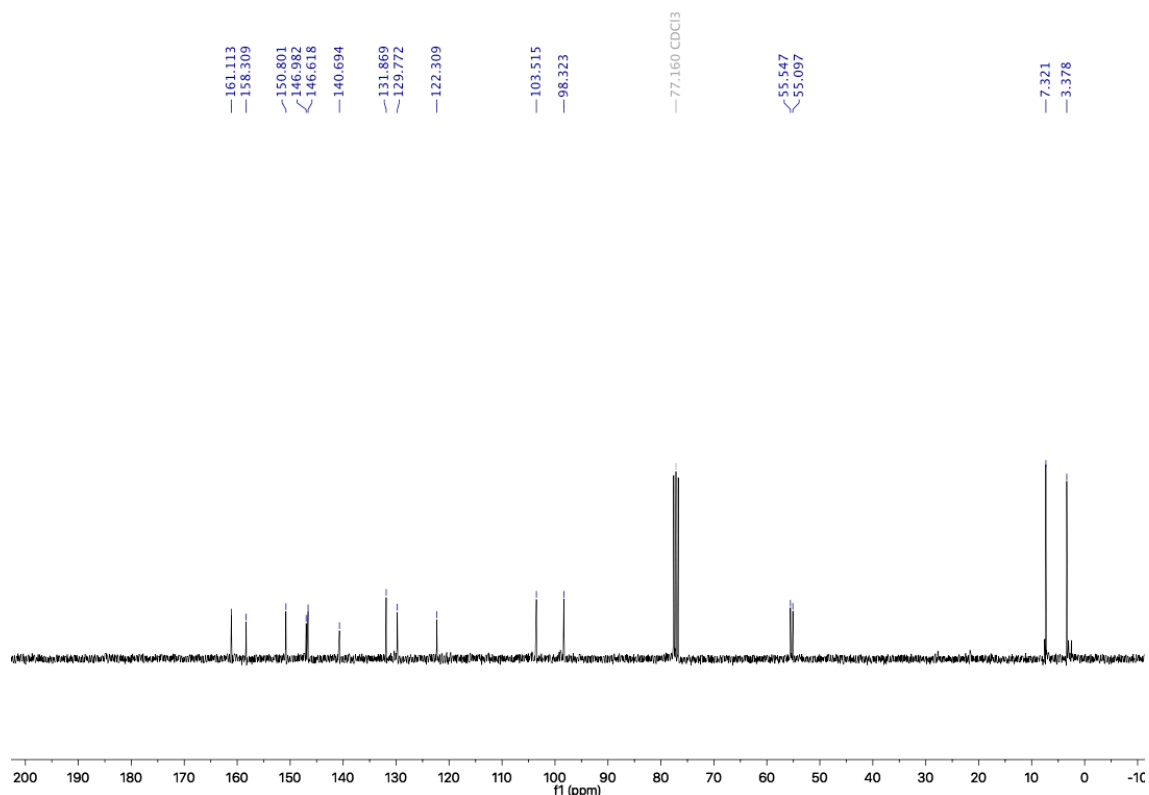
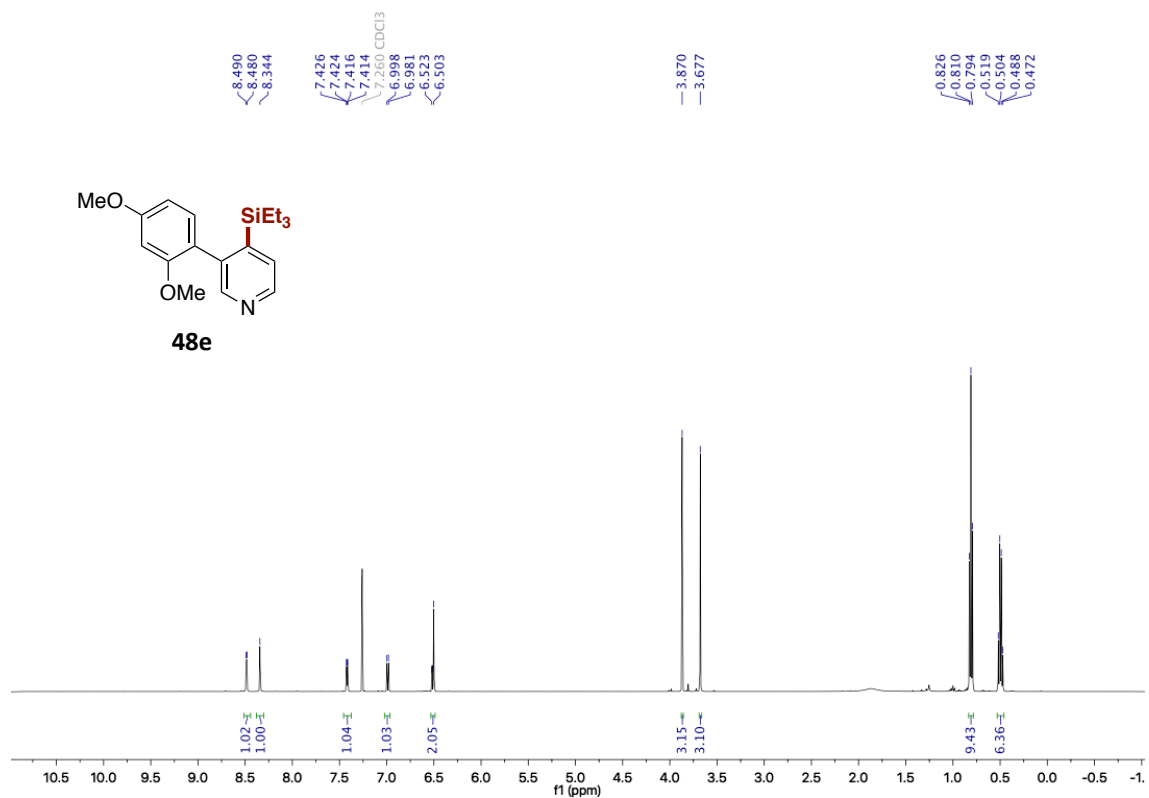


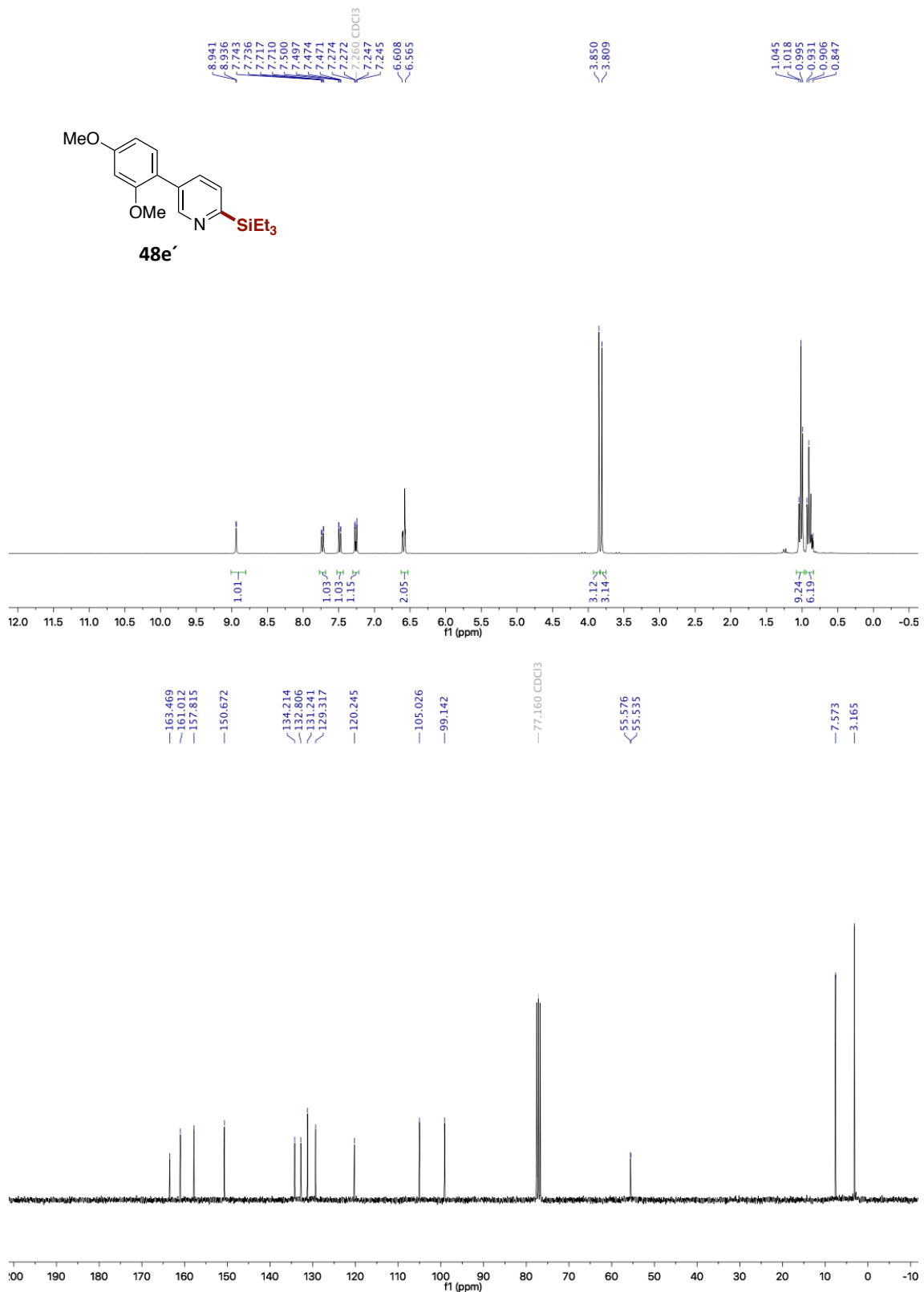
A Mild and Site-Selective sp^2 C-H Silylation of (Poly)Azines



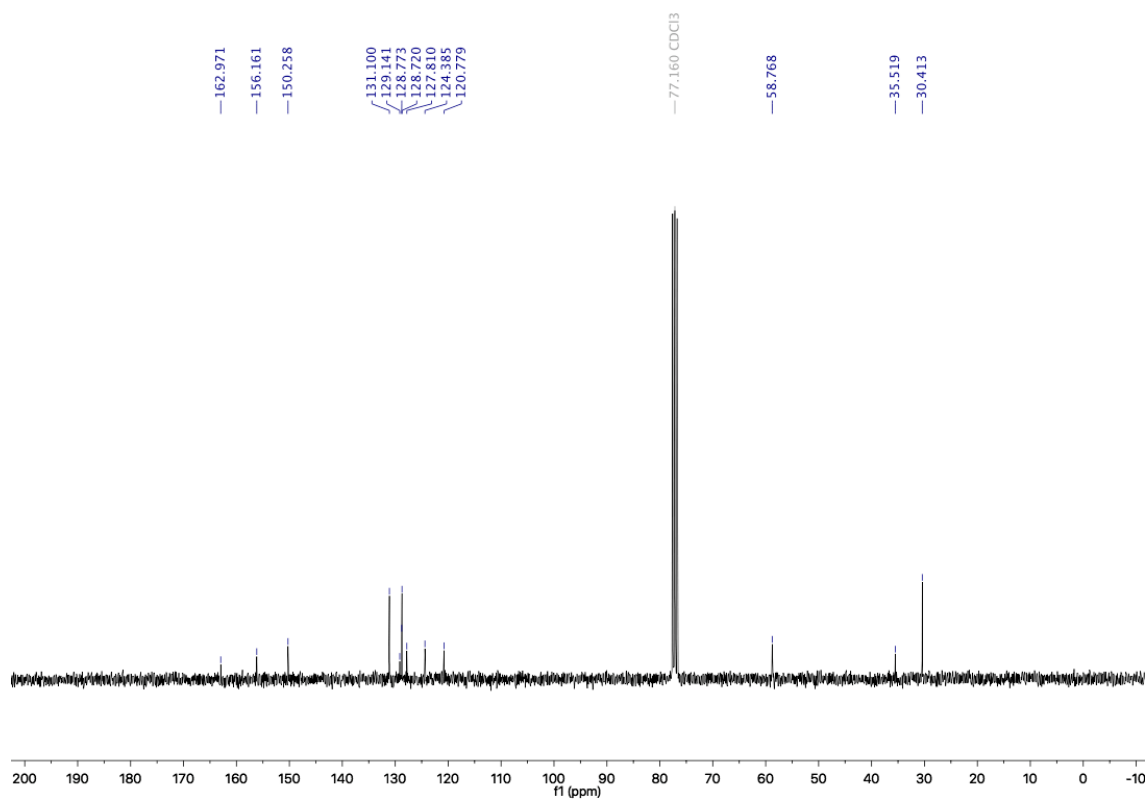
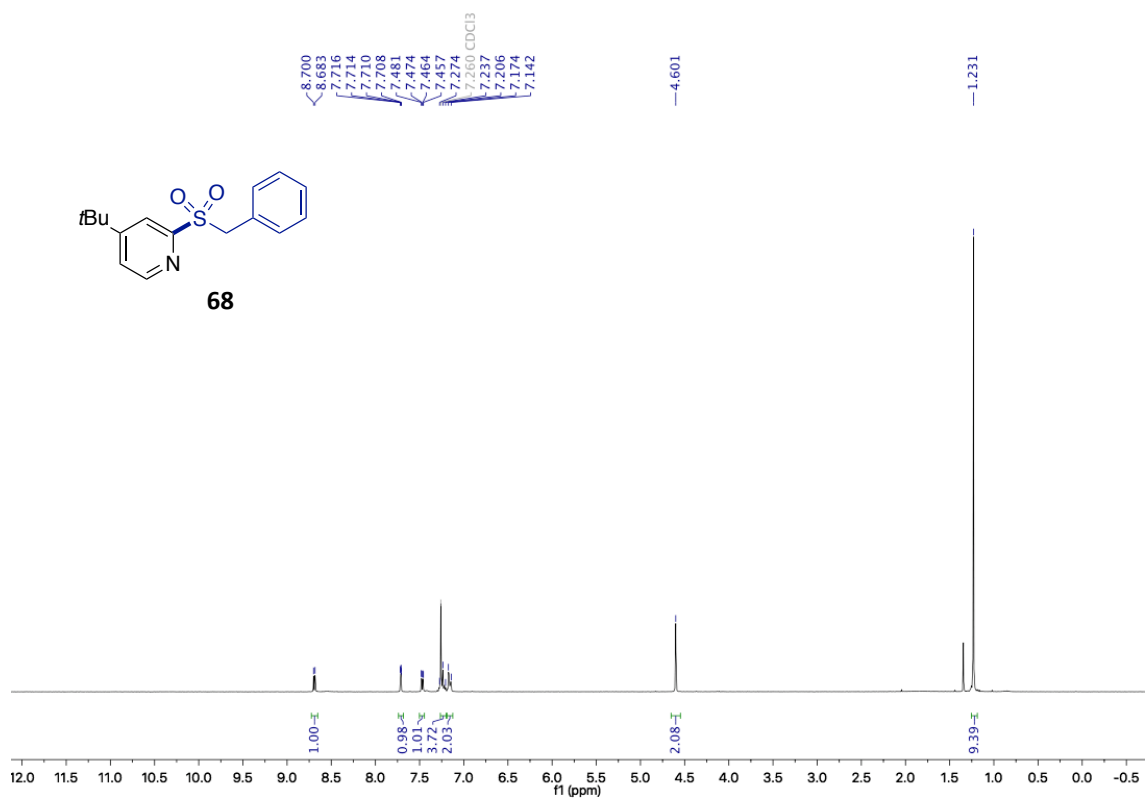


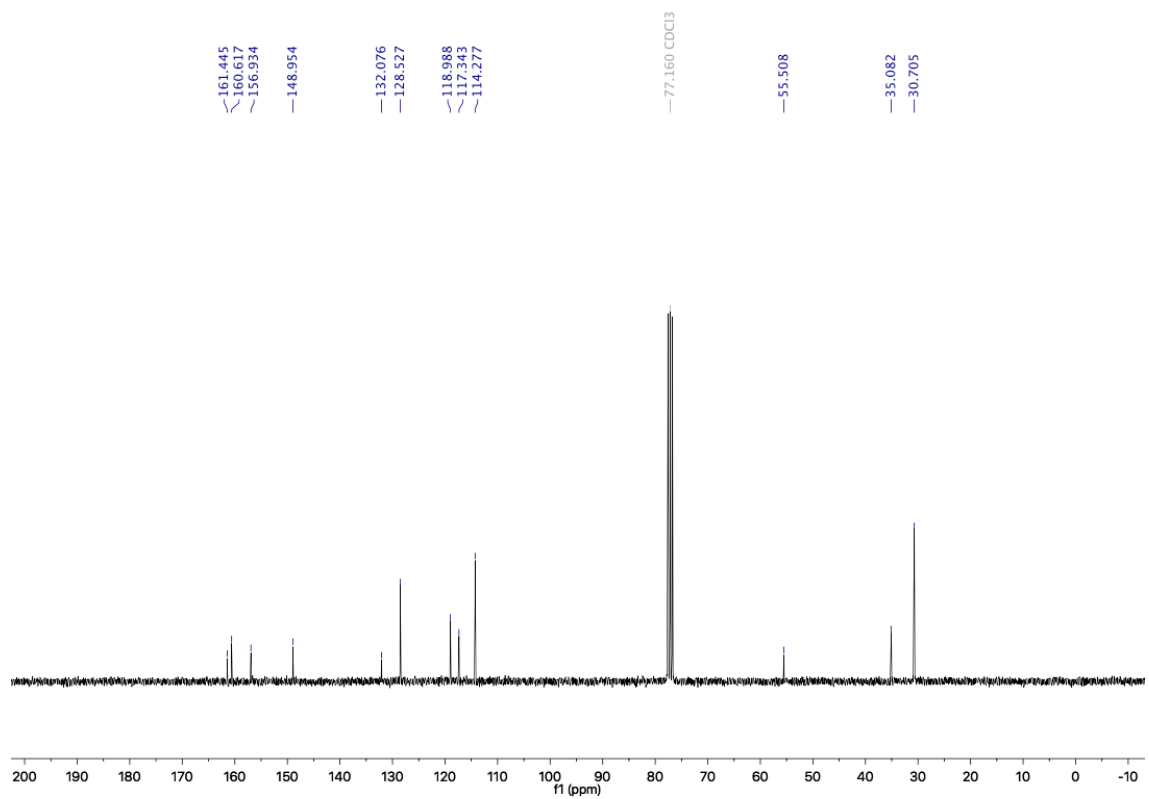
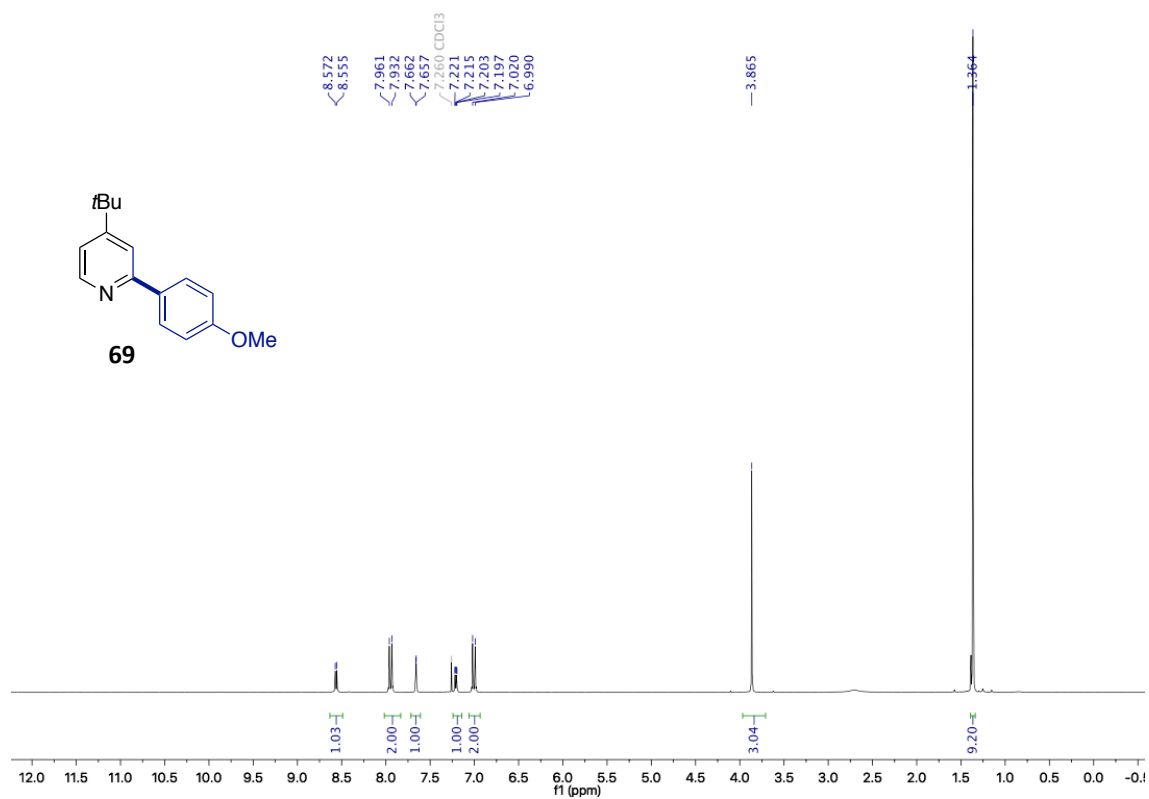
A Mild and Site-Selective sp^2 C-H Silylation of (Poly)Azines



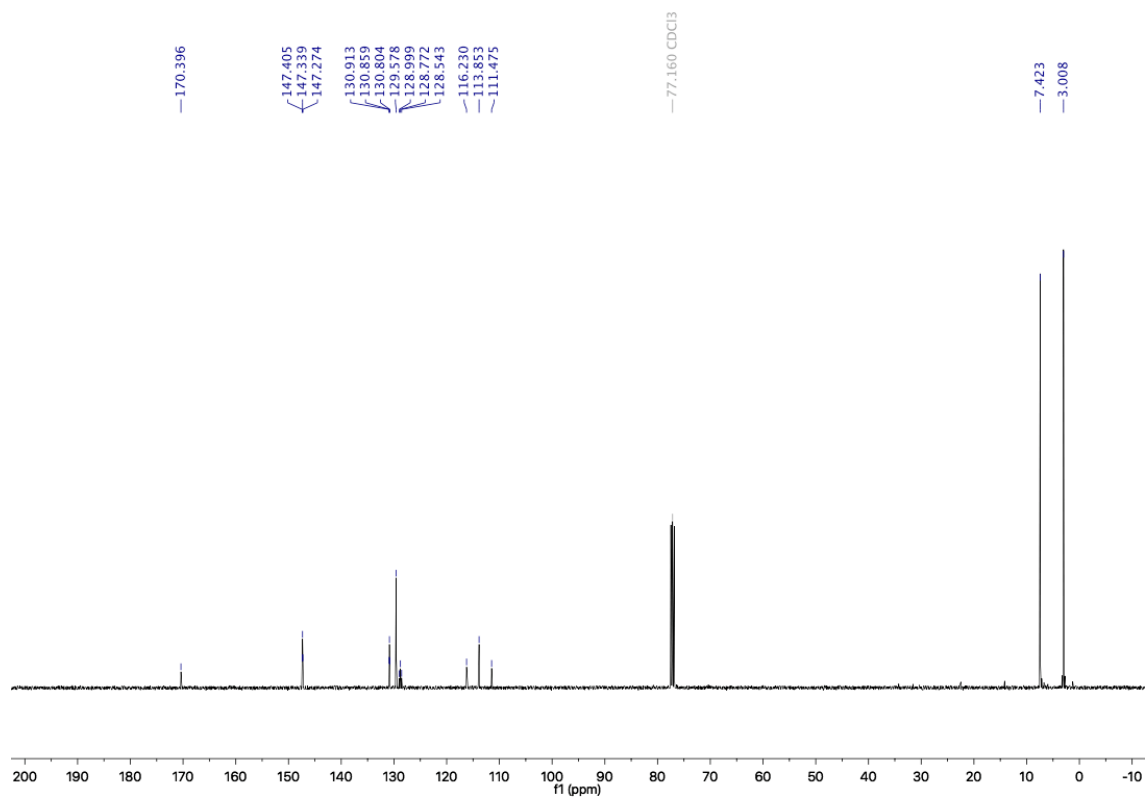
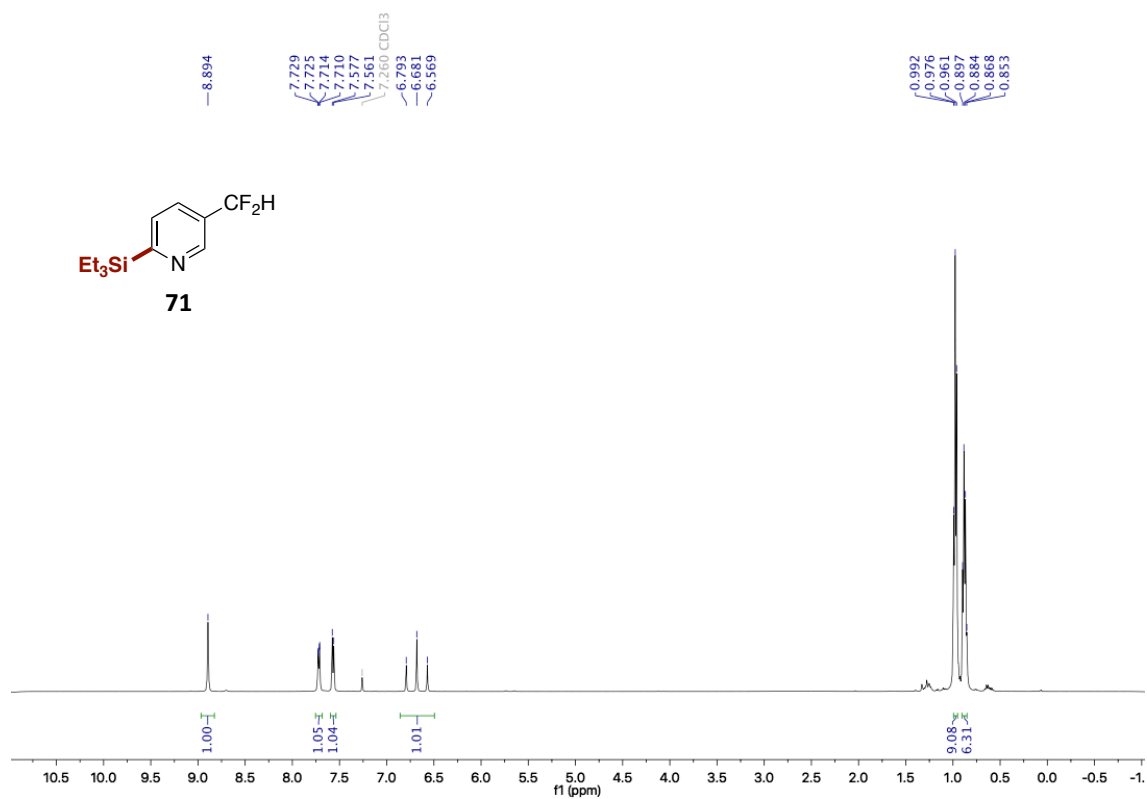


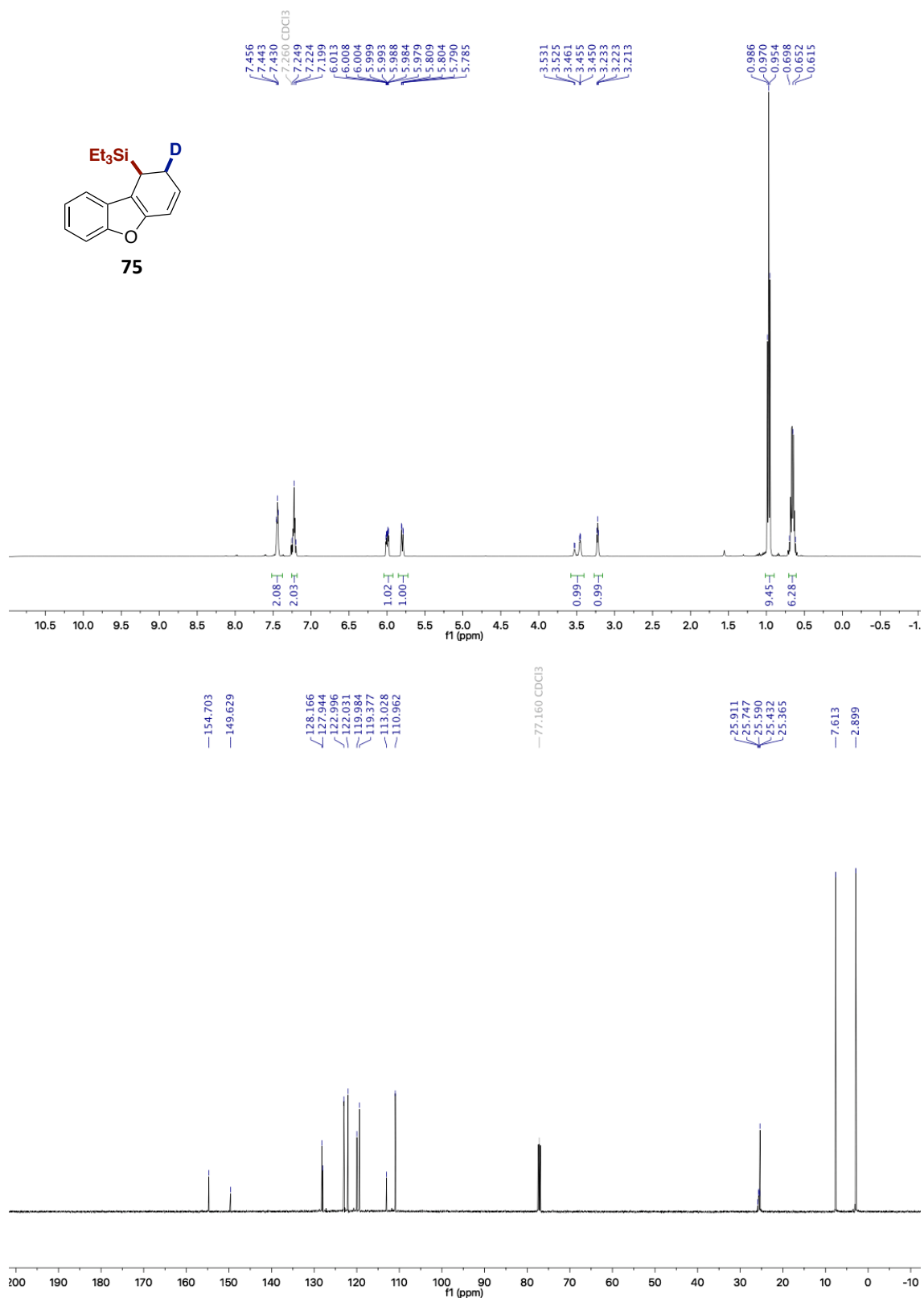
A Mild and Site-Selective sp^2 C-H Silylation of (Poly)Azines



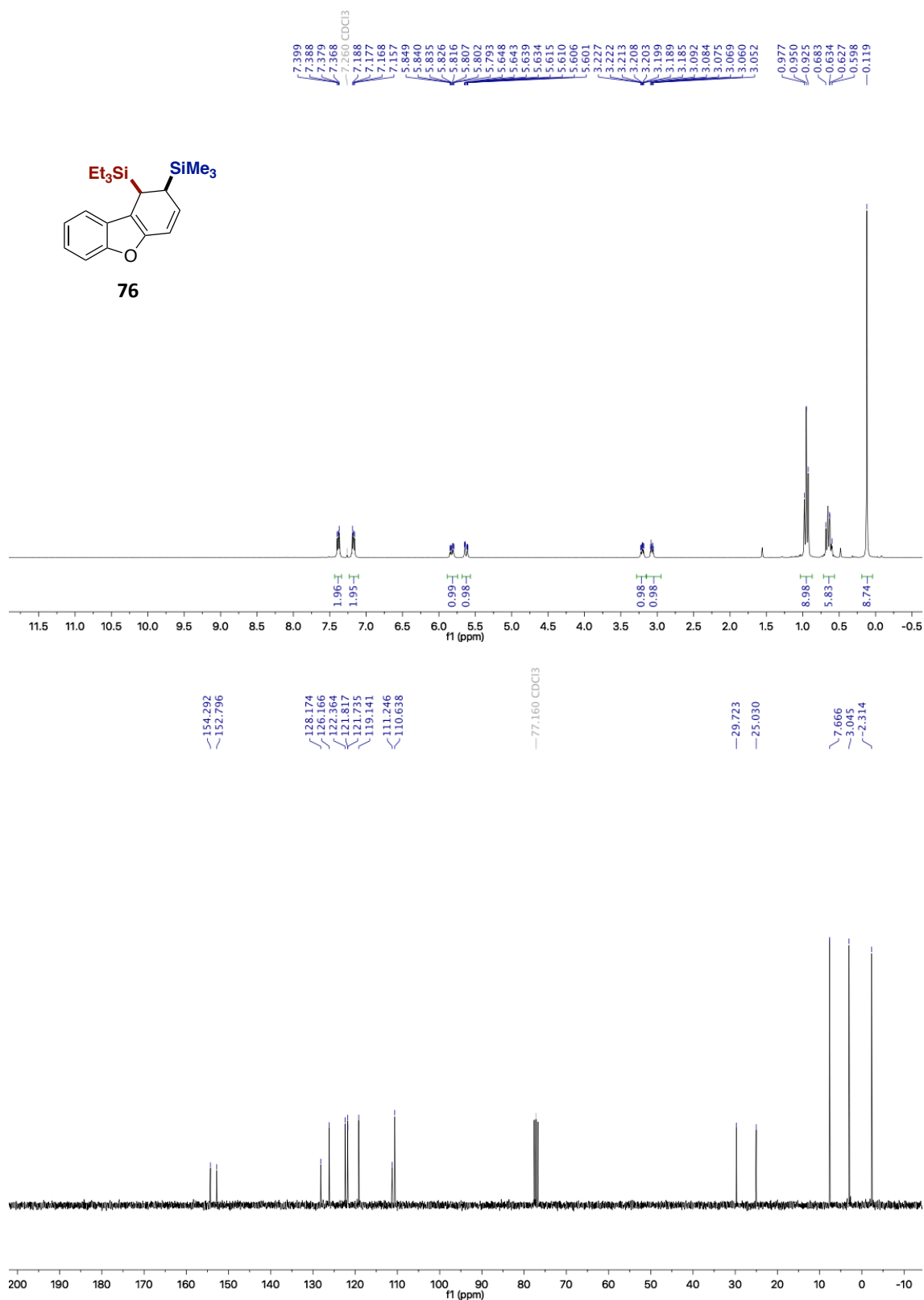


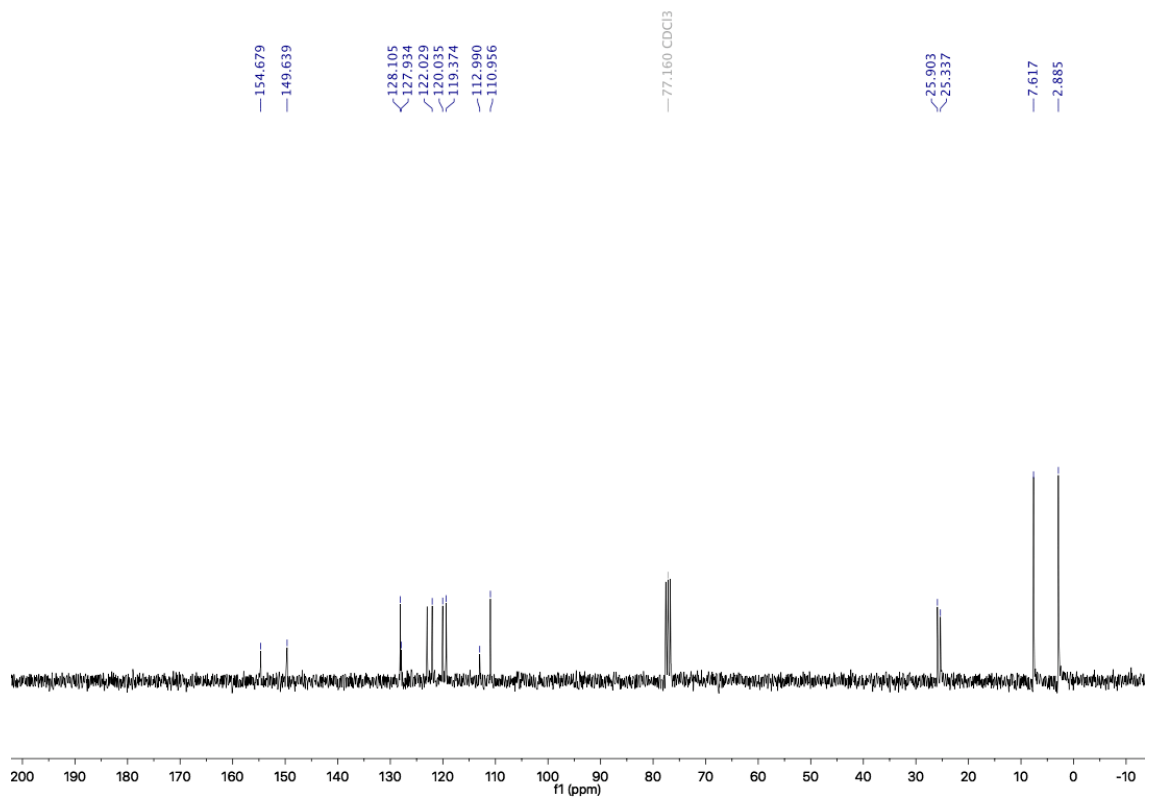
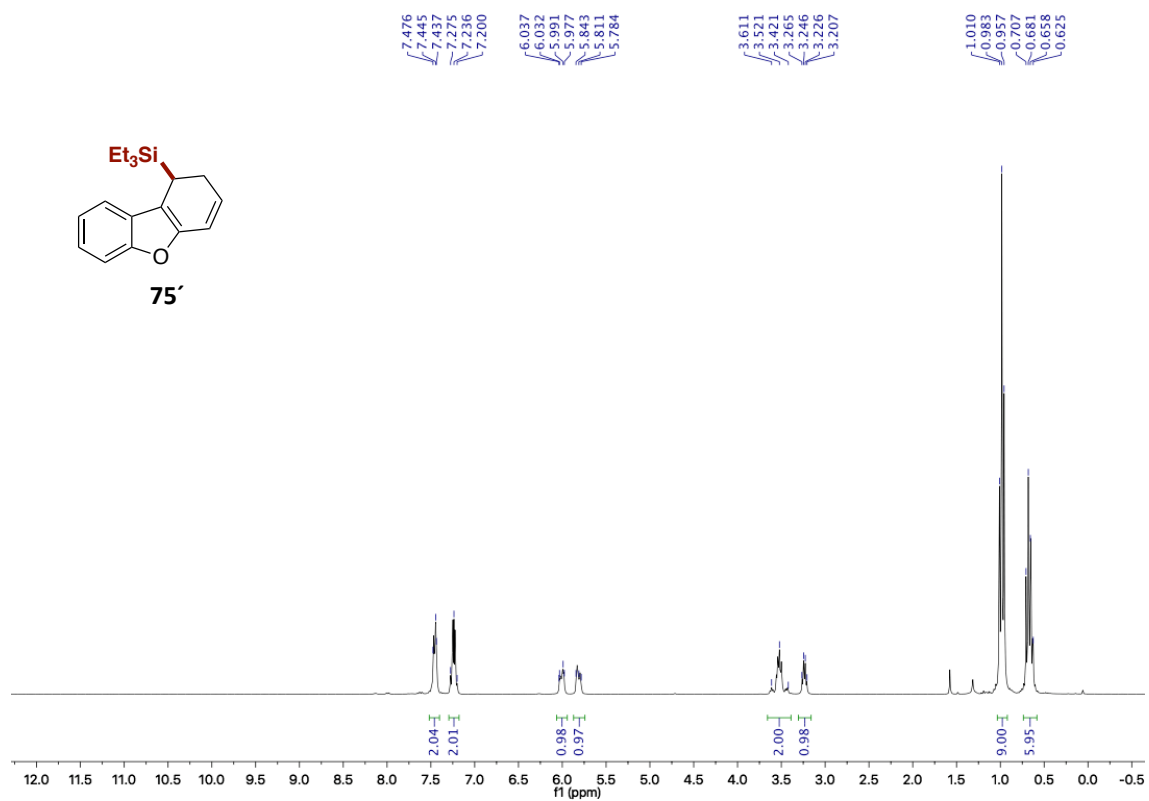
A Mild and Site-Selective sp^2 C-H Silylation of (Poly)Azines



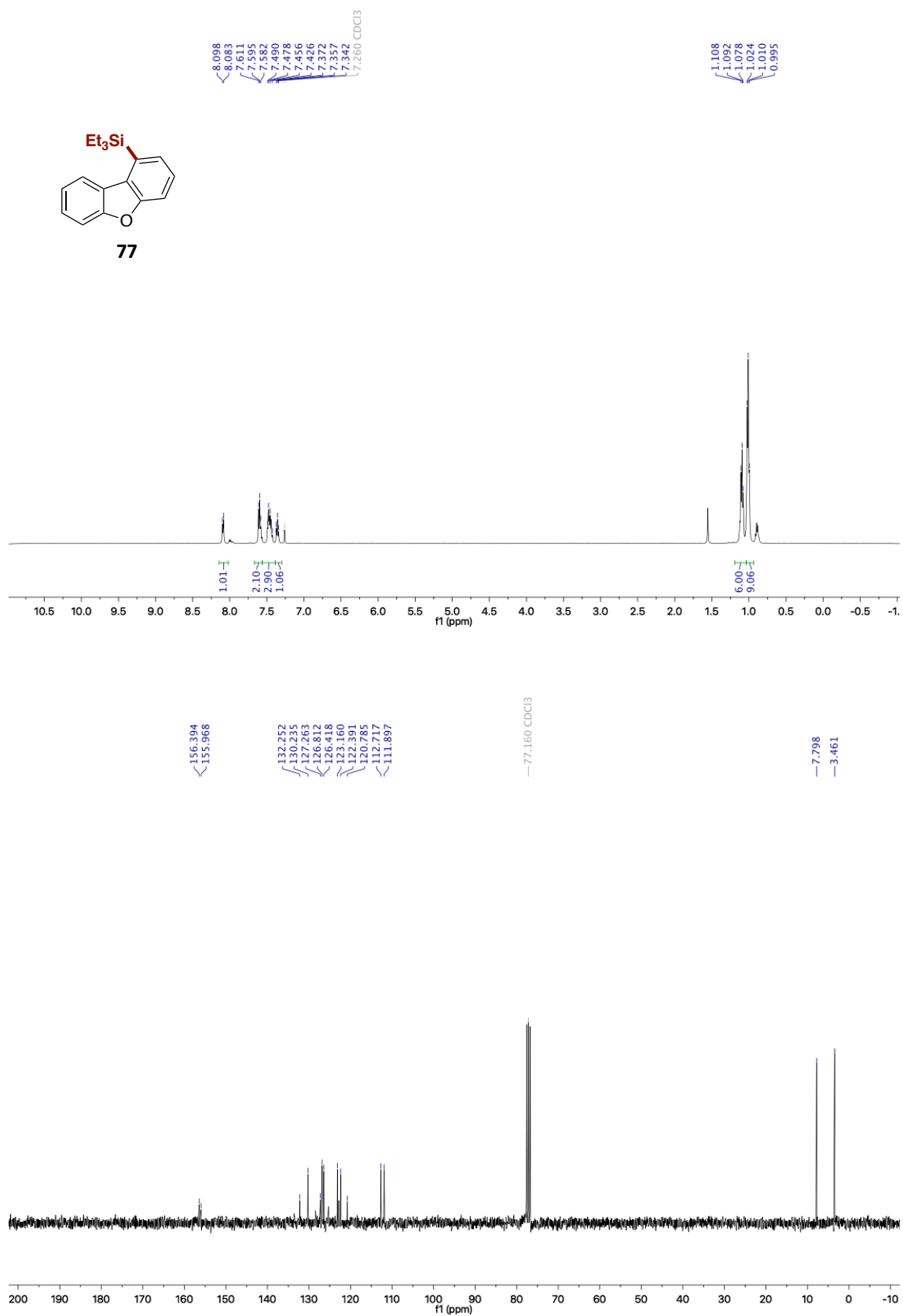


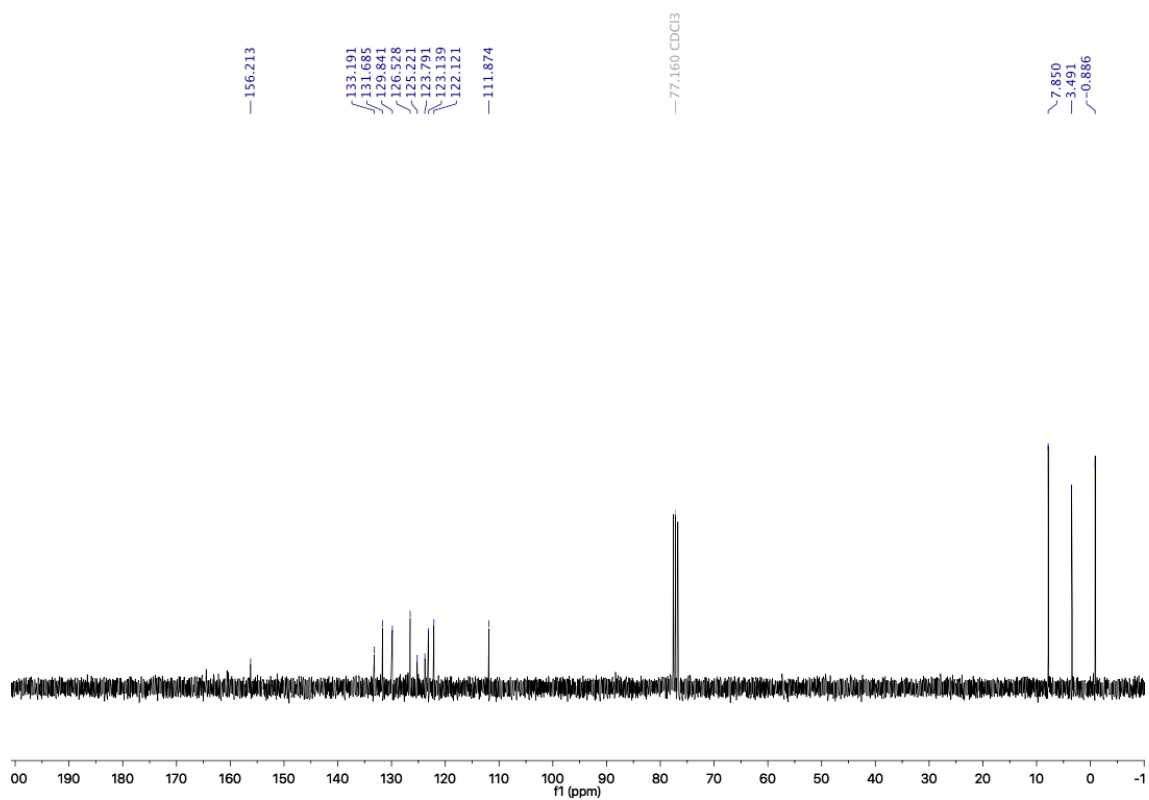
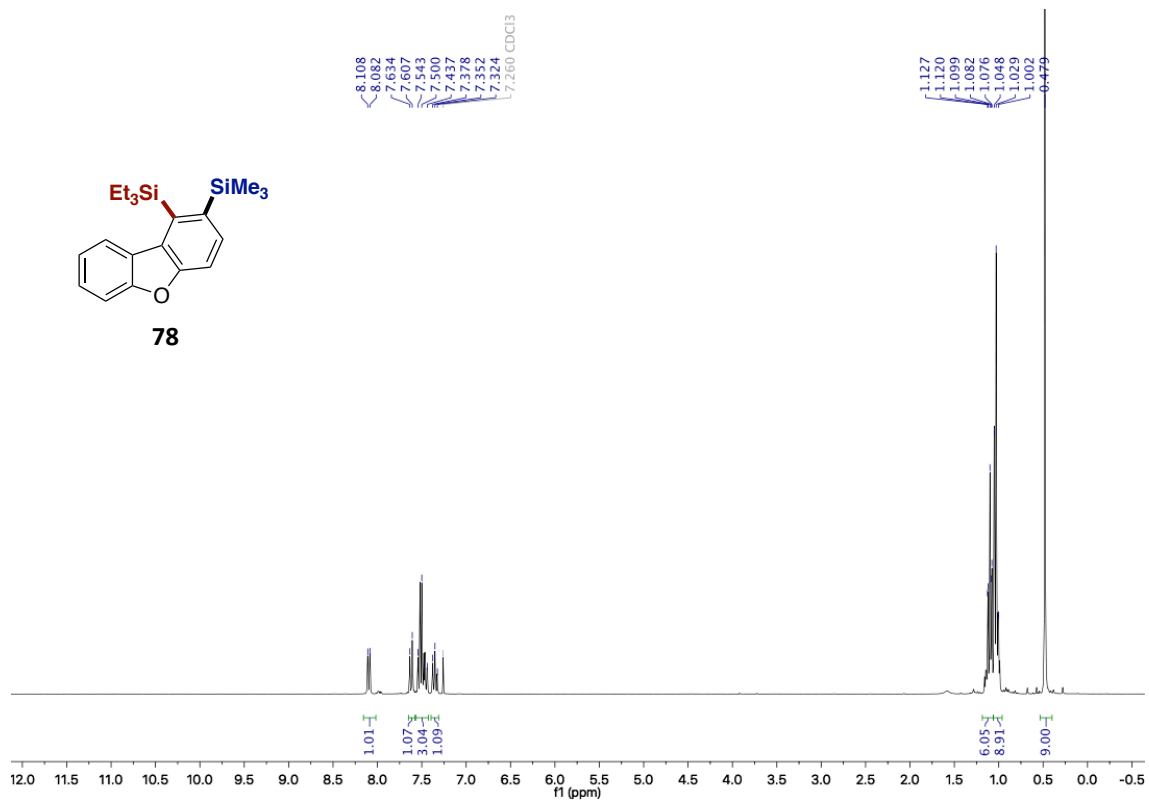
A Mild and Site-Selective sp^2 C-H Silylation of (Poly)Azines



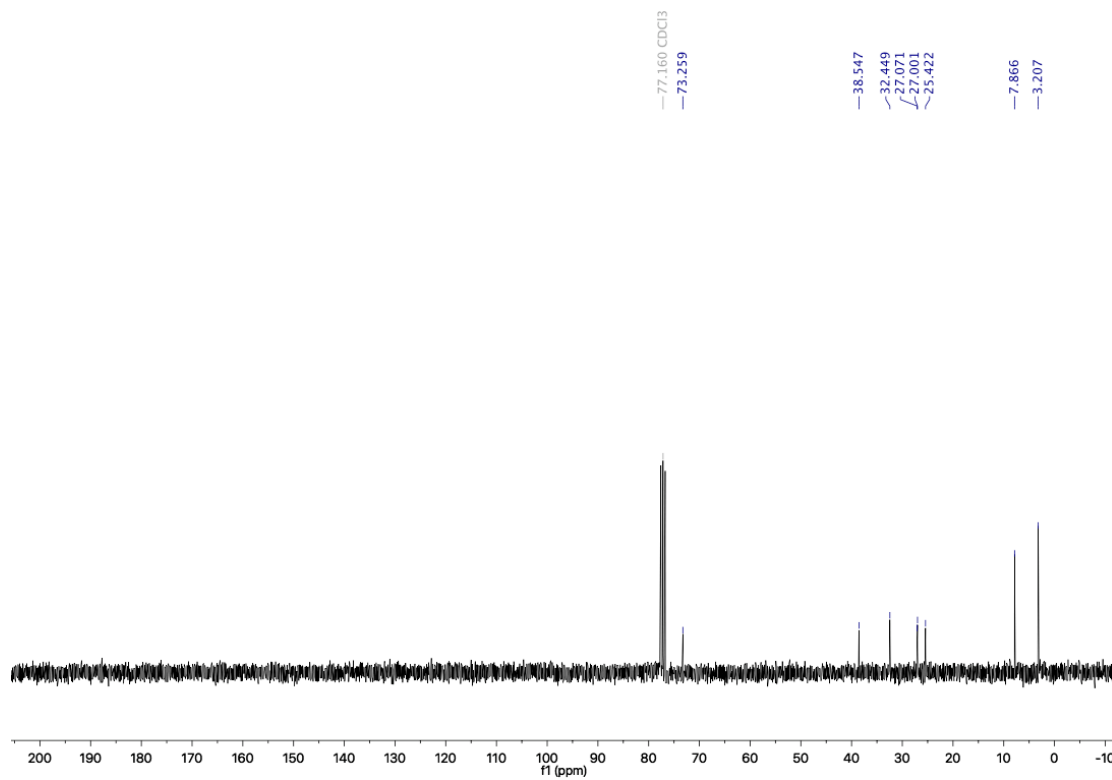
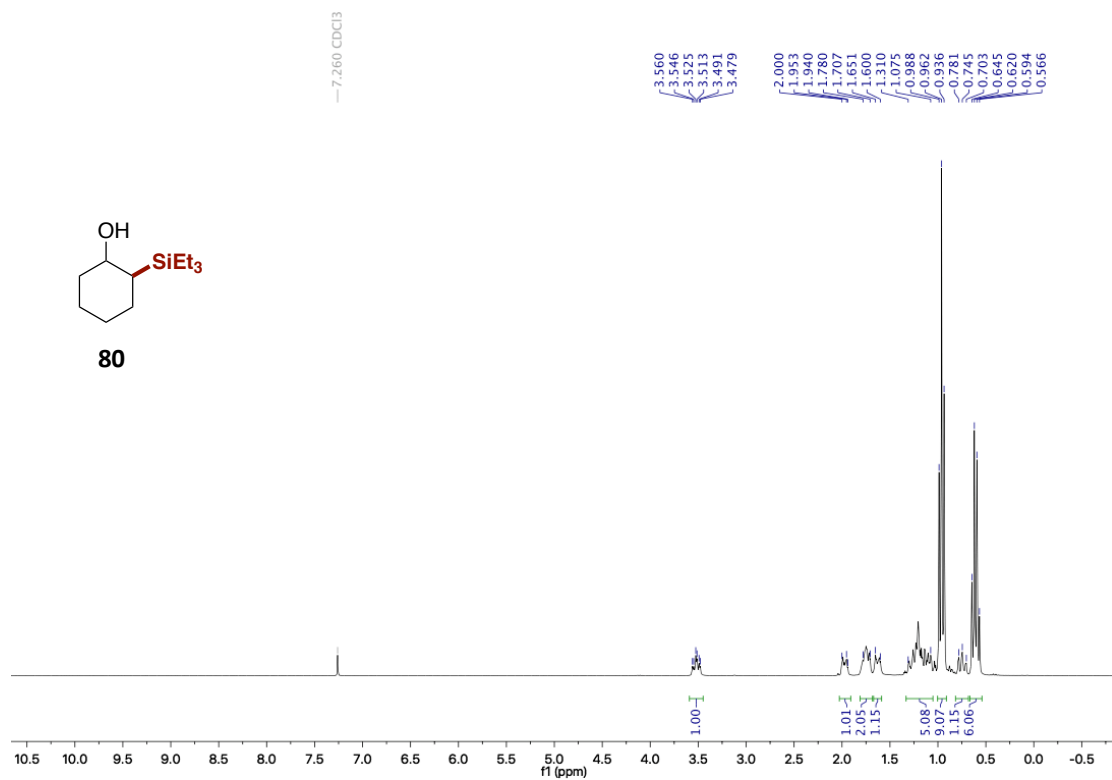


A Mild and Site-Selective sp^2 C-H Silylation of (Poly)Azines





A Mild and Site-Selective sp^2 C-H Silylation of (Poly)Azines

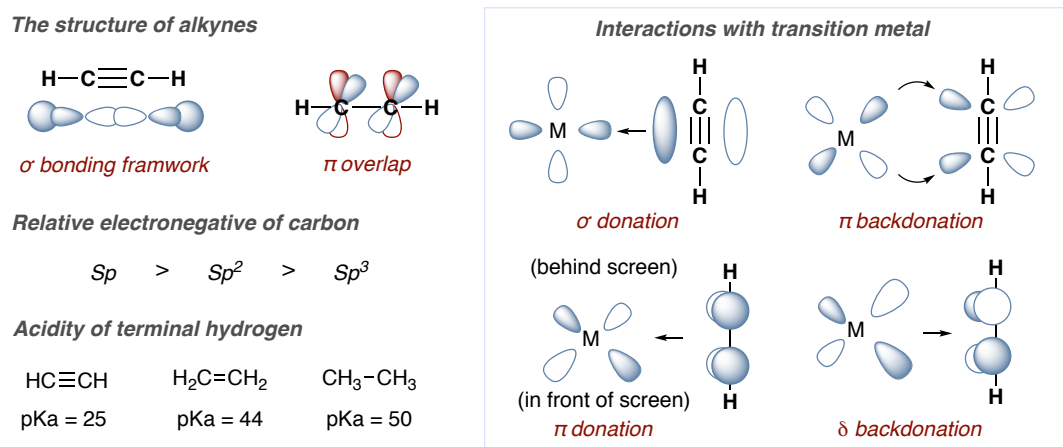


Chapter 4.

Stereoselective Base-Catalyzed 1,1-Silaboration of Terminal Alkynes

4.1. 1,1-Difunctionalization of Terminal Alkynes

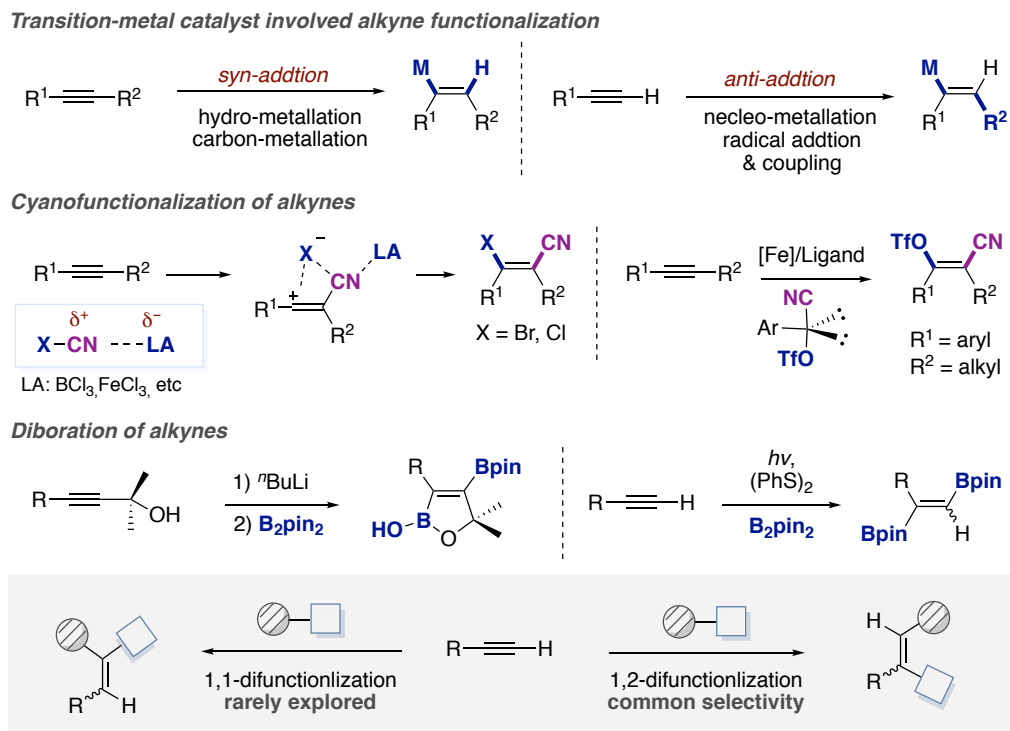
The C≡C triple bond ranks amongst the most basic functional groups in organic synthesis. Each carbon of acetylene is sp hybridized (Scheme 4.1). One sp orbital overlaps the s orbital of a hydrogen, and the other overlaps an sp orbital of the other carbon. Because the sp orbitals are oriented as far from each other as possible to minimize electron repulsion, acetylene is a linear molecule with bond angles of 180° . Due to the higher s orbital character, terminal alkynes are mildly acidic, with pK_a values of around 25, thus leaving ample space for deprotonation-functionalization chemistry.¹⁻³ Indeed, terminal alkynes are far more acidic than alkenes and alkanes, which have pK_a values of around 44 and 50, respectively. The C≡C triple bond is very strong with a bond strength of 200.6 kcal/mol, in which the sigma bond contributes 88.2 kcal/mol while the π bonds have bond strengths of 64.1 kcal/mol and 48.3 kcal/mol, respectively. The relatively weak π -bonds make the alkyne functionality 'vulnerable' to the addition of hydrogen, halogens, oxidations and cycloadditions.^{4,5}



Scheme 4.1. Structure of terminal alkyne and interaction with metal

One of the most attractive methodologies in the alkyne functionalization arena is the ability to generate heavily functionalized alkenes in a highly stereoselective manner. As judged by the wealth of literature data, the utilization of alkynes in chemical endeavors has witnessed a renaissance due to not only its prevalence in biochemistry or material sciences, but also as a versatile synthon to build up molecular complexity.⁶ Such interest has been fueled by the development of new powerful synthetic methodologies based on transition metal catalysis such as Pd, Ni, Au, Fe or Cu, among others.⁷⁻⁹ Indeed, the marriage of alkynes with transition metals creates an avalanche of progress in triple bond functionalization, thus providing numerous tools for organic synthesis. Such reactivity arises from the fact that a metal catalyst binds to the π -orbitals of the alkyne and transferring a group via *syn* migratory insertion such as hydrometallation, carbon-metallation or via an external *anti* nucleophilic attack. Alternatively, transition-metal-catalyzed radical addition/coupling reaction of alkynes, typically favoring anti-addition, is dominated by steric factors of vinyl radicals in the coupling step.¹⁰ As expected, the

resulting nucleophilic vinyl-metal species can undergo a range of further reactions to form 1,2-functionalized alkenes.



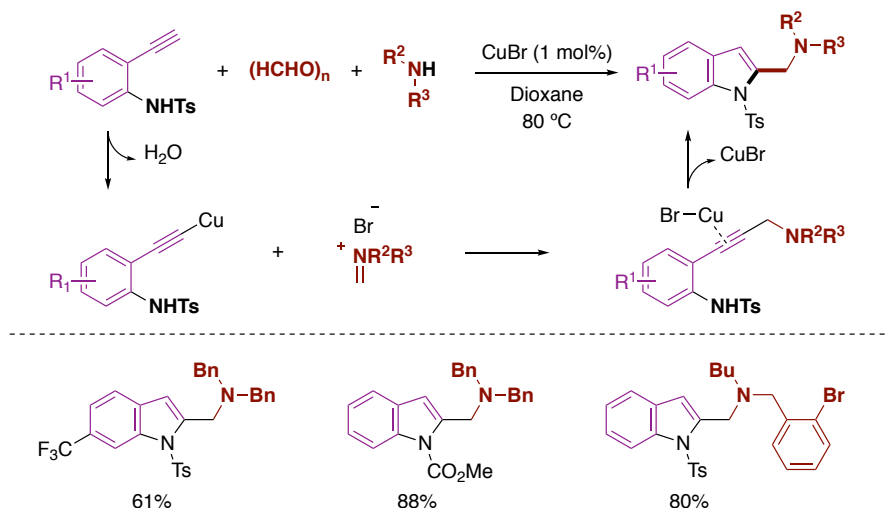
Scheme 4.2. Difunctionalization of terminal alkyne

In recent years, a non-negligible number of methods have been designed for the difunctionalization of terminal alkynes by means of transition-metal catalysts, Lewis acid catalysis or Lewis basic catalysis, among others (Scheme 4.2)¹¹⁻¹⁷ Regardless of the synthetic route employed, these methods almost exclusively result in 1,2-difunctionalization, a common reactivity mode for addition to C≡C multiple bonds. By contrast, only a few reports are related to the 1,1-difunctionalization of terminal alkynes. To the best of our knowledge, the 1,1-difunctionalization of terminal alkynes by one-step process is still of great challenge although several elegant disclosures have been made in the area of 1,1-diboration of alkynes.^{18, 19} In this chapter, recent advances of the 1,1-difunctionalization of terminal alkynes for the preparation of multifunctionalized alkenes are presented.

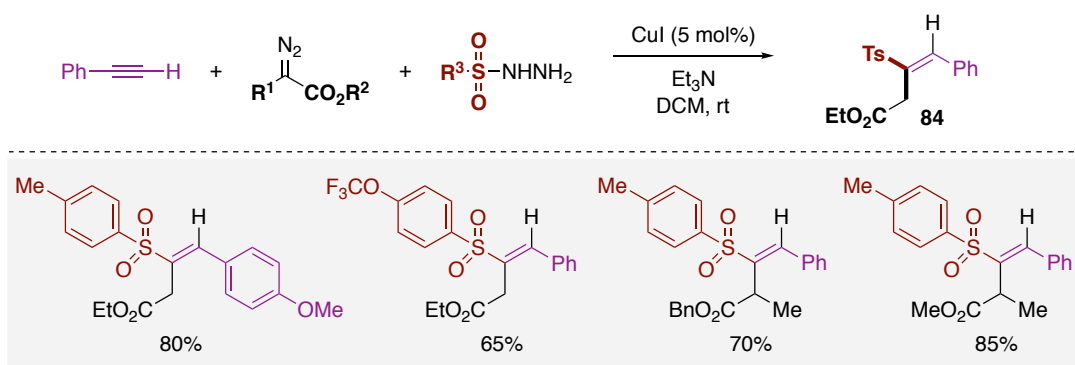
4.1.1. TM-catalyzed three-component 1,1-difunctionalization of terminal alkynes

Driven by the rapid buildup of molecular complexity, multicomponent reactions (MCRs) have been rapidly adopted within the context of alkyne functionalization.²⁰ Unlike commonly applied 1,2-difunctionalization reactions, extensions to the 1,1-site-selective pattern are rather rare. In 2007, the Fujii group presented a copper(I)-catalyzed domino three-component coupling/cyclization reaction of *N*-protected ethynylaniline derivatives (Scheme 4.3).²¹ With water as the only by-product, this reaction led to functionalized 2-aminomethylindoles in a high

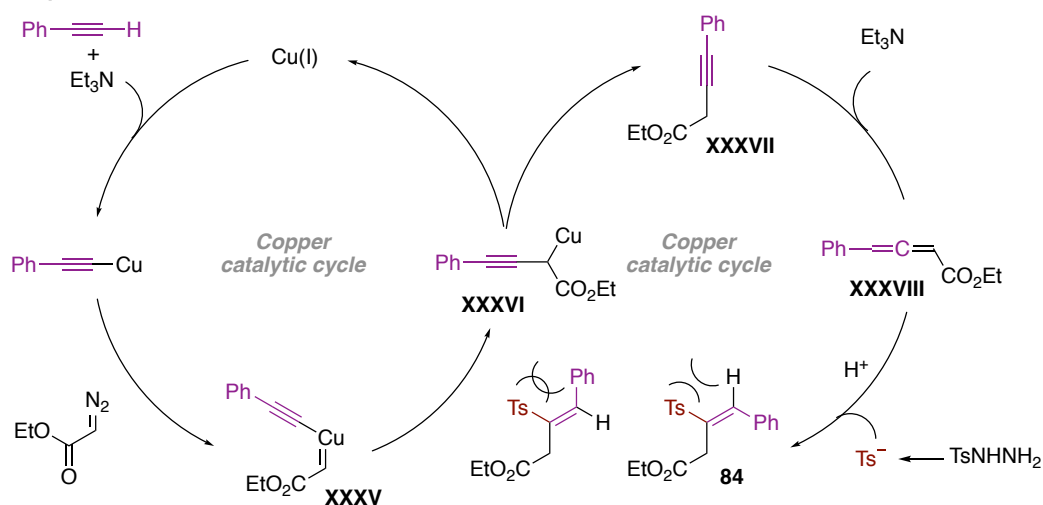
atom-economical fashion. The reaction presumably proceeded through a Mannich-type MCR followed by the formation of an indole ring. Subsequently, it was believed that the Cu catalyst acted as a π acid to activate the alkyne, yielding the final product via an intramolecular alkyne hydroamination reaction while regenerating the CuBr catalyst.



Scheme 4.3. Cu-catalyzed coupling/cyclization in the synthesis of 2-(aminomethyl)indoles

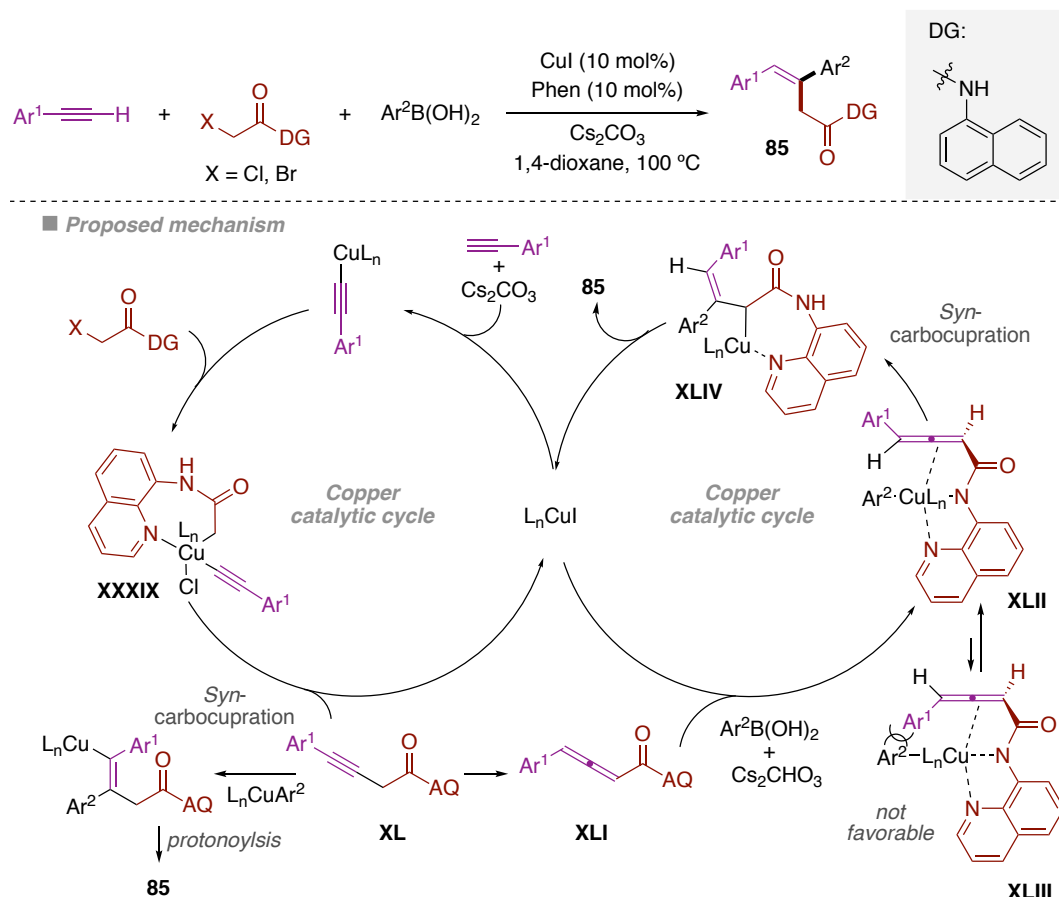


■ Proposed mechanism



Scheme 4.4. Cu-catalyzed three-component reaction for the construction of vinyl sulfones

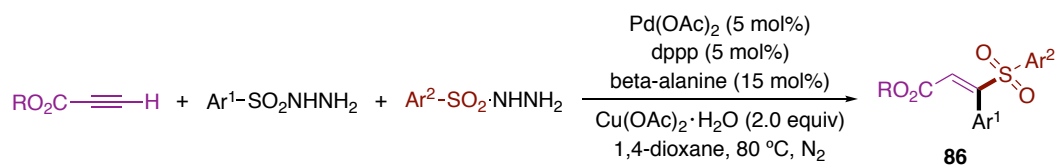
More recently, a copper-catalyzed three-component reaction of phenylacetylene, diazo ester and sulfonyl hydrazine has been designed, delivering a variety of vinyl sulfones with high stereoselectivity (Scheme 4.4).²² Preliminary mechanistic studies suggested that the reaction operates via Cu-catalyzed formal C–H insertion to produce **XXXVI**. After protonation of **XXXVI**, the presence of TEA results in an allene intermediate **XXXVIII**, which could be trapped by the sulfonyl anion to give the formal 1,1-difunctionalization product. The stereoselectivity of the reaction can be explained by steric effects between the sulfonyl group and the phenyl moiety at the alkyne terminus.



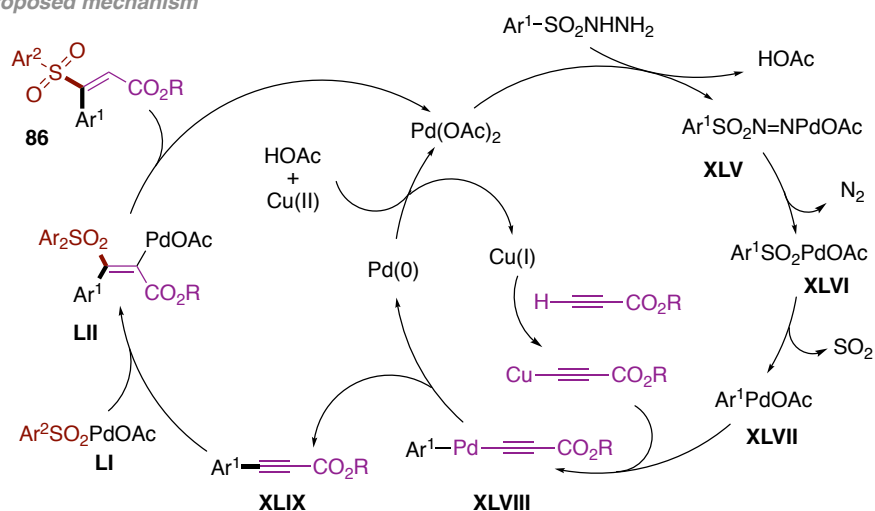
Scheme 4.5. Cu-catalyzed dicarbofunctionalization of terminal alkynes

A copper-catalyzed selective 1,1-arylation of alkynes with α -haloacetamides and organoboronic acids by the addition of both alkyl and aryl groups to the terminal carbon of alkynes was realized by Shi by using a removable, bidentate 8-aminoquinoline auxiliary (Scheme 4.5).²³ The plausible mechanism is believed to proceed via a copper acetylide generated from L_nCuI and the alkyne under basic conditions. Subsequently, interaction with α -haloacetamides affords intermediate **XXXIX**, which can be converted to intermediate **XL** through a reductive elimination. The bidentate 8-aminoquinoline auxiliary and the carbonyl within the α -haloacetamide may serve both as the auxiliary group and as electron-withdrawing group to facilitate the cross-coupling. Then, allenamide **XLI** is rapidly generated *in situ* from intermediate **XL** followed by transmetalation with arylboronic acid to form copper-aryl complex **XLII** or **XLIII**

with the assistance of a bidentate 8-aminoquinoline. Subsequently, **XLII** undergoes *syn*-carbocupration to afford **XLIV**, thus explaining the regioselectivity and stereoselectivity of the reaction. Alternatively, a L_nCuI could participate in a transmetalation to generate an L_nCuAr^2 complex followed by *syn*-carbocupration with **XL** en route to vinylcopper intermediate, which undergoes protonolysis to give product **85** and regenerate the copper catalyst.



■ Proposed mechanism



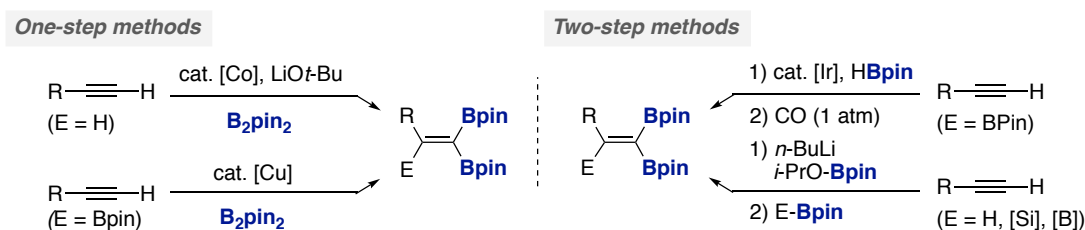
Scheme 4.6. Pd-catalyzed coupling-addition of propiolates with arylsulfonyl hydrazides

Yin and co-workers reported a novel strategy for one-pot 1,1-difunctionalization of terminal alkynes via Pd-catalyzed cross-coupling reaction of propiolates with readily available arylsulfonyl hydrazides, providing a broad range of highly functionalized (*E*)-vinylsulfones.²⁴ The reaction mechanism is depicted in Scheme 4.6. The reaction of Pd(OAc)₂ with arylsulfonyl hydrazide gives intermediate **XLVII**, which is formed via successive dehydrogenation of arylsulfonyl hydrazide, together with the release of N₂ and SO₂. Transmetalation of **XLVII** with copper acetylides gives palladium arylacetylides **XLVIII**, which undergoes reductive elimination to generate the cross-coupling product, simultaneously releasing Pd(0) catalyst. Intermediate **LI** undergoes *syn* migratory insertion into the internal alkynes **XLIX**, followed by protonolysis to afford product **86** and the Pd(II) catalyst. Different electronic effects occurred in the desulfonative cross-coupling and sulfonative addition. Indeed, the electron-withdrawing groups on the aryl group facilitate the cross-coupling reaction via cleavage of the Ar(C)-S bond, but disfavor the subsequent addition reaction via cleavage of the S-N bond.

4.1.2. Transition-metal-catalyzed 1,1-diboration of terminal alkynes

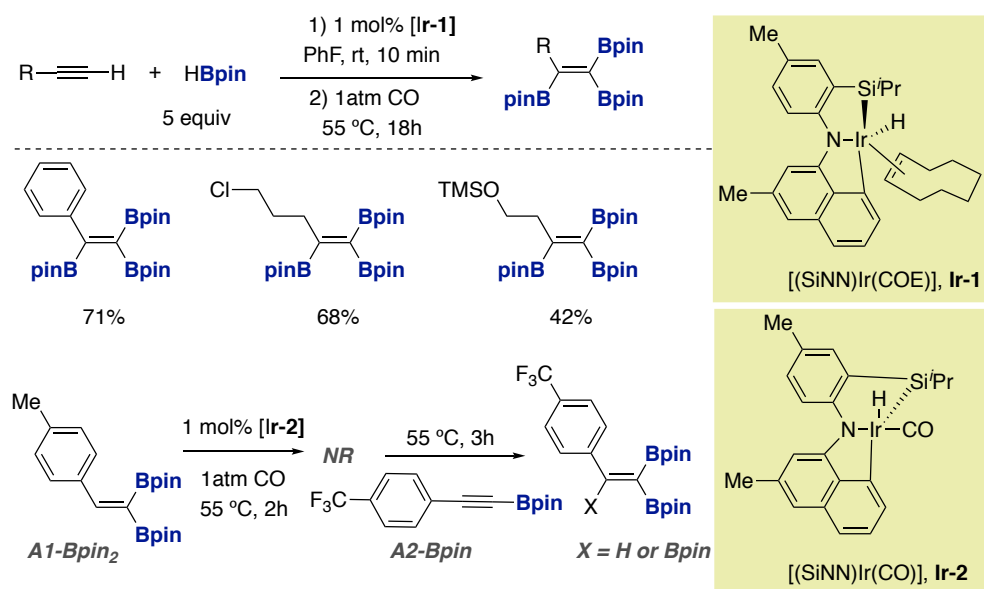
Driven by the inherent synthetic potential of organoboron reagents as linchpins in organic chemistry endeavors, considerable research has been devoted to generate well-defined

organoborane intermediates by using alkynes as coupling acceptors.²⁵⁻²⁸ Indeed, the ability to access a gem-diborylalkene from the corresponding alkyne will be particularly attractive given the possibility of transforming these intermediates into highly substituted, stereodefined alkenes by means of subsequent C–B bond-cleavage reactions.²⁹⁻³² Among these, particularly attractive is the development of a transition metal-catalyzed 1,1-diboration of terminal alkynes en route to the corresponding diborylated alkene.

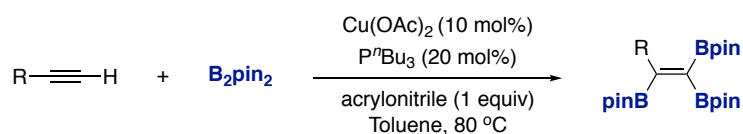


Scheme 4.7. Methods for the synthesis of 1,1-diborylalkenes

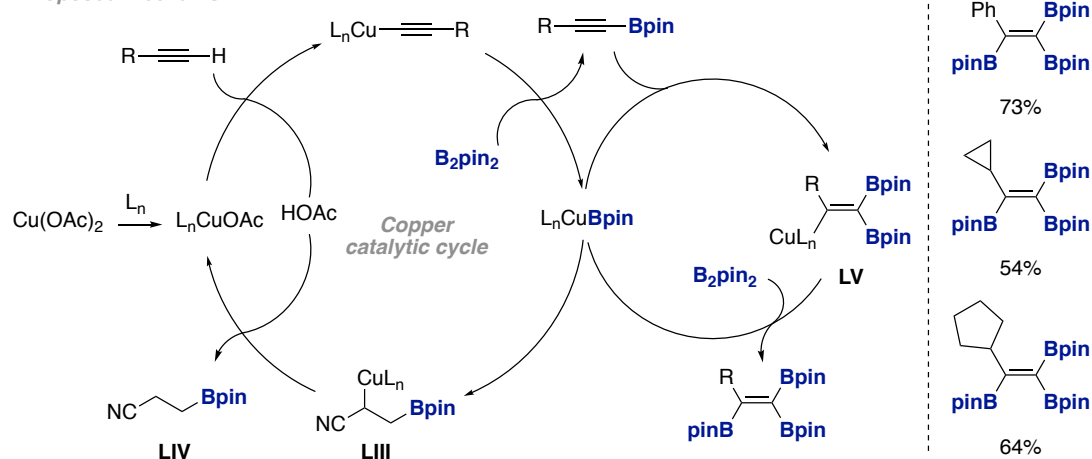
Ozerov and co-workers reported a one-pot, two-step protocol to convert terminal alkynes into triborylalkenes using a SiNN pincer cyclooctene iridium complex with HBpin under an atmosphere of CO (Scheme 4.8).³³ In the first step, the terminal alkyne and pinacolborane are converted into an 1-alkynylboronate by means of Ir catalysis. Subsequently, treatment of the reaction mixture with CO promotes the carbonylation of the [(SiNN)Ir(COE)] catalyst, thus generating a new species that triggered a dehydrogenative diboration of 1-alkynylboronate with pinacolborane. The plausible active [(SiNN)Ir(CO)] (**Ir-2**) catalyst could be isolated and characterized, showing its catalytic competence as reaction intermediate in the dehydrogenative diboration of alkynylboronate. Preliminary mechanistic studies by treating **A1-Bpin₂** with HBpin under 1 atm CO, resulting in no reaction, suggesting that triborylalkenes are not produced from the borylation of free diborylalkenes. Unfortunately, this method suffers from weak functional group tolerance, tedious procedures and expensive catalysts.



Scheme 4.8. Iridium-catalyzed tandem C–H borylation and diboration



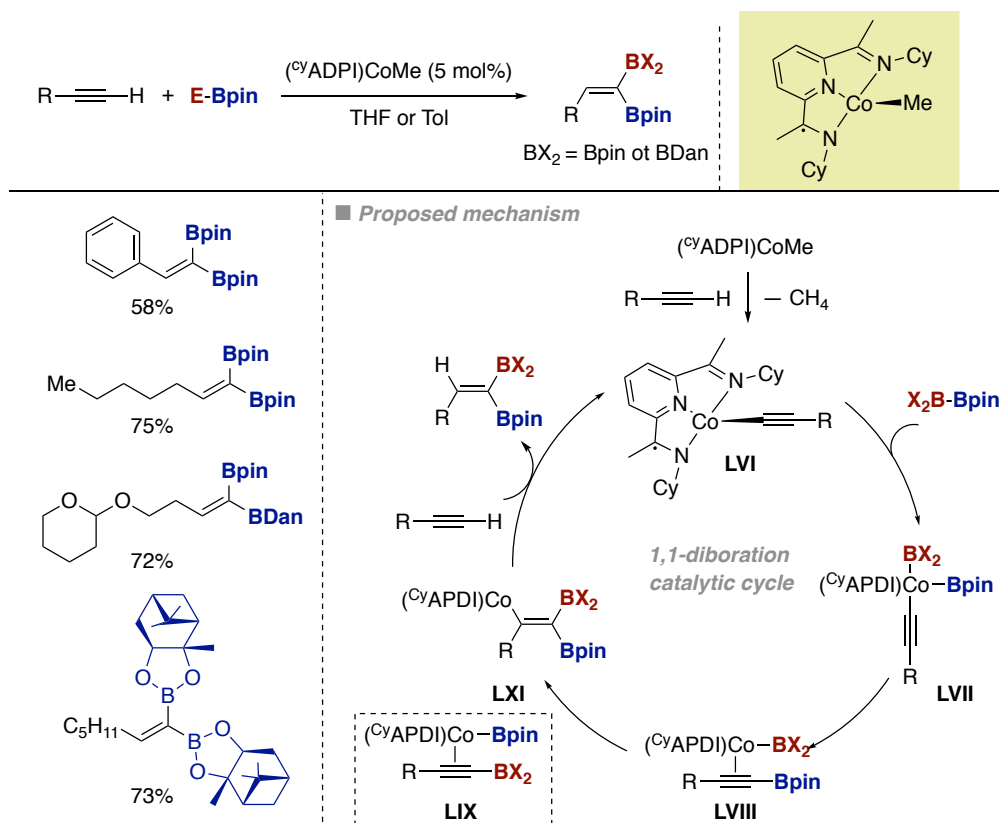
■ *Proposed mechanism*



Scheme 4.9. Copper-catalyzed triborylation of terminal alkyne

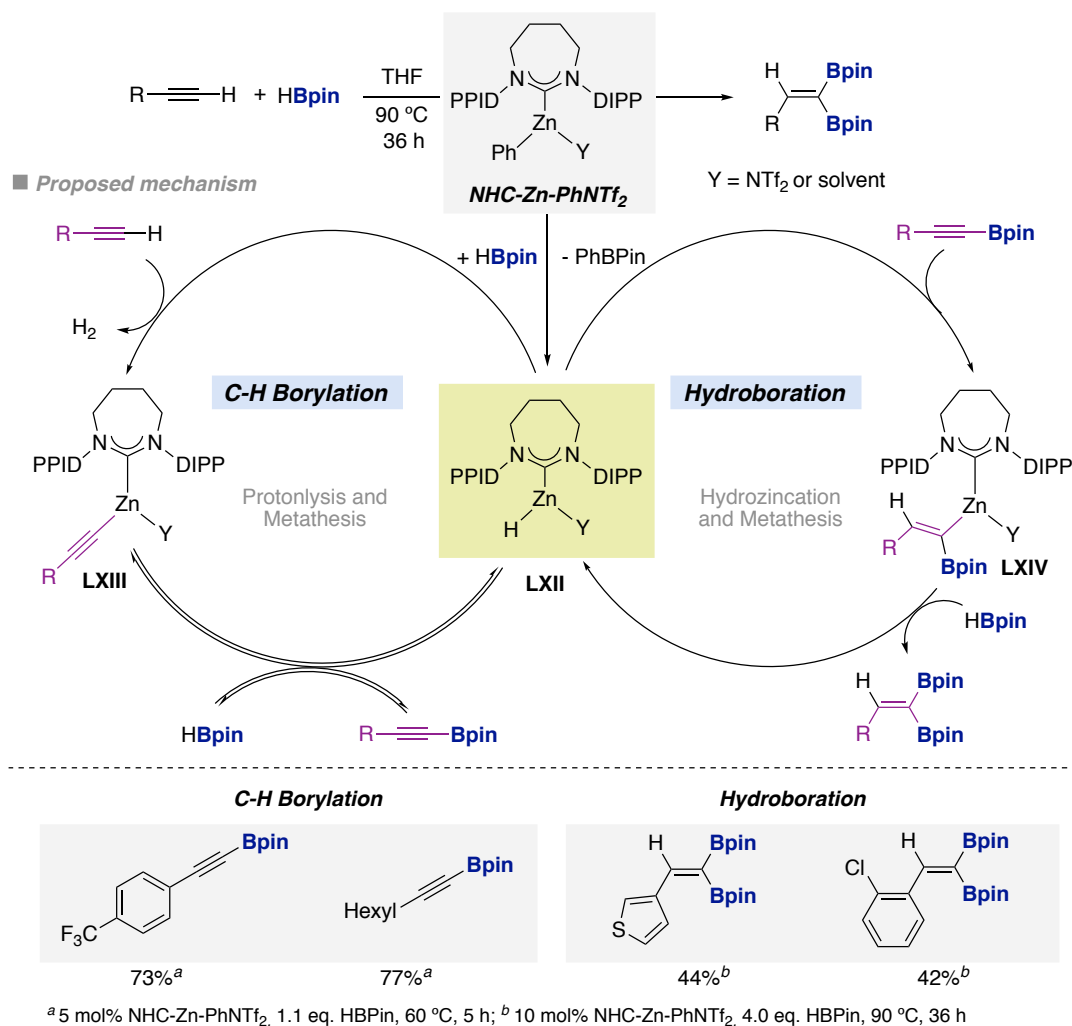
Recently, Marder and co-workers disclosed a copper-catalyzed triborylation of terminal alkynes using readily available Cu(OAc)_2 and B_2pin_2 .³⁴ The process features mild reaction conditions, broad substrate scope and can be conducted on a gram scale. A plausible mechanism is proposed in Scheme 4.9. The terminal alkyne reacts with L_nCuOAc species to afford copper acetylides, setting the basis for a σ -bond metathesis with B_2pin_2 to afford the alkynylboronate and a copper-boryl complex. Insertion of alkynylboronate into a Cu–B bond generates alkenylcopper species **LV**, giving rise to the desired product after σ -bond metathesis with B_2pin_2 . It is worth noting that hydroboration of acrylonitrile is faster than that of alkynes, thus suppressing alkyne hydroboration while improving the efficiency of the triborylation process.

Stereoselective Base-Catalyzed 1,1-Silaboration of Terminal Alkynes



Scheme 4.10. Cobalt-catalyzed 1,1-diboration of terminal alkyne

In 2017, Chirik and co-workers developed a novel protocol aimed at preparing 1,1-diborylated alkenes from the corresponding alkyne by using a cyclohexyl-substituted pyridine diamine cobalt complex (Scheme 4.6).¹⁹ The reaction features mild reaction conditions and exclusive 1,1-selectivity, thus furnishing various 1,1-diborylalkenes with excellent functional group tolerance. The authors proposed an initial formation of a cobalt acetylide **LVI** from which an alkynyl diboronate cobalt(III) complex **LVII** is generated upon oxidative addition of B-B bond. Then, an alkynylboronate complex **LVIII** is formed upon reductive elimination. A *syn*-functionalization then affords vinylcobalt intermediate **LXI**, ultimately leading to the corresponding Z-configured compound. The high stereo-selectivity observed in the 1,1-diboration with PinBBDan could be a result of selective reaction of one vinylcobalt intermediate over another (**LVIII** vs **LIX**), but is also consistent with the more Lewis acidic boron substituent (Bpin) being transferred to the alkyne first and the resulting **LVIII** to undergo *syn*-functionalization. Formal deprotonation with another terminal alkyne is believed to deliver the targeted 1,1-diborylalkene product. The proposed mechanism was supported by the isolation of cobalt intermediates **LVI** and **LIX** and their full characterization by X-ray diffraction analysis.

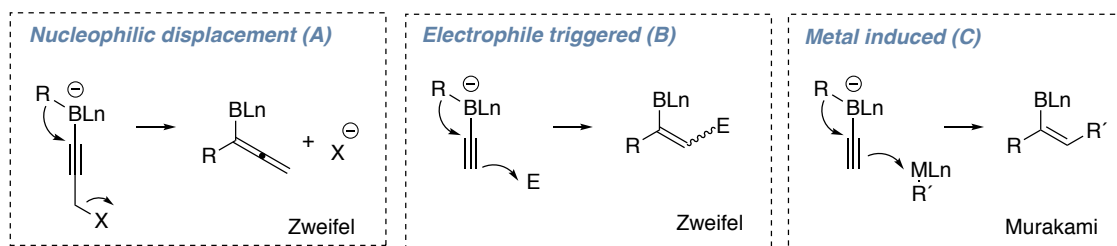


Scheme 4.11. NHC-Zinc-hydride complex catalyzed alkyne C-H borylation and hydroboration

Recently, the Ingleson group reported a low coordinate NHC-zinc-hydride complex catalyzed C-H borylation and hydroboration with pinacolborane.³⁵ In this transformation a Zn-C/H-B metathesis step is key to enabling a Zn-catalyzed borylation and internal alkyne hydroboration in one pot, thereby converting terminal alkynes into 1,1-diborylated alkenes without isolation of sensitive alkynyl boronate ester intermediates. The proposed mechanism is shown in Scheme 4.11. Firstly, NHC-Zn-PhNTf undergoes transmetalation with HBpin to afford a low-coordinate [(7-DIPP)ZnH]⁺ cationic species **LXII**, from which Zn-alkynyl species **LXIII** could be formed upon reaction with the terminal alkyne. Subsequently, **LXIII** further reacts with HBpin through σ -bond metathesis to produce the C-H borylation product and regenerate **LXII**. In the second cycle, alkynyl boronate esters are proposed to undergo hydrozincation followed by metathesis with HBpin to form the diborylated alkenes. Isolation of intermediates, stoichiometric experiments and DFT calculations supported the intermediacy of organozinc species, zinc hydrides, and Zn-C/H-B σ -bond metathesis. Bulky *N*-heterocyclic carbenes are critical for success, as their steric hindrance enhances the stability of NHC-Zn species and provides access to low coordinate (NHC)Zn-H cations.

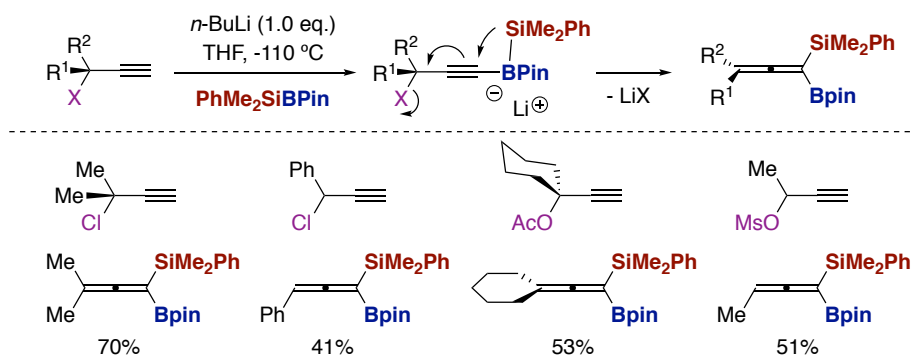
4.2. 1,2-Metallate Shift from Boron to an *sp* Center

The anionotropic 1,2-migration of an organic substituent from a tetrasubstituted borate ion – often referred to as an “ate” complex – to an acceptor atom is the basis of the most useful application of organoboranes in organic synthesis.³⁶ Since its discovery over 50 years ago,³⁰ the 1,2-metallate rearrangement of a boronate complex has been developed and refined into a powerful and versatile method for chemical invention.³⁷⁻⁴⁰ Not surprisingly, the rearrangement of alkynylboronate complexes to access alkenylboronates has also attracted much attention in recent years. In line with this context, the 1,2-metallate shift of an ate complex from boron to an *sp* center has been developed with remarkable results. For example, Zweifel and coworkers demonstrated, for the first time, the 1,2-migration by nucleophilic displacement requiring a leaving group (Scheme 4.12, A).⁴¹ They also reported another type of 1,2-metallate shift triggered by addition of an external electrophile (Scheme 4.12, B).⁴² In 2009, the Murakami group discovered the π -acidic late transition metal-induced 1,2-metallate shift of alkynyl boronates (Scheme 4.12, C).⁴³



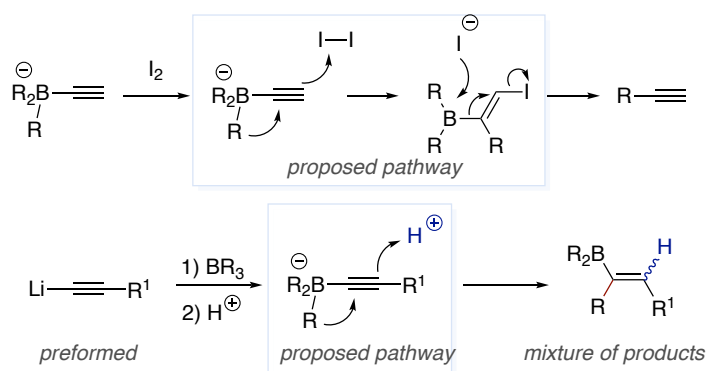
Scheme 4.12. Three types of 1,2 metallate shift to an *sp* center

A gem-silylborylation of terminal alkynes in the presence of stoichiometric base through nucleophilic displacement in the presence of an appropriate leaving group was discovered by Hiyama in 2003 (Scheme 4.13).⁴⁴ The reaction proceeds via 1,2-migration of the silyl group from the negatively charged boron atom to the terminal acetylenic carbon. If methanesulfonyl derivatives are employed as leaving groups, the addition of chlorotrimethylsilane – formally considered as a Lewis acid that promotes the elimination of the mesyloxy group – is necessary to accelerate the reaction.



Scheme 4.13. Gem-silylborylation of an *sp* carbon to synthesize 1-boryl-1-silyllallene

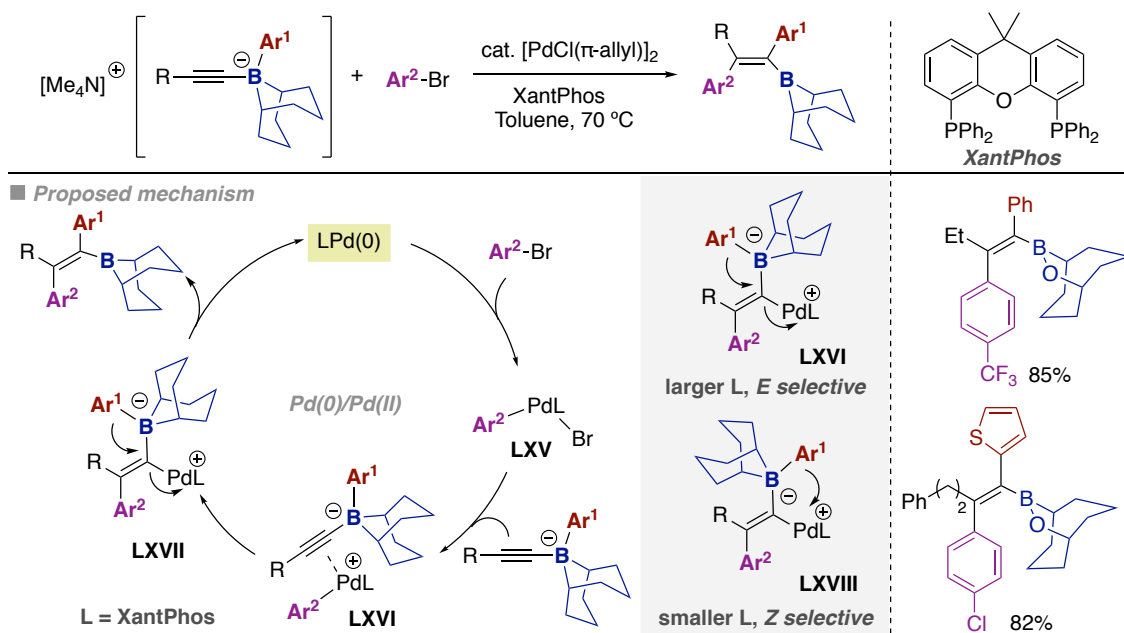
Electrophile induced 1,2-metallate shifts in alkenylborates was first proposed by Zweifel in iodine-promoted rearrangements of trialkylborane-derived substrates, where the corresponding alkyl-substituted alkyne was obtained upon spontaneous deiodoboration.⁴⁵ In 1975, Brown showed that lithium acetylides readily add to alkylboranes to form borate complexes.⁴⁶ Further reaction of the borate with a variety of electrophiles induces an alkyl group migration from boron to carbon leading to the formation of both isomers of alkenyl borane. The stereochemical outcome has been attributed to the nature of the 1,2-metallate shift, which is proposed to proceed through a carbocation intermediate. Subsequent protodeboration provided a mixture of Z- and E- alkenes.



Scheme 4.14. Reaction of lithium ethynyltrialkylborates with Brønsted acid

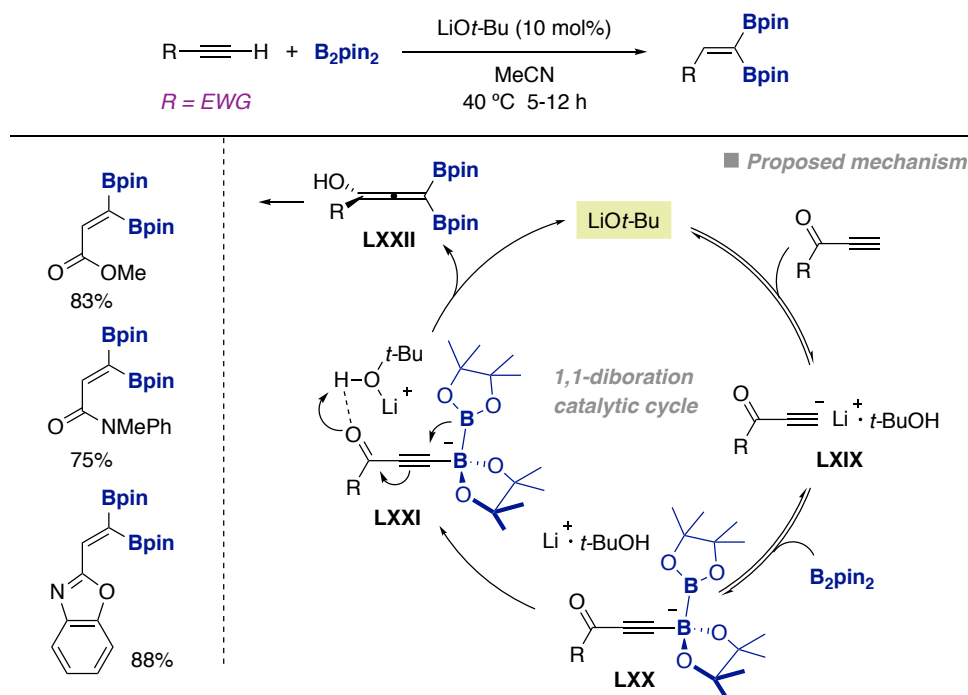
Murakami and co-workers reported a Pd-catalyzed biarylation of alkynylborates with aryl halides in which the two aryl groups were introduced *trans* to each other.^{47, 48} A proposed mechanism for the stereoselective *trans*-addition reaction is shown in Scheme 4.15. Oxidative addition of Ar²Br to LPd(0) gives arylPd(II) bromide **LXV**. Alkynylborate then coordinates to **LXV** to form intermediate **LXVI**. Carbopalladation across the C≡C triple bond occurs in a *cis* fashion to provide alkenylpalladium **LXVII**, followed by the migration of the phenyl group with formal inversion of stereochemistry, resulting in the formation of *trans*-addition product and the regeneration of the propagating active Pd(0)(XantPhos) species within the catalytic cycle. The stereochemical outcome was largely dependent on the ligand: With XantPhos, transmetalation is inhibited and 1,2-migration of the phenyl group onto the carbon occurs, resulting in the E product. In contrast, the utilization of tri(*o*-tolyl)phosphine results in 1,3-migration of the phenyl group from boron to palladium (**LXVIII**), thereby delivering the Z isomer.

Stereoselective Base-Catalyzed 1,1-Silaboration of Terminal Alkynes



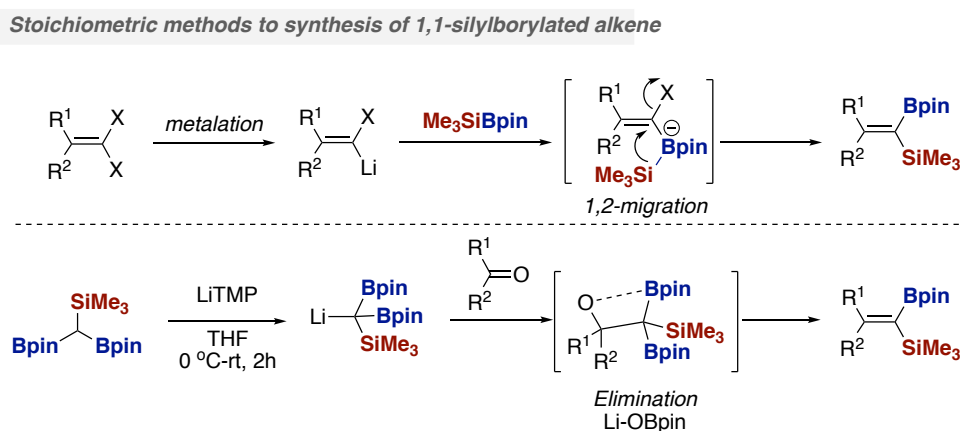
Scheme 4.15. Pd-catalyzed stereoselective reaction of alkynylborates with aryl halides

In 2015, a transition-metal-free 1,1-diboration between terminal alkynes and B₂pin₂ using LiOt-Bu as catalyst was reported by Ohmiya and Sawamura (Scheme 4.16).¹⁸ The authors proposed a mechanism consisting of deprotonation of the terminal alkyne with LiOt-Bu to give a lithium acetylide **LXIX** in which they proposed the coordination with *t*-BuOH. Subsequently, reaction with B₂pin₂ led to an alkynyl borate intermediate **LXX** followed by 1,2-migration of the terminal boryl group into the *sp*-hybridized carbon atom. An allenol or allenamine intermediate, generated by the protonation of the carbonyl or the azole group in **LXXI** with the Li cation-coordinated *t*-BuOH, would immediately isomerize to **LXXII** and regenerate the catalytically competent species. Unfortunately, this reaction was limited to activated alkynes bearing electron-withdrawing substituents such as propiolates.



Scheme 4.16. LiOt-Bu-catalyzed 1,1-diboration of activated terminal alkynes

The preparation of gem-silaborated alkenes by the utilization of organolithium intermediates and lithium carbenoid species has been developed (Scheme 4.17). In 2001, Hiyama and Shimizu showed that 1,1-dihaloalkene or 1-haloalkenes can react with either *n*-BuLi or LiTMP to afford 1-boryl-1-silylalkenes via 1,2-migration, resulting in inversion of configuration at the *sp*² carbon centre.^{49, 50} Subsequently, Fernández and co-workers discovered a new olefination reagent, HC(Bpin)₂(SiMe₃), which can be deprotonated in the presence of LiTMP to generate boron and silicon stabilized carbanions.⁵¹ This reagent was able to subsequently undergo addition to a carbonyl functionality, followed by the *syn* B–O elimination to access the gem-silaborated olefins. Noteworthily, HC(Bpin)₂(SiMe₃) can be efficiently prepared on gram scale from B₂pin₂ and commercially available (trimethylsilyl)diazomethane.

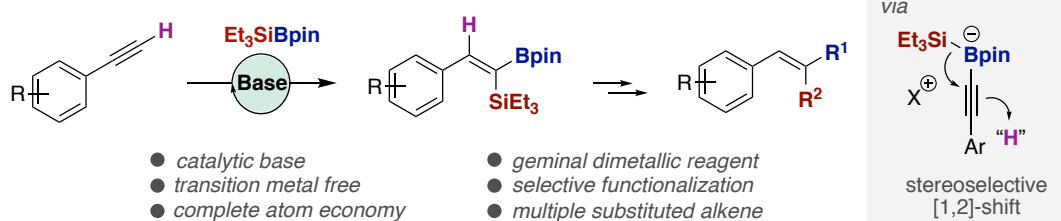


Scheme 4.17. Synthesis of gem-silaborated alkenes with lithium carbenoid

4.3. General Aim of the Project

At the outset of our investigations, 1,1-difunctionalization of terminal alkynes was a relatively unknown area of expertise, and mainly limited to the utilization of transition metal catalysts or stoichiometric organolithium reagents. We wondered whether we could implement a transition-metal-free 1,1-heterodifunctionalization of terminal alkynes. Among different scenarios, we focused on the possibility of enabling the simultaneous incorporation of both C–Si and C–B atoms in a 1,1-fashion with total control of the diastereoselectivity. If successful, we anticipated that such a technology will allow for preparing densely functionalized alkenes via site-selective C–Si & C–B bond-cleavage, thus offering new techniques for converting useful building blocks into valuable compounds from simple precursors.

□ Base-catalyzed stereoselective 1,1-silaboration of terminal alkynes (**this chapter**)

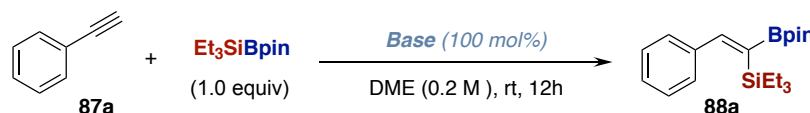


Scheme 4.18. Base-catalyzed stereoselective 1,1-silaboration of terminal alkynes

4.4. Catalytic Base-Catalyzed Site-Selective 1,1-Silaboration of Terminal Alkynes

4.4.1. Optimization of the reaction conditions

We initiated our study by reacting phenylacetylene (**87a**) with Et₃SiBpin in DME in the presence of an appropriate base. After systematic screening of the reaction conditions (Table 4.1), we detected the desired product **88a** when LiHMDS, NaHMDS, KHMDS, or KOt-Bu were employed as bases (entries 1-4, 7). As expected from the acidity of the acetylenic C-H bond (pK_a~25), weaker bases such as KOMe, K₂CO₃, and CsF failed to promote the targeted 1,1-silaboration. Furthermore, the amount of KHMDS could be reduced to 20 mol% while maintaining a similar yield of **88a** (entry 4). Importantly, in all cases analysed we only obtained a single diastereoisomer, with the silyl group and the arene being in a *cis*-fashion.

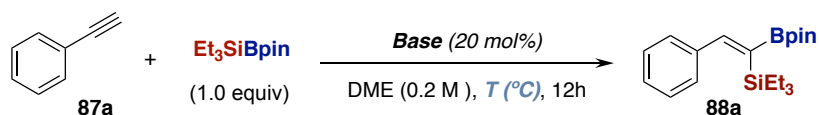


Entry	Base	Conversion of 87a (%)	Yield of 88a (%) ^a
1	LiHMDS	65	28
2	NaHMDS	61	37
3	KHMDS	66	44
4	KHMDS	43	38 ^b
5	LiOt-Bu	11	0
6	NaOt-Bu	15	0
7	KOt-Bu	34	12
8	KOMe	6	0
9	KOTM	9	0
10	KOH	12	0
11	Zn(HMDS) ₂	8	0
12	Mg(HMDS) ₂	2	0
13	K ₃ PO ₄	5	0
14	K ₂ CO ₃	4	0
15	Cs ₂ CO ₃	2	0
16	CsF	7	0
17	KF	4	0

Reaction conditions: **87a** (0.40 mmol), Et₃SiBpin (0.40 mmol), base (100 mol%) in DME (2.0 mL) at room temperature, 12h. ^a GC yields using decane as internal standard. ^b 20 mol% of KHMDS was used.

Table 4.1. Screening of bases

Stereoselective Base-Catalyzed 1,1-Silaboration of Terminal Alkynes

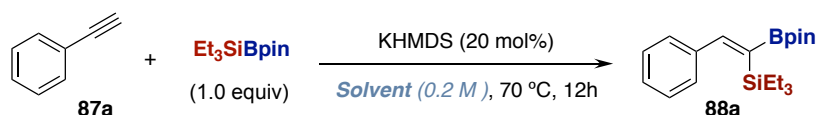


Entry	Base (0.2 equiv)	T ($^\circ\text{C}$)	Conversion of 87a (%)	Yield of 88a (%) ^a
1	KHMDS	rt	52	50 ^b
2	KHMDS	40	71	65
3	KHMDS	50	88	80
4	KHMDS	60	90	86
5	KHMDS	70	96	94
6	KHMDS	80	96	95
7	KHMDS	90	100	96
8	LiHMDS	90	42	39
9	NaHMDS	90	79	70
10	KOt-Bu	90	51	50
11	KHMDS	90	60	49 ^c
12	KHMDS	70	64	51 ^c

Reaction conditions: **87a** (0.40 mmol), Et_3SiBpin (0.40 mmol), base (20 mol%) in DME (2.0 mL), 12h. ^a GC yields using decane as internal standard. ^b 48h instead of 12h. ^c 10 mol% KHMDS was used.

Table 4.2. Screening of temperature

Next, we evaluated the reaction temperature in order to further improve the conversion of **87a** and the yield of **88a** (Table 4.2). The yield of the desired product was increased when the reaction temperature was raised beyond room temperature, resulting in yields up to 96% (entries 1-7). As expected, the nature of the base and the counterion had marked effects on reactivity (entries 7-10). The highest yield of **88a** was detected when 20 mol% of KHMDS was used (entries 5-7), but a lower yield was observed when the amount of KHMDS was reduced to 10 mol% (entry 11, 12). As the identity of the solvent has a strong influence on the aggregation and solubility of KHMDS,⁵²⁻⁵⁴ the effect of different solvents was studied (Table 4.3). As expected, better results were observed in DME, toluene and MeCN (entry 1, 8, 10), probably due to the good solubility of KHMDS in these solvents. In contrast, nonpolar solvents such as pentane or other ether solvents led to moderate yields of the desired product. The reaction also occurred in the absence of solvent to give the desired product in a decent yield (entry 12).

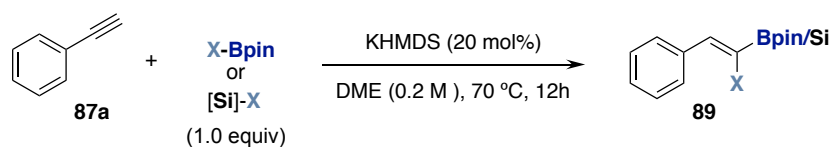


Entry	Solvent	Conversion of 87a (%)	Yield of 88a (%) ^a
1	DME	100	97
2	Dioxane	45	32
3	Et ₂ O	69	65
4	<i>t</i> -BuOMe	46	42
5	THF	68	65
6	Pentane	32	29
7	Cyclohexane	37	33
8	Toluene	100	96
9	DMF	100	58
10	MeCN	100	94
11	DCM	9%	0
12	none	81	76

Reaction conditions: **87a** (0.40 mmol), Et₃SiBpin (0.40 mmol), KHMDS (20 mol%) in solvent (2.0 mL) at 70 °C, 12h. ^a GC yields using decane as internal standard.

Table 4.3. Screening of solvents

As shown in Table 4.4, Et₃SiBpin was found to be the most efficient reagent among all X-Bpin or X-Si compounds utilized. Indeed, changing the electronic properties of the silyl group did not improve the yield (entry 2), whereas the inclusion of bulky groups at silicon shut down the reactivity (entry 3). Likewise, no reactivity was found for either (Et₃Si)₂ or B₂pin₂ (entries 4, 7).



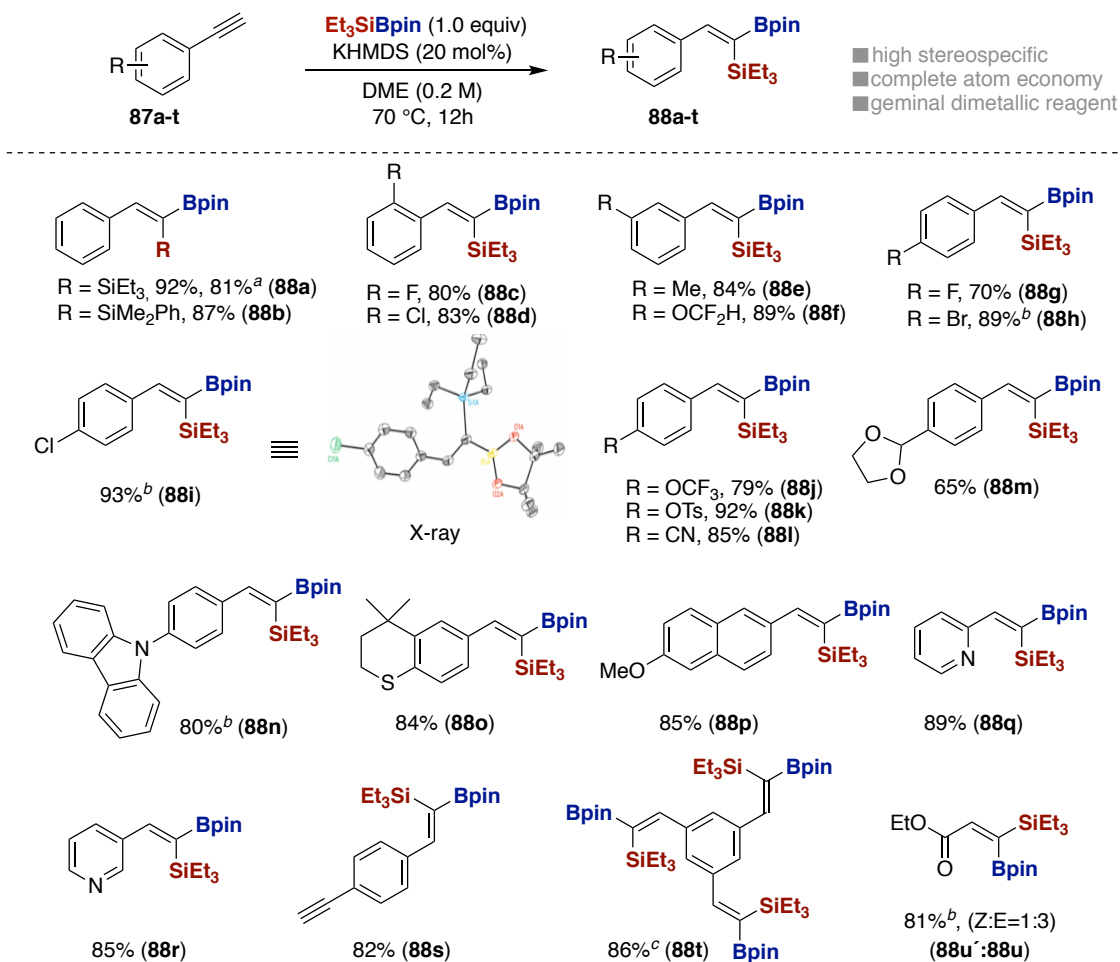
Entry	X-Bpin or [Si]-X	Conversion of 87 (%)	Yield of 89 (%) ^a
1	Et ₃ SiBpin	100	92
2	Ph ₂ MeSiBpin	100	80
3	(TMS) ₃ SiBpin	60	ND
4	Et ₃ SiSiEt ₃	32	ND
5	TMS ₄ Si	16	ND
6	HBpin	15	ND
7	B ₂ pin ₂	25	ND
8	HSiEt ₃	13	ND

Reaction conditions: **87a** (0.40 mmol), Et₃SiBpin (0.40 mmol), KHMDS (20 mol%) in solvent (2.0 mL) at 70 °C, 12h. ^a GC yields using decane as internal standard.

Table 4.4. Screening of X-Bpin or X-[Si] reagents

4.4.2. Preparative substrate scope

4.4.2.1. Scope of terminal alkyne



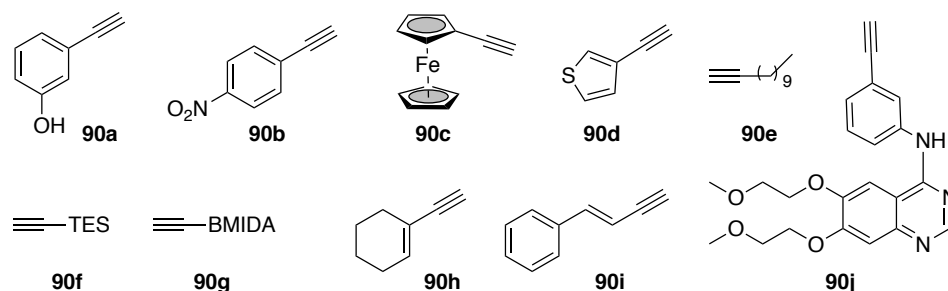
Reaction conditions: As Table 4.3, entry 1; yield of isolated product, average of at least two independent runs ^a 10 mol scale. ^b T = rt. ^c Et_3SiBpin (3.5 equiv).

Scheme 4.19. Scope of terminal alkyne

The generality of the stereoselective silaboration was studied by applying the optimized conditions to a diverse set of substituted phenylacetylenes, most of which were commercially available. As becomes evident from the results compiled in Scheme 4.19, the scope of alkyne partner turned out to be rather wide regardless of the electronic and steric environments on the aryl ring. Substrates containing halide entities at the *ortho*-position were tolerated without noticeable side-reactions (**88c** and **88d**). Furthermore, nitriles (**88l**), ethers (**88f**, **88j**, **88p**), carbazoles (**88n**), ketones (**88m**), or thiochromane (**88o**) could all perfectly be accommodated. Notably, the silaboration of **87a** could be executed on a gram scale (10 mmol) without significant erosion in yield. The presence of nitrogen-containing heterocycles did not interfere with the targeted 1,1-silaboration (**88q** and **88r**). Interestingly, a substrate bearing two terminal alkynyl moieties (**87s**) underwent 1,1-diboration at only one alkynyl group; However, three-fold

silaboration was within reach after carefully adjusting the stoichiometry of the reaction (**88t**). Notably, E/Z mixtures of propiolate (**87u**) were observed if **87u** was used as starting material. This result could be explained by a pathway similar to that shown by Ohmiya and Sawamura's,¹⁸ in which an allene intermediate is involved in.

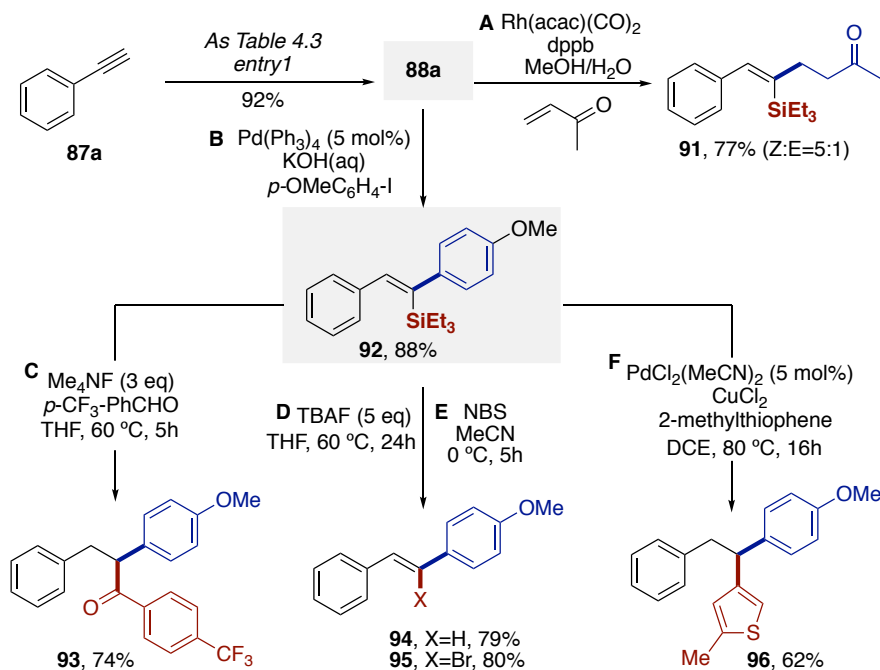
4.4.2.2. Unsuccessful substrates



Scheme 4.20. Unsuccessful substrates of aryl pivalates

The limitations on the alkyne partner were identified while studying the scope of the reaction (Scheme 4.20). For example, unprotected phenols (**90a**), nitro groups (**90b**) and ferrocenes (**90c**) were not compatible under our reaction conditions. 3-ethynylthiophene (**90d**) was decomposed during the reaction, leading to low yields of the final silaboration event and no improvement was found upon lowering down the temperature. Unfortunately, no reactivity was found with unactivated alkyl-substituted acetylenes (**90e**) even by changing all reaction parameters or stronger bases. Likewise, the use of (triethylsilyl)acetylene (**90f**) resulted in a complex mixture of unidentified by products and alkynyl MIDA boronate (**90g**) was recovered under the reaction condition. In the case of Erlotinb derivative (**90j**), no reaction took place, presumably by sequestering the potassium cation by the ethereal environment. Likewise, enynes could not be employed as substrates, suggesting that the conjugated arene was essential for promoting our 1,1-silaboration.

4.4.3. Synthetic Application of 1-boryl-1-silylalkene

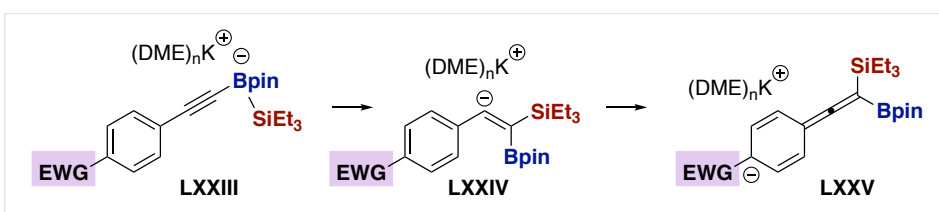
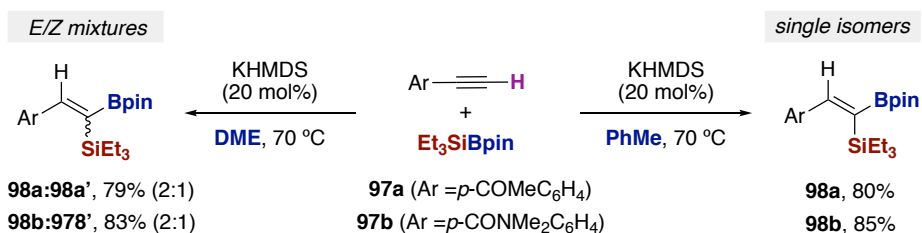


Scheme 4.21. Scope of benzyl and allyl pivalates

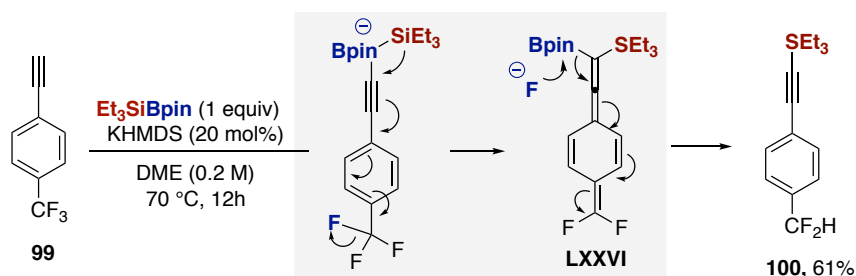
With a powerful methodology in hand for accessing silaborated alkenes, we next wondered whether we could access densely substituted alkenes by means of site-selective C–Si or C–B bond-cleavage. As shown in Scheme 4.21, the Bpin group could first be converted to an aryl or alkyl group by means of a Pd-catalyzed Suzuki-Miyaura coupling or a Rh-catalyzed 1,4-addition to an appropriate Michael acceptors (Scheme 4.21, A, B).⁵⁵ Subsequently, a nucleophilic addition of **92** to an aldehyde or protodesilylation of the silyl group could be achieved, leading to **93** and **94** respectively (Scheme 4.21, C, D).⁵⁶ In addition, halogen exchange by exposing **92** to NBS delivered **95** in high yield (Scheme 4.21, E) whereas a Hiyama-type cross-coupling reaction was within reach by synergistic Pd/Cu catalysis if coupled with 2-methyl thiophene under oxidative conditions (Scheme 4.21, F).⁵⁷ Although a trisubstituted alkene should be obtained upon oxidative C–H functionalization, the formation of **96** can tentatively be interpreted on the basis of a subsequent metal hydride insertion into the π -system followed by protonolysis.

It is worth noting that substrates possessing electron withdrawing groups such as CONEt₂ or Ac (**97a**, **97b**) at the *para* position delivered E/Z mixtures (Scheme 4.22). Note, however, that a single isomer could be obtained by simply changing the solvent from DME to toluene. In these two particular cases, it becomes apparent that the non-coordinating solvent favors the generation of the Z isomer. The reason behind this remains unclear so far, but the result can tentatively be interpreted on the basis of the strong coordination of DME to the escorting potassium counterion, thus generating a separated silylboronated ion pair **LXXIII** that precedes the formation of allene-type intermediates **LXXV** via [1,2]-shift from the boron ate complex.^{18, 58}

Solvent-dependent stereoselectivity pattern



Defluorosilylation of *p*-CF₃-phenylacetylene

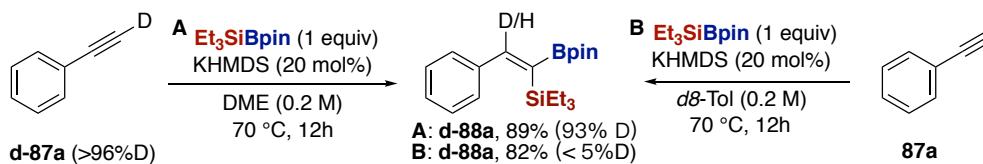


Scheme 4.22. Solvent-dependent selectivity and intermediacy of allene species

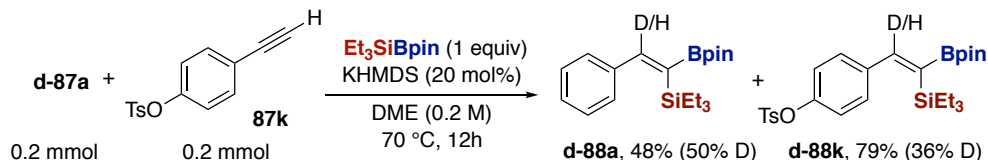
In addition, we found an intriguing defluorosilylation reaction when *p*-CF₃-phenylacetylene was used under our optimized condition. Specifically, defluorosilylation of **99** was observed instead in a 61% yield (Scheme 4.22). The mechanism of the transformation is believed to proceed via a boronate complex, leading to the formation of a silaborallene **LXXVI** upon fluoride extrusion. Subsequent nucleophilic attack of the fluoride anion at the boron followed by rearomatization resulted in the formal defluorosilylated product. In a formal sense, the formation of **LXXVI** serves as a testament that a migration might occur through allene intermediates, suggesting a similar reaction pathway to that compounds possessing electronwithdrawing groups at the *para* position such as **97a** and **97b**.

4.4.4. Mechanistic considerations

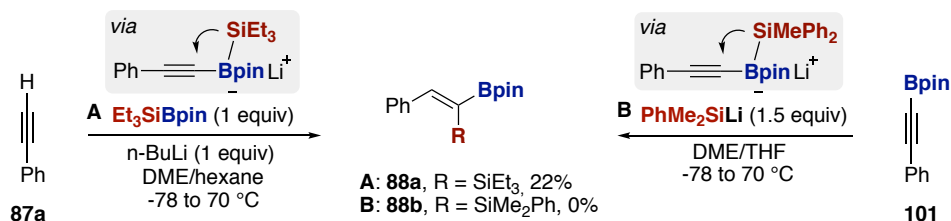
A ■ deuterium labeling experiment



B ■ deuterium-labeled crossover experiment



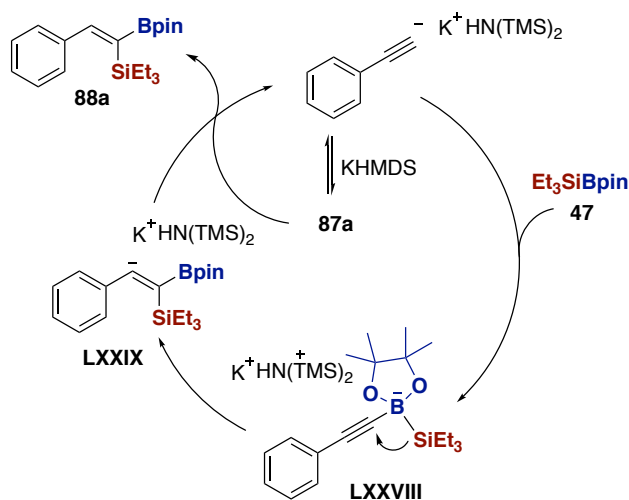
C ■ Stoichiometric reaction using *n*-BuLi and PhMe_2SiLi



Scheme 4.23. Mechanistic studies

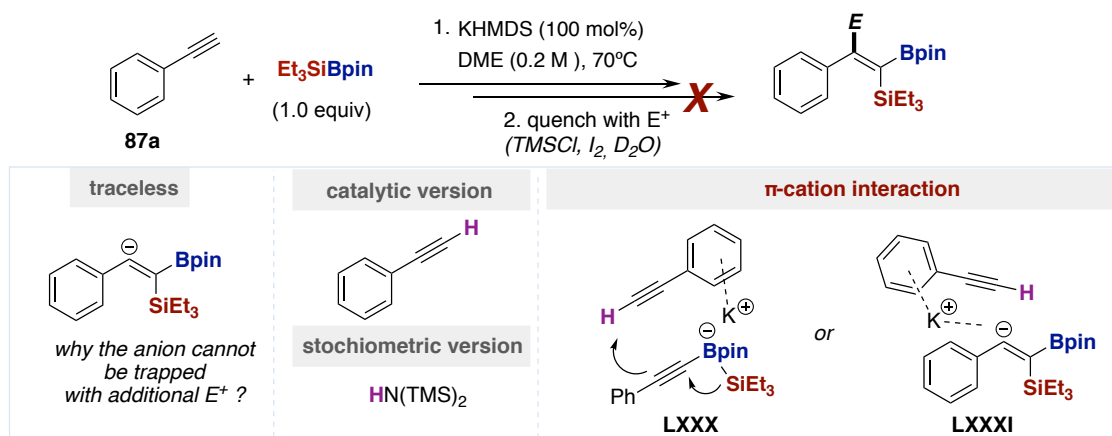
To gain insight into the mechanism, a deuterium labeling experiment was conducted (Scheme 4.23, A). The reaction with **d-87a** (>96 % D) afforded **d-88a** with 93% incorporation of deuterium at the vinylic motif. In line with our expectations, the reaction of unlabeled acetylene **87a** with d^8 -toluene led to the final product with no deuterium incorporation. Taken together, these results suggest that the hydrogen atom derives exclusively from the acetylenic *sp* C–H bond. Interestingly, a deuterium-labeled crossover experiment between **d-87a** (>96 % D) and **87k** resulted in nearly complete H/D scrambling in both products **d-88a** and **d-88k**, suggesting that the final protonolysis of the vinylic motif takes place via intermolecular events (Scheme 4.23, B). In line with these experiments, we propose that the reaction was initiated by deprotonation of the acetylenic *sp* C–H bond ($\text{pK}_a \sim 25$) by KHMDS ($\text{pK}_a = 27$). This assumption was tested by reacting **87a** with *n*-BuLi in a stoichiometric fashion followed by reaction with Et_3SiBpin (Scheme 4.23, C). Although a moderate 22 % of **88a** was isolated after the reaction was stirred at 70 °C for 3h, we presume that such low yield is due to the use of lithium rather than potassium cation and also the lack of proton source to induce the migration. Notably, no desired product was obtained when the reaction mixture was treated at room temperature instead of 70 °C; in the absence of further kinetic studies, we believe that these observations suggest that the proposed 1,2-shift is likely endothermic. Interestingly, no reaction was found when exposing **101** to PhSiMe_2Li . It seems there is no driving force in the absence of proton, thus favoring a concerted 1,2-shift/deprotonation pathway.

■ Proposed mechanism



Scheme 4.24. Plausible mechanistic scenario

Although additional studies should await further investigations, our results are consistent with a mechanism occurring via initial deprotonation followed by addition of Et_3SiBpin , leading to a silylboronate adduct (Scheme 4.24). A subsequent 1,2-metallate shift likely gives access to the final product by abstracting a hydrogen atom from the starting alkyne, thus leading to the final product and generating back the key potassium acetylide.



Scheme 4.25. Attempts to trap intermediary anion

In light of these observations, one might argue whether the intermediate vinyl anion might be trapped with a different electrophile other than simple protonolysis in the presence of excess amounts of an alkyne. All our efforts to trap the nucleophilic entity with TMSCl , I_2 or D_2O were unsuccessful regardless of whether catalytic or stoichiometric amounts of KHMDS or even KH were used or not (Scheme 4.25).⁵⁹⁻⁶² Although tentative, this observation might indicate that the 1,2-migration is triggered with concomitant protonolysis in a concerted pathway. Alternatively, such a pathway might be triggered by cation π -interactions.⁶³ in that the potassium ion

coordinates to the arene of the phenylacetylene so that the deprotonation occurs in a concerted manner (**LXXX** or **LXXXI**). Although further experiments should be conducted to find whether this pathway occurs or not, this hypothesis is in line with the lack of reactivity found for alkyl-substituted acetylenes in our silaboration. Certainly, DFT calculations and in depth NMR studies⁶⁴ should be conducted to unravel whether such pathways intervene or not.

4.5. Conclusions

In summary, we have reported the development of a catalytic 1,1-silaboration of terminal alkynes that operates with excellent stereoselectivity catalyzed by KHMDS. This method does not only provide rapid access to rather useful 1,1-dimetallated building blocks, but also establish a platform to generate densely functionalized olefins by subsequent C-Si and C-B transformation. Our protocol is characterized by its mild conditions, accessing compounds in an atom-economical fashion in the absence of either stoichiometric organolithium species or transition metal complexes. Unfortunately, the reaction is mainly restricted to acetylenes end-capped with arenes, but efforts to incorporate alkyl substituted acetylenes are currently ongoing in our lab. A preliminary mechanistic pathway based on 1,2-metallate rearrangement from boron to the *sp* carbon has been proposed, although further studies are necessary to unravel the underpinnings of these processes.

4.6. References

1. Zhang, X.; Zhang, W. Z.; Ren, X.; Zhang, L. L.; Lu, X. B. Ligand-Free Ag(I)-Catalyzed Carboxylation of Terminal Alkynes with CO₂. *Org. Lett.* **2011**, *13*, 2402.
2. Gooßen, L. J.; Rodríguez, N.; Manjolinho, F.; Lange, P. P. Synthesis of Propiolic Acids via Copper-Catalyzed Insertion of Carbon Dioxide into the C–H Bond of Terminal Alkynes *Adv. Synth. Catal.* **2010**, *352*, 2913.
3. Chinchilla R.; Nájera, C. Recent Advances in Sonogashira Reactions. *Chem. Soc. Rev.* **2011**, *40*, 5084.
4. Stang, P. J., Diederich, F. Modern Acetylene Chemistry. VCH: Weinheim, **1995**.
5. Diederich, F., Stang, P. J., Tykwinski, R. R. Acetylene Chemistry. Wiley-VCH: Weinheim, **2005**.
6. Chinchilla, R.; Nájera, C. Chemicals from Alkynes with Palladium Catalysts. *Chem. Rev.* **2014**, *114*, 1783.
7. Au: (a) Chen, Q.; Zhao, J.; Ishikawa, Y.; Asao, N.; Yamamoto, Y.; Jin, T. Remarkable Catalytic Property of Nanoporous Gold on Activation of Diborons for Direct Diboration of Alkynes. *Org. Lett.* **2013**, *15*, 5766.
8. Fe: Nakagawa, N.; Hatakeyama, T.; Nakamura, M. Iron-Catalyzed Diboration and Carboboration of Alkynes. *Chem. - Eur. J.* **2015**, *21*, 4257.
9. Cu: Yoshida, H.; Kawashima, S.; Takemoto, Y.; Okada, K.; Ohshita, J.; Takaki, K. Copper-Catalyzed Borylation Reactions of Alkynes and Arynes. *Angew. Chem. Int. Ed.* **2012**, *51*, 235.
10. Guo, L.; Song, F.; Zhu, S.; Li, H.; Chu, L. *syn*-Selective Alkylarylation of Terminal Alkynes via the Combination of Photoredox and Nickel Catalysis. *Nat Comm*, **2018**, *9*, 4543.
11. (a) Yoshida, H. Borylation of Alkynes under Base/Coinage Metal Catalysis: Some Recent Developments. *ACS Catal.* **2016**, *6*, 1799. (b) Wille, U. Radical Cascades Initiated by Intermolecular Radical Addition to Alkynes and Related Triple Bond Systems. *Chem. Rev.* **2013**, *113*, 813.
12. Zhurakovskiy, O.; Dias, R. M. P.; Noble, A.; Aggarwal, V. K.; Stereo- and Regiocontrolled Methylboration of Terminal Alkynes. *Org. Lett.* **2018**, *20*, 3136.
13. Nagao, K.; Ohmiya, H.; Sawamura, M. Anti-Selective Vicinal Silaboration and Diboration of Alkynoates through Phosphine Organocatalysis. *Org. Lett.* **2015**, *17*, 1304.
14. Barrado, A. G.; Zieliński, A.; Goddard, R.; Alcarazo M. Regio- and Stereoselective Chlorocyanation of Alkynes. *Angew. Chem. Int. Ed.* **2017**, *56*, 13401.
15. Wang X.; Studer, A. Regio- and Stereoselective Cyanotriflation of Alkynes Using Aryl(cyano)iodonium Triflates. *J. Am. Chem. Soc.* **2016**, *138*, 2977.
16. Nagashima, Y.; Hirano, K.; Takita, R.; Uchiyama, M. Trans-Diborylation of Alkynes: Pseudo-Intramolecular Strategy Utilizing a Propargylic Alcohol Unit. *J. Am. Chem. Soc.* **2014**, *136*, 8532.
17. Yoshimura, A.; Takamachi, Y.; Han, L.-B.; Ogawa, A. Organosulfide-Catalyzed Diboration of Terminal Alkynes under Light. *Chem. - Eur. J.* **2015**, *21*, 13930.
18. Morinaga, A.; Nagao, K.; Ohmiya, H.; Sawamura, M. Synthesis of 1,1-Diborylalkenes through a Brønsted Base Catalyzed Reaction between Terminal Alkynes and Bis(pinacolato)diboron. *Angew. Chem. Int. Ed.* **2015**, *54*, 15859.
19. Krautwald, S.; Bezdek, M. J.; Chirik, P. J. Cobalt-Catalyzed 1,1-Diboration of Terminal Alkynes: Scope, Mechanism, and Synthetic Applications. *J. Am. Chem. Soc.* **2017**, *139*, 3868.
20. Dömling, A.; Wang, W.; Wang, K. Chemistry and Biology of Multicomponent Reactions. *Chem. Rev.* **2012**, *112*, 3083.
21. Ohno, H.; Ohta, Y.; Oishi, S.; Fujii, N. Direct Synthesis of 2-(Aminomethyl)indoles through Copper(I)-Catalyzed Domino Three-Component Coupling and Cyclization Reactions. *Angew. Chem. Int. Ed.* **2007**, *46*, 2295.
22. Sun, Q.; Li, L.; Liu, L.; Yang, Y.; Zha, Z.; Wang, Z. Copper-Catalyzed 1,1-Difunctionalization Of Terminal Alkynes: A Three-Component Reaction For The Construction Of Vinyl Sulfones. *Sci. China Chem.* **2019**, *62*, 904.
23. Lv, Y.; Pu, W.; Shi, L. Copper-Catalyzed Regio- and Stereoselective 1,1-Dicarbonylfunctionalization of Terminal Alkynes. *Org. Lett.* **2019**, *21*, 6034.

24. Liu, L.; Sun, K.; Su, L.; Dong, J.; Cheng, L.; Zhu, X.; Au, C.; Zhou, Y.; Yin, S. Palladium-Catalyzed Regio- and Stereoselective Coupling-Addition of Propiolates with Arylsulfonyl Hydrazides: A Pattern for Difunctionalization of Alkynes. *Org. Lett.* **2018**, *20*, 4023.
25. Neeve, E. C.; Geier, S. J.; Mkhaliid, I. A. I.; Westcott, S. A.; Marder, T. B. Diboron Compounds: From Structural Curiosity to Synthetic Workhorse. *Chem. Rev.* **2016**, *116*, 9091.
26. Barbeyron, R.; Benedetti, E.; Cossy, J.; Vasseur, J.-J.; Arseniyadis, S.; Smietana, M. Recent developments in alkyne borylations. *Tetrahedron* **2014**, *70*, 8431.
27. Takaya, J.; Iwasawa, N. Catalytic, Direct Synthesis of Bis(boronate) Compounds. *ACS Catal.* **2012**, *2*, 1993.
28. Shimizu, M.; Nakamaki, C.; Shimono, K.; Schelper, M.; Kurahashi, T.; Hiyama, T. Selective And Catalytic Arylation Of N-Phenylpyrrolidine: (Sp^3) C-H Bond Functionalization In The Absence Of A Directing Group. *J. Am. Chem. Soc.* **2005**, *127*, 12506.
29. Iwasaki, M.; Nishihara, Y. Synthesis of Multisubstituted Olefins through Regio- and Stereoselective Addition of Interelement Compounds Having B-Si, B-B, and Cl-S Bonds to Alkynes, and Subsequent Cross-Couplings. *Chem. Rec.* **2016**, *16*, 2031.
30. Wang, J. Stereoselective Alkene Synthesis in Topics in Current Chemistry. Springer: Berlin, **2012**.
31. Negishi, E.; Huang, Z.; Wang, G.; Mohan, S.; Wang, C.; Hattori, H. Recent Advances In Efficient And Selective Synthesis Of Di-, Tri-, And Tetrasubstituted Alkenes Via Pd-Catalyzed Alkenylation-Carbonyl Olefination Synergy. *Acc. Chem. Res.* **2008**, *41*, 1474.
32. Royes, J.; Cuenca, A. B.; Fernández, E. Access to 1,1-Diborylalkenes and Concomitant Stereoselective Reactivity. *Eur. J. Org. Chem.* **2018**, 2728. (b) Cuenca, A. B.; Shishido, R.; Ito H.; Fernández, E. Transition-Metal-Free B-B and B-Interelement Reactions with Organic Molecules. *Chem. Soc. Rev.* **2017**, *46*, 415.
33. Lee, C.-I.; Shih, W.-C.; Zhou, J.; Reibenspies, J. H.; Ozerov, O. V. Synthesis of Triborylalkenes from Terminal Alkynes by Iridium-Catalyzed Tandem C-H Borylation and Diboration. *Angew. Chem., Int. Ed.* **2015**, *54*, 14003.
34. Liu, X.; Ming, W.; Friedrich, A.; Kerner, F.; Marder, T. B. Copper-Catalyzed Triboration of Terminal Alkynes Using B_2pin_2 : Efficient Synthesis of 1,1,2-Triborylalkenes. doi.org/10.1002/anie.201908466.
35. Richard J. Procter, Marina Uzelac, Jessica Cid, Philip J. Rushworth, and Michael J. Ingleson Low coordinate NHC-Zinc-Hydride Complexes Catalyze Alkyne C-H Borylation and Hydroboration using Pinacolborane. *ACS Catal.* **2019**, *9*, 5760.
36. Aggarwal, V. K.; Fang, G.-Y.; Ginesta, X.; Howells, D. M.; Zaja, M. Toward an Understanding of the Factors Responsible for the 1,2-migration of Alkyl Groups in Borate Complexes. *Pure Appl. Chem.* **2006**, *78*, 215.
37. (a) Matteson, D. S.; Mah, R. W. H. Neighboring Boron in Nucleophilic Displacement. *J. Am. Chem. Soc.* **1963**, *85*, 2599. (b) Matteson, D. S. Asymmetric Synthesis with Boronic Esters. *Acc. Chem. Res.* **1988**, *21*, 294. (c) Matteson, D. S. α -Halo Boronic Esters in Asymmetric Synthesis. *Tetrahedron* **1998**, *54*, 10555. (d) Matteson, D. S. Boronic Esters in Asymmetric Synthesis. *J. Org. Chem.* **2013**, *78*, 10009.
38. A. Fawcett, A. Murtaza, C. H. U. Gregson, V. K. Aggarwal, Strain-Release-Driven Homologation of Boronic Esters: Application to the Modular Synthesis of Azetidines. *J. Am. Chem. Soc.* **2019**, *141*, 4573.
39. He, F. Song, H. Sun, Y. Huang, Transition-Metal-Free Suzuki-Type Cross-Coupling Reaction of Benzyl Halides and Boronic Acids via 1,2-Metalate Shift. *J. Am. Chem. Soc.* **2018**, *140*, 2693.
40. M. Burns, S. Essafi, J. R. Bame, S. P. Bull, M. P. Webster, S. Balieu, J. W. Dale, C. P. Butts, J. N. Harvey, V. K. Aggarwal, Assembly-line Synthesis of Organic Molecules with Tailored Shapes. *Nature* **2014**, *513*, 183.
41. (a) Leung, T.; Zweifel, G. Allenic Boranes. Their Preparation and Conversion into Alkylallenes. *J. Am. Chem. Soc.* **1974**, *96*, 5620. (b) Zweifel, G.; Backlund, S. J.; Leung, T. Synthesis of Homopropargylic and α -allenic Alcohols from Lithium Chloropropargylide, Trialkylboranes, and Aldehydes. *J. Am. Chem. Soc.* **1978**, *100*, 5561.
42. (a) Suzuki, A.; Miyaura, N.; Abiko, S.; Itoh, M.; Brown, H. C.; Sinclair, J. A.; Midland, M. M. Convenient and General Synthesis of Acetylenes via the Reaction of Iodine with Lithium I-alkynyltriorganoborates. *J. Am. Chem. Soc.* **1973**, *95*, 3080. (b) Ganesh, V.; Odachowski, M.; Aggarwal, V. K. Alkynyl Moiety for

- Triggering 1,2-Metallate Shifts: Enantiospecific sp^2 - sp^3 Coupling of Boronic Esters with *p*-Arylacetylenes. *Angew. Chem. Int. Ed.* **2017**, *56*, 16318.
43. (a) Ishida, N.; Miura, T.; Murakami, M. Stereoselective Synthesis of Trisubstituted Alkenylboranes by Palladium-Catalysed Reaction of Alkynyltriarylborates with Aryl Halides. *Chem. Commun.* **2007**, 4381. (b) Ishida, N.; Ikemoto, W.; Narumi, M.; Murakami, M. Synthesis of Pyridine-N-oxide–Borane Intramolecular Complexes by Palladium-Catalyzed Reaction of 2-Bromopyridine-N-oxides with Alkynyltriarylborates. *Org. Lett.* **2011**, *13*, 3008.
 44. Shimizu, M.; Kurahashi, T.; Kitagawa, H.; Hiyama, T. gem-Silylborylation of an *sp* Carbon: Novel Synthesis of 1-Boryl-1-silylallenes. *Org. Lett.* **2003**, *5*, 225.
 45. Zweifel, G.; Arzoumanian, H.; Whitney, C. C. A Convenient Stereoselective Synthesis of Substituted Silkenes via Hydroboration-Iodination of Alkynes. *J. Am. Chem. Soc.* **1967**, *89*, 3652.
 46. Brown, H. C.; Levy, A. B.; Midland, M. M. Reaction of Lithium Ethynyl- and Ethenyltriarylborates with Acid. Valuable Route to the Markovnikov Alkenyl- and Alkylboranes. *J. Am. Chem. Soc.* **1975**, *97*, 5017.
 47. Ishida, N.; Shimamoto, Y.; Murakami, M. Stereoselective Synthesis of (*E*)-(Trisubstituted alkenyl)borinic Esters: Stereochemistry Reversed by Ligand in the Palladium-Catalyzed Reaction of Alkynylborates with Aryl Halides. *Org. Lett.* **2009**, *11*, 5434.
 48. Ishida, N.; Narumi, M.; Murakami, M. Synthesis of Amine–Borane Intramolecular Complexes through Palladium-Catalyzed Rearrangement of Ammonioalkynyltriarylborates. *Org. Lett.* **2008**, *10*, 1279.
 49. Hata, T.; Kitagawa, H.; Masai, H.; Kurahashi, T.; Shimizu, M.; Hiyama, T. Geminal Difunctionalization of Alkenylidene-Type Carbenoids by Using Interelement Compounds. *Angew. Chem., Int. Ed.* **2001**, *40*, 790.
 50. Kurahashi, T.; Hata, T.; Masai, H.; Kitagawa, H.; Shimizu, M.; Hiyama, T. Geminal Dimetalation of Alkylidene-Type Carbenoids With Silylboranes And Diborons. *Tetrahedron* **2002**, *58*, 6381.
 51. Cascia, E. L.; Cuenca, A. B.; Fernandez, E. Opportune gem-Silylborylation of Carbonyl Compounds: A Modular and Stereocontrolled Entry to Tetrasubstituted Olefins. *Chem. Eur. J.* **2016**, *22*, 18737.
 52. Algera, R. F.; Ma, Y.; Collum, D. B. Sodium Diisopropylamide: Aggregation, Solvation, and Stability. *J. Am. Chem. Soc.* **2017**, *139*, 7921.
 53. Lucht, B. L.; Collum, D. B. Lithium Ion Solvation: Amine and Unsaturated Hydrocarbon Solvates of Lithium Hexamethyldisilazide (LiHMDS). *J. Am. Chem. Soc.* **1996**, *118*, 2217.
 54. Lucht, B. L.; Collum, D. B. Ethereal Solvation of Lithium Hexamethyldisilazide: Unexpected Relationships of Solvation Number, Solvation Energy, and Aggregation State. *J. Am. Chem. Soc.* **1995**, *117*, 9863.
 55. Masaaki Sakai, Hiroyuki Hayashi, and Norio Miyaura Rhodium-Catalyzed Conjugate Addition of Aryl- or 1-Alkenylboronic Acids to Enones. *Organometallic* **1997**, *16*, 4229.
 56. Kurahashi, T.; Hata, T.; Masai, H.; Kitagawa, H.; Shimizu, M.; Hiyama, T. Geminal Dimetalation of Alkylidene-Type Carbenoids With Silylboranes And Diborons. *Tetrahedron* **2002**, *58*, 6381.
 57. Funaki, K.; Sato, T.; Oi, S. Pd-Catalyzed β -Selective Direct C–H Bond Arylation of Thiophenes with Aryltrimethylsilanes. *Org. Lett.* **2012**, *14*, 6186.
 58. Ganesh, V.; Odachowski, M.; Aggarwal, V. K. Alkynyl Moiety for Triggering 1,2-Metallate Shifts: Enantiospecific sp^2 - sp^3 Coupling of Boronic Esters with *p*-Arylacetylenes. *Angew. Chem. Int. Ed.* **2017**, *56*, 9752.
 59. Schlosser, M.; Bosshardt, H.; Walde, A.; Stahle, M. A Facile Route to a Sensitive Terpene Alcohol–Regio- Unselective Metalation of α -Terpinene as Key Step. *Angew. Chem. Int. Ed.* **1980**, *19*, 303.
 60. Sun, C.-L.; Li, H.; Yu, D.-G.; Yu, M.; Zhou, X.; Lu, X.-Y.; Huang, K.; Zheng, S.-F.; Li, B.-J.; Shi, Z.-J. An Efficient Organo-catalytic Method for Constructing Biaryls through Aromatic C–H Activation. *Nat. Chem.* **2010**, *2*, 1044.
 61. Midya, G. C.; Paladhi, S.; Dhara, K.; Dash, J. Iron Catalyzed Highly Regioselective Dimerization of Terminal Aryl Alkynes. *Chem. Commun.* **2011**, 47, 6698.
 62. Midya, G. C.; Parasar, B.; Dhara, K.; Dash, J. Ligand Mediated Iron Catalyzed Dimerization of Terminal Aryl Alkynes: Scope and Limitations. *Org. Biomol. Chem.* **2014**, *12*, 1812.
 63. For selected reviews, (a) Yamada, S. Cation- π Interactions in Organic Synthesis. *Chem. Rev.* **2018**, *118*, 11353. (b) Dougherty, D. A. The Cation- π Interaction. *Acc. Chem. Res.* **2013**, *46*, 885. (c) Mahadevi, A.

- S.; Sastry, G. N. Cation- π Interaction: Its Role and Relevance in Chemistry, Biology, and Material Science. *Chem. Rev.* **2013**, *113*, 2100–2138. (d) Dougherty, D. A. Cation- π Interactions in Chemistry and Biology: A New View of Benzene, Phe, Tyr, and Trp. *Science* **1996**, *271*, 163.
64. Banerjee, S.; Yang, Y.F.; Jenkins, I. D.; Liang, Y.; Toutov, A. A.; Liu, W.-B.; Schuman, D. P.; Grubbs, R. H.; Stoltz, B. M.; Krenke, E. H.; Houk, K. N.; Zare, R. N. Ionic and Neutral Mechanisms for C-H Bond Silylation of Aromatic Heterocycles Catalyzed by Potassium tert-Butoxide. *J. Am. Chem. Soc.* **2017**, *139*, 6880.

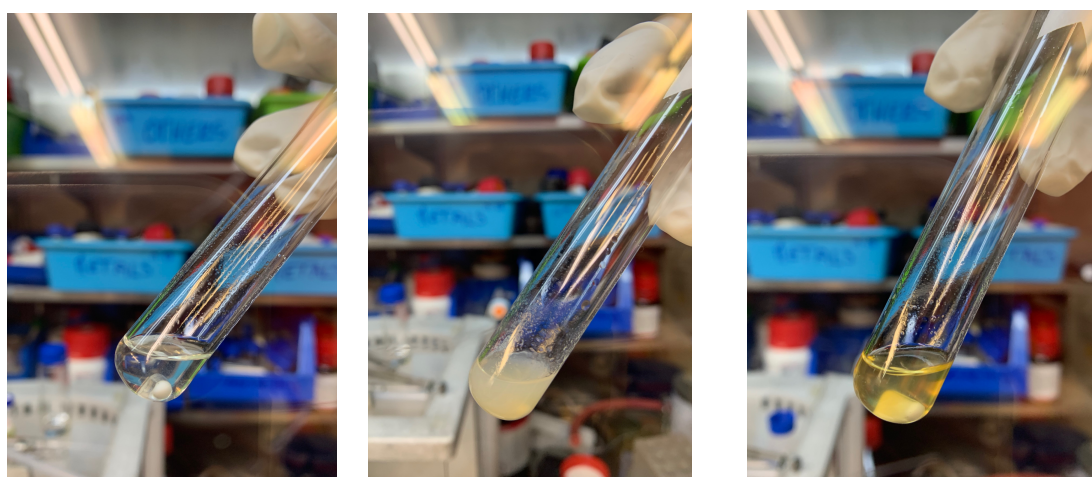
4.7. Experimental Section

4.7.1. General considerations

Reagents. Commercially available materials were used without further purification. KHMDS was purchased from Strem Chemicals. Anhydrous DME and Dioxane were purchased from Alfa Aesar. Silylborane Et₃SiBpin was prepared in bulk quantities in one-step from Et₃SiH and B₂pin₂ according to a known literature procedure. All the other reagents were purchased from commercial sources and used as received. Flash chromatography was performed with EM Science silica gel 60 (230-400 mesh). Thin layer chromatography was carried out using Merck TLC Silica gel 60 F254.

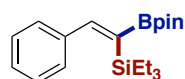
Analytical methods: ¹H-NMR, ¹³C-NMR, and ¹⁹F-NMR spectra and melting points (where applicable) are included for all new compounds. ¹H-NMR, ¹³C-NMR, and ¹⁹F-NMR spectra were recorded on a Bruker 300 MHz, a Bruker 400 MHz or Bruker 500 MHz. All ¹H-NMR spectra are reported in parts per million (ppm) downfield of TMS and were measured relative to the signals for CHCl₃ (7.26 ppm). All ¹³C-NMR spectra were reported in ppm relative to residual CHCl₃ (77.2 ppm) and were obtained with ¹H decoupling. Coupling constants, *J*, are reported in hertz (Hz). Melting points were measured using open glass capillaries in a Büchi B540 apparatus. Infrared spectra were recorded on a Bruker Tensor 27. Specific optical rotation measurements were carried out on a Jasco P-1030 model polarimeter equipped with a PMT detector using the Sodium line at 589 nm. Mass spectra were recorded on a Waters LCT Premier spectrometer. Gas chromatographic analyses were performed on HewlettPackard 6890 gas chromatography instrument with a FID detector using 25m x 0.20 mm capillary column with cross-linked methyl siloxane as the stationary phase. EPR signals were recorded with EMX Micro EPR spectrometer. The yields reported refer to isolated yields and represent an average of at least two independent runs. The procedures described in this section are representative. Thus, the yields may differ slightly from those given in the tables of the manuscript.

4.7.2. General procedure for base-catalyzed 1,1-silaboration of terminal alkynes

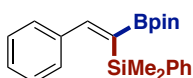


(Left) KHMDS dissolved in DME. **(Middle)** alkyne was added, deprotonation occurs immediately. **(Right)** TESBpin was added in the end.

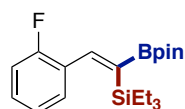
General procedure A: An oven-dried 10 mL screw-capped test tube containing a stirring bar was transferred to a nitrogen-filled glove-box where KHMDS (16.0 mg, 0.08 mmol), and dry ethylene glycol dimethyl ether (DME, 0.2 M, 2mL) were added. (*left*) The corresponding alkyne (1.0 eq, 0.4 mmol) was subsequently added. (*middle*) Then, Et₃SiBpin (96.9 mg, 0.4 mmol) was added in the end. (*right*) The reaction mixture was taken out of the glovebox and heated to 70 °C. After rigorously stirred for 12 h, the reaction was diluted with EtOAc (8 mL). the mixture filtered through a Celite® plug and concentrated under reduced pressure, the desired product was directly purified by flash column chromatography in silica. The product was isolated by column chromatography to give the corresponding 1,1-silaborylalkenes



(Z)-triethyl(2-phenyl-1-(4,4,5,5-tetramethyl-1,3,2-dioxaborolan-2-yl)vinyl)silane (88a). Following the general procedure, using ethynylbenzene (40.8 mg, 0.4 mmol), the title compound was obtained in 91% yield (125.3 mg) as colorless oil. *R*_f 0.65 (Hex: EtOAc 50:1). ¹H NMR (300 MHz, CDCl₃) δ 8.14 (s, 1H), 7.29 (s, 5H), 1.32 (s, 12H), 0.85 (t, *J* = 7.8 Hz, 9H), 0.55 (q, *J* = 7.8 Hz, 6H) ppm. ¹³C NMR (75 MHz, CDCl₃) δ 158.5, 141.9, 128.1, 127.7, 127.6, 83.2, 24.9, 7.8, 5.0 ppm. IR (neat, cm⁻¹): 2953, 2874, 1562, 1353, 1321, 1144, 860, 756. HRMS (ESI) [C₂₀H₃₄BO₂Si] (M+H) *calcd.* 334.2443, *found* 334.2364.



(Z)-dimethyl(phenyl)(2-phenyl-1-(4,4,5,5-tetramethyl-1,3,2-dioxaborolan-2-yl)vinyl)silane (88b). Following the general procedure, using ethynylbenzene (40.8 mg, 0.4 mmol), the title compound was obtained in 87% yield (126.6 mg) as colorless oil. *R*_f 0.62 (Hex: EtOAc 50:1). ¹H NMR (300 MHz, CDCl₃) δ 8.12 (s, 1H), 7.58-7.54 (m, 2H), 7.41-7.24 (m, 3H), 7.18 (s, 5H), 1.25 (s, 12H), 0.22 (s, 6H) ppm. ¹³C NMR (75 MHz, CDCl₃) δ 158.4, 140.9, 134.1, 128.6, 128.5, 127.8, 127.7, 127.7, 83.5, 24.9, -0.4 ppm. IR (neat, cm⁻¹): 2977, 1427, 1352, 1321, 1211, 249, 1142, 814. HRMS (ESI) [C₂₃H₂₉BO₂SiNa] (M+Na) *calcd.* 386.1958, *found* 386.1962.

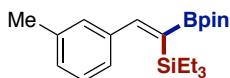


(Z)-triethyl(2-(2-fluorophenyl)-1-(4,4,5,5-tetramethyl-1,3,2-dioxaborolan-2-yl)vinyl)silane (88c). Following the general procedure, using 1-ethynyl-2-fluorobenzene (48.1 mg, 0.4 mmol), the title compound was obtained in 80% yield (115.8 mg) as colorless oil. *R*_f 0.55 (Hex: EtOAc 20:1). ¹H NMR (300 MHz, CDCl₃) δ 8.04 (s, 1H), 7.32-7.14 (m, 2H), 7.14-6.93 (m, 2H), 1.32 (s, 12H), 0.85 (t, *J* = 7.8 Hz, 9H), 0.53 (q, *J* = 7.9 Hz, 6H) ppm. ¹³C NMR (75 MHz, CDCl₃) δ 160.0 (d, *J* = 246.6 Hz), 151.5 (d, *J* = 2.3 Hz), 130.5 (d, *J* = 3.6 Hz), 129.6 (d, *J* = 16.3 Hz), 129.4 (d, *J* = 8.0 Hz), 123.3 (d, *J* = 3.6 Hz), 115.1 (d, *J* = 21.7 Hz), 83.3, 24.9, 7.7, 4.6 ppm. ¹⁹F NMR (376 MHz, CDCl₃) δ -114.48 ppm. IR (neat, cm⁻¹): 2952, 2874, 1739, 1481, 1317, 1270, 1143, 735. HRMS (ESI) [C₂₀H₃₂BF₂O₂SiNa] (M+Na) *calcd.* 384.2177, *found* 384.2177.

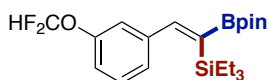


(Z)-[2-(2-chlorophenyl)-1-(4,4,5,5-tetramethyl-1,3,2-dioxaborolan-2-yl)vinyl]triethylsilane (88d). Following the general procedure, using 1-chloro-2-ethynylbenzene (54.6 mg, 0.4 mmol), the title

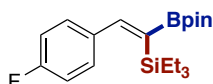
compound was obtained in 83% yield (125.4 mg) as colorless oil. R_f 0.58 (Hex: EtOAc 20:1). ^1H NMR (300 MHz, CDCl_3) δ 8.05 (s, 1H), 7.45-7.30 (m, 1H), 7.28-7.14 (m, 3H), 1.32 (s, 12H), 0.85 (t, $J = 7.8$ Hz, 9H), 0.49 (q, $J = 7.9$ Hz, 6H) ppm. ^{13}C NMR (75 MHz, CDCl_3) δ 155.9, 140.5, 133.0, 130.3, 128.9, 126.0, 83.2, 24.9, 7.7, 4.6 ppm. IR (neat, cm^{-1}): 2951, 2873, 1573, 1463, 1316, 1269, 1143, 1003, 857, 721. HRMS (ESI) [$\text{C}_{20}\text{H}_{32}\text{BClO}_2\text{SiNa}$] (M+Na) *calcd.* 400.1882, *found* 400.1874.



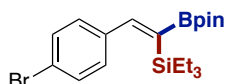
(Z)-triethyl(1-(4,4,5,5-tetramethyl-1,3,2-dioxaborolan-2-yl)-2-(m-tolyl)viny)triethylsilane (88e). Following the general procedure, using 1-ethynyl-3-methylbenzene (46.5 mg, 0.4 mmol), the title compound was obtained in 73% yield (104.6 mg) as colorless oil. R_f 0.43 (Hex: EtOAc 50:1). ^1H NMR (300 MHz, CDCl_3) δ 8.08 (s, 1H), 7.20-7.16 (m, 1H), 7.15-7.00 (m, 3H), 2.33 (s, 3H), 1.29 (s, 12H), 0.82 (t, $J = 7.8$ Hz, 9H), 0.52 (q, $J = 8.5, 7.9$ Hz, 6H) ppm. ^{13}C NMR (75 MHz, CDCl_3) δ 158.7, 141.8, 137.1, 128.9, 128.3, 127.6, 125.2, 83.2, 25.0, 21.5, 7.8, 5.0 ppm. IR (neat, cm^{-1}): 2951, 1873, 1564, 1316, 1270, 1143, 855, 734. HRMS (ESI) [$\text{C}_{21}\text{H}_{35}\text{BO}_2\text{SiNa}$] (M+Na) *calcd.* 380.2428, *found* 380.2432.



(Z)-triethyl(1-(3-(difluoromethoxy)phenyl)-1-(4,4,5,5-tetramethyl-1,3,2-dioxaborolan-2-yl)viny)triethylsilane (88f). Following the general procedure, using 1-(difluoromethoxy)-3-ethynylbenzene (67.2 mg, 0.4 mmol), the title compound was obtained in 87% yield (141.8 mg) as colorless oil. R_f 0.66 (Hex: EtOAc 20:1). ^1H NMR (300 MHz, CDCl_3) δ 8.03 (s, 1H), 7.31-7.25 (m, 1H), 7.14-7.05 (m, 1H), 7.05-6.98 (m, 2H), 6.49 (t, $J = 74.0$ Hz, 1H), 1.29 (s, 12H), 0.82 (t, $J = 7.8$ Hz, 9H), 0.51 (q, $J = 8.2$ Hz, 6H) ppm. ^{13}C NMR (75 MHz, CDCl_3) δ 156.7, 150.8, 143.9, 129.2, 125.2, 119.1, 118.6, 83.4, 24.9, 7.7, 4.8 ppm. ^{19}F NMR (376 MHz, CDCl_3) δ 80.58 ppm. IR (neat, cm^{-1}): 2954, 2875, 1738, 1372, 1320, 1234, 1142, 1047, 734. HRMS (ESI) [$\text{C}_{21}\text{H}_{33}\text{NaBF}_2\text{O}_3\text{Si}$] (M+Na) *calcd.* 432.2189, *found* 432.2203.



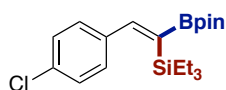
(Z)-triethyl(1-(4-fluorophenyl)-1-(4,4,5,5-tetramethyl-1,3,2-dioxaborolan-2-yl)viny)triethylsilane (88g). Following the general procedure, using 1-ethynyl-4-fluorobenzene (48.1 mg, 0.4 mmol), the title compound was obtained in 70% yield (101.3 mg) as colorless oil. R_f 0.63 (Hex: EtOAc 20:1). ^1H NMR (400 MHz, CDCl_3) δ 8.03 (s, 1H), 7.26-7.18 (m, 2H), 6.97 (t, $J = 8.7$ Hz, 2H), 1.29 (s, 12H), 0.82 (t, $J = 7.9$ Hz, 9H), 0.52 (q, $J = 7.8$ Hz, 6H) ppm. ^{13}C NMR (101 MHz, CDCl_3) δ 168.84 (d, $J = 229.2$ Hz), 157.2, 137.9 (d, $J = 3.7$ Hz), 129.8 (d, $J = 8.1$ Hz), 114.7 (d, $J = 21.4$ Hz), 83.3, 24.9, 7.8, 5.0 ppm. ^{19}F NMR (376 MHz, CDCl_3) δ -114.44 ppm. IR (neat, cm^{-1}): 2982, 1733, 1504, 1373, 1237, 1045, 910, 729. HRMS (ESI) [$\text{C}_{21}\text{H}_{33}\text{BNO}_2\text{Si}$] (M+H) *calcd.* 369.2404, *found* 369.2403.



(Z)-triethyl(1-(4-bromophenyl)-1-(4,4,5,5-tetramethyl-1,3,2-dioxaborolan-2-yl)viny)triethylsilane (88h). Following the general procedure, using 1-bromo-4-ethynylbenzene (72.4 mg, 0.4 mmol), the title compound was obtained in 89% yield (150.6 mg) as colorless oil. R_f 0.49 (Hex: EtOAc 50:1). ^1H NMR (300 MHz, CDCl_3) δ 7.99 (s, 1H), 7.41 (d, $J = 8.3$ Hz, 2H), 7.12 (d, $J = 8.2$ Hz, 2H), 1.29 (s, 12H), 0.82 (t, $J = 7.8$ Hz,

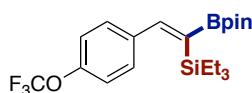
Stereoselective Base-Catalyzed 1,1-Silaboration of Terminal Alkynes

9H), 0.52 (q, $J = 7.8$ Hz, 6H) ppm. ^{13}C NMR (75 MHz, CDCl_3) δ 156.9, 140.7, 130.9, 129.8, 121.7, 83.4, 24.9, 7.8, 4.9 ppm. IR (neat, cm^{-1}): 2955, 2856, 1496, 1355, 1144, 1045, 1008, 735. HRMS (ESI) [$\text{C}_{20}\text{H}_{32}\text{BrBO}_2\text{SiNa}$] ($\text{M}+\text{H}$) *calcd.* 444.1377, *found* 444.1366.



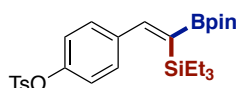
(Z)-(2-(4-chlorophenyl)-1-(4,4,5,5-tetramethyl-1,3,2-dioxaborolan-2-yl)vinyl)triethylsilane (88i).

Following the general procedure, using 1-chloro-4-ethynylbenzene (54.6 mg, 0.4 mmol), the title compound was obtained in 93% yield (140.9 mg) as colorless oil. R_f 0.54 (Hex: EtOAc 20:1). ^1H NMR (300 MHz, CDCl_3) δ 8.03 (s, 1H), 7.31-7.24 (m, 2H), 7.21-7.18 (m, 2H), 1.31 (s, 12H), 0.84 (t, $J = 7.7$ Hz, 9H), 0.54 (q, $J = 7.7$ Hz, 6H) ppm. ^{13}C NMR (75 MHz, CDCl_3) δ 157.0, 140.2, 133.4, 129.5, 127.9, 83.4, 24.9, 7.8, 5.0 ppm. IR (neat, cm^{-1}): 2952, 2874, 1486, 1318, 1143, 1092, 1014, 734. HRMS (ESI) [$\text{C}_{20}\text{H}_{32}\text{BClO}_2\text{SiNa}$] ($\text{M}+\text{Na}$) *calcd.* 400.1882, *found* 400.1876.



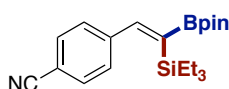
(Z)-triethyl(1-(4,4,5,5-tetramethyl-1,3,2-dioxaborolan-2-yl)-2-(4-(trifluoromethoxy)phenyl)vinyl)silane (88j).

Following the general procedure, using 1-ethynyl-4-(trifluoromethoxy)benzene (74.5 mg, 0.4 mmol), the title compound was obtained in 79% yield (135.2 mg) as colorless oil. R_f 0.56 (Hex: EtOAc 20:1). ^1H NMR (300 MHz, CDCl_3) δ 8.05 (s, 1H), 7.28 (d, $J = 5.4$ Hz, 2H), 7.14 (d, $J = 8.3$ Hz, 2H), 1.30 (s, 12H), 0.82 (t, $J = 7.8$ Hz, 9H), 0.51 (q, $J = 7.8$ Hz, 6H) ppm. ^{13}C NMR (75 MHz, CDCl_3) δ 156.6, 148.7, 140.6, 129.5, 120.2, 83.4, 24.9, 7.7, 4.9 ppm. ^{19}F NMR (376 MHz, CDCl_3) δ -57.96 ppm. IR (neat, cm^{-1}): 2954, 1734, 1502, 1372, 1252, 1144, 1045, 731. HRMS (ESI) [$\text{C}_{21}\text{H}_{33}\text{BF}_3\text{O}_3\text{Si}$] ($\text{M}+\text{H}$) *calcd.* 428.2278, *found* 428.2276.



(Z)-4-(2-(4,4,5,5-tetramethyl-1,3,2-dioxaborolan-2-yl)-2-(triethylsilyl)vinyl)phenyl 4-methylbenzenesulfonate (88k).

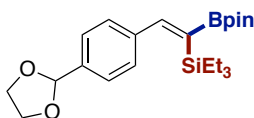
Following the general procedure, using 4-ethynylphenyl 4-methylbenzenesulfonate (108.9 mg, 0.4 mmol), the title compound was obtained in 92% yield (189.3 mg) as colorless oil. R_f 0.62 (Hex: EtOAc 10:1). ^1H NMR (300 MHz, CDCl_3) δ 8.01 (s, 1H), 7.67 (d, $J = 8.3$ Hz, 2H), 7.29 (d, $J = 8.1$ Hz, 2H), 7.15 (d, $J = 8.4$ Hz, 2H), 6.89 (d, $J = 8.5$ Hz, 2H), 2.44 (s, 3H), 1.29 (s, 12H), 0.81 (t, $J = 7.8$ Hz, 9H), 0.47 (q, $J = 7.8$ Hz, 6H) ppm. ^{13}C NMR (75 MHz, CDCl_3) δ 156.7, 149.1, 145.5, 140.9, 132.2, 129.8, 129.2, 128.7, 121.8, 83.4, 24.9, 21.8, 7.7, 4.9 ppm. IR (neat, cm^{-1}): 2955, 1626, 1500, 1348, 1176, 1143, 863, 715. HRMS (ESI) [$\text{C}_{27}\text{H}_{39}\text{BO}_5\text{SSiNa}$] ($\text{M}+\text{Na}$) *calcd.* 536.2309, *found* 536.2326.



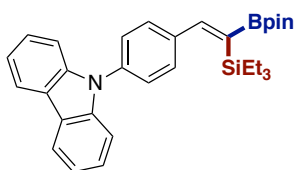
(Z)-4-(2-(4,4,5,5-tetramethyl-1,3,2-dioxaborolan-2-yl)-2-(triethylsilyl)vinyl)benzotrile (88l).

Following the general procedure, using 4-ethynylbenzotrile (50.8 mg, 0.4 mmol), the title compound was obtained in 85% yield (125.2 mg) as colorless oil. R_f 0.63 (Hex: EtOAc 30:1). ^1H NMR (300 MHz, CDCl_3) δ 8.03 (s, 1H), 7.58 (d, $J = 8.2$ Hz, 2H), 7.33 (d, $J = 8.1$ Hz, 2H), 1.29 (s, 12H), 0.81 (t, $J = 7.8$ Hz, 9H), 0.48 (q, $J = 7.8$ Hz, 6H) ppm. ^{13}C NMR (75 MHz, CDCl_3) δ 155.8, 146.6, 131.7, 128.8, 111.1, 83.6, 24.9, 7.7, 4.9 ppm. IR (neat, cm^{-1}):

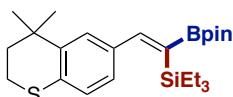
¹): 2982, 1737, 1372, 1320, 1235, 1144, 1045, 733. HRMS (ESI) [C₂₁H₃₃BNO₂Si] (M+H) *calcd.* 369.2404, *found* 369.2403.



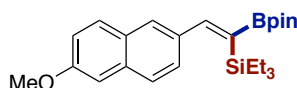
(Z)-2-(2-(4-(1,3-dioxolan-2-yl)phenyl)-1-(4,4,5,5-tetramethyl-1,3,2-dioxaborolan-2-yl)vinyl)triethylsilane (88m). Following the general procedure, using 2-(4-ethynylphenyl)-1,3-dioxolane (69.7 mg, 0.4 mmol), the title compound was obtained in 65% yield (108.1 mg) as colorless oil. *R*_f 0.69 (Hex: EtOAc 10:1). ¹H NMR (300 MHz, CDCl₃) δ 8.09 (s, 1H), 7.42 (d, *J* = 7.9 Hz, 2H), 7.29 (d, *J* = 7.5 Hz, 2H), 5.82 (s, 1H), 4.29-3.84 (m, 4H), 1.31 (s, 12H), 0.83 (t, *J* = 7.8 Hz, 9H), 0.53 (q, *J* = 7.8 Hz, 6H) ppm. ¹³C NMR (75 MHz, CDCl₃) δ 157.9, 142.8, 137.0, 128.2, 126.0, 103.8, 83.3, 65.4, 24.9, 7.8, 4.9 ppm. IR (neat, cm⁻¹): 3284, 2955, 1718, 1607, 1271, 1076, 858, 770. HRMS (ESI) [C₂₃H₃₈BO₄Si] (M+H) *calcd.* 417.2627, *found* 417.2629.



(Z)-9-(2-(2-(4-(4,4,5,5-tetramethyl-1,3,2-dioxaborolan-2-yl)-2-(triethylsilyl)vinyl)phenyl)-9H-carbazole (88n). Following the general procedure, using 9-(4-ethynylphenyl)-9H-carbazole (106.9 mg, 0.4 mmol), the title compound was obtained in 80% yield (163.0 mg) as colorless oil. *R*_f 0.65 (Hex: EtOAc 50:1). ¹H NMR (300 MHz, CDCl₃) δ 8.23 (s, 1H), 8.16 (d, *J* = 7.7 Hz, 2H), 7.50 (s, 4H), 7.46-7.37 (m, 4H), 7.30 (ddd, *J* = 8.0, 6.3, 1.9 Hz, 2H), 1.34 (s, 12H), 0.90 (t, *J* = 7.8 Hz, 9H), 0.62 (q, *J* = 7.4 Hz, 6H) ppm. ¹³C NMR (75 MHz, CDCl₃) δ 157.3, 141.3, 141.0, 136.9, 129.6, 126.4, 126.1, 123.5, 120.4, 120.0, 109.9, 83.4, 25.0, 7.9, 5.1 ppm. IR (neat, cm⁻¹): 2952, 1714, 1602, 1509, 1315, 1219, 1142, 723. HRMS (ESI) [C₃₂H₄₁BNO₂Si] (M+H) *calcd.* 509.3030, *found* 509.3013.



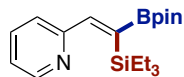
(Z)-2-(2-(4,4-dimethylthiochroman-6-yl)-1-(4,4,5,5-tetramethyl-1,3,2-dioxaborolan-2-yl)vinyl)triethylsilane (88o). Following the general procedure, using 6-ethynyl-4,4-dimethylthiochromane (80.9 mg, 0.4 mmol), the title compound was obtained in 84% yield (124.1 mg) as colorless oil. *R*_f 0.44 (Hex: EtOAc 50:1). ¹H NMR (300 MHz, CDCl₃) δ 8.01 (s, 1H), 7.27 (s, 1H), 7.08-6.82 (m, 2H), 3.19-2.83 (m, 2H), 2.06-1.84 (m, 2H), 1.32 (s, 6H), 1.30 (s, 12H), 0.84 (t, *J* = 7.8 Hz, 9H), 0.57 (q, *J* = 8.5, 8.0 Hz, 6H) ppm. ¹³C NMR (75 MHz, CDCl₃) δ 158.5, 141.1, 137.6, 131.2, 126.6, 126.1, 125.9, 83.2, 37.9, 33.2, 30.3, 25.0, 23.3, 7.8, 5.0 ppm. IR (neat, cm⁻¹): 2955, 1741, 1469, 1315, 1238, 1143, 1050, 854, 730. HRMS (ESI) [C₂₅H₄₂BO₂Si] (M+H) *calcd.* 444.2799, *found* 444.2797.



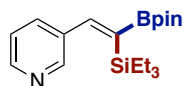
(Z)-triethyl(2-(6-methoxynaphthalen-2-yl)-1-(4,4,5,5-tetramethyl-1,3,2-dioxaborolan-2-yl)vinyl)silane (88p). Following the general procedure, using 2-ethynyl-6-methoxynaphthalene (75.3 mg, 0.4 mmol), the title compound was obtained in 85% yield (144.8 mg) as colorless oil. *R*_f 0.66 (Hex: EtOAc 20:1). ¹H NMR

Stereoselective Base-Catalyzed 1,1-Silaboration of Terminal Alkynes

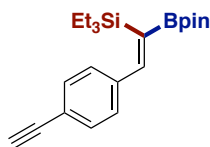
(300 MHz, CDCl_3) δ 8.22 (s, 1H), 7.76-7.58 (m, 3H), 7.39 (dd, $J = 8.4, 1.7$ Hz, 1H), 7.19-7.07 (m, 2H), 3.92 (s, 3H), 1.32 (s, 12H), 0.83 (t, $J = 7.8$ Hz, 9H), 0.57 (q, $J = 8.6, 8.2$ Hz, 6H) ppm. ^{13}C NMR (75 MHz, CDCl_3) δ 158.6, 157.9, 137.1, 134.1, 129.8, 128.4, 127.2, 127.1, 126.1, 119.0, 105.9, 83.3, 55.4, 25.0, 7.9, 5.1 ppm. IR (neat, cm^{-1}): 2971, 1619, 1481, 1392, 1356, 1320, 1260, 1148, 843. HRMS (ESI) [$\text{C}_{25}\text{H}_{37}\text{BO}_3\text{SiNa}$] ($\text{M}+\text{Na}$) *calcd.* 446.2534, *found* 446.2552.



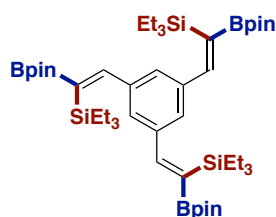
(Z)-2-(2-(4,4,5,5-tetramethyl-1,3,2-dioxaborolan-2-yl)-2-(triethylsilyl)vinyl)pyridine (88q). Following the general procedure, using 2-ethynylpyridine (41.2 mg, 0.4 mmol), the title compound was obtained in 89% yield (122.8 mg) as colorless oil. R_f 0.51 (Hex: EtOAc 10:1). ^1H NMR (300 MHz, CDCl_3) δ 8.57 (d, $J = 4.6$ Hz, 1H), 7.85 (s, 1H), 7.63 (td, $J = 7.6, 1.6$ Hz, 1H), 7.26 (d, $J = 7.9$ Hz, 1H), 7.14 (dd, $J = 7.5, 4.8$ Hz, 1H), 1.31 (s, 12H), 0.88 (t, $J = 7.6$ Hz, 9H), 0.71 (q, $J = 9.0, 8.3$ Hz, 6H) ppm. ^{13}C NMR (75 MHz, CDCl_3) δ 157.2, 154.0, 148.5, 136.0, 124.2, 122.4, 83.4, 25.0, 8.2, 5.4 ppm. IR (neat, cm^{-1}): 2949, 2872, 1735, 1426, 1372, 1320, 1238, 1144, 731. HRMS (ESI) [$\text{C}_{19}\text{H}_{33}\text{BNO}_2\text{Si}$] ($\text{M}+\text{H}$) *calcd.* 345.2404, *found* 345.2404.



(Z)-3-(2-(4,4,5,5-tetramethyl-1,3,2-dioxaborolan-2-yl)-2-(triethylsilyl)vinyl)pyridine (88r). Following the general procedure, using 3-ethynylpyridine (41.2 mg, 0.4 mmol), the title compound was obtained in 85% yield (117.3 mg) as colorless oil. R_f 0.45 (Hex: EtOAc 10:1). ^1H NMR (300 MHz, CDCl_3) δ 8.62 (d, $J = 2.2$ Hz, 1H), 8.44 (dd, $J = 4.8, 1.5$ Hz, 1H), 7.69 (dt, $J = 7.9, 1.9$ Hz, 1H), 7.21-7.09 (m, 2H), 1.25 (s, 12H), 0.97 (t, $J = 7.8$ Hz, 9H), 0.71 (q, $J = 8.6, 7.8$ Hz, 6H) ppm. ^{13}C NMR (75 MHz, CDCl_3) δ 149.2, 148.6, 147.4, 136.1, 134.8, 122.9, 83.7, 25.2, 7.5, 3.6 ppm. IR (neat, cm^{-1}): 2952, 2874, 1591, 1371, 1330, 1297, 1139, 1005, 856, 706. HRMS (ESI) [$\text{C}_{19}\text{H}_{33}\text{BNO}_2\text{Si}$] ($\text{M}+\text{H}$) *calcd.* 345.2404, *found* 345.2390.

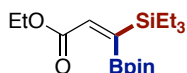


(Z)-triethyl(2-(4-ethynylphenyl)-1-(4,4,5,5-tetramethyl-1,3,2-dioxaborolan-2-yl)vinyl)silane (88s). Following the general procedure, using 1,4-diethynylbenzene (50.5 mg, 0.4 mmol), the title compound was obtained in 81% yield (119.2 mg) as colorless oil. R_f 0.65 (Hex: EtOAc 20:1). ^1H NMR (300 MHz, CDCl_3) δ 8.04 (s, 1H), 7.42 (d, $J = 8.2$ Hz, 2H), 7.21 (d, $J = 8.0$ Hz, 2H), 3.09 (s, 1H), 1.29 (s, 12H), 0.82 (t, $J = 7.8$ Hz, 9H), 0.52 (q, $J = 7.8$ Hz, 6H) ppm. ^{13}C NMR (75 MHz, CDCl_3) δ 157.4, 142.4, 131.6, 128.2, 121.2, 83.9, 83.4, 77.7, 24.9, 7.8, 5.0 ppm. IR (neat, cm^{-1}): 3299, 2952, 2873, 1573, 1499, 1318, 1270, 1144, 1005, 738. HRMS (ESI) [$\text{C}_{22}\text{H}_{34}\text{BO}_2\text{Si}$] ($\text{M}+\text{H}$) *calcd.* 368.2436, *found* 368.2452.

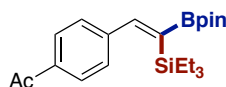


1,3,5-tris((Z)-2-(4,4,5,5-tetramethyl-1,3,2-dioxaborolan-2-yl)-2-(triethylsilyl)vinyl)benzene (88t).

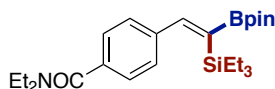
Following the general procedure, using 1,3,5-triethynylbenzene (60.1 mg, 0.4 mmol), the title compound was obtained in 84% yield (294.2 mg) as colorless oil. R_f 0.59 (Hex: EtOAc 20:1). ^1H NMR (300 MHz, CDCl_3) δ 8.05 (s, 3H), 6.99 (s, 3H), 1.29 (s, 36H), 0.81 (t, $J = 7.8$ Hz, 27H), 0.51 (q, $J = 7.8$ Hz, 18H) ppm. ^{13}C NMR (75 MHz, CDCl_3) δ 158.6, 140.8, 126.9, 83.2, 24.9, 7.8, 4.9 ppm. IR (neat, cm^{-1}): 2952, 2874, 1557, 1312, 1269, 1143, 1005, 854. HRMS (ESI) [$\text{C}_{48}\text{H}_{88}\text{B}_3\text{O}_6\text{Si}$] (M+H) *calcd.* 876.6199, *found* 876.6233.



Following the general procedure, using ethyl propiolate (39.2 mg, 0.4 mmol), the title compound was obtained in 20.2% of ZZ and 60.8% of EE as colorless oil. R_f 0.43 (Hex: EtOAc 10:1). **ethyl (Z)-3-(4,4,5,5-tetramethyl-1,3,2-dioxaborolan-2-yl)-3-(triethylsilyl)acrylate (88u).** ^1H NMR (300 MHz, CDCl_3) δ 6.91 (s, 1H), 4.17 (q, $J = 7.1$ Hz, 2H), 1.27 (s, 15H), 0.92 (t, $J = 7.7$ Hz, 9H), 0.85-0.70 (m, 6H) ppm. ^{13}C NMR (75 MHz, CDCl_3) δ 166.4, 143.1, 83.9, 60.5, 24.9, 14.4, 8.0, 4.0 ppm. IR (neat, cm^{-1}): 2953, 2874, 1724, 1368, 1319, 1189, 1142, 851, 736. HRMS (ESI) [$\text{C}_{17}\text{H}_{33}\text{NaBO}_4\text{Si}$] (M+Na) *calcd.* 362.2170, *found* 362.2178. **ethyl (E)-3-(4,4,5,5-tetramethyl-1,3,2-dioxaborolan-2-yl)-3-(triethylsilyl)acrylate (88u').** ^1H NMR (300 MHz, CDCl_3) δ 6.40 (s, 1H), 4.19 (q, $J = 7.1$ Hz, 2H), 1.35 (s, 12H), 1.27 (t, $J = 7.1$ Hz, 3H), 0.95 (t, $J = 7.8$ Hz, 9H), 0.68 (q, $J = 8.7$, 8.3 Hz, 6H) ppm. ^{13}C NMR (75 MHz, CDCl_3) δ 166.3, 138.1, 83.9, 60.8, 25.3, 14.4, 7.3, 3.3 ppm. IR (neat, cm^{-1}): 2955, 1717, 1350, 1301, 1187, 1139, 1007, 852, 731. HRMS (ESI) [$\text{C}_{17}\text{H}_{33}\text{NaBO}_4\text{Si}$] (M+Na) *calcd.* 362.2170, *found* 362.2177.



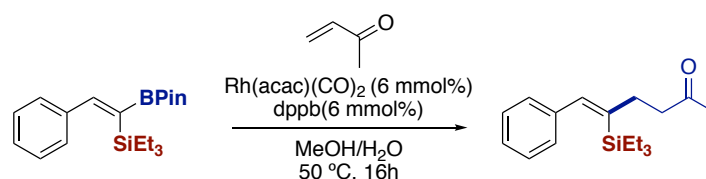
Following the general procedure, using 1-(4-ethynylphenyl)ethan-1-one (57.7 mg, 0.4 mmol) in DME, the title compound was obtained in 52% yield of **98a**, 25% of **98a'** separately. While 2 mL of Toluene was used as solvent instead of DME, the only Z isomer was obtained in 79% yield. **(Z)-1-(4-(2-(4,4,5,5-tetramethyl-1,3,2-dioxaborolan-2-yl)-2-(triethylsilyl)vinyl)phenyl)ethan-1-one (98a).** Following the general procedure, using 1-(4-ethynylphenyl)ethan-1-one (57.7 mg, 0.4 mmol) in Toluene, the title compound was obtained in 78% yield (120.1 mg) as colorless oil. R_f 0.63 (Hex: EtOAc 10:1). ^1H NMR (300 MHz, CDCl_3) δ 8.07 (s, 1H), 7.89 (d, $J = 8.3$ Hz, 2H), 7.34 (d, $J = 8.0$ Hz, 2H), 2.61 (s, 3H), 1.30 (s, 12H), 0.81 (t, $J = 7.8$ Hz, 9H), 0.51 (q, $J = 8.2$ Hz, 6H) ppm. ^{13}C NMR (75 MHz, CDCl_3) δ 198.0, 156.9, 146.8, 136.1, 128.3, 128.0, 83.5, 26.8, 24.9, 7.8, 4.9 ppm. IR (neat, cm^{-1}): 2952, 2873, 1685, 1575, 1317, 1263, 1142, 722. HRMS (ESI) [$\text{C}_{22}\text{H}_{35}\text{BO}_3\text{SiNa}$] (M+Na) *calcd.* 408.2377, *found* 408.2378. **(E)-1-(4-(2-(4,4,5,5-tetramethyl-1,3,2-dioxaborolan-2-yl)-2-(triethylsilyl)vinyl)phenyl)ethan-1-one (98a').** R_f 0.58 (Hex: EtOAc 10:1). ^1H NMR (300 MHz, CDCl_3) δ 7.90 (d, $J = 8.4$ Hz, 2H), 7.51 (d, $J = 8.2$ Hz, 2H), 7.28 (s, 1H), 2.60 (s, 3H), 1.29 (s, 12H), 1.01 (t, $J = 7.8$ Hz, 9H), 0.74 (q, $J = 8.3$ Hz, 6H) ppm. ^{13}C NMR (75 MHz, CDCl_3) δ 197.9, 149.7, 145.2, 136.1, 128.4, 128.1, 83.7, 26.8, 25.3, 7.5, 3.7 ppm. IR (neat, cm^{-1}): 2953, 1738, 1683, 1602, 1372, 1297, 1139, 1005, 732. HRMS (ESI) [$\text{C}_{22}\text{H}_{35}\text{BO}_3\text{SiNa}$] (M+Na) *calcd.* 408.2377, *found* 408.2385.



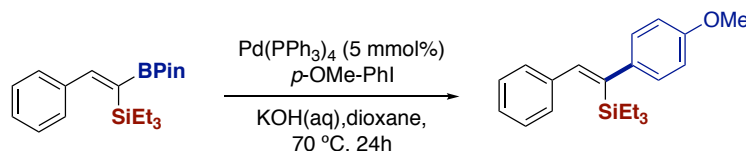
Following the general procedure, using *N,N*-diethyl-4-ethynylbenzamide (80.5 mg, 0.4 mmol) in DME, the title compound was obtained in 53% of **98b** and 27% of **98b'** as colorless oil. While 2 mL of Toluene was used as solvent instead of DME, the only Z isomer was obtained in 85% yield. **(Z)-N,N-diethyl-4-(2-(4,4,5,5-**

tetramethyl-1,3,2-dioxaborolan-2-yl)-2-(triethylsilyl)vinyl)benzamide (98b). R_f 0.49 (Hex: EtOAc 2:1). ^1H NMR (300 MHz, CDCl_3) δ 8.09 (s, 1H), 7.29 (s, 4H), 3.54 (s, 2H), 3.23 (s, 2H), 1.29 (s, 12H), 1.26-0.97 (m, 6H), 0.81 (t, $J = 7.8$ Hz, 9H), 0.51 (q, $J = 7.8$ Hz, 6H) ppm. ^{13}C NMR (75 MHz, CDCl_3) δ 171.3, 157.5, 142.7, 136.3, 128.0, 125.8, 83.3, 43.4, 39.4, 24.9, 14.2, 13.0, 7.7, 4.9 ppm. IR (neat, cm^{-1}): 2951, 2873, 1634, 1575, 1424, 1317, 1144, 1094, 722. HRMS (ESI) [$\text{C}_{25}\text{H}_{43}\text{NO}_3\text{BSi}$] (M+H) *calcd.* 443.3136, *found* 443.3118. **(E)-N,N-diethyl-4-(2-(4,4,5-tetramethyl-1,3,2-dioxaborolan-2-yl)-2-(triethylsilyl)vinyl)benzamide (98b')**. R_f 0.44 (Hex: EtOAc 2:1). ^1H NMR (300 MHz, CDCl_3) δ 7.45 (d, $J = 8.1$ Hz, 2H), 7.34-7.24 (m, 3H), 3.53 (s, 2H), 3.24 (s, 2H), 1.28 (s, 12H), 1.25-1.04 (m, 6H), 1.00 (t, $J = 7.8$ Hz, 9H), 0.73 (q, $J = 7.8$ Hz, 6H) ppm. ^{13}C NMR (75 MHz, CDCl_3) δ 150.3, 141.5, 136.5, 127.9, 126.2, 83.6, 43.4, 39.5, 25.2, 14.2, 12.9, 7.5, 3.7 ppm. IR (neat, cm^{-1}): 2972, 2884, 1634, 1373, 1294, 1234, 1141, 731. HRMS (ESI) [$\text{C}_{25}\text{H}_{43}\text{NO}_3\text{BSi}$] (M+H) *calcd.* 443.3136, *found* 443.3115.

4.7.3. Synthetic application profile

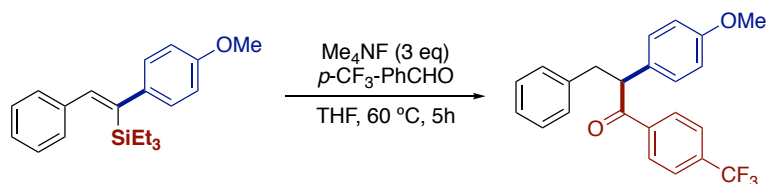


(Z)-6-phenyl-5-(triethylsilyl)hex-5-en-2-one (91). A general procedure for Rhodium catalyzed conjugate addition of **88a** to enone. Methanol (1 mL) was added to an oven-dried schlenk tube containing $\text{Rh}(\text{acac})(\text{CO})_2$ (1.5 mg, 0.006 mmol), dppb (2.5 mg, 0.006 mmol), and **88a** (34.4 mg, 0.10 mmol). After being stirred for 15 min at room temperature, the mixture was treated with water (0.20 mL) and methyl vinyl ketone (28 mg, 0.40 mmol). The resulting mixture was stirred at 50 °C for 24h, diluted with diethyl ether (10 mL), and washed with water (3 mL). The organic layer was then separated, dried over MgSO_4 , and concentrated. The resulting crude product was purified by column chromatography on silica gel to give desired product as a colorless oil (22.2 mg, 77% yield, Z:E = 5:1). R_f 0.36 (hexane/ethyl acetate 5:1). ^1H NMR (300 MHz, CDCl_3) δ 7.42 -7.16 (m, 4H), 7.21-7.10 (m, 2H), 5.52 (t, $J = 1.4$ Hz, 1H), 2.77-2.68 (m, 2H), 2.56-2.47 (m, 2H), 2.11 (s, 3H), 0.81 (t, $J = 7.9$ Hz, 9H), 0.29 (q, $J = 7.9$ Hz, 6H) ppm. ^{13}C NMR (101 MHz, CDCl_3) δ 208.4, 158.6, 143.7, 128.6, 128.5, 128.0, 127.9, 127.3, 124.5, 42.5, 37.1, 30.0, 7.6, 4.5 ppm. IR (neat, cm^{-1}): 2951, 2873, 1717, 1594, 1359, 1158, 1014, 771, 702. HRMS (ESI) [$\text{C}_{18}\text{H}_{28}\text{NaOSi}$] (M+Na) *calcd.* 311.1799, *found* 311.1794.

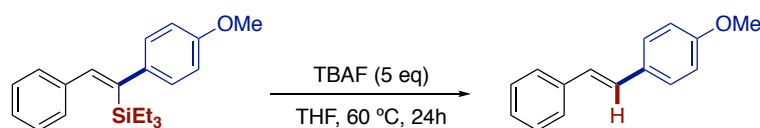


(Z)-triethyl(1-(4-methoxyphenyl)-2-phenylvinyl)silane (92). A general procedure for Suzuki coupling of **88a** with 1-iodo-4-methoxybenzene. A mixture of **88a** (68.8 mg, 0.20 mmol), 1-iodo-4-methoxybenzene (70.5 mg, 0.30 mmol), $\text{Pd}(\text{PPh}_3)_4$ (11.6 mg, 0.01 mmol), and 3 M KOH aqueous solution (0.20 mL, 0.60 mmol) in dioxane (2 mL) was heated at 90 °C for 12h. The reaction mixture was diluted with diethyl ether (10 mL), washed with water (3 mL). The organic layer was then separated, dried over anhydrous MgSO_4 , and concentrated. The crude product was purified by column chromatography on silica gel to give the desired product as colorless oil in 88% (57.1 mg). R_f 0.67 (Hex: EtOAc 10:1). ^1H NMR (300 MHz, CDCl_3) δ 7.34-7.27 (m, 6H), 7.12 (d, $J = 8.7$ Hz, 2H), 6.86 (d, $J = 8.7$ Hz, 2H), 3.82 (s, 3H), 0.80 (t, $J = 7.8$ Hz, 12H), 0.41

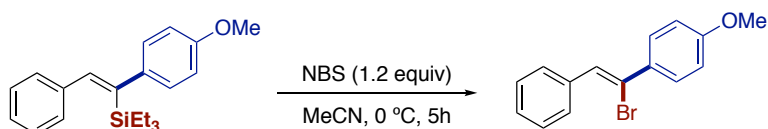
(q, $J = 7.9$ Hz, 9H) ppm. ^{13}C NMR (75 MHz, CDCl_3) δ 157.9, 146.2, 144.6, 140.2, 140.2, 128.5, 128.5, 127.9, 127.2, 113.4, 55.4, 7.7, 4.8 ppm. Spectroscopic data for **92** match those previously reported in the literature.²



2-(4-methoxyphenyl)-3-phenyl-1-(4-(trifluoromethyl)phenyl)propan-1-one (93). A THF solution of anhydrous Me_4NF (55.8 mg, 0.60 mmol) was added to 4-(trifluoromethyl)benzaldehyde (69.6 mg, 0.40 mmol) and (Z)-triethyl(1-(4-methoxyphenyl)-2-phenylvinyl)silane (64.9 mg, 0.20 mmol) under an argon atmosphere. The resulting solution was stirred at 60 °C for 24 h. The reaction mixture was diluted with diethyl ether (10 mL) and washed with saturated aq. NH_4Cl (6 mL). The organic layer was then separated, dried over MgSO_4 , and concentrated. The crude product was purified by column chromatography to give the title compound as a colorless oil in 74% (56.8 mg). R_f 0.44 (Hex: EtOAc 10:1). ^1H NMR (300 MHz, CDCl_3) δ 7.96 (d, $J = 8.1$ Hz, 2H), 7.60 (d, $J = 8.1$ Hz, 2H), 7.24-6.99 (m, 7H), 6.80 (d, $J = 8.7$ Hz, 2H), 4.72 (t, $J = 7.2$ Hz, 1H), 3.75 (s, 3H), 3.53 (dd, $J = 13.7, 7.4$ Hz, 1H), 3.04 (dd, $J = 13.7, 7.1$ Hz, 1H) ppm. ^{13}C NMR (101 MHz, CDCl_3) δ 198.7, 159.0, 139.7, 139.7, 134.13 (d, $J = 32.7$ Hz), 130.5, 129.5, 129.3, 129.1, 128.4, 126.4, 125.67 (q, $J = 3.8$ Hz), 114.7, 55.7, 55.4, 40.1 ppm. ^{19}F NMR (376 MHz, CDCl_3) δ -63.3 ppm. IR (neat, cm^{-1}): 3029, 2935, 1686, 1509, 1321, 1126, 1065, 830, 699. HRMS (ESI) [$\text{C}_{23}\text{H}_{19}\text{F}_3\text{NaO}_2$] ($\text{M}+\text{Na}$) *calcd.* 407.1229, *found* 407.1225.

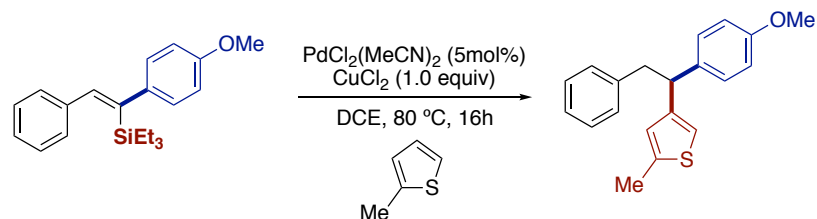


(E)-1-methoxy-4-styrylbenzene (94). To a solution of (Z)-triethyl(1-(4-methoxyphenyl)-2-phenylvinyl)silane (64.9 mg, 0.20 mmol) in THF (2 mL) was added 1 M solution of TBAF in THF (1 mL), and the resulting solution was heated at 60 °C for 3 h. The mixture was diluted with diethyl ether (3 mL) and treated with water (3 mL). The organic layer was separated, dried over anhydrous MgSO_4 , and concentrated. The crude product was purified by column chromatography on silica gel to afford (E)-1-methoxy-4-styrylbenzene as colorless oil in 79% (33.7 mg). R_f 0.54 (Hex: EtOAc 40:1). ^1H NMR (300 MHz, CDCl_3) δ 7.53-7.41 (m, 4H), 7.35 (t, $J = 7.5$ Hz, 2H), 7.26-7.20 (m, 1H), 7.15-6.94 (m, 2H), 6.91 (d, $J = 8.8$ Hz, 2H), 3.84 (s, 3H) ppm. ^{13}C NMR (75 MHz, CDCl_3) δ 159.5, 137.8, 130.3, 128.8, 128.4, 127.9, 127.4, 126.8, 126.4, 114.3, 55.5 ppm. Spectroscopic data for **94** match those previously reported in the literature.³

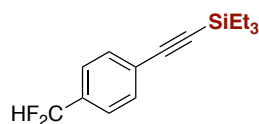


(Z)-1-(1-bromo-2-phenylvinyl)-4-methoxybenzene (95). To a solution of NBS (53.2 mg, 0.24 mmol, 1.2 equiv) in 1.0 mL dry MeCN, (Z)-triethyl(1-(4-methoxyphenyl)-2-phenylvinyl)silane (64.9 mg, 0.2 mmol) in 1.0 mL dry MeCN was added. After the reaction was stirring at 0 °C for 4 h, the resulting mixture was extracted with EtOAc (10 mL) and the organic layer was dried over MgSO_4 . After filtration and evaporation of all volatiles, the residue was purified by column chromatography. The title compound was isolated as

a colorless oil in 80 % (46.1 mg) after chromatography on silica. R_f 0.63 (Hex: EtOAc 50:1). ^1H NMR (300 MHz, Chloroform-*d*) δ 7.30 (d, J = 8.9 Hz, 2H), 7.19–7.11 (m, 3H), 7.12 (s, 1H), 7.04–6.95 (m, 2H), 6.83 (d, J = 8.8 Hz, 2H), 3.82 (s, 3H) ppm. ^{13}C NMR (101 MHz, CDCl_3) δ 160.0, 136.4, 132.5, 131.9, 130.9, 128.8, 128.4, 127.5, 123.8, 114.1, 55.4 ppm. Spectroscopic data for **95** match those previously reported in the literature.⁴

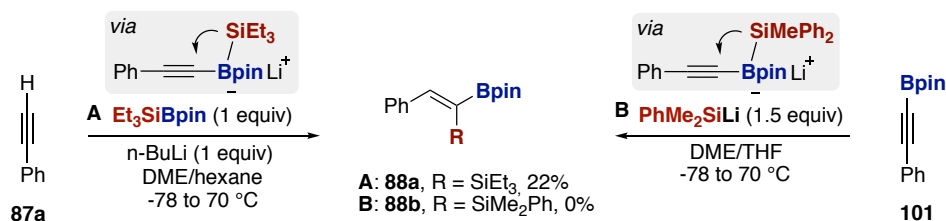


(S)-4-(1-(4-methoxyphenyl)-2-phenylethyl)-2-methylthiophene (96). In a glove box, a reaction tube was charged with $\text{PdCl}_2(\text{MeCN})_2$ (1.3 mg, 5 mol %, 0.005 mmol), CuCl_2 (13.4 mg, 0.1 mmol). Then, 0.4 mL of dry 1,2-dichloroethane, (*Z*)-triethyl(1-(4-methoxyphenyl)-2-phenylvinyl)silane (32.5 mg, 0.1 mmol), and thiophene substrate (17.8 mg, 0.2 mmol) were added, and the resulting mixture was stirred at 80 °C for 16 h. The reaction mixture was cooled to room temperature, and passed through a silica gel short column. After the volatile was removed in *vacuo*, the residue was purified by silica gel flash column chromatography to give the corresponding product in 62% (18.9 mg) as colorless oil. R_f 0.54 (Hex: EtOAc 20:1). ^1H NMR (400 MHz, CDCl_3) δ 7.23–7.06 (m, 5H), 7.02 (d, J = 7.8 Hz, 2H), 6.80 (s, 2H), 6.58–6.53 (m, 1H), 6.54–6.47 (m, 1H), 4.30 (t, J = 7.7 Hz, 1H), 3.77 (s, 3H), 3.39 (dd, J = 13.6, 6.9 Hz, 1H), 3.22 (dd, J = 13.6, 8.5 Hz, 1H), 2.39 (s, 3H) ppm. ^{13}C NMR (101 MHz, CDCl_3) δ 158.3, 147.1, 140.1, 138.2, 136.4, 129.2, 128.9, 128.2, 126.1, 124.6, 123.8, 113.8, 55.3, 48.2, 43.8, 15.5 ppm. IR (neat, cm^{-1}): 2955, 2863, 1713, 1609, 1455, 1249, 1167, 1032, 779, 754. HRMS (ESI) [$\text{C}_{20}\text{H}_{20}\text{SO}$] ($\text{M}+\text{H}$) *calcd.* 308.1238, *found* 308.1236.



((4-(difluoromethyl)phenyl)ethynyl)triethylsilane (100). Following the general procedure, using 1-ethynyl-4-(trifluoromethyl)benzene (68.2 mg, 0.4 mmol), the title compound was obtained in 61% yield (64.7 mg) as colorless oil. R_f 0.49 (Hex: EtOAc 20:1). ^1H NMR (300 MHz, CDCl_3) δ 7.55 (d, J = 8.5 Hz, 2H), 7.44 (d, J = 8.3 Hz, 2H), 6.63 (t, J = 56.4 Hz, 1H), 1.06 (t, J = 7.8 Hz, 9H), 0.69 (q, J = 8.4, 7.9 Hz, 6H) ppm. ^{13}C NMR (101 MHz, CDCl_3) δ 134.2 (t, J = 22.5 Hz), 132.4, 126.1, 125.6 (t, J = 6.1 Hz), 114.5 (t, J = 239.1 Hz), 105.4, 93.9, 7.6, 4.5 ppm. ^{19}F NMR (376 MHz, CDCl_3) δ -111.0 ppm. IR (neat, cm^{-1}): 2957, 2876, 2159, 1737, 1374, 1234, 1043, 729. HRMS (ESI) [$\text{C}_{15}\text{H}_{20}\text{NaF}_2\text{Si}$] ($\text{M}+\text{Na}$) *calcd.* 288.1131, *found* 288.1140.

4.7.4. Mechanistic studies



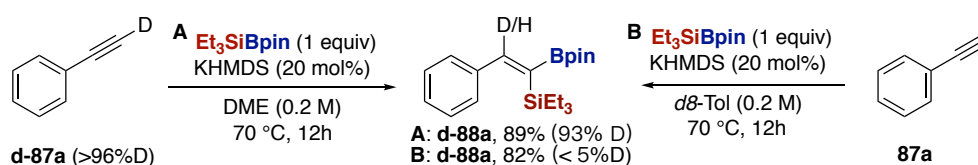
Reaction between 87a and Et₃SiBpin in the presence of stoichiometric Amount of *n*-BuLi.

phenylacetylene (**87a**) (20.4 mg, 0.2 mmol) was placed in an oven-dried 10 mL screw-capped test tube containing a magnetic stirring bar. DME (1.0 mL) and *n*BuLi (200 μL, 0.2 mmol, 1.0 M hexane) were sequentially added to the vial at -78 °C. After stirring for 30 min at -78 °C, Et₃SiBpin (**47**) (48.4 mg, 0.2 mmol) was added, and the mixture was warmed to room temperature. After 12 hours, no desired product **88a** was detected from GC and GC-MS. After Et₃SiBpin was added, if the reaction mixture was directly warmed to 70 °C with stirring for 3h. Then the mixture was quenched with EtOAc, filtered through a Celite® plug and concentrated under reduced pressure. The desired product was directly purified by flash column chromatography in silica to give the corresponding product in 22% (15.1 mg) as colorless oil.

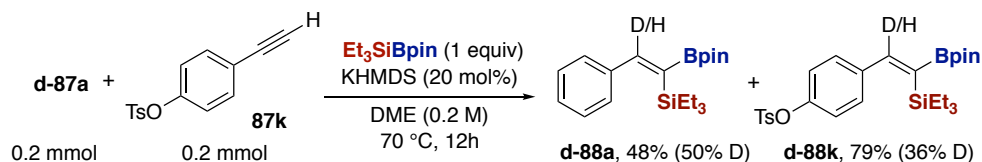
Reaction between 87a and PhMe₂SiLi

To a solution of naphthalene (12.8 mg, 0.1 mmol) in THF (10 mL), were added lithium clippings (70 mg, 10 mmol). The resulting mixture started turning dark green and was stirred at room temperature for 1 h under an argon atmosphere. Then PhMe₂SiCl (341.4 mg, 2 mmol) was added dropwise and the mixture was stirred at room temperature for 3 h. The resulting 10 mL solution was transferred via cannula to a Schlenk reaction vessel under argon and then stored at room temperature. A portion of 1.5 mL of the above solution (0.3 mmol) was added into a solution of **101** (45.6 mg, 0.2 mmol) in 1.0 mL DME at -78 °C. The reaction was warmed to 70 °C. After 3 h, the reaction quenched with 2 equiv of H₂O. No desired product was detected from GC and GC-MS.

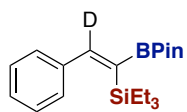
■ deuterium labeling experiment



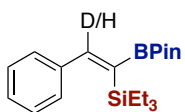
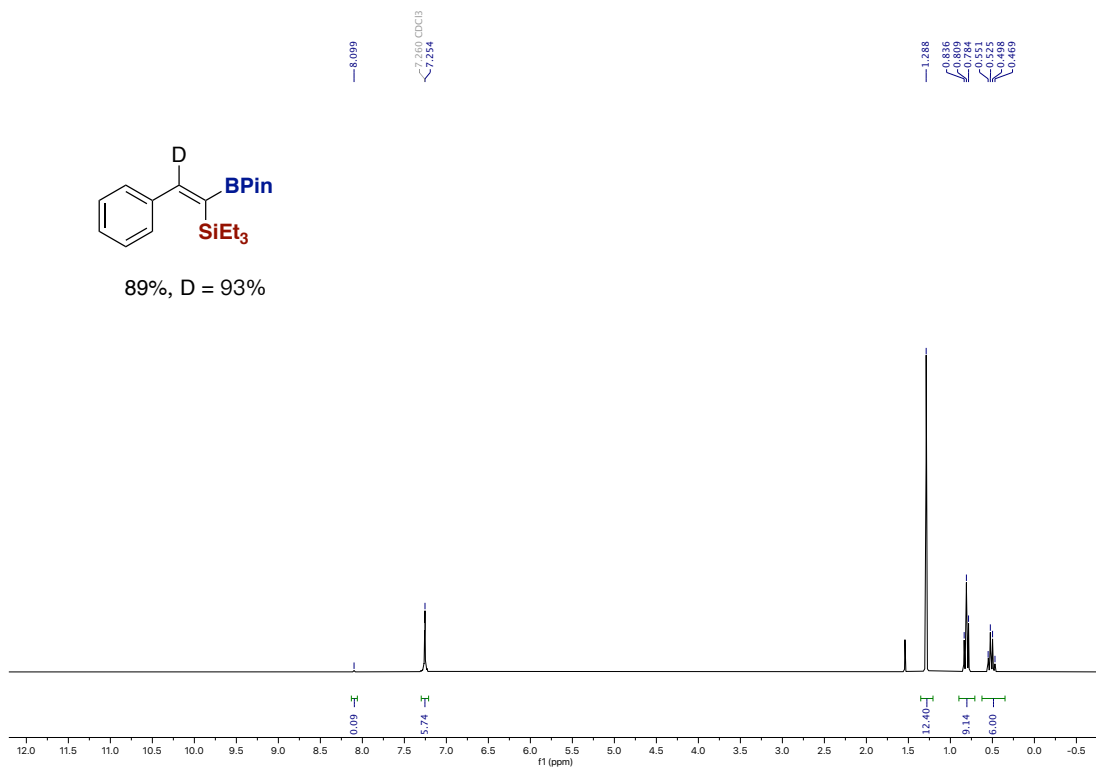
■ deuterium-labeled crossover experiment



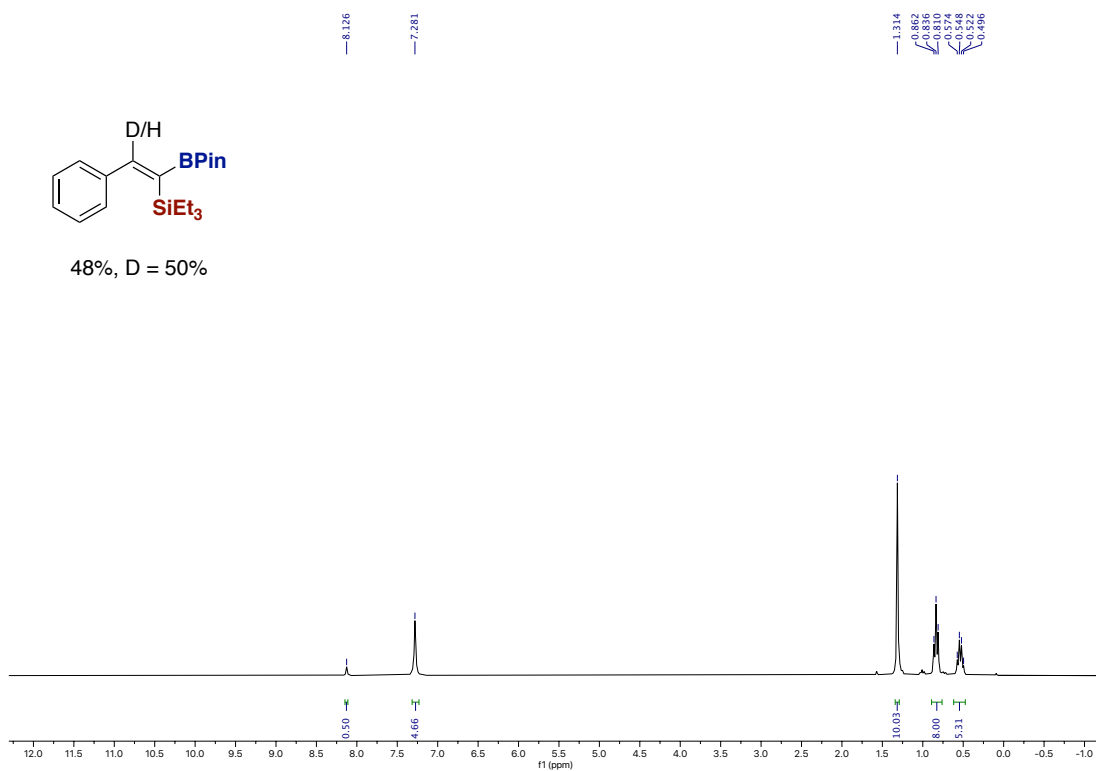
Stereoselective Base-Catalyzed 1,1-Silaboration of Terminal Alkynes

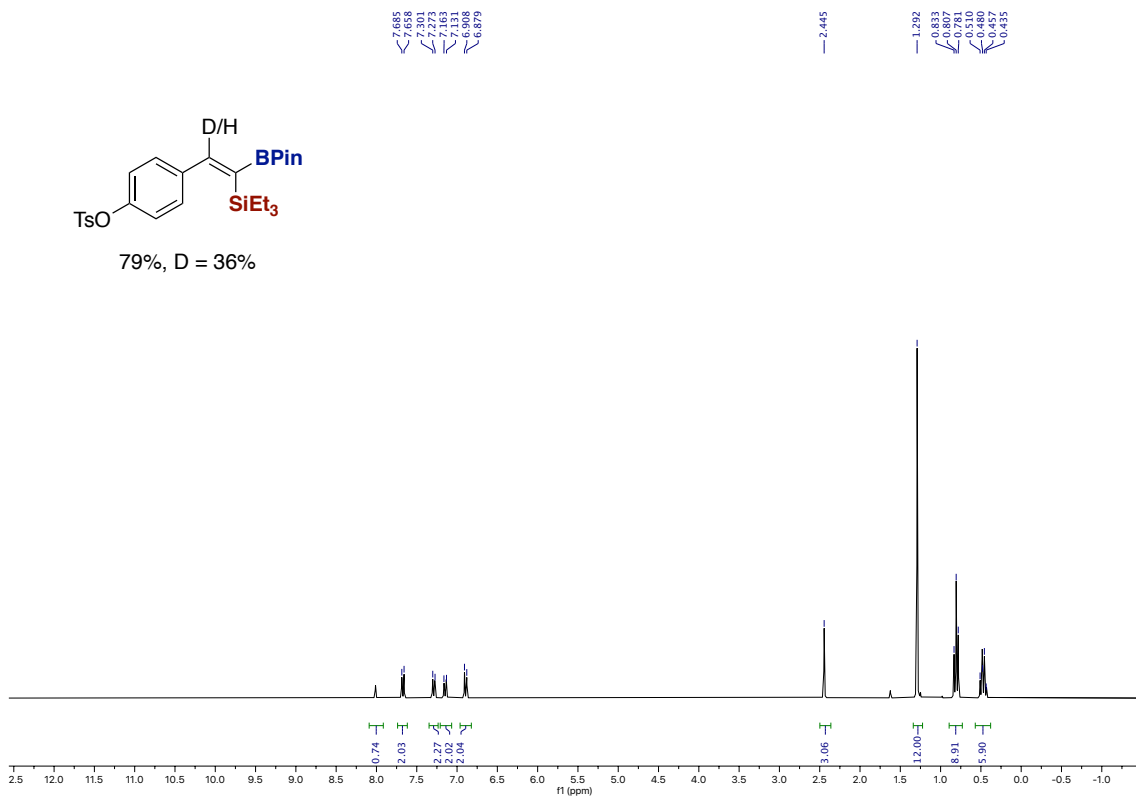


89%, D = 93%



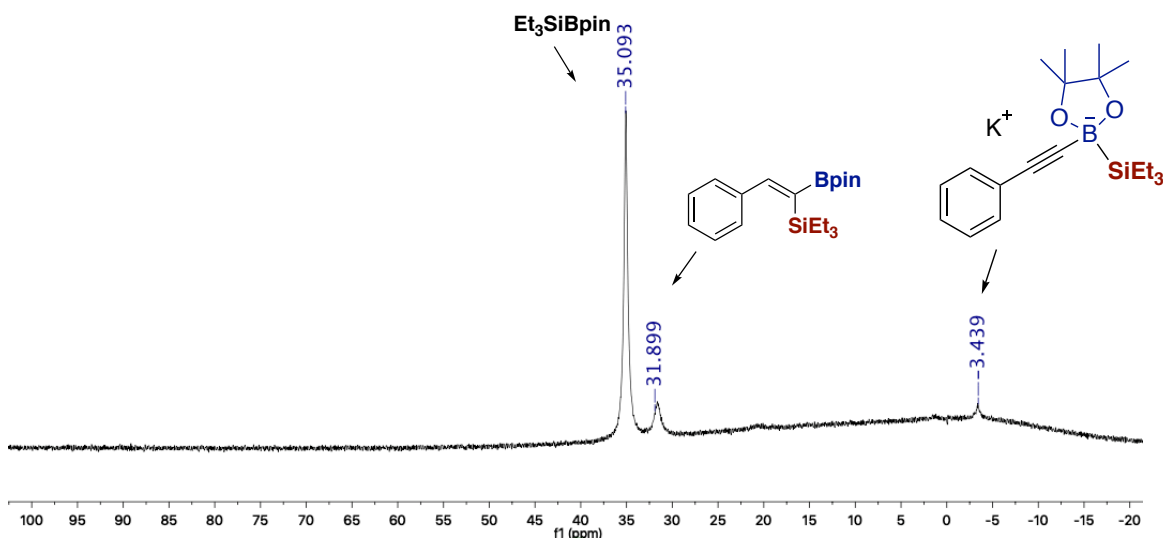
48%, D = 50%





NMR experiment of Et₃SiBpin and KHMDS

*d*8-Toluene



To gain insights into the nature of the active nucleophilic component, we monitored the model reaction using a mixture of Phenylacetylene (15.3 mg, 1.0 eq, 0.15 mol), KHMDS (1.8 mg, 0.2 eq, 0.03 mmol) and Et₃SiBpin (34.7 mg, 1.0 eq, 0.15 mmol) in 0.6 mL *d*8-Toluene at 90 degrees. After 30 min by ¹¹B NMR spectroscopy, three peaks at $\delta = 3.4$, 31.8 and 35.1 ppm were observed. These peaks could be assigned as tetracoordinated anionic boron species, silaborated product and Et₃SiBpin. And the formation of tetracoordinated anionic boron species might support the plausible reaction mechanism.

4.7.5. X-ray diffraction of 88i

Table 1. Crystal data and structure refinement for mo_88i_0m.

Identification code	mo_YGU928_0m	
Empirical formula	C20 H32 B Cl O2 Si	
Formula weight	378.80	
Temperature	100(2)K	
Wavelength	0.71073 Å	
Crystal system	triclinic	
Space group	P -1	
Unit cell dimensions	a = 7.2616(11)Å b = 15.344(3)Å c = 20.498(3)Å	a = 70.227(4)°. b = 81.937(4)°. g = 88.840(5)°.
Volume	2127.2(6) Å ³	
Z	4	
Density (calculated)	1.183 Mg/m ³	
Absorption coefficient	0.246 mm ⁻¹	
F(000)	816	
Crystal size	0.150 x 0.100 x 0.050 mm ³	
Theta range for data collection	1.066 to 28.888°.	
Index ranges	-9<=h<=5,-20<=k<=20,-27<=l<=27	
Reflections collected	29061	
Independent reflections	11058[R(int) = 0.0720]	
Completeness to theta =28.888°	98.9%	
Absorption correction	Multi-scan	
Max. and min. transmission	0.74 and 0.41	
Refinement method	Full-matrix least-squares on F ²	
Data / restraints / parameters	11058/ 0/ 465	
Goodness-of-fit on F ²	1.013	
Final R indices [I>2sigma(I)]	R1 = 0.0648, wR2 = 0.1659	
R indices (all data)	R1 = 0.1016, wR2 = 0.1945	
Largest diff. peak and hole	0.849 and -0.696 e.Å ⁻³	

Table 2. Bond lengths [Å] and angles [°] for mo_YGU928_0m.

Bond lengths----

C1B	C1B	1.743(2)
Si1B	C13B	1.878(2)
Si1B	C9B	1.881(2)
Si1B	C11B	1.886(3)
Si1B	C8B	1.897(2)
O1B	B1B	1.369(3)
O1B	C15B	1.459(3)
O2B	B1B	1.381(3)
O2B	C16B	1.460(3)
C1B	C2B	1.383(3)
C1B	C6B	1.387(3)
C2B	C3B	1.386(3)
C3B	C4B	1.399(3)
C4B	C5B	1.403(3)
C4B	C7B	1.465(3)
C5B	C6B	1.379(3)
C7B	C8B	1.355(3)
C8B	B1B	1.557(3)
C9B	C10B	1.535(3)
C11B	C12B	1.520(4)
C13B	C14B	1.528(3)
C15B	C17B	1.506(3)
C15B	C18B	1.523(3)
C15B	C16B	1.557(3)
C16B	C20B	1.514(3)
C16B	C19B	1.519(3)
Cl1A	C1A	1.743(3)
Si1A	C13A	1.876(2)
Si1A	C11A	1.876(2)
Si1A	C9A	1.890(2)
Si1A	C8A	1.894(2)
O1A	B1A	1.371(3)
O1A	C15A	1.464(3)
O2A	B1A	1.376(3)
O2A	C16A	1.466(3)
C1A	C2A	1.377(3)
C1A	C6A	1.383(4)
C2A	C3A	1.378(3)
C3A	C4A	1.396(3)
C4A	C5A	1.390(3)
C4A	C7A	1.474(3)

Stereoselective Base-Catalyzed 1,1-Silaboration of Terminal Alkynes

C5A C6A 1.382(4)
C7A C8A 1.352(3)
C8A B1A 1.557(3)
C9A C10A 1.531(3)
C11A C12A 1.529(3)
C13A C14A 1.529(3)
C15A C17A 1.508(3)
C15A C18A 1.524(3)
C15A C16A 1.553(3)
C16A C20A 1.510(3)
C16A C19A 1.522(3)

Angles-----

C13B Si1B C9B 107.80(11)
C13B Si1B C11B 107.76(11)
C9B Si1B C11B 109.97(11)
C13B Si1B C8B 113.76(10)
C9B Si1B C8B 104.57(10)
C11B Si1B C8B 112.83(11)
B1B O1B C15B 107.67(17)
B1B O2B C16B 106.85(17)
C2B C1B C6B 121.7(2)
C2B C1B C11B 119.04(19)
C6B C1B C11B 119.27(18)
C1B C2B C3B 118.7(2)
C2B C3B C4B 121.5(2)
C3B C4B C5B 117.7(2)
C3B C4B C7B 122.9(2)
C5B C4B C7B 119.3(2)
C6B C5B C4B 121.7(2)
C5B C6B C1B 118.7(2)
C8B C7B C4B 130.5(2)
C7B C8B B1B 113.1(2)
C7B C8B Si1B 128.12(18)
B1B C8B Si1B 118.56(16)
C10B C9B Si1B 115.24(17)
C12B C11B Si1B 115.72(18)
C14B C13B Si1B 115.43(17)
O1B C15B C17B 109.26(19)
O1B C15B C18B 106.82(18)
C17B C15B C18B 110.6(2)
O1B C15B C16B 101.62(16)
C17B C15B C16B 115.18(18)
C18B C15B C16B 112.66(19)

Chapter 4.

O2B C16B C20B 108.59(19)
O2B C16B C19B 106.53(18)
C20B C16B C19B 110.37(19)
O2B C16B C15B 102.14(16)
C20B C16B C15B 115.07(19)
C19B C16B C15B 113.36(19)
O1B B1B O2B 112.2(2)
O1B B1B C8B 124.5(2)
O2B B1B C8B 123.2(2)
C13A Si1A C11A 110.70(11)
C13A Si1A C9A 107.28(11)
C11A Si1A C9A 110.81(11)
C13A Si1A C8A 114.50(10)
C11A Si1A C8A 108.27(10)
C9A Si1A C8A 105.14(10)
B1A O1A C15A 107.22(17)
B1A O2A C16A 106.98(17)
C2A C1A C6A 121.0(2)
C2A C1A C11A 119.3(2)
C6A C1A C11A 119.62(19)
C1A C2A C3A 119.5(2)
C2A C3A C4A 121.0(2)
C5A C4A C3A 118.0(2)
C5A C4A C7A 120.0(2)
C3A C4A C7A 121.8(2)
C6A C5A C4A 121.5(2)
C5A C6A C1A 118.8(2)
C8A C7A C4A 129.5(2)
C7A C8A B1A 114.06(19)
C7A C8A Si1A 129.42(18)
B1A C8A Si1A 116.49(16)
C10A C9A Si1A 116.51(17)
C12A C11A Si1A 116.55(17)
C14A C13A Si1A 114.80(17)
O1A C15A C17A 109.1(2)
O1A C15A C18A 106.53(18)
C17A C15A C18A 110.7(2)
O1A C15A C16A 101.87(17)
C17A C15A C16A 114.81(19)
C18A C15A C16A 113.0(2)
O2A C16A C20A 108.70(19)
O2A C16A C19A 106.57(19)
C20A C16A C19A 110.58(19)
O2A C16A C15A 102.04(16)

C20A C16A C15A 114.9(2)

C19A C16A C15A 113.2(2)

O1A B1A O2A 112.5(2)

O1A B1A C8A 123.6(2)

O2A B1A C8A 123.9(2)

Table 3. Torsion angles [°] for mo_YGU928_0m.

C6B	C1B	C2B	C3B	1.5(3)
C1B	C1B	C2B	C3B	-179.44(16)
C1B	C2B	C3B	C4B	-0.6(3)
C2B	C3B	C4B	C5B	-1.2(3)
C2B	C3B	C4B	C7B	-177.5(2)
C3B	C4B	C5B	C6B	2.2(3)
C7B	C4B	C5B	C6B	178.6(2)
C4B	C5B	C6B	C1B	-1.3(3)
C2B	C1B	C6B	C5B	-0.6(3)
C1B	C1B	C6B	C5B	-179.65(17)
C3B	C4B	C7B	C8B	-38.5(4)
C5B	C4B	C7B	C8B	145.4(3)
C4B	C7B	C8B	B1B	172.9(2)
C4B	C7B	C8B	Si1B	-12.1(4)
C13B	Si1B	C8B	C7B	-23.9(3)
C9B	Si1B	C8B	C7B	-141.3(2)
C11B	Si1B	C8B	C7B	99.2(2)
C13B	Si1B	C8B	B1B	150.87(18)
C9B	Si1B	C8B	B1B	33.5(2)
C11B	Si1B	C8B	B1B	-86.0(2)
C13B	Si1B	C9B	C10B	49.4(2)
C11B	Si1B	C9B	C10B	-67.9(2)
C8B	Si1B	C9B	C10B	170.75(18)
C13B	Si1B	C11B	C12B	-165.22(17)
C9B	Si1B	C11B	C12B	-48.0(2)
C8B	Si1B	C11B	C12B	68.3(2)
C9B	Si1B	C13B	C14B	65.40(18)
C11B	Si1B	C13B	C14B	-175.95(16)
C8B	Si1B	C13B	C14B	-50.06(19)
B1B	O1B	C15B	C17B	-147.08(19)
B1B	O1B	C15B	C18B	93.3(2)
B1B	O1B	C15B	C16B	-24.9(2)
B1B	O2B	C16B	C20B	-147.40(19)
B1B	O2B	C16B	C19B	93.7(2)
B1B	O2B	C16B	C15B	-25.4(2)
O1B	C15B	C16B	O2B	30.2(2)
C17B	C15B	C16B	O2B	148.1(2)
C18B	C15B	C16B	O2B	-83.8(2)
O1B	C15B	C16B	C20B	147.60(19)
C17B	C15B	C16B	C20B	-94.4(3)
C18B	C15B	C16B	C20B	33.7(3)
O1B	C15B	C16B	C19B	-84.0(2)

Stereoselective Base-Catalyzed 1,1-Silaboration of Terminal Alkynes

C17B C15B C16B C19B 33.9(3)
C18B C15B C16B C19B 162.0(2)
C15B O1B B1B O2B 10.1(3)
C15B O1B B1B C8B -172.6(2)
C16B O2B B1B O1B 10.9(3)
C16B O2B B1B C8B -166.5(2)
C7B C8B B1B O1B -157.3(2)
Si1B C8B B1B O1B 27.1(3)
C7B C8B B1B O2B 19.7(3)
Si1B C8B B1B O2B -155.86(18)
C6A C1A C2A C3A 1.8(4)
C1A C1A C2A C3A -179.34(18)
C1A C2A C3A C4A -0.4(3)
C2A C3A C4A C5A -1.9(3)
C2A C3A C4A C7A -177.6(2)
C3A C4A C5A C6A 2.9(4)
C7A C4A C5A C6A 178.7(2)
C4A C5A C6A C1A -1.6(4)
C2A C1A C6A C5A -0.8(4)
C1A C1A C6A C5A -179.7(2)
C5A C4A C7A C8A 143.4(3)
C3A C4A C7A C8A -41.0(4)
C4A C7A C8A B1A 172.5(2)
C4A C7A C8A Si1A -9.5(4)
C13A Si1A C8A C7A -23.2(3)
C11A Si1A C8A C7A 100.8(2)
C9A Si1A C8A C7A -140.7(2)
C13A Si1A C8A B1A 154.72(17)
C11A Si1A C8A B1A -81.2(2)
C9A Si1A C8A B1A 37.2(2)
C13A Si1A C9A C10A 34.9(2)
C11A Si1A C9A C10A -86.0(2)
C8A Si1A C9A C10A 157.23(18)
C13A Si1A C11A C12A -75.0(2)
C9A Si1A C11A C12A 43.9(2)
C8A Si1A C11A C12A 158.7(2)
C11A Si1A C13A C14A -173.10(16)
C9A Si1A C13A C14A 65.88(18)
C8A Si1A C13A C14A -50.4(2)
B1A O1A C15A C17A -147.2(2)
B1A O1A C15A C18A 93.3(2)
B1A O1A C15A C16A -25.4(2)
B1A O2A C16A C20A -146.5(2)
B1A O2A C16A C19A 94.3(2)

Chapter 4.

B1A O2A C16A C15A -24.7(2)
O1A C15A C16A O2A 30.0(2)
C17A C15A C16A O2A 147.7(2)
C18A C15A C16A O2A -83.9(2)
O1A C15A C16A C20A 147.4(2)
C17A C15A C16A C20A -94.8(3)
C18A C15A C16A C20A 33.5(3)
O1A C15A C16A C19A -84.2(2)
C17A C15A C16A C19A 33.6(3)
C18A C15A C16A C19A 161.9(2)
C15A O1A B1A O2A 10.9(3)
C15A O1A B1A C8A -171.2(2)
C16A O2A B1A O1A 9.8(3)
C16A O2A B1A C8A -168.0(2)
C7A C8A B1A O1A -158.3(2)
Si1A C8A B1A O1A 23.4(3)
C7A C8A B1A O2A 19.3(3)
Si1A C8A B1A O2A -159.00(19)

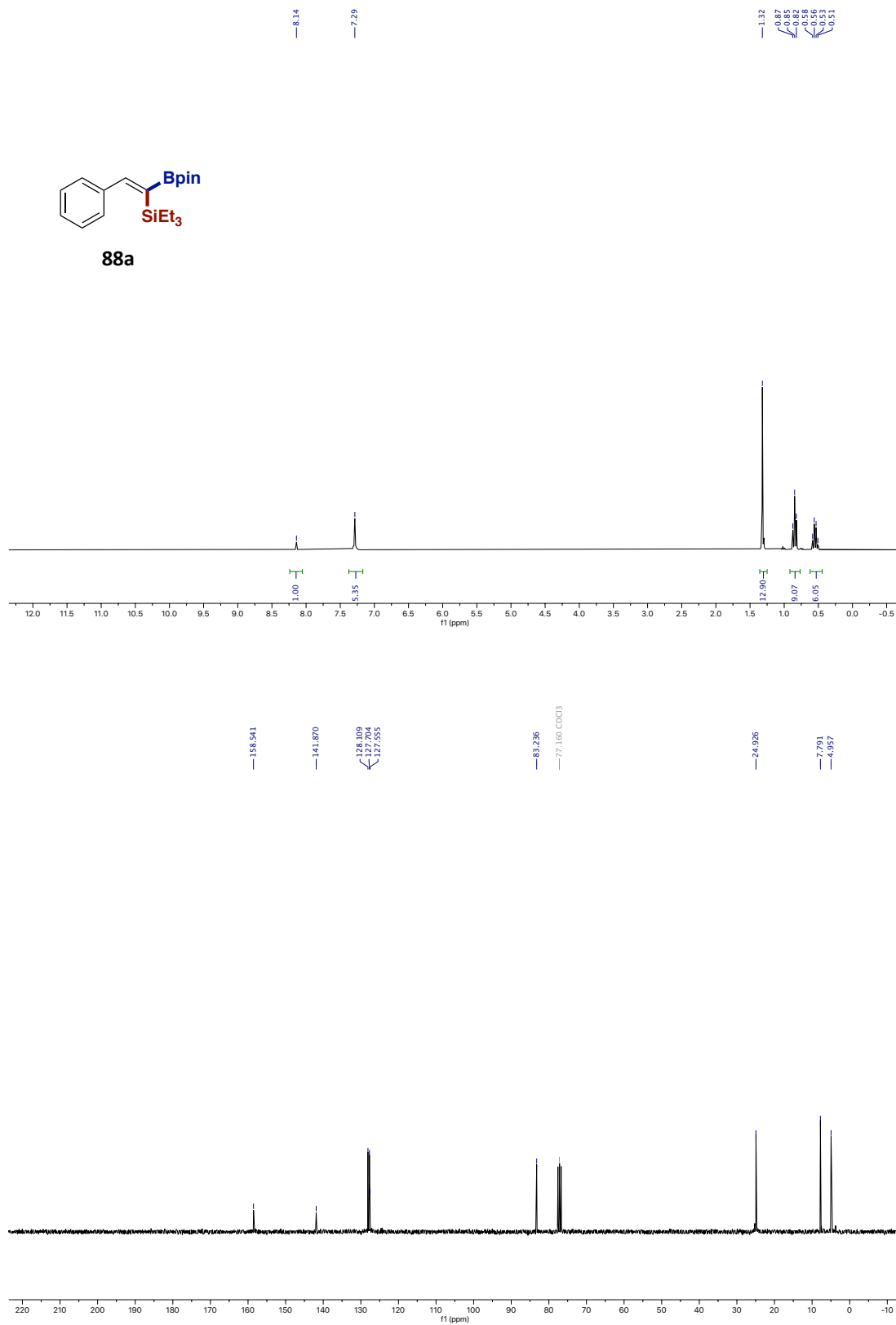
Symetry operations

- 1 'x, y, z'
- 2 '-x, -y, -z'

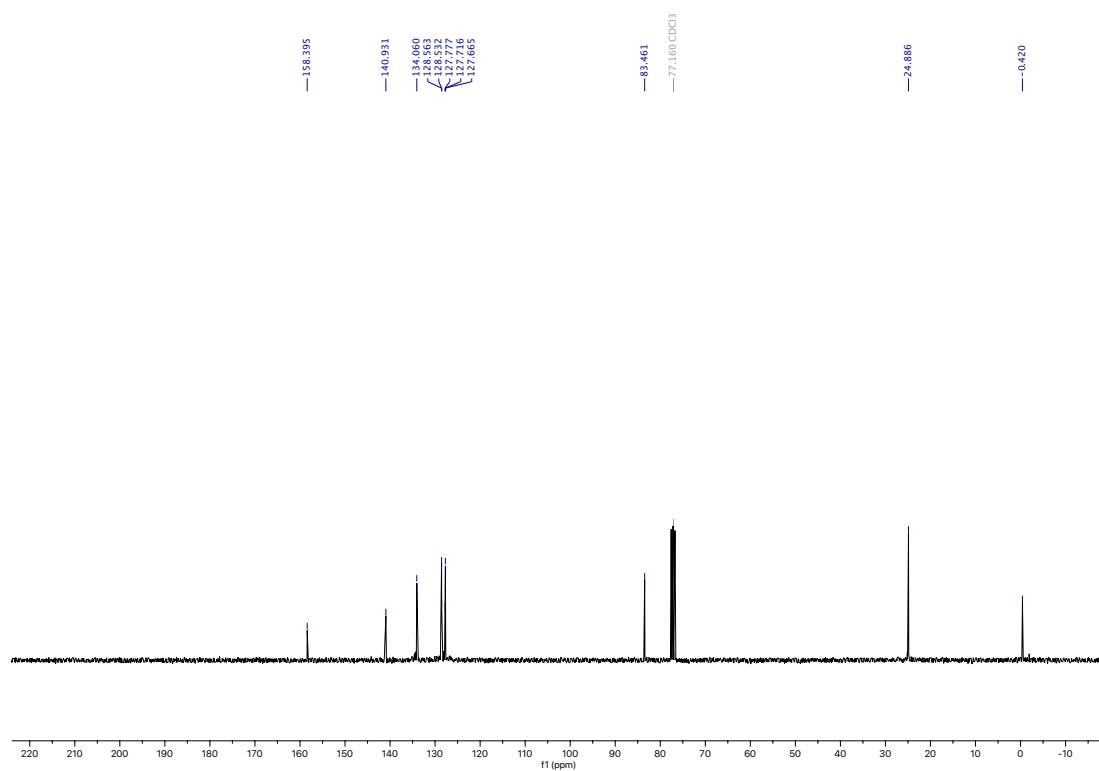
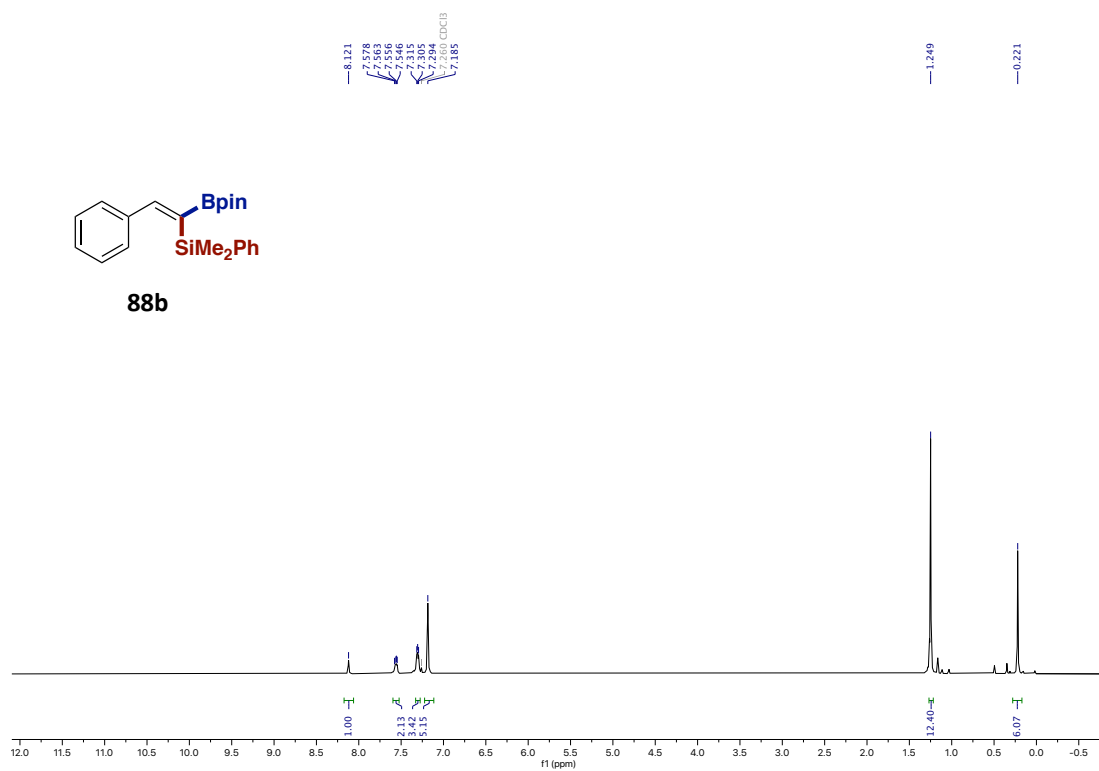
4.7.6. Bibliography of known compounds

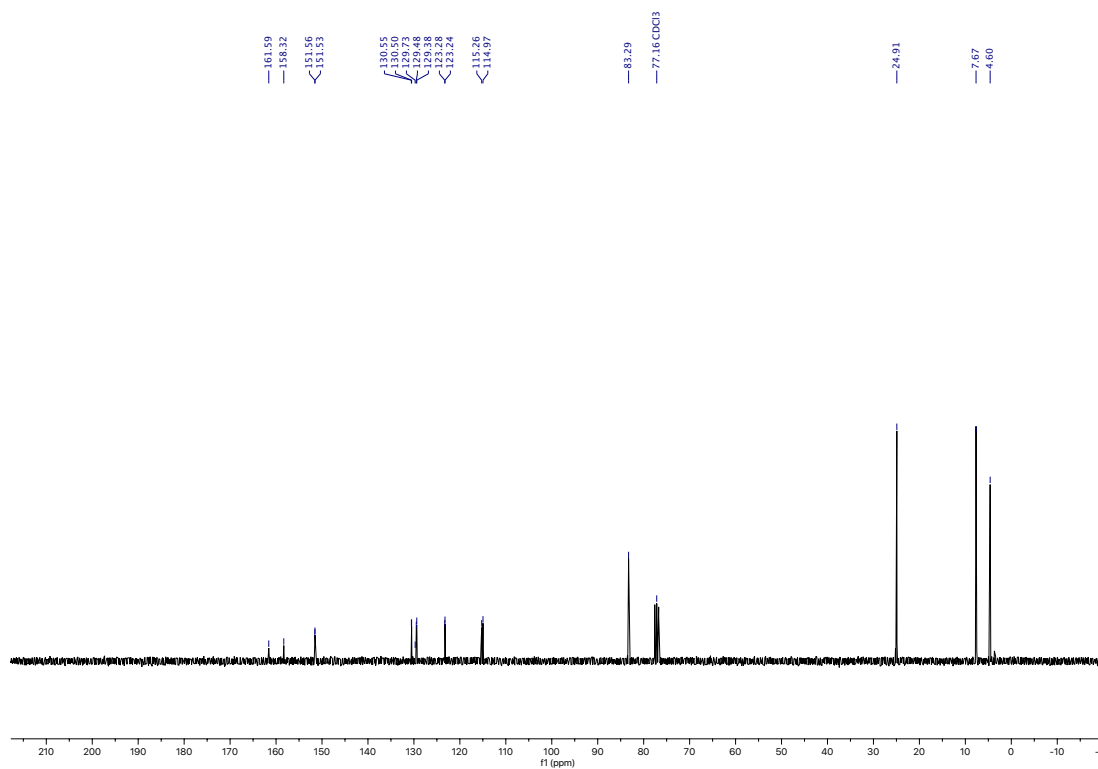
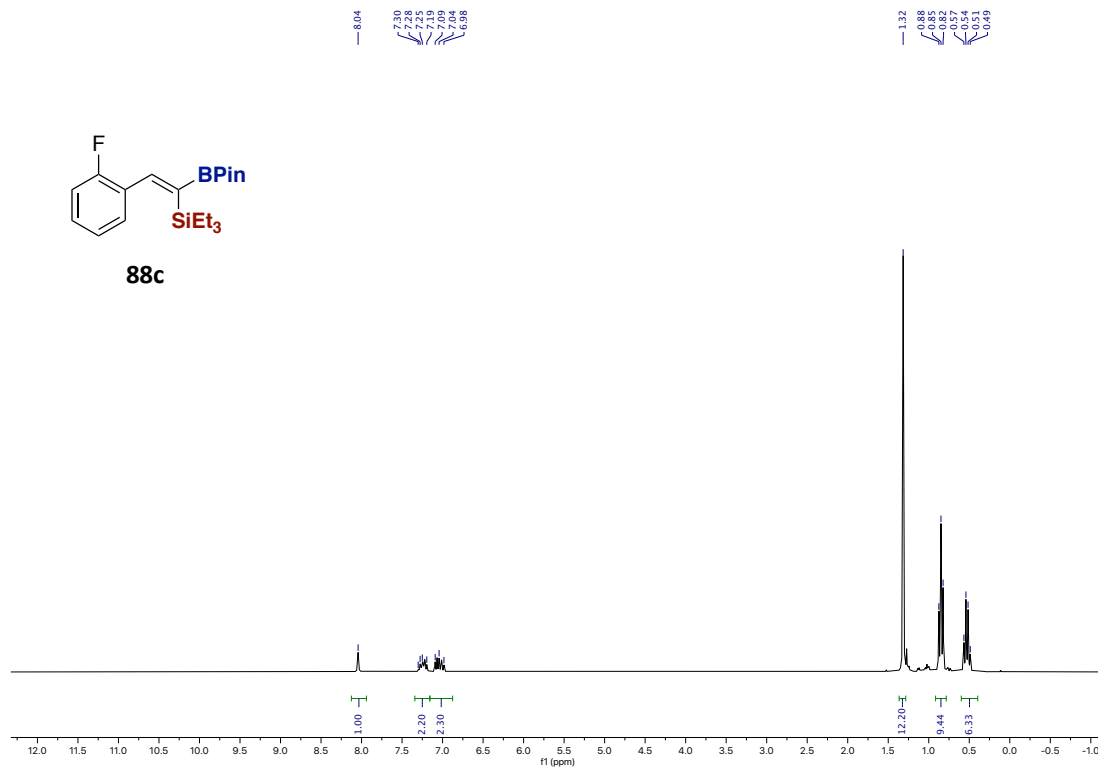
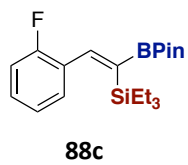
1. Boebel, A. B.; Hartwig, J. F. *Organometallics* **2008**, *27*, 6013.
2. Guo, W.; Pleixats, R.; Shafir, A.; Parella, T. *Advanced Synthesis & Catalysis*, **2015**, *357*, 89.
3. Richmond, E.; Moran, J. *J. Org. Chem.*, **2015**, *80*, 6922.
4. Suta, K.; Turks, M. *ACS Omega* **2018**, *3*, 18065.

4.7.7. NMR spectra

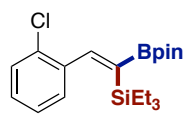


Stereoselective Base-Catalyzed 1,1-Silaboration of Terminal Alkynes

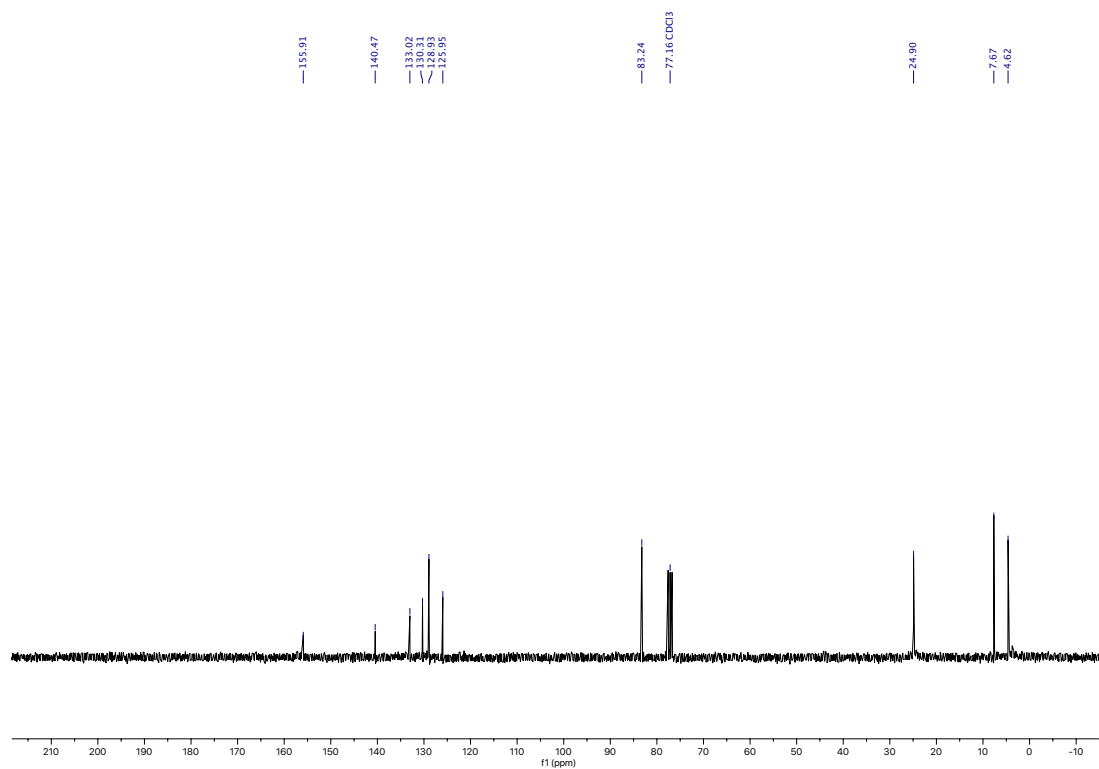
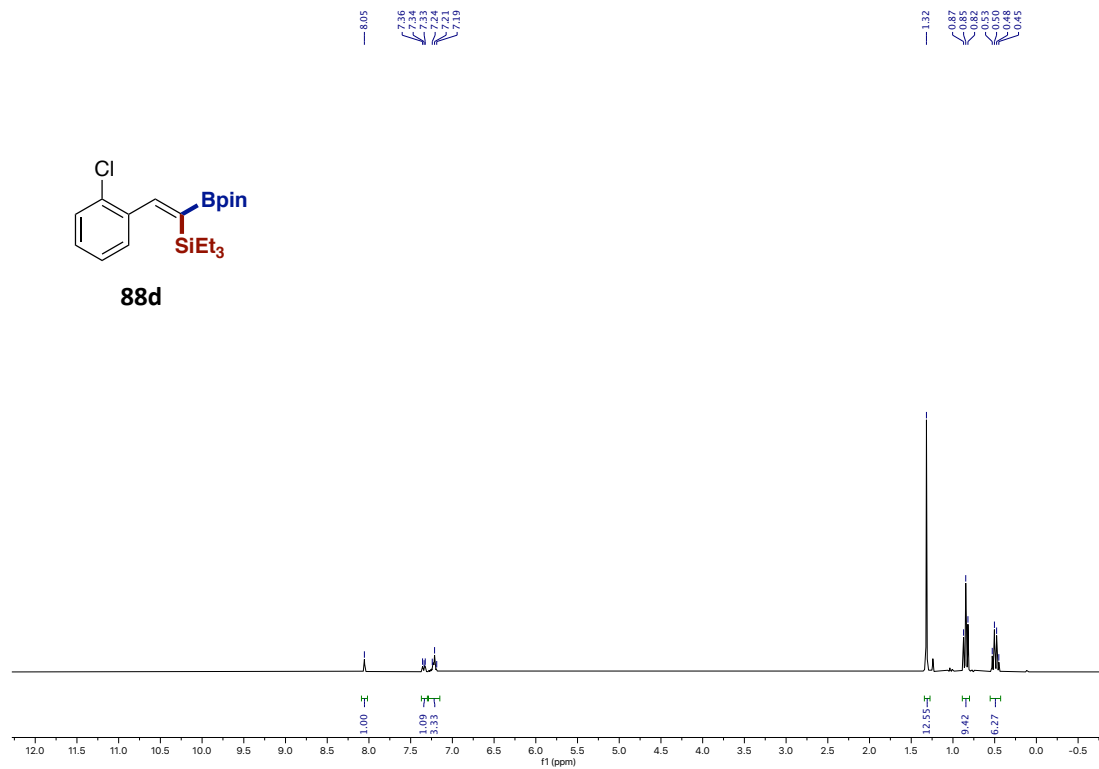


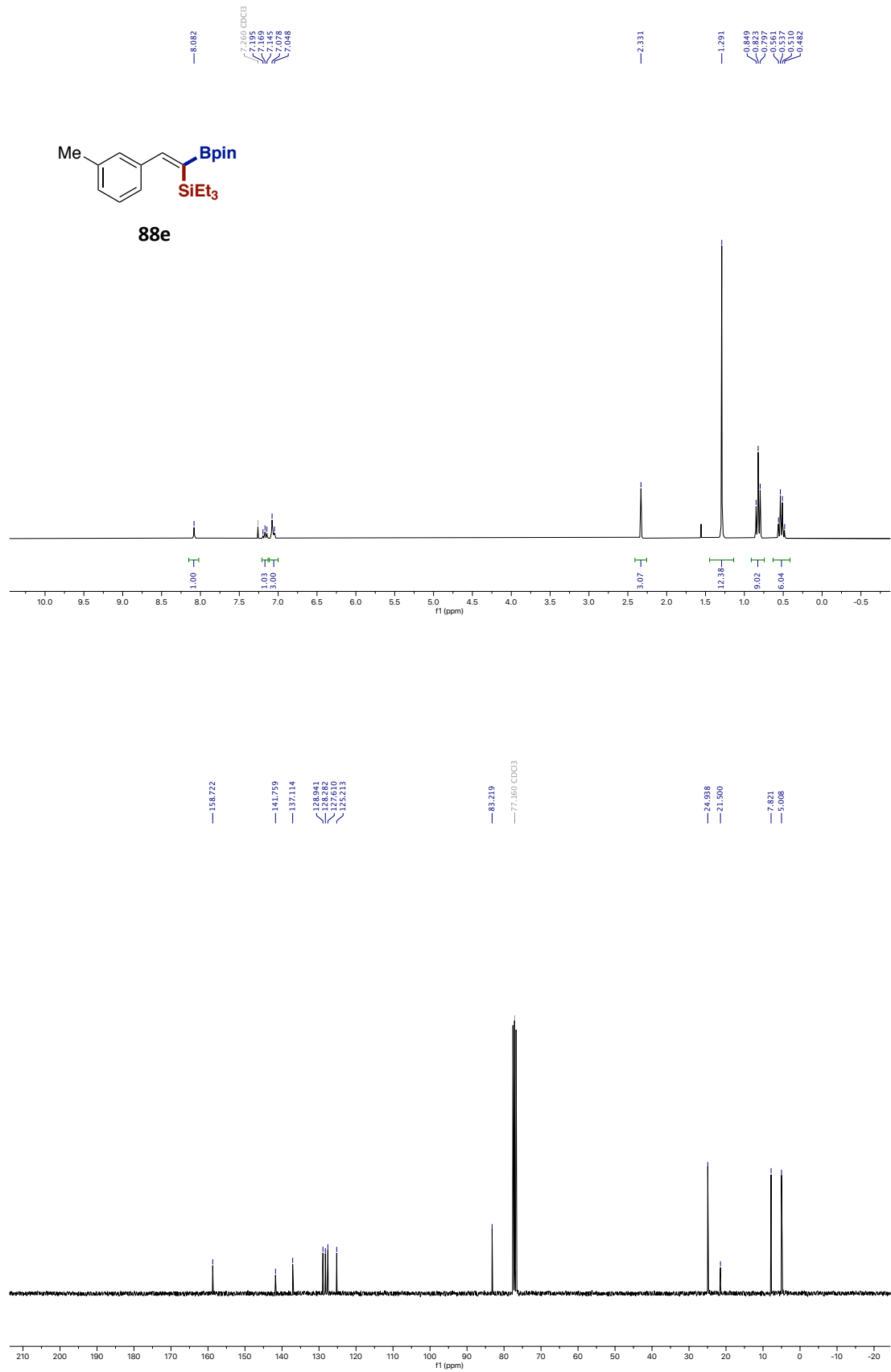


Stereoselective Base-Catalyzed 1,1-Silaboration of Terminal Alkynes

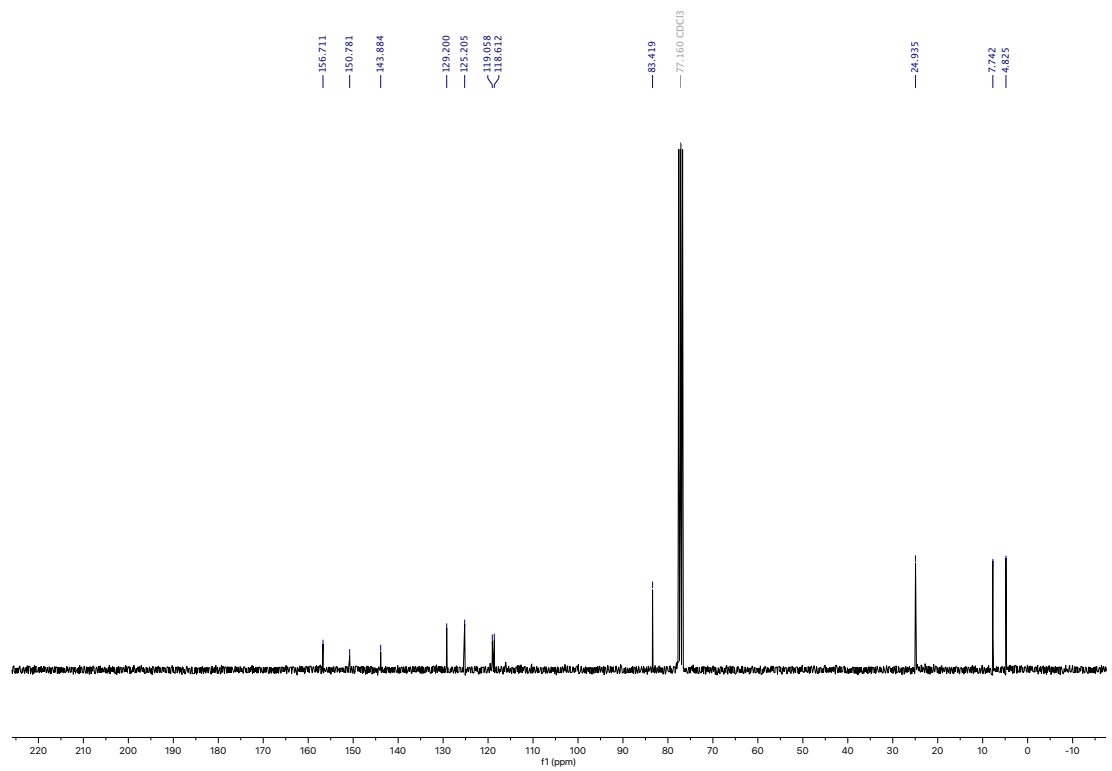
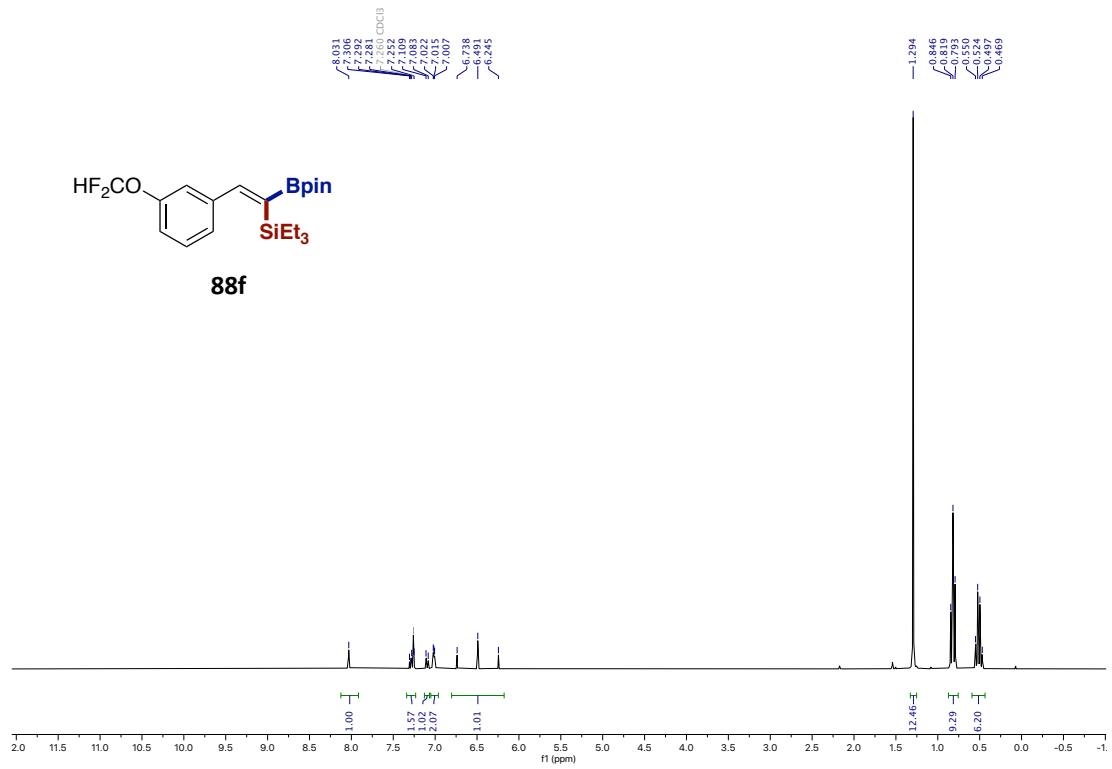


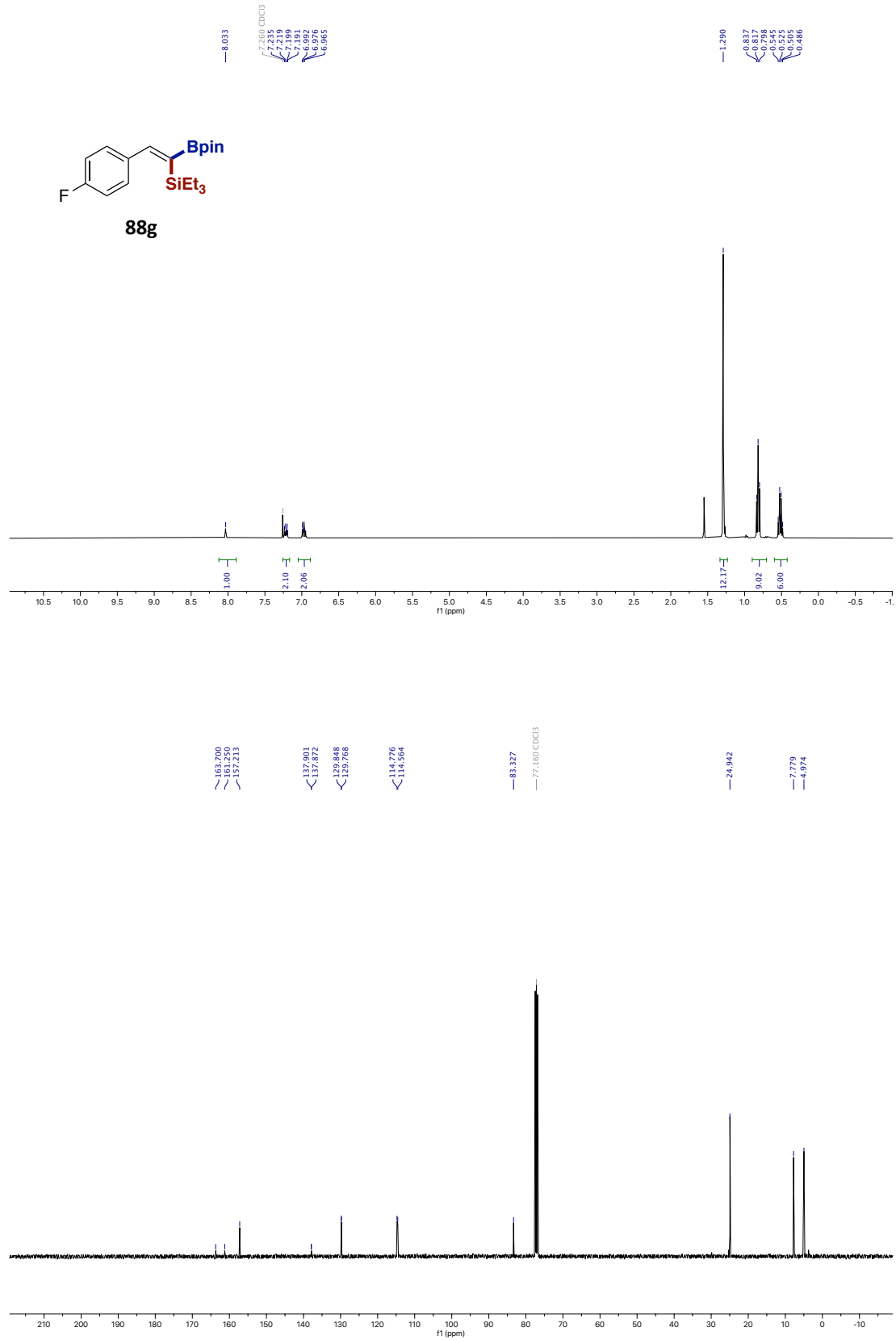
88d



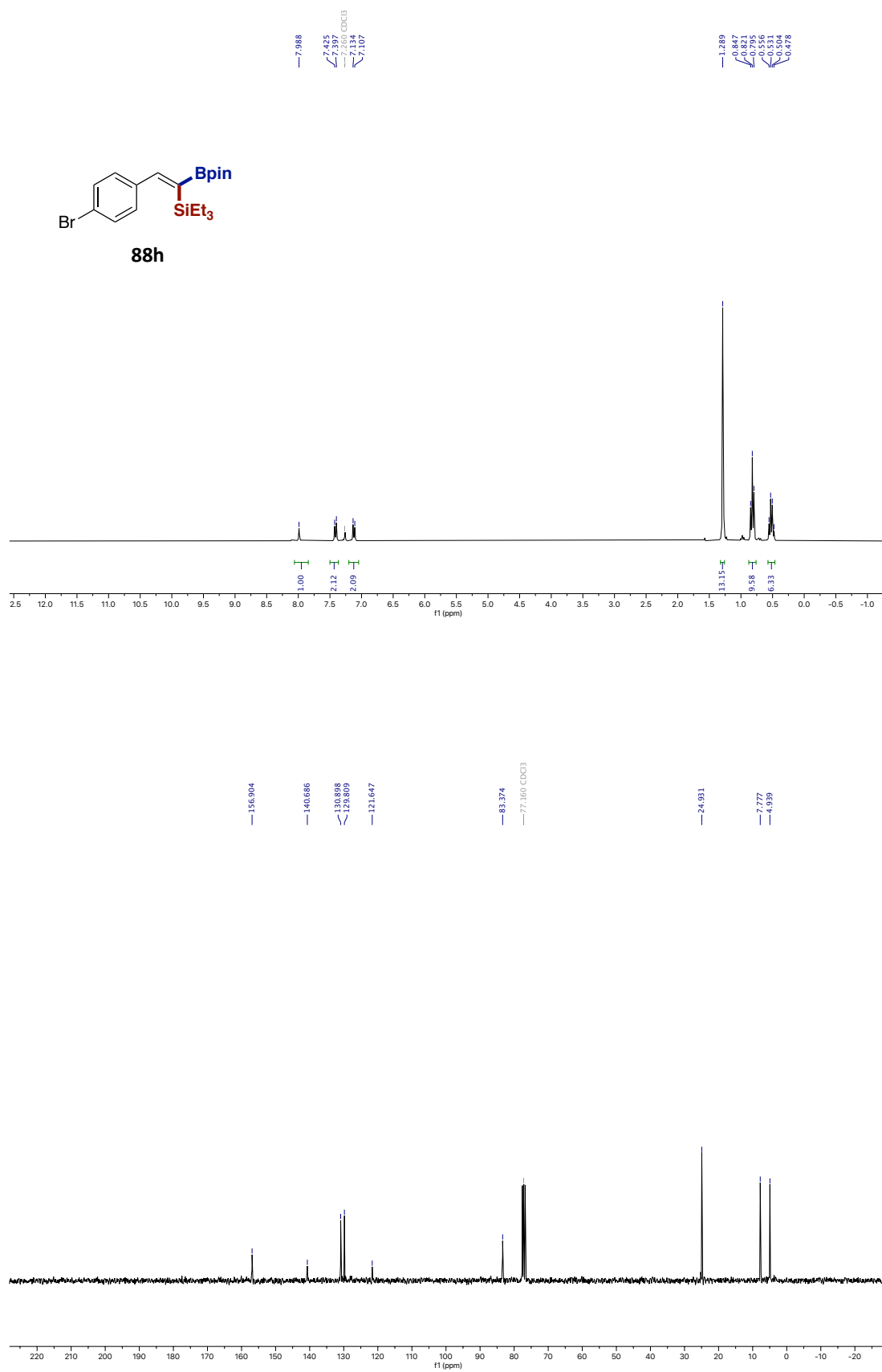


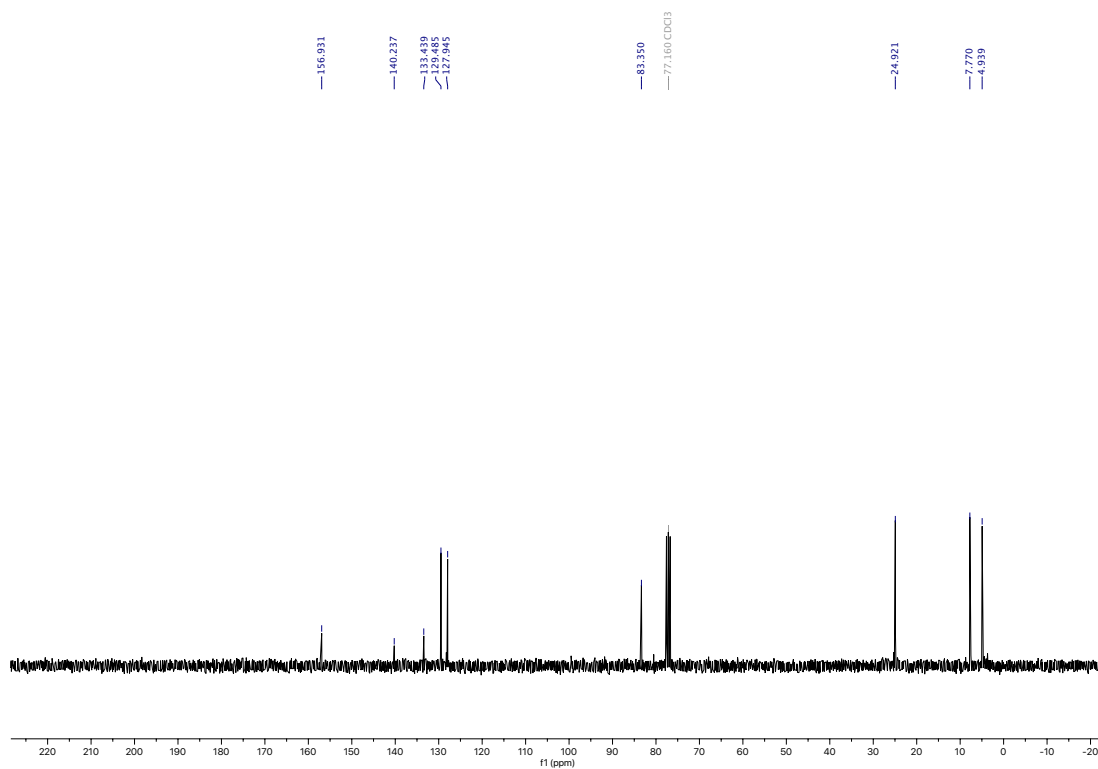
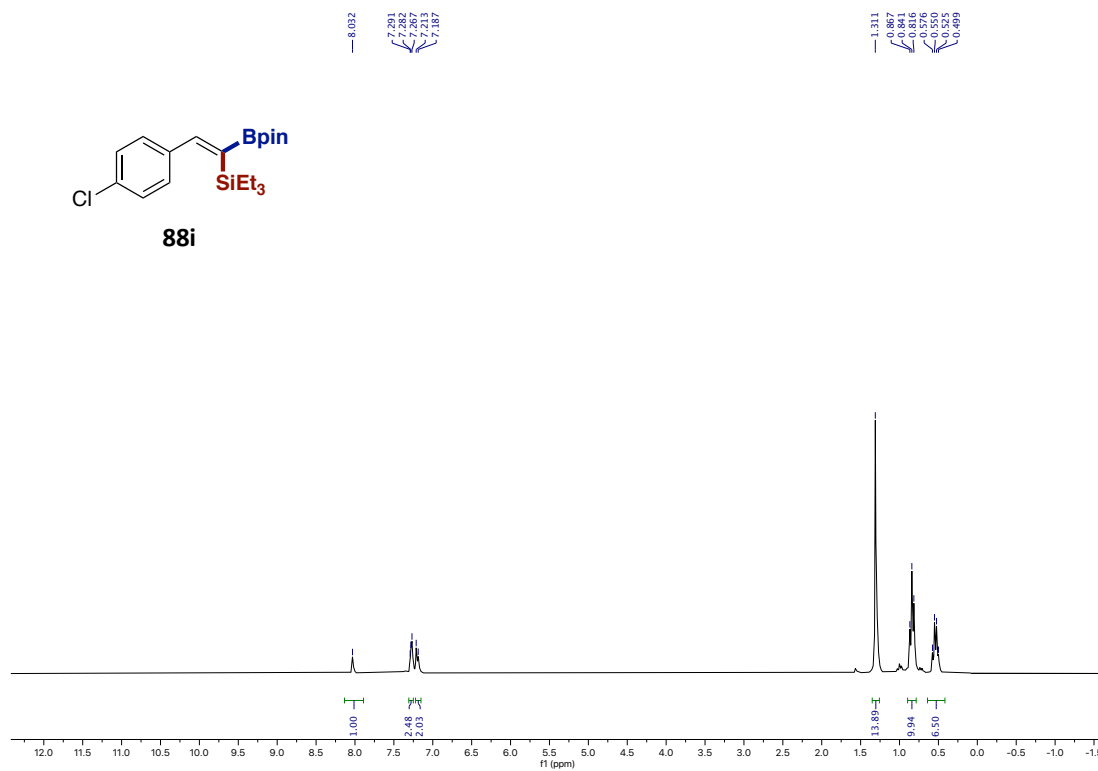
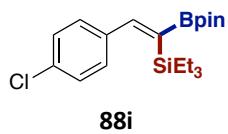
Stereoselective Base-Catalyzed 1,1-Silaboration of Terminal Alkynes



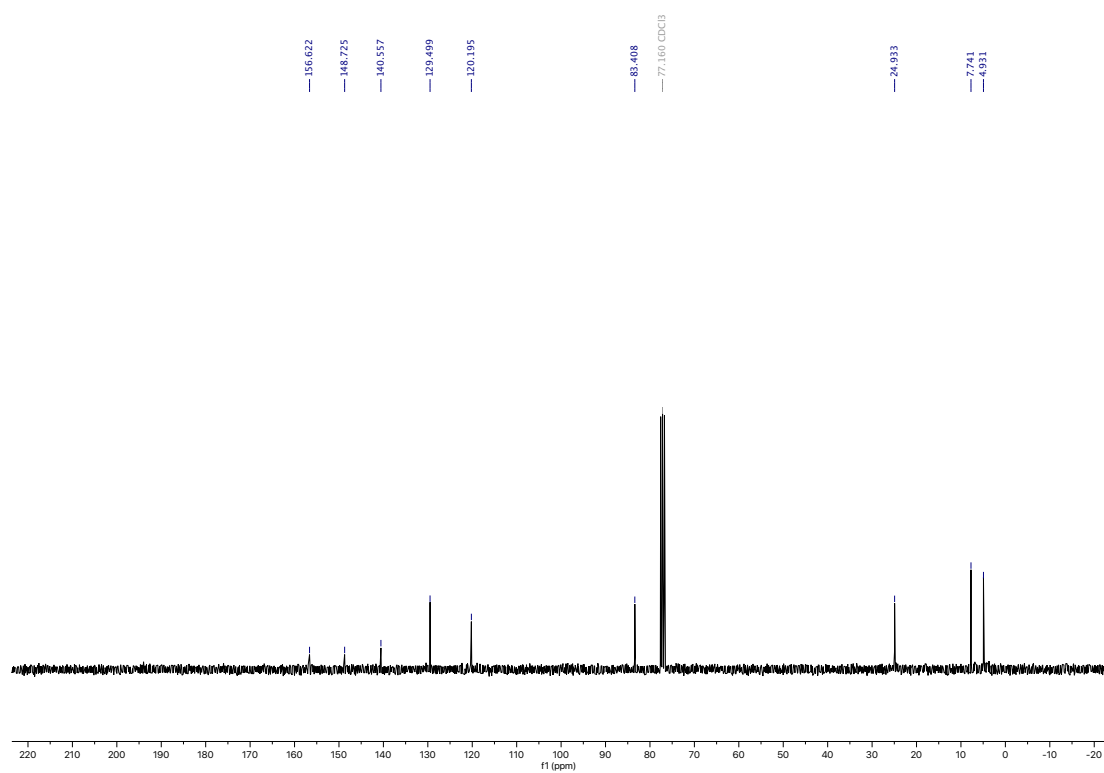
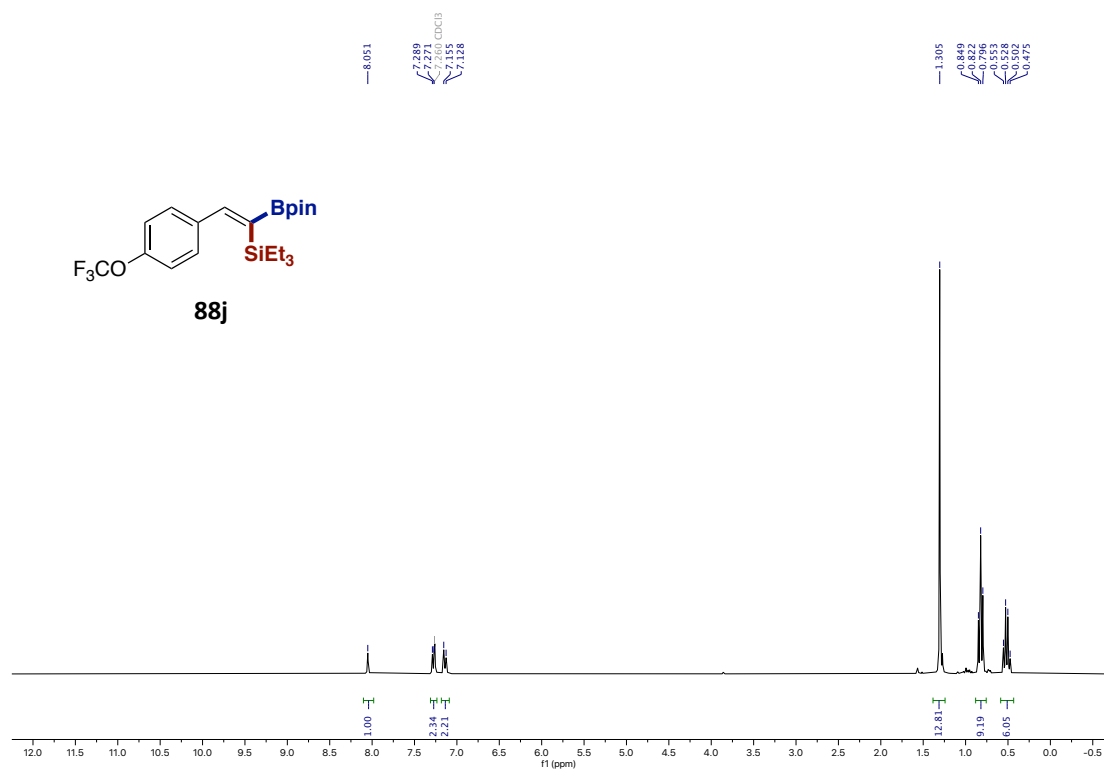


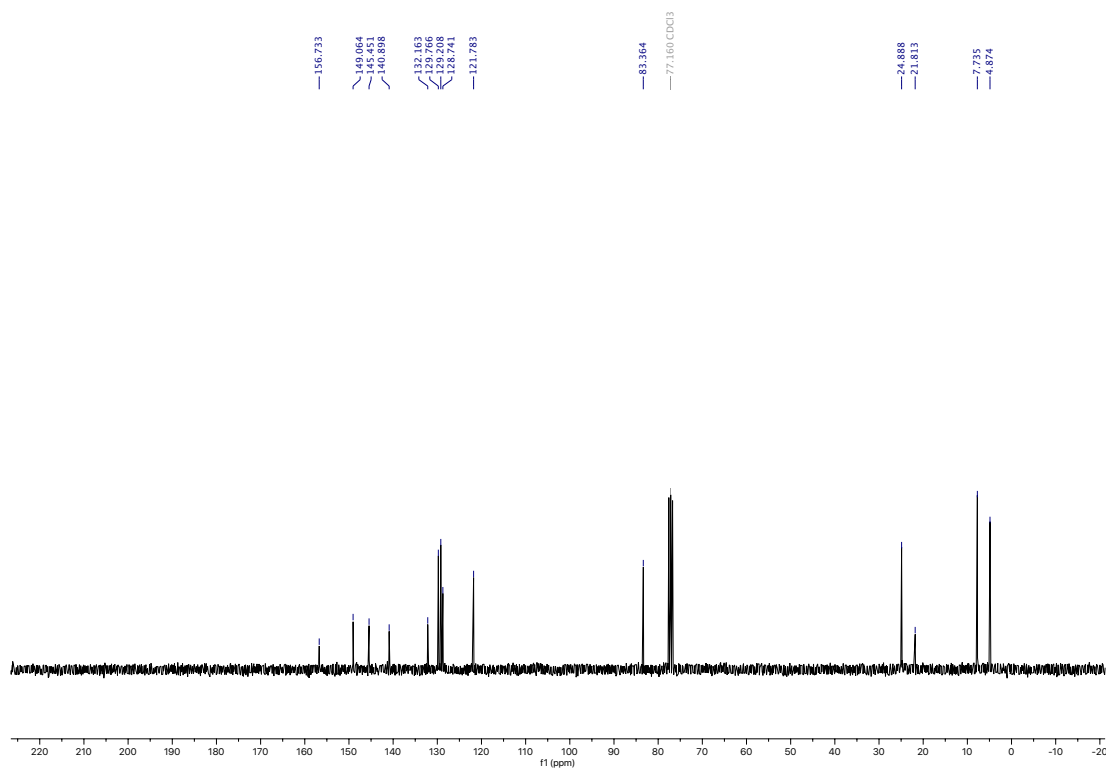
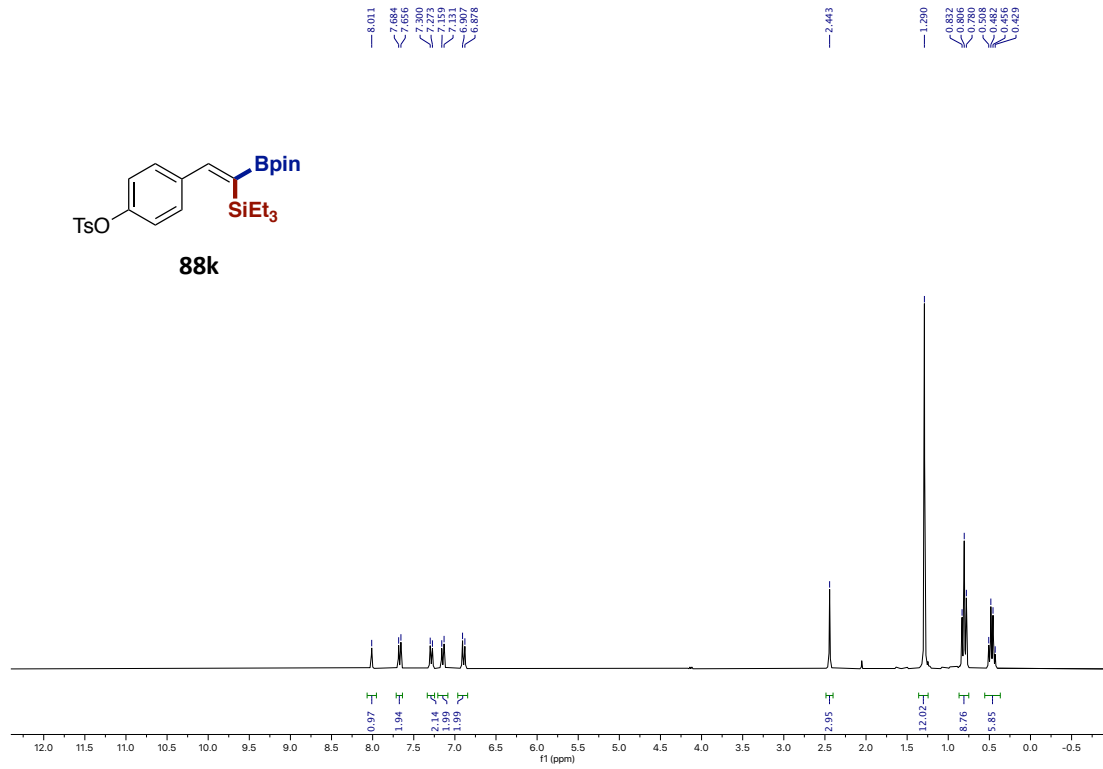
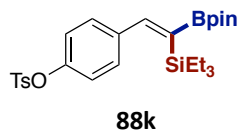
Stereoselective Base-Catalyzed 1,1-Silaboration of Terminal Alkynes



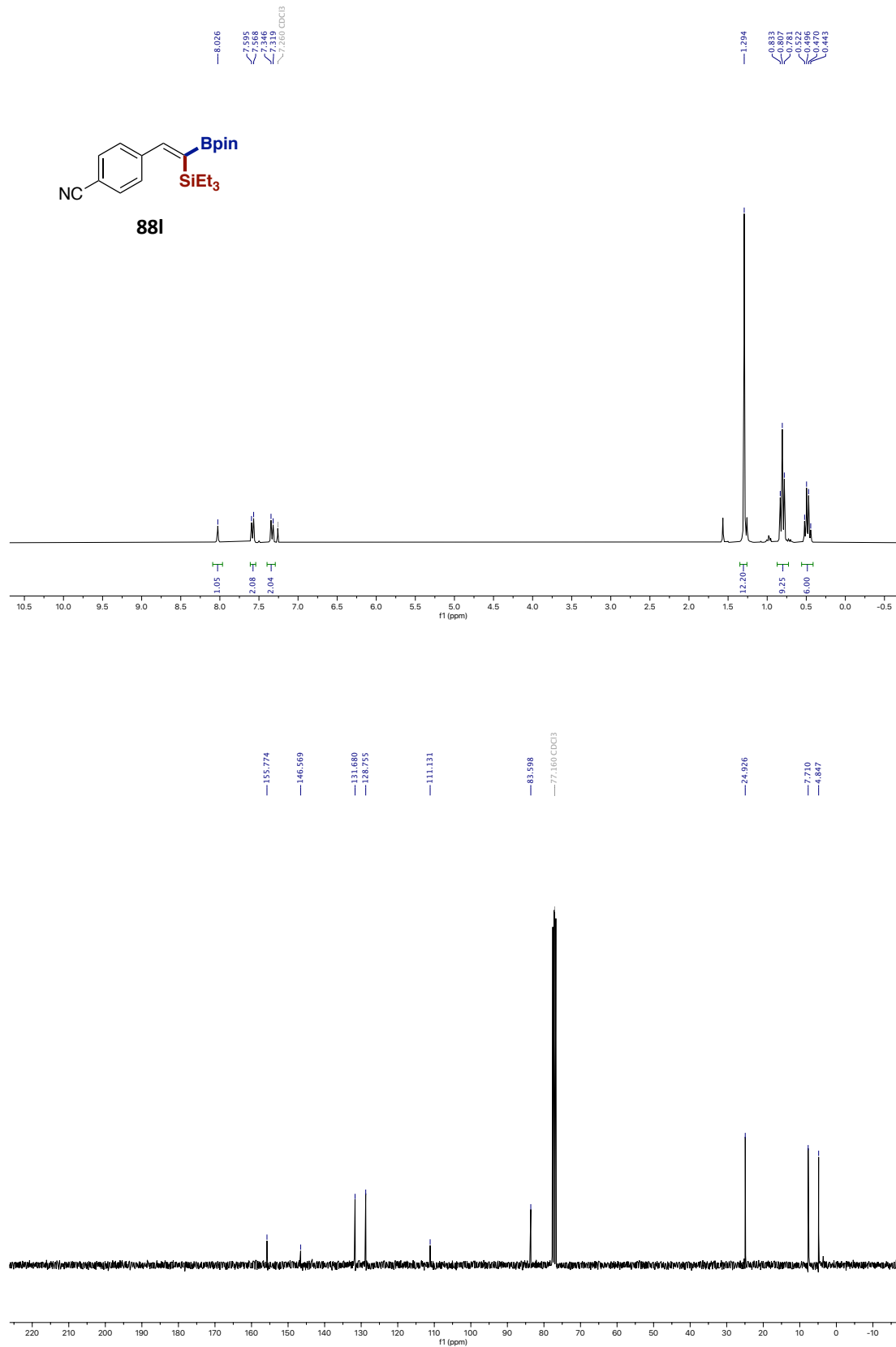


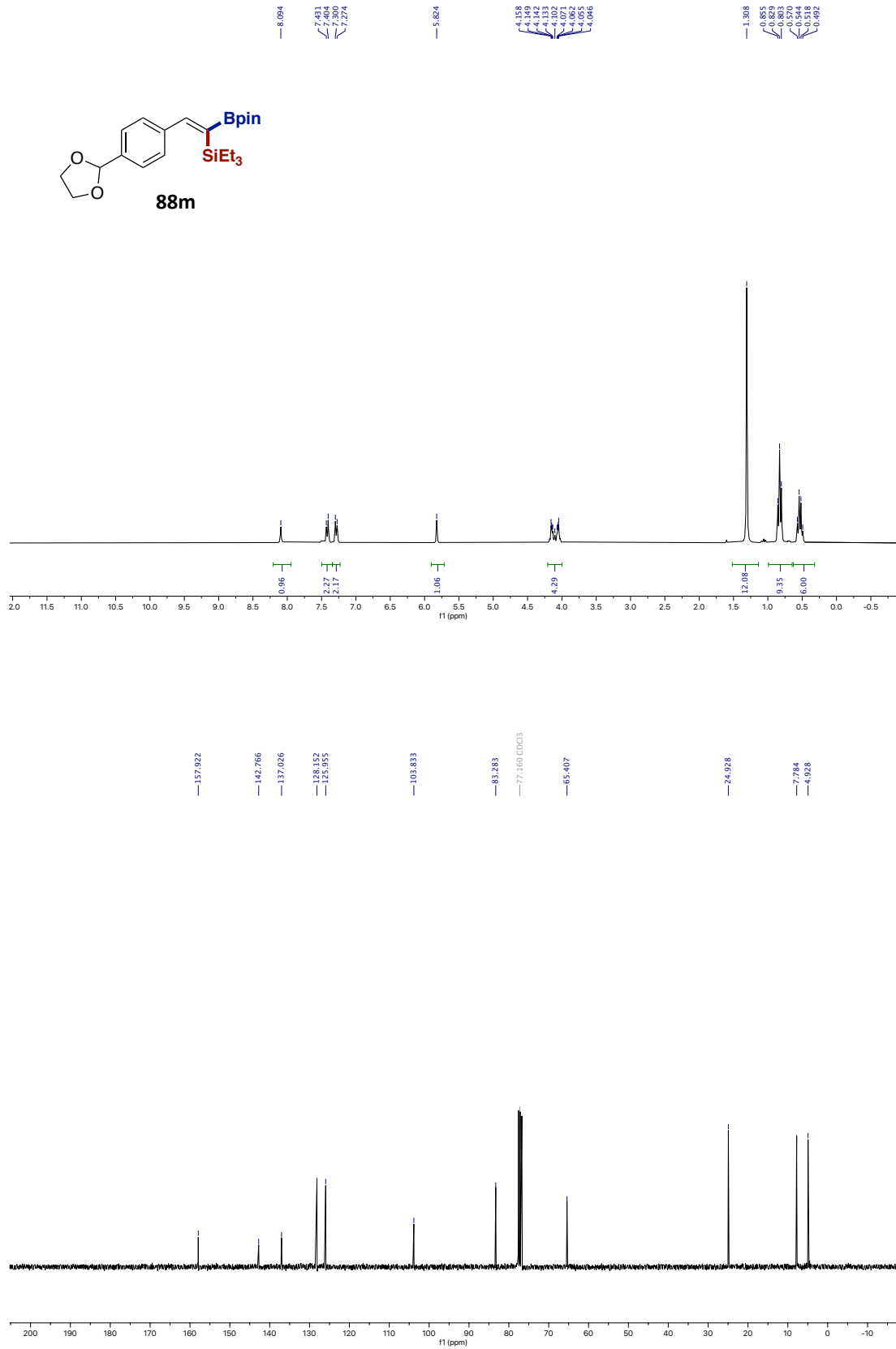
Stereoselective Base-Catalyzed 1,1-Silaboration of Terminal Alkynes



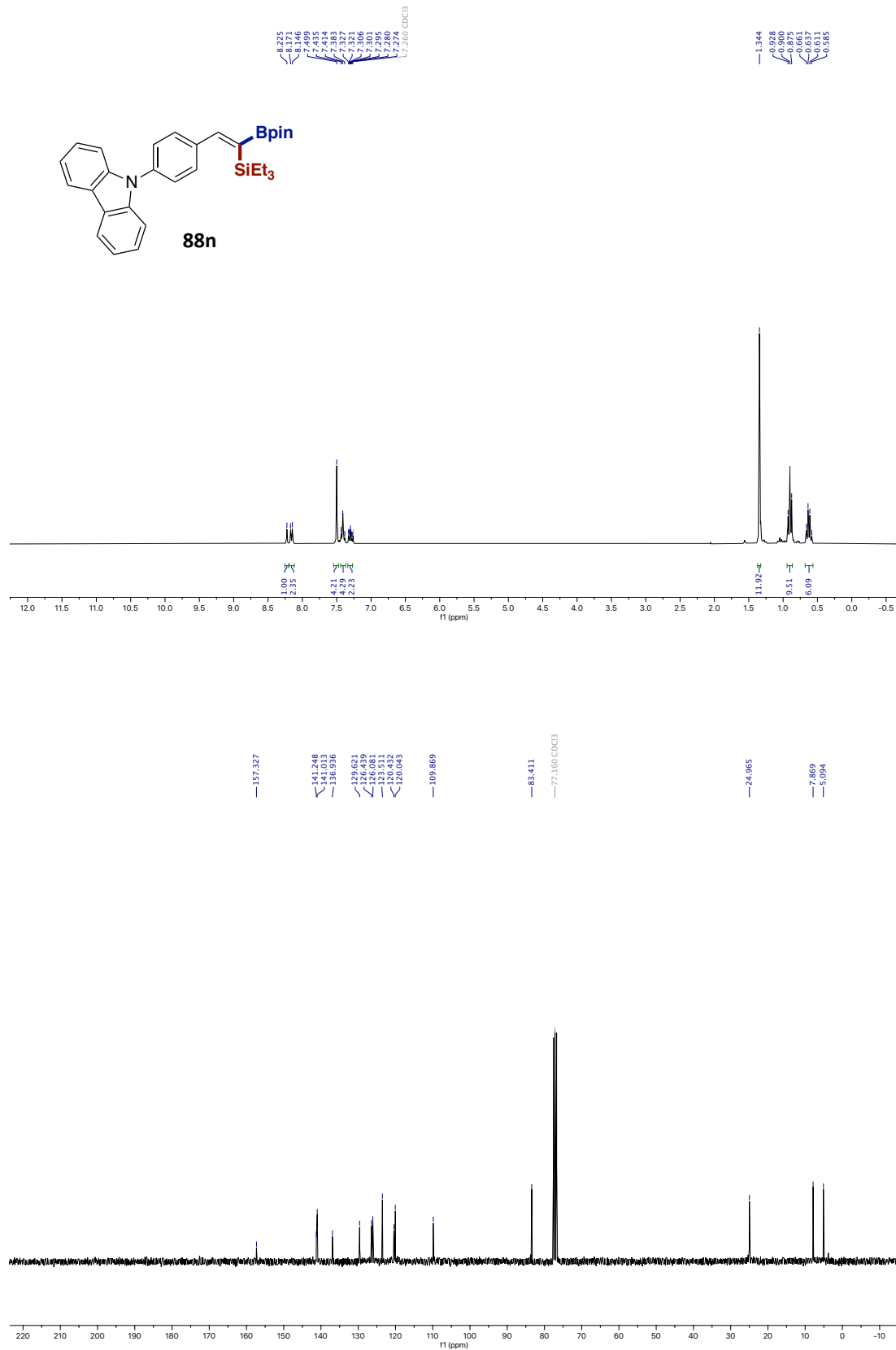


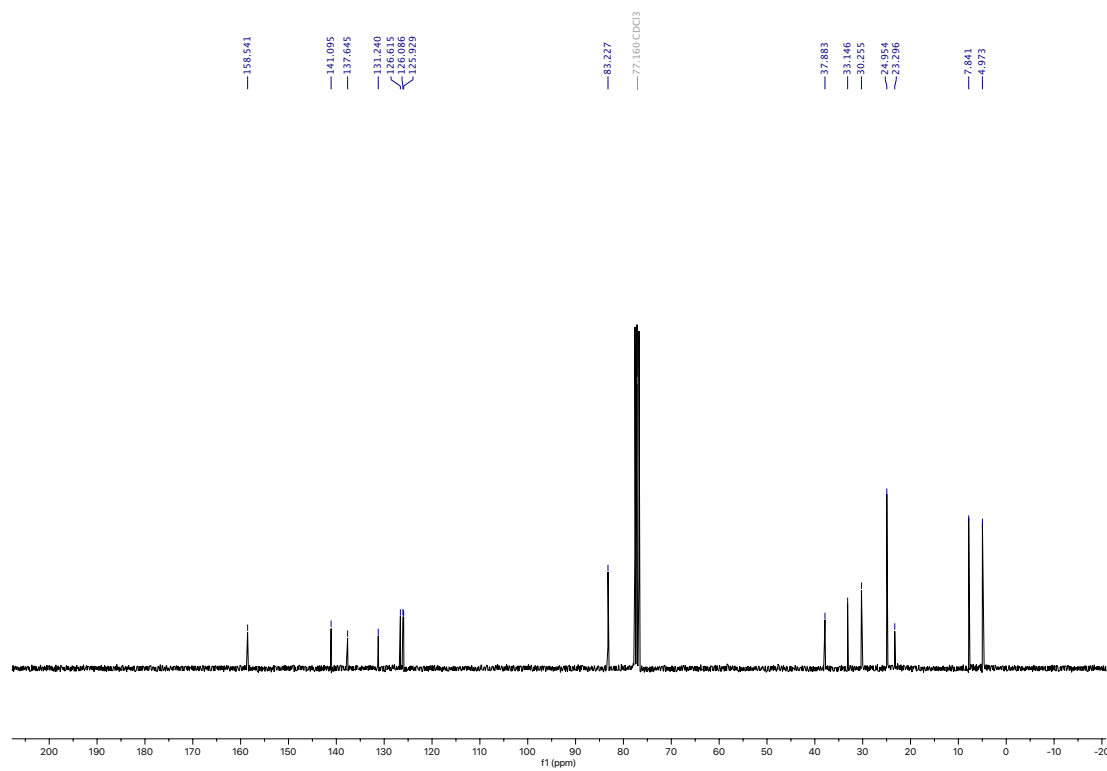
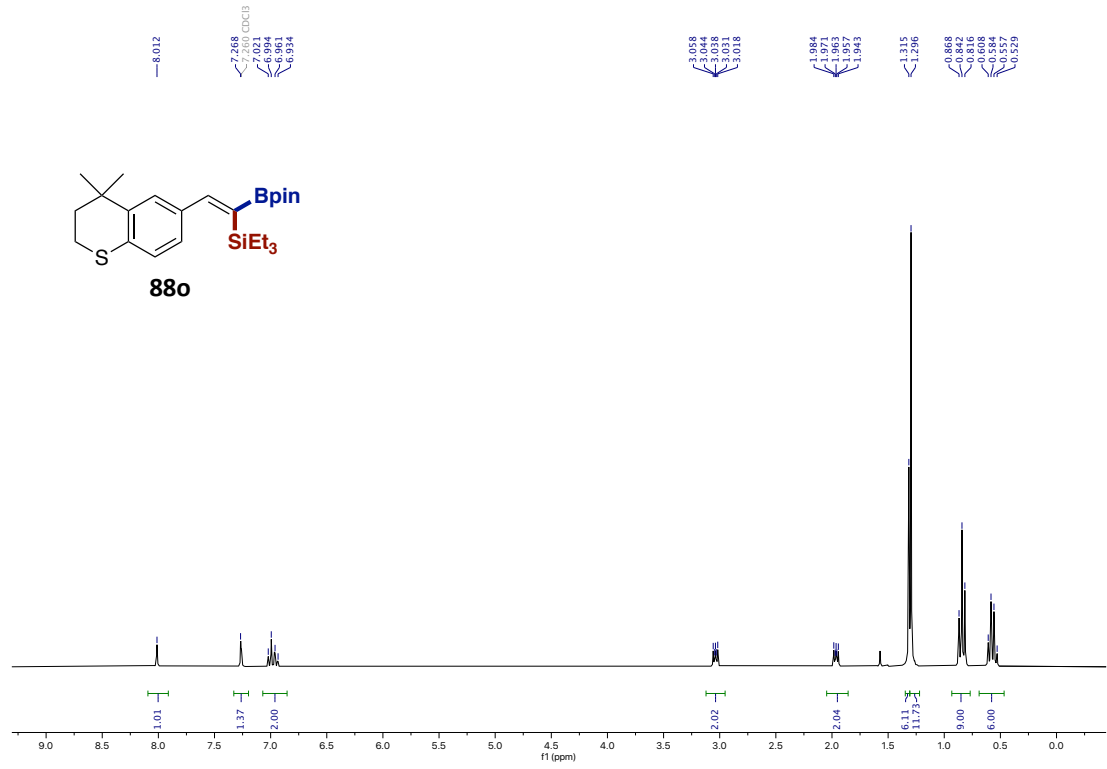
Stereoselective Base-Catalyzed 1,1-Silaboration of Terminal Alkynes



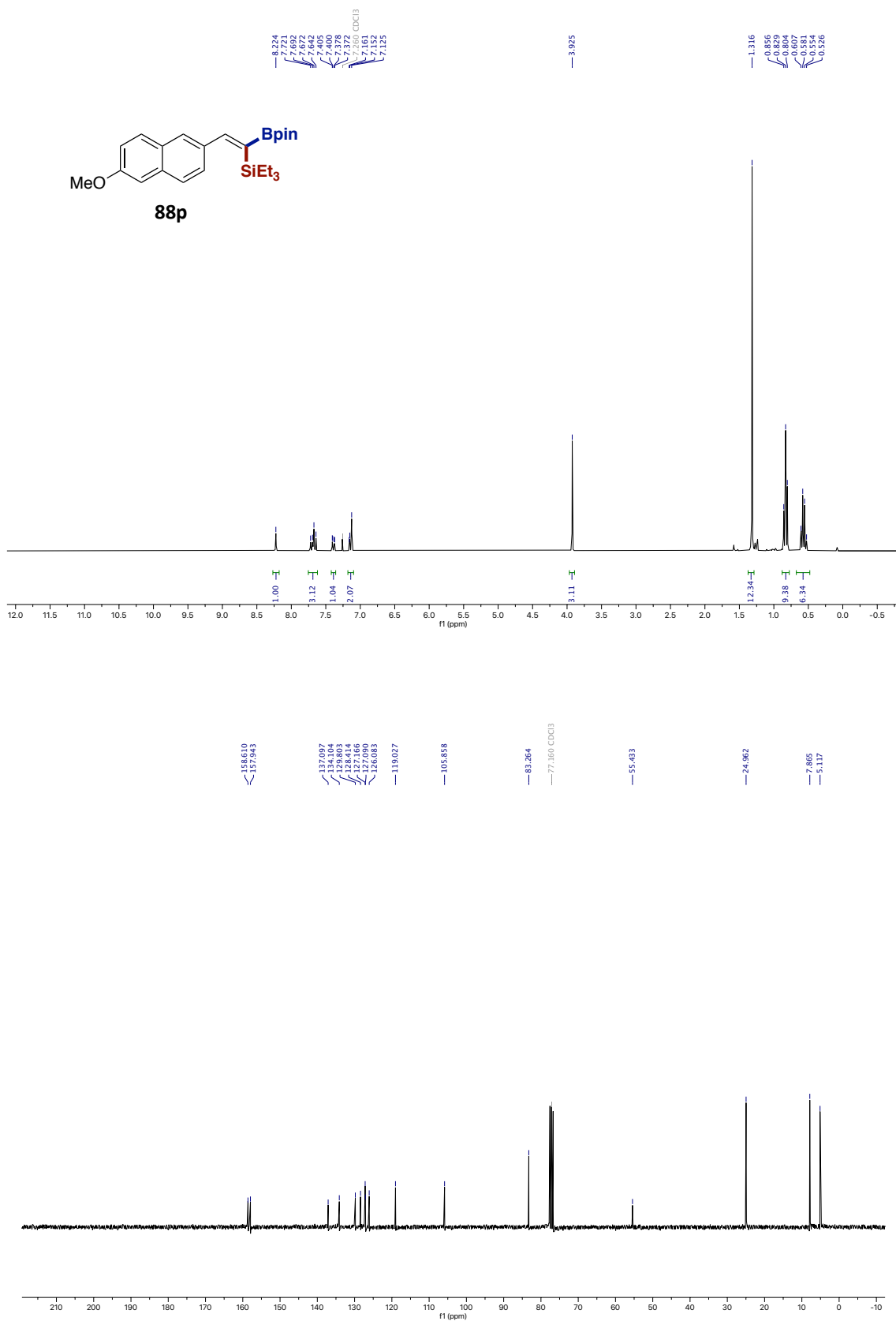


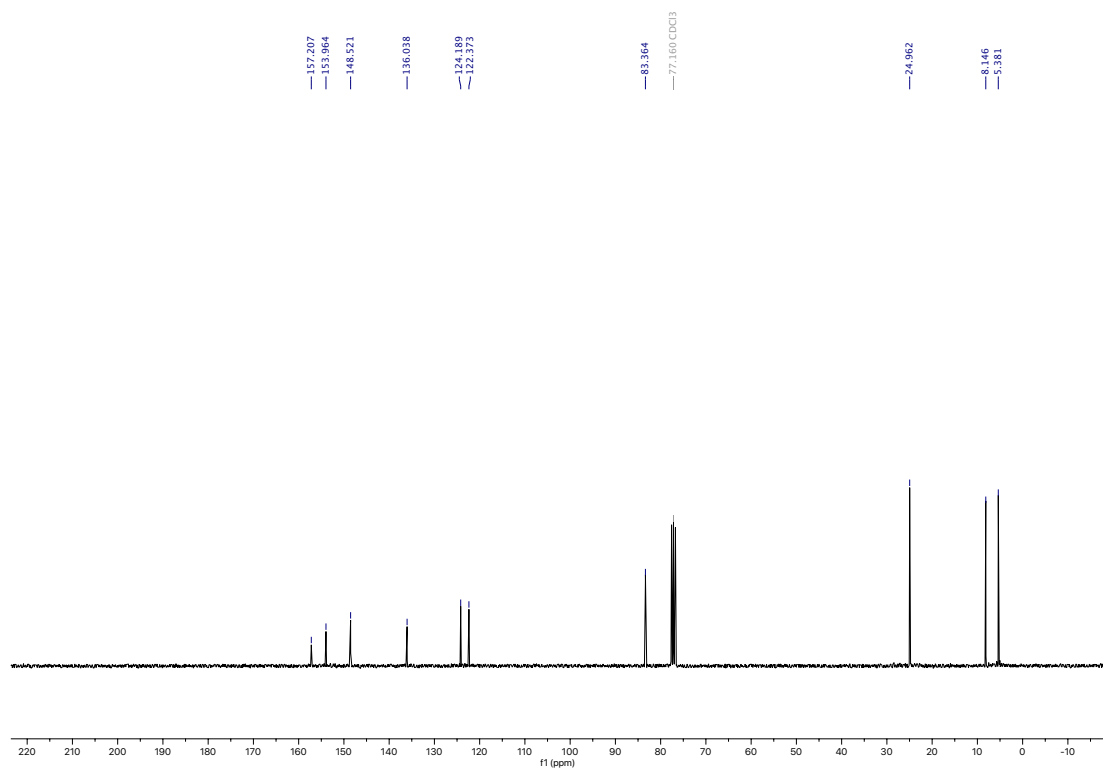
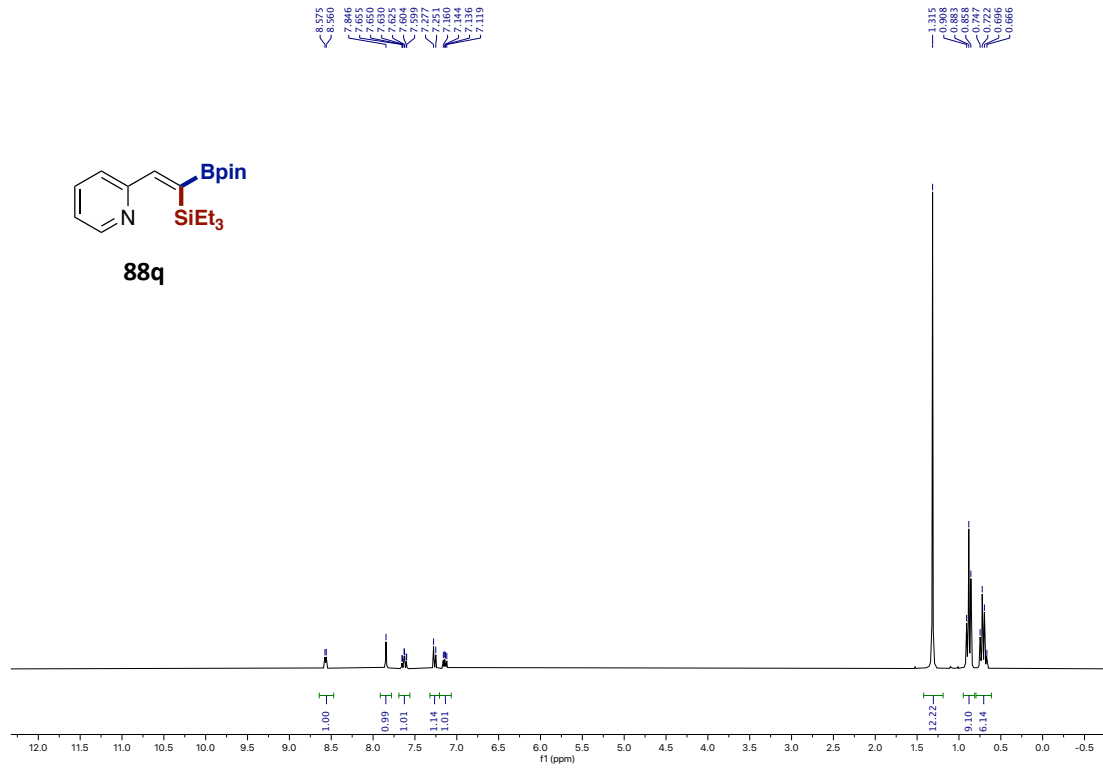
Stereoselective Base-Catalyzed 1,1-Silaboration of Terminal Alkynes



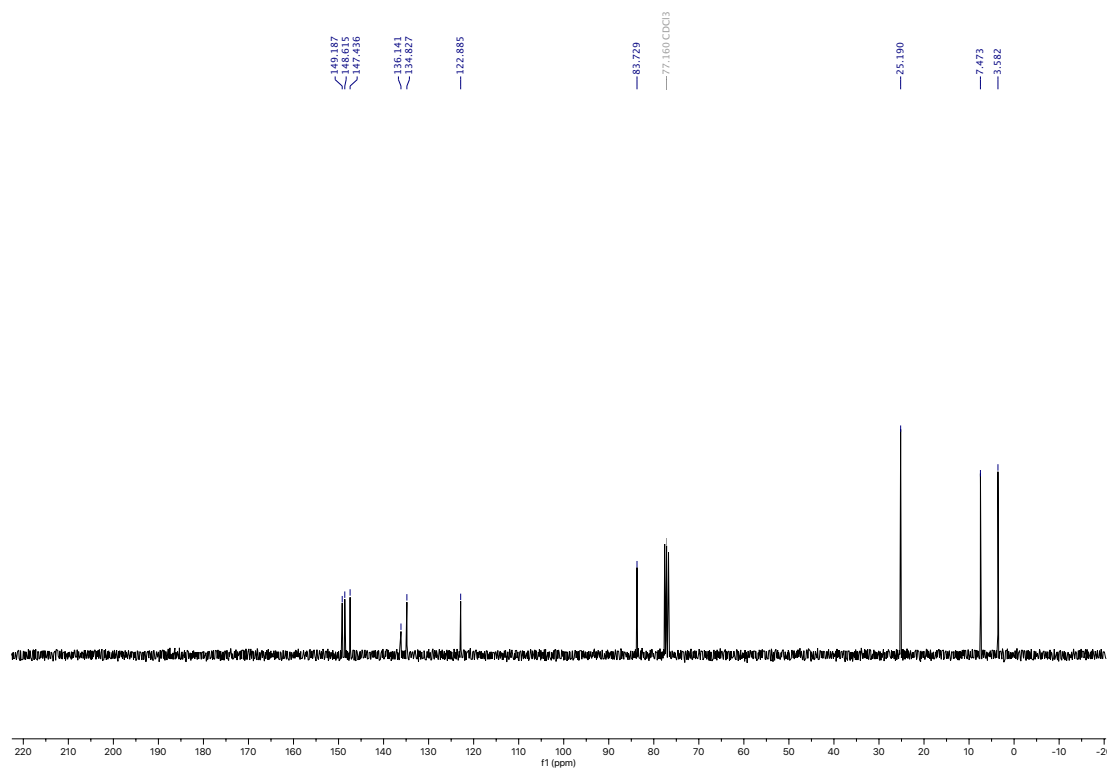
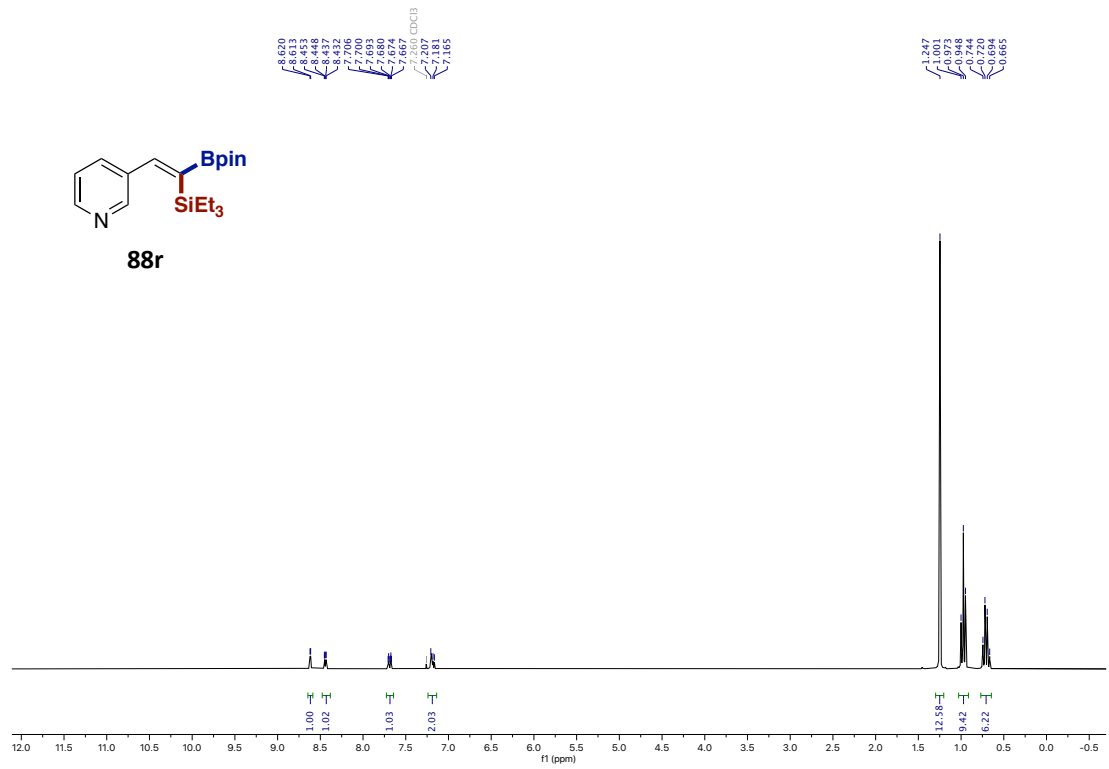


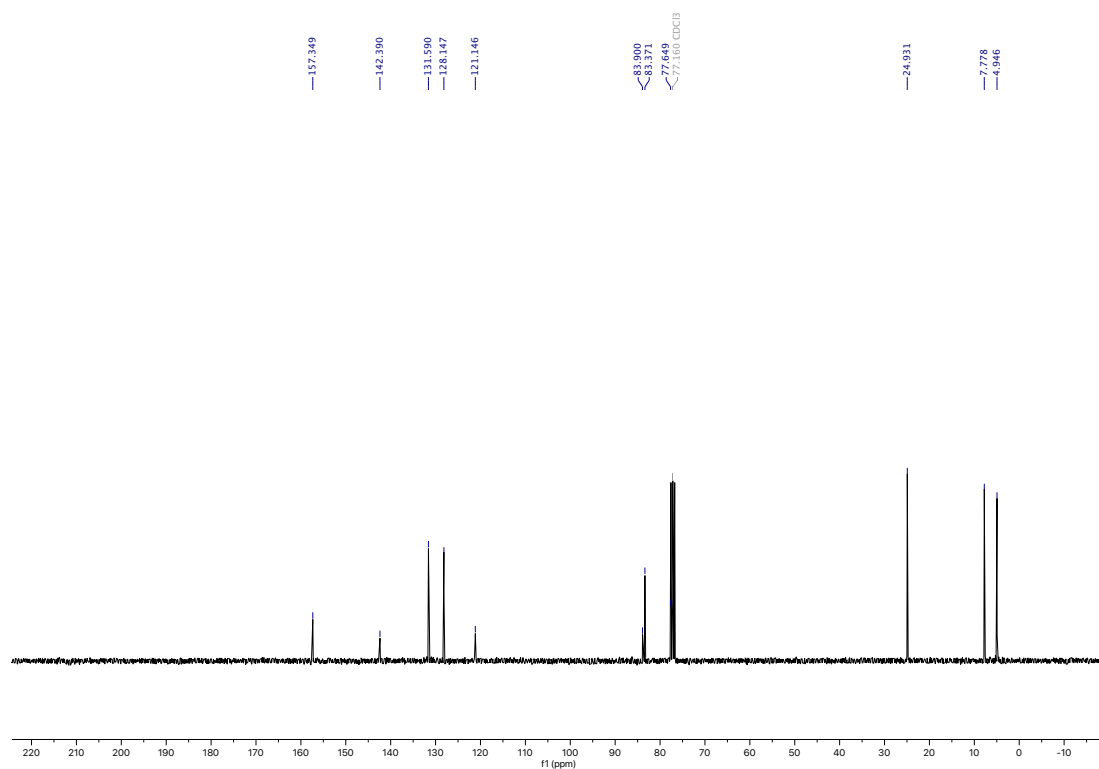
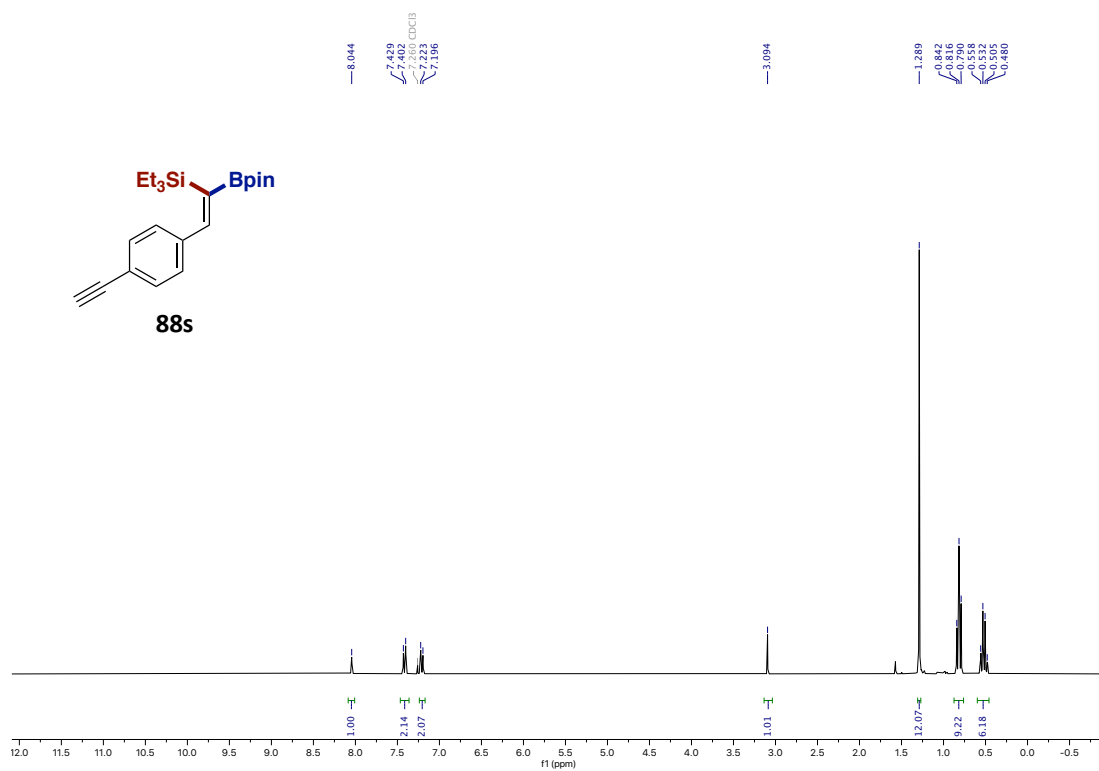
Stereoselective Base-Catalyzed 1,1-Silaboration of Terminal Alkynes



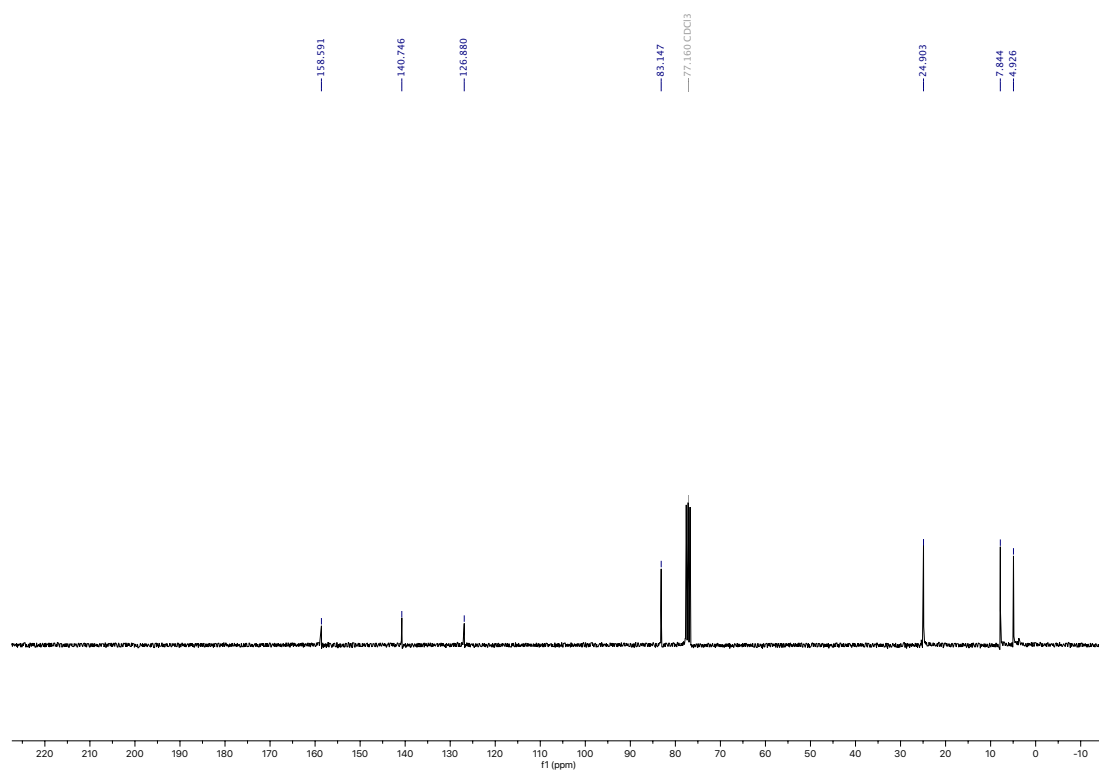
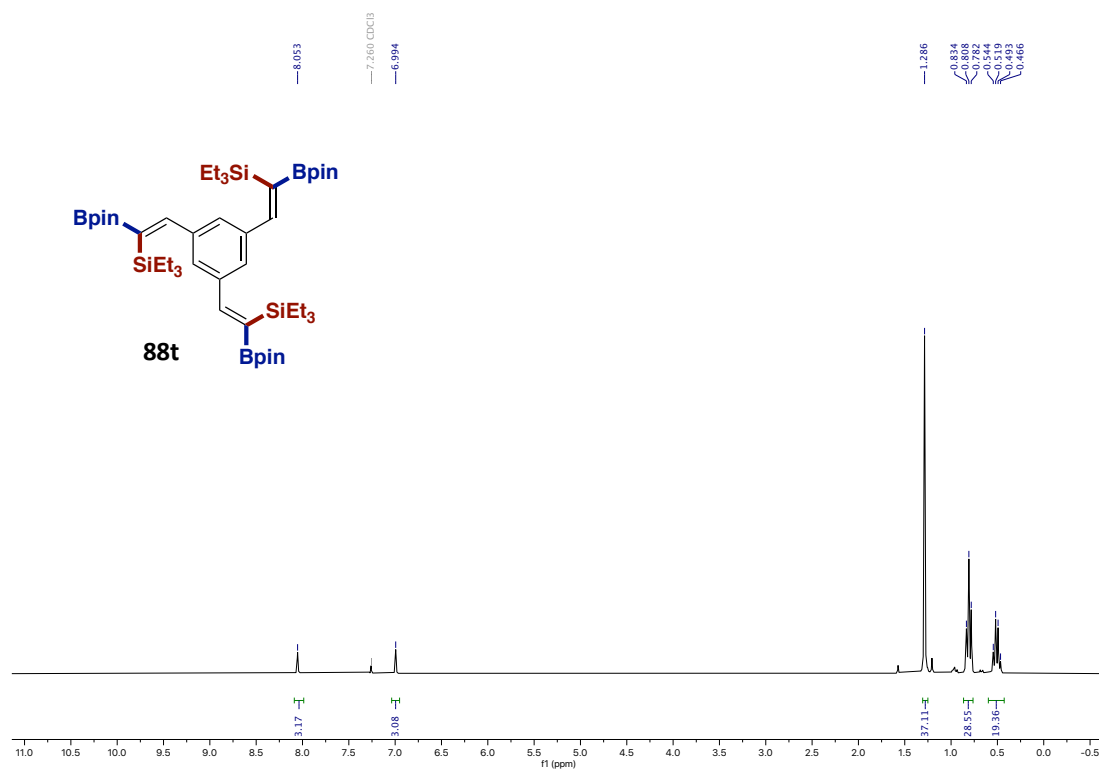


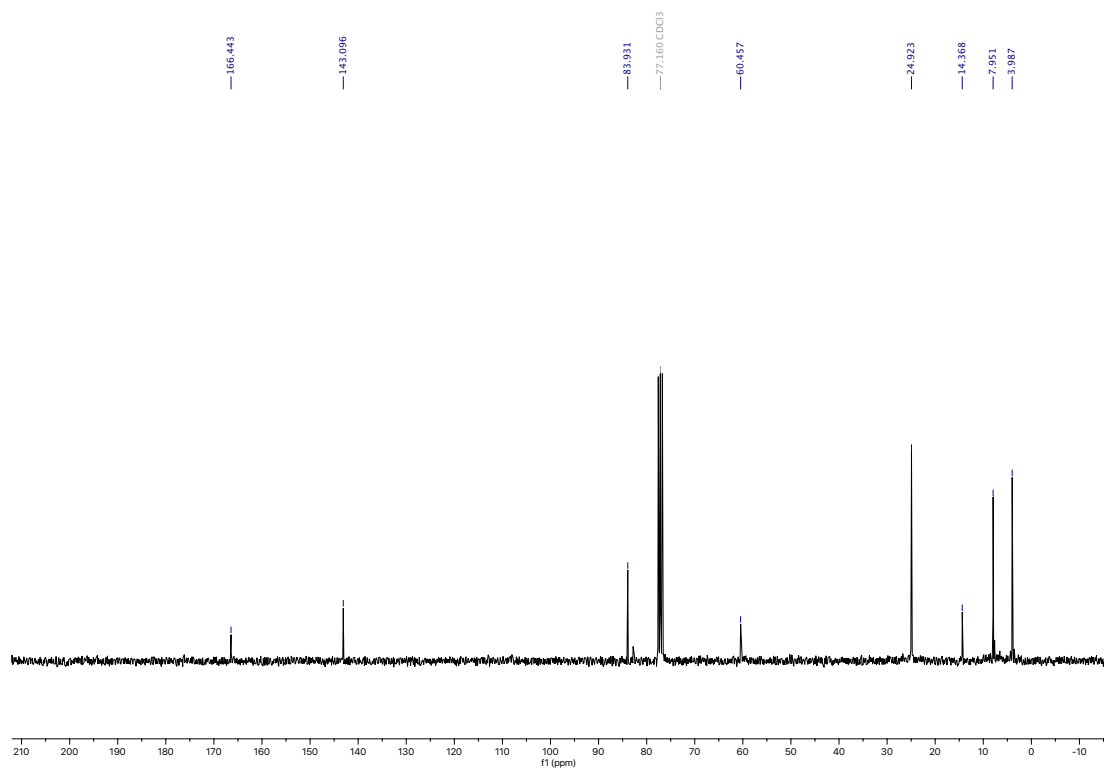
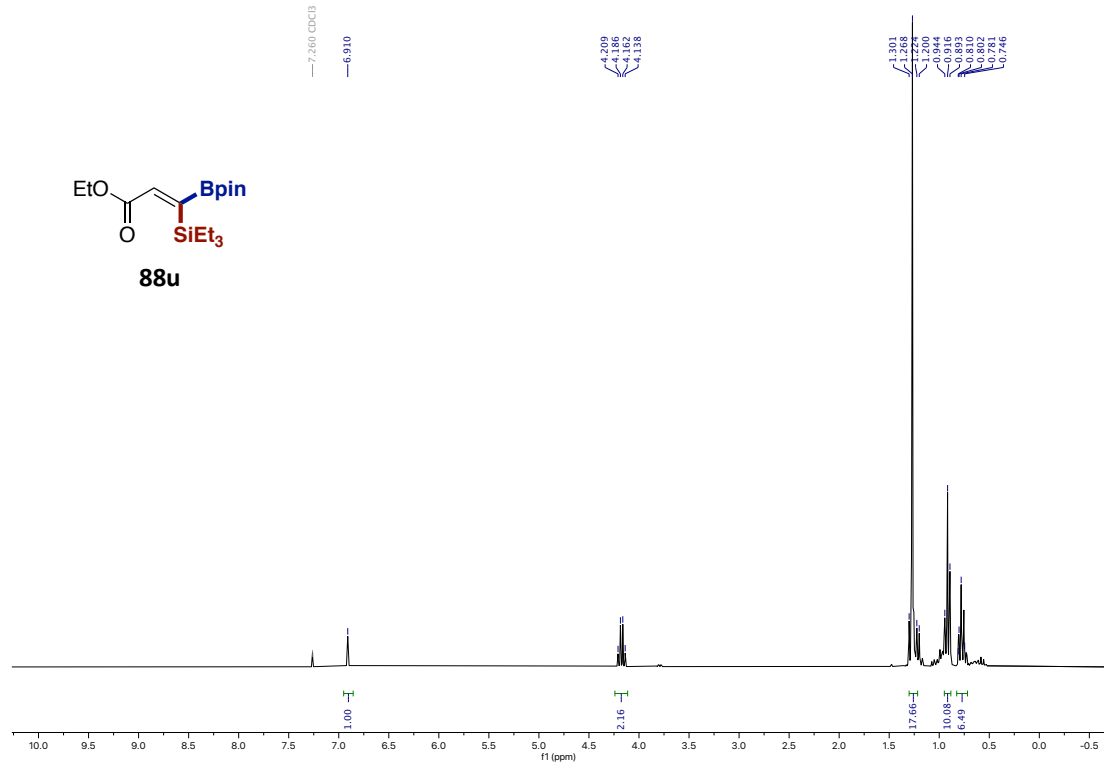
Stereoselective Base-Catalyzed 1,1-Silaboration of Terminal Alkynes



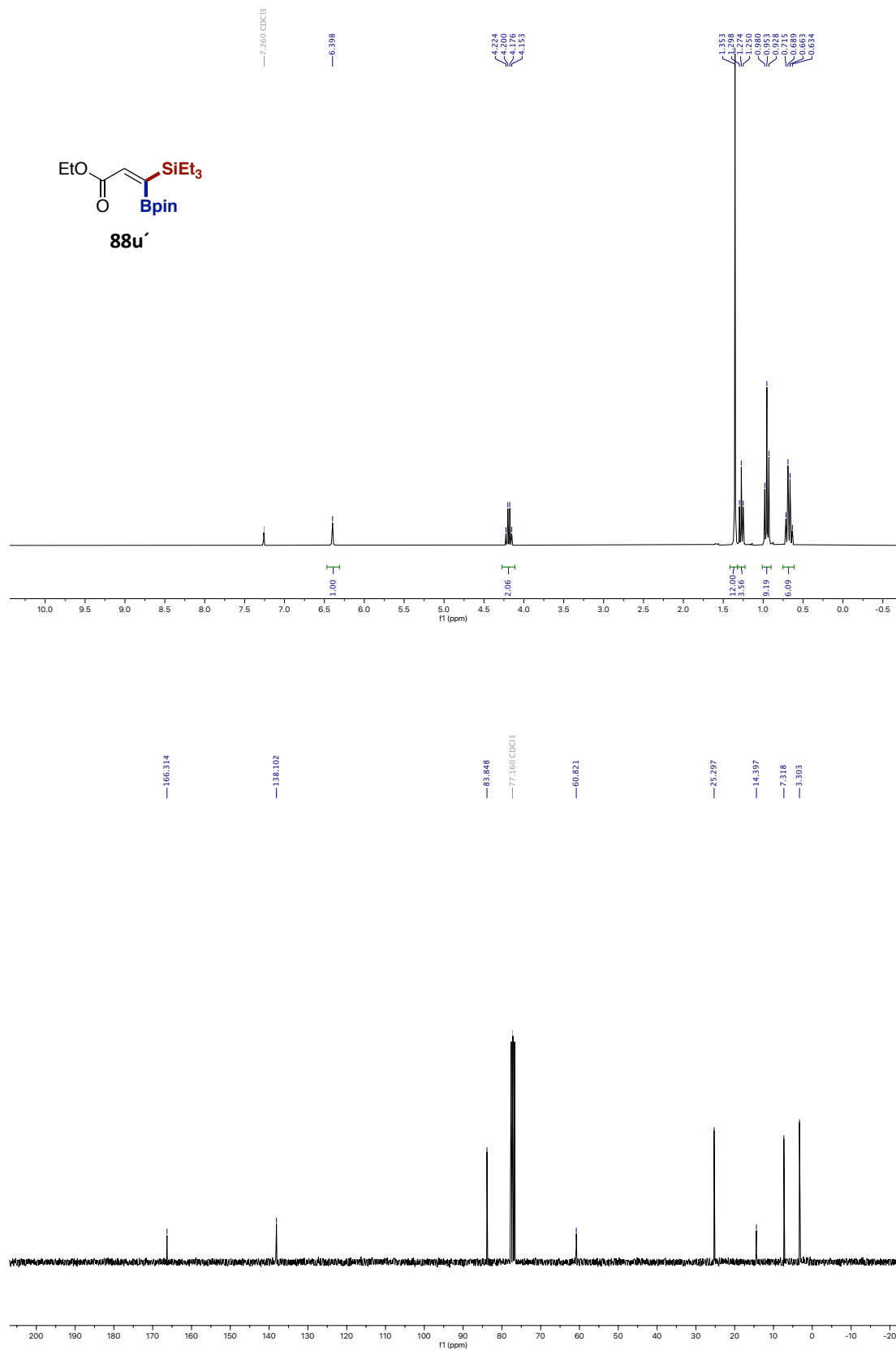


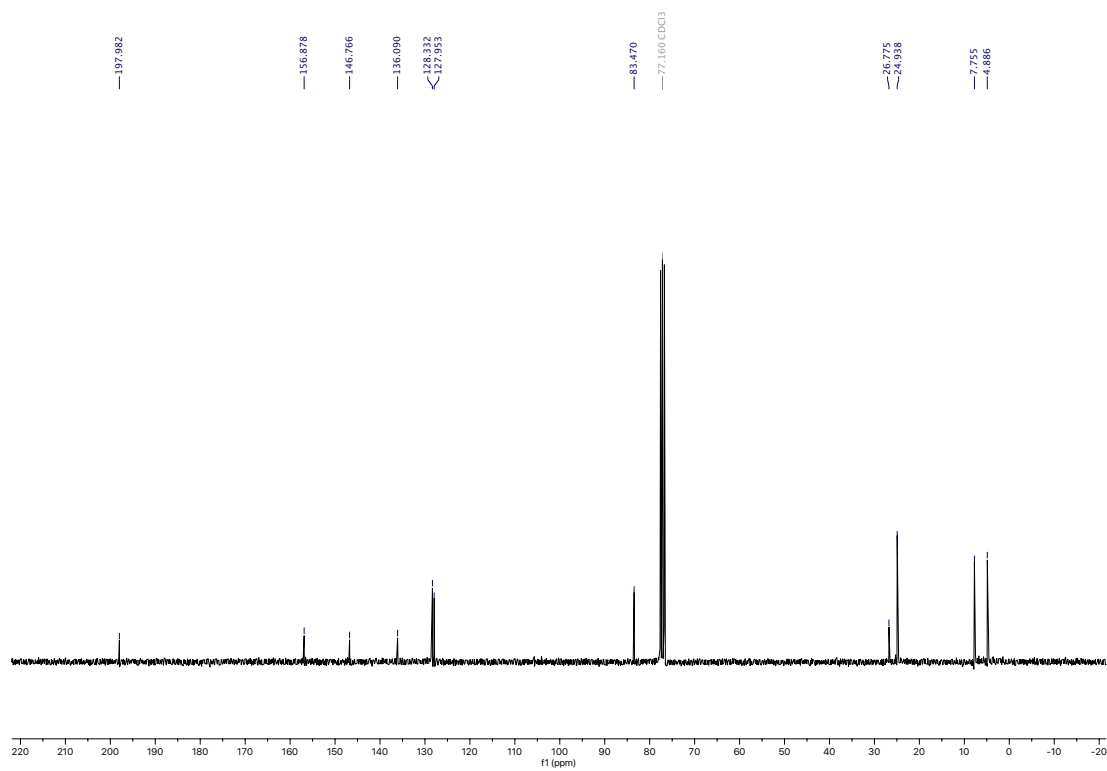
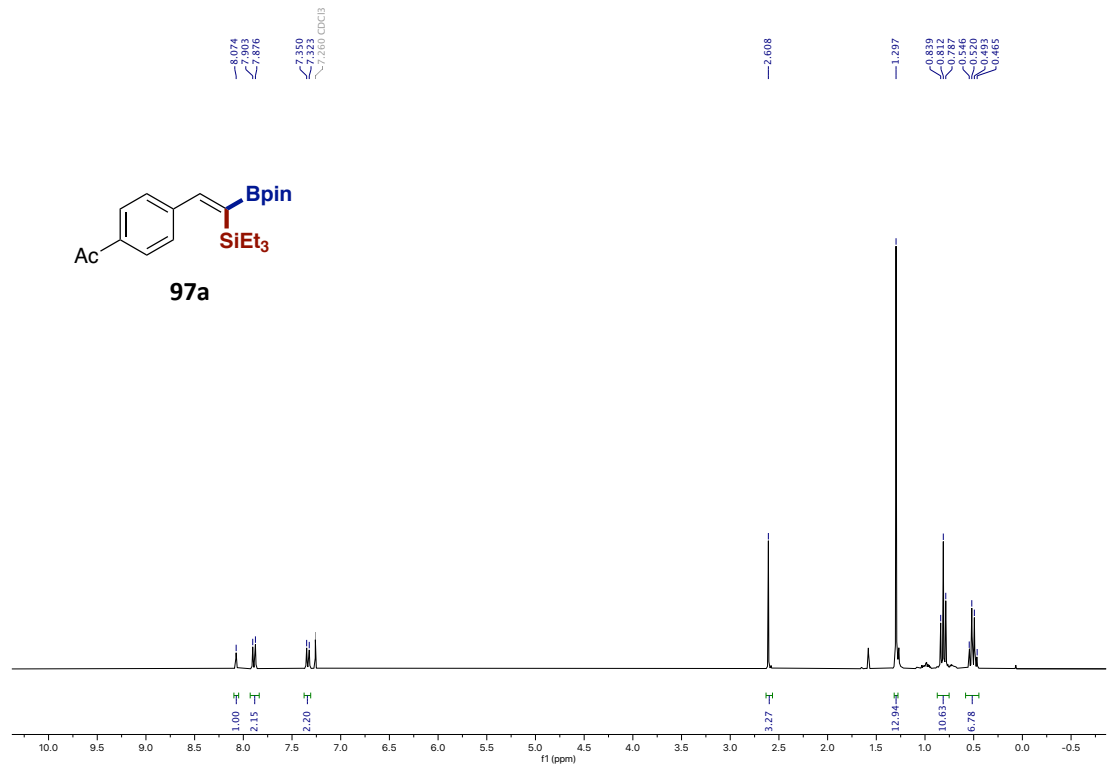
Stereoselective Base-Catalyzed 1,1-Silaboration of Terminal Alkynes



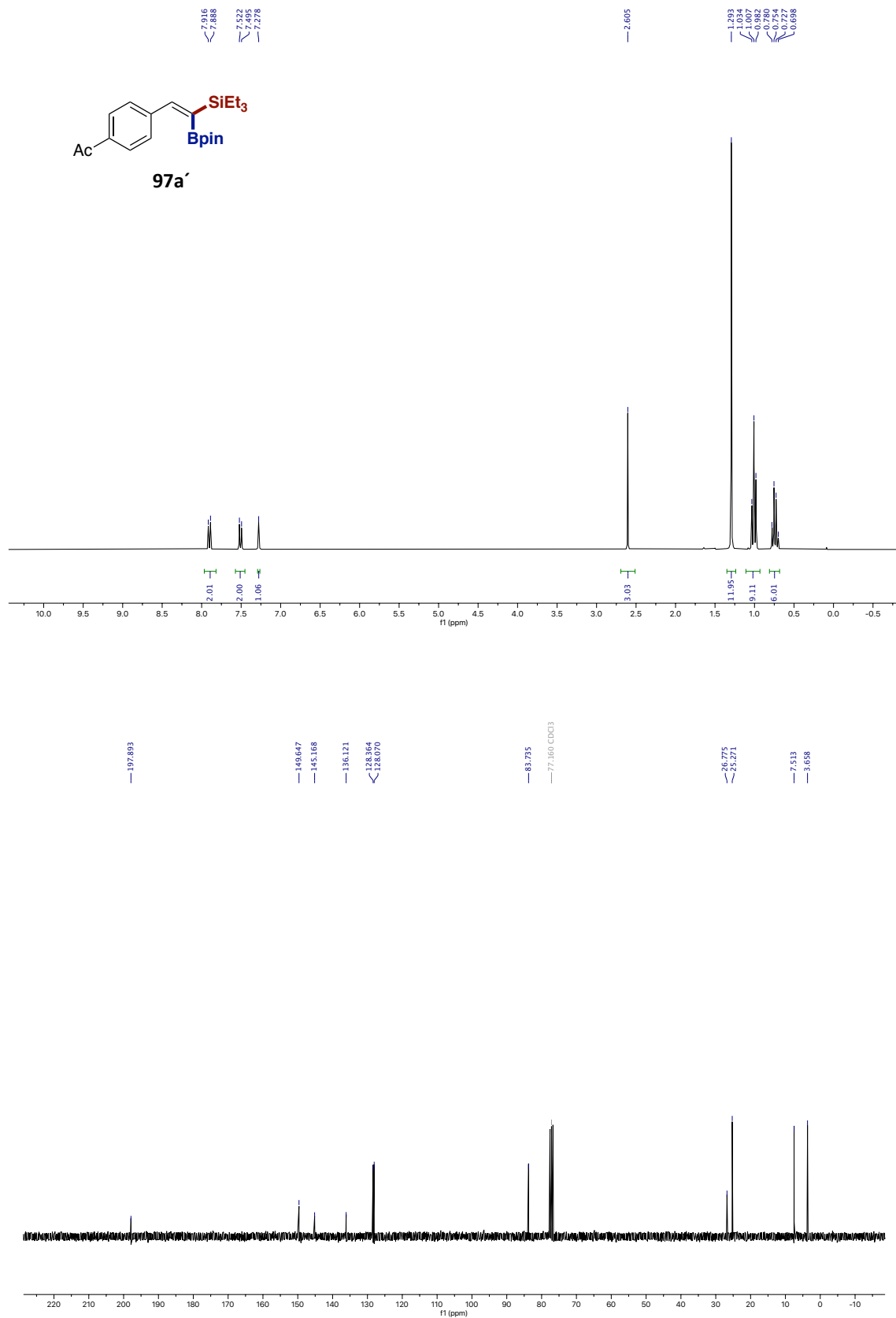


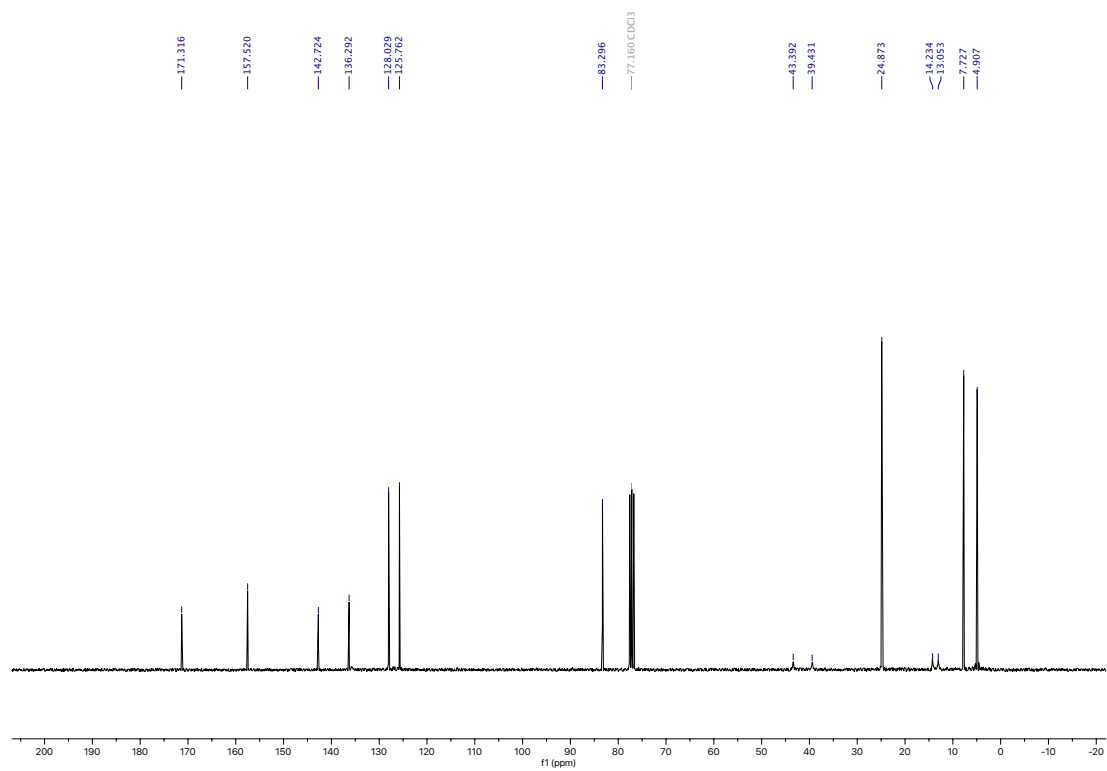
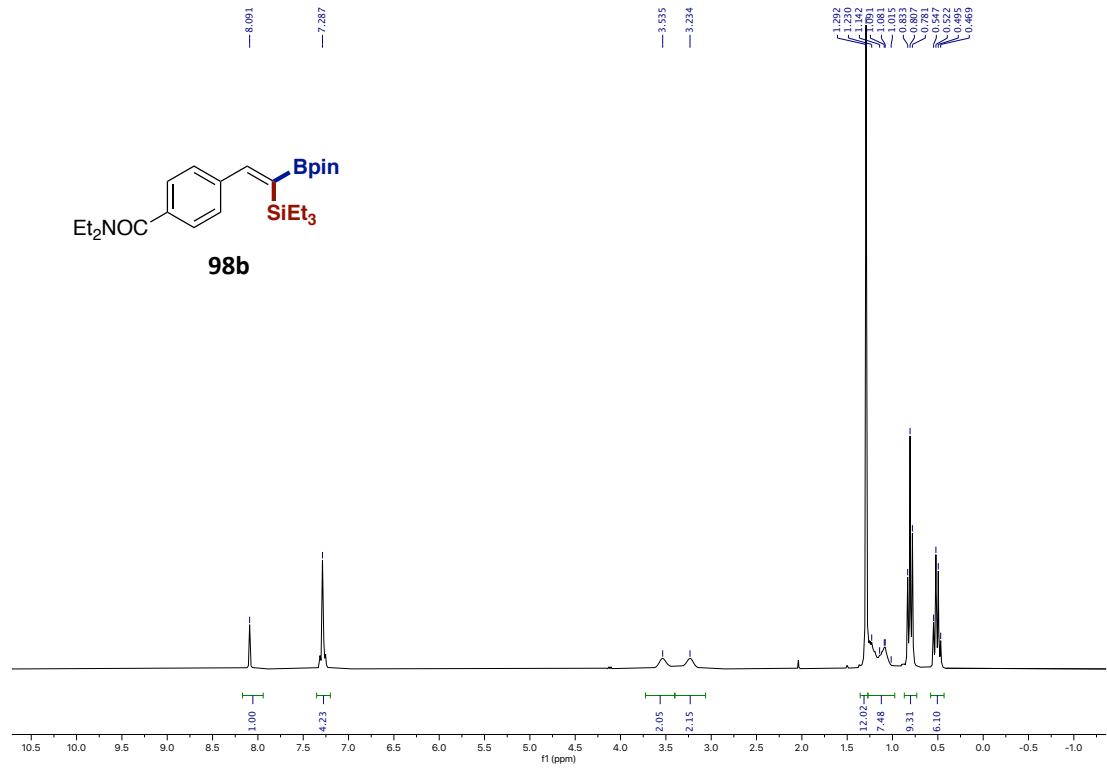
Stereoselective Base-Catalyzed 1,1-Silaboration of Terminal Alkynes



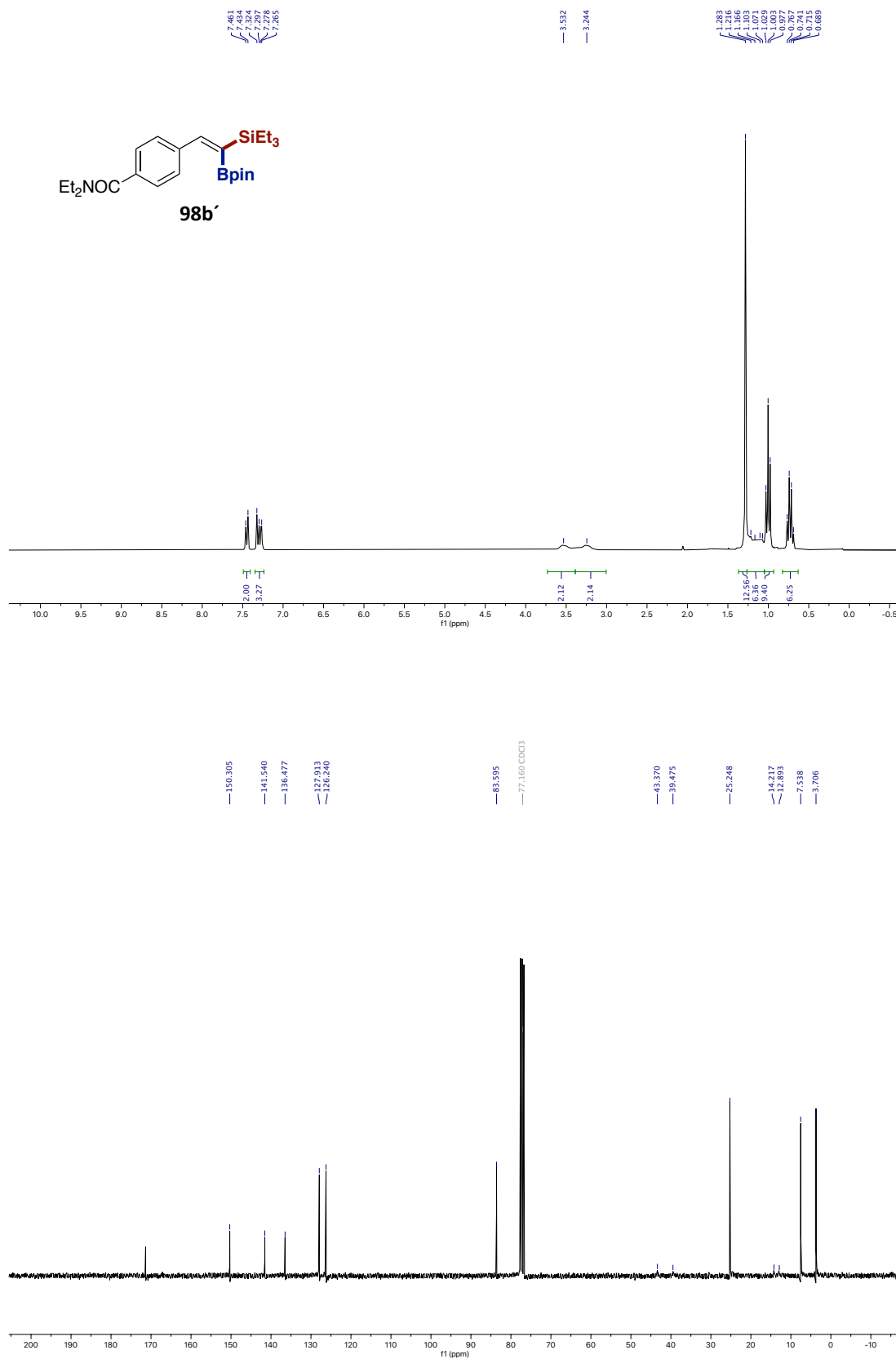


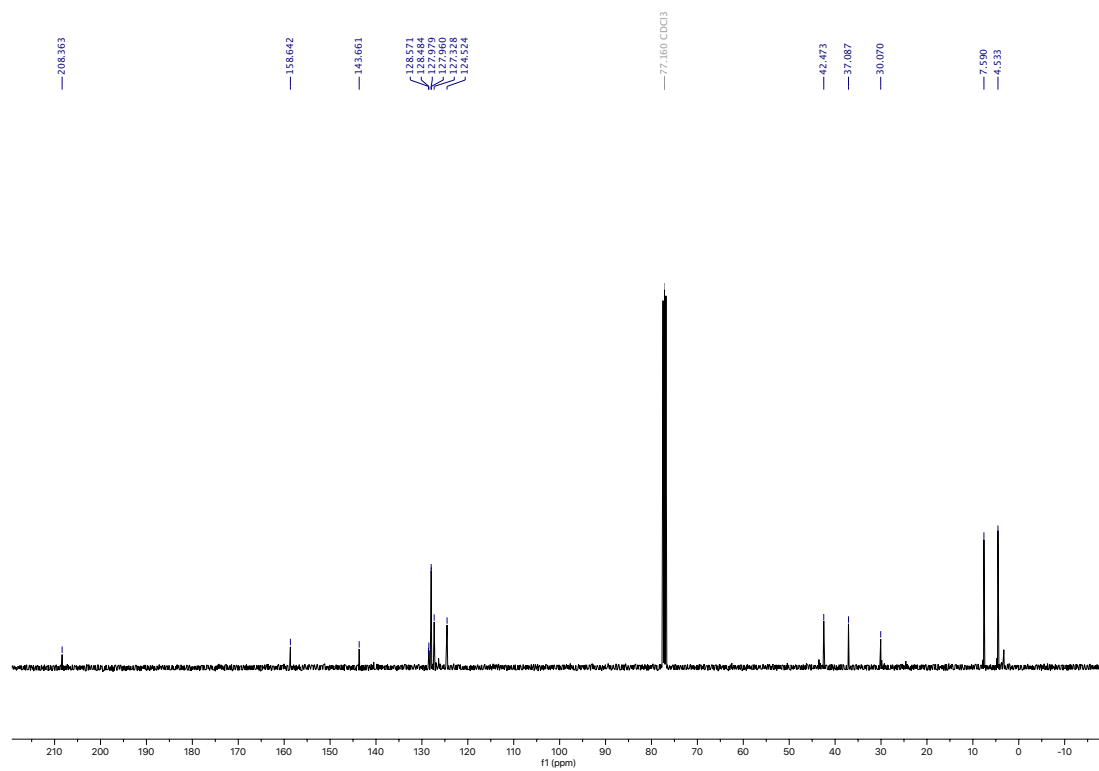
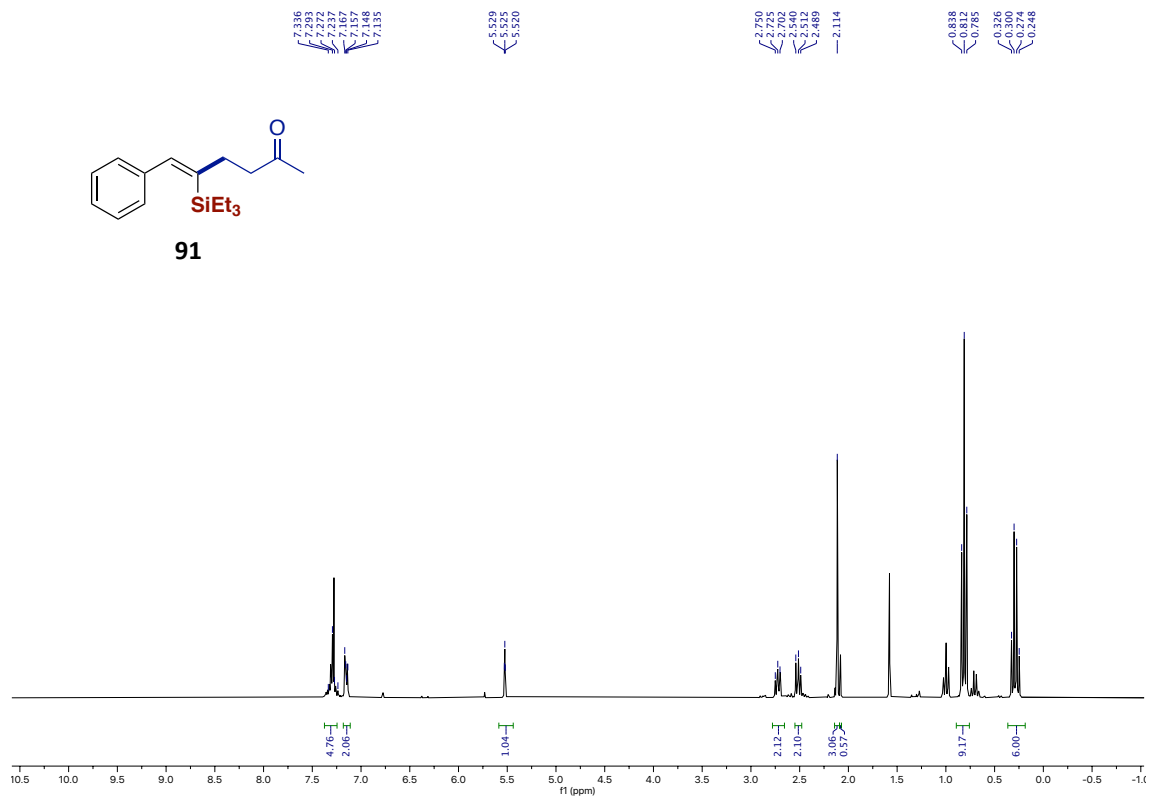
Stereoselective Base-Catalyzed 1,1-Silaboration of Terminal Alkynes



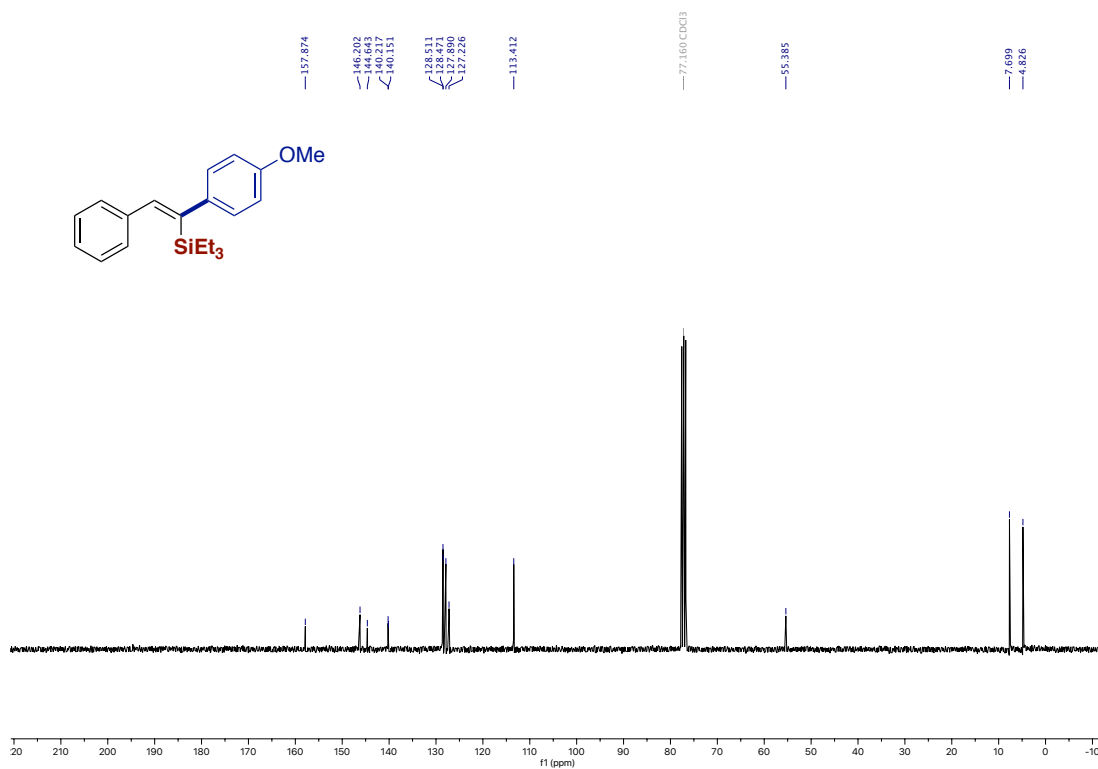
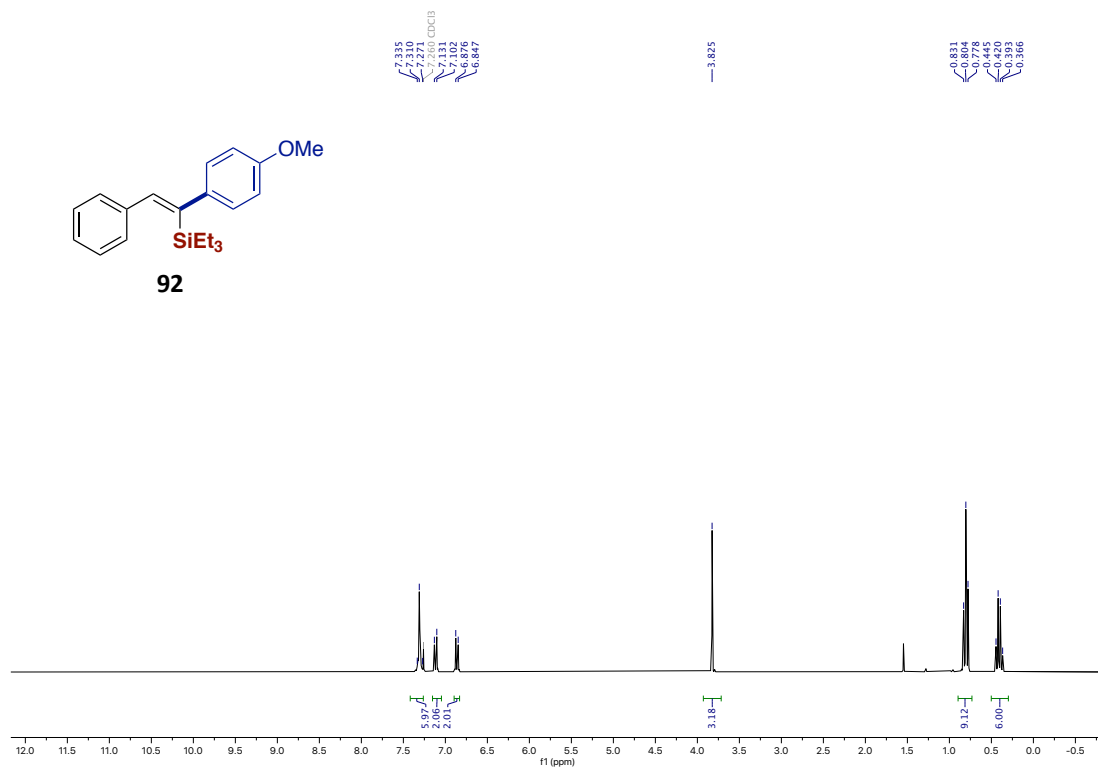


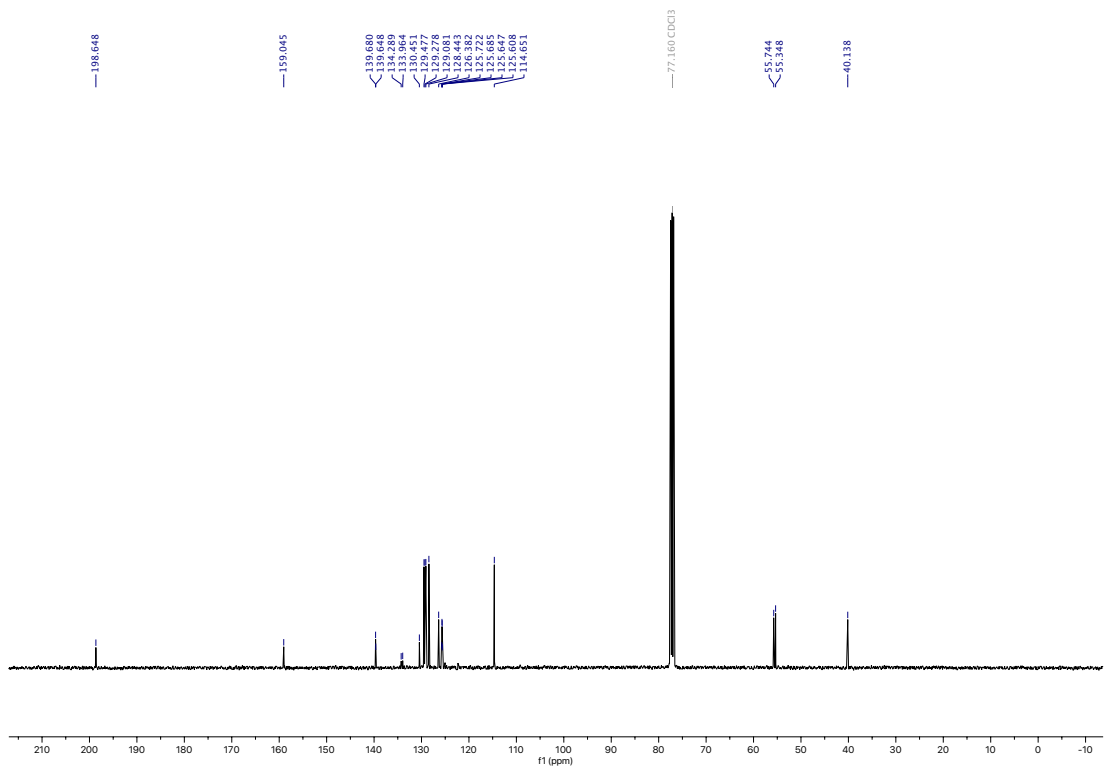
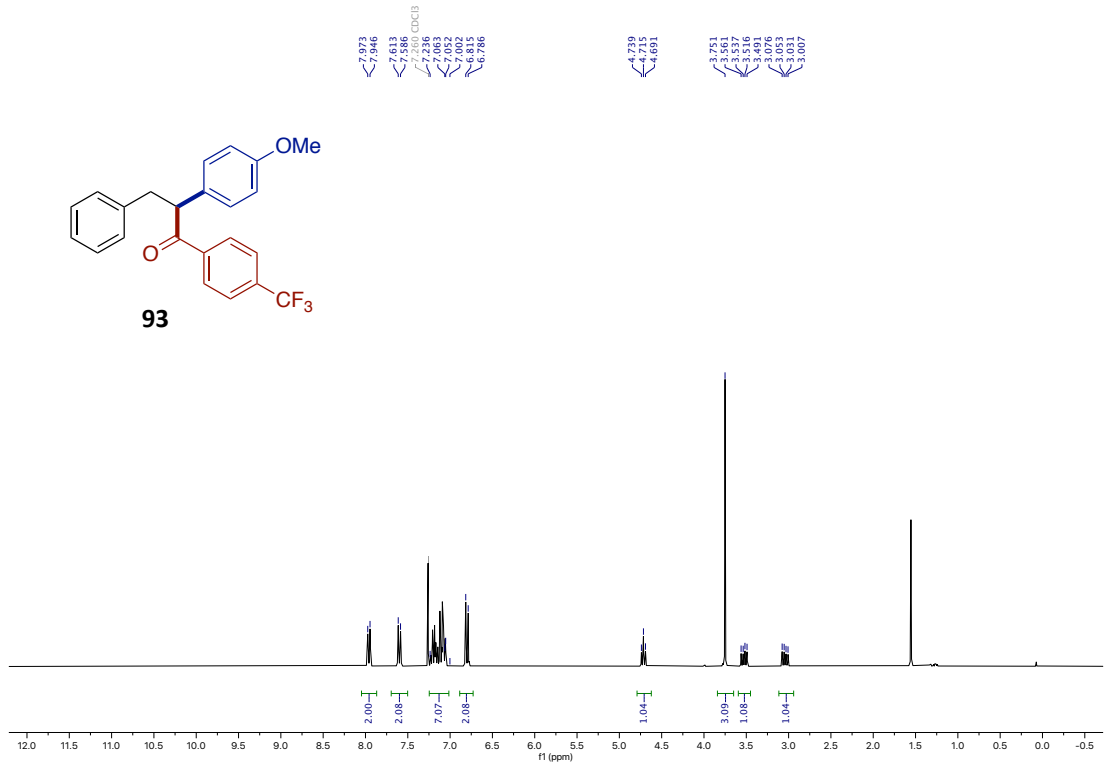
Stereoselective Base-Catalyzed 1,1-Silaboration of Terminal Alkynes



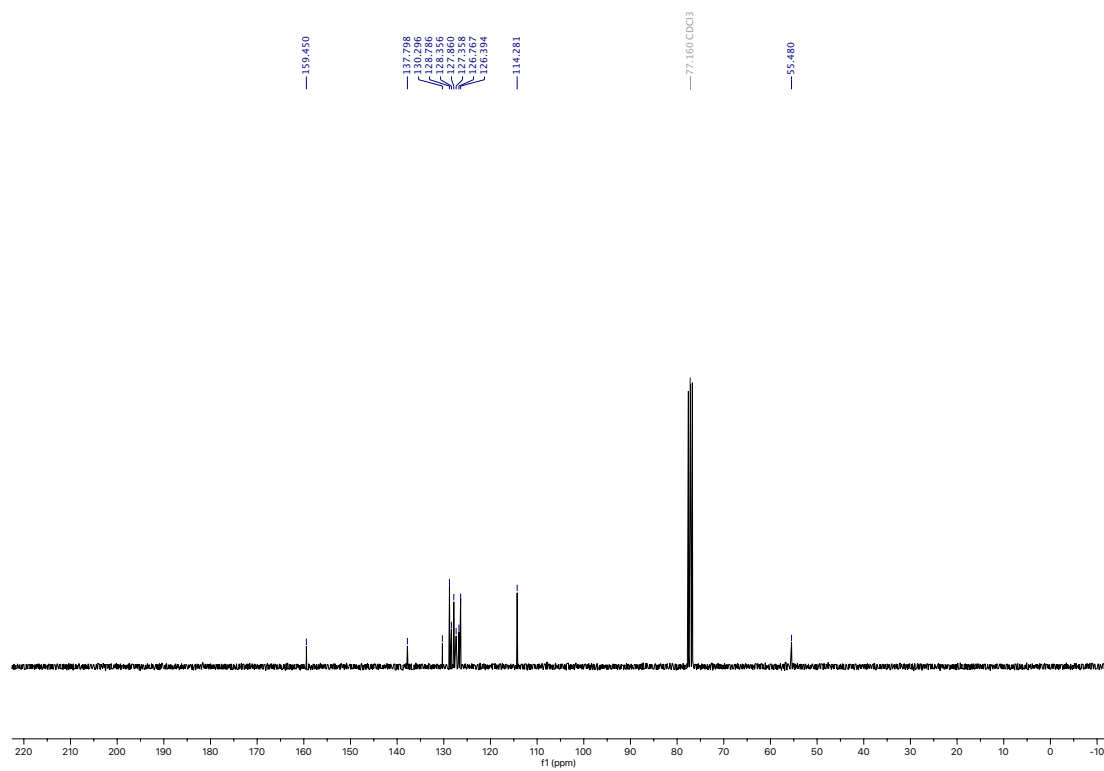
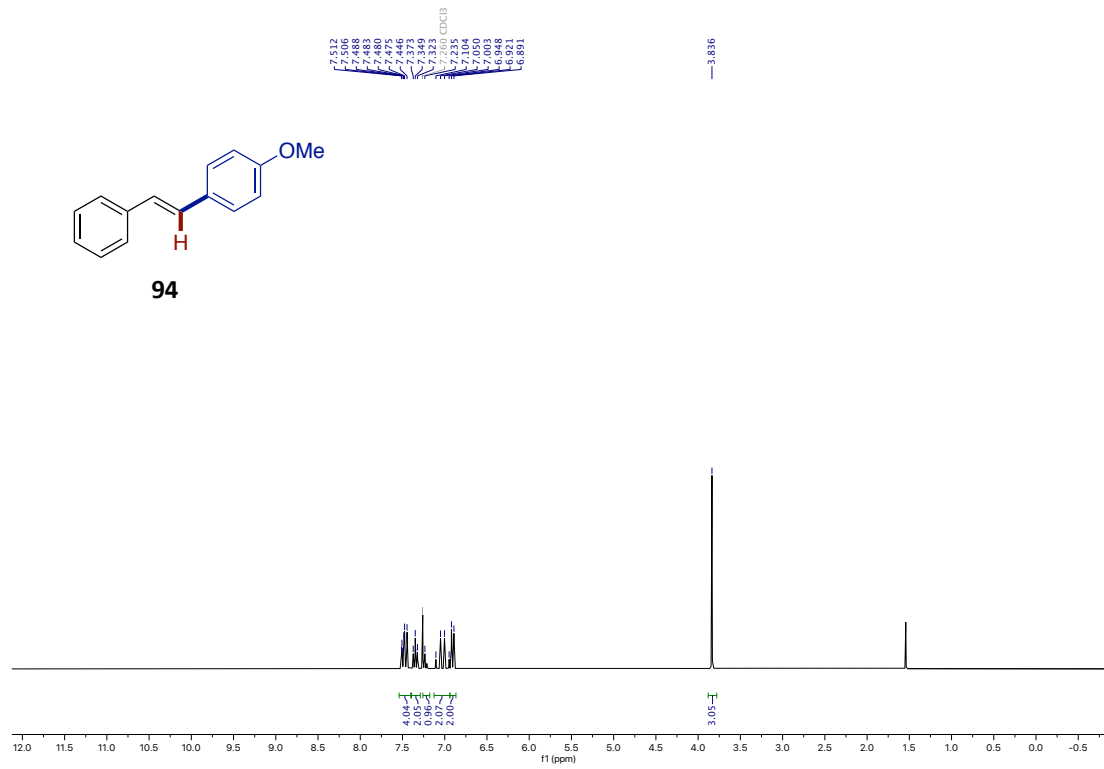


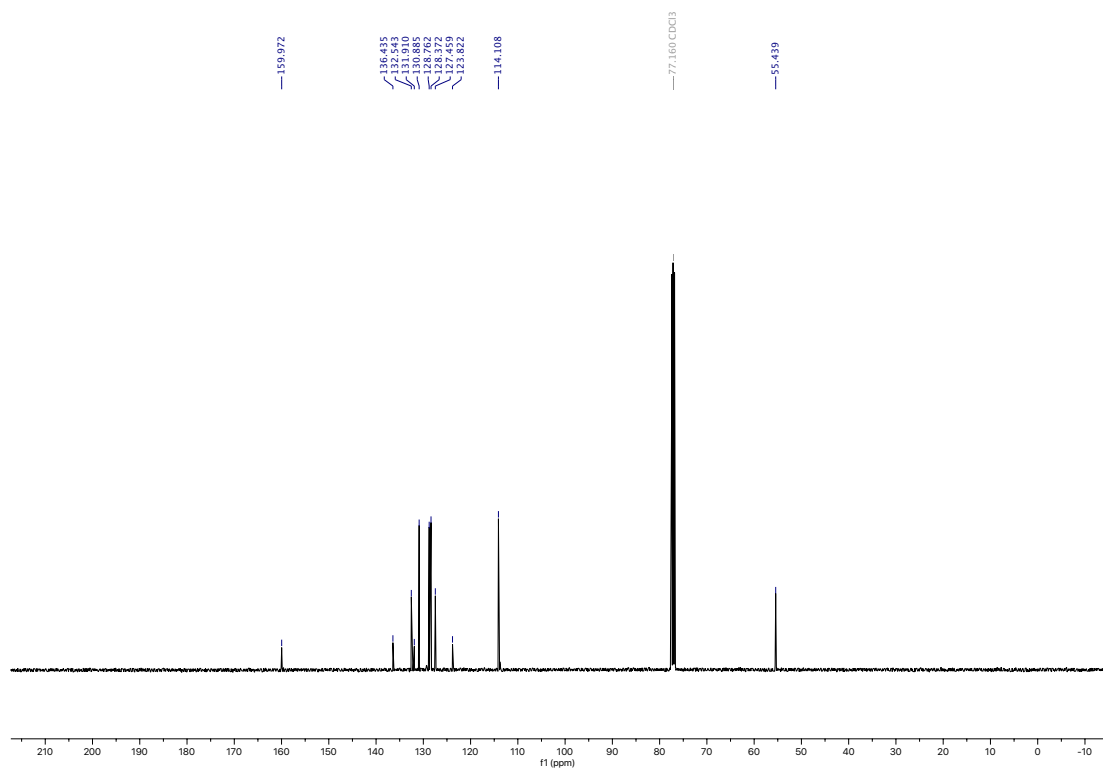
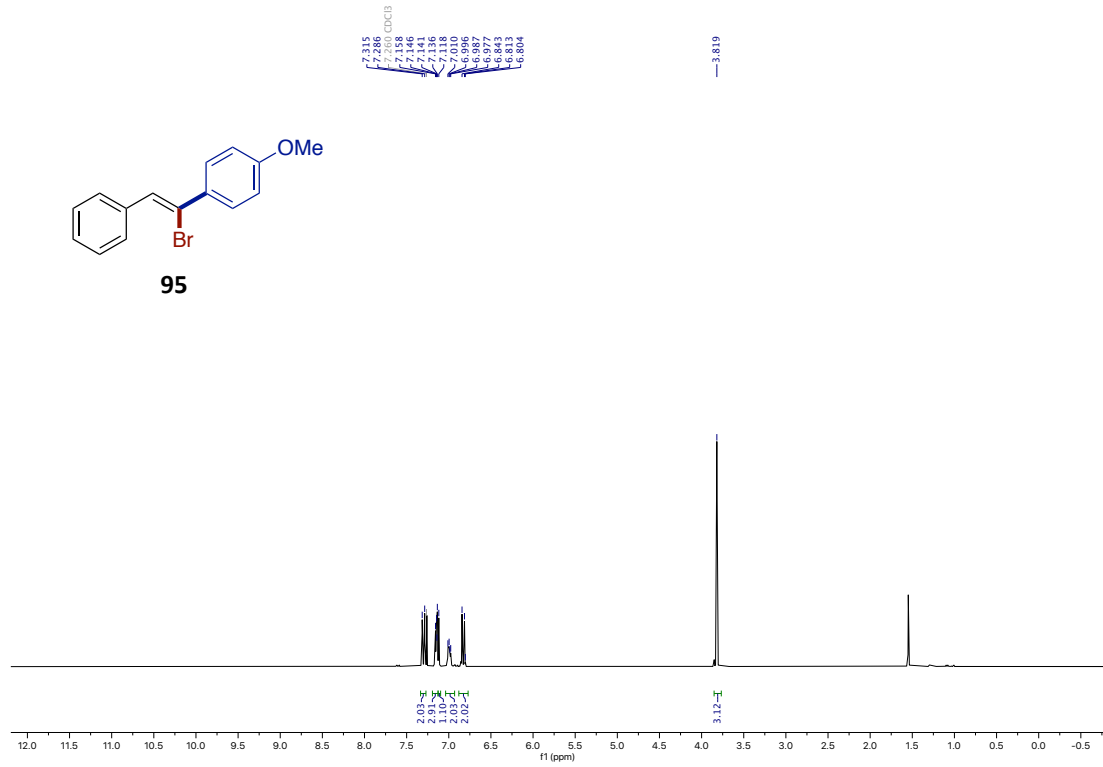
Stereoselective Base-Catalyzed 1,1-Silaboration of Terminal Alkynes

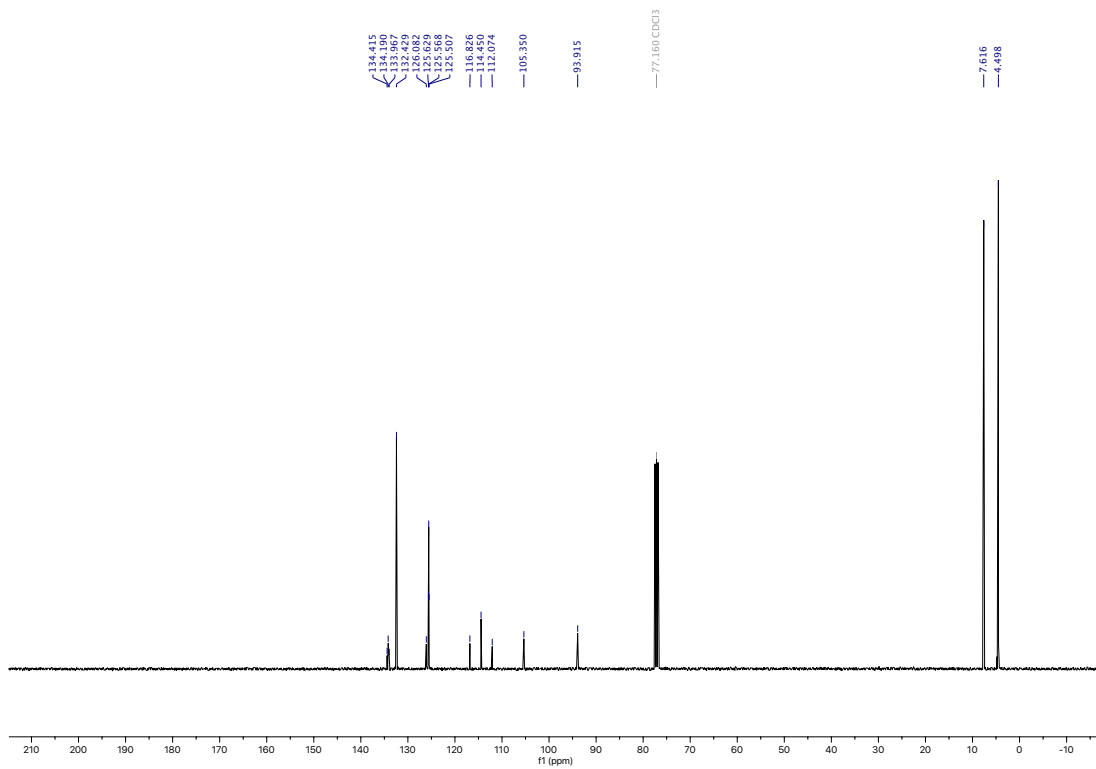
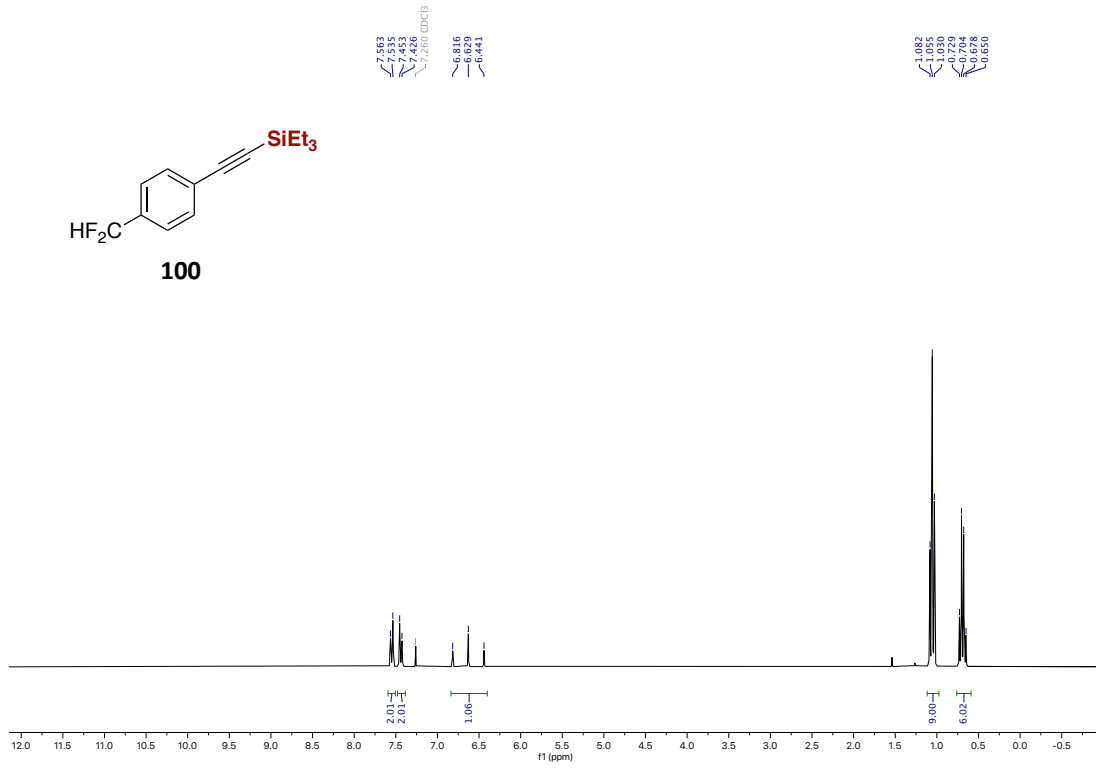
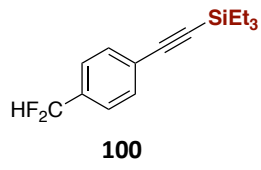




Stereoselective Base-Catalyzed 1,1-Silaboration of Terminal Alkynes







Chapter 5.

General Conclusions

The methods realized in this Doctoral Thesis showed wide utilization of silicon-heteroatom interelement linkage in functionalization of inert chemical bonds, enabling access value compounds via manifold activation pathways. It would be useful to highlight what we have achieved in our initial aims.

Chapter 2:

- A mild Ni-catalyzed stannylation of aryl pivalates via sp^2 C–O bond cleavage has been developed.
- This transformation represents an alternative methodology for efficient synthesis of arylstannes, various intermediates in organic synthesis; and is characterized by its wide substrate scope including rather sensitive functionalities.
- The applicability of the transformation is demonstrated with further functionalization of the synthesized arylstannanes, and orthogonal C–heteroatom bond formations.
- Based on experimental studies and precedent literatures, a Ni(0)-Ni(II) catalytic cycle was proposed to further understand the mechanism.

Chapter 3:

- A direct site-selective sp^2 C–H silylation of (poly)azines is described using stoichiometric KHMDS and silylboranes.
- The method features as its simplicity and mild reaction conditions, enabling late-stage silylation of drug molecules.
- It is also demonstrated that regioselectivity between C4 and C2 could be simply tuned by a judicious choice of corresponding ethereal solvents.
- Detailed mechanistic studies suggest the initially formation of intermediacy silyl anion species and a plausible catalytic cycle including dearomatized intermediates is presented.

Chapter 4:

- A KHMDS-catalyzed stereoselective 1,1-silaboration of terminal alkynes under surprisingly mild reaction conditions has been documented.
- The method is characterized by no transition metal catalyst, complete atom economy, and exquisite stereoselectivity, thus offering a convenient route to densely functionalized trisubstituted olefins.
- Although more rigorous mechanistic investigations are required in order to draw a catalytic cycle with full confidence, a 1,2-metallate shift from tetracoordinated boron atom to an sp carbon center is proposed to deliver geminal bimetallic alkenes.
- The potential usage of our protocol is illustrated by further transformation of silaborylated alkenes which could serve as versatile building blocks in stereoselective synthesis.

UNIVERSITAT ROVIRA I VIRGILI

C-H & C-O FUNCTIONALIZATION BY SILICON-HETEROATOM INTERELEMENT LINKAGES

Yiting Gu



UNIVERSITAT
ROVIRA i VIRGILI

